INSTITUT INTERNATIONAL DE PHYSIQUE SOLVAY

NEUVIÈME CONSEIL DE PHYSIQUE

tenu à l'Université Libre de Bruxelles
du 25 au 29 septembre 1951

L'ÉTAT SOLIDE

RAPPORTS ET DISCUSSIONS

publiés par les Secrétaires du Conseil
sous les auspices de la Commission Administrative de l'Institut

R. STOOPS
Editeur
76-78, COUDENBERG, BRUXELLES

—

1952

INTRODUCTION

RAPPORTS
ET
DISCUSSIONS

LE NEUVIÈME CONSEIL DE PHYSIQUE

Le neuvième des Conseils de Physique, prévus à l'article 10 des statuts de l'Institut International de Physique fondé par Ernest Solvay, a tenu ses séances à Bruxelles, du 25 au 29 septembre 1951, dans les locaux mis obligeamment à la disposition de l'Institut par l'Université Libre de Bruxelles, siège social de l'Institut.

Le Comité Scientifique de l'Institut était représenté par :

Sir Lawrence Bragg (Cambridge), *président*, et MM. H.A. Kramers (Leiden), C. Møller (København), N.F. Mott (Bristol), W. Pauli (Zurich), *membres*.

MM. F. Perrin (Paris), et J.R. Oppenheimer (Princeton), membres du Comité, étaient absents.

Les rapporteurs étaient :

MM. W.G. Burgers (Technische Hogeschool, Delft), F.C. Frank (H.H.Wills Physical Laboratory, Bristol), A. Guinier (Conservatoire National des Arts et Métiers, Paris) W. Köster (Max-Planck Institut für Metallkungde, Stuttgart), N.F. Mott (H.H. Wills Physical Laboratory, Bristol), F. Seitz (University of Illinois, U.S.A.), W. Shockley (Bell Telephone Laboratories, Murray Hill, U.S.A.), C.S. Smith (University of Chicago, U.S.A.), E. Rudberg (Mettallografiska Institutet, Stockholm).

Ont fait des exposés complémentaires :

MM. C.O.G. Borelius (Royal Technical University, Stockholm), A.H. Cottrell (The University-Edgbaston, Birmingham), C. Crussard (Ecole Nationale Supérieure des Mines, Paris), U. Dehlinger (Institut für Theor. und Angew. Physik der Techn. Hochschule, Stuttgart), J. Laval (Collège de France, Paris), E. Orowan (Massachusetts

Intitute of Technology, U.S.A.), G.W. Rathenau (Philips Research Laboratories, Eindhoven).

Etaient également invités :

Mlle Yvette Cauchois (Laboratoire de Chimie physique, Paris), MM. N.P. Allen (National Physical Laboratory, Teddington), J.H. Hollomon (General Electric Co., Schenectady, U.S.A.), G. Homes (Université de Bruxelles).

M. C. Zener (University of Chicago) n'a pas pu accepter l'invitation qui lui avait été faite.

L'United States Office of Naval Research qui prêta son concours à la Commission administrative de l'Institut pour arranger le voyage de certains invités des centres de recherches américains, était représenté par M. L.M. McKenzie (Washington).

Mlle L. de Brouckère, MM. G. Balasse, R. Gaspars, J. Geheniau, L. Groven, I. Prigogine de la Faculté des Sciences de l'Université Libre de Bruxelles et MM. M. Cosyns, L. Flamache, P. Kipfer, O. Goche de la Faculté des Sciences appliquées de la même Université étaient invités comme membres auditeurs.

Le Secrétariat du Conseil a été assuré par MM. H. Curien (Paris), W.M. Lomer (Cambridge), P.V. Pâquet (Bruxelles).

La Commission administrative de l'Institut se composait de M. Jules Bordet, *président*, MM. E.J. Solvay, Dr. F. Heger-Gilbert, E. Henriot, *membres* et M. F.H. van den Dungen, *secrétaire*.

Le jeudi 27 septembre les membres du Conseil ont visité le château de Gaasbeek où ils ont été reçus par M. G. Lockem, conservateur de ce musée de l'Etat.

Suivant la tradition, un banquet offert par la famille Solvay et la Commission administrative de l'Institut a réuni la plupart des membres du Conseil le soir du vendredi 28 septembre; des toasts ont été portés par M. E.J. Solvay et Sir Lawrence Bragg.

Interfaces Between Crystals

by Cyril Stanley Smith *

**Professor of Metallurgy and Director,*
Institute for the Study of Metals, University of Chicago
Chicago, Illinois, U. S. A.

INTRODUCTION

A discussion of the interfaces between crystals must at the present time be limited mainly to empirical facts. Though the interface between fluids has been experimentally studied for three centuries and satisfactory theories have existed for nearly one, crystal boundaries have until very recently been ignored by the theorist.

Metallurgists have long been aware of the practical consequences of intercrystalline « hot-short » fracture, of the slow intercrystalline flow of metal when exposed to steady loads at elevated temperatures, and of the migration of grain boundaries to produce an increase of grain size on annealing. However, even the metallurgist has generally paid more attention to the structure, deformation, and properties of the grains themselves than to the interfaces between them.

King and Chalmers ([1]) in their excellent review of the properties of grain boundaries discuss briefly the development of ideas concerning their structure, commencing with the amorphous metal theory which flourished under the protagonism of Rosenhain. The idea of a spatially-concentrated disorganized zone rather than a progressive change of orientation from one crystal to its neighbor was supported by the observations on the mechanical behavior of polycrystalline metals at elevated temperatures, which act as if the crystals are joined by a cement whose viscosity varies with temperature in the manner of a normal liquid. However, as King and Chalmers point out :

« The hypothesis that the amorphous material must be in equili-

brium with the crystals at any temperature below the melting point demands that the free energy of the boundary material must vary with temperature according to a different law from that followed by the liquid. Thus some property of the boundary material must change with temperature. This cannot be the structure if this resembles that of the supercooled liquid. It must therefore be some function of the thickness, but since the thickness would have no effect on the free energy of the atoms that are not very close to the limiting surfaces of the boundary, it follows that the boundary must be so thin that the whole of it is affected by the neighbouring crystals. It is difficult to see how a layer of this kind differs from a transitional lattice. »

The argument for a transitional lattice in preference to a layer of amorphous metal is essentially one of dimensions and the two concepts become identical if all disorder is regarded as being concentrated in a two-dimensional layer (or, more correctly, a layer only one atom thick) of complete or partial disorder. In the absence of long-range elastic strain externally imposed, it is obvious that there must be either missing or added atoms between two extended crystalline regions of different orientation, and it is equally apparent that many of the atoms at the boundary may be regarded as belonging to both lattices and having the normal number of neighbors even though the atomic volumes and the angles between nearest neighbors may be abnormal. In considering a grain boundary it is useful to regard the topological and the elastic strain features separately. Strain may decrease rapidly away from a boundary but at least to an infinitesimal extent it must influence the entire crystal. Topologically the missing or added lattice sites — i. e., the atoms of abnormal coordination — do not need to form a separate three-dimensional cell but can exist in a two-dimensional interface between the three-dimensional cells of uniform lattices. The interface is not necessarily plane; in fact, it is unlikely that it should be so. If a separate three-dimensional non-crystalline phase should form between the crystals there would of necessity be at least two interfaces, i. e., at least one more than needed for the minimum solution. There is no reason to regard the interface as more than two-dimensional. All phenomena connected with grain boundaries can be accounted for if the grain boundaries are regarded as having properties that depend only on extent and are independent of thickness.

Though many of the physical, chemical, and thermodynamic

descriptions of the interface between immiscible fluids can be applied to the boundary between two crystals of the same phase, there are certain essential differences. Crystals differing in orientation are thermodynamically the same phase, have identical free energies, and no change of energy or entropy occurs as material is transferred from one to the other across a plane interface. Yet the interface is indestructible at any temperature and pressure provided that the crystalline phase itself is stable; it has two-dimensional continuity and though it can be distorted it cannot be pierced. It has free energy associated with it and seeks a minimum-energy configuration just like the interface between two immiscible fluids, although unlike the interface between fluids, the crystal boundary does not necessarily tend to a configuration of minimum area, and it may, of course, be made to disappear entirely by giving the adjacent two crystals the same orientation.

In many respects intercrystalline boundaries behave as thin films of a liquid phase separating discrete cells of another fluid. The boundaries in a polycrystalline solid can be geometrically duplicated by models in either two or three dimensions consisting of an emulsion of oil with a minor aqueous phase or more simply by a froth of air bubbles separated by soapy septa (*). However, unlike such two-phase systems, the grain boundary acts as if it had no volume, and nothing accumulates as the area of grain boundary diminishes during grain growth. In many respects the grain boundary represents the surface phase that students of Gibbs are told must *not* be assumed to have physical reality. Its existence is in very essence two-dimensional. In ordinary liquid solutions there is tolerance for some concentration gradient near an interface, but in the case of, for example, large polar molecules in water the gradient of chemical potential with concentration may be so steep that, in an attempt to maintain constant chemical potential throughout the system, the composition varies discontinuously on a molecular scale and a true surface phase may result. Similarly in crystals, the change in energy resulting from local lattice imperfections must be very high and atoms of abnormal coordination necessary at a grain boundary must be limited to extremely small layers, probably even to monatomic ones.

(*) It should be noted that such films are stable only if they contain a surface-absorbed polar molecule oriented normal to the surface, so that as the film becomes thinner the two surfaces repel each other. In the absence of this the film can locally become progressively thinner under even a slight pressure gradient until it eventually perforates and allows the fluid in adjacent cells to merge.

VARIATION OF GRAIN BOUNDARY ENERGY WITH ORIENTATION

An examination of the miscrostructure of an annealed metal or single phase alloy reveals a high proportion of 120° angles between smoothly curved boundaries, which suggests that the energy of a boundary is independent both of the orientation of the crystals that it separates and of the direction of the boundary in relation to the crystal axes. Although in a random aggregate most of the boundaries are in the range where this is approximately true, it is not so when the crystals approach identical or twin orientations.

The theoretical treatment by Shockley and Read in their important papers [2] [3] is in excellent agreement with the experimental determinations of relative grain boundary energy as a function of orientation made by Dunn *et al* [4] [5] and by Aust and Chalmers [6] [7] Shockley and Read used the simple dislocation model proposed independently by Burgers [11] and Bragg [10] and considered the energy of a dislocation as being divisible into two components, a fixed energy associated with a volume of about atomic size and a shear strain energy which can interact with the strain field of adjacent dislocations. Their simple treatment for a boundary between two crystals which have a principal crystallographic direction in common gives the following relation :

$$E = \frac{Ga\,(\cos\varphi + \sin\varphi)}{4\pi\,(1-\sigma)}\;\theta\,(A - ln\;\theta) \qquad (1)$$

for an isotropic cubic metal where E is total grain boundary energy; G is the shear modulus; σ Poisson's ratio; a is the slip vector of the dislocation; A is an arbitrary constant and represents the energy associated with each dislocation in the small volume wherein the number of neighbors is incorrect and the strain is beyond the range where Hooke's Law holds; θ is the orientation difference between the lattices; and φ represents the inclination of the boundary from the position of exact symmetry. This relation suggests (for symmetrical boundaries between crystals differing not greatly in orientation) a linear relation between E/θ and log θ, the slope being

$$\frac{Ga}{4\pi}\,(1-\sigma).$$

Though it is a matter of considerable difficulty to obtain absolute

measurements of grain boundary energies, it is relatively simple to obtain the relative energies between interfaces which can be brought into equilibrium with each other at a three-grain corner. The dihedral angle of such crystals (Figure 1) is given by the simple triangle-of-forces relation:

$$\frac{\gamma_{23}}{\sin\theta_1} = \frac{\gamma_{13}}{\sin\theta_2} = \frac{\gamma_{12}}{\sin\theta_3}. \qquad (2)$$

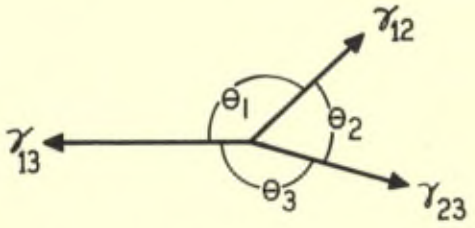

Fig. 1. — Three interfaces in equilibrium geometry under surface forces.

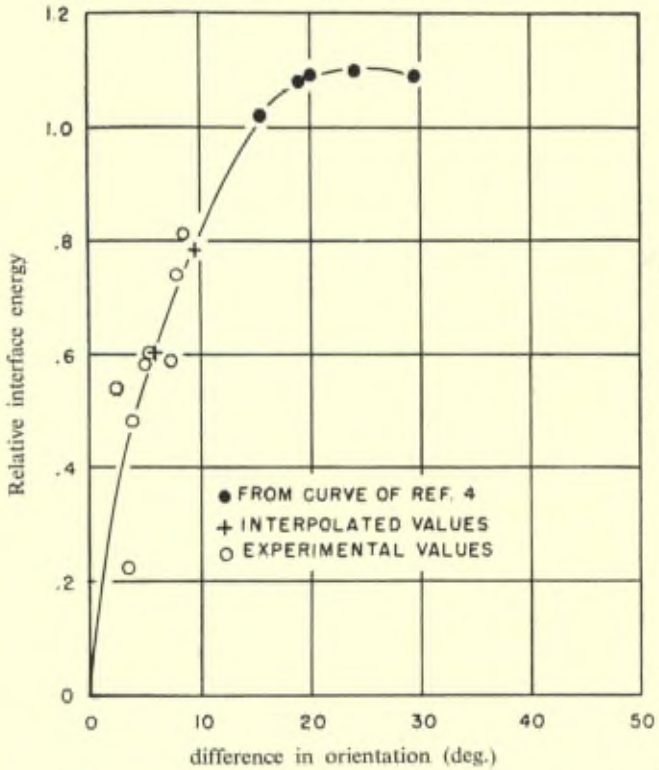

Fig. 2. — Variation of relative boundary energies in α silicon iron with difference in orientation of grains. 110 axes in common. (Dunn *et al*) [5].

If one boundary is known or used in successive experiments as a constant reference value, the others are obtainable in relative terms and the effect of orientation may be seen. This technique has been applied by Dunn and Lionetti to silicon-iron ([4]), ([5]) and by Aust and Chalmers to lead ([7]) and tin ([8]) with results shown in Figures 2, 3, 4 and 5. Figure 6 shows the silicon-iron values, and Figure 7 the Aust and Chalmers' values for lead and tin plotted as γ/θ *vs* log θ. There is remarkable agreement with the prediction from the Shockley-Read theory that straight lines should result. Figure 8 shows Aust and Chalmers' results converted to absolute surface energy by arbitrarily selecting an appropriate value of A to give the best fit with accepted values of G, a, and σ and ignoring the difference between free energy, which they measured and total energy, which Equation 2 gives. The factor A was $+ 0.2$ in the case of lead, $- 0.6$ for tin. As Aust and Chalmers point out, it is remarkable that the adjusted experimental data agree with predictions so well even for high angle boundaries, for the theory should not apply when dislocations are numerous and close together. The negative value of A for tin may result from the non-cubic nature of its lattice. It will be noticed that the high-angle boundary in lead and tin corresponds to energies of about 200 and 100 erg/cm^2, respectively, if the theory is correct and the constants properly interpreted. Shockley and Read proposed a value of about 1300 ergs/cm^2 for the silicon-iron boundary of Dunn and Lionetti, using $A = 0.5$. Though the tin and lead values are reasonable this silicon-iron boundary seems to be improbably high. *

Read and Shockley show that on the simple dislocation model a series of cusps should occur since dislocations can be evenly spaced only at a few critical angles. Figure 9, reproduced from their paper, shows the variation to be expected due to this cause and the particularly low cusps occuring at a twin orientation. They show that when the crystals are related in twin orientations the energy varies

(*) Reference should be made to the paper by Greenough and King ([42]) published after the present paper was written. By measuring the dihedral angle of surface grooves resulting from the equilibration of grain boundaries against the surface of silver, they obtained the relative value of grain boundary energy as a function of orientation difference in three series of bi-crystals, each with a common axis progressively rotated. In all three cases the energy rapidly increases at first as the angle between lattices increases, following the general pattern of Fig. 2 to 5. Although the results are not inconsistent with a decrease of energy for angles above about 20°, as called for by equation (1), the experimental scatter is such that they could with equal precision represent a nearly constant value.

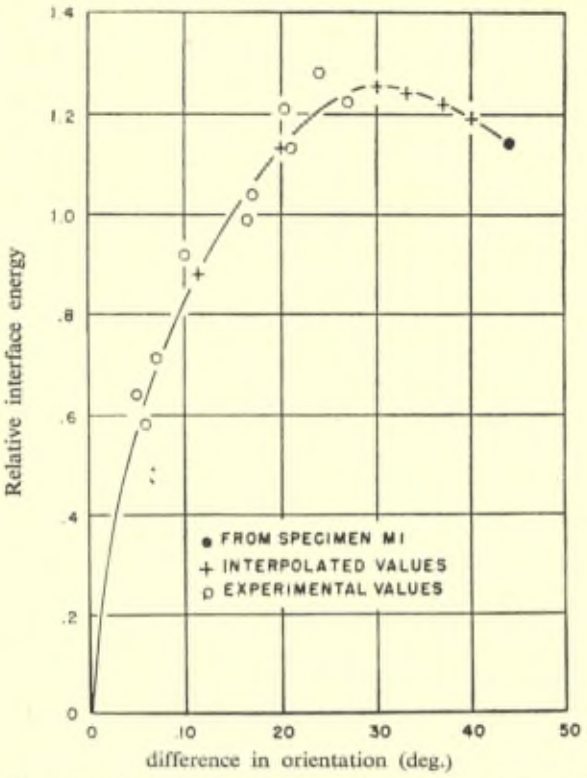

Fig. 3. — Variation of relative boundary energies in α silicon iron with difference in orientation of grains. 100 axes in common. (Dunn *et al*) [5].

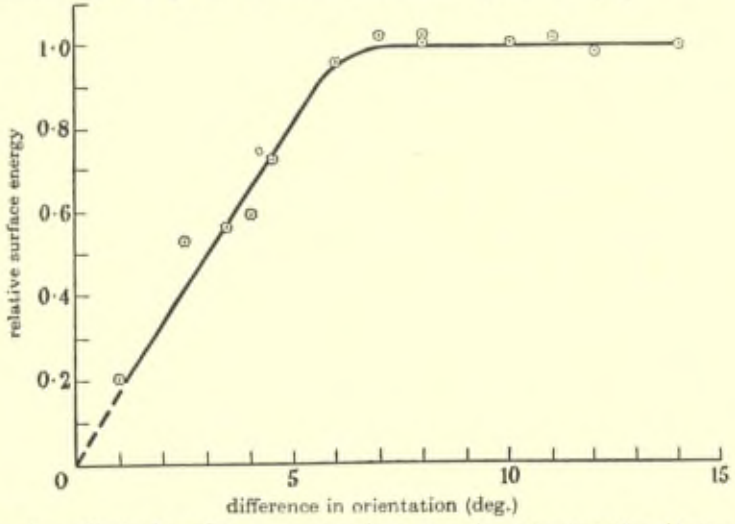

Fig. 4. — Grain boundary energy in tin as function of orientation (Aust and Chalmers) [6, 7].

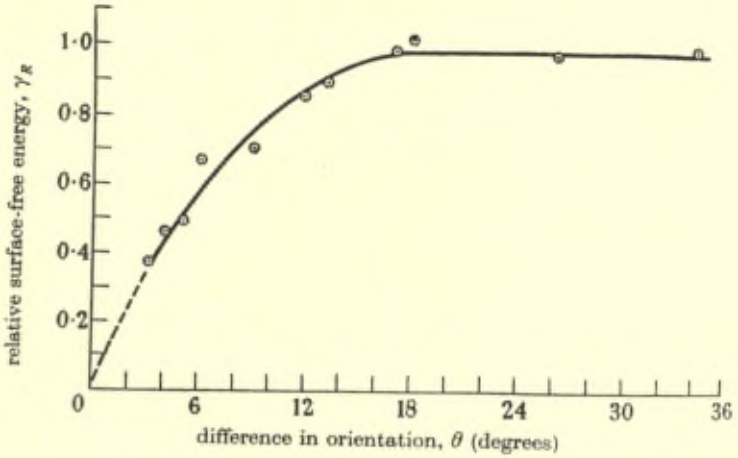

Fig. 5. — Grain boundary energy in lead as function of orientation (Aust and Chalmers) [6] [7].

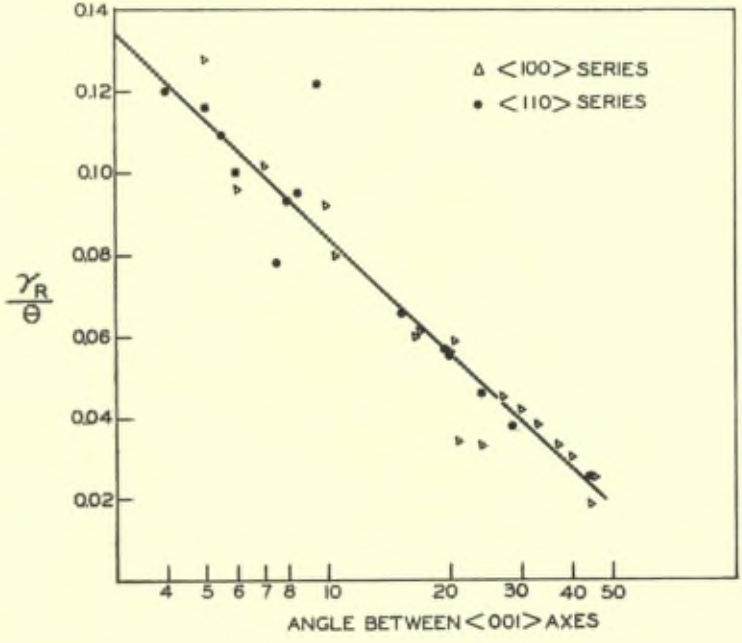

Fig. 6. — Grain boundary energy of 3.3 % silicon-iron. (Dunn *et al* [5], replotted as γ_R/θ *vs* log θ).

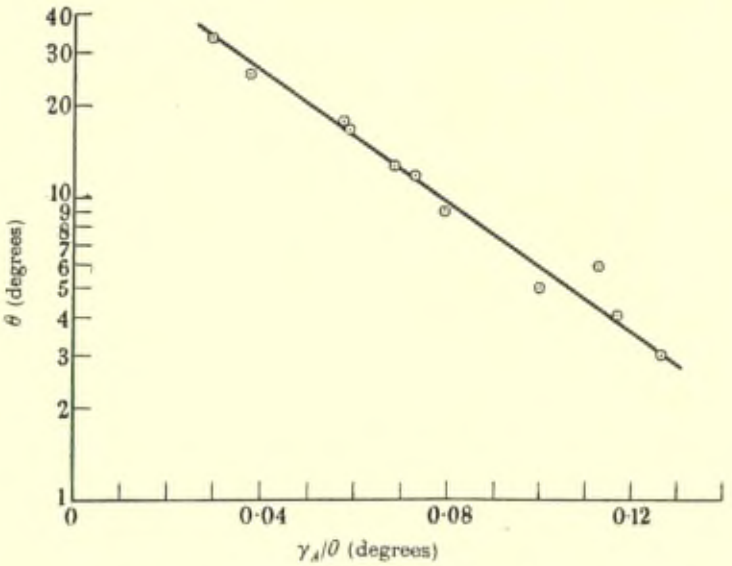

Fig. 7. — A. Grain boundary energies of lead plotted as γ_B/θ *vs* log θ. (Aust and Chalmers) (7).

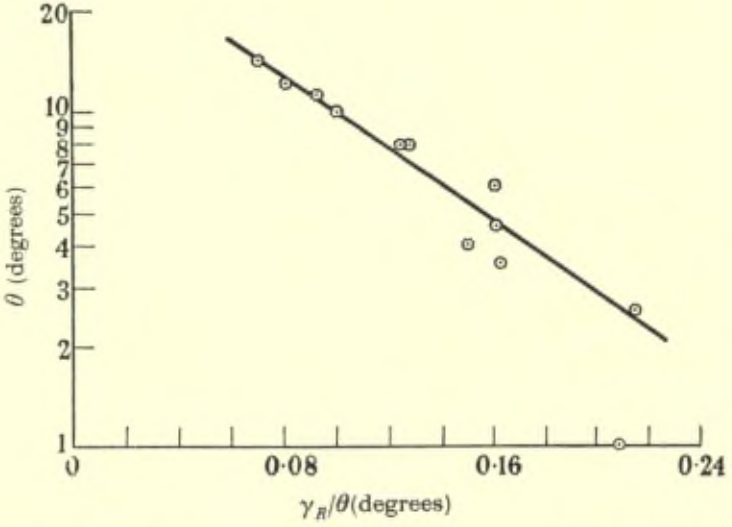

B. Grain boundary energies of tin plotted as γ_B/θ *vs* log θ. (Aust and Chalmers) (7).

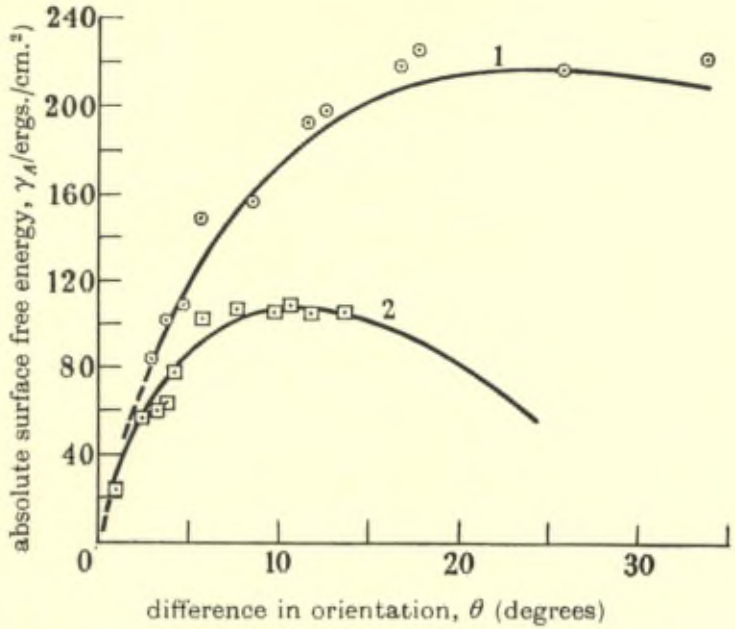

Fig. 8. — Comparison between theoretical curves for Pb and Sn (A = + 0.2 and — 0.6, respectively) with experimental results adjusted to best fit. (Aust and Chalmers) (7).

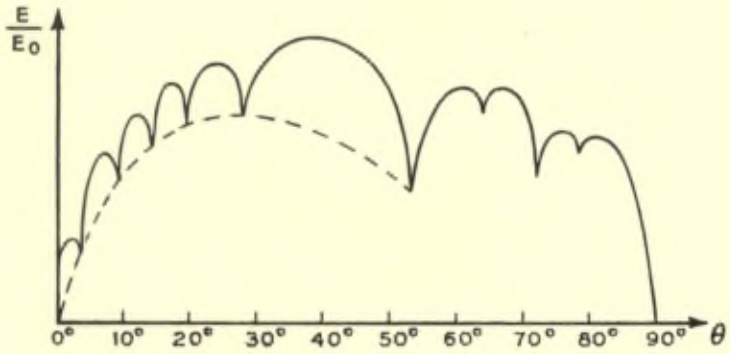

Fig. 9. — Theoretical variation of grain boundary energy with orientation, showing fine structure and twin boundary cusp. (Read and Shockley) (2).

steeply as the boundary orientation varies from the symmetrical one, and that the symmetrical boundary is nearly as strongly dependent on slight departures from the twin orientation as in the case of crystals with small deviations from identical orientation. Although

there is plenty of qualitative evidence in the appearance of microstructures of metals for the low energy of twin-boundaries and their sensitivity to orientation, random boundaries generally do not appear to be as directionally sensitive as suggested by Figure 8.

When the boundary energy varies with its spatial orientation the simple triangle-of-forces relation of equation (2) does not hold (*) but, as Bardeen ([10]) has shown, the relation becomes.

$$\gamma_1 - \gamma_2 \cos \alpha_2 - \gamma_3 \cos \alpha_3 + \sin \alpha_2 \frac{\partial \gamma_2}{\partial \alpha_2} + \sin \alpha_3 \frac{\partial \gamma_3}{\partial \alpha_3} = 0 \qquad (3)$$

where α_3 and α_2 are the angles between interfaces 3 and 2, respectively, and the extension of interface 1. It has been shown by Burke ([12]) that twins in alpha-brass or copper cannot move normal to the twinning plane, and the writer ([13]) has shown photomicrographs of twinned grains surrounded with liquid in which, parallel twin boundary migration does not occur although it would produce a large reduction of surface area. The correct mechanical analogue is therefore not that of three strings free to reach equilibrium as in Figure 1, but that of a stiff rod free to move only in the direction of its length, as in Figure 10 (taken from Fullman ([14]), who has developed this concept). Under these conditions, the following equation holds :

$$\gamma_{12} \cos \theta_1 + \gamma_{t2} \cos \theta_2 + \gamma_t = 0 \qquad (4)$$

which is identical with Equation (3) if the two parts of the principle crystal boundary are assumed to be themselves independent of orientation. Applying this to actual dihedral angle measurements in copper, Fullman found that the ratio of the twin boundary energy to that of the average grain boundary was 0.045 ± 0.0030. Another figure, obtained by a more devious route, will be given later.

In another paper Fullman ([15]) has found the ratio of twin to boundary energy in the case of aluminium to be 0.21 ± 0.05, a much higher value than in copper and in line with the relative rarity of twins in the microstructure of aluminium compared with their fre-

(*) There has been much discussion regarding the use of surface-tension equilibrium concepts in the case of solids. Although surface free energy and surface-tension are dimensionally identical, they are not necessarily numerically equal in the case of solids. However, as Gurney ([11]) has shown, if any atomic mobility exists at the interfaces the two must be identical at equilibrium, and it is only in the lack of mobility that any distinction can be drawn. Under the annealing conditions customarily used there is no possibility of maintaining shear stresses across an interface and Gurney's condition is certainly met.

quency in copper and its alloys. Similarly, Dunn, Daniels and Bolton [16] measured angles opposite twin boundaries in sillicon-iron (3.3 % Si) and obtained 0.22 as the ratio of twin energy to that of a general grain boundary.

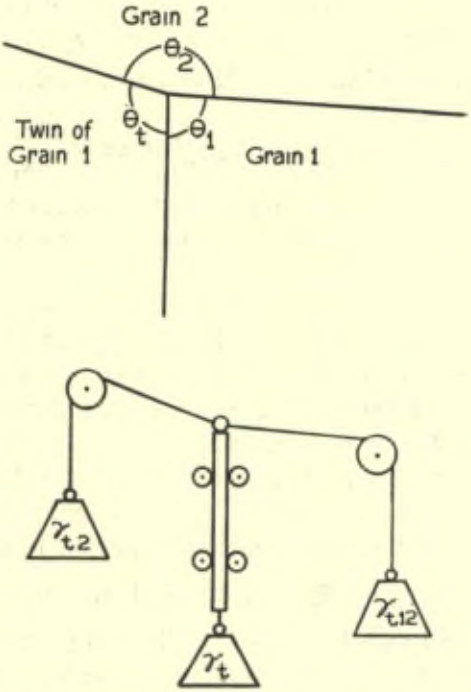

Fig. 10. — Mechanical analogue of interface tension equilibrium at junction of twin boundary and grain boundary (after Fullman) [14].

ABSOLUTE MEASUREMENTS OF GRAIN BOUNDARY ENERGIES

Although relative grain boundary energies are easy to obtain, absolute energies are more difficult. Calorimetric measurements have not been made and are, in fact, likely to prove extremely difficult since the grain boundary free energy is small — for example only about 0.05 calories for 1 cubic cm. of copper at 0.01 mm. grain size — and the total heat, including entropy, is not likely to be more than twice the free energy. It is possible, however, to measure the free

energy of liquid surfaces or interfaces by standard capillary techniques and to equilibrate such interfaces with solid/liquid interfaces whose relative energies are then obtained by measuring the equilibrium angles and using Equation 1. These in turn can be balanced against a solid-solid interface whose energy is to be obtained. This method, though correct in principle, is not capable of high precision. It has been used to measure the copper grain boundary energy (derived from liquid lead via the copper/lead interface) and the gamma-iron boundary (from the molten copper/copper-sulphide interface via both Fe/Cu and Fe/Cu_2S interfaces).

The first investigators to use this technique were Bailey and Watkins [17]. They measured the contact angle of copper-saturated liquid lead against a plane copper surface and the dihedral angle of the groove in a copper surface in equilibrium with lead vapor against a grain boundary. From these values, together with the known surface tension of lead and a previous value [21] for the ratio of grain boundary energy to that of the copper-lead interface, they obtained the value of 640 ergs/cm^2 for the grain boundary energy. Their data are summarized in Table I.

TABLE I

Some Absolute Measurements of Free Energies of Interfaces in the Cu-Pb System. (Bailey and Watkins) [17]

Interface	Interface Free Energy			
	800 °C erg/cm^2	900 °C in H_2 erg/cm^2	900 °C in Argon erg/cm^2	B and W Selected Value erg/cm^2
Lead/lead vapour (assumed) . .	435	466	466	
Copper/lead vapour	780 810*	810 880*	740 720*	780
Copper/copper vapour	1750 1840*	2000 2170*	1600 1350*	1800
Copper/liquid lead	380 400*	360 420*	290 260*	340
Copper/copper.	670 700*	700 750*	560 470*	640

(*) Value obtained by reinterpretations by Fisher and Dunn [19].

Fisher and Dunn ([19]) suggested that Bailey and Watkins' contact angle did not correspond to a strictly plane surface and they introduced corrections for local changes in geometry due to solution and transfer of copper, thereby obtaining the values marked with an asterisk in Table I.

Sears ([20]) used a slightly different approach to the same system. By placing small drops of lead on the surface of copper crystals and measuring the diameter and height of the lens-shaped drops formed at equilibrium he estimated the angles at the edge of the lens and so obtained the ratio of the three interfaces. From this the lead/copper interface was found to have an energy of 510 ergs/cm^2 and, using the known dihedral angle of lead against a copper boundary, 860 ergs/cm^2 for the grain boundary energy. Because the copper surface surrounding the drops was not strictly plane, this measurement is probably not as accurate as that of Bailey and Watkins. Fisher and Dunn ([19]) have critically reviewed all the data in this system and have selected most probable values for all of the energy ratios involved. Their conclusions are shown in Table II, together with all other absolute values for copper grain boundary energies.

A second type of interface available for equlibrating with grain boundaries and whose energy is known absolutely is the surface of the crystals themselves. The surface free energy of copper has been measured by Udin, Schaler and Wulff ([22]) by the method (in principle easy but in practice difficult) of determining that stress which a fine wire will withstand without either extending or shortening at a temperature where microcreep occurs. They obtained the value of about 1410 ergs for copper at 1000 °C, and later ([43]), after allowing for the effects of grain boundaries, they suggested a revised value of 1650 ± 100 ergs/cm^2 at the melting point with a temperature coefficient of —0.55 ergs/cm^2/°C. This corresponds to about 1600 ergs/cm^2 at 1000 °C. Utilizing the surface dihedral angle against a grain boundary [(the significance of which was realized by Chalmers, King and Shuttleworth ([23]) and by the writer ([21]) but first measured by Bailey and Watkins ([17])] grain boundary energies may be directly obtained, as reported in Table II. Since the dihetral angle is about 160° the results are extremely sensitive to experimental error and cannot be regarded as reliable. Moreover, the work of Alexander, Dawson and King ([44]) showed that polycrystalline wires under low stress at high temperatures bulge, bend and undergo complicated

changes of shape which render surface tension measurements by Udin's method very unreliable.

All the above measurements relate to interfaces in the copper or copper-lead system. The only other values that have been obtained absolutely are those of Van Vlack (24) working in the writer's labo-

TABLE II

Absolute Grain Boundary Energies of Copper.

Interface	Derivation	Energy ergs/cm^2	Refer.
Random grain boundary	$\gamma_{10}\frac{\gamma_{11}}{\gamma_{10}} = 1700 \times 0.36$	610	43,17
	$\gamma_{23}\frac{\gamma_{12}}{\gamma_{23}}\frac{\gamma_{11}}{\gamma_{12}} = 435 \times 0.79 \times 1.72$	590	19
	$\gamma_{23}\frac{\gamma_{13}}{\gamma_{23}}\frac{\gamma_{11}}{\gamma_{13}} = 435 \times 1.78 \times .65$	505	19
	See Table III	595	24
	Average value	575	
Coherent twin boundary	$\gamma_{11}\frac{\gamma_t}{\gamma_{11}} = 550 \times 0.045$	24.7	14
Coherent twin boundary	$\gamma_{13}\frac{\gamma_t}{\gamma_{11}} = 760 \times 0.0168$	12.7	14
	Average value	19	
Incoher. twin boundary	$\gamma_{11}\frac{\gamma_{t'}}{\gamma_{11}} = 550 \times 0.80$	440	14

Phases : 0 = copper vapour
1 = copper crystal
2 = lead (liquid)
3 = lead vapour
4 = copper (liquid)
5 = copper sulphide (liquid)
6 = gamma iron crystal
7 = alpha iron crystal
t = twin interface in copper
t' = non-coherent twin in copper.

NOTE : The value used for γ_{10} is the average between Udin's corrected value (43) and Bailey and Watkins' (17) value. The other values are taken directly from the references cited.

ratory. Using the standard capillary technique with radiography to disclose the height of the interface, Van Vlack measured the interface tension of the interface between molten copper and molten copper-sulphide (both phases saturated with iron). The interfacial tension thus directly determined at 1105 °C was 100 dynes/cm. By dihedral angle measurements in microsamples of ternary alloys heat treated and quenched, Van Vlack then obtained energies for the other interfaces in this system with the results given in Table III. By measuring the equilibrium angle between various groups of phases it is possible to find the ratio of any two interfaces in the system. In a three-phase alloy it is possible to compute ratios for any two interfaces in at least three different ways and the values used in Table III

TABLE III

Interface Energies in the Copper-Iron-Sulphur System.

(Computed from data given by Van Vlack) [24]

Interface	Route of Computation	Free Energy ergs/cm²	Temp. °C
Cu_2S/Cu (both liquid)	Direct capillary measurem.	100	
gamma-iron (solid)/Cu (liq.)	$\gamma_{45}\frac{\gamma_{64}}{\gamma_{45}} = 100 \times 4.30$	430	
gamma-iron (sol.)/CuS (liq.)	$\gamma_{45}\frac{\gamma_{65}}{\gamma_{45}} = 100 \times 4.70$	470	1105
gamma-iron/gamma-iron (solid)	$\gamma_{64}\frac{\gamma_{66}}{\gamma_{64}} = 470 \times 1.94$	850	
gamma-iron/copper (solid)	$\gamma_{66}\frac{\gamma_{61}}{\gamma_{66}} = 850 \times 0.61$	520	
copper/copper (solid)	$\gamma_{61}\frac{\gamma_{11}}{\gamma_{61}} = 520 \times 1.15$	595	1000
alpha-iron/copper (solid)	$\gamma_{11}\frac{\gamma_{71}}{\gamma_{11}} = 595 \times 0.86$	510	
alpha-iron/alpha-iron (solid)	$\gamma_{71}\frac{\gamma_{77}}{\gamma_{71}} = 510 \times 1.42$	720	825

See footnote to Table II for key to interface numbers. All interface energy ratios computed by at least three independent routes which were averaged. It is assumed that γ_{61} and γ_{71} do not change with temperature and that the metallic interfaces are not changed by the presence or absence of sulphur.

represent Van Vlack's averages. Although the final figure in the table — for the alpha-iron boundary — depends on the product of seven ratios, none of which are themselves very accurately known, the errors are not cumulative. It is estimated to be accurate to about 20 %. It should be pointed out that Van Vlack assumed that the gamma-iron boundary did not change between 1105 and 1000 °C, that the copper grain boundary did not change between 1000 and 825 °C, and that the presence of sulphur did not change the values.

COMPOSITION CHANGES AT SINGLE PHASE CRYSTAL INTERFACES

In considering concentration changes in the vicinity of grain boundaries in polycrystalline bodies with two or more components, the standard Gibbs-Guggenheim treatment ([25]) ([26]) can be applied, although, unlike liquid interfaces, the proper value of $\partial\gamma_g/\partial C$ cannot in any way be deduced from the variation of surface tension with the composition of the bulk phase concerned but applies only to the boundary material itself. The Gibbs equation for solutions that are both ideal and dilute is :

$$\Gamma_2 = -\frac{C_2}{RT}\frac{\partial\gamma}{\partial C_2} \qquad (5)$$

where Γ_2 is the total excess concentration associated with the interface, C_2 is the concentration of the minor component, γ the interfacial free energy. Although the grain boundary is not three-dimensional, it can be considered thermodynamically as a thin layer of a second phase and $\frac{\partial\gamma_g}{\partial C}$ the combined effect of two surfaces a vanishingly small distance apart and incapable of separate existence. Spretnak and Speiser ([27]) have discussed the thermodynamics of grain boundaries at some length, but rigourous treatment is badly needed.

Unfortunately, no measurements have as yet been made of the influence of solute elements on grain boundary energies even for nominally pure substances. Impurities (particularly those that are relatively insoluble in the crystals themselves) would be expected to have a great effect on boundary energies, and grain boundaries in nominally pure materials are probably quite different from those in really pure substances. Decker and Harker ([28]) have shown indeed that the activation energy for grain boundary migration

in recrystallizing high purity copper (99.999 %) is 22,400 cal compared with 29,900 for OFHC copper analyzing 99.98 %. It is not certain, however, whether their grain boundary orientations were in both cases identical or that there were no disturbing influences from precipitate particles varying in solubility with temperature.

INTERFACES BETWEEN DIFFERENT CRYSTALLINE PHASES

It would be expected that the interface between two different crystalline phases in equilibrium with each other would differ from the single-phase grain boundary energy by an additional energy of chemical origin similar to that existing between two immiscible liquid phases. This prediction is in actuality not always fulfilled, indeed in the case of crystal phases of reasonable chemical similarity the interphase interface almost always has a *lower* energy than the random grain boundary in either phase.

The writer ([21]) has pointed out that the dominant factor in determining the microstructure of annealed polyphase alloys is the dihedral angle resulting from the equilibrium between the tensions of the interphase interfaces and those of the grain boundaries. The matter is thus of considerable practical importance and a number of such relative energies have been determined.

In a two-phase system, if the interfaces are regarded as having energies independent of orientation, then, in Figure 11 :

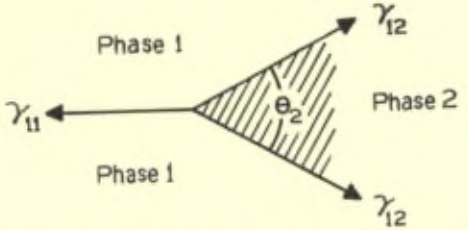

Fig. 11. — Geometry of interfaces at junction of two grains of one phase with one of a second phase in equilibrium with it.

$$\frac{\gamma_{12}}{\gamma_{11}} = \frac{1}{2 \cos \theta/2} \tag{6}$$

and :

$$\theta = 2 \cos^{-1} \left(\frac{\gamma_{11}}{2\gamma_{12}} \right) \tag{7}$$

The ratio of energies is plotted as a function of the dihedral angle θ, in Figure 12, taken from reference (21). Measurements of these angles

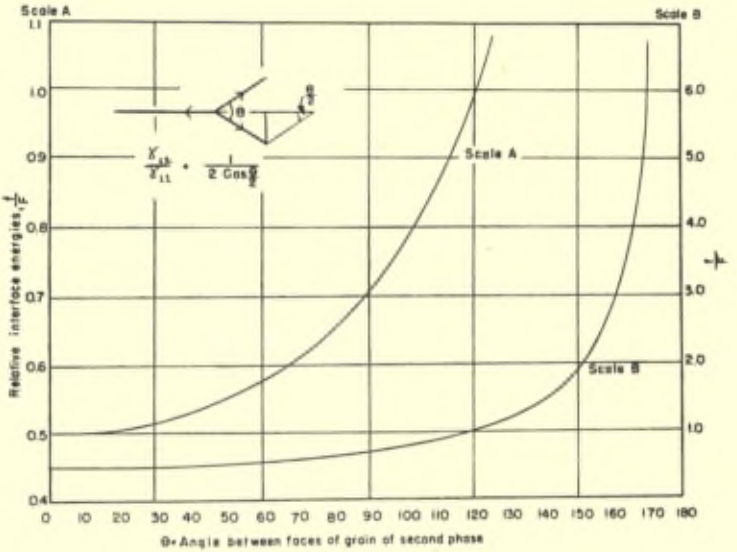

Fig. 12. — Ratio of interface energies as function of dihedral angle (Smith) (21).

have been made under the microscope on polished and etched specimens of a number of two-phase alloys (cf. Fig. 15-19) and the resulting ratio of interphase energy to grain boundery energy obtained. Table IV summarizes all published values relating to the interfaces between two crystalline phases in equilibrium (*).

The remarkable thing about these results is that in almost all cases the interphase-interface has a lower energy than does the grain boundary in either phase. A theoretical explanation for this is much to be desired. It has been pointed out (29) that it is possible to have a coherent interface between dissimilar lattices, while similar ones differing in orientation must have discontinuities. It is also true that a difference in atomic radius, which limits solubility in a lattice even though the atoms may be chemically tolerant of each other has no adverse effect at a grain boundary where there must be space for atoms of varying size and ionization. However, neither of these

(*) This table is reproduced with a few corrections from a paper by the writer (29) presented before the U. S. National Research Council conference on crystal imperfections in 1950.

TABLE IV

Relative Interfacial Energies Between Various Alloy Phases.

System	Temperatur °C	Interface between		Grain Boundary Used As A Comparison Interface, C	$\frac{\gamma\ A/B}{\gamma_C}$	Reference
		Phase A	Phase B			
Cu-Zn	700	αFCC	βBCC	α/α	0.78	21
	»	αFCC	βBCC	β/β	1.00	»
Cu-Al	600	αFCC	βBCC	α/α	0.71	»
	»	βBCC	γ CC	γ/γ	0.78	»
Cu-Sn	750	αFCC	βBCC	α/α	0.76	»
	»	αFCC	βBCC	β/β	0.93	»
Cu-Sn-Pb	600	αFCC	βBCC	β/β	1.00	»
	»	αFCC	βFCC	α/α	0.75	»
Cu-Sb	600	αFCC	βBCT	α/α	0.71	29
Cu-Ag	750	α(Cu)FCC	β(Ag)FCC	α/α	0.65	»
	»	α(Cu)FCC	β(Ag)FCC	β/β	0.74	»
Cu-Si	845	αFCC	βBCC	α/α	0.53	»
	»	αFCC	βBCC	β/β	1.18	»
	830	αFCC	ϰHCP	α/α	0.82*	»
	»	αFCC	ϰHCP	ϰ/ϰ	0.87*	»
Fe-C	690	αBCC	Fe_3 C OR	α/α	0.93	21
	750	αBCC	γFCC	α/α	0.71	»
	950	αBCC	γFCC	γ/γ	0.74	24
Fe-Cu	825	αBCC	«Cu»FCC	α/α	0.74	»
	»	αBCC	«Cu»FCC	Cu/Cu	0.86	»
	1000	γFCC	«Cu»FCC	γ/γ	0.61	»
	1000	γFCC	«Cu»FCC	Cu/Cu	0.87	»
Zn-Cu-Al	375	η_1HCP	εHCP	ε/ε	0.93	21
(Three	»	η_1HCP	εHCP	η_1/η_1	0.93	»
phase	»	εHCP	β_1FCC	β_1/β_1	0.87	»
alloy)	»	εHCP	β_1FCC	ε/ε	0.74	»
	»	η_1HCP	β_1FCC	β_1/β_1	1.00	»
	»	η_1HCP	β_1FCC	η_1/η_1	0.87	»
Zn-Sn	160	β(Sn)BCT	α(Zn)HCP	α/α	0.74	29
	»	β(Sn)BCT	α(Zn)HCP	β/β	1.18	»

Key to structures of phases :
FCC = Face centered cubic.
BCC = Body centered cubic.
CC = Gamma-brass structure.
HCP = Hexagonal close packed.
BCT = Body centered tetragonal.
OR = Orthorhombic.

21. C. S. Smith, 1948.
24. L. H. Van Vlack, 1950
29. C. S. Smith, unpublished.

(*) This applies only to randomly oriented ϰ from decomposition of β. The oriented α/ϰ interface is of extremely low energy, probably lower than a twin in a FCC structure.

can be important factors since (*a*) interfaces between phases of the same crystal structure but differing in parameter are found also to have lower energies than either boundary (*cf.* Cu/Ag and Cu/γ-iron in Table IV) and (*b*) the grain boundary of a solid solution alloy, would already have benefited from the freedom of chemical substitution at the boundary and hence would not be able to gain further advantage on contact with another phase (*cf.* α/β brass in Table IV).

At the present writing there are no measurements of grain boundary energies in any but metallic crystals, and there are no studies of the boundaries between two crystals differing considerably in type of bonding. It is probable that an oxide layer formed on a metal is protective only if the interface energy is very low, and this which must depend on the possibility of forming an interface which is intermediate between the true metal and the oxide both structurally and in electron configuration. Inclusions in steel, except for sulphides, frequently show very high dihedral angles against the γ-iron boundaries and thus possess very high interface energies. The metallic and non-metallic phases in some meteorites (for example, the Brenham pallasite) have geometries which seem to correspond to surface-tension equilibrium with a dihedral angle of about 70° for the FeNi (supposedly liquid when equilibrium was attained) against grain boundaries in the olivine. This indicates that the metal-olivine interface has appreciably *less* energy than the grain boundary between the olivine crystals themselves — a surprising fact considering the completely different nature of the materials.

It must not be expected that all alloys will conform to the simple surface-tension picture outlined above. There is no doubt that the energy of the interface between dissimilar crystals is considerably dependent upon the relative orientation. There are probably cases where such an oriented interface has a lower energy than even a twin in either phase, for example, the α/ϰ interface in the copper-silicon system. If, in slowly cooled or heat treated alloys a second phase appears, it will generally nucleate and grow only in those orientations where the interface energies are particularly favorable. Although the minimum surface energy requirement will always determine the equilibrium geometry, this will not result in the simple curved shapes of liquid phases in those cases where the energy is critically dependent on the relative orientation of the phases and the direction of the boundary between them. Widmanstatten structures are generally of this type and are stable on annealing. Van Vlack [24] has shown

that the α-phase that occurs in plate-like form in a casting of an iron carbon alloy maintains its orientation and high-area configuration even after annealing for 48 hours at 1005 °C although after deformation it assumed a surface-tension equilibrium shape in only 30 minutes. The matter is of considerable complexity. Many structures are, of course, not in surface energy equilibrium at all but result principally from the anisotropy of surface or bulk diffusion during growth. These approach equilibrium geometry on annealing. The microstructure of metals is discussed again in the last section of this paper.

THE INTERFACE BETWEEN A CRYSTAL AND A LIQUID

The fact that the liquid in a partly melted metal generally has a zero dihedral angle shows (from equation 6) that the interface between a crystal and liquid of the same composition in equilibrium at the melting point has less than half the energy of the grain boundary. A relatively slight difference in composition between liquid and solid in an alloy often brings the dihedral angle into the measurable range above 0°, which suggests that in a pure metal the solid/liquid interface has an energy only very slightly less than half that of the grain boundary. Qualitatively copper seems to be more tolerant of a composition change than is aluminium. In an alloy system the energy of the solid/liquid interface increases as the solid and liquid differ more in concentration. If the composition of the liquid changes rapidly as a function of temperature, the interface energy will also change, and, with it, the dihedral angle of the liquid against a grain boundary. There is little change in dihedral angle with temperature when the liquidus is not highly sloped. The great difference in behavior of the liquid phases in the aluminium-tin and copper-lead alloys illustrates this (Figure 13). The dihedral angle of the liquid in copper-lead alloys remains constant to 800 °C and drops, first slowly, and at 960°, rapidly to zero; while the dihedral angle of the liquid in the aluminium-tin alloys decreases progressively as temperature is increased. The constitution diagrams show why. In the copper-lead system ([30]) the amount of copper in the liquid-lead-rich phase in equilibrium with solid copper, though it increases smoothly, is relatively small (10 at. %) at all temperatures below 850 °C, but it increases rapidly thereabove to become 53 at. % at 960 °C (the

monotectic temperature) where it discontinuously changes to a copper-rich liquid. The liquid in aluminium-tin alloys, on the other hand (31), continuously increases in aluminium content with temperature, starting with almost pure tin and ending with pure aluminium at its melting point.

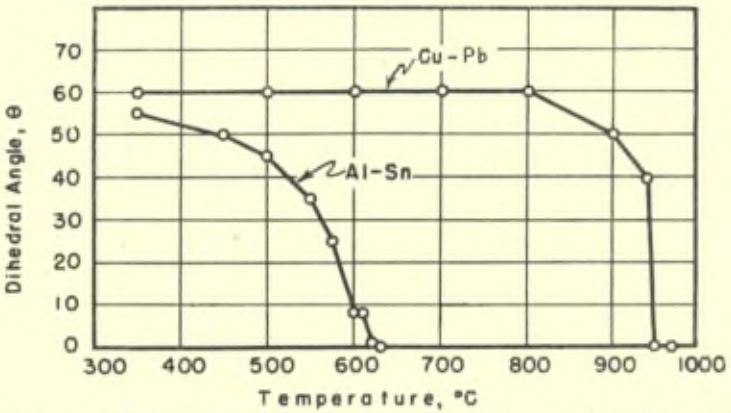

Fig. 13. — Variation of dihedral angle with annealing temperature. Copper-lead and aluminium-tin alloys (Ikeuye and Smith) (18).

If the relative interface energy is plotted (regardless of temperature) as a function of the composition of the liquid, it varies in a manner strongly reminiscent of the variation of surface energy of a liquid alloy with composition (Figure 14).

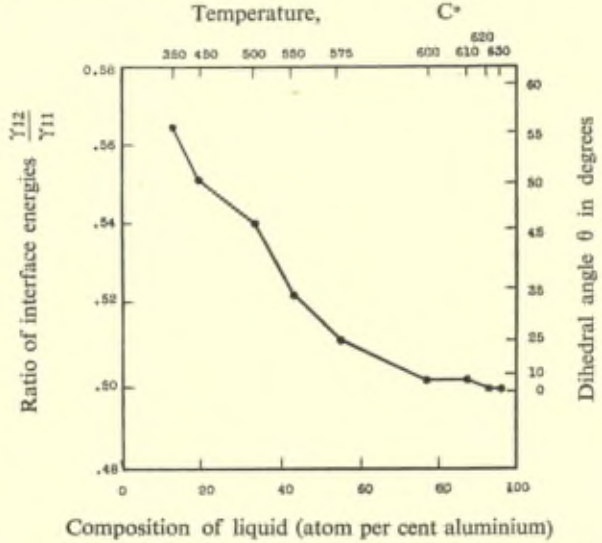

Fig. 14. — Relative interface energy as function of composition of liquid phase in Al-Sn alloys (Smith) (35).

The dihedral angle of liquid phases is of great importance in connection with solidification mechanism of alloys, for a continuous path for feeding solidification shrinkage will be maintained only as long as the dihedral angle is 60 °C, or below.

Turnbull and Fisher ([32]) and Turnbull ([33]) have discussed the role of solid/liquid interface energy in determining nucleation of the solid from the liquid. Turnbull's important paper showed that the degree of undercooling possible in metals free from external nuclei is a constant fraction of the melting point. Applying his nucleation theory, he shows that this would result if the liquid/solid interface energy were proportional to the heat of fusion and if the entropy of fusion were constant in all systems. In actual fact he finds that the ratio of interface energy per gram-atom of surface (computed in all cases from undercooling experiments) to the heat of fusion per gram-atom is 0.45 for all metals except for antimony, bismuth, and germanium which fall on a second line of slope 0.32, and aluminium which, as in many things, is abnormal.

THE MELTING OF GRAIN BOUNDARIES

The fact that many polycrystalline alloys became extremely hot-short at temperatures somewhat below their melting point has been known and both deplored and utilized for many centuries. When first scientifically studied it was attributed to the presence at the grain boundary of a low-melting eutectic resulting from impurities. The temperature at which brittleness first appears, which is extremely sharp and reproducible, has been used for studying the solidus in alloy systems (Homer and Plummer) ([34]), although it has been pointed out ([35]) that only if the ratio of the energy of the grain boundary to that of the liquid/crystal interface is over 2 will the liquid completely separate the grains. Molten metals will often cause intergranular failure of stressed structures — the cracking of brass wet with mercury or molten tin, and the cracking of nickel or steel with molten brazing solder being well-known examples. The effect seems to occur under stress even in cases where surface-tension alone would not cause complete penetration. The interaction between mechanical and surface forces is a complex matter of considerable industrial importance and in need of further study.

Chalmers ([36]) measured the difference between the melting point of crystalline tin and the temperature at which a grain boundary failed under a normal tensile stress of 1 to 3 kg/cm^2. This amounted to about 0.2 °C and was not critically dependent on purity and hence seemed not to be due to a low-melting composition at the boundary. Lacombe and Yanaquis ([35]) haves hown that high purity aluminium heated in a slight temperature gradient shows superficial signs of grain boundary melting in areas estimated as about a quarter of a degree below the true melting point.

It is well known that grain boundaries yield to shear stresses in a viscous manner, the viscosity varying with temperature in a manner much like a liquid ([38]). There have been no measurements on boundaries in shear which would show whether or not the viscosity varies suddenly shortly below the melting point, as it would if real grain boundary melting took place. Failure under tension stresses, as observed by Chalmers and others, could be a result of the lowering of the melting point that occurs locally due to stress concentration along the line where the boundary meets the surface. The melting point of a crystal depends upon its size according to the following relation :

$$\frac{dT}{dr} = \frac{2\,\gamma^{V}}{r^2\,(S_l - S_s)} \tag{8}$$

where r is the radius of curvature of the surface, V the molal volume, S_s, S_l, T, and γ the entropy of the liquid and solid respectively, the temperature, and the free energy of the solid-liquid interface, If we assume that, for small ΔT, V and γ are not a function of T, and that the difference in entropy between solid and liquid is $\Delta H_f/T_m$ where ΔH_f is the heat of fusion, then the change of melting point due to curvature is :

$$\Delta T = T - T_m = -\frac{2\,\gamma\,VT_m}{r\,\Delta H_f} \tag{9}$$

This applies to an isolated spherical crystal in equilibrium with

liquid (*). Wherever four grains meet the corners will not be infinitely sharp but will be rounded to a spherical radius corresponding to the above. Three grains meeting along an edge will be cylindrically curved with half the radius of the sphere. The space between the convex surfaces of the grain edges and corners will be filled with liquid — *equilibrium* liquid — unless this is displaced by a pressure sufficient to overcome normal capillary forces and viscosity.

Substituting reasonable values for the various constants for aluminium :

$$r = \frac{5.64 \times 10^{-4}}{-\Delta T} \text{ cm.} \qquad (10)$$

With extremely small curvatures the relation is meaningless, but it is interesting to note that curvatures of a micron (10^{-4} cm) correspond to undercooling of 0.6 °C, and that under cooling of 0.001° gives radii of over half a millimeter. This liquid must exist on all grain edges and form a completely continuous network throughout an entire polycrystalline sample. It provides a system of undoubted notches which, under tension, would cause local high stresses and permit progressive failure of the type observed by Chalmers. It should be noticed, however, that this liquid can only exist on a highly curved surface (the radius depending on ΔT), and must solidify if it encounters a less curved crystal surface. It does not correspond to grain boundary melting but only to grain edge melting.

(*) The writer wishes to thank Professor J. W. Stout for this derivation. The objection has been raised that V in equations (8) and (9) should be replaced by $(V_l - V_s)$. On this point Dr. Stout writes:

In the ordinary equation for the change in melting point with pressure :

$$\Delta T = \frac{\Delta P \, T_m (V_l - V_s)}{\Delta H_f}.$$

The pressure increment ΔP is applied to both phases and hence the difference in the volumes of liquid and solid enters. If, however, it were possible to apply the pressure increment only to the solid phase, keeping the pressure on the liquid unchanged, then the expression would become :

$$\Delta T = -\frac{\Delta P \; T_m \; V_s}{\Delta H_f}$$

(See, e. g., Lewis and Randall, *Thermodynamics*, p. 184.)

The effect of surface energy on a spherical crystal is effectively to increase the pressure in the crystal by an amount $\Delta P = \frac{2\gamma}{r}$, while the pressure on the liquid is unchanged, and hence one obtains the expression : $\Delta T = -\frac{2\gamma}{r} \frac{V_s \; T_m}{\Delta H_f}$.

NOTE ADDED IN PROOF : From private discussion with Messrs Harvey Brooks and D. Turnbull it appears that the basic assumption of a pressure difference between solid and liquid is not appropriate at a three- or four-grain equilibrium corner. Liquid will appear only to the extent that its free energy can be provided by de replacement of some area of grain boundary by solid-liquid interface of lower energy. If the dihedral angle is greater than 60°, no liquid will appear.

It is possible to have liquid at a grain boundary below its true freezing point if it is under negative hydrostatic pressure which could result from an external force opposed by surface tension acting on a strongly curved meniscus. The pressure change is :

$$\frac{dp}{dT} = \frac{\Delta H_f}{T (V_l - V_s)}$$

This amounts to —113 atm/ °C for aluminium, —205 atm/ °C for tin and +281 atm/ °C for bismuth. The pressure necessary to depress the melting point of aluminium by 0.2 °C could be balanced by the surface-tension of the liquid at a meniscus having a negative curvature of approximately 5×10^{-4} mm. It may be, therefore, that liquid formed at grain edges without stress can continually advance between plane grain surfaces under the influence of tension at temperatures perceptibly below the melting point. One would anticipate somewhat different behavior in the case of substances whose freezing point is lowered by pressure, for example, bismuth and ice : It is perhaps significant that, although most substances become mushy at their melting points when some liquid is present, ice once frozen seems tomelt only superficially and does not disintegrate into a granular mush.

When a bi-crystal is immersed in a liquid with which it is in equilibrium, it will be corroded until the dihedral angle is the correct one for equlibrium. There will be no change thereafter if the dihedral angle is above zero or if the grain boundary has exactly twice the energy of the solid-liquid interface. However, if the surface work required to replace the boundary by liquid (defined as $2 \gamma_{sl} - \gamma_b$) is negative the liquid will continue to advance, albeit at a slow rate limited by diffusion and deformation, unless the two crystals are held together by an external mechanical force equivalent to this work divided by the area in which the system effectively changes from one to two interfaces.

THE MICROSTRUCTURE OF METALS

It is very easy when dealing with two-dimensional micro-sections of metals and alloys to focus attention on the grains themselves and to overlook the extreme importance of the interfaces between the grains. Actually, however, the structures result mostly from the requirements of local equilibrium between interface tensions working

within the framework of topological requirements. The grains themselves are of only secondary importance.

In a single phase material the grain boundaries form a network virtually indistinguishable from a froth of soap bubbles, an analogy which Desch ([39]) in particular has discussed. The interface tension eliminates any contact of more than three grains along an edge, or four grains at a corner. The writer has elsewhere shown ([40]) that under these conditions the number of corners and faces on an array of three-dimensional space-filling polyhedra are related as follows :

$$\Sigma\,(6-n)P_n = 6\,(B+1) \tag{10}$$

$$\frac{C}{B} = \frac{\bar{n}}{6-n} \tag{11}$$

$$\frac{P}{B} = \frac{6}{6-\bar{n}} \tag{12}$$

$$\bar{n} = 6\,(1-\frac{B}{P}) \tag{13}$$

$$\frac{P}{B} - \frac{C}{B} = 1. \tag{14}$$

In these, C is the number of corners, B is the number of three-dimensional cells, P the number of polygons (i. e., two-dimensional septa, each of which would form the faces on two polyhedra if the cells were separated), and $\bar{n}$ is the number of edges to the average polygon. The first relation is rigourously true, the others hold only when a large number of cells is considered so that the unshared faces at the periphery are negligible.

The total interface area for a given number of cells is minimum when the number of faces or corners shared by adjacent cells is a maximum. The number of corners per cell $\left(\frac{C}{B}\right)$ can never exceed 6, but the nearer it approaches 6 the lower the total number of interfaces and hence, in general, the lower the total interface energy. Under these conditions $\bar{n}$ approaches 5 1/7, a curious number that is the three-dimensional equivalent of the hexagon in two dimen-

sions (*). The prevalence of pentagons among the faces of grains, bubbles, and cells in undifferentiated biological tissue has long been known, as well as the fact that it is impossible to fill space with polyhedra having only pentagonal faces.

Because the angles required by local equilibrium of surfaces can only be reconciled with the topological requirements for numbers of point and linear contacts by the introduction of curvature, a random froth or grain aggregate is basically unstable. If diffusion can occur the smaller, convex, cells will shrink and disappear while the larger ones grow. It is this fundamental conflict between the geometric and topological needs that provides the mechanism for grain growth on annealing metals and alloys ([40]).

It is striking to observe in three dimensions the true structure of a metal. A two-dimensional photomicrograph or even a study of a solid intergranular fracture or a group of separated grains quite fails to convey a concept of the basic structural unit. This is not a grain but a junction of six nearly plane interfaces meeting along four edges which themselves join at a point at angles of 109½° with each other. The accompanying stereoscopic radiomicrograph (Figure 15),

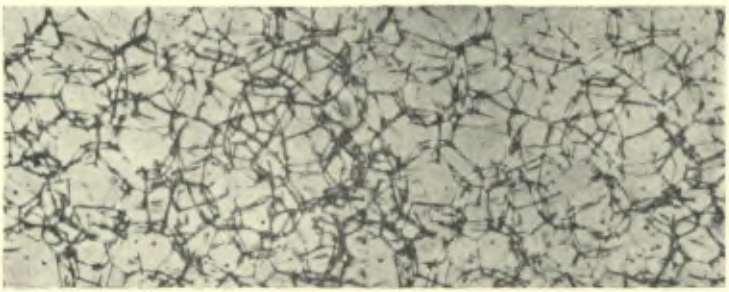

Fig. 15. — Stereoscopic pair of microradiographs showing actual shape in three dimensions of grains in aluminium-tin alloy (2 volume per cent Sn) annealed 18 hours at 575° C. Magnification 25 diam. (Photograph by W. M. Williams).

obtained by W. Williams in the Institute for the Study of Metals at Chicago, shows the configuration in three dimensions of the grain edges in aluminium. The edges were made visible by the addition to the aluminium of 2 volume per cent tin, which, being insoluble and, having a dihedral angle of about 30° at the annealing tempera-

(*) In two dimensions, under the limitation that polygon edges meet always and only three at each corner, then $\Sigma\,(6-n)P_n = E_b + 6$, where E_b is the number of cell edges at the boundary of the array.

ture used, collects at grain edges only without significant spreading over the grain faces. The structure is virtually indistinguishable from that of a soap froth except for the places where the tin occurs out of contact with any boundary, when it is spherical, or when it is isolated in the middle of a single grain boundary when it is lens-shaped. There is a complete lack of any crystallographic features in the structure. A two-dimensional section of a polycrystalline metal will give only a pale reflection of the three-dimensional network.

On a two-dimensional section through a polycrystalline metal the grains have on the average almost exactly six sides, and the most frequent angle at which the three boundaries meet is 120° However, partly as a result of the random angle of sectioning which introduces a distribution around the true angle at which the boundaries meet in the three dimensions (Harker and Parker) ([41]) and partly because surface energy does vary somewhat with orientation, there will be some departure from 120°.

The variation of surface energy with orientation also makes it possible for there to be occasional four-grain corners (in three dimensions five-grain corners) which are stable for it may happen that the new interface that would otherwise form woult have a higher energy than the resultant of the four old interfaces in its direction. It is this phenomenon which, together with the influence of inclusions in restraining grain boundary migration, is responsible for the cessation of grain growth when the grains have become large and uniform so that grain boundary curvatures are small. Abnormal grain growth, « secondary recrystallization », and perhaps even primary recrystallization, occurs only when the interfaces are blocked at a fairly uniform grain size but when for some reason a certain grain gets larger than its neighbors and its boundary, being everywhere concave, can advance rapidly through the surrounding interfaces.

In a two-phase alloy some of the three-grain contacts in two dimensions will be replaced by edges at which two grains of one phase will meet one grain of a second phase. Depending on the ratio of the grain boundary and interphase boundary energies, the dihedral angle of the crystal differing from the other two may be anything between 0 and nearly 180°. This angle is the feature of the microstructure that metallurgists have for decades subconsciously realized to be the characteristic difference between various structures. The second phase need not, of course, be a crystal. Figures 16, 17 and 18

show the microstructures of copper alloys containing a small amount of liquid, but with the ratio of solid/liquid interface energy to that of the grain boundary progressively increasing. It should be noted that the second phase forms a circular drop, regardless of the interface energy, whenever it is not in contact with a grain boundary, while if it occurs at a three-grain corner it must establish equilibrium

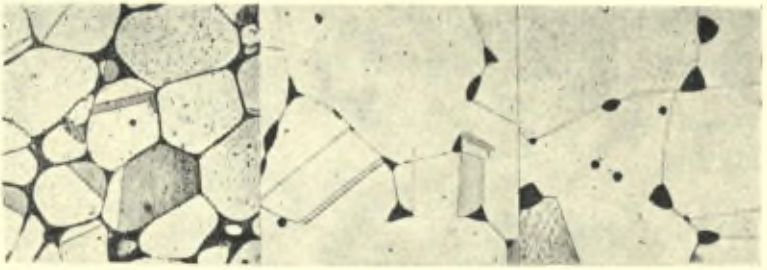

Microstructure of Copper Alloys Containing a Liquid Phace.

Fig. 16. — Cu-Ag (15 % Ag). Quenched from 850 °C. X250. Liquid phase has dihedral angle of 0°.

Fig. 17.— Cu-Pb (3% Pb). Quenched from 900 °C. X500. Didheral angle of liquid 50°.

Fig. 18. — Cu-Zn-Pb (67-30-3). Quenched from 750 °C. X500. Dihedral angle of liquid 80°.

with the three adjacent grain boundaries and hence forms triangles with more and more acute edges as the interface energy decreases. If the volume of liquid increases the number of contacts will increase and the curvature of the surfaces between them will change, but there is no change of equilibrium angle.

If the dihedral angle of a second phase in relation to grain boundaries of the first is zero it will penetrate completely between the grains; if it is between zero and 60° it will penetrate continuously along grain edges in three dimensions but will not separate grain faces, while if the angle is over 60° the second phase will exist discretely as separate polyhedra ([21]).

When the alloy is composed of two crystalline phases the structure is still composed of connected three-grain corners, but these can consist, two-dimensionally, of two grains of either phase and one of the other. Although the interphase interface is identical in both types of corner, the energies of the grain boundary in the two phases may be different and the structure is then composed of two kinds of corner, each with a characteristic angle, and also corners with three grains of a single-phase which will meet at approximately

120° regardless of which phase is concerned. Four-grain contacts will be much more common in two-phase alloys than in single phase ones because of the higher probability of two migrating low energy corners giving rise to a new high energy boundary. These principles can easily be seen in examining Figures 19 and 20 showing two-phase structures.

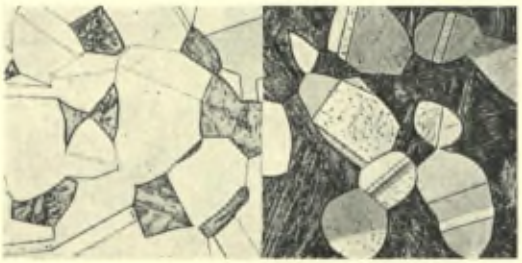

Microstructure of Alloys with Two Solid Phases

Fig. 19. — Cu-Sn alloy (16 % Sn). Quenched from 750 °C. X250.

Fig. 20. — Cu-Sn alloy (21 % Sn). Quenched from 750 °C. X250.

Note small angle where a β grain abuts against an α boundary and larger angle where α grain meets a β boundary.

$$\gamma_{\alpha\alpha}/\gamma_{\alpha\beta}/\gamma_{\beta\beta} = 1.3/1.0/1.0$$

This discussion of microstructure is highly idealized and assumes that the energy of an interface is independent of the orientation of the crystals on the two sides of it. Nevertheless, it does account in a very satisfactory fashion for the microstructure of most worked and annealed alloys. The principles of fluid-like equilibrium of interfaces are much less evident in cast or heat-treated alloys because of the frequent occurrence of interfaces of highly selected orientation possessing critically low energies. The general ideas can probably be applied to other polycrystalline bodies, including rocks, ceramics and organic polycrystals. Most minerals occur in nature under conditions where their shape is determined by the mechanisms and accidents of growth. Nevertheless, there are many rocks (particularly metamorphosed sedimentary deposits, such as quartzite, marble or ice) wherein nearly equi-axed grains are found possessing smoothly cured interfaces joining at 120° in a manner displaying no crystallinity and geometrically identical with grains in a metal or cells in a soap froth.

REFERENCES

(1) R. King and B. Chalmers, « Crystal Boundaries » *Progress in Metal Physics* (Ed. B. Chalmers), Vol. I, p. 127-162 (1949).

(2) W. T. Read and W. Shockley, « Dislocation Models of Crystal Grain Boundaries », *Physical Review*, **78,** pp. 275-289 (1950).

(3) W. T. Read, « Dislocation Models of Grain Boundaries », paper presented at U. S. National Research Council Conference on Crystal Imperfections, October 1950. (To be published in book form.)

(4) C. G. Dunn and F. Lionetti, « The Effect of Orientation Difference on Grain Boundary Energies, » *Trans. A. I. M. E.*, **185,** pp. 125-132 (1949).

(5) C. G. Dunn, F. W. Daniels and M. J. Bolton, « Relative Energies of Grain Boundaries in Silicon Iron », *Trans. A. I. M. E.*, **188,** pp. 1245-1248 (1950).

(6) K. T. Aust and B. Chalmers, « The Specific Energy of Crystal Boundaries in Tin », *Proc. Roy. Soc.* **201***A*, pp. 210-215 (1950).

(7) K. T. Aust and B. Chalmers, « Surface Energy and Structure of Crystal Boundaries in Metals », *Proc. Roy. Soc.* **204***A*, pp. 359-366 (1950).

(8) W. L. Bragg Discussion of J. M. Burgers' Paper « Geometrical Considerations Concerning the Structural Irregularities to be Assumed in a Crystal », *Proc. Phys. Soc.*, **52,** pp. 54-55 (1940).

(9) J. M. Burgers « Geometrical Considerations Concerning the Structural Irregularities to be Assumed in a Crystal », *Proc. Phys. Soc.*, **52,** pp. 23-33 (1940).

(10) C. Herring, Appendix 2 to « Surface Tension as a Motivation for Sintering » *The Physics of Powder Metallurgy*, (Ed. W. E. Kingston, New York, McGraw-Hill), pp. 176-177 (1950).

(11) C. Gurney, « Surface Forces in Liquids and Solids », *Proc. Phys. Soc.*, **62***A*, pp. 639-648 (1949).

(12) J. E. Burke, « The Formation of Annealing Twins », *Trans. A. I. M. E.*, **188,** pp. 1324-1328 (1950).

(13) C. S. Smith, Discussion of Paper by W. R. Hibbard, Jr., Y. C. Liu, and S. F. Reiter, « Annealing Twins in Copper and 70-30 Alpha Brass », *Trans. A. I. M. E.*, **188,** pp. 1021-1022 (1950).

(14) R. L. Fullman, « Interfacial Free Energy of Coherent Twin Boundaries in Copper »; « Crystallography and Interfacial Free Energy of Noncoherent Twin Boundaries in Copper », *Journ. Appl. Phys.*, **22,** pp. 448-460 (1951).

(15) R. L. Fullman, *General Electric Company Research Report No. RL422*, September, 1950 (Private communication).

(16) C. G. Dunn, F. W. Daniels and M. J. Bolton, « Measurement of Relative Interface Energies in Twin Related Crystals », *Trans. A. I. M. E.*, **188,** pp. 368-377 (1950).

(17) G. L. J. Bailey and H. C. Watkins, « Surface Tensions in the System Solid Copper-Molten Lead », *Proc. Phys. Soc.*, **63***B*, pp. 350-358 (1950).

(18) K. K. Ikeuye and C. S. Smith, « Studies of Interface Energies in Some Aluminium and Copper Alloys ». *Trans. A. I. M. E.*, **185,** pp. 762-768 (1949).

(19) J. C. Fisher and C. G. Dunn, « Surface and Interfacial Tensions of Single Phase Solids », paper presented at U. S. National Research Council Conference on Crystal Imperfections, October 1950. (To be published in book form.)

(20) G. W. Sears, « An Absolute Measurement of Copper-Copper Interfacial Free Energy », *Journ. Appl. Phys.*, **21,** p. 721 (1950).

(21) C. S. Smith, « Grains, Phases, and Interfaces: An Interpretation of Microstructure », *Trans. A. I. M. E.*, **175,** pp. 15-51 (1948).

(22) H. Udin, A. S. Shaler and J. Wulff, « The Surface Tension of Solid Copper », *Trans. A. I.. M. E*, **185,** pp. 186-190 (1949).

(23) B. Chalmers, R. W. King and R. Shuttleworth, *Nature*, **158,** pp. 482-483 (1946).

(24) L. Van Vlack « Intergranular Energy of Iron and Some Iron Alloys », *Trans. A. I. M. E.*, pp. 251-258 (1951).

(25) J. Willard Gibbs, *Collected Works of J. Willard Gibbs*, **1,** pp. 219-237 (1931).

(26) E. A. Guggenheim, « An Elementary Deduction of Gibbs' Adsorption Theorem », *J. Chem. Phys.*, **4,** pp. 689-695 (1936); « Thermodynamics of Interfaces in Systems of Several Components », *Trans. Faraday Soc.*, **36,** pp. 397-412 (1940).

(27) J. W. Spretnak and R. Speiser, « Grain and Grain-Boundary Compositions : Mechanism of Temper Brittleness », *Trans. Amer. Soc. Metals*, **43,** pp. 734-748 (1951).

(28) B. F. Decker and D. Harker, « Activation Energy for Recrystallization in Rolled Copper », *Trans. A. I. M. E.*, **188,** pp. 887-890 (1950).

(29) C. S. Smith, « Interphase Interfaces », paper presented at U. S. National Research Council Conference on Crystal Imperfections, October 1950. (To be published in book form.)

(30) O. J. Kleppa and J. A. Weil, « The Solubility of Copper in Liquid Lead Below 950° », *J. A. C. S.*, **73,** pp. 4848-4850 (1951).

(31) A. H. Sully, H. K. Hardy and T. J. Heal, « The Aluminium-Tin Phase Diagram and the Characteristics of Aluminium Alloys Containing Tin as an Alloying Element », *J. Inst. Metals*, **76,** pp. 269-281 (1949).

(32) D. Turnbull and J. C. Fisher, « Rate of Nucleation in Condensed Systems », *J. Chem. Phys.*, **17,** pp. 71-73 (1949).

(33) D. Turnbull, « Formation of Crystal Nuclei in Liquid Metals », *J. Appl. Phys.*, **21,** pp. 1022-1028 (1950).

(34) C. E. Homer and H. Plummer, « Embrittlement of Tin at Elevated Temperatures and its Relation to Impurities », *J. Inst. Metals*, **64,** pp. 169-200 (1939).

(35) C. S. Smith, Discussion of J. Crowther's Paper, « Overheating Phenomena in Aluminium-Copper-Magnesium-Silicon Alloys of the Duralumin Type », *J. Inst. Metals*, **76,** pp. 726-728 (1949-1950).

(36) B. Chalmers, « Crystal Boundaries in Tin », *Proc. Roy. Soc.*, *A***175,** pp. 100-110 (1940).

(37) P. Lacombe and N. Yannaquis, « La corrosion intercristalline de l'aluminium de haute pureté et ses conséquences au sujet de la nature des joints de grains », *Métaux et Corrosion*, **22,** pp. 35-37 (1947).

(38) T. S. Kê, « Stress Relaxation Across Grain Boundaries in Metals », *Phys. Rev.*, **72,** pp. 41-46 (1947).

(39) C. H. Desch, « The Solidification of Metals from the Liquid State », *J. Inst. Metals*, **22,** pp. 241-263 (1919).

(40) C. S. Smith, « The Shape of Metal Grains, with Some Other Metallurgical Applications of Topology », paper presented at American Society for Metals Symposium on Metal Interfaces, October 1951.

(41) D. Harker and E. Parker, « Grain Shape and Grain Growth », *Trans. Amer. Soc. Metals*, **34,** pp. 156-195 (1945).

(42) A. P. Greenough and R. King, « Grain Boundary Energies in Silver », *J. Inst. Metals*, **79,** pp. 415-427 (1951).

(43) H. Udin, « Grain Boundary Effect in Surface Tension Measurement », *Trans. A. I. M. E.*, **189,** p. 63 (1951).

(44) B. H. Alexander, M. H. Dawson and H. P. Kling, « Deformation of Gold Wire at High Temperature », *J. Appl. Phys.*, **22,** pp. 439-443 (1951).

Discussion du rapport de M. C. S. Smith

Prof. Bragg. — Prof. Smith's report of Turnbull's observation that the interface energy per gram atom for crystals of a pure metal is proportional to the latent heat of fusion has an interesting relation to the law that the latent heat of fusion per cc of a metal is itself proportional to Young modulus. This can be explained by supposing that the distortions created at the interface, or in the passage from solid to liquid state, are geometrically similar in all true metals, and therefore the energy per cc is proportional to the elastic constant of the metal.

Hollomon. — Smith has referred to the work of our Laboratory in measuring the interface free energy between solid and liquid metals. The justification for the validity of such measurements obtained from supercooling experiments rests upon the adequacy of the description of the kinetics of the process by nucleation

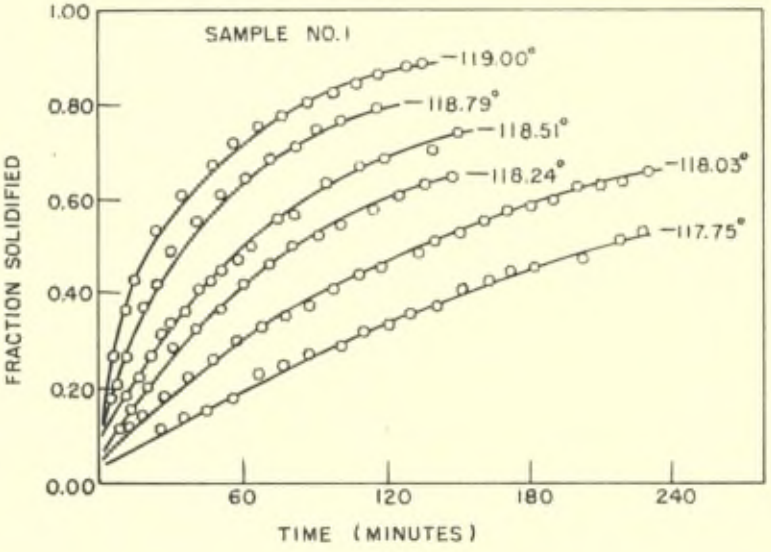

Fig. 1

theory. The isothermal experiments (fig. 1) of Turnbull (1) on the homogeneous solidification of mercury droplets at nearby 80 °C supercooling can be described within the experimental accuracy by such theory. In figure 2 (1) a comparison of the theory and the

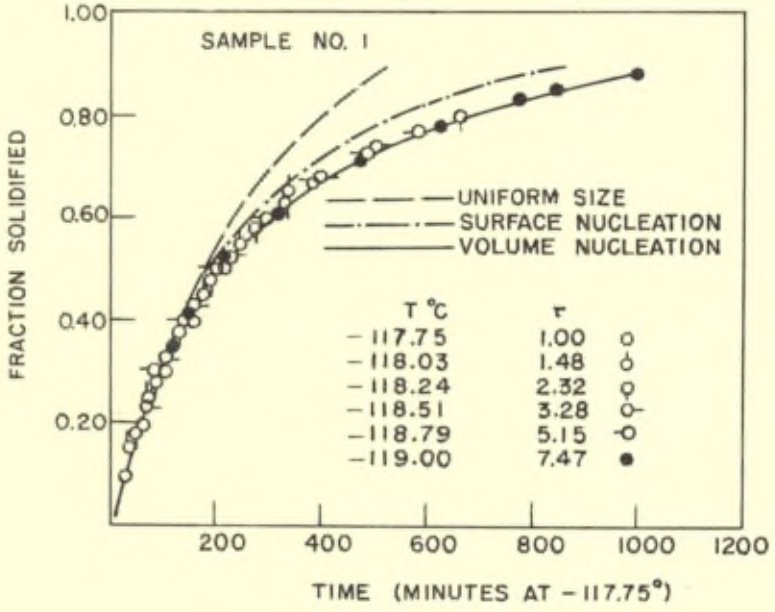

Fig. 2

assembled experimental results is shown. In making this comparison, it is necessary to assign the value 32.1 ergs/cm^2 to the interfacial free energy between solid and liquid mercury. Having justified the analysis, the interfacial free energy has been determined for a number of elementary metals; from them the surface energy per gram atom was calculated and found to be nearby 1/2 the gram atomic heat of fusion (Table I) (2).

M. Grussard. — (1) Du point de vue thermodynamique, si l'on considère une surface ou une interface comme à deux dimensions, est-il possible de définir correctement les potentiels thermodynamiques? En particulier, comment définit-on l'entropie (superficielle

(1) D. Turnhull, « Kinetics of Solidification of Supercooled Liquid Mercury Droplets » (accepted for publication in the *Journal of Chemical Physics*).
(2) D. Turnhull, « Formation of Crystal Nuclei in Liquid Metals », *Journal of Applied Physics*, **21**, No. 10, 1022-1028, October 1950.

TABLE I (*)

Interfacial energies between various crystal nuclei and the corresponding liquid calculated from frequency of nucleation in small droplets.

Metal	Crystal structure	Interfacial energy σ ergs/cm^2	σ_g Cal./g. atom	$\sigma_g/\Delta Hf$	σ_g/T_0
Mercury	Hexagonal	24.4	296	0.53	1.32
Water	Hexagonal	32.1	461	0.32	1.69
Gallium	Orthorhombic	55.9	581	0.436	1.91
Tin	Tetragonal	54.5	720	0.418	1.47
Bismuth	Rhombohedral	54.4	825	0.33	1.52
Lead	Face centered cubic	33.3	479	0.386	0.80
Antimony	Rhombohedral	101	1430	0.302	1.59
Aluminium	Face centered cubic	93	932	0.364	1.00
Germanium	Diamond	181	2120	0.348	1.71
Silver	Face centered cubic	126	1240	0.457	1.00
Gold	Face centered cubic	132	1320	0.436	0.99
Copper	Face centered cubic	177	1360	0.439	1.01
Manganese	Tetragonal	206	1660	0.480	1.11
Nickel	Face centered cubic	255	1860	0.444	1.08
Cobalt	Face centered cubic	234	1800	0.490	1.02
Iron	Body centered cubic	204	1580	0.445	0.88
Palladium	Face centered cubic	209	1850	0.450	1.01
Platinum	Face centered cubic	240	2140	0.455	1.05

(*) Heats of fusion and absolute melting points used in the computations summarized in Tables I and II are those recommended by K. K. Kelley [« Contributions to the Data on Theoretical Metallurgy. V. Heats of Fusion of Inorganic Substances » Bureau of Mines Bulletin No. 393 (1936)] with the exception of the heat of fusion of germanium (6100 cals/g atom) that was calculated by R. A. Oriani of this Laboratory from equilibrium data on the binary systems Ge-Au, Ge-Pb, Ge-Ag.

ou interfaciale) du point de vue probabiliste, en tenant compte de ce que l'agitation thermique se produit par ondes?

(2) Le fait que la tension superficielle entre deux phases différentes est en général plus faible que celle entre deux grains d'une même phase, ne peut-il s'expliquer par l'hypothèse suivante :

Les joints peuvent être de deux types :

(a) *joints « véritables »* formés par un réseau à deux dimensions de défauts lacunaires très localisés;

(b) *paroi de dislocations* au sens de Shockley et Read.

Les joints entre deux phases seraient du type (a); ceux entre deux grains d'une même phase du type (b). Ces derniers peuvent avoir une énergie supérieure à ceux du premier type; ils seraient alors dans un état métastable préservé par les impuretés qui sont inévitablement concentrées dans les joints du type (b), et pas forcément dans ceux du type (a).

M. Prigogine. — En réponse à la première partie de la question

de Mr. Crussard, je voudrais rappeler qu'il existe deux méthodes pour introduire les grandeurs thermodynamiques superficielles. La première, due à Gibbs, consiste à les rapporter à une surface fictive unique, la surface de division, tandis que les phases volumiques sont supposées homogènes jusqu'au contact de cette surface.

L'inconvénient de cette méthode est que l'énergie superficielle Fa devient l'excès de l'énergie libre du système sur l'énergie de ses phases volumiques prolongées de manière homogène jusqu'à la surface de Gibbs. De même les autres grandeurs thermodynamiques deviennent des excès sur des valeurs dans un système homogène.

Au contraire, la seconde méthode due à Vershaffelt (*Ac. Roy. Belg. — Cl. Sc.*, **22**, p. 273, 390, 402 [1936]) et reprise par Guggenheim (*Tr. Far. Soc.*, **36**, p. 357 [1940]) définit directement les fonctions thermodynamiques superficielles comme les propriétés de la couche capillaire. Mais alors apparaissent d'autres inconvénients, par exemple le choix des limites de la couche. Mon collègue, M. Defay et moi, nous avons étudié les rapports entre les deux méthodes de manière détaillée dans un livre récent (R. Defay et I. Prigogine, *Tension superficielle et absorption*, Desoer, Liège, 1951). De toute manière, les relations macroscopiques utilisées par le professeur Smith sont conservées dans les deux modèles de sorte qu'aucune difficulté ne peut apparaître du fait du passage de la conception « surface » à la conception « couche ».

La seconde difficulté mentionnée par M. Crussard concernant l'interprétation probabiliste de l'entropie superficielle ne me paraît pas fondée. Même si l'on inclut les phénomènes superficiels, l'énergie libre reste liée à la somme d'états Z par la relation classique $exp(-EIRT) = Z$. La difficulté est plutôt d'ordre pratique en ce sens qu'il faut, pour déduire les grandeurs superficielles, utiliser une évaluation asymptotique plus poussée pour Z.

M. Crussard. — La difficulté de calculer l'entropie interfaciale ne provenait pas, dans mon esprit, d'une question de principe relative à la définition de l'entropie, mais bien d'une question pratique relative au calcul de la somme d'états. Plus précisément, je me demandais, pour le choix des coordonnés, si l'on avait le droit de décrire les mouvements des atomes de l'interface par un système d'ondes capillaires à deux dimensions, comme le fait Léon Brillouin pour la tension superficielle.

M. Smith. — Professor Crussard points out that there are two possible types of boundaries between crystals — that between phases differing in coordination number being possibly coherent, while that between identical lattices differing in orientation or parameter being essentially incoherent. I do not believe, however, that this provides a sufficient explanation for the relatively low energy of interfaces between different phases since crystals of the same structure type differing only in parameter and composition also give rise to an interface of low energy, as can be seen in the case of all the face-centered cubic pairs in Table IV of my report.

M. Frank. — An analysis of a boundary into dislocations is *formally* possible either for two similar lattices, differently oriented, or for two lattices of different parameter, or even of different structure, when they meet on planes of low crystallographic index : and I presume that it could even be extended to the general case of different lattices in arbitrary orientation meeting in an arbitrary plane. However, unless the disorientation is small (say, less than about 15°) or the difference in lattice parameter is small (say less than about 25 %) this analysis remains only formal: it is fraught with subtleties and ambiguities. For example, in the case of a boundary between two like lattices, of cubic symmetry, with different orientation, there are in general twenty-four different ways of specifying the difference of orientation as a rotation, to each of which corresponds a different analysis of the boundary into dislocations. If one always chooses to describe the difference in orientation by a rotation about that axis which makes the angle of rotation least, that angle may be as large as 63 ½°. But it is only when the angle is less than perhaps about 15°, and then when the boundary has attained a state of low energy, that it can be unambiguously analysed into a specific set of discrete dislocations. Since the grain boundaries of which professor Smith is speaking mostly involve much larger disorientations than 15°, I do not think that professor Crussard's suggested explanation of the difference between single phase and two phase boundaries — that the former consist of dislocations whereas the latter do not — can be supported.

M. Lomer. — Read and Shockley have assumed in their paper that there is a certain small radius r_0 within which the energy is unaffected by the presence of other dislocations, and that this is

equal to that value of r_0 which makes the energy of a finite cylindrical crystal of radius R equal to that of a cylinder of same radius, with a axial hole of radius r_0. Foreman, Jaswon and Wood (*Proc. Phys., 64A*, 1951, 156) have suggested that a dislocation in a real metal is quite long and an extension of this work shows that r_0 may be some $4\lambda_0$. This would make the energy maximum of Read and Shockley's curve come at an angle

$$\theta_m = \frac{\lambda_0}{2\pi\gamma_0} \sim 1/25 \sim 2^0$$

Pictures of the boundary structures seen in bubble rafts show that in fact at such a value of D interactions between the dislocations become very significant and thus the quantities results of Read and Shockley are inapplicable. The dislocations retain their identity but change their form; misfit along the slip plane diminishes and cracking on the tensile side of the edge dislocations increases so that at about 15° to 20° the dislocation picture becomes inappropriate.

In reply to a question by professor A.H. Cottrell, it was pointed out that Van der Merwe (*Proc. Phys. Soc., 63A*, 1950, 616) assumed the Peierls law of force between slip planes, which made r_0 less than λ_0, and so $\theta_m \sim 15^0$ in agreement with Read and Shockley.

M. Shockley. — I have no answer to Dr. Lomer's very interesting comment but I shall consider it between now and the time of my report and attempt a rejoinder then (1).

M. Seitz. — The importance of the influence of imperfections on the change of lattice entropy through a change in lattice vibrational frequencies, that is, through entropy terms other than those associated with mixing, seems to be illustrated by recent work of professor Lawson and Dr. Kurnick at the University of Chicago (as yet unpublished).

They have studied the influence of temperature and pressure on the atomic conductivity of silver chloride. Their results indicate that, although Frenkel defects predominate below 300 °C, Schottky

(1) A discussion of Dr. Lomer's point will be found in Dr. Shockley Report p. 431. In particular, details can be found there concerning Dr. Shockley's remark that for small angle boundaries there is little difference between energy and free energy. (Note de l'éditeur.)

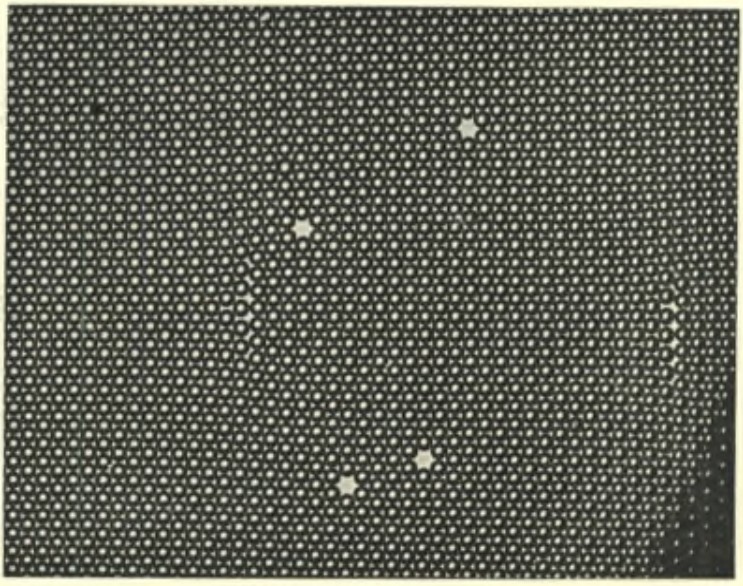

Fig. 1. — Part of boundary separating regions of lattice disoriented by 2°.

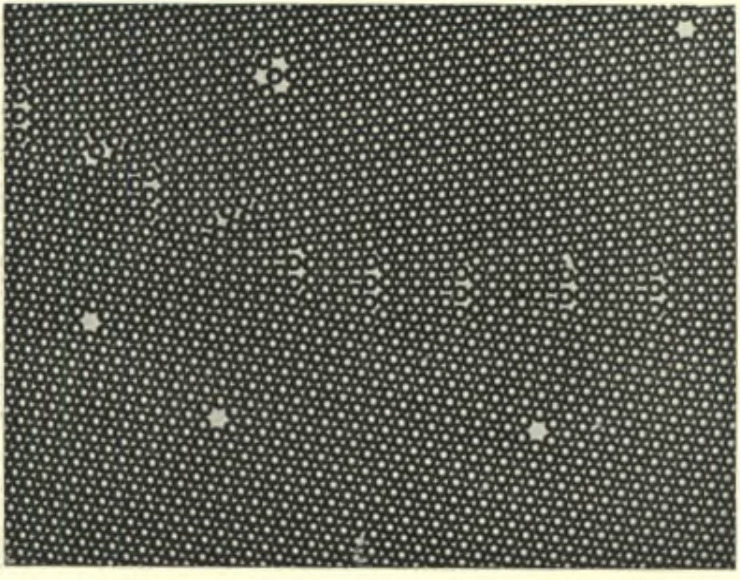

Big. 2. — Boundary between regions disoriented by 10°.

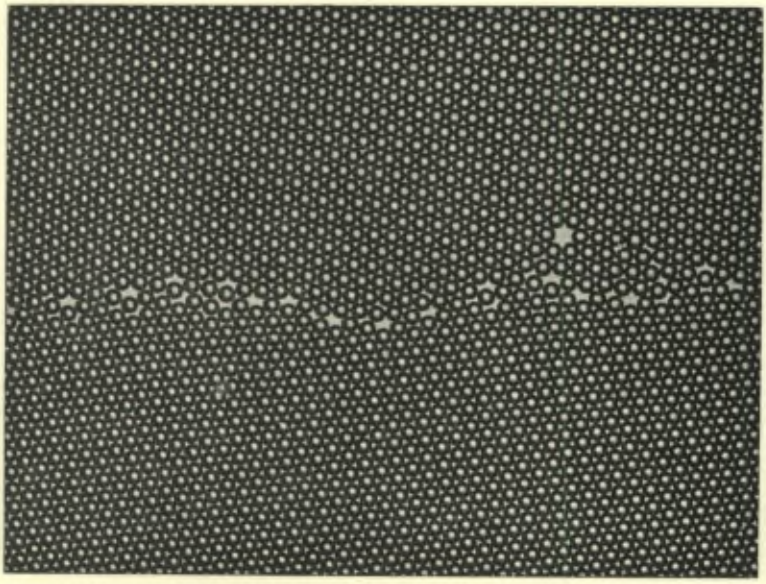

Fig. 3. — Boundary between regions disoriented by 25°.

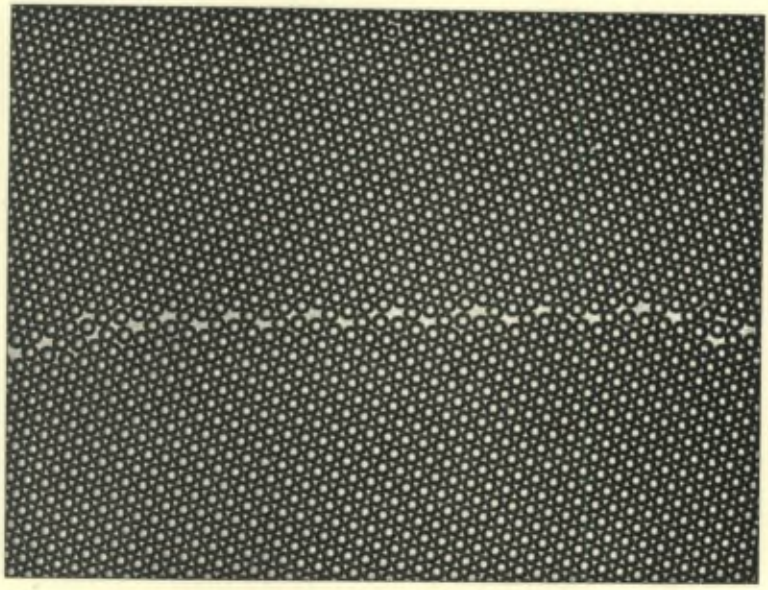

Fig. 4. — Boundary between regions disoriented by 35°.

defects succeed in dominating above 300 °C in spite of the fact that the heat of formation of the latter is greater. It appears that the entropy gained by the lattice through the introduction of Schottky defects, which have a loosening influence and presumably lower the lattice frequencies as a result, is sufficient to compensate for the higher heat of formation of Schottky defects relative to that of Frenkel defects. These measurements suggest that entropy effects, other than those associated with mixing, become important in determining the equilibrium form of imperfections as soon as one is within twenty per cent of the melting temperature.

Grain Growth Observed by Electron Optical Means

by G.W. Rathenau

Philips Research Laboratories
N. V. Philips' Gloeilampenfabrieken
Eindhoven-Netherlands.

Whereas the profound influence of interfacial tensions on the microstructure of solids has been well proved, comparatively little work has been done with the aim to determine how local equilibrium at grain boundaries is actually established.

Though electron emission microscopy furnishes only qualitative results it allows of direct observation of grain boundary movement and of straightforward information regarding the factors by which it is influenced.

A. THE EMISSION MICROSCOPE

In the emission microscope the grain structure of a metal surface is rendered visible by evaporation onto it of a thin film of an electropositive metal such as Ba or Cs. The atoms of these activating metals are preferentially absorbed by certain crystal faces. Therefore on heating the metal to a suitable temperature in the region 400 to 1250 °C the intensity of thermal electron emission varies with the orientation of the crystal faces at the surface of the metal. On focussing the emitted electrons one obtains an image of the metal surface in which the grains are clearly differentiated. Because of the high velocity of surface diffusion of the activator atoms, changes in grain structure of the metal under consideration are immediately observable.

This method of observation has been used with small resolution and magnification as early as 1932 by Brüche and coworkers (1) and later by Burgers and Ploos van Amstel (2) who applied it to several metallurgical problems.

Fig. 1*a*

Fig. 1*b*

Fig. 1*c*

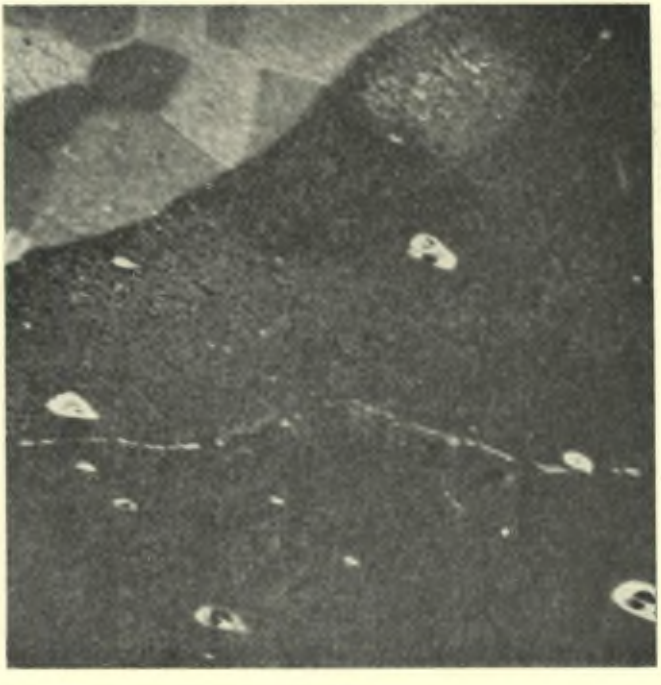

Fig. 1*d*

Fig. 1*a*-1*d*. — Growth of a large secondary crystal S in an array of similarly oriented grains (cubic orientation). NiFe 48/52 % by weight. The temperature was about 1090 °C.

B. GRAIN GROWTH IN A WELL PRONOUNCED TEXTURE OF ONE LARGE GRAIN OF DEVIATING ORIENTATION

It seemed interesting to study grain growth in an array of small grains of very similar orientation, which is in contact with only one large grain of deviating orientation. This has been done in the following way. Many face centered cubic metals und alloys can after cold rolling be made te recrystallize in the so-called cubic orientation. In this recrystallization texture the cubic planes of the small crystals (maximum dimension about 50 μ) are parallel to each other within a few degrees, while one (100) plane approximately coincides with the rolling plane. Under certain conditions a few large crystals of well defined orientations, which are different from that of the cubic orientation and its twins can be made to grow fairly quickly within the texture ([3], [4], [5]).

The growth of these large so called « secondary crystals » has been followed electronmicroscopically in face centered NiFe alloys ([6]). As can be seen from figures 1*a*—1*d* the boundary of the secondary crystal is generally concave towards the grains of the matrix it is going to absorb. It curves with a small radius of curvature around a large crystal of the matrix : *a*. From the angles formed by the boundaries between two so-called cubic crystals and the boundary of the secondary crystal it can be deduced that the ratio of the surface (free) energy of the interface between cubic crystals γ_{cc} and the surface energy belonging to the secondary crystal γ_{sc} is smaller than unity. It amounts to about $\gamma_{cc}/\gamma_{sc} = 1/2$.

These observations are to be expected. As shown by Smith ([7]) concavity of the grain boundary of a large grain within a matrix of small grains should occur if the ratio of the diameters D/*d* of the large grain (D) and of the grains of the matrix (*d*) exceeds : $2\,\gamma_{sc}/\gamma_{cc}$ which in our case is about 4. The ration D/*d* which has been observed is certainly larger than 4. According to Harker and Parker's ([8]) considerations it is the concavity of a grain boundary which stimulates its movement towards the centre of curvature.

It seems probable that the high specific surface energy of the boundary which we have measured is a stringent condition for its motion. According to Mott's picture ([9]) an interface between crystals consists of regions of good fit and of bad fit. If the surface energy is small a good fit area is large and a high activation energy would

be needed to loosen its atoms simultaneously. On the contrary little activation energy is needed to « melt » the small good fit areas of a high energy boundary. In this connection the experiments of Burgers, Lacombe and coworkers should be mentioned who found unrecrystallized islands of nearly identical or nearly twin orientation within recrystallized grains ([10]). These experiments point equally to the stability of low energy surfaces during grain growth.

C. GRAIN GROWTH AT LOW ENERGY BOUNDARIES

It seemed interesting to investigate the grain growth at a boundary of two crystals in nearly identical or in nearly twin position.

The same NiFe alloy which after severe cold rolling and recrystallization develops a rather perfect pseudo-unicrystalline texture contains when cold rolled to a lesser degree besides the crystals in cubic orientation, their twins and near twins and also crystals orientated at random.

Grain boundary movement at the boundary of two crystals with about the same orientation and at the boundary of a cubic crystal and its (near) twin has been studied electron-optically ([6]).

Grain boundary movement at an interface between two nearly indentically oriented crystals proved always to be very restricted. At the boundary of a crystal and its (near) twin one must distinguish between two kinds of faces : the common twinning plane (111) which because of the perfect fit of the atoms on both sides of the boundary is a surface of very low energy, and faces differing from the twinning plane, having considerably higher surface energies ([11]). The faces of high surface energy of a boundary between a crystal and its near twin proved to move, while the low energy boundary (111) was never observed to move in the direction of its normal. In figures 2*a*-2*d* a typical case is reproduced.

Mott's picture once more accounts for the observations : high activation energies would be required to displace boundaries with large good fit areas in the direction of their normal, as are the boundaries between crystals of about the same orientation, or low-energy (111)-twin boundaries.

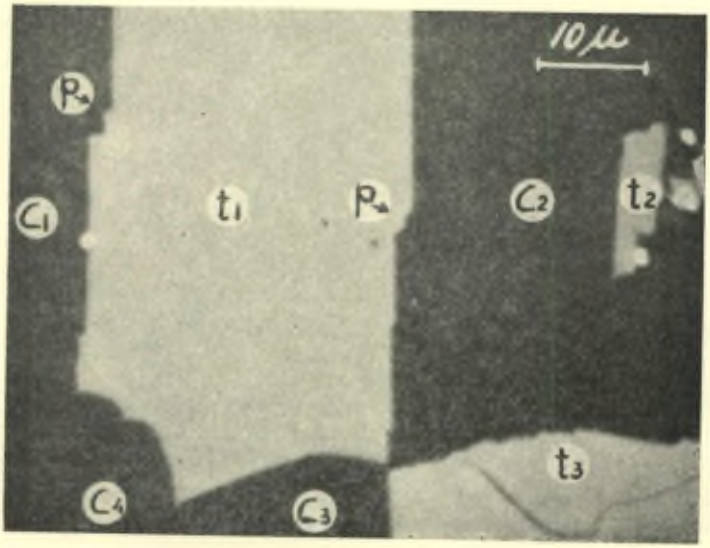

Fig. 2*a*

Fig. 2*b*

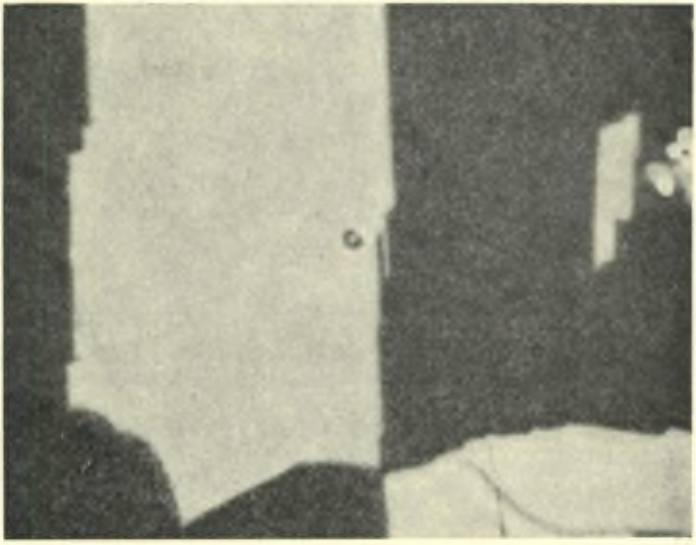

Fig. 2*c*

Fig. 2*d*

Fig. 2*a*-2*d*. — Crystal growth at the boundary of (nearly) twin-related crystals. The same alloy as in figure 1. Temperatures of heating : 1145-1205 °C. Crystals in cubic orientation are denoted by C_1, C_2 ... (near) twins of crystals in cubic orientation by t_1, t_2.

Movement of the boundary occurs at high-energy surface parts (*p*) only.

D. GRAIN GROWTH IN AN IMPERFECT TEXTURE

The material dealt with in section *c)*, a face centered Nickel-Iron alloy, which contained, besides crystals in a preferred orientation (the cubic texture), the four types of (near) twins belonging to this orientation and random oriented crystals, served as an object for studying grain growth in an imperfect texture ([6]).

The following results have been obtained. Grains of random orientation are preferentially absorbed by the grains in cubic orientation and their twins. The grain boundary shift is localized, these « unstable » crystals being simultaneously and rapidly ($\sim$ 100 μ/sec) invaded by almost all of the adjoining crystals. The grain boundaries, which the absorbing crystals had in common before the attack, generally do not move, or only very little, during the absorption of the disappearing crystal (figures 3*a*-3*b*). Therefore after completion of the absorption lowest local surface energy is often not immediately established. Steps may be formed at the new interfaces, which only gradually disappear.

The explanation of these observations may probably once more be given along the lines of Mott's theory. The stable crystals are crystals in cubic orientation and their twins. The former mutually form low energy interfaces along arbitrary directions in space. Also twins of similar orientation form mutually low energy interfaces. Cubic crystals and their twins have low energy interfaces along the (111) — twinning plane only. However, all boundaries, which the unstable arbitrary oriented crystal forms with the crystals in cubic orientation and their twins, are high energy interfaces.

If an unstable crystal is attacked by movement of one of these high energy boundaries in the direction of the centre of this crystal, the equilibrium of surface forces cannot immediately be restored by rearrangement of the low energy interfaces between the surrounding grains. Therefore the required equilibrium angles are roughly maintained by movement into the unstable grain of almost all of the adjoining grains. Complete adaptation of the low energy interfaces follows slowly.

This explanation once more suggests, that the existence of high

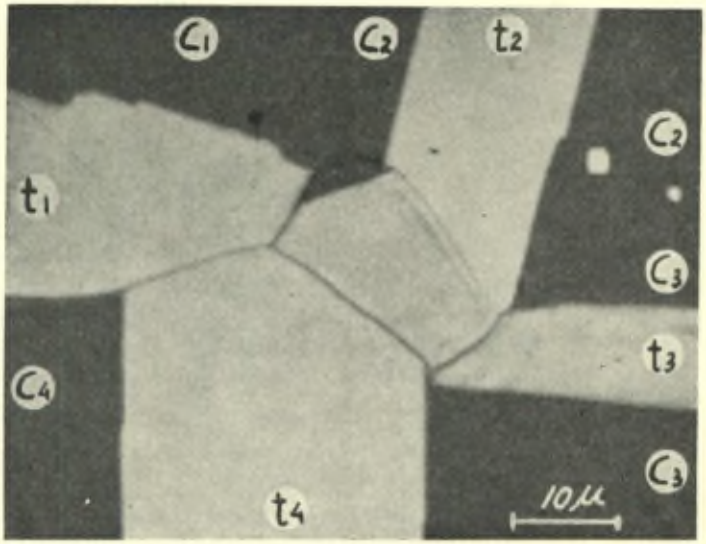

Fig. 3*a*

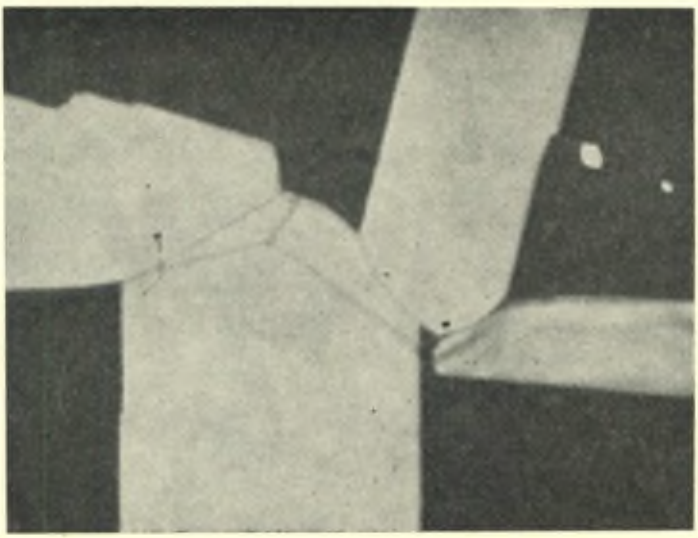

Fig. 3*b*

Fig. 3*a*-3*b*. — Crystal growth in an imperfect texture. Alloy as in figures 1 and 2. Temperature of heating : 1145 °C. Crystals in cubic orientation denoted by *c*, (near) twins by *t*. One crystal in the centre differing in orientation from the crystals in cubic orientation and probably their twins is rapidly absorbed. The former boundaries are still visible because of thermal etching.

energy interfaces is a stringent condition for grain growth. It does not account for the fact, that a small crystal of deviating orientation does not grow but is absorbed by the crystals of the texture. It is of course clear that grains, much smaller than the average grain of the texture, are unstable.

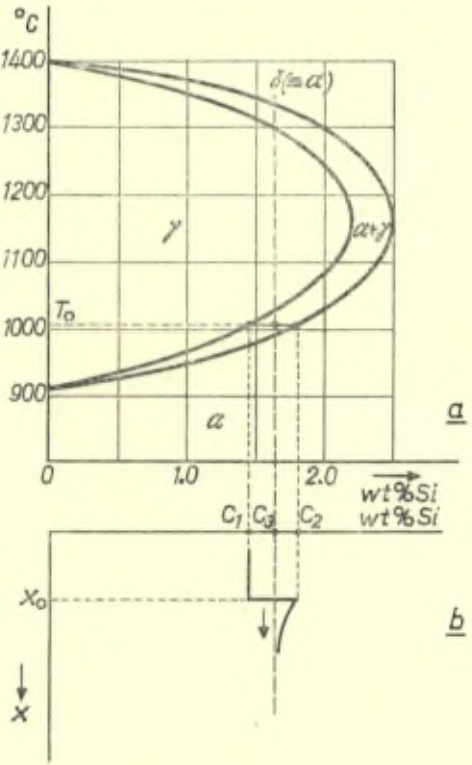

Fig. 4*a* — 4*b*

Fig. 4*a*. — Part of the phase diagram of Fe-Si alloys. The dashed line at 1.64 % Si indicates the composition of the alloy to be discussed.

Fig. 4*b*. — Schematical drawing (following Zener) of the change in concentration at a moving phase boundary. It is assumed that by quick heating to temperature T_0 a homogeneous Si-Fe alloy of Si content C_3 which has the alpha structure, develops growing gamma crystals. C_1 and C_2 stand for the Si-concentrations of the phases in which the homogeneous alloy C_3 would separate if kept for a long time at the temperature T_0.

Vertical : a distance X along the normal to the phase boundary. X_0 represents the actual place of the moving boundary.

E. GRAIN GROWTH ACCOMPANYING THE PHASE TRANSFORMATION OF ALLOYS

In studying grain growth that is caused by phase transformation other factors than interfacial tensions have to be considered also. The grain growth which is connected with the phase transformation alpha/gamma in silicon — iron alloys has been followed by electron-optical means. Figure 4*a* shows the pertinent part of the phase diagram. It is seen, that at temperatures, where the phases alpha and gamma are in equilibrium, the gamma-phase contains a lower percentage of Si. It is therefore whenever a homogeneous alloy is quickly brought to a temperature at which under equilibrium conditions separation into two phases of different composition occurs, that the growing grains of the new phase must get rid of Si (if the gamma phase grows in an alpha matrix) or absorb it from the matrix (if the alpha phase is growing in a gamma matrix). As the number of atoms per cm^3 within the matrix and the separating phases is nearly equal, a countercurrent of Fe atoms flows in the opposite direction to the current of the Si-atoms.

Zener ([12]) has treated the case, for which the rate at which the phase boundary advances is solely determined by the diffusion of atoms in the disappearing parent phase while at the interface the equilibrium concentrations are maintained (figure 4*b*). The velocity of the boundary displacement is written as follows :

$$v_b \sim \frac{-D}{(c_2 - c_1)_b} \cdot \left(\frac{\partial c_2}{\partial x}\right)_b$$

where D stands for the coefficient of diffusion in the parent phase, c_2 and c_1 for the concentrations of the solute atoms in the parent and the new phase respectively and x for the distance along the normal of the phase boundary pointing into the disappearing parent phase.

The gradient $(\partial c_2/\partial x)_b$, which provides the driving force for diffusion generally decreases at constant temperature, during the growth of the new phase at the expense of the parent phase, because this phase gets nearer to its equilibrium concentration. If f.i. two grains of the new phase approach eachother the value of the gradients $(\partial c_2/\partial x)$ at both phase boundaries approaches zero.

On comparing different shapes of the advancing boundary, the concentration gradient is found to be maximum for thin rods or plates growing — convex towards the parent phase — along the

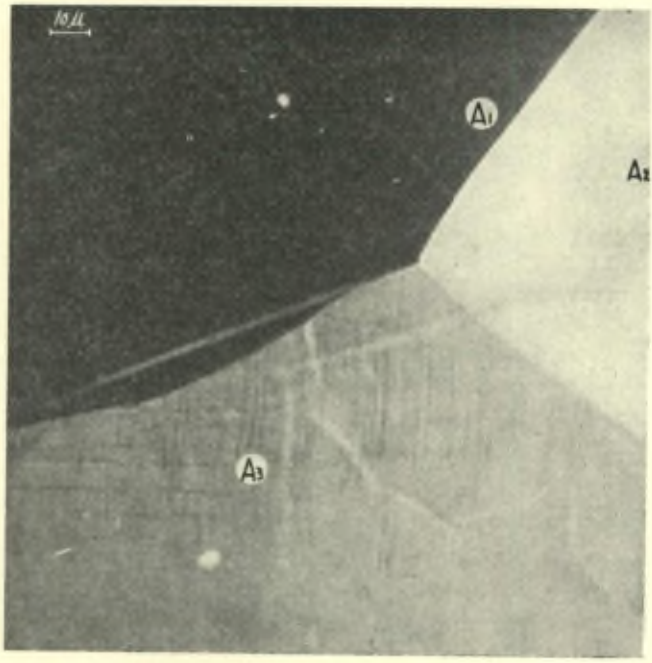

Fig. 5*a*

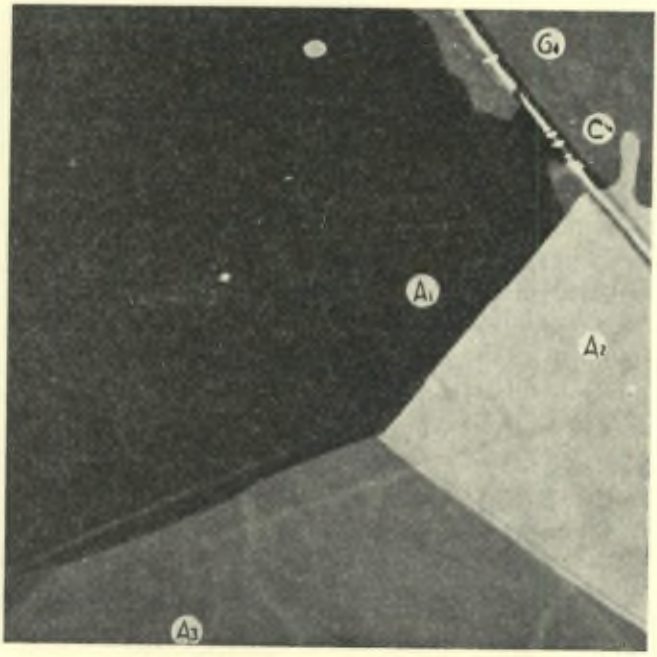

Fig. 5*b*

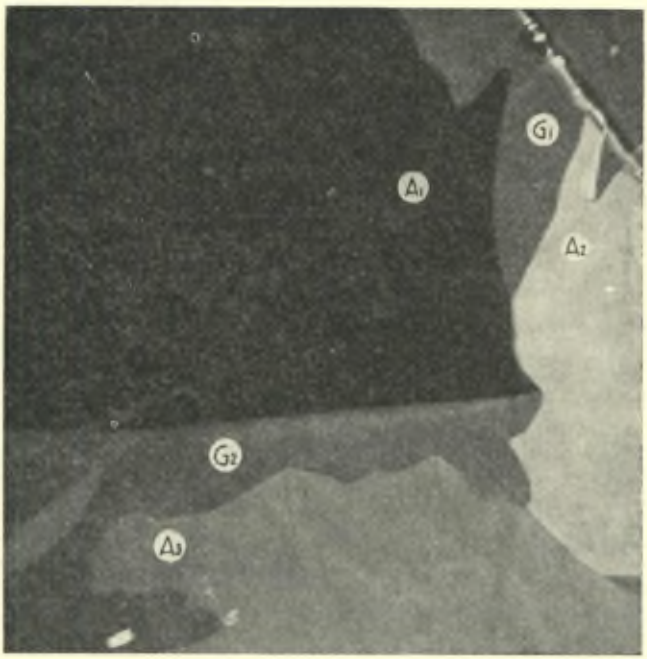

Fig. 5c

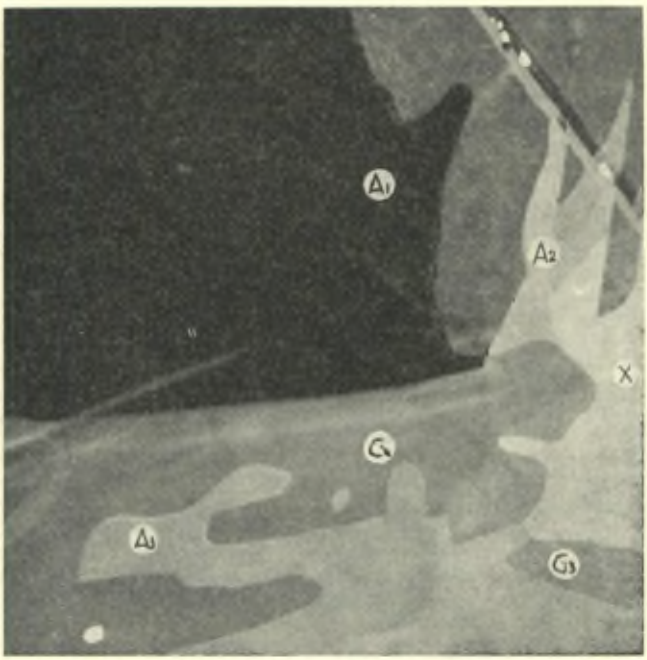

Fig. 5d

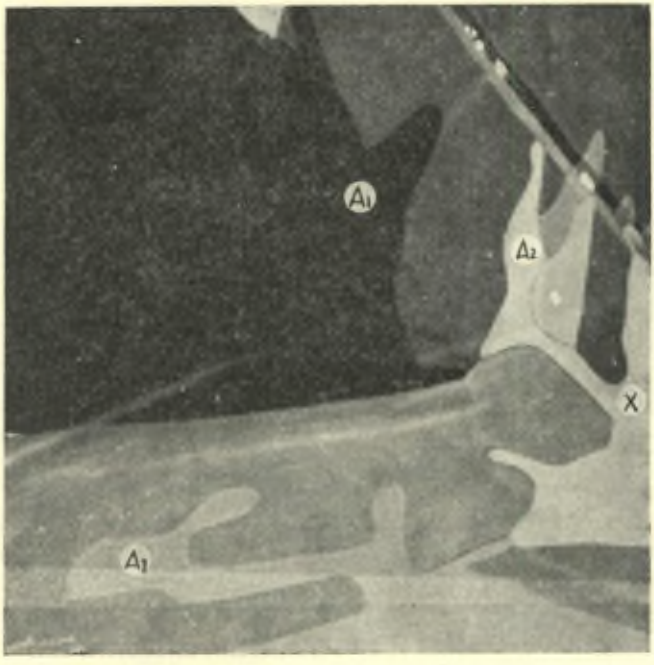

Fig. 5*e*

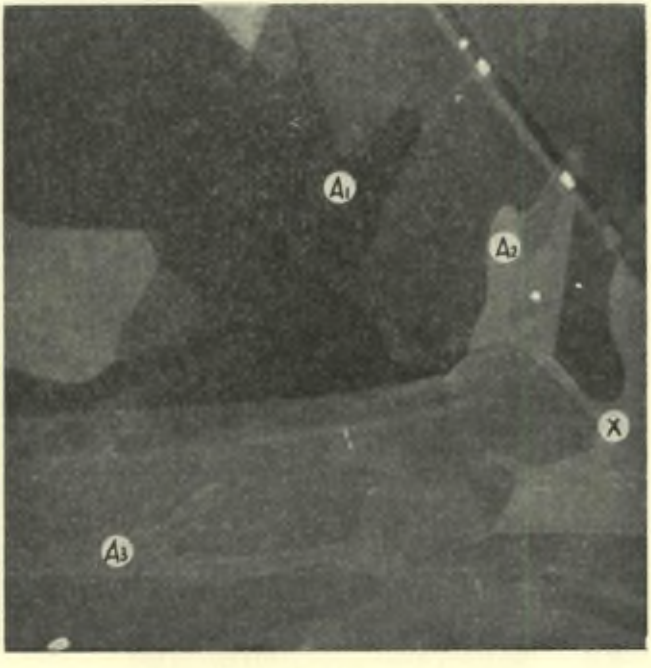

Fig. 5*f*

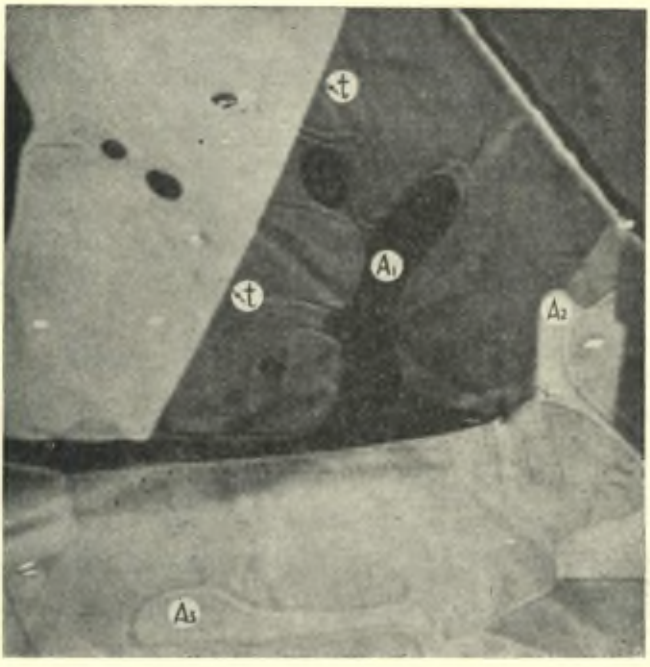

Fig. 5*g*

Fig. 5*h*

Fig. 5. — Fe-Si alloy (1.64 % Si by weight) transforming on heating slowly from the homogeneous alpha into the gamma phase (*a-g*). Decreasing the temperature results in nearly the same alpha structure which has been present in the beginning of the experiment (*h*). The alpha grains are indicated by A_1, A_2, A_3, the grains in gamma structure by G_1, G_2, G_3. The spots A_1, A_2, A_3 indicate on every photograph the same places of the metallic surface.

direction of their maximum extension, while it is small for large plane boundaries moving in the direction of their normal and still smaller for concave boundaries. It might be anticipated, that on phase transformation in alloys extremely fine grains would develop growing convex towards the matrix. It is because of the opposing influence of surface energy, which as shown above almost solely controls the growth in homogeneous materials, that the convex curvature of the advancing boundary remains finite.

A homogenized Fe — Si alloy (3,2 at %, 1,64 weight % of Si) of high purity has been investigated electron-optically. The type of grain growth which is expected from Zener's calculations has often been found to take place in our experiments when the alloy is slowly heated so as to transform from the homogeneous alpha phase into the gamma phase. Figure 5 which shows some stages of the transformation of the alpha into the gamma phase may serve as an example. The phase boundary advances sufficiently slowly as to allow of appreciable diffusion near this boundary. In the structure of figure 5 initially three alpha grains (A) are to be seen (figure 5*a*). From the upper right part of the image a gamma grain (G_1) invades two alpha grains (figure 5*b*). The phase boundary is generally heavily curved. The parts of the boundary which are most heavily curved convex towards the disappearing alpha matrix advance at the highest rate (figures 5*c*—5*d*), leaving at first unattacked channels of Si — rich alpha phase with concave interfaces towards the alpha phase (*c* in figures 5*b*—5*d*). In a later stage of growth these channels are generally cut off, thus leaving isolated islands of Si — rich alpha phase within the gamma grain. In figures 5*f* and 5*g* it can be clearly seen that the islands within the gamma grains are remnants of the original alpha grains of which they were formerly a part.

As shown in figures 5 *d*, *e*, *f* at X two gamma grains, which have come near each other tend to turn aside, apparently because of the high Si - concentration of the remaining alpha phase in between these grains. It is in this way that the grains of the growing phase are enveloped by material having the structure and orientation of the disappearing phase as is clearly seen in figure 5*g*. Only at the boundary between twins of the new phase, which have grown coordinately (twin boundary *t* in figure 5*g*) there remains no Si-rich alpha phase.

On lowering the temperature the alpha phase inclusions, at grain boundaries and within the grains, grow at the expense of the gamma

structure. This leads to about the same structure of alpha grains (figure 5*h*) which has been present in the very beginning of the experiment (figure 5*a*).

The following observations are remarkable. The alloy was heated to the gamma region such, that the alpha inclusions at the gamma grain boundaries or within the gamma grains had seemingly disappeared — and should have disappeared according to the phase diagram. On cooling to the alpha region or heating to the so called delta region (figure 4*a*), where alpha crystals again are stable, alpha germs of *one* definite orientation seemed to originate at *several* places of the gamma grain boundary. These places were generally those at which on heating to the gamma region the alpha structure was consumed latest and which consequently have had been richest in silicon content. The germs at gamma grain boundaries have been seen to grow to an alpha grain, which sometimes had clear indications of having the same structure as the alpha grain present *before* the transformation to the gamma phase had taken place.

It can of course not be ruled out that the new alpha- and delta phase germs are actually formed below the surface of the alloy which only is visible in the electronoptical image. Moreover the observations in the delta region are troubled due to excessive evaporation of the alloy.

However, it seems fairly certain that boundaries of grains grown during phase transformation may not always be considered simply as two dimensional interfaces.

Eindhoven, 9 November 1951.

REFERENCES

(1) E. Brüche und H. Johannson, *Phys. Z.*, **33**, p. 898 (1932).
(2) W. G. Burgers and J. J. A. Ploos van Amstel, *Nature*, **136**, p. 721 (1935).
Physica **4**, pp. 5, 15 (1937); *Nature*, **141**, p. 330 (1938).
Physica, **5**, p. 305 (1938); *Erg. Techn. Röntgenk.*, **6**, p. 165 (1938).
Physica, **5**, p. 313 (1938).
Philips Techn. Rev., **1**, p. 317 (1936).
W. G. Burgers, *Z. Metallkunde*, **29**, p. 250 (1937); *Metallwiss.*, **17**, p. 648 (1938).
(3) P. A. Beck and Hsun Hu, *Trans. A. I. M. E.*, **185**, p. 627 (1949).
(4) J. S. Bowles and W. Boas, *J. Inst. Metals*, **74**, p. 501 (1948).
M. L. Kronberg and F. H. Wilson, *Trans. A. I. M. E.*, **185**, p. 501 (1949).
(5) G. W. Rathenau and J. F. H. Custers, *Philips Research Reports*, **4**, p. 241 (1949).
(6) G. W. Rathenau and G. Baas, *Physica*, **17**, p. 117 (1951).
(7) C. S. Smith, Preprint 37, *Am. Soc. Metals*, October, 15, (1951).
(8) D. Harker and E. R. Parker, *Trans. A. S. M. E.*, **34**, p. 156 (1945).
(9) N. F. Mott, *Proc. Phys. Soc.* (London), **60**, p. 391 (1948).
(10) T. J. Tiedema, W. May and W. G. Burgers, *Acta Cryst*, **2**, p. 151 (1949).
W. G. Burgers and V. Dalitz, *Proc. Kon. Akad. Wet.*, **52**, p. 623 (1949).
P. Lacombe and A. Berghezan, *C. R. Acad.* (Paris), **228**, p. 93 (1949); *Métaux et Corrosion*, Jan. 1949.
(11) R. L. Fullman, *J. Appl. Physics*, **22**, pp. 448, 456, (1951).
(12) C. Zener, *A. I. M. M. E; T. P.* 1925, (1946).

Recrystallization and Grain Growth in Solid Metals

by W. G. Burgers

Department of Physical Chemistry
Technical University, Delft (Holland)

CHAPTER I

INTRODUCTION

I, 1. Definition of Subject.

In this report we shall discuss results obtained in recent years (*) concerning structural changes taking place in metals during heat treatment, in so far they have an influence on the number, size, shape, state or orientation of the constituent crystallites. Structural changes, which are due to allotropic transition or in general to transgression of a boundary line in the phase diagram of a system will not be considered, or only in so far the considerations given apply to recrystallization phenomena occurring within the range of thermodynamic stability of a given phase. This implies that changes in actual crystal structure, in the sense as this expression is commonly used in X-ray crystallography, are not discussed, but only changes in what we may call the grain structure and texture (German : Gefüge) of crystalline solids. It are these changes which in metallurgical practice are indicated by the general expression recrystallization. The phenomena falling under this head are already so complicated and present so many problems that limitation to this restricted field seems appropriate.

(*) An extensive discussion of recrystallization research up till 1940 is given by Burgers (1941).

I, 2. Restriction in Treatment.

It will appear in what follows that attention is especially given to the « geometric » side of the recrystallization mechanism, meaning by this that phenomena connected with the orientation relationships existing between matrix and growing crystals are extensively discussed. The statistical reproducibility of these relationships is often so pronounced that one cannot help thinking that they must be based on some general law, governing the atomic processes underlying the formation and growth of crystals. Less attention is given to papers dealing with the kinetic side of recrystallization. Partly this is due to the circumstance that it proved to be no easy task to get so thoroughly to the bottom of the various theories proposed that their contents might be stated and weighed in a proper way. Besides, the formulae developed although capable of describing more or less accurately the course of a recrystallization process are commonly based on general assumptions which donot directly help to form a picture of the actual atomic processes underlying the observed phenomena.

Our considerations are restricted in another sense, as they deal almost exclusively with phenomena in « pure » metals or alloys. Of course, this restriction has to be taken with reserve, because a certain percentage of foreign atoms, be it perhaps very small, is practically always present. As it is well known that structure sensitive properties of solids can be strongly influenced by such small additions, it must be kept in mind that the observed phenomena may be related to their presence and be different in the truly « pure » state of the metal or alloy studied.

I, 3. Sintering.

Finally, we must remark that we have not discussed the phenomena occurring during « sintering » of powder aggregates. Actual crystal growth (i. e. increase in size of coherent lattice regions) plays only a minor part in the processes underlying this procedure. Preponderant is the increase in density and strength of the material, and the change in shape of its « holes ». Apart from surface and internal diffusion, plastic flow seems to be the principal process in sintering. In recent years the atomic mechanism of the sintering process has

been treated in various fundamental papers. The following may be quoted :

Kieffer and Hotop (1943), McKee (1948), Schwarzkopf (1948), Dedrick and Gerds (1949), Geach and Jones (1949), Kuczynski (1949), Mackenzie and Shuttleworth (1949), Shaler (1949), Cabrera (1950), Herring (1950), Skaupy (1950). A short survey of the subject is given by Shaler and Wulff (1948).

Moreover, quite recently a collection of papers presented at a symposium held at Bayside, N. Y., has been published in bookform under the title : « The Physics of Powder Metallurgy » (New York 1951).

I, 4. General Course of the Report.

The general course of the report runs as follows : First the atomic processes taking place during annealing are considered in general terms (Chap. II). This is followed by a short exposition of the nomenclature of recrystallization phenomena as used in the current literature (Chap. III). Then follows a discussion on the fundamental phenomena recovery (Chap. IV), polygonization (Chap. V), nucleation (Chap. VI) and boundary migration (crystal growth) (Chap. VII). The origin of recrystallization textures (Chap. VIII) and the formation of annealing twins (Chap. IX) are treated next. Some stray remarks on the influence of impurities on recrystallization close the discussion proper (Chap. X).

However, considering the fact that several of the experimental results reviewed in the report have been obtained by applying either not-commonly used variations of in itself well-known techniques or techniques which have only recently been developed, a *Supplement* is added, in which a survey is given of some newer methods used for the investigation of structural changes in metals (Chap. XI). A second chapter (Chap. XII) contains an exposition of some novel methods used for preparing test-pieces consisting of one or a few crystals with prechosen orientation, as such crystals have been applied for researches dealing with definite aspects of the problems treated in the report.

Delft, March 1951.

CHAPTER II

ATOMIC PROCESSES TAKING PLACE DURING ANNEALING*

II, 1. Definition of Conceivable Types.

Ultimately the atomic displacements taking place during annealing of a cold-worked matrix are due to its tendency to attain the state of minimal free energy, i. e. a « perfect » single crystal in thermodynamic equilibrium possessing its appropriate number of lattice defects of the Frenkel and Schottky types. Annealing in its most complete sense might then be described as a process of elimination of structural imperfections, on the one hand those existing at the « boundaries » between lattice domains with deviating orientation (grains, mosaic-blocks) and further irregularities in the atomic array existing inside coherent lattice domains not belonging to the equilibrium state.

A priori it seems possible to discriminate between different types of atomic displacement processes taking place in the course of the annealing procedure. One way of looking at these phenomena is to assume that all the structural irregularities resulting from cold-work can be analyzed into terms of dislocations of well-defined type, such as line dislocations (Taylor dislocations) or screw dislocations (sometimes called Burgers (**) dislocations). Such dislocations are the seats of stress fields and give rise to the presence of strain energy in the surrounding lattice regions. The resulting stresses may act over short distances and cause a direct interaction between neighbouring dislocations. It is also possible, however, that the stresses due to definite arrays of dislocations extend over larger distances, so that they can exert a cooperative action upon sets of dislocations present at positions relatively far away in the matrix. If the temperature is sufficiently raised to cause atomic movements to occur in reasonable times, we may expect both mutual movements

(*) After this section was written, the author by the courtesy of Professor F. Seitz received a manuscript of his paper on the generation of vacancies by moving dislocations for perusal. From this it becames apparent that the movement and particularly the dissolution of aggregates of vacancies may be one of the fundamental processes taking place during recovery. Unfortunately, it has not been possible to take these views into account when writing this report. It may be well possible that they lead to important modifications of the considerations given here.

(**) After J. M. Burgers.

of « individual » dislocations or cooperative movements of whole arrays of dislocations.

Reasoning along these lines, we might consider the following processes :

a) mutual elimination (« neutralization ») of two suitably « oriented » dislocations of opposite sign (edge dislocations), c. q. opposite sense (screw dislocations);

b) rearrangement of a set of dislocations inside a coherent lattice region, for example an accumulation into definite planes of dislocations originally scattered throughout the domain considered;

c) collective migration of an array of « parallel » dislocations of « equal sign » or of two « non-parallel » arrays under the influence of over-all stresses (cf. Read and Shockley, 1950).

All these movements will take place in a sense ultimately leading to a decrease in free energy.

II, 2. Elimination of Dislocations.

Processes of type *a)* occur within lattice regions of relatively restricted extension : the structural changes involved in these processes will generally be too small to make themselves « visible », although it is obvious that this depends on the sensivitity of the method applied to detect them (ordinary microscope, electron miscroscope, X-ray diffraction, etc.). On the other hand the release of stress and strain, which accompanies these changes, may influence mechanical and physical properties considerably and in general cause a return of their values to those existing in the completely annealed state. Dependent on the correlation between the property considered and the characteristics (« wave length ») of the stress strain state, its « redress » will be more or less intensive. We are thus inclined to say that processes of this type belong to the annealing stage commonly denoted as « recovery » (cf. Thorley, 1950).

II, 3. Rearrangement of Dislocations.

A similar effect may be expected to be the result of processes considered under *b)*. Here, however, visible structural changes are more likely to appear, due to the formation of transition surfaces which transform the originally coherent strained lattice region into a series of « polygons » with slightly different orientations.

This process is what Orowan (1947) and Cahn (1949) call « polygonization ».

The processes considered under *a)* and *b)* may, moreover, have another effect on the course of the annealing process, as they give rise to the formation of lattice domains, inside which the « density » of dislocations has greatly diminished. Regions are therefore created in the matrix, where areas of small dislocation density are surrounded by areas of far greater density and thus strain energy. As will be discussed in chapter VI, such dislocation-poor lattice regions serve probably as nuclei for new crystals (Cahn, 1949, 1950). If so, recovery and nucleation occur to some extent simultaneously and form part of the same processes. Such a view would fit in with ideas put forward by Thorley (1950).

II, 4. Migration of Dislocations.

The collective movement of dislocation arrays, considered under *c)*, is of a different type, in so far it does not diminish the number of dislocations, but only displaces them, the displacement being equivalent to the migration of a boundary between two adjoining lattice blocks of different orientation (J. M. Burgers, 1940; Bragg, 1940). As pointed out by Read and Shockley (1950), dependent on the « structure » of the boundary in terms of dislocations, the exact mechanism of the dislocation displacement can be different : both movements parallel and perpendicular to their « glide planes » have to be considered. Moreover these authors, while considering allowable the conception of the process of growth as a collective displacement of dislocation arrays when describing boundary displacements between blocks including *small* angles, doubt whether it is still permitted (or has still sense) to describe a boundary between blocks including large angles by definite sets dislocations. Probably, as Mott (1948, 1949) has suggested, such a boundary is better described as a sequence of places of « good » and « bad » fit. The transition process taking place on displacement of such a boundary is then considered by Mott as being due to a local melting, followed by readjustment of the atoms. As the number of places of bad fit will presumably increase with the angle between adjoining lattices, at least within certain limits (cf. Chap. VII, 2), the probability of these local melting processes, and so the rate of boundary displacement, may be expected to increase at the same time. This alternative conception

is the more important because, as we shall see later (Chap. VII, 6), actual boundary migration is in the main restricted to boundaries between domains with *large* differences in orientation.

In yet another way Beck, Sperry and Hsun Hu (1950) consider self-diffusion along the grain boundary as an essential feature of the mechanism of grain boundary migration. They expect that the difference in lattice orientation has a strong effect on the rate of self-diffusion along the boundary, the latter being relatively high along a boundary with high disorientation. This, according to Beck (private communication) has recently been confirmed for self-diffusion in tin by Fensham (1950) and for diffusion of copper along grain boundaries of nickel by Barnes (1950). Also observations by Achter and Smoluchowski (1951) on the penetration of silver along grain boundaries in a copper matrix indicate that the rates of precipitation differ in the various grain boundaries.

Leaving this question as it stands, the resulting effect of boundary migration can in any case be described as growth of one lattice block at the cost of an adjoining block and so represents the basal phenomenon observed during actual « recrystallization » of the matrix structure.

CHAPTER III

NOMENCLATURE OF RECRYSTALLIZATION PHENOMENA

Purely phenomenologically, when considering the visible course of recrystallization, one can discern various stages, which we shall call *primary recrystallization*, *grain growth* and *secundary recrystallization*. As these expressions are currently used in the literature, but not always in exactly the same sense, it seems appropriate to define them as well as possible, in order to avoid confusion when using them in this report.

As long as we observe the growth of new crystals at the cost of the deformed matrix up till the stage that they impinge upon each other, we speak of *primary recrystallization*. Various metals in this stage show considerable differences in appearance. In aluminium, for example, the new crystallites show generally curved contours, the occurrence of straight boundaries, although observed under special circumstances (cf. Dalitz and Burgers, 1949), being rather

exceptional. With other metals, like copper and brass, or nickel iron, straight boundaries are always present in great number ; generally these boundaries form the traces of octahedral planes, separating two lattice regions in mutual twin position.

If, as is the case with severely deformed test-pieces, the size of the primary crystallites is sufficiently small, for example with diameters of the order of 0,01-0,1 mm, then, on prolonged heating, a gradual coarsening of the grain structure may occur, due to the growth of some crystallites at the cost of neighbouring ones. This phenomenon we shall denote, in concord with common use, as *grain growth* (by some authors coalescence, in German : Kornvergrösserung).

There are cases, however, that on prolonged heat treatment of a primarily recrystallized fine-grained matrix a general coarsening does not take place, but only one or a few crystals develop, these crystals growing at the expense of the primary matrix grains, which, in the main, donot increase in size. This phenomenon, which gives the impression that the test-piece, although not subjected to a new cold-working, recrystallizes anew in a similar way as during primary recrystallization by « nucleation and growth », will be called « *secundary recrystallization* ». In the literature it is sometimes denoted as « exaggerate grain growth », or (by Beck and co-workers, 1947) as « discontinuous » grain growth, as contrasted to « continuous » grain growth in the normal case (*).

Of course the distinction between the three stages mentioned above must not be taken to be so narrow that two of the processes mentioned may not to some extent occur simultaneously. For example in a not too severely deformed test-piece one may observe, beside the formation of new grains by primary recrystallization, simultaneously in another part of the test piece the growth of an already existing grain at the cost of an adjoining grain by « grain growth »:

(*) It is essential to take notice that in the above nomenclature the two phenomena indicated as « primary » and « secundary » recrystallization represent two successive stages of the annealing process of a cold-worked matrix. Naturally a recrystallized test-piece can again be cold-worked and once more subjected to a heat treatment causing recrystallization. In that case we should speak of a second « primary » recrystallization, followed perhaps by a second « secundary » recrystallization. It seems useful to call attention to this distinction, as it may forestall confusion when studying older literature : for example Tammann (1929, 1930) used the expressions « primary » and « secundary » for what we would call here a « first » and a « second » recrystallization (see further Burgers, 1941, paragraph 6-8).

in that case Beck and Sperry (1950) speak of « strain induced » grain boundary migration.

We shall repeatedly refer to these various stages in the course of the following chapters.

CHAPTER IV

RECOVERY (*)

IV, 1. Local Atomic Displacements.

The conception that recovery involves only local atomic displacements is discussed in several papers. In the first place we wish to point to Nye's investigation (1948, 1949*a*, 1949*b*) on plastically deformed silverchloride in polarized light (cf. Chap. XI, 3). Nye found that annealing without recrystallization causes no alteration in the position of the light places appearing under crossed nicols, but only a reduction in their intensity. This indicates, as the author states, that recovery does not bring about any large-scale redistribution of stress, but only a general reduction of its magnitude.

Burgers (1947) advanced the view that mutual elimination of dislocations is the fundamental atomic process lying at the base of this stage of the annealing process, whereas Cook and Richards (1951, 1946) suggest that polygonization is probably identical with lattice recovery (cf. also Greenough and Smith, 1950, Thorley, 1950 and others).

IV, 2. Course of Recovery as a Function of Time and Temperature of Heating. Meta- and Ortho-Recovery.

In Burgers' paper an effort was made to understand on this basis at least qualitatively some features of the recovery process, such as its dependance on time and temperature of heating and on degree of deformation by assuming :

1) the presence in the cold-worked test-piece of groups of dislocations with different « neutralization energies », and

(*) This phenomenon is the subject of a separate report, therefore only a few salient points will be brought forward here.

2) a dependence of this energy on the « density » of neutralizable dislocation pairs in each group.

In this connection it is of interest to consider more recent work by Cherian, Pietrowsky and Dorn (1949) on the recovery of cold-worked aluminium (99^+ %). These authors found two types of recovery of the stress-strain curve of extended test-pieces. For a given extension (true strain 0.092) annealing at low temperatures (33 °C and 100 °C) brought about a partial but nevertheless considerable recovery of the initial flow stress; upon restraining, however, the stress-strain curve of the recovered material coincided again with that of the original material. At higher temperatures (150 °C and 205 °C) on the other hand not only a lowering of the *initial* stress, but also a *permanent* decrease in the flow stress was obtained in such a way that the complete stress-strain curve for the recovered material was *below* that for the virgin metal at the same total strain. Fig. IV,1 and IV, 2, taken from the paper quoted, illustrate this behaviour. The two phenomena are distinguished as meta- and ortho-recovery.

The kinetics of both processes appear to be different, in this sense that for a given temperature ortho-recovery appears to continue until complete restoration, whereas meta-recovery practically ceases short of complete recovery, the « end value » being closer to the completely annealed state for higher temperature of annealing. The authors consider this to be an indication that two kinds of imperfection are introduced by cold-work, one which is rapidly recoverable and a second, which is more slowly recoverable. The former kind (Fig. IV, 3), responsible for meta-recovery, is assumed to have activation energies extending over a fairly wide range, or, alternatively, to have values which increase with diminishing number of dislocations left (*). Those of the second kind responsible for ortho-recovery, are thought to have a narrow range of (higher) activation values.

The question might be raised whether a correlation exists between the phenomena of meta- and ortho-recovery and the two types of processes considered above, neutralization and rearrangement of dislocations. If so, ortho-recovery must be accompanied by changes in X-ray pictures as observed in polygonization. Although some

(*) In Burgers (1947, p. 721/722) it is assumed, on the basis of considerations developed in the earlier days of recrystallization research by Dehlinger (1929), that the energy required to dissolve a dislocation pair *decreases* with decreasing density.

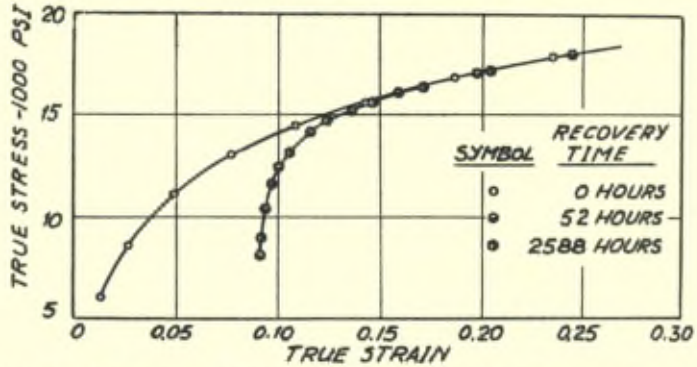

Fig. IV, 1. — Recovery of 99 % aluminium at 100 °C after a prestrain of 0.092.

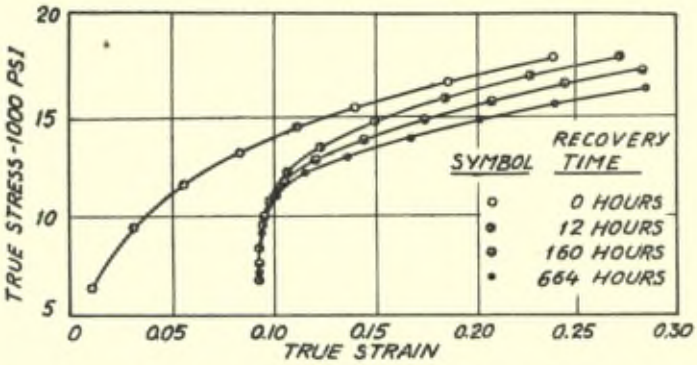

Fig. IV, 2. — Recovery of 99 % aluminium at 205 °C after a prestrain of 0.092.

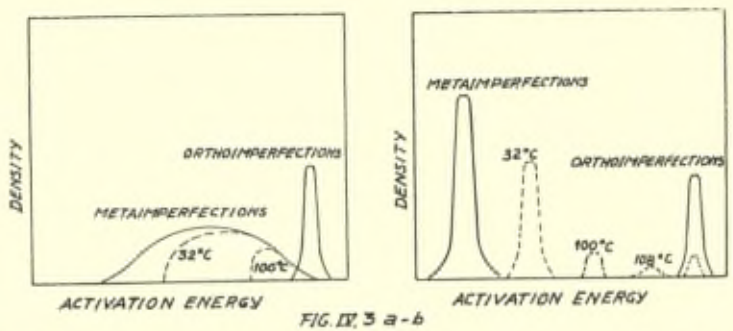

Fig. IV, 3 *a-b*. — Schematic representation of distributions of imperfections induced by cold work as a function of activation energy for recovery [after Cherian, Pietrowsky and Dorn (1949)].

X-ray photographs are given by Cherian c.s., these are not sufficiently detailed to decide this point (*).

IV, 3. Recovery versus Recrystallization.

Leaving aside the question whether recovery itself comprises two different atomic displacement processes of the types mentioned under *a)* and *b)* in Chap. II, 1, the question has often been discussed (cf. Burgers, 1941, paragraph 65 ff.; 1947) whether recovery, seen as strain release and redress of properties without « visible » structural changes, and actual recrystallization are two consecutive and fundamentally different stages of the complete annealing process, or whether « recovery » is in reality « recrystallization » on such a small scale that there would be no reason to discriminate between the two phenomena in a more fundamental way.

With regard to this question an investigation of Averbach and Warren (1949) on cold-worked α-brass is of special interest. These authors measured the integrated intensity of various X-ray reflections before and after annealing. At temperatures up to 200 °C a small reduction of the strongest reflection (111) was observed, the reduction increasing appreciably at higher temperatures up to 350 °C. As the continuous lines did not yet show any spottiness, nor did metallographic observation show a clear indication of actual recrystallization, the observations are therefore mainly restricted to what we may call the recovery range (although according to Averbach the sharper drop above 200 °C may be the onset of recrystallization).

The observed intensity effect is considered to be due to primary extinction and to indicate an increase in particle size. On the basis of these results Averbach (1949) concludes that recovery may be a process analogous to recrystallization, during which small strain free grains are already formed. This view would fit in with that put forward in Chap. II, 3.

The point is again discussed by Thorley (1950), in a paper reviewing the « one-stage » theory supported by Krupkowski and Balicky (1937, 1939, 1951) and the « two-stage » theory brought forward

(*) A correlation between meta- and ortho-recovery and the coalescence of vacancies c. q. the removal of vacancy clusters is brought forward by Professor Seitz in the manuscript paper, mentioned at the beginning of Chapter II.

by Cook and Richards (1946). Whereas according to the first-mentioned authors the redress of a physical property (for example hardness) with time of heating at constant temperature can be adequately described by the simple equation of a « monomolecular reaction » (rate of redress at any moment proportional to fraction not-yet recovered resp. recrystallized) with only one activation energy, according to Cook and Richards the data require a more complex formula in which the rate of redress depends on two consecutive processes, being proportional both to the fraction not-yet « recrystallized » and to the degree of « recovery »; moreover, the analysis leads to two different values of the activation energy for the two stages.

Thorley, extending Cook and Richards' formula, arrives at the conclusion that, although a two-stage process is actually required to explain the occurrence of an incubation period during which no observable change in the property considered takes place (*), both stages possess the same value of the activation energy. As, however, different regions of a cold-worked test-piece may have different amounts of strain energy, and recrystallization may start immediately in the regions where the strain is already sufficiently low, recovery and recrystallization of the test-piece as a whole take place simultaneously throughout the whole period of anneal, each starting at zero time.

IV, 4. Recovery of Sheared Crystals.

Kuhlmann, Masing and Raffelsieper (1949) have considered recovery in sheared crystals. These authors hold the view that recovery is due to dissolution of dislocations arrested at the ends of their « free-paths » along the glide planes. The assumption that the activation energy for dissolution is decreased by the shear stress leads to a time dependence which is different from that given by Krupkowski and Balicky (simple exponential law) and also from that given by Cook and Richards. It approaches the former for small values of the shear stress.

(*) The incubation time appears to be very short for higher-temperature anneals and can therefore easily escape detection.

CHAPTER V

POLYGONIZATION

V, 1. Experimental Evidence.

Polygonization is caused by an accumulation of dislocations along more or less well-defined planes, forming the boundaries of lattice regions (« polygons ») with generally slightly different orientations, up to for exemple a few tenth of a degree. Cahn (1949), in his fundamental paper on this process, studied it particularly in bent single crystals. Here it is due to the displacement of dislocations of like sign along the glide planes and causes a transformation, under release of strain energy, of a continuously bent lattice into the « poligonized » state of discontinuous blocks (fig. V, 1). This

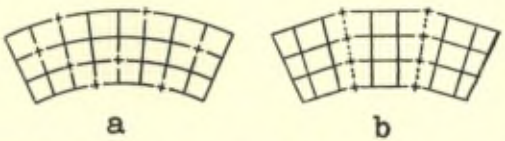

Fig. V, 1. — *a* Bending of a crystal by randomly distributed dislocations of the same sign. *b* Assembly of the dislocations into sheets, producing crystallites (after Cottrell, 1949).

effect shows itself in the breaking-up of the asterism striae visible in a Laue photograph in separate spots and in the appearance of boundary lines perpendicular to the glide lines in carefully polished and etched metallographic samples. On a finer scale these discontinuities (up to angular differences of less than half a minute of arc) can be made visible by the focussing technique of Guinier and Tennevin (1948, 1949*a*), discussed in Chap. XI, 9.

From subsequent work it is clear that polygonization is not limited to macroscopically bent crystals, but can generally be rought about by careful annealing in cold-worked test-pieces. For example Lacombe and Berghezan (1949*c*) (cf. also Guinier and Lacombe, 1948) describe polygonization in slightly extended specimens of aluminium and aluminium-zinc solid solutions, Beck and Hsun Hu (1950) and also Kellar, Hirch and Thorp (1950) in rolled aluminium, and, quite recently, Dunn and Daniels (1951) in bent and rolled silicon-iron.

Kellar, Hirsch and Thorp, applying the «micro-beam» method mentioned in Chap. XI, 10, counted the number of spots on the diffraction rings and, in this way, concluded to a decrease in « particle size » from about 3.6 μ a few weeks after rolling to about 2.2 μ a few months afterwards. As this decrease was accompanied by a decrease in radial broadening of the spots, these results are, in the view of the authors, compatible with the occurrence of polygonization (*).

V, 2. Mobility of Sub-Boundaries.

The results obtained by Guinier and Lacombe and also by Dunn and Daniels, show that the sub-boundaries are far more mobile than ordinary grain boundaries and that annealing produces a coarsening of the sub-structure. (In Dunn and Daniels' experiments this was accompanied by a sharpening of the asterism of the Laue spots and thus a reduction in spread of the orientations of the polygons). We shall refer to this again in Chapter VII, 3, when discussing grain boundary migration. Here we wish only to suggest the possibility of a connection between this observation and that of Heidenreich (1948, 1949), by means of the electron microscope, of the structure of rolled aluminium, mentioned in the Supplement (Chap. XI, 4). Heidenreich found that directly after rolling a granular structure of about 200 — 800 Å width exists inside domains of about a few micron diameter, which structure, after keeping the samples some time at room temperature, disappears before the growth of the larger domains is observed (**).

V, 3. Polygonization and Type of Deformation.

From the foregoing the impression is gained that polygonization, meaning by this the building-up, by agglomeration of dislocations, of surfaces separating lattice regions with slightly different orientations under release of stress, is not restricted to the special simple

(*) According to Greenough and Smith (1950) the phenomenon of cell formation, reported by Wilms and Wood (1949), Wood and Rachinger (1949) and Wood and Scrutton (1950) to occur during slow deformation (creep) of polycrystalline aluminium, has to be considered as polygonization as well (cf. also Calnan and Burns, 1950 and Cottrell and Aytekin, 1950).

(**) It is not clear to us whether this result is compatible with that obtained by Kellar, Hirsch and Thorp, mentioned in the foregoing section.

type of bending originally applied by Cahn. Wether « arbitrarily » curved lattice regions can polygonize, or whether special types of deformation are required, is a matter of great interest with regard to nucleation theory (Chap. VIB) and, in connection herewith, the origin of recrystallization textures (Chap. VIIIA, 2). In this relation a short note by Snoek (1951) seems important, in which the question has been raised whether uniform arrays of screw dislocations, such as have to be assumed in twisted single crystals, may agglomerate and cause a special type of polygonization. Snoek points to experiments by Jillson (1950) with zinc single crystals, twisted about the hexagonal axis. According to Jillson, there is no tendency to form any discontinuity under these conditions. Snoek takes this to indicate that screw dislocations of equal sign tend to repel each other, contrary to edge dislocations (at least in a *finite* crystal : see Cottrell, 1949), so that no polygonization would occur in this case (*).

CHAPTER VI

NUCLEATION

As remarked in the introduction, this report deals primarily with the geometric side of the nucleation process. An effort, however, will be made to bring forward the trend of thought lying at the base of some recent fundamental « kinetic » papers (see also Burgers, 1949; Cahn, 1950).

A. KINETICS OF NUCLEATION AND GROWTH

VIA, 1. Isothermal Recrystallization Curves.

If a fine-grained test-piece with no preferential orientation of its crystallites is subjected to a deformation of a few percent and then heated for various periods, we see, after etching, the formation of new crystals with an approximately circular (or spherical) shape. Following the course of the recrystallization process with time of heating at constant temperature, one finds that the circular crystals

(*) In the note Dr. Snoek announced that experiments to verify this point were being started, but most probably his untimely death has rendered this impossible.

grow with an approximately constant rate in all directions. Extrapolation of the growth lines, in a diameter versus time diagram, to the time axis shows that the crystals have started their growth (at least the period of constant rate) at different moments, apparently statistically distributed over the time of heating. These features of the primary recrystallization process allow it to be described in terms of rate of nucleation (N) and rate of growth (G), quite apart from the question as to the underlying atomic processes. Part of the work on recrystallization has gone along these lines, former work by Von Göler and Sachs (1932), more recently by Johnson and Mehl (1939), Anderson and Mehl (1945) (*), Avrami (1939, 1940) and, most recently, by Cahn (1950).

In these papers, starting from assumptions of the type outlined above, formulae have been developed which give the fraction recrystallized as function of time for constant temperature (the so-called « isothermal recrystallization curve »). Inversely, these formulae have been applied to severely deformed test-pieces, which, on recrystallization, develop large numbers of grains. By counting these numbers, combined with planimetric measurements of the recrystallized fractions of the test-pieces and with measurements of the size of the largest grains, the dependence of both fundamental factors, rate of nucleation and rate of growth, on the variables temperature, degree of deformation and time of heating, could be deduced. The essential difficulty in this type of work is to know the exact way in which such factors as the mutual impingement of growing crystals are to be introduced in the formulae.

As to the process of nucleation itself, Anderson and Mehl merely assume that nuclei are formed either at points of lowest or, what they consider more probable, points of highest energy with a certain probability, given by an activation energy (see for an extensive discussion of experimental arguments in favour of one or other of these two possibilities : Burgers, 1941). Cahn (1950), on the other hand, gives a clear picture of what he considers actually to happen during nucleation, namely polygonization of a local lattice curvature. To each curvature he attributes, for a given annealing temperature, a definite nucleation time, inversely proportional to the radius of the curvate. He then shows that, by assuming a normal frequency distribution of curvatures, a formula can be deduced for the course

(*) Extensively discussed by Lücke (1950).

of rate of nucleation (N) with time of heating at constant temperature which fits well the curve deduced by Anderson and Mehl from their actual experiments. In particular the observed increase of N in the beginning of the annealing treatment, the explanation of which was left open by Anderson and Mehl, is well accounted for (*).

VIA, 2. Transient Nucleation.

This last point, which is of special interest, is considered from a completely different point of view by Turnbull (1948) in a paper on « Transient Nucleation ». This paper forms part of a series, written in collaboration with Fisher and Hollomon, on nucleation in condensed systems in which a new phase is formed (Fisher, Hollomon and Turnbull, 1948; Turnbull and Fisher, 1949; Turnbull and Hollomon, 1951). Although partly falling outside the restricted range of recrystallization in cold-worked metals, the general importance of the subject justifies to give a brief outline of the point of view given by these authors.

Their considerations start from the Volmer-Becker theory of nucleus formation in vapours and solids (Becker and Döring, 1935; Volmer, 1939; Becker, 1940; again summarized in Nabarro, 1947). In this theory the free energy change ΔF_i associated with the formation of a nucleus of i atoms of a new phase, contains a positive term due to the formation of a new surface (c. q. interface) and a negative term, due to the gain in free energy of the atoms « inside » the nucleus (**). As the first term is proportional to the surface of the nucleus and the second to its volume, a plot of the free energy change versus number of atoms for a chosen undercooling temperature shows a maximum. (Fig. VI, 1). For the corresponding « critical » size an equal chance exists to increase or to decrease in the next instant. Domains of the new phase, which have attained this size, are supposed to grow continuously and are called *nuclei*; whereas domains of subcritical size are denoted as *embryos*.

(*) So are also other features, such as the influence of a preliminary anneal (recovery) on N. For details we refer to Cahn's paper.

(**) In Fisher, Hollomon and Turnbull's paper (1948), a third positive term, taking account of strain energy between nucleus and matrix, is introduced, whereas it is pointed out that for other types of transformation, f. i. magnetic, a corresponding energy term may be taken into consideration.

It is further assumed that for each undercooling temperature a *steady state* exists, for which the relative concentration of embryos and nuclei is given by a Boltzmann-factor, determined by the corresponding values of the activation energies. If in this state the concentration of nuclei is appreciably different from zero, a definite rate of transformation exists, proportional to this concentration which, taken per unit volume of untransformed matrix, remains constant with time. This type of nucleation is called «*thermal nucleation*» (*) (fig. VI, 2).

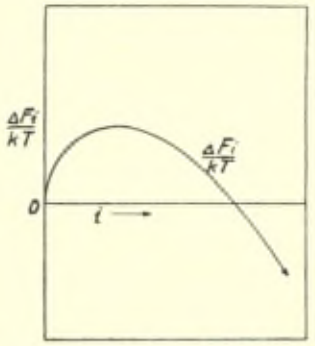

Fig. VI, 1. — $\Delta F_i/kT$ versus i (number of atoms of nucleus) for transformation to a more stable phase.

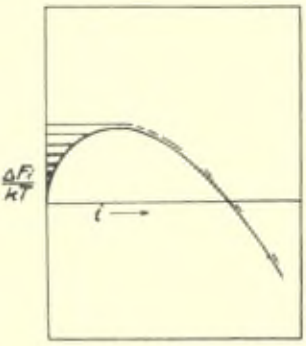

Fig. VI, 2. — Steady-state nucleation for transformation to a more stable phase.

We now consider different undercooling temperatures. As follows from the quantities involved, the critical nuclear size decreases continuously with increasing undercooling, starting from « infinite »

(*) In the final expression for the rate of nucleation Becker (1940) introduces, besides the Boltzamnn-factor containing the activation energy for nucleus formation, a second similar factor taking into account the general mobility of the atoms, i. e. a normal diffusion factor.

A third factor has been introduced by Borelius (1945, 1947, 1949) in the course of studies on the formation of nuclei in supercooled solid solutions (see again Nabarro, 1948). When this process takes place in an alloy with a concentration so close to the saturation region that $\partial^2 F/\partial \alpha^2$ (F = free energy, α = concentration) is still positive, then diffusion tends to *remove* actual fluctuations of concentration. This circumstance requires an extra term in the activation energy for formation of a stable nucleus, proportional to the number of atoms. Borelius estimates this free energy from the phase diagram of the system. His consideration leads also to an estimation for the number of atoms of a stable nucleus (in this connection see also Becker, 1937). For precipitation of Sn in PbSn-alloys, depending on the range of concentration and temperature, nuclear sizes of 100-200 atoms are found to be stable.

Hobstetter (1948) has considered the critical conditions for nucleus formation both with regard to size and concentration.

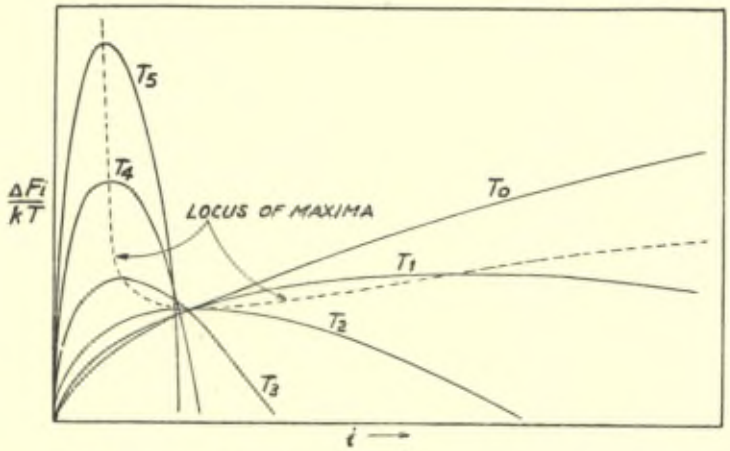

Fig. VI, 3. — Plot of $\Delta F_i/kT$ versus at various temperatures T_1 — T_5 below the transition temperature T_0.

Figures VI, 1-3. — After Fisher, Hollomon and Turnbull (1948).

size at the transition temperature. The same holds for the corresponding activation energy. However, on account of the factor $1/kT$ in the exponent of the Boltzmann-factor, the quantity $\Delta F_i/kT$ for the critical size passes through a minimum at a definite undercooling temperature : Fig. VI, 3, again taken from Fisher, Hollomon and Turnbull (1948) illustrates this. This means that the concentration of critical nuclei, which is zero at the transition temperature (and above this temperature), first increases, then decreases with increasing undercooling, being again zero at temperature zero. This is shown in a schematic way in fig. VI, 4, which gives the steady-state distribution of embryos for various temperatures as function of embryo size, from the transition temperature T_0 downwards to lower temperatures T_1 ... T_5. The curves have been broken off at the (arbitrarily chosen) critical size of the embryo (nucleus), larger domains for these temperatures being supposed to be stable and grow. For each undercooling temperature the rate of nucleation is proportional to the corresponding critical concentration.

If, on cooling a stable phase to a temperature below the transition temperature, or when changing from a definite undercooling temperature to a lower one, the concentration of critical nuclei at the new undercooling temperature is *larger* than its value at the original temperature (this applies to the temperature range $T_0 \rightarrow T_2$ of

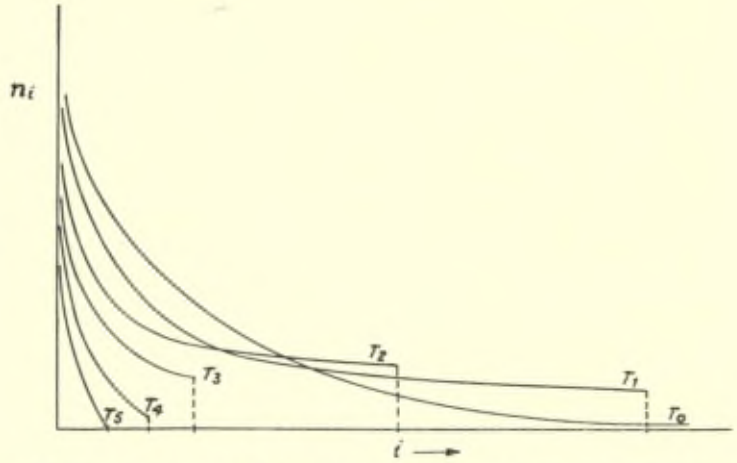

Fig. VI, 4. — Steady-state distributions of embryo-sizes at various temperatures $T_1 \ldots T_5$ below the transition temperature T_0.

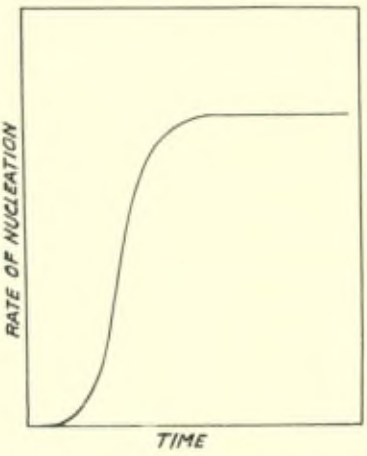

Fig. VI, 5. — Incubation period in thermal nucleation after quenching from T_0 to T_1 in fig. VI, 4.

Figures VI, 4-5. — After Fisher, Hollomon and Turnbull (1948).

figure VI, 4) the rate of transformation will increase; if it is lower (f. i. when changing from T_2 to T_3), it will decrease.

If we chose the second temperature very low (T_4 or T_5), it will

practically come to a stop. However, due to the fact that the critical nuclear *size* at the lower temperature is smaller than that corresponding to the higher temperature, a number of embryos present at the starting temperature are of super-nuclear size at the lower temperature. These embryos can therefore become nuclei of the new phase and cause a sudden transformation to take place during cooling (*).

Now for the problem which interests us here, namely the variation of rate of nucleation in the course of annealing at constant temperature, it is important to realize that in the considerations of Volmer and Becker it is tacitly assumed that at each « undercooling temperature » the corresponding steady-state is *immediately* established. This leads to a constant rate of nucleation for a given temperature. Turnbull, however, introduces as a fundamental idea the assumption that, contrary to what may be expected to occur in the gaseous or liquid states, the attainment of a new steady-state distribution of embryos and nuclei in the solid state on changing the temperature may take some time, due to the limited mobility of its atoms. This involves that *transient phenomena* can be observed : f. i., on changing the undercooling temperature, the corresponding change in the rate of transformation will take some time. This may give the impression of an inconstancy of the (supposed) isothermal rate of nucleation at the new temperature, which might be interpreted as an « incubation period » (fig. VI, 5).

Turnbull, in his paper cited in the beginning of this section (1948), applies these considerations to pure recrystallization i. e. the transition of the cold-worked into the fully annealed state. Here the two energy terms governing the formation of nuclei include surface energy and strain energy. If we consider the cold-worked state as « undercooled » with regard to the fully annealed state, then, for a given cold-worked matrix a definite steady-state distribution of

(*) If the new temperature is so low that these nuclei do not grow and moreover the steady-state concentration of nuclei corresponding to that temperature is practically zero (T_5 in fig. VI 4), we observe a transition process characterized by the sudden appearance of domains of the new phase during the actual cooling, not accompanied by a growth process of these domains. This type of nucleation is called *athermic nucleation* by Fisher, Hollomon and Turnbull and can be considered as characteristic for processes of the « martensitic type », whereby sudden transformations of coherent lattice domains from one crystalline structure into another take place. For examples of such processes and further literature we refer to Burgers and Jacobs (1934); Barrett (1943, 1948); Cohen, Machlin and Paranpje (1950); Kulin and Cohen (1950); Bowles (1951).

« strain free » embryos may be supposed to exist at each temperature, corresponding to a definite rate of nucleation. This rate is in general neglectable at sufficiently low temperatures (for metals with a not too low melting point for example at room temperature) and has a measurable value at the « recrystallization temperature ». If, therefore, the metal is annealed, it will take a certain time before the steady-state corresponding to that temperature is realized, during which « incubation period » N increases with time.

In this connection it must be mentioned that Laurent (1945), in a to some extent analogous treatment of nucleation during phase transformations, has taken into account the formation of nuclei of *all* sizes, from the critical size up to infinity. This, combined with his idea that a « nucleus » is only actually « visible » after having attained a certain size, seems to lead to a formula for the « rate of nucleation » as a function of time, which also may explain a changing rate at constant temperature.

VIA, 3. Exhaustion of Germ Nuclei.

A third possibility to understand the existence of a variable, in casu decreasing, rate of nucleation with time can be based on the assumption that originally a *given* number of « germ nuclei » is present, which, by thermal fluctuations, transform into « growth nuclei », and so bring about the progression of the transformation process. In such a theory a decrease of rate of isothermal nucleation is caused by an exhaustion of the number of germ nuclei originally present. A consideration of this type lies at the base of the nucleation theory put forward by Avrami (1939; 1940).

VIA, 4. Conception of Petersen.

We conclude this chapter with a reference to a paper by Lücke and Masing (1948), in which, following a suggestion made by Petersen (1947), a « germ nucleus » is conceived as a spherical lattice region, embedded into a hole in the surrounding matrix of somewhat smaller size. The germ has thus a definite energy, composed of two

terms, one due to its volume compression, and one to its surface energy (*). The total energy is given by :

$$U = 3\pi(1 - \mu)/E \cdot p_0^2 r_0^2 r^{-3} + 4\pi r^2\sigma$$

where E is the modulus of elasticity, μ Poisson's ratio, p_o and r_o the original pressure and radius of the « germ region » and σ the surface energy. Putting $dU/dr = 0$, one finds a value $r = r_{min.}$ for which the energy is a minimum ($U_{min.}$). Assuming definite values for the quantities involved ($\mu = 1/3$, $p_o = 10^{10}$ dyn. cm^{-2}, $E = 10^{12}$ dyn. cm^{-2}, $\sigma = 10^{-2}$ dyn. cm^{-1}), Lücke and Masing calculate that for values of r_o between 10^{-7} and 10^{-5} cm, $r_{min.}$ is of the order of 4-10 times r_o whereas $U_{min.}$ lies between 1/20 and 1/300 U_o. This means, according to these authors, that a steep decrease in energy is obtained after a small increase in size of the germ region, and that therefore a stress-free « growth nucleus » is rather suddenly formed.

It may, however, be questioned whether the value taken for σ is not far too low. If this had to be of the order of 10^3 dyn. cm^{-1} (cf. Shockley and Read, 1949), then, corresponding to the same values of p_0, one would have to take considerably larger values for r_0 (the size of the « germ region »), e. g. 10^{-2} cm, to obtain a decrease in energy after its growth. This size seems too large.

B. NATURE OF RECRYSTALLIZATION NUCLEI (**)

VIB, 1. Presence of « Potential Nuclei » in the Cold-Worked Matrix. Experiments with « Homogeneously » Compressed Single Crystals.

Considerable thought has been given to the question of the nature of the nuclei of crystals growing in deformed metals by the process of recrystallization (see for a discussion of the litterature up to 1940

(*) We must make here the following remark. Petersen's paper deals with the whole field of recrystallization phenomena and contains many valuable considerations and suggestions. For example the considerations given below on « stimulated » growth (Chap. VI*B*, 4), enclosed grains (Chap. VI*B*, 6), grain growth and secundary recrystallization (Chap. VII) are in several respects related to those developed in Petersen's paper. To follow the reasoning given, one has, however, to be fully aware of the author's meaning of the conceptions he introduces. These are not always lucid to the present reviewer. For example in considering the energy state of the nucleus, not the surface energy as considered by Lücke and Masing, but a term comparable to a molecular pressure in a fluid with a curved surface is introduced. This circumstance makes it difficult to treat the paper so thoroughly as it is due to.

(**) Parts of this and of some following sections are taken from Burgers and Tiedema (1950).

Burgers, 1941). Generally speaking, several authors, though differing perhaps in details of their conception, favour the view that nuclei are small lattice regions already present in the deformed matrix, which, for some reason or other, obtain the faculty to grow during heat treatment. Based on the assumption that a lattice region could grow only at the expense of surrounding regions if it is more stable (less strained), it was assumed that those lattice blocks could serve as « potential nuclei » which, being originally in a strained state, on heat treatment suffered some stress-releasing process, which transformed them from « potential » into « actual » growth nuclei (Van Arkel, 1930, 1936; Van Liempt, 1931).

To find evidence for this, Burgers and Louwerse (1931, 1934) subjected aluminium single crystal discs to homogeneous compression between flat blocks, thus causing almost pure shear parallel to definite combinations (glide plane [111], glide direction in this plane [110]). After recrystallization the (then fine-grained) samples possessed a pronounced texture, the crystal orientation of which could be deduced from those of the deformed crystals by a rotation about the normal to the glide direction (a [112]-direction), c. q. by a combination of rotations about the perpendiculars to various glide directions. Lattice blocks with these orientations were supposed to be produced by the deformation process as « local curvatures » of glide planes at places where moving dislocations are hold up by lattice irregularities, for example mosaic block boundaries (*). Moreover, such lattice regions may be expected to possess a particularly strained state.

(*) In this connection it seems of interest to remark that, as set forth by Kochendörfer (1950) (cf. also Bilby, 1950), shear along a [111] plane may be produced as well by propagation in a direction parallel to the glide direction of a « Taylor » or « line » dislocation, as by a sideways displacement of a screw dislocation. Whereas the holding-up of line dislocations gives rise to local curvatures about the normal to the glide direction [112], considered above, the holding-up of screw dislocations will presumably cause local lattice rotations about the normal to the glide plane [111] (cf. J. M. Burgers, 1940). Only the first type of curvatures was considered at the time of the Burgers and Louwerse 1931-paper. If gliding in these experiments was also produced by the second mechanism, rotations about the [111]-axis normal to the active glide planes might be expected. They were apparently observed by Heidenreich and Shockley (1948) (cf. also Frank, 1948). If such local rotations actually existed, the presence of [111]-related deformation and recrystallization textures could be expected. This remark is of interest in connection with Beck and Hsun Hu's observation (1949), discussed in Chap. VIIIB, 2, that the orientations observed by Burgers and Louwerse in compressed aluminium single crystals can actually be described by [111]-rotations with regard to the deformed matrix. However, the [111]-axes applied by Beck and Hsun Hu to explain the recrystallization textures, were *not* the [111]-axes perpendicular to the prominent glide planes (cf. also Barrett, 1940).

VIB, 2. Apparently Different Behavious of Stretched Single Crystals.

It is worth noting that similar experiments with carefully stretched aluminium single crystals by Burgers and Basart (1928), Cahn (1950) and Laloeuf and Crussard (1950) show such a large scattering in the positions of the new crystals that a preferential orientation can hardly be recognized. In these cases, naturally, only a small number of new crystals (of the order of 10 say) is formed, so that the orientation of each individual crystal has to be determined. Laloeuf and Crussard associate the scattering in the positions with the many possible ways according to which in the cubic system a given lattice position may be « rotated » into another position. Cahn attributes it to the incidence of « pencil glide » in aluminium, this process fixing only the glide direction and not the glide plane, and thus leaving a wide variation for axes of « local curvatures ».

According to the view of Tiedema and the present author, however, the possibility must also be considered that in such slightly deformed crystals the orientations found for the new crystals are more or less accidental. It was namely observed by Tiedema that a stretched single crystal, after careful etching-away the sides of the test-piece, (and, of course, also the parts which had been clamped in the holders), often did not recrystallize at all (see Chap. VIII-A, 3). This, and the fact that nearly all single crystals, prepared by recrystallization, contain small inclusions left over from the original deformed matrix (Ch. VIB, 6), suggests the possibility that the new crystals originate from nuclei formed either at sides or at the « boundary » of inclusions in « curvatures » about undefined axes. If so, a large scattering in their orientations does not seem strange. For this reason the original experiments of Burgers and Louwerse (1931) mentioned above where *large* « homogeneous » deformations were applied, so that *many* new grains were formed after recrystallization, the orientation of which could be viewed *statistically*, are perhaps more reliable.

VIB. 3. Nucleation by Elimination of Dislocations.

In Van Arkel and Van Liempt's conception of the nucleation process, mentioned in Chap. VIB, 1, the potential nucleus had to be « activated » in order to become transformed into an actual growth nucleus. The necessity of such an activation may account

for the occurrence of an incubation period before visible growth starts, as observed in recrystallization experiments. Considerations regarding the atomic character of the activation process have been given, as early as 1929 by Dehlinger (1929, 1933) and, more recently, by Burgers (1947, 1949). The latter, starting from the assumption that recrystallization was essentially a process of elimination of structural imperfections (Chap. II), advanced the idea that by a proper elimination of dislocations of « opposite sign » somewhere in the deformed matrix, stresses could be reduced locally and so create a « remaining » stress, capable of displacing a dislocation layer between two adjoining domains, initiating crystal growth. It was thought that a lattice block such as *b* in the schematic figure VI, 6, lying in the inflexion point of a S-curved region, was particularly favorably placed for such a local neutralization process, as it is separated from the neighbouring blocks *a* and *c* by dislocations of opposite sign. This conception of the nucleation process and of the most probable nuclear spot is much akin to Dehlinger's conception of 1929. The « S » curved regions were considered to be a direct consequence of the occurrence of the « local curvatures » of the active glide lamellae about the normal to the glide direction, considered in section VIB, 1.

VIB, 4. Nucleation by « Stimulation ».

The conception that an elimination of dislocations, involving a release of strain energy, may lie at the root of the process required to « activate » a potential nucleus to growth, was considered to be supported by the phenomenon of « stimulation » of crystal growth. As set forth in various papers (ref. in Burgers, 1947), in recrystallized aluminium plates crystals may be found of a special « pointed » shape (fig. VI, 7, Plate I), the occurrence of which can be understood on the assumption (fig. VI, 8) that growth of such a « stimulated » crystal starts at the moment that an already growing « stimulating » crystal comes into contact with its nucleus.

By means of Laue-photographs (Burgers and May, 1945) and application of Guinier and Tennevin's focussing method (Supplement Chap. XI, 9), it was found that such crystal pairs were mutually oriented as spinel twins with a precision of less than a minute of arc (Guinier and Tennevin, 1949; May, 1950). A practically perfect fit

is therefore possible between the growing crystal and the potential nucleus of the stimulated crystal. This lead to the suggestion that the sudden elimination of dislocations produced when contact was established was the actual cause of the stimulating process and thus constituted a direct example of the growth activation of a potential nucleus (that of the stimulated crystal), this time not brought about by thermal agitation as such, as in spontaneous nucleation, but in a kind of « artificial » way.

In the light of this phenomenon, a conception of spontaneous nucleation might be conceived, which is somewhat different from that advanced in the foregoing section. As will be discussed in Chap. VII, 2, it follows from theoretical work by Read and Shockley (1950) that the energy content of the boundary layer between two adjoining lattice regions with special mutual orientations is extremely sensitive for slight variations in the orientation of the boundary layer, in this sense that it increases at an infinite rate with deviations from a special position. If then, in a deformed test-piece, adjoining lattice regions happen to be present in such mutual positions, it seems reasonable to assume that on heating a release of strain energy may occur by such slight displacements at their boundary, and so cause transformation of a potential nucleus into a growth nucleus.

There may be some relation between this conception and that brought forward by Kronberg and Wilson (1949) in connection with their investigation of the growth of large crystals on prolonged annealing of fine-grained copper with cube texture by « secundary recrystallization » (abnormal grain growth). These authors point out that the orientation relationship existing between the new crystals and the primary texture (they are related by a rotation about either a [111] or a [100] — axis over approximately definite angles) is such that the atoms in the (111) resp. (100) planes show definite coincidences or near-coincidences in both orientations, so that the atoms of one net can be brought into the sites of the new net by simple movements. If, reasoning along the lines set forth above, two such lattice regions were adjacent in the deformed state, it might be envisaged that such movements, bringing about better fit, were apt to give a stress release and to initiate growth (*).

(*) The fact that, according to their experiments, secundary recrystallization occurs only in twin-bearing material, leads Kronberg and Wilson to the assumption that « nucleation » occurs preferentially at twin boundaries and is connected with stacking faults existing at such boundaries.

VIB, 5. Nucleation by Polygonization.

A more defined conception of the nucleation process has been given by Cahn (1950). Cahn starts from the assumption given above that the growth nuclei are actually formed in the most distorted parts of the lattice, i. e. in the « local curvatures » and postulates (as is also done in a note by Beck, 1949) that the process which transforms the potential nuclei in growth nuclei is essentially the process of « polygonization » (Orowan, 1947; Cahn, 1949); discussed in Chap. V. As set forth there, and illustrated schematically in fig. V, 1, this process, taking place in curved lattice regions, is considered to consist of a diffusion of dislocations parallel to the slip planes, thus producing a redistribution of dislocations causing a change of a continuously bent lattice into a number of polygon elements, each keeping the orientation of that part of the bent lattice from which it is formed but free of elastic strain (*). Figure VI, 9, taken from Cahn's paper,

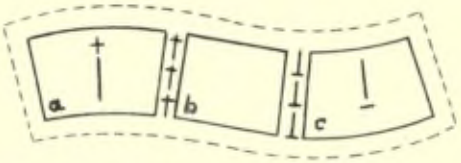

Fig. VI, 6. — Three adjoining lattice blocks, which, taken together, can be considered to form a « S-curved » lattice region. Block *b* in the « inflexionpoint » can presumably function as a moleus for recrystallization.

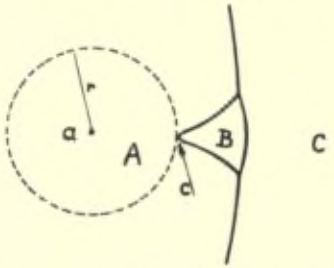

Fig. VI, 8. — Form of the grain boundary between two crystals *A* and *B*, originated under the following conditions : Crystal *B* did not start to grow from its nuclear spot at *c* before crystal *A*, starting from *a*, had attained a size indicated by the circle with radius *r*; the average rate of growth for *B* is somewhat larger than for *A*. (C is an arbitrary crystal, which stops the growth of both *A* and *B*).

(*) It was pointed out to us by Dr. W. Shockley that also local redistributions of dislocations in a somewhat different way may involve a release of strain energy. For example under special conditions a displacement of two sets of dislocations along intersecting glide planes can built up a boundary between lattice elements including a definite angle under release of strain.

illustrates the effect of polyganization of a local curvate, representing a potential nucleus (PP in figure *a*) and suggests (figure *b*) that a strain-free element formed in this way is able to grow at the expense of the surrounding lattice.

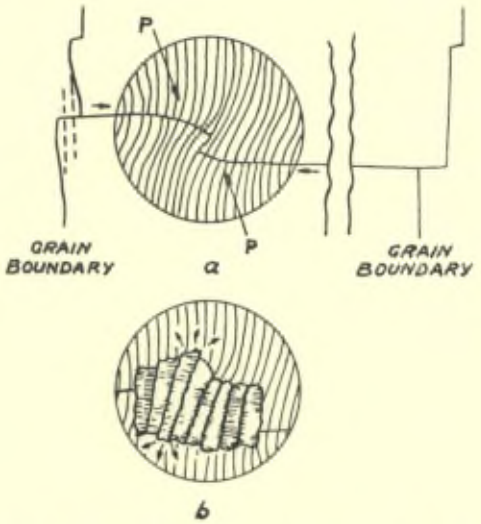

Fig. VI, 9. — Local curvate in a deformed crystal : *a)* as deformed; *b)* after annealing. PP = potential nuclear spot. (After Cahn, 1950).

VIB. 6. Experimental Evidence for the Polygonised State of the Nuclear Region.

The conceptions of the process of nucleation, discussed in the foregoing paragraphs, are in our view supported by X-ray diffraction results recently obtained by Tiedema (1950). These results show that Laue photographs of the « center » (the nuclear region) of aluminium crystals formed by recrystallization have a peculiar striated appearance, as if they are accompanied by satellite spots, these pecularities being absent on photographs of parts of the crystal *outside* the nuclear spot region (fig. VI, 10*a* and 10*b*, Plate I). This fact points to the presence, in the nuclear region, of lattice elements differing in orientation of the order of a degree of arc from the main body of the crystal, which have been left unconsumed by the growing nucleus.

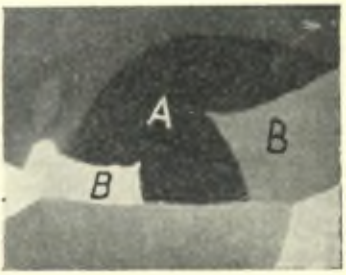

Fig. VI, 7. — Stimulated crystals *(B)* in recrystallized aluminium : the pointed crystals *(B)* are perfect twins with regard to the stimulating crystal *A*. Natural size.

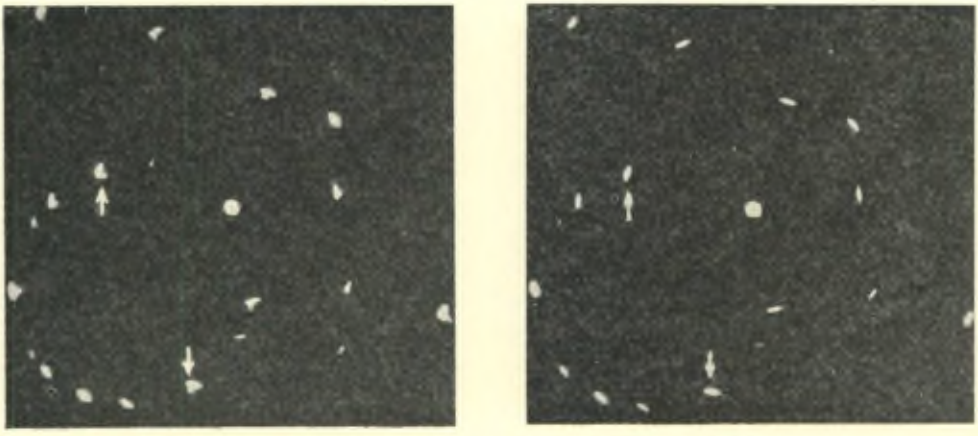

Fig. VI, 10. — *a)* Laue photograph of the nuclear spot of an aluminium crystal. *b)* Laue photograph of the same crystal but now made 0,5 mm beside the centre. *(Tiedema,* 1950)

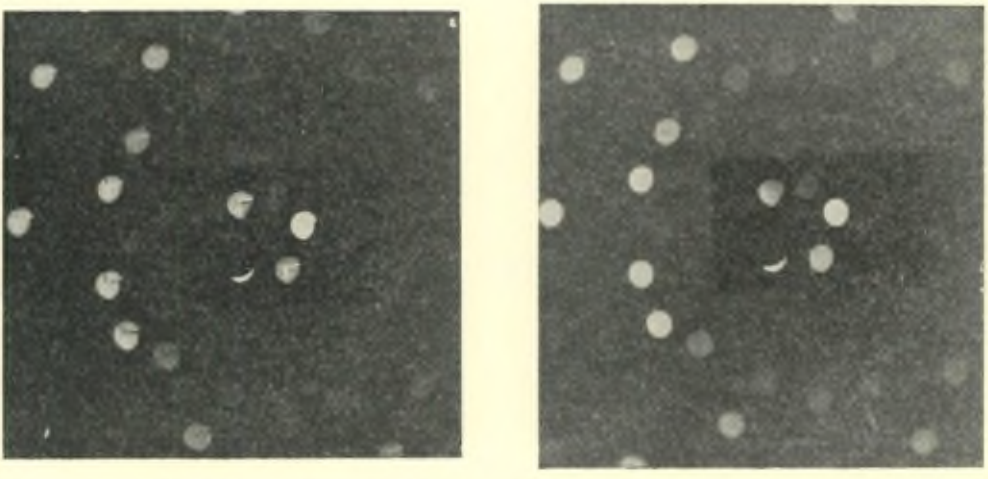

Fig. VI, 11. — Photographs made after the Laue variant of Guinier and Tennevin. The time of exposure was 5 hours : *a)* Nuclear spot of a roundish crystal showing sub-division of the Laue-interferences; *b)* Photograph of only one part of the full-grown crystal showing no « boundary ». *(Tiedema,* 1950.)

Now it is well established that a growing crystal cannot, or in any case only very reluctantly, consume lattice regions of approximately parallel orientation : such regions are left over as inclusions (« cristaux insulaires ») (Tiedema, May and Burgers, 1949; Lacombe and Berghézan, 1949*a*, 1949*b*; Burgers and Dalitz, 1949). In view of this experimental fact, the above result is in excellent agreement with the idea that a crystal grows from a lattice element which forms part of a local curvature, as schematically shown in figure VI, 9, leaving unabsorbed some neighbouring elements of approximately the same orientation and growing at the expense of the deformed matrix outside the local curvature, which differs from it far more in lattice orientation.

Moreover, the non-focussed Laue photographs taken by Tiedema according to Guinier and Tennevin's method (see Supplement Chap. XI, 9) and shown in fig. VI, 11*a* and *b* (Plate I), show that *not one but a few elements* of the local curvature, with *slightly* deviating orientation (of the order of minutes of arc), may function simultaneously as actual growth nuclei, growing as it where side by side and producing a crystal consisting of as many parts with the same slight orientation differences (*).

Such a behaviour seems compatible with either of the two conceptions of nucleation discussed above,

1) by elimination or

2) by redistribution of dislocations.

In fact, it seems a priori very well possible that in both cases more than one element of the original local curvature becomes sufficiently free of strain to obtain the faculty to grow. These, due to their approximately coinciding orientations, can grow at equal rate at the expense of the surrounding matrix, thus forming a straight « boundary » between them as observed in Tiedema's photographs,

(*) These regions of *macroscopic* size, dividing the final crystal in a few parts only, must not be confused with the very much smaller lattice regions (dimensions $\sim$ 0.1 mm) with still smaller (less than one minute of arc) orientation differences existing over the whole extension of the crystal and therefore inside each of the larger blocks, as discussed by Lacombe and Guinier and co-workers (see f. e. references in Chaudron, 1949).

while leaving unabsorbed those elements of the original local curvature, which differ from them in orientation to a larger degree (*).

CHAPTER VII

BOUNDARY MIGRATION (CRYSTAL GROWTH)

VII, 1. Surface Energy as Driving Force.

The displacement of the boundary layer between two non-parallel lattice blocks, which is equivalent to growth of one block at the cost of the other, constitutes the basal phenomenon observed during actual recrystallization. Phenomenologically it may show itself under the various « forms » summed-up when discussing the nomenclature of recrystallization phenomena in Chap. III : primary recrystallization, grain growth and secundary recrystallization. Moreover, as mentioned in Chap. V, 2, the sub-boundaries between the polygons inside a polygonized grain can migrate so as to produce a coarsening of the sub-structure.

A consideration of the phenomenon of boundary migration may start from the conception that a crystal aggregate, or, more generally speaking, an aggregate of lattice blocks is in a certain light comparable to a froth structure. In analogy herewith, the boundary surfaces have the tendency to arrange themselves in such a way that they include definite angles, corresponding to a state of equlibrium between the surface tensions acting in the boundary planes. This point of view has been brought forward by various authors (Desch, 1919, 1923; Benedicks, 1940; Harker and Parker, 1945) and was advanced particularly by C. S. Smith (1948) in a fundamental paper : « Grains, Phases and Interfaces. An Interpretation of Microstructure ».

(*) In this connection it seems of interest to remark that in rapidly heated samples Kronberg and Wilson often observed roughly elliptical grains containing a twin boundary near the center and along the major axis, the occurrence of which they take as an indication that in that case growth develops a twinned crystal as the first unit of growth, which continues to grow most rapidly parallel to the twin boundary. This may perhaps be compared with the occurrence of two or three side-by-side growing parts of slightly different orientation observed by Tiedema in aluminium crystals. We are, however, aware that this comparison is highly speculative and that the possibility exists that the origin of the crystal parts must be explained in quite a different way.

The actual attainment of equilibrium angles between undeformed crystals was studied in detail by Dunn and co-workers (Dunn and Lionetti, 1949; Dunn, Daniels and Bolton, 1950*a*, 1950*b*) with silicon iron, using specimens consisting of a few crystals only with prechosen orientations, prepared according to their method mentioned in Chap. XIII, 1. Fig. VII, 1 shows one of their results.

For tin a similar study was carried out by Aust and Chalmers (1950 : *Proc. Roy. Soc., A 201*, p. 210), using three-crystal specimens prepared from the melt (cf. Chap. XII, 1). In agreement with the conception that the boundary possesses a definite surface tension, is the fact that very often in normal grain growth a boundary between two grains displaces itself in the direction *towards* its center of curvature, as has to be expected on the basis of surface tension theory. This is most clearly illustrated in fig. VII, 2, which is a drawing after an actual observation by Beck and Sperry (1950) on grain growth in high putiry aluminium, obtained by applying the electrolytic etching technique developped by Sperry (1950) (see Supplement Chap. XI, 1.)

The same conception makes one expect, as pointed out by Smith, that grain growth will be a discontinuous process, requiring at a definite stage a sudden readjustment of several boundaries to conform to a new equilibrium state. This also is confirmed by several researches; it is for example shown in Carpenter and Elam's « classical » study (1920) of grain growth in a tin antimony alloy; and, most recently, by direct observation in the emission electron microscope by Rathenau and Baas (1951) (Supplement Chap. XI, 5). This work, moreover, shows directly the formation of grooves at the surface of the specimen between two crystals, and their gradual disappearance after grain growth, due to the tendency of intergranular and actual surface tension to attain equilibrium.

VII, 2. Dependence of Boundary Energy on Degree of Misfit between Adjacent Lattice Regions.

In order to understand other features observed during boundary migration it is important to realize that the excess energy in the boundary depends on the misfit between the two adjacent lattices, i. e. both on the difference in relative orientation of the lattices and on the position of the boundary plane.

This is a direct consequence of the conception, brought forward by J. M. Burgers (1940), W. L. Bragg (1940) and others that the boundary layer represents the best-possible « fit » between the two adjacent lattices and possesses a definite « structure », either in terms of definite dislocation arrangements, or merely as a sequence of places of good and bad fit (cf. Mott's conception, discussed in Chap. II, 4). This structure may be expected to vary with the relative orientation and position of the boundary and to possess different physical and chemical properties according to its precises state. This is confirmed by experiment : various boundaries are differently attacked by etching reagents (cf. Lacombe, 1948) or even show a different « melting point » (Chaudron, Lacombe and Yannaquis, 1948; Chalmers, 1940). Also the rate of self-diffusion differs for different boundaries, as follows from experiments with tin by Fensham (1950) (cf. Chap. II, 4). In particular the low surface energy of twin boundaries, due to their near-equivalence to perfect fit, is apparent from all this work, as they show no attack by etching, no premelting, no increased diffusion rate (*), no grooves in the electron image. Also the fact, pointed out by Smith (1948) that a twin boundary can meet a grain boundary at virtually any angle without much deviation of the latter, is an exponent of its low energy.

Calculations of the dependence of boundary energy on misfit, based on dislocation models in a simple cubic lattice, have been made by Read and Shockley (1950). For the case that the two lattices are rotated with regard to each other about the common z-axis over a small angle θ, the resulting expression is :

$$E = E_0\theta\,[A - \ln\theta] \qquad (1)$$

where E_0 and A are constants depending to some extent on the orientation of the grain boundary and the macroscopic elastic constants. The complete dependence of energy on « misfit » is, however, very complicated : even for constant position of the boundary plane with regard to the lattice axes the energy $\longleftrightarrow\theta$ curve shows « cusps » for definite angles between the lattices, namely those at which dislocations are separated by an integral number of atomic planes; moreover, the energies for these relative lattice orientations are very sensitive for the exact position of the boundary plane.

(*) For example the intercrystalline diffusion of liquid bismuth in copper (which causes embrittlement) does not take place along twin boundaries (E. Scheil and K. E. Schiessl, 1949. *Z. Naturforsch*, **4***a*, 584).

Considering these facts, one does not wonder that for the « practical » case of, for example, a cubic face-centred metal it is at present not possible to survey in detail the variation of energy with misfit between two arbitrary lattice regions. Nevertheless, the results of the measurements of relative energy values for silicon iron (cubic body-centred) by Dunn and co-workers (see above) are in agreement with the general course of the calculations and show that at small angles the energy approaches zero value and increases with angle of misfit to maxima at angles of about 26-30°; moreover, these measurements confirm the presence of lower energy « cusp positions ».

Aust and Chalmers, in their research with three-crystal specimens of tin, mentioned in the foregoing section, found an approximately constant boundary energy for orientation differences between two crystals of 6-15°, whereas for smaller angles between the crystal lattices the energy decreases progressively to zero value.

VII, 3. Boundary Displacement and Orientation Difference.

A connection between boundary displacement and orientation difference of the adjoining lattice regions may be traced both by taking into consideration the change in energy due to the displacement and by considering the actual mobility of the boundary.

With regard to the first point, Read and Shockley's calculations of grain boundary energies and the experimental measurements of Dunn and co-workers obtained so far help to understand various phenomena observed in grain growth studies. For example, Rathenau and Baas (1951), by applying their electron emission microscope, observed during grain growth in recrystallized nickel iron foil an almost simultaneous invasion of one grain by all its surrounding grains. In this material, with a well-developed cube texture, all the invading grains (N_1 — N_7) had approximately the same orientation : such grains are separated by low energy boundaries. The disappearance of an enclosed grain (1) of strongly different orientation replaces therefore a number of large energy boundaries by low energy boundaries (cf. fig. VII, 3) and thus causes a gain in free energy. Moreover, according to Rathenau and Baas, one has to take into account that low energy boundaries have a low mobility (see below). If, therefore, only *one* grain invaded the enclosed grain, equilibrium could not

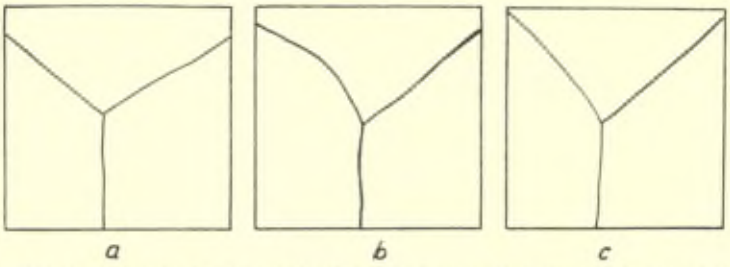

Fig. VII, 1. — Gradual attainment of equilibrium angles between the boundaries in a three-grain specimen of silicon iron.
a) Specimen as prepared
b) After 24 hours at 1200 °C
c) After 66 hours at 1400 °C
× 500.
(Drawing after microphotographs by Dunn, Daniels and Bolton, 1950*b*).

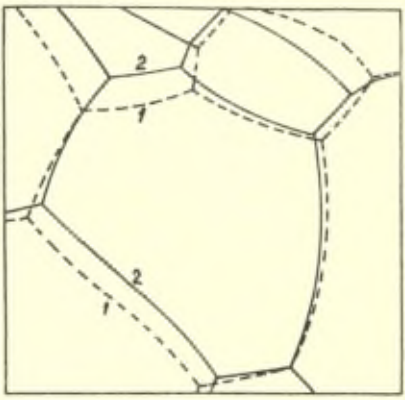

Fig. VII, 2. — Migration of boundary surfaces *towards* their centers of curvature during normal grain growth in high-purity aluminium, after annealing 2 minutes at 600 °C : 1) (dashes); and after an additional anneal of 30 seconds at 600 °C; 2) (full line). Magnification 75 ×. (Drawing after photographs by Beck and Sperry, 1950).

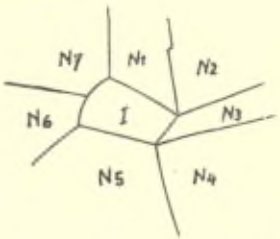

Fig. VII, 9. — Schematic representation of grain growth in a texture. It is assumed that the disappearing crystal I forms high-energy boundaries crystals N, while the crystals N form with each other low-energy grain boundaries. (After Rathenau and Baas, 1951).

easily be restored by rearrangement of low energy boundaries alone.

As another outcome of Read and Shockley's formula we may see (cf. Dunn and Daniels, 1951) the coarsening of the sub-structure inside a polygonized grain, mentioned in Chap. V, 2. In fact, the coalescence of the boundary between two polygons replaces *two* « θ^o-boundaries » by *one* « $2\theta^o$-boundary », which, according to the formula, means a gain in free energy.

With regard to the actual mobility of a boundary, on general grounds it seems natural to expect a layer between bad-fitting lattice regions to be more mobile than between well-fitting regions. That actually a *small* difference in orientation appears to be unfavorable for displacement may be concluded from the experimental fact, already mentioned in chapter VIB, 6, that lattice regions in approximate parallel or approximate twin-position (deviations up to a few degrees) are generally left unabsorbed by a growing crystal. Also when material with a « cube texture » is subjected to prolonged annealing, one never observes, as far as we know, that this texture coalesces into *one* crystal with *this* orientation. If large crystals are formed (by secundary recrystallization) they have orientations which differ considerably from the cube position.

Apparently an exception forms the observation on coarsening of a sub-boundary structure in a polygonized grain, considered above. Dunn and Daniels (1951), following a discussion with D. Turnbull, consider it possible that the ease of boundary migration decreases at first with difference in orientation, reaches a minimum value for a relatively small value of θ (they estimate at one degree) and then increases again. One may also ask whether at very small angles the influence of *both* orientation difference of the adjoining lattices *and* position of the boundary has not to be taken into account (*).

It is often observed that general grain growth comes to a stoppage after prolonged heating. According to Rathenau and Baas this might be ascribed to the gradual disappearance of high-energy grain boundaries, thus of grains with considerably deviating orientations. According to experiments by Beck, Kremer, Demer and

(*) Dunn and Daniels, on p. 153 of their paper, refer to the presence of interaction points in the metallographic picture, where two not perfectly parallel sub-boundaries meet. They remark that such interactions may play a part in the displacement of the sub-boundaries. In this connection we wish also to point to the « mechanism » of sideways displacement of a twin boundary as observed by Rathenau and Baas in the electron emission microscope, discussed in Chapter IX, 5.

Holzworth (1948) with high-purity aluminium, however, stoppage occurs only when the average grain size reaches a value approximately equal to or slightly larger than the strip thickness, whereas it proceeds in thicker specimens of the same material. Of course, in such cases a growing grain could devour its neighbours only «from the side» and not also, by following a detour, via smaller grains «from above», a fact, which would certainly limit the allowable movements of boundaries and so decrease at least the rate of growth.

VII, 4. Influence of a Difference in Internal State of Adjoining Lattice Regions on Boundary Displacement.

So far we have supposed that adjacent grains were both «undeformed», so that we had only to consider the interaction of the proper grain boundaries from the point of view of surface energy. The situation will, however, be different when a difference in «internal state» of adjoining grains exist. In the first place this holds for growth of primary grains in a cold-worked matrix. But also the grains in a primary recrystallized test-piece, in particular if they are of small size, may possess different states of internal strain, be it in a very much weaker degree. This may be due to various causes, one of them being the fact, demonstrated by Polanyi and Sachs (1925) and brought forward again by Rathenau and Custers (1949) that in an inhomogeneously deformed partially recrystallized test-piece the uncompensated stresses still existing in the not-yet recrystallized part may cause the first recrystallized grains to become strained anew, whereas those which are formed in a later stage of the recrystallisation process are strain-free, or at least less strained. That actually crystals formed by recrystallization can become strained in such a way may be concluded from Cahn's observation (1949) that coarse grains of copper and magnesium, produced by primary recrystallization, show signs of distortion and polygonization. Cahn considers this due to the progressive redistribution of the intercrystallines stresses present in the cold-worked polycrystalline specimen by the growth of the new grains. This redistribution caused the new grains themselves te become slightly distorted and during the remaining period of the annealing they underwent polygonization. In agreement herewith, grains formed by recrystallization of deformed *single crystals* of magnesium were strain-free.

Another argument in favour of the idea that crystals formed by recrystallization may be differently strained, may be based on Dunn and Daniel's observation (1951) that in silicon iron sub-boundaries move along with the grain boundaries. Assuming that new crystals grow from polygonized nuclei, this behaviour may also cause new grains to differ in internal state, depending on the state of the nucleus from which they are formed (*).

Now, again on general grounds, it can be expected that a less-deformed lattice region will have the tendency to grow at the cost of an adjoining more-deformed region. It seems to us at present not possible to visualize this process in terms of atomic displacements more precisely than is done in the general terms put forward in Chap. II, 4. It is probably not fundamentally different from what happens in normal grain growth, namely a perpetual rearrangement of boundary surfaces to conform with changing surface energy conditions : if we consider a deformed block merely as an aggregate of very small mosaic blocks, the phenomenon could be the same on a much finer scale.

It is, however, perhaps more adequate to consider the process from an energetic point of view, as is done in Dunn and Daniel's 1951-paper and to say that boundary migration occurs when there is a difference in sub-boundary energy (we might perhaps say in density of dislocations) inside adjoining grains. Dunn and Daniels show definitely by the following experiment that a lack of balance in the « density » of sub-boundaries adjacent to a boundary between two crystals promotes migration of this latter. By their controled method of growth (see Chap. XII, 1) they transformed one half of a fine-grained test-piece into a single crystal, then bent the test-piece and transformed the other half into a second crystal. In this second step the first crystal undergoes polygonization due to its bent state. The specimen is now bent a second time and again polygonized by suitable heat treatment. One so obtains two crystals differing in sub-boundary energy per unit volume. The test-piece was finally subjected to a 3 hour anneal at 1.300 °C and it was observed that the second crystal, which is bent only *once*, and thus after polygonization possesses

(*) A similar reasoning lead May (1949, 1950) to investigate by precision X-ray methods (intensity measurements; sharpness of « divergent pattern »), whether differences in mosaic structure could be traced between *large* crystals formed by primary recrystallization in fine-grained aluminium at a different growth rate. Within the limits of the accuracy attained, no difference could be detected in this case.

the lowest sub-boundary energy per unit volume, grew at the expense of the first crystal, which had suffered bending twice. This proves the capacity for growth of a less-deformed crystal at the cost of an adjoining more-deformed one.

The above accounts for the increase in rate of growth with degree of deformation of the matrix, is well-known from experiments on primary recrystallization.

It may also interfere with the direction of boundary displacement in normal grain growth, in so far as this would be expected on the ground of its curvature alone. For example, a movement *away from* instead if *towards* its centre of curvature is often observed, so in Carpenter and Elam's paper (cf. figures 119-122 in Burgers, 1941; an example is given in fig. VII, 4); also Petersen (1947), in his article mentioned in Chap. VI*A*, 4, refers in a somewhat different way

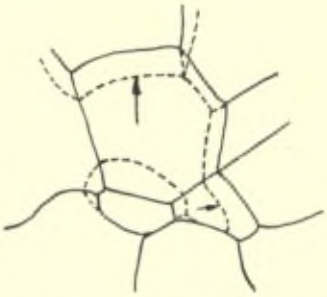

Fig. VII, 4. — Structural changes in tin antimony test-piece caused by heat treatment at about 2000 °C during 1/2 hour. The original boundaries are *dotted*, those after annealing full-drawn. Boundaries indicated by an arrow are displaced *away from* their center of curvature. (After Carpenter and Elam, 1902).

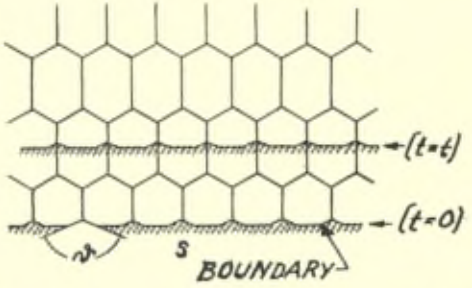

Fig. VII, 5. — Schematic representation of secundary growth of a large crystal (S) at the cost of a large number of small grains with approximately the same orientation. The total surface energy diminishes continuously. (After Rathenau and Baas, 1951).

to the influence of remaining stresses on the direction of boundary displacement in normal grain growth (*). Also the fact that in slightly deformed polycrystalline test-piece grain growth may proceed, or

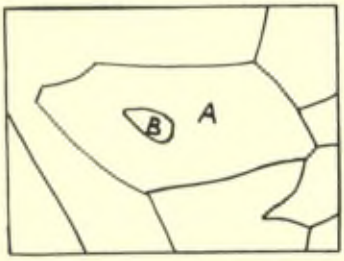

Fig. VII, 6. — Pear-shaped crystal *(B)* inside a large crystal *(A)*. Both crystals are grown by primary recrystallization in fine-grained aluminium plate, the rate of growth of *A* was larger than that of *B*. About *natural* size. (After Burgers, 1947).

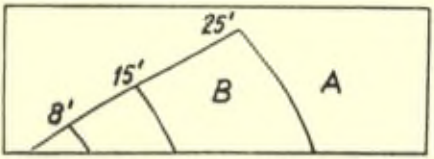

Fig. VII, 1. — Directional growth of a new crystal *(B)* in a stretched single crystal *(A)* of aluminuim. The boundary position is indicated after 8, 15 and 25 minutes of heating at 600 °C. About *natural* size. (After Burgers and May 1945).

occur simultaneously, with primary recrystallization, as observed by Burke and Shiau (1948) in α-brass and by Beck and Sperry (1950) in high-purity aluminium (denoted by these authors as « strain induced grain boundary migration »), has to be seen in this way (Dunn and Daniels, 1951) (**).

(*) Burke (1948), however, in experiments with brass, observed that grain growth continued only as long as the specimen was completely solid but came to a stop as soon as some melting at the grain boundaries had occurred; whereas it continued again if the specimen was reheated just below the solidus line. This means, according to this author, that the driving force for boundary migration is interfacial energy and not differential lattice energy, because, when melting has occurred, the surfaces of all grains could develop a convex curvature and the tendency for surfaces to loose atoms would be nearly equal.

(**) The phenomenon was already observed by Van Arkel and Van Bruggen in 1928. Also Chevigny's observation (1946) that in aluminium test-pieces which had undergone a weak degree of rolling before being annealed, « la recristallisation primaire succède à une recristallisation de rassemblement déjà amorcée » belongs probably to this category of phenomena.

Finally the remarkable observations by Van Arkel, Van Bruggen and Ploos van Amstel (1927, 1930) that growth of a large primary grain in a deformed fine-grained matrix could be stopped by subjecting the large crystal to a slight deformation (extension), may fall under this head. As suggested by Burgers (1941, paragraph 96), such a deformation will presumably affect the large undeformed grain far more than the surrounding smaller grains. Therefore, by creating a substructure near its boundary (where glide is hindered), a balance in (sub-)boundary energy at both sides of the boundary of the large grain may be established (cf. also Dunn and Daniels, 1951).

VII, 5. Secundary recrystallization.

The growth of large secundary crystals in a primary recrystallized fine-grained matrix may also be ascribed to a difference in « internal state » between growing crystal and to-be-consumed matrix. This phenomenon occurs in a pronounced degree only in case the primary matrix has a sharp texture with a limited range of lattice orientations as exists in rolled single crystals (experiments with aluminium by Van Arkel and Van Bruggen, 1928; Burgers and Basart, 1929) or in nickel iron or copper sheet with cube texture (Custers and Rathenau, 1949; Boas and Bowles, 1948; Kronberg and Wilson, 1949; older references in Burgers, 1941). So the matrix possesses very many grain boundaries with relatively low interfacial energy. If a large crystal with deviating orientation, and therefore large boundary energy with regard to the texture crystals, grows at their expense, in a way as schematically represented in fig. VII, 5 (taken from Rathenau and Baas, 1951; cf. also Harker and Parker, 1945), the final effect comprises the elimination of a large number of low-energy boundaries without considerable increase of high-energy boundary. Therefore, taken as a whole, the interfacial energy will decrease (*).

One may ask, however, whether this energy difference is the only driving force or whether one has to assume that the primary crystals

(*) From the fact that the angle θ in their electron emission pictures has an average value of 150°, Ratheanu and Baas estimate the boundary energy of secundary crystal versus cubic crystal to be about twice that between two cubic crystals.

are moreover less perfect than the growing secundary crystal. Moreover, the question arises, why do only a few secundary crystals develop in the primary texture? Concerning these points different assumptions can be made. One way of looking at it (Burgers and Sandee, 1942; Rathenau and Custers. 1949) is to assume in the deformed matrix, apart from the main rolling texture,

a) a *large* number of « equivalent » nuclear spots of *strong* local curvature and approximately the same orientation (for example the cube-orientated regions in rolled nickel iron) and

b) a *small* number of only *slightly* deformed (or practically undeformed) lattice regions.

On annealing, the *a*-spots will polygonize first and become transformed into actual growth nuclei, capable to consume the main rolling texture, but, so we assume, not the *b*-spots, on account of the slightly deformed state of these latter. As a result the primary cube texture is formed. If the primary crystals, due to their small size, should not reach a perfect state, or become restrained in the way suggested in section VII, 4, when discussing Polanyi and Sachs' experiment (cf. a similar suggestion by Boas and Bowles, 1948), the possibility might be envisaged that on prolonged annealing the *b*-spots polygonizing in their turn (*), attain such a strain-free state that they become capable of consuming again the primary grains. Once the secundary crystal has obtained the faculty to grow, growth will proceed indefinitely, as, due to the sharp primary texture, it encounters always grains with the same orientation, so that conditions for growth remain constant.

As an alternative one may assume with Dunn (1948) that during primary recrystallization some grains are formed of somewhat larger than average size in positions deviating from the primary texture. In this case one would expect these grains to have been

(*) It might for example be thought possible that polygonization of the secundary nuclei is « stimulated » when contacted by the primary grains : this would require, as set forth in section VI*B*, 4, an *exact* twin relationship between secundary grain and stimulating cubic grain. As will be mentioned in section VIII*B*, 1, orientations of secundary crystals can often be deduced from the primary texture by a rotation about an 111 axis, be it over angles often considearbly different from that required for exact twinning. It must, however, be realized that such angles relate generally to *centres of gravity* of pole regions of fairly large scattering, so that it seems not wholly impossible that *individually* a *perfect* twin relationship between a definite primary grain and a secundary grain might exist.

nucleated *before* the primaries! Whereas the primary grains, due to their approximately similar orientation, would be stable against normal grain growth, these larger grains, if present, would tend to grow slowly at first, then more rapidly, until large compared with the matrix grains they would continue at a constant rate.

We do not know how to decide between such possibilities. The fact, for example, that secundary recrystallization in rolled foil occurs within a restricted range of rolling degrees limited to both sides (cf. ref. in Burgers, 1941, also Ratheanu and Custers, 1949) is understandable on the basis of both « theories », as both conceptions require the simultaneous occurrence in the deformed matrix of many nuclear spots in *one* orientation and a small number of « other » nuclear spots in a *different* orientation. This may be expected to occur for an intermediate degree of rolling, as, for low degree of deformation, the texture is not well enough developed, whereas for too high deformations it may be too uniform.

Guinier and Tennevin (1949*b*), by applying their « focussing technique » mentioned in the Supplement, Chap. XI, 9, tried to show that actually secundary crystals are more « perfect » than the primary crystals at the cost of which they grow. Although the authors were able to show that the secundary crystals, formed in nickel iron with a primary cube texture, had a perfect lattice in so far that within the entire space occupied by a secundary crystal with dimensions of $3 \times 1 \times 0.1$ mm the disorientation of the reflecting lattice plane was of the order of 1 minute of arc, the experiment could not establish a difference in perfection between primary and secundary crystals. As the authors state, however, the sensitivity of their method was not sufficient to reach a definite conclusion regarding the point in question.

VII, 6. Growth Selectivity.

We consider once again the growth of a large crystal at the cost of a fine-grained matrix, as occurs in primary or secundary crystal growth. In that case a lattice with a « constant » state of perfection meets during its growth lattice domains varying both with regard to orientation and position of boundary, and, in primary growth, moreover in degree of deformation.

If growth occurs in a quasi-isotropic fine-grained slightly deformed matrix (primary growth), the growing crystal, as already mentioned in section VI*A*, 1, has approximately a circular shape, indicating an overall equal rate of growth in all directions. The boundary line is, however, often corrugated, which is an indication that the individual crystals are consumed at a different rate. This may be due to various causes such as differences in the size or state of deformation (*), but probably also to a dependence of the mobility of the boundary layer on the difference in orientation of the two lattice regions which it separates, and on its position with regard to these two lattices. The fact that grains with approximately coinciding or approximately twin orientation are left unconsumed as « inclusions » (see section VI*B*, 6), is an argument in favour of this suggestion.

If we assume such a dependence, then, considering that a matrix is never wholly quasi-isotropic as to the orientations of its grains, one would anticipate that the average rates of growth of differently oriented primary crystals in the same matrix must be different. Such differences actually show themselves by the fact that a large crystal may grow around another primary crystal growing at a somewhat smaller overall rate; this gives rise to pear- and heart-shaped enclosed crystals, as described by Sandee (1942) and in subsequent papers by Burgers (1945, 1947, 1947*a*) and May (1950). An example is shown in fig. VII, 6. A mathematical analysis of these leads to an estimation of the ratio of rates of growth for different crystals, which amount to perhaps some 10-20 % maximally.

More direct measurements can be made (Dunn, 1949) by sending a sample at the proper speed into a furnace with a high temperature gradient, thus causing crystals to grow from one side to the other. For silicon iron the experiments point again to possible differences of about 20-30 % for crystals growing in a matrix with a nonrandom, fairly weak texture. Analogous experiments by Tiedema with aluminium would put this value rather lower.

Larger differences can, however, be expected if growth of a large crystal takes place in a matrix with a pronounced preferential orientation of its constituent grains, such as may be obtained by stretching

(*) Perhaps variations in impurity content have also to be considered (cf. Dunn, 1949).

a single crystal. In agreement herewith, Tiedema (unpublished) applying the method of « growing a crystal over a curvature » (see Chap. XII, 1), was able to confirm on the one hand that a growing crystal cannot consume a matrix with approximately the same or approximately twin orientation : it was, for example, impossible to grow in a matrix obtained by stretching a single crystal wire with a [111]-direction parallel to its axis, a new crystal with approximately this orientation. On the other hand it proved possible to grow in this matrix crystals with orientations differing from it by say 30°, whereby, as far as these experiments go, it was rather immaterial by what rotation the orientation of the crystal was related to that of the matrix. This result suggests that growth, so far as orientation of crystal and matrix lattice is concerned, requires a rather large difference without further specification.

For a *given* orientation of growing crystal with regard to the matrix, however, the anisotropy in the rate of growth can be considerable : crystals may, for example, develop more or less straight boundaries, parallel to certain directions (see fig. VII, 7). This has been observed for aluminium in case of growth in deformed single crystals (see e. q. Kornfeld and Rybalko, 1937; Barrett, 1940); it is further shown in secundary growth in copper foil with cubic texture (e. g. Cook and Richards, 1940; Bowles and Boas, 1948), where growth parallel to octahedral planes of the secundary crystals seems to be preferential.

It is not easy to conclude from these and similar experiments what position of the boundary plane is either most or least mobile, as one has to take into account the possibility that single crystals, on deformation, often develop « deformation bands » (cf. Barrett, 1943) which constitute inhomogeneities in their deformation on a « macroscopical » scale, and which may influence the development and the shape of new crystals (Karnop and Sachs, 1937; Collins and Mathewson, 1940). Also the presence of insoluble impurities along definite planes in the deformed matrix influences the development of anisotropic crystal forms (cf. Kornfeld, 1934, discussed in Burgers, 1941, paragraph 90).

Nevertheless, considering the available evidence on growth selectivity altogether, one gets the impression that it is *not the relative orientation* of the adjoining lattices as such, but the *« structure » of the plane of contact* between them, which is the controling factor,

in this sense that a definite (or some definite) structure(s) of this plane possess(es) the strongest tendency to migrate. Perhaps these structures are characterized by special coincidences of atoms in the adjacent lattices, of the type discussed by Kronberg and Wilson (1949) and, with regard to twin structures, by Ellis and Treuting (1951). They may also be related to the « cusp positions » in the interfacial energy curve (or to the maxima in this curve lying intermediate between these positions) deduced by Read and Shockley and encountered in the experimental work of Dunn and co-workers, as discussed in section VII, 2. Such « mobile » interfaces can, we think, be constructed for various relative positions of the lattices. *Growth selectivity would then be insufficiently characterized by the relative orientations of these lattices, for example, as given by the rational movement (specified by direction of axis and amount of rotation) required to transform one position into the other.*

Conversely, easy mobility would not be confirmed to a definite relative orientation of growing crystal and disappearing matrix.

We shall return to this questions in Chap. VIII*B*, when discussing the influence of growth selectivity on the formation of definite recrystallization textures.

CHAPTER VIII

ORIGIN OF RECRYSTALLIZATION TEXTURES

A. INFLUENCE OF ORIENTED NUCLEATION

VIIIA, 1. Coincidence of Lattice Orientations before and after Recrystallization.

A direct consequence of the conception of nucleation put forward in Chap. VI*B* is the assumption that the orientations of the crystals formed after recrystallization correspond to those of definite lattice regions already present in the deformed matrix, independently thereof whether the crystals are formed by what we called in Chap. III primary or secundary recrystallization. In those cases in which the recrystallization texture closely resembles the deformation texture this condition presents no difficulties. Moreover, in several instances

of clearly different textures, it has been found that the recrystallization texture can be traced, be it weakly, in the texture of the cold-worked test-piece. This holds particularly for rolled copper and nickel iron foil, which generally recrystallize in the so-called cube orientation (Cu : Iweronowa and Schdanow, 1934; NiFe : Sachs and Spretnak, 1940; Burgers and Ploos van Amstel, 1941; Custers and Rathenau, 1941; Schmid and Thomas, 1950. *Z. Metallk.* 41, 45) (*). As to rolled aluminium foil, this recrystallizes mostly in the « as-rolled » texture and only occasionally recrystallization in the cubic texture has been observed by various investigators (Schmid and Wassermann, 1931; Coheur and Lejeune, 1949; Beck and Hsun Hu, 1950). If so, then, at least according to Coheur and Lejeune's observations, the cube position could again be traced in the rolling texture. Moreover, Coheur and co-workers (private communication) obtained a similar result with rolled zinc : whereas normally the recrystallization texture coincides with the rolling texture (basal planes predominantly at angles of about 20° to the plane of rolling), these authors found that material rolled in a special way produced a recrystallization texture with the basal planes parallel to the plane of rolling. On further investigation it appeared that in the surface layer of *this* rolled material basal planes with this orientation were actually present.

Inversely, the giving-away of the cube texture for the rolling texture when recrystallizing very thinly etched rolled nickel iron foil (thickness $\sim$ 1 μ) was attributed by Custers and Rathenau (1941) to a gradual disappearance of lattice domains in cube orientation in this thin material.

As to secundary recrystallization, a survey of the results obtained with aluminium (cf. Burgers, 1941, paragraph 119), nickel iron (Rathenau and Custers, 1949) and copper (Bowles and Boas, 1948; Kronberg and Wilson, 1949) gives the impression that the orientations of at least part of the large secundary crystals can be refound, or lie closely to, orientations clearly present in the (in general considerably spread-out) rolling texture.

If the recrystallization orientations are *not* explicity refound in

(*) The presence of the cube position in rolled nickel iron is apparently not observed in a recent determination by Seymour and Harker (1950).

the cold-worked texture, the proposed conception requires that nevertheless these orientations are present in lattice domains of such small size (or in such limited quantity) that they are not detected by means of the method applied to determine the deformation texture (for example by X-rays) (*).

However, in order to explain on the above basis the occurrence of recrystallization textures which are different from the deformation texture from which they are formed, at least two other assumptions have to be made :

1) those lattice domains in the cold-worked matrix, which correspond in orientation to the recrystallization texture, are more favorable for « nucleation » than lattice domains occupying the main orientations present in the deformed matrix, i. e. nucleation is « oriented »;

2) the polygonized nuclei can actually grow.

VIIIA, 2. Oriented Nucleation.

As to the first point, although it is not known what type of deformation (bending) is most favorable for polygonization to occur, it seems reasonable that this capacity varies with the character of the deformation. We raised this point already in section V, 3 when discussing Snoek's note on the impossibility of polygonization in crystals deformed by torsion. Further we remind of Cahn's assumption, mentioned in section VI*A*, 1, according to which the incubation period, for a given heat treatment, is inversely proportional to the radius of curvature. Nye (1949), in his paper on stresses in silverchloride (cf. Chap. IV, 1), points to the necessity of a bent lattice region to straighten out when it forces dislocations to its edges. For a grain embedded in a polycrystalline aggregate this straightening out cannot occur without stresses being set up in neighbouring grains.

(*) This, for example, according to our view, must be assumed when considering the results of recrystallization experiments with deformed aluminium single crystals as carried out by Burgers, Basart and Louwerse (1928, 1931, 1934) and more recently by Cahn (1950) and by Laloeuf and Crussard 1950), to which we refered in section VI*B*, 2. In all these cases the observed range of orientations found for the new crystals exceeds considerably (by tens of degrees) the orientation spread detectable in the deformed matrix, as shown by the Laue-asterism of the extended crystals.

In an analogous way polygonization of definite lattice regions may be hindered by neighbouring regions and it seems possible that those regions are privileged, the polygonization of which doesnot require a relatively large « straightening-out » in a definite « direction », but a more restricted change of shape. Reasoning along these lines it might be conceived that a lattice region, which has suffered glide along *one* definite set of glide planes and which thus is curved rather strongly about one definite axis, is less apt for polygonization than regions, which have been subjected to several intersecting glide systems and therefore possess a more « all-round » curvature. Such a behaviour could perhaps make understandable that lattice domains in « symmetrical » orientations, for example cube orientations in rolled foil, are privileged for polygonization and have the shortest incubation period (*).

One is, however, far from understanding why the orientations actually observed in various recrystallization textures are those which have to be expected on these grounds and why not another « symmetrical » orientation doesnot appear (**).

VIIIA, 3. Influence of Rate of Growth of Nuclei.

The second point, mentioned above, the ability to grow, is as important as the first. Although the way in which growth of one domain at the cost of a neighbouring domain actually proceeds is not at all clear (cf. chapter II, 4), it seems certain from the discussion on growth selectivity in chapter VII, 6 that a considerable difference in orientation between growing and grown-into domain is required. In any case a growing crystal appears unable to consume a lattice region in approximately the same or in approximately twin position. For this reason it is possible that even in case strain-released nuclei are formed, crystal growth cannot take place.

(*) The general idea underlying this argument can already be found in Dehlinger's « classic » paper on recrystallization (1929); see also Burgers (1941, paragraphs 49 and 149).

(**) If we assume that a potential nucleus is a lattice region which has been subjected to the maximal number of glide combinations, then perhaps a measure might be obtained by calculating for example the mean value of the relative shear stress for all possible glide combinations for the special type of deformation applied. For extension or compression of cubic face centred crystals this can easily be achieved, for example with the aid of the diagrams given by Boas and Schmid (1931). The [100]- and [210]-directions are very favorable from this point of view, but so are also for example [113] and [520].

An example of such behaviour was apparently met with by Tiedema (unpublished) in the following experiment : An aluminium single crystal with a (111)-plane parallel to the surface (prepared by the method discussed in Chap. XII, 1) was stretched in a direction approximately parallel to [112]. This deformation didnot produce any appreciable Laue-asterism even after 20 % extension, indicating that notwithstanding its severe shear hardening the deformed crystal had an extremely sharp texture with only weak « local lattice curvatures ». Annealing the deformed crystal (after first removing all the « side parts » by etching) at the highest possible temperature, although causing appreciable softening, didnot give rise to growth of new crystals, evidently through lack of « nuclei » with an orientation sufficiently different from that of the matrix (*).

Therefore, if rolled nickel iron crystallizes in the cube orientation, it doesnot only mean, according to the view set forth here, that cube oriented nuclei are formed by polygonization, but moreover that these nuclei are capable of growing at the cost of the main rolling texture.

VIIIA, 4. Change of Texture.

Of course, the formation of the cube texture doesnot exclude the possibility that also lattice domains with the orientation of the main rolling texture may become polygonized and thus transformed into actual nuclei. In fact it is found (Custers and Rathenau, 1941; also Tiedema, unpublished; cf. also Müller's 1939-investigation of nickel-iron-copper alloys) that nickel iron foil at relatively low temperatures (500-600 °C) develops a recrystallization texture which closely resembles the main rolling texture. However, even in this case, nuclei in cube position seem to form first, as appears both from the X-ray photographs and from the metallographic investigation (**). So we have to assume, with Custers and Rathenau, that the *rate of growth* of the cube nuclei at these low temperatures is so small that the lattice domains in the main rolling orientation, which are far in abundance, obtain the possibility to polygonize before the matrix

(*) It was certainly *not* due to lack of recrystallization power of the stretched crystal, as new crystals could easily grow into it from a scratch.

(**) The same was observed by E. Schmid and H. Thomas (1950. *Z. Metallk.* **41**, 45).

is consumed by the cube grains; whereas at high temperatures (1000-1100 °C), in which case the cube texture immediately predominates, the rate of growth of the primarily formed cube nuclei is so large that the matrix is consumed before the domains with main rolling orientation obtain a chance to polygonize.

In special cases it appears to be possible to influence the « nucleation capacity » of lattice domains by « exterior » means : Smoluchowski and Turner (1949) found a change of texture when recrystallizing rolled iron cobalt alloy *without* and *with* a magnetic field. This is thought to be due to the anisotropic character of the magnetostriction, which causes differently oriented domains to become differently strained and thus differently influenced as to their capacity to function as « nucleation centers ».

B. INFLUENCE OF GROWTH SELECTIVITY ON THE FORMATION OF RECRYSTALLIZATION TEXTURES

VIIIB, 1. Conception of Beck and Co-workers.

From the considerations given in Chap. VII, 6, it seems certain that a definite selectivity is inherent to the process of boundary displacement, in that sense that, under for the rest similar circumstances, definite boundary layers are more mobile than others. This point is of interest because recently Beck and co-workers (Beck, Hsun Hu, Sperry, 1949, 1950) have advanced the idea that the occurrence of definite recrystallization textures in recrystallized matrices is due to such an « oriented growth » and not to what may be called an « oriented nucleation », as advanced in the foregoing section, which implied that the orientations of the new crystals correspond to those of « potential nuclei » formed as a direct consequence of the foregoing deformation process.

The arguments in favour of the oriented growth theory are based on the experimental fact that, with cubic face centred metals, pronounced orientation relationships have been found between the grains growing in a matrix with a strong single orientation texture and the matrix itself, namely a rotation of 30-40° around a [111]-axis.

For aluminium, according to Beck c. s., this relationship exists as well for primary recrystallization when the matrix is a cold-worked

single crystal deformed by compression, rolling or local scratching, as for secundary recrystallization when the matrix is an annealed primarily recrystallized material with a pronounced preferential orientation. Similar relationships, particularly for crystals grown by secundary recrystallization in material with cube texture, have been found in copper by Bowles and Boas (1948) and by Kronberg and Wilson (1949) and in nickel iron by Custers and Rathenau (1949).

The occurrence of the same relationship in all these cases is considered by Beck c. s. as an indication that grains with definite orientations with respect to the matrix grow much faster than others. Taking this as starting point, and assuming that in a deformed matrix, and also in a recrystallized material, even when a strong texture is present, there are always some lattice elements in practically any orientation (*), is is supposed that only those domains can serve as actual nuclei, which are favorably oriented with regard to the matrix for their growth. The resulting texture would thus be caused by « selective growth » and not by « selective nucleation » of domains in special positions only. A similar view was tentatively advanced by Barrett (1940), and discussed by Dunn (1948).

VIIIB, 2. Divergent Views.

In contradistinction to this conception, Tiedema and the present author (1950), considering the data on selective growth set forth in Chap. VII, 6, hold that growth selectivity, as defined by a definite orientation difference between two adjacent lattices, is in itself insufficient to cause such sharp orientation relationships as are often found in recrystallized fine-grained matrices. This view is, in their opinion, supported by a closer examination of the results obtained by Beck c. s. with aluminium, according to which a 30-40° rotation about an [111]-axis between growing grain and matrix is particularly favorable for growth, as it appears that deviations from such positions up to at least 15° in some direction are present. This is a considerable amount in a lattice with cubic symmetry and means that crystals

(*) There is no doubt that this is certainly true in most cases (cf., however, footnote in Chapter VIII*B*, 3), as X-ray photographs apart from the interference spots due to the prefered orientation, practically always show at least some intensity along the Debye-Scherrer rings outside the intense reflection region due to the texture.

with a quite different crystallographic orientation with regard to the matrix can also grow with a comparable rate.

The same conclusion can be drawn from Kronberg and Wilson's work with copper and from Rathenau and Custers' work with nickel iron. In both cases, apart from [111]-rotated crystals, also large crystals with *other* orientations with regard to the matrix occur, for example crystals rotated about a [001]-axis. Furthermore Becker (1951), when recrystallizing single crystals of α-brass, found that the new crystals, growing from saw cuts or from the end of the tensile specimens, never showed a [111]-orientation, but appeared quite random (*).

The argument can be illustrated in another way. As set forth in section VI*B*, 1, the recrystallization texture of homogeneously compressed aluminium single crystals was interpreted by Burgers and Louwerse on the basis of oriented nucleation in lattice regions rotated about an axis [112], perpendicular to the glide direction [110]. In the original paper it is shown that the observed orientations could approximately be ascribed to rotations around the perpendiculars to the various active glide directions. Beck and Hsun Hu (1949), in an effort to fit these results into the theory of selective growth, show decidedly that the same orientations, at least the prominent groups, can also be described, perhaps even somewhat better, by a rotation around [111]-direction. As far as this statement goes, the argument may be taken as an example that the scattering of the observed orientations is so considerable that they can approximately be described by rotations about different sets of axes (**).

We finally point to two other phenomena which seem difficult to understand on the basis of oriented growth alone.

Becker (1951), in his recent note refered to above, points to the fact that recrystallization textures may vary with the temperature of annealing (cf. Chap. VIII*A*, 4). This, according to Becker, would

(*) In this connection we refer also to a result obtained by Schmid and Thomas (1950. *Z. Metallk.*, **41**, 45) when recrystallizing (at 1000 °C) nickel iron sheet with cube texture after deforming it by extension. Although this mode of deformation left the texture essentially unaltered, yet it recrystallized into a random texture.

(**) One may say also that a description of a scattered texture by a rotation about a definite axis or set of axes has in itself not much value. It derives this value from the interpretation : either (Burgers and Louwerse) on the basis of « oriented nucleation » in local curvatures, or (Beck and Hsun Hu) in terms of growth selectivity.

imply that the anisotropy of growth rates is a suddenly varying function of temperature which seems unlikely.

Then there exists the phenomenon of « stimulated crystal growth », discussed in Chap. VI*B*, 4. Here we find an example of two crystals growing both at the cost of the same fine-grained matrix, of which the one with the faster rate of growth, viz. the « stimulated » crystal, starts to grow at a *later* moment than the one with the slower rate of growth, viz. the « stimulating » crystal. Therefore, notwithstanding its faster rate, which undoubtedly means that its orientation with respect to the matrix texture is more favorable for consuming this texture, the « stimulated » crystal would perhaps not have developed at all, if not, according to our view, the *establishing of contact* with the approaching « stimulating » crystal had « activated » its « potential » growth nucleus to a centre actually capable to grow (*).

VIIIB, 3. Combined Influence of Oriented Nucleation and Growth Selectivity.

If, assuming that a difference in mobility between definite boundary layers certainly exists, we ask what effect growth selectivity may exert on the development of recrystallization textures, then, following our trend of thought at the end of Chap. VII, 6, we feel inclined to say that, ceteris paribus, it will promote growth of those crystals, which are « separated » from the matrix by highly movable boundaries. Growth selectivity in this sense, however, if we see it rightly, need not give rise to a definite relationship in lattice *orientations*. We can only say that, if actually the deformation process produces potential nuclei in all possible orientations and with nearly equal « incubation periods », growth selectivity may be expected to further the displacement of easy movable boundaries and so co-determine the final texture, this expression taken not merely in the sense of the *orientations* of the grains but of the « structure » of the whole of the array of intergranular boundaries.

The above, however, is only valid if actually potential nuclei are present in all possible positions.

(*) This argument must be abandoned if the formation of a « stimulation twin » takes place according to the mechanism suggested for the formation of annealing twins by Fisher, discussed in Chapter IX.

In other cases, however, the deformation process may have a less allround character and produce « local curvatures » or adjacent lattice elements with « unstable » boundaries only in special positions with regard to the matrix, either because the « curvatures » are directly correlated to the orientation of the glide planes, or because unstable boundaries require quite definite orientation relationships between two adjacent lattice elements. In such cases the orientation of the new crystals, according to our view, is determined by the orientation of the potential nuclei produced by the deformation process, i. c. by oriented nucleation. If these orientations do not conform to that which is most favorably oriented with respect to the matrix from the point of view of growth selectivity, then such « favorable » orientations cannot develop and (to quote Cahn, 1950, footnote, p. 333) growth must necessarily occur from the available nuclei, whatever their orientations. Again the selectivity of the growth process seems to us to be sufficiently weak to allow such growth, if only the orientation of the available nuclei is sufficiently different from that of the matrix (*).

Something similar would hold if nuclei are present with all possible orientations but with *widely varying* incubation periods. In such cases potential nuclei with the shortest periods become actual growth nuclei and start their growth before nuclei with longer periods. If the « short period nuclei » happen to possess an orientation different from that most favorable for growth, then, due to the fact that growth selectivity is not so very pronounced, such nuclei may consume a considerable part of the matrix before nuclei with a longer incubation period (and perhaps more favorable orientation with respect to the matrix) may start their growth, or such nuclei may even be consumed by the already growing crystals. In such a case, again the final texture

(*) That actually a deformation process apparently not always produces growth nuclei in every possible orientation, from which the recrystallizing matrix may « chose » those best fitted to grow, is clear from the following experiment (Tiedema, unpublished) : A drawn and annealed aluminium wire, on prolonged heating, often shows the formation of large crystals with a [210]-direction parallel to the wire axis (Burgers and Sandee, 1942).

If, however, a *single* crystal wire, with a [111]-direction parallel to the wire axis, is extended circa 8 %, and then subjected to prolonged annealing, then among the large crystals developed by « secundary recrystallization », the formation of a [210]-crystal was in no case observed. Yet, by the method of « growth round the corner », it was found that such a crystal, if presented to the matrix, could consume the deformed [111]-crystal readily. This can be interpreted that, in this case, 8 % extension of the single crystal did not produce potential nuclei in the [210]-orientation.

is not that to be expected according to the growth selectivity conception. The occurrence of a large scattering in the observed textures as well as that of large crystals with orientations different from that of the main group can be understood in this way.

Of course, the considerations given above do not pretend in any way to give a definite solution to the problem of the origin of recrystallization textures. We think it impossible at the present state of our knowledge to decide with certainty between the various possibilities. However, it seems opportune to draw attention to some experimental facts, which, at least in our opinion, are not readily explained on the basis of the selective growth theory *alone*.

CHAPTER IX

FORMATION OF ANNEALING TWINS

A few remarks will be made about the origin of annealing twins, a subject which has puzzled metallographers for a long time. Quite recently, however, two papers have appeared which may throw considerable light on this remarkable phenomenon.

Burke (1950) discusses the two possible causes for twinning advanced in the literature, viz. :

1) the mechanical nucleation hypothesis, which suggests that the preceding cold-work has given rise to small mechanical twins, which serve as « nuclei » for the annealing twins formed on subsequent recrystallization; and

2) the growth fault hypothesis, which assumes that twins are formed in the course of the annealing process itself, when the advancing grain boundary encounters some kind of discontinuity, which will induce a twinning accident.

Burke brings forward several arguments in favour of the second hypothesis, for example the fact that twins can be found within a grain with sides parallel to octahedral planes, which the grain has *not* in common with the original matrix.

Furthermore the paper gives evidence that twin boundaries cannot migrate laterally. This follows from the fact that the width of a twin band *enclosed within a grain*, such as illustrated schematically in fig. IX, 1 at *a*, does not increase during grain growth. Microphoto-

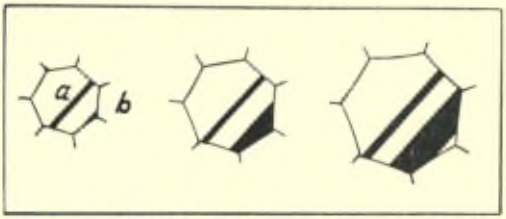

Fig. IX, 1. — Schematic representation of grain growth in a material containing twin bands. *a* The width of a twin band enclosed within a grain remains unchanged. *b* A twin band can increase in width in case one side coincides with a grain boundary. (After Burke, 1950).

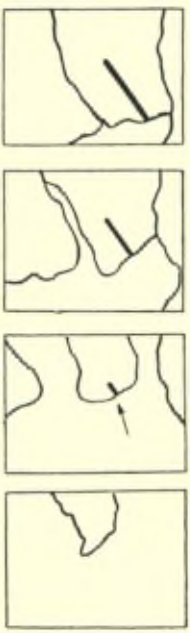

Fig. IX, 2. — Direct observation, by means of the electron emission microscope, of the growth of a twin band «parallel» to the band direction. Drawing after photographs of emission patterns at about 1100 °C × 25. (After Burgers and Ploos van Amstel, 1938).

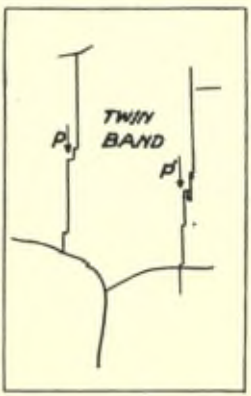

Fig. IX, 3. — *Apparent* sideways displacement of twin boundaries. Actually growth takes place parallel to the twin planes, starting from high-energy surface parts, projecting from the straight boundaries, such as P and P' (Drawing after electron emission pattern obtained by Rathenau and Baas, 1951.)

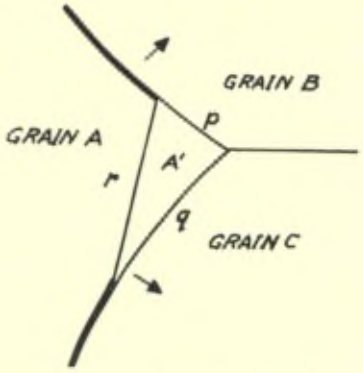

Fig. IX, 4. — Schematic representation of the changes in grain boundary energy associated with the formation of a twin, A', in an infinitesimal region in the corner of a growing grain. Grain boundaries with high interfacial energy are represented by wide lines.

The free energy will decrease by formation of a twin A' if

$$p\sigma_{A'B} + q\sigma_{A'C} + r\sigma_{AA'} < p\sigma_{AB} + q\sigma_{AC}$$

where p, q and r represent the areas and σ the interfacial free energies, respectively of the boundaries indicated by the subscripts (figure and text taken from Fullman, 1950).

graphs of α-brass in Burke's paper show this clearly. The same can be seen for nickel in electron emission pictures at 1000 °C obtained by Burgers and Ploos van Amstel (see Burgers, 1941, fig. 3). By this last method also the growth of a twin band « parallel » to the band direction could be made directly visible for crystal growth in nickel iron and iron (Burgers and Ploos van Amstel, 1948, *Metallwirtschaft*; also Burgers, 1941, fig. 179-181). Fig. IX, 2 is a drawing after some of their photographs.

Newer results, obtained by this method by Rathenau and Baas (1951) at much larger magnification (cf. Supplement, Chap. XI, 5), show, however, that an *apparent* sideways displacement of a twin boundary may be achieved starting from high-energy parts projecting from the straight boundary, such as P or P' in fig. IX, 3, which is again a drawing after actual photographs of the electron emission image. Actually, also in this case growth takes place parallel to the twin plane (*).

(*) Rathenau and Baas remark that possibly the boundary separates in this case two crystals in *approximate* twin position.

Important in Burke's paper is the observation that twin lamellae can increase in width in case one face coincides with a grain boundary, in the way indicated schematically in fig. IX, 1 at *b*.

With regard to this observation, a suggestion published in a recent note by Fullman (1950) and ascribed to J. C. Fisher, is of great interest. It is there suggested that an annealing twin forms in the corner of a growing grain, when the orientation relationships between the twin and the grains' neighbours lead to a smaller total interfacial energy than do the orientation relationships between the grain itself and neighbours. This condition is elucidated with the aid of fig. IX, 4, taken from Fullman's note.

Such a behaviour would make understandable, at least in principle, that twin formation is of necessity related to « lattice faults » (grain boundaries included), which explains why a definite metal which forms generally annealing twins after recrystallization, can also « crystallize » without considerable twinning (for example from the melt).

It would also allow for the fact that the frequency of twinning depends to a large extent on the « texture » of the matrix in which recrystallization or grain growth takes place. For example the large copper crystals obtained by Cook and Macquarie (1938) by secundary recrystallization in strip rolled in one direction, show many straight lamellae, which are not present in the crystals developed in an analogous way in cross-rolled strip.

Finally one could understand from this point of view that different cubic face-centred metals, like copper and aluminium, may differ so much in their twinning frequency. This might be due to a different degree of anisotropy of grain boundary energy. According to Fullman, the anisotropy is for aluminium much smaller than for copper, so that for aluminium a possible gain in energy by transforming into a twin is less likely and the twinning less frequent.

In connection with Fisher's suggestion it may be remarked that the present author thought it possible that annealing twins were due to « stimulation » of a lattice domain in the matrix by a growing grain in exact twin position, as discussed in Chap. VI*B*, 4. Also this mechanism would make twinning dependent on the texture of the matrix, as the latter would influence the chance for a growing grain to meet an exact twin. Whether such an effect could play

a part might be investigated by making, in a frequently twinning metal like copper, a crystal grow over a certain distance in a matrix with prefered orientation; then, before proceeding the growth, bending the matrix over a certain angle, so that the crystal in the further course of its growth meets the matrix grains « under a different angle ». This ought to influence the stimulation frequency (*).

That twin relationships can exist between the various orientations present in a recrystallized matrix follows from a research by Coheur and Lejeune (1945) and Coheur and Barrett (1946) on annealed copper strip.

CHAPTER X

INFLUENCE OF IMPURITIES ON RECRYSTALLIZATION PHENOMENA

We shall leave this subject undiscussed, notwithstanding its great importance. At present, however, it seems not well possible to give a reasoned-out account of all the effects encountered. An effort to achieve this regarding the data published up to 1940 has been given in Burgers (1941 : paragraphs 79-81 and 153-161). This survey shows that especially the *rate* of recovery and recrystallization can be altered considerably by the presence of even minute percentages of foreign atoms. This is particularly evident from researches by Calvet, Trillat and Paič (1935) on the influence of a few 0.001 % of iron and silicon on high purity aluminium. It appears again in newer work by Decker and Harker (1950) with copper samples containing different amounts of impurities.

In connection with this very important question, it may suffice to point to the fundamental considerations by Cottrell (1948) (**) on the influence of foreign atoms on the mobility of dislocations. These considerations help to understand why large effects may be

(*) However, also most probably the twinning tendency according to Fisher's view point.

(**) A. H. Cottrell, 1948. Report Conference on Strenght of Solids, p. 30; cf. also F. R. N. Nabarro, *ibid.* p. 38; J. S. Koegler, 1947, *J. Appl. Mechan.* **14**, 217.

expected for processes connected with the displacement of such lattice disturbances.

In order to mention one example of the complexity of the phenomenon here involved it is perhaps adequate to mention a research by Beck, Holzworth and Sperry (1948) on recrystallization of a manganese aluminium alloy. Here is a case of restricted solubility so that heat treatment may occur both in the homogeneous range and at temperatures where segregation of a second phase occurs. It appears from the paper that the capacity for developing large crystals by secundary recrystallization is fundamentally influenced by this phenomenon. This may be understood in this way that on the one hand a sufficient quantity of finely dispersed phase must initially be present to cause considerable inhibition of normal gain growth, whereas on the other hand heating must be continued at a temperature where partial redesolving takes place. Consequently the temperature must be chosen just below the solvus point for the special composition in hand.

SUPPLEMENT

CHAPTER XI

RECENT DEVELOPPEMENT IN THE METHODS USED FOR THE INVESTIGATION OF STRUCTURAL CHANGES IN METALS

As set forth in the introduction to this report, in this chapter a review is given of newer developments in the techniques applied for the investigation of structural changes in metals. The following techniques will be discussed :

Chemical Attack;
Cathodic Bombardment;
Optical Methods;
Electron Microscope;
Emission Microscope;
Field Emission;
X-ray Diffraction;
Electron Diffraction.

XI, 1. Chemical Attack (Etching, Electro-polishing, Oxidation).

The application of electrolytic polishing and etching, originally brought forward by Jacquet (1938), finds now general application : as an example we mention Maddin, Mathewson and Hibbard's investigation of « cross-slip » in extended brass-crystals (1949). Surveys of the procedures to be followed for various metals and alloys are a. o. given in Smithells' « Metals Reference Handbook » (1949). In research dealing with recrystallization of aluminium, the method is extensively used, for example when studying grain boundary migration by applying alternately annealing and electrolytic etching treatments (Sperry, 1950).

Moreover, starting with an electrolytically polished surface, application of a special reagent (containing a mixture of hydrofluoric, hydrochloric and nitric acids) gives rise to the development of small etchpits, bounded by the cube planes of the crystal lattice (*). Their formation is of help when studying various properties of the crystals. In the first place they can be used to fix the orientation of the crystal lattice (applied for example by Walton, 1944; Barrett and Levensohn, 1940; Tiedema, May and Burgers, 1949; Kostron, 1950). Secondly as they accumulate at intragrain « block boundaries », they can give indications regarding the internal « mosaic » structure of crystals and the changes this structure undergoes during heat treatment (Lacombe and Beaujard, 1947*e*). Finally, when a crystal with cubic etchpits is subsequently deformed, glide lines often pass through the pits and from their directions conclusions regarding the slip mechanism have been deduced (Lacombe and Beaujard, 1947; Heidenreich and Shockley, 1948; Kostron, 1950) : see fig. XI. 1.

Electrolytic dissolution has also been applied with success to obtain very thin metallic foils, suitable for observation of electron diffraction transmission photographs (Heindenreich, 1949).

Interesting « line structures » have been developed on metal surfaces by heating in gases, in particular oxygen, by Elam (1936)

(*) This, at least, is true for aluminium. Etchipts with octahedral planes are apparently developed with nickel iron, as found by Seymour and Harker (1950), using a mixture of hydrochloric acid and hydrogen-peroxide. According to Mahl and Stranski (1942) octahedral planes can also be developed with aluminium, if only etching is carried out in absence of oxygen, with dry hydrochloric acid gas.

on copper and more recently by Chalmers, King and Shuttleworth (1948) on silver. This is of importance, as Graf (1942) in an extensive research on the « line structure » visible on crystals and test-pieces solidified from the melt, observed a regular lining without having applied any etching which he ascribed to a fundamental lamellar structure of the crystals. In view of the fact just mentioned it may be asked whether oxygen does not play a part in Graf's work also.

XI, 2. « Etching » by Cathodic Bombardment.

According to preliminary results obtained by McCutcheon (1949) with silver alloys and steel, cathodic sputtering may be applied for rendering visible the crystalline structure of metals.

XI, 3. Optical Methods.

Of great importance for metallographic research, in particular for investigations on crystal growth, is the possibility of direct microscopic observation of test-pieces at high temperatures. A furnace for high-temperature miscrocopy, adapted to an ordinary microscope and allowing the investigation of surface structures up to temperatures of over 900 °C, was applied by Chalmers, King and Shuttleworth (1948) in their above-mentioned research on oxidation of silver.

Another field of application of the microscope is based on the use of polarized light. It is well-known that observation of crystalline surfaces under such circumstances is capable of revealing details not readily visible in unpolarized light (see f. i. Sachs, 1925; Von Schwarz, 1932). For aluminium, this is particularly true if the test-piece is first subjected to anodic oxidation (Lacombe and Beaujard, 1944, 1945; Hone and Pearson, 1948; Sperry, 1950). The oxide films formed in this way appear in different colours when viewed under crossed nicols. According to Perryman and Lack (1951) the polarization effects are due to a surface structure and are not caused by optical anisotropy of the oxidized film.

An interesting recent application of polarized light is made by

Woodart (1949) in an investigation of the deformation of monel metal : in the photographs published in the paper the gradual development of inhomogeneous distortions inside individual grains is clearly visible. The method is of course especially suited for investigating stress development when deforming non-metallic transparent crystals : in this field important work has been done with silver-chloride by Nye (1948; 1949*a*; 1949*b*).

Very promising is Tolansky and Holden's recent application (1949) of multiple-beam interference methods to the study of surface displacements occurring when straining metal crystals. By this method displacements of a few Å can be evaluated. Good results were obtained with aluminium and tin crystals, where slip lines were clearly visible and average slip steps were of the order of 900 Å for aluminium and 50-350 Å for tin, which is of the same order of magnitude as observed by Heinderich and Shockley for aluminium (see below). With aluminium it could moreover be concluded that the blocks between slip zones were tilted through angles of the order of 6′.

Concluding this section we mention the technique used by Beck and co-workers (1948) for counting grain numbers in recrystallized metal plates by illuminating the surface by differently coloured light beams emerging from different points, a technique also applied in former work by Van Arkel (unpublished).

XI, 4. Electron Microscope.

A recent collection of papers on *Metallurgical Applications of the Electron Microscope* has been edited by the Institute of Metals (London 1949). The number of such applications using a replica method generally combined with shadow casting, increases continuously. A simple replica technique is described by Shaefer and Harker (1942) and, somewhat modified, by Radevitch (1949). In the hands of Heidenreich and Shockley (1948) the method has given important results concerning the fine-mechanism of the development of glide bands during plastic deformation of aluminium crystals. The thickness of individual lamellae was found to be about 200 Å and the relative displacement of adjacent lamellae about 2000 Å, a number of lamellae gradually filling-up a « visible » glide band.

These results were confirmed and extended by Brown (1949). Moreover, Heidenreich (1948; 1949) found that cold-worked aluminium possesses a « granular » structure of somewhat variable size of the order of 200-800 Å, existing within domains of about 1-2 μ in diameter. This is of special interest in connection with Buckwell and Geach's observation (1949) of an extremely parallel striation on the surface of electrolytically polished crystals of high-purity aluminium at distances of about 600 $\pm$ 100 Å. Castaing and Guinier (1949), in an investigation of the age-hardening of copper aluminium alloys, observed a selective segregation of the phase Al_2Cu θ' at points about 1000 Å apart along the boundaries of sub-grains inside the polygonized crystals, revealing perhaps the individual dislocations between the slightly disoriented polygons with orientation differences of the order of a few minutes of arc.

XI, 5. Emission Microscope.

The above relates to the « normal » electron microcope. As to the application of the emission microscope in physical metallurgy, it is rather astonishing that after the preliminary results obtained in this field with low magnification (about 30 — 100 times) by Brüche, Mahl, Schenk, Knecht and others in Germany, Burgers and Ploos van Amstel in Holland, Johnson and Shockley, Ahearn and Becker in the United States, not very much progress has been made. References to these older researches (up to about 1938) can be found in Burgers and Ploos van Amstel (1937; 1938) (see also Allen, 1950).

Yet, when reviewing the results obtained in these first applications, as well with regard to the direct observation of allotropic changes and recrystallization phenomena as to the mechanism of activation and surface diffusion, one feels justified to expect that this method must be able to yield valuable information about metallographical problems. Papers have actually been published regarding the possibility of developing a high-resolving emission microscope by Boersch (1942) Kinder (1942), Mahl (1942), Mecklenburg (1942) and Recknagel (1941; 1942) (a survey is given by Brüche, 1942), from which it appears that, for suitably shaped cathodes and suitable magnitudes of the applied accelerating field ($\sim$ 100 KV/cm), a resolving power of the order of 100 Å may be expected. At present an emission microscope for practical application, up to a magnification of about

5000 times, is in state of construction in the Philips Research Laboratories by Rathenau. Preliminary results obtained with this instrument were reported at the Conference on Electron Microscopy held at Delft (1949) and at that at Paris (1950) by Rathenau and, more in detail, in a paper by Rathenau and Bass (1951) to which we referred several times in foregoing chapters when discussing boundary migration and twinning.

In this section it seems adequate to refer also to a new electron microscope developed for the intervention of oxide cathodes by Jacob (1949), which enables the selection and exploration of small emitting areas by applying a modulating electrode placed in front of the cathode, which functions as an image diafragm.

XI, 6. Field Emission.

This survey would be incomplete without calling attention to the extremely interesting results obtained by studying the field emission from single-metalcrystal points, at first by Müller (1937; 1938; 1949) in Germany and somewhat later by Benjamin and Jenkins (1938; 1940; 1942) in England (see also the survey given by Suhrmann, 1950).

Benjamin and Jenkins obtained the required high field strengths of for example 10^8 V/cm by mounting a metal point with a radius of the order of 10^{-5} cm in the centre of a glass bulb with a diameter of a few cm and applying a voltage of a few thousand volts between metal point and bulb surface. The emission patterns were directly observed on a fluorescent screen covering the inside surface of the bulb. The metals were investigated both in the clean state and when covered with minute quantities of for example thorium, barium and sodium. The changes in emission pattern with time at constant temperatures were a direct indication for surface migration, either of the atoms of the metal proper or of those of the evaporated metals. On pure tungsten for example migration occurred already at temperatures as low as 1170° K; for molybdenum at 770° K and for nickel at 370° K. Moreover, Benjamin and Jenkins observed in their apparatus the actual activation of tungsten, due to diffusion of thorium atoms through the tungsten crystal to its surface. It was so found

that the thorium diffuses in the tungsten lattice along preferential directions, such as [311] and [111] (*).

XI, 7. X-Ray Diffraction.

The study of structural irregularities *inside* coherent lattice domains has been the subject of much research in recent years, both theoretical and experimental, partly in connection with the study of the segregation mechanism taking place in age-hardening alloys. It is impossible, and falls also somewhat outside the scope of this report, to discuss these researches and it may suffice to give some references.

For theoretical considerations of lattice distortions in general we refer to a comprehensive paper by Bouman (1951); for research on age-hardening to papers by Guinier and co-workers (see Guinier 1942; 1945; 1949). The study of diffuse bands in Laue photographs, so-called Preston-Guinier zones, plays an important part in this type of investigations. This is particularly evident from a paper by Geisler and Hill (1948) on aged Al-Ag and Al-Mg-Si alloys.

We call also attention to important work by Bertaut (1949; 1950) and by Warren and Averbach (1949; 1950), which shows that Fourier analysis of the profile of diffraction lines may yield important conclusions regarding the size and state of perfection of lattice domains.

In what follows we restrict ourselves to the discussion of some diffraction techniques, which differ from « classical » diffraction methods and which have been applied in recent years for obtaining information concerning the mosaic character of crystals. Among these we must mention particularly the *divergent beam technique* and the *focussing technique*.

XI, 8. Divergent Beam Technique.

The application of a divergent X-ray beam with large aperture gives rise to the appearance, on the photographic plate, of dark and white lines in the general background, known as *reflection* and *extinction* lines. The principle of their formation is due to the fact

(*) Direct observations concerning surface migration by means of electron emission patterns have been observed by several investigators : Brüche and Mahl (1935; 1936); Johnson and Shockley (1936); Ahearn and Becker (1936); Burgers and Ploos van Amstel (*Physica* 1937; 1938); Becker and Moore (1940); Daniel (1942); Nichols (1942).

that monochromatic rays, coming from a point source and falling on the crystal, are reflected by a definite lattice plans under a definite angle of incidence. All rays fulfilling this condition form the surface of a cone. Fig. XI, 2, due to Lonsdale (1947), will help to make this clear. The transmitted rays form the continuation of this cone. They suffer by the reflection an extra loss in intensity as compared with rays going in non-reflecting directions and therefore give rise

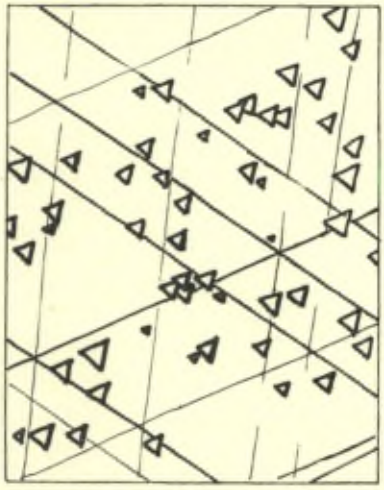

Fig. XI, 1. — Parallelism of the three slip lines with the sides of the equilateral etch figures obtained on an aluminium crystal surface parallel to a 111-plane × 650; reduced 25 % in reproduction. (Drawing after a photograph by Lacombe and Beaujard, 1947).

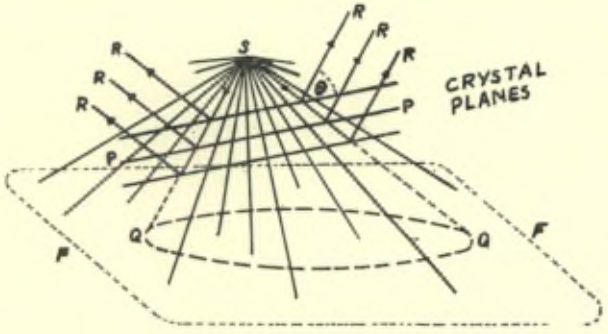

Fig. XI, 2. — Removal of a cone of X-rays, by reflection, from the general divergent beam, emitted by the point source at S. PP : reflecting planes; RR : reflected rays; QQ : extinction line of lower photographic density as compared with the general background; F : photographic film. (After Lonsdale, 1947).

Fig. XI, 3. — A small relative displacement of two extinction lines which intersect nearly tangentially, causes a considerable change in the distance between their points of intersection PQ → P'Q'.

to a line of lower density on the photographic plate, QQ in fig. XI, 2, this line being the intersection of the film (F) with the said cone. Similarly, the reflected « cone » will produce a line of higher density on the film. The resulting effect has been produced in various ways by different authors and has been applied to the study of structural features of crystals, particularly by Lonsdale (1943; 1944*a*; 1944*b*; 1947), by Geisler, Hill and Newkirk (1947; 1948) and by May (1949; 1950). Older references are given in these papers.

The applications of this method, which interest us here, are twofold. Firstly it appears that the sharpeness and intensity of the lines can be taken as an indication of the lattice (im) perfection : perfect crystals, due to the fact that the angular reflection region is so extremely narrow, do not give visible or in any case very indistinct divergent patterns, whereas « mosaic » crystals, with blocks small enough to exhibit only secundary extinction, give clear patterns. The sharpness of the lines allows to draw conclusions regarding the angular deviation of lattice blocks within a crystal. For example, for aluminium crystals obtained by recrystallization of cold-worked metal the extinction lines produced by Mo-$K\alpha_1$- and $K\alpha_2$-radiation were distinctly resolved at a distance ca 1 1/2 m from the point-source, from which fact May (1950) could deduce that the angular orientation differences between the separate mosaic blocks of the crystal under investigation could not exceed 1/2 minute of arc (*).

To other application is based on the fact that the extinction lines may serve to determine the lattice parameter of the crystal with very great accuracy : this is due to the fact that the position of the lines originating from a definite plane changes with changing Bragg-angle, and therefore with a change in lattice constant. Lines due to high-order reflections are particularly sensitive in this respect. If two lines on the film can be found which intersect nearly tangentially, then a relative small displacement of both lines may cause a consi-

(*) Plastic deformation of the crystals again destroys the pattern.

derable change in the distance between their points of intersection (cf. fig. XI, 3) and so enable an accurate measurement of the corresponding change in spacing. By applying this method Lonsdale (1947) could detect differences in spacing between various diamond crystals of the order of 0.01 ‰, whereas May (1949; 1950) in a search for possible differences in lattice constant between a « stimulating » and a « stimulated » crystal in recrystallized aluminium plate (cf. Chap. VI*B*, 4), could establish in this way that such differences, if present, must be less than 0.01 ‰. In a similar way Geisler, Hill and Newkirk (1948) determined small changes in parameter accompanying segregation in alloys.

XI, 9. Focussing Technique.

Guinier and Tennevin (1948; 1949*a*) applied a focussing X-ray beam, which permitted them to detect differences in parallelism existing inside a family of parallel lattice planes in a crystal slab. In this case a narrow beam of *polychromatic* X-rays, with *small* angular divergence, emitted by a point source S in fig. XI, 4, fall upon the crystal slab PP′ which is placed at a distance of about 50-100 cm from the X-ray source. It can be shown that the reflections of planes nearly perpendicular to the crystal slab are approximately focussed in a line, passing through a point M situated « at the other side » of the crystal at a distance approximately equal to its distance from the point source. Small deviations of parallelism between the reflecting planes cause a broadening of the reflection which, in general, shows a « fine-structure » made-up of separate lines. The method enables to detect angular differences smaller than 1/2 minute of arc, similar to those obtained by the divergent-beam method mentioned above.

The same experimental set-up was used by Guinier and Tennevin (1949*a*) in an alternative way : whereas in fig. XI, 4 the X-rays still came from the point source S at about 1/2 — 1 m distance in front of the crystal, the photographic film was now placed only a few cm behind the crystal, at F′ in fig. XI, 4. By means of a screen QQ′ placed in front of the crystal the exposed region was limited to about 5×5 mm. Under these circumstances, due to the focussing arrangement, a point-to-point correlation exists between a reflecting point of the crystal and the corresponding point of the « Laue spot ». If

therefore the exposed region contains more than one crystal, the shape of the different Laue spots due to a definite crystal is conform with the shape of this crystal in the slab. Different crystals thus give rise to differently-shaped spots and can be easily recognized (cf. fig. XI, 5). Moreover, if the crystal lattice is in some way or other irregular, for example it consists of somewhat differently oriented regions, this betrays itself in an unequal intensity distribution (« fine-structure ») of the « Laue spots ». An application hereof is shown in Chap. VI*B*, 6 on Plate 1.

The procedure is akin to that used by Barrett (1945). Here a fine-grained photographic plate is placed in contact with or very close to the specimen to be examined and reflections are recorded, produced by an X-ray beam striking the surface of the specimen. The image so obtained corresponds also point-to-point to the surface of the specimen and the intensity variations in the reflection record the distribution of inhomogeneous strain throughout the specimen. In this case the use of a fine-grained plate allows a proper magnification, so that strain inhomogeneities occupying distances of a few microns may be detected.

A modification of Barrett's method is described by Honeycombe (1950. *J. Inst. Metals*, *76*, 734) and applied by this author to the investigation of structural changes accompanying the deformation of single crystals. We mention in this connection also a microradiographic method described by Smoluchowski, Lucht and Hurd (1946). In this method the combination of selective absorption and diffraction in various grains of a test-piece reveals interesting structural details.

XI, 10. Micro-Camera Technique.

To get information about the size of individual lattice domains in a *fine-grained* test-piece, Kellar, Hirsch and Thorp (1950) applied a micro-camera with very narrow beam (about 35 μ), illuminating such a small volume of material that the continuous rings obtained with the usual techniques split up into individual diffraction spots. From the number of spots and their shapes, estimates of particle size and distortion could be obtained. The narrow beam was produced by means of fine-bore leadglass capillaries.

This technique was already applied earlier by Kreger (1945), who developped a micro-beam camera with X-ray beams down to a few μ for the structure investigation of biological objects. A full description of this camera is given in Kreger (1951).

For other micro-techniques we refer to Frevel and Anderson (1950).

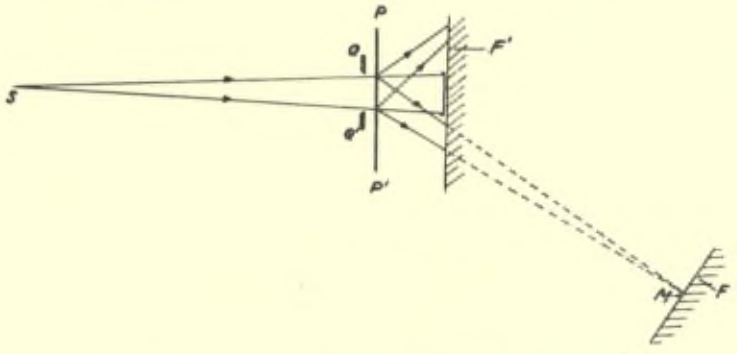

Fig. XI, 4. — Schematic representation of the focussing method and the Laue-variant of Guinier and Tennevin (1949).
S : point source of X-rays
PP' : crystal slab
QQ' : screen limiting the exposed region to a few mm width
M : focussing point
F : film in focussing position
F' : film in « Laue-position ».

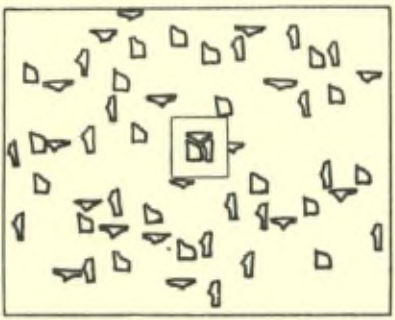

Fig. XI, 5. — « Laue-photograph » taken by Guinier and Tennevin with their method described in the foregoing figure, of a part of an aluminium test-piece containing three crystals (shown in centre of figure). Each crystal produces spots conforming to its shape. (Drawing after actual photograph in Guinier and Tennevin, 1949).

XI, 11. Geiger-Counter Technique.

This section would be incomplete without mentioning the increasing application of Geiger-counter technique for quantitative measurement of X-ray intensity in metallographic research. Averbach and Warren (1949) applied it when studying the structural changes accompanying cold-work and recovery (discussed in Chapt. IV, 3; cf. also Chapt. XI, 7); Decker, Seymour and Harker (1950) in a study of the course of recrystallization in rolled copper and nickel iron. It is also used in recent determinations of prefered orientations in textures by Decker, Asp and Harker (1948); Norton (1948); Field and Merchant (1949) and Schulz (1949). In the lastmentioned group of researches special mounting techniques are in some cases used to enable the complete pole-figure to be determined under constant absorption conditions. This is alzo realized by Custers (1948).

A movable-film camera technique for texture determination was developed by Smoluchowski and Turner (1950).

XI, 12. Electron Diffraction.

As to the application of electron diffraction to the study of recrystallization phenomena in metals, Heidenreich and Shockley (1948) applied electron diffraction to produce « Kichuchi lines », which, at least geometrically, are to some extent similar to the extinction and reflection lines in photographs taken with a divergent X-ray beam, although the cause of their formation is not the same. In analogy with what was said for X-rays, also the sharpness of the Kichuchi pattern can be used to get insight in the perfection of crystals : deformation causes them to disappear.

In a more recent paper, Heidenreich (1949) analyses the electron diffraction effect of thin metal foils on the basis of the dynamic theory of diffraction and shows that the combined study of electron microscopic *and* electron diffraction photographs may yield valuable indications about the finest details of their structure.

SUPPLEMENT

CHAPTER XII

PREPARATION OF TEST-PIECES CONTAINING ONE OR A FEW CRYSTALS WITH PRE-CHOSEN ORIENTATION

It appeared in the course of this report that it is of great value in recrystallization research to dispose of test-pieces consisting of one or more crystals with a pre-chosen orientation.

When preparing crystals from the melt this may be achieved by applying suitably oriented seed crystals, as was done by Chalmers (1937; 1940; 1949) and, more recently, by Aust and Chalmers (1950. *Proc. Roy. Soc. A 201*, 210) when preparing specimens of tin consisting of two or three crystals.

A note-worthy method to grow large flat crystals from the melt was developed by Lacombe and Beaujard (1947*a*; 1947*b*) for aluminium. The metal was melted in a furnace on top of a horizontal plate of kaoline of about 10-15 cm width and 1-3 mm thickness. The furnace was so constructed that a temperature gradient of about 10° was maintained along the length of the plate. The molten metal was surrounded by an oxide layer and so prevented from flowing. It was cooled from 700 °C down to 600 °C in 15 minutes. Large crystals were produced in this way, in particular in high-purity aluminium. The presence of « impurities », as iron and silicon, causes the development of smaller crystals, as they act apparently as nuclei for crystallization.

By feeding with suitably oriented germs, also this method is probably suited for the production of crystals with pre-chosen orientations.

Recently, however, the same result has been realized directly in the solid state by a special recrystallization method, originally due to Fujiwara (1939; 1941) and elaborated by Dunn (1949) for silicon iron and by Tiedema (1949) for aluminium.

In Tiedema's method the growth of a new crystal is started at one end of a critically deformed test-piece by pulling this end through a heating zone. The orientation of the crystal with regard to the test-piece (f. i. with regard to the surface plane of a flat piece or the

axis of a wire) is then determined by means of X-rays. Then, with the aid of a special holder (fig. III, 1) the not-yet recrystallized part of the test-piece is locally, in the immediate neighbourhood of the boundary of the crystal, subjected to a combination of bending and twisting so that the desired parallelism between the chosen directions of crystal lattice and text-piece is attained in the not-yet recrystallized part. If now the whole test-piece is again subjected to a suitable anneal by letting it pass through a furnace, the crystal continues its growth over the « curvature » into the fine-grained part of the test-piece : in this way (cf. fig. XII, 2) the desired correlation of directions is realized.

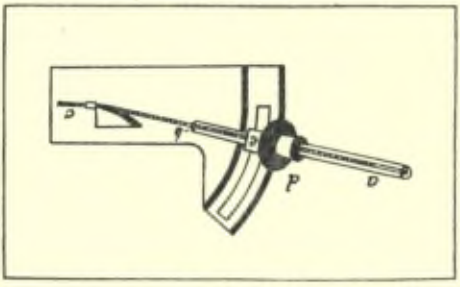

Fig. XII, 1. — Bending apparatus for aluminium wire. The single crystal wire (*c*) of length some cm, is fixed in the glass capillary (*a*) by means of a drop of molten wax (*b*). The wire can be rotated about its axis by means of the disc (*d*) and bent by means of the slide (*e*). (After Tiedema, 1949).

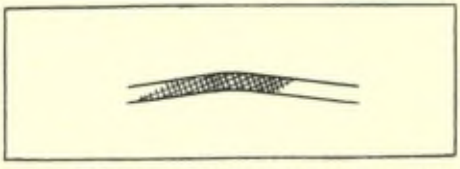

Fig. XII, 2. — Position of the crystal lattice in a bent wire. (After Tiedema, 1949).

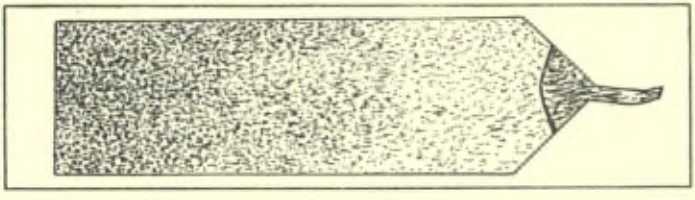

Fig. XII, 3. — Fine-grained specimen with reoriented seed crystal in the form of a small flag on end of narrow twisted part of the specimen. Nat. size (after Dunn, 1949).

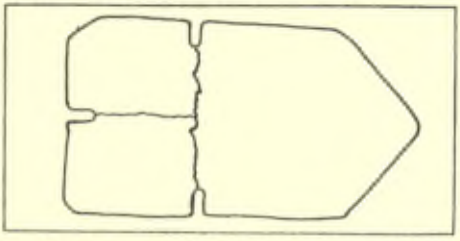

Fig. XII, 4. — Specimen composed of three grains, each having a pre-chosen orientation. The notches are introduced to anchor the grain boundaries during subsequent annealing operations which should bring the grain boundaries to the lowest energy configuration (after Dunn, 1949).

Dunn and Lionetti (1949) used test-pieces of the type schematically shown in fig. XII, 3 : a crystal was grown in the far end of the little « tail ». Then the tail, in its fine-grained part, was twisted at a point situated closely to the broader part, as indicated. By using test-pieces (sheets) with more than one « tail », this method made it possible to prepare sheets consisting of two or three crystals with previously chosen orientations (fig. XII, 4), which were used for the study of boundary displacement and boundary energy as function of the relative orientation of adjacent lattices, discussed in Chap. VII,1.

Tiedema (1949) prepared aluminium crystals both in wire and in plate form and used them in investigations on crystal growth and nucleation in material with a « narrow » texture : see Chap. VII, 6, Chap. VIII*A*, 3 and Chap. VIII*B* 3.

Moreover, the plate-shaped cristal could be prepared in a « curved » shape and used as monochromators for X-ray spectrographic work, for example in the Cauchois spectograph (Cauchois, Tiedema and Burgers, 1950).

REFERENCES

Achter, M. R. and R. Smoluchowski, Paper in « The Physics of Powder Metallurgy » (New York), p. 77 (1951).

Ahearn, A. J. and J. A. Becker, *Phys. Rev.*, **49**, (1936).

Allen, N. P., « Metall. Applic. of the Electr. Microsc. » (London : Institute of Metals), p. 1 (1950).

Anderson, W. A. and R. F. Mehl, *Trans. A. I. M. E. Inst. Met. Div.*, **161**, p. 140 (1945).

Arkel, A. E. (van), *Z. Metallk.*, **22**, p. 217 (1930).

Arkel, A. E. (van), *Polyt. Weekblad*, **26**, p. 397 (1932) (ref. in *Hdb. Metallphysik* III, **2**, p. 294 (1941).

Arkel, A. E. (van), *Rev. Métall.*, **33**, p. 197 (1936).

Arkel, A. E. (van) and M. G. Bruggen (van), *Z. Physik.*, **42**, p. 795 (1927).

Arkel, A. E. (van) and M. G. Bruggen (van), *Z. Physik*, **51**, p. 520 (1928).

Arkel, A. E. (van) and J. J. A. Ploos van Amstel, *Z. Physik.*, **62**, p. 43 (1930).

Averbach, B. L., *Metals Trans.*, **185**, p. 491 (1949).

Averbach, B. L. and B. E. Warren, *J. Appl. Physics*, **20**, p. 1066 (1949).

Avrami, M., *J. Chem. Physics*, **7**, p. 1103 (1939).

Avrami, M., *J. Chem. Physics*, **8**, p. 212 (1940).

Balicki, M., Chapter IV in « The Physics of Powder Metallurgy » (New York) (1951).

Barnes, R. S., *Nature*, **166**, p. 1032 (1950).

Barrett, C. S., *Metals Technol.*, **7**, *Tech. Publ.*, Nr. 1141 (1940).

Barrett, C. S., *Trans. A. I. M. E., Inst. Met. Div.*, **137**, p. 128 (1940).

Barrett, C. S., « Structure of Metals » (New York : Mac Graw Hill) (1943).

Barrett, C. S., *Trans. A. I. M. E., Techn. Publ.*, Nr. 1865 (1945).

Barrett, C. S., « Transformations in Pure Metals », Symposium on Transformations in Solids, Cornell University (1948).

Barrett, C. S. and L. H. Levenson, *Trans. A. I. M. E.*, **137**, p. 112 (1940).

Beck, P. A. *J. Appl. Physics*, **20**, p. 633 (1949).

Beck, P. A. L, M. L. Holzworth and Ph. R. Sperry, *Trans. A. I. M. E., Techn. Publi.*, Nr. 2475 (1948).

Beck, P. A. and Hsun Hu, *Metals Trans.*, **185**, p. 627 (1949).

Beck, P. A. and Hsun Hu, *Metals Trans., J. Metals*, **188**, p. 1215 (1950).

Beck, P. A., J. C. Kremer, L. Demer and M. L. Holzworth, *Trans. A. I. M.E., Metals Technol.*, **175**, p. 372 (1948).

Beck, P. A. and Ph. R. Sperry, *J. Appl. Physics*, **21**, p. 150 (1950).

Beck, P. A., Ph. R. Sperry and Hsun Hu, *J. Appl. Physics*, **21**, p. 420 (1950).

Becker, J. A. and G. E. Moore, *Phil. Mag.*, **29**, p. 129 (1940).

Becker, J. J., *Trans. A. I. M. E., J.Metals*, **191**, p. 115 (1951).

Becker, R., *Z. Metallk.*, **29**, p. 245 (1937).

Becker, R., *Proc. Phys. Soc.*, **52**, p. 71 (1940).

Becker, R. and W. Döring, *Ann. Phys.*, **24**, p. 719 (1935).

Benedicks, C., *Koll. Z.*, **91**, p. 217 (1940).

Benjamins, M. and R. O. Jenkins, *Phil. Mag.*, **26**, p. 1049 (1938).

Benjamins, M. and R. O. Jenkins, *Proc. Roy. Soc.* (London), *A* **176**, p. 262 (1940).

Benjamins, M. and R. O. Jenkins, *Proc. Roy. Soc.* (London), *A* **180**, p. 225 (1942).

Bertaut, E. F., *C. R.*, **228**, p. 492 (1949).

Bertaut, E. F , *Acta Cryst.*, **3**, p. 14 (1950).

Bilby, B. A., *J. Inst. Metals*, **76**, p. 613 (1950).

Boas, W. and E. Schmid, *Z. Techn. Physik*, **12**, p. 71 (1931).

Boersch, H., *Naturwiss.*, **30**, p. 120 (1942).

Borelius, G., *Arkiv för Matematik, Astronomi och Fysik*, K. Svenska Vetenskapsakademien, **32** *A*, p. 1 (1945).
Borelius, G., *J. Inst. Metals*, **73**, p. 17 (1947).
Borelius, G., *Physica*, **15**, p. 135 (1949).
Bouman, J., « Selected Topics in X-ray Crystallography » (Amsterdam), p. 80 ff. (1951).
Bowles, J. S., *Trans. A. I. M. E., J. Metals*, **191**, p. 44 (1951).
Bowles, J. S., *Acta Cryst.*, **4**, p. 162 (1951).
Bowles, J. S. and W. Boas, *J. Inst. Metals*, **74**, p. 501 (1948).
Bragg, W. L., *Proc. Phys. Soc.*, **52**, p. 54 (1940).
Brown, A. F., *Nature*, **163**, p. 961 (1949); « Symp. Metall. Applic. of the Electron Microscope » (London), p. 103.
Brüche, E., *Koll. Z.*, **100**, p. 192 (1942).
Brüche, E. and H. Mahl, *Z. Techn. Physik*, **16**, p. 623 (1935).
Brüche, E. and H. Mahl, *Z. Techn. Physik*, **17**, pp. 81 and 262 (1936).
Bucknell, G. L. and G. A. Geach, *Nature*, **164**, p. 231 (1949).
Burke, J. E., *Metals Technol.*, October, Techn. Publ., Nr. 2472 (1948).
Burke, J. E., *Trans. A. I. M. E., J. Met.*, **188**, p. 1324 (1950).
Burke, J. E. and Y. G. Shiau, *Trans. A. I. M. E.*, **175**, p. 141 (1948).
Burgers, J. M., *Proc. Phys. Soc.* (London), **52**, p. 23 (1940).
Burgers, W. G., « Pap. Disc. Internat. Conf. Physics », Vol. II, (London), p. 139 (1934).
Burgers, W. G., « Rekristallisation, Verformter Zustand und Erholung », in Masing : « Handbuch der Metallphysik », Vol. III, 2 (Leipzig : Becker and Erler. (1941).
Burgers, W. G., *Physica*, **9**, p. 987 (1942).
Burgers, W. G., *Rec. Trav. Chim.* (Pays-Bas), **64**, p. 20 (1945).
Burgers, W. G., *Proc. Acad. Sc.* (Amsterdam), **50**, p. 452 ff. (1947); *J. Chimie Physique*, **44**, p. 292 (1947*a*).
Burgers, W. G., *Physica*, **15**, p. 92 (1949).
Burgers, W. G. and J. C. M. Basart, *Z. Physik.*, **51**, p. 545 (1928).
Burgers, W. G. and J. C. M. Basart, *Z. Physik.*, **54**, p. 74 (1929).
Burgers, W. G. and V. Ch. Dalitz, *Proc. Kon. Ned. Akad. v. Wetensch.* (Amsterdam), **52**, p. 623 (1949).
Burgers, W. G. and F. M. Jacobs, *Physica*, **1**, p. 561 (1934).
Burgers, W. G. and P. C. Louwerse, *Z. Physik.*, **67**, p. 605 (1931).
Burgers, W. G. and W. May, *Rec. Trav. Chim.* (Pays-Bas), **64**, p. 5 (1945).
Burgers, W. G. and J. J. A. Ploos van Amstel, *Physica*, **4**, p. 5 and 15 (1937).
Burgers, W. G. and J. J. A. Ploos van Amstel, *Physica*, **5**, p. 305; *Metallwirtschaft*, **17**, p. 648 (1938).
Burgers, W. G. and J. J. A. Ploos van Amstel, « Handbuch der Metallphysik » III, 2 (Leipzig), p. 84 (1941).
Burgers, W. G. and J. Sandee, *Physica*, **9**, p. 996 (1942).
Burgers, W. G. and T. J. Tiedema, *Proc. Acad. Sc.* (Amsterdam), **53**, p. 1525 (1950).
Cabrera, N., « Sintering of Metallic Particles », *J. Metals*, **188**, p. 667 (1950).
Cahn, R. W., *J. Inst. Metals*, **76**, p. 121 (1949).
Cahn, R. W., *Proc. Phys. Soc.* (London), **63**, p. 323 (1950).
Calnan, E. A. and B. D. Burns, *J. Inst. Metals*, **77**, p. 445 (1950).
Calvet, J.. *C. R. Acad. Sci.* (Paris), **200**, p. 66 (1935).
Calvet, J., Trillat J. J. and M. Paic, *C. R. Acad. Sci.* (Paris), **201**, p. 426 (1935).
Carpenter, H. C. H. and C. F. Elam, *J. Inst. Metals*, **24**, p. 83 (1920).
Castaing, R. and A. Guinier, *C. R. Acad. Sci* (Paris), **228**, p. 2033 (1949).
Cauchois, Y., T. J. Tiedema and W. G. Burgers, *Acta Cryst.*, **3**, p. 372 (1950).
Chalmers, B., *Proc. Roy. Soc., A* **162**, p. 120 (1937).
Chalmers, B., *Proc. Roy. Soc. ,A* **175**, p. 100 (1940).
Chalmers, B., *Proc. Roy. Soc., A* **196**, p. 64 (1949).
Chalmers, B., King R. and R. Shuttleworth, *Proc. Roy. Soc., A* **193**, p. 465 (1948).
Chaudron, G., *J. Inst. Metals*, **76**, p. 1 (1949).

Chaudron, G., Lacombe P. and N. Yannaquis, *C. R. Acad. Sci.* (Paris), **226**, p. 1372 (1948).
Cherian, T. V., Pietrokowsky P. and J. E. Dorn, *Metals Trans.*, **185**, p. 948 (1949).
Chevigny, R., *Rev. de l'Aluminium*, **23**, p. 153 (1946).
Cohen, M., Machlin E. S. and V. G. Paranpje, *Trans. A. S. M.*, **42A**, p. 242 (1950).
Coheur, P. and C. S. Barrett, *Trans. A. I. M. E., Techn. Publ.*, p. 2104 (1946).
Coheur, P. and J. M. Lejeune, *Rev. Univ. des Mines*, **9**, p. 3 (1945).
Coheur, P. and J. M. Lejeune, *Rev. Mètall.*, **46**, p. 439 (1949).
Collins, J. A. and C. H. Mathewson, *Metals Techn.*, **7**, *Techn. Publ.*, Nr. 1145 (1940).
Cook, M. and C. Macquarie, *Met. Techn.*, **5**, *Techn. Publ.*, Nr. 974 (1938).
Cook, M. and T. L. Richards, *J. Inst. Metals*, **66**, p. 1 (1940).
Cook, M. and T. L. Richards, *J. Inst. Metals*, **73**, p. 1 (1946).
Cook, M. and T. L. Richards, *J. Inst Metals*, **78**, p. 463 (1951).
Cottrell, A. H., in B. Chalmers : « Progress in Metal Physics », I (London), pp. 93-94 (1949).
Cottrell, A. H. and V. Aytekin, *J. Inst. Metals*, **77**, p. 389 (1950).
Custers, J. F. H., *Physica*, **14**, pp. 453 and 461 (1948).
Custers, J. F. H. and G. W. Rathenau, *Physica*, **8**, p. 759 (1941).
Dalitz, V. Ch. and W. G. Burgers, *Proc. Acad. Sc.* (Amsterdam), **52**, p. 627 (1949).
Daniel, J. H., *Phys. Rev.*, **61**, p. 657 (1942).
Decker, B. F., Asp E. J. and D. Harker, *J. Appl. Physics*, **19**, p. 388 (1948).
Decker, B. F. and D. Harker, *Trans. A. I. M. E., J.Metals*, **188**, p. 887 (1950).
Dedrick, J. H. and A. Gerds, *J. Appl. Physics*, **20**, p. 1042 (1949).
Dehlinger, U., *Ann. Physik* (5), **2**, p. 749 (1929).
Dehlinger, U., *Metallw.*, **12**, p. 48 (1933).
Desch, C. H., *J. Inst. Metals*, **22**, p. 241 (1919).
Desch, C. H., *Rec. Trav. Chim.* (Pays-Bas), **42**, p. 822 (1923).
Dunn, C. G., « Symposium on Cold Working of Metals A. S. T. M. » (1948).
Dunn, C. G. and F. W. Daniels, *Trans. A. I. M. E., J. Metals*, **191**, p. 147 (1951).
Dunn, C. G., Daniels F. W. and M. J. Bolton, *Trans. A. I M. E., J. Metals* **188**, p. 368 (1950*a*).
Dunn, C. G., Daniels F. W. and M. J. Bolton, *Trans. A. I. M. E., J. Metals*, **188**, p. 1245 (1950*b*).
Dunn, C. G., Lionetti, F. *Trans. A. I. M. E., J. Metals*, **185**, p. 125 (1949).
Elam, C. F., *Trans. Faraday Soc.*, **32**, p. 1604 (1936).
Ellis, W. C. and R. G. Treuting, *Trans. A. I. M. E., J. Metals*, **189**, p. 53 (1951).
Fensham, F. J., *Australian J. Scient. Res., A* **3**, p. 105 (1950).
Field, M. and M. E. Merchant, *J. Appl Physics*, **20**, p. 741 (1949).
Fisher, J. C., Hollomon J. H. and D. Turnbull, *J. Appl. Physics*, **19**, p. 715 (1948).
Frank, F. C., « Report Conference on Strength of Solids », p. 46 (1948).
Frevel, L. K. and H. C. Anderson, *Acta Cryst.*, **4**, p. 186 (1951).
Fullman, R. L., *J. Appl. Physics*, **21**, p. 1069 (1950), also **22**, p. 1350 (1951).
Fujiwara, T., *J. Sc. Hiroshima Univ., A* **9**, p. 227 (1939).
Fujiwara, T., *J. Sc. Hiroshima Univ., A* **11**, p. 89 (1941).
Geach, G. A. and F. O. Jones, *Research*, **11**, p. 493 (1949).
Geisler, A. H., and J. K. Hill, *Acta Cryst.*, **1**, p. 238 (1948).
Geisler, A. H., Hill J. K. and J. B. Newkirk, *Phys. Rev.*, **72**, p. 983 (1947).
Geisler, A. H., Hill J. K. and J. B. Newkirk, *J. Appl. Physics*, **19**, p. 1041 (1948).
Göler, Frhr. (von) and G. Sachs, *Z. Physik*, **77**, p. 281 (1932).
Graf, L., *Z. Elektrochemie*, **48**, p. 181 (1942).
Greenough, G. B. and E. M. Smith, *J. Inst. Metals*, **77**, p. 435 (1950).
Guinier, A. J., *J. Phys. Radium*, (8), **3**, p. 124 (1942).
Guinier, A. J., *Proc. Phys. Soc.* (London), **57**, p. 310 (1945).
Guinier, A. J., *Physica*, **15**, p. 148 (1949).
Guinier, A. J., and P. Lacombe, *Métaux et Corrosion*, **24**, p. 212 (1948).

Guinier, A. J. and J. Tennevin, *C. R. Acad. Sci.* (Paris), **226**, p. 1530 (1948).
Guinier, A. J. and J. Tennevin, *Acta Cryst.*, **2**, p. 133 (1949*a*).
Guinier, A. J. and J. Tennevin, *Philips Res. Rep.*, **4**, p. 316 (1949*b*).
Harker, D. and E. R. Parker, *Trans. Am. Soc. Metals*, **34**, p. 156 (1945).
Heidenreich, R. D., Symposium « Cold Working of Metals », *Am. Soc. Met.*, **87**, p. 57 (1948).
Heidenreich, R. D., *J. Appl. Physics*, **20**, p. 993 (1949).
Heidenreich, R. D. and W. Shockley, « Report of a Conference on Strength of Solids, Bristol », p. 57 (1947).
Herring, C., *J. Appl. Physics*, **21**, p. 301 (1950).
Hobstetter, J. N., *Metals Techn., Techn. Publ.*, Nr. 2447 (1948).
Hone, A. and E. C. Pearson, *Metal Progress*, **53**, p. 363 (1948).
Iweronowa, W. and G. Schdanow, *Techn. Physics U. S. S. R.*, **1**, p. 64 (1934).
Jacob, L., *J. Scient. Instr.*, **26**, p. 262 (1949).
Jacquet, P., *Métaux et Corrosion*, **13**, p. 86 (1938).
Jillson, D. C., *Trans. A. I. M. E., J. Metals*, **188**, p. 1009 (1950).
Johnson, R. P. and W. Shockley, *Phys. Rev.*, **49**, p. 436 (1936).
Johnson, W. A. and R. F. Mehl, *Trans. A. I. M. E., Inst. Met. Div.*, **135**, p. 416 (1939).
Karnop, R. and G. Sachs, *Z. Physik*, **42**, p. 283 (1927).
Kellar, J. N., Hirsch P. B. and J. S. Thorp, *Nature*, **165**, p. 554 (1950).
Kieffer, R. and W. Hotop, « Pulvermetallurgie und Sinterwerkstoffe » (Berlin) (1943).
Kinder, E., *Naturwiss.*, **39**, Heft 38-39 (1942).
Kochendörfer, A., *Z. Metallk.*, **41**, p. 33 (1950).
Kornfeld, M., *Phys. Z. Sowj. Union*, **6**, p. 170 (1934).
Kornfeld, M. and F. Rybalko, *Phys. Z. Sowj. Union*, **12**, p. 658 (1937).
Kostron, H., *Z. Metallk.*, **41**, p. 370 (1950).
Kreger, D. R., *Proc. Acad. Sc.* (Amsterdam), **48**, p. 336 (1945).
Kreger, D. R., in J. Bouman : « Selected Topics in X-ray Crystallography » (Amsterdam), p. 340 (1951).
Kronberg, M. L. and F. H. Wilson, *Metals Trans., J. Metals*, **185**, p. 501 (1949).
Krupkowski, A. and M. Balicky, *Ann. Acad. Sci. Techn.* (Varsovie), **4**, p. 270 (1937).
Krupkowski, A. and M. Balicky, *Rev. Métall.*, **36**, p. 21 (1939).
Kuczynski, G. C., *J. Appl. Physics*, **20**, p. 1160 (1949).
Kuhlmann, D., G. Masing and J. Raffelsieper, *Z. Metallk.*, **40**, p. 241 (1949).
Kulin, S. A. and M. Cohen, *Trans. A. I. M. E.*, **186**, p. 1139 (1950).
Lacombe, P., « Report Bristol Conference », p. 91 (1948).
Lacombe. P. and L. Beaujard, « Etudes sur les aspects des pellicules d'oxydation anodique formée sur l'aluminium et ses alliages » (Paris), p. 73 (1944).
Lacombe, P. and L. Beaujard, « Journées des Etats de Surface » (Paris), p. 44 (1945).
Lacombe, P. and L. Beaujard, *C. R. Acad. Sci.* (Paris), **224**, p. 116 (1947*a*).
Lacombe, P. and L. Beaujard, *J. Chim. Physique*, **44**, p. 269 (1947*b*).
Lacombe, P. and L. Beaujard, *J. Inst. Metals*, **74**, p. 1 (1947*c*).
Lacombe, P. and A. Berghezan, **228**, p. 93 (1949*a*).
Lacombe, P. and A. Berghezan, *Métaux et Corrosion*, Janvier (1949*b*).
Lacombe, P. and A. Berghezan, *Physica*, **15**, p. 161 (1949*c*).
Laloeuf, A. and C. Crussard, *Rev. Métall.* **48**, p. 461 (1951).
Laurent, P., *Rev. Métall.*, **42**, p. 22 (1945).
Liempt (van), J. A. M., *Z. Anorg. Allg. Chem.*, **195**, p. 366 (1931).
Lonsdale, K., *Nature*, **151**, p. 52 (1943).
Lonsdale, K., *Nature*, **153**, p. 22 (1944*a*).
Lonsdale, K., *Nature*, **153**, p. 433 (1944*b*).
Lonsdale, K., *Phil. Trans. Roy. Soc.* (London), *A* **240**, p. 219 (1947).
Lücke, K., *Z. Metallk.*, **41**, p. 114 (1950).
Lücke, L. and G. Masing, *Z. Metallk.*, **39**, p. 291 (1948).
Mackenzie, J. K. and R. Shuttleworth, *Proc. Phys. Soc. B* **62**, p. 833 (1949).

Maddin, R., Mathewson, C. H. and Hibbard, W. R. *Metals Trans.*, **185,** p. 527 (1949).
Mahl, H., *Z. Techn. Phys.*, **17,** p. 653 (1936).
Mahl, H., *Z. Techn. Phys.*, **23,** p. 117 (1942).
Mahl, H. and I. N. Stranski, *Z. Physik. Chem.*, **52,** p. 257 (1942).
May, W., *Nature*, **163,** p. 569 (1949).
May, W., Thesis (Delft) (1950).
McCutcheon, M., *J. Appl. Physics*, **20,** p. 414 (1949).
McKee, J. H., « Phys. Soc. Conference » (Bristol), p. 106 (1948).
Mecklenburg, W., *Z. Phys.*, **120,** p. 21 (1942).
« Metallurgical Applications of the Electron-Microscope » (London : Institute of Metals) (1949).
Mott, N. F., *Proc. Phys. Soc.* (London), **60,** p. 391 (1948).
Mott, N. F., *Physica*, **15,** p. 119 (1949).
Müller, E., *Z. Physik*, **106,** p. 541 (1937).
Müller, E., *Z. Physik*, **108,** p. 668 (1938).
Müller, E., *Z. Physik*, **126,** p. 642 (1949).
Müller, H. G., *Z. Metallk.*, **31,** p. 322 (1939).
Nabarro, F. R. N., « Symposium on Internal Stresses in Metals and Alloys » (London : Institute of Metals), p. 237 (1947).
Nichols, M. H., *Phys. Rev.*, (abstr.), **61,** p. 390 (1942).
Norton, J. T., *J. Appl. Physics*, **19,** p. 1176 (1948).
Nye, J. F., *Nature*, **161,** p. 367 (1948).
Nye, J. F., *Proc. Roy. Soc.* (London), *A* **198,** p. 190 (1949*a*).
Nye, J. F., *Proc. Roy. Soc.* (London), *A* **200,** p. 47 (1949*b*)
Orowan, E., Comm. Congr. Soc. Franç. Mét. (Paris) (1947).
Perryman, E. W. C. and J. M. Lack, *Nature* **167,** p. 479 (1951).
Petersen, C., *Metallforschung* **2,** p. 289 (1947).
Polanyi, M. and G. Sachs *Z. Metallk.* **17,** p. 227 (1925).
Radevich, J. F. *Metals Trans.* **185,** p. 395 (1949).
Rathenau, G. W., « Proc. Internat. Conf. on Electron-Microscopy » (Delft), p. 81 (1949).
Rathenau. G. W., « Journées Métallurgiques d'Automne » (Paris) (1950).
Rathenau, G. W. and G. Baas *Physica* **17** p. 117 (1951).
Rathenau, G. W. and J. F. H. Custers, *Philips Res. Rep.*, **4,** p. 241 (1949).
Read, W. T. and W. Shockley, *Phys. Rev.*, **78,** p. 275 (1950).
Recknagel, A., *Z. Phys.*, **117,** p. 689 (1941).
Recknagel, A., *Z. Phys.*, **120,** p. 331 (1942).
Sachs, G., *Z. Metallk.*, **17,** p. 299 (1925).
Sachs, G. and J. Spretnak, *Met. Techn.*, 7, *Techn. Publ.*, Nr. 1143 (1940).
Sandee, J., *Physica*, **9,** p. 741 (1942).
Schmid, E. and G. Wassermann, *Metallw.*, **10,** p. 409 (1931).
Schwarz (von), M., *Z. Metallk.*, **24,** p. 97 (1932).
Schwarzkopf, P., *Powder Metallurgy Bulletin*, **3,** p. 74 (1948).
Schulz, L. G., *J. Appl. Physics*, **20,** pp. 1030-1033 (1949).
Seymour, W. E, and D. Harker, *Trans. A. I. M. E., J. Metals*, **188,** p. 1001 (1950).
Shaefer, V. J. and D. Harker, *J. Appl. Physics*, **13,** p. 427 (1942).
Shaler, A. J., *Metals Trans.*, **185,** p. 796 (1949).
Shaler, A. J. and J. Wulff, *Ind. Eng. Chem.*, **40,** p. 838 (1948).
Shockley, W., and W. T. Read, *Phys. Rev.*, **75,** p. 692 (1949).
Skaupy, F., *Z. Metallk.*, **41,** p. 301 (1950).
Smith, C. S., *Trans. A. I. M. E.*, **175,** p. 15 (1948).
Smithells, C. J., « Metals Reference Book » (London), p. 238 (1949).
Smoluchowski, R., C. M. Lucht and J. M. Hurd, *J. Appl. Phys.*, **17,** p. 864 (1946).
Smoluchowski, R., and R. W. Turner, *J. Appl. Physics*, **20,** p. 745 (1949).
Smoluchowski, R., and R. W. Turner, *Physica*, **16,** p. 397 (1950).
Snoek, J. L., *J. Appl. Physics*, **22,** p. 109 (1951).
Sperry, Ph. R., *Trans. A. I. M. E., J.Metals*, **188,** p. 103 (1950).

Suhrmann, R., *Naturwiss*, **37**, p. 329 (1950).
Tammann, G., *Z. Anorg. Allg. Chem.*, **185**, p. 1 (1929).
Tammann, G., *Z. Metallk.*, **22**, p. 224 (1930).
Thorley, N., *J. Inst. Metals*, **77**, p. 141 (1950).
Tiedema, T. J., *Acta Cryst.*, **2**, p. 261 (1949).
Tiedema, T. J,. *Proc. Acad. Sc.* (Amsterdam), **53**, p. 1422 (1950).
Tiedema, T. J., W. May and W. G. Burgers, *Acta Cryst.*, **2**, p. 151 (1949).
Tolansky, S. and J. Holden, *Nature*, **164**, p. 754 (1949).
Turnbull, D., « *Metals Technol., Techn. Publ.* », Nr. 2365 (1948).
Turnbull, D. and J. C. Fisher, *J. Chem. Physics*, **17**, p. 71 (1949).
Turnbull, D. and J. H. Hollomon, Chapter VII in « The Physics of Powder Metallurgy » (New York) (1951).
Volmer, M., « Kinetic der Phasenbildung » (Dresden, Leipzig) (1939).
Walton, C. J., *Trans. Am. Electrochem. Soc.*, **85**, p. 239 (1944).
Warren, B. E. and B. L. Averbach, *J. Appl. Physics*, **20**, p. 885 (1949).
Warren, B. E. and B. L. Averbach, *J. Appl. Physics*, **21**, p. 595 (1950).
Wilms, G. R. and W. A. Wood, *J. Inst Metals*, **75**, p. 693 (1949).
Wood, W. A. and W. A. Rachinger, *J. Inst. Metals*, **76**, p. 237 (1949).
Wood, W. A. and R. F. Scrutton, *J. Inst. Metals*, **77**, p. 423 (1950).
Woodard, D. H., *Metals Trans.*, **185**, p. 722 (1949).

Discussion du rapport de M. W.G. Burgers

M. Guinier. — Avec la collaboration de J. Blin, nous avons étudié la diffusion des rayons X aux très faibles angles pour un métal à l'état écroui, restauré, recristallisé. Nous avons trouvé avec le cuivre et le nickel qu'un fort écrouissage (laminage) produit une diffusion s'annulant à quelques degrés. Jusqu'ici, pour l'aluminium, un tel effet n'a pas été trouvé. Cette diffusion n'est pas changée quand le métal est restauré (c'est-à-dire quand il donne des raies D.S. fines). Elle est à peu près supprimée par une recristallisation complète (fig. 1).

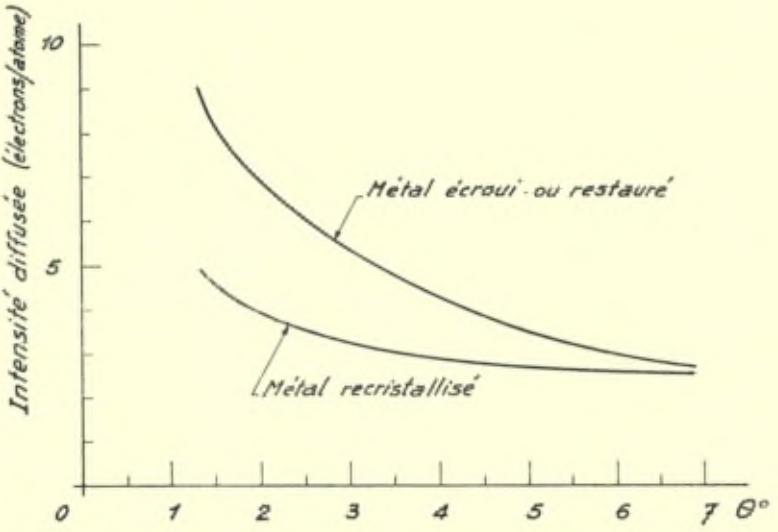

Fig. 1

La diffusion aux petits angles est caractéristique de la présence de variations locales de densité électronique. Les dislocations isolées (Wilson) n'ont aucun effet. L'interprétation la plus simple de l'effet observé est que l'écrouissage, quand il est assez violent, produit des vides, ou tout au moins des régions à faible densité. L'étendue

angulaire de la diffusion détermine le rayon de giration de ces lacunes. Pour le cuivre, nous avons trouvé 6 Å. Nous ne connaissons pas la forme de ces lacunes; en tout cas, elles comprendraient moins de 100 atomes. L'intensité absolue de la diffusion (extrapolée à l'angle O), donne le nombre de ces lacunes; cela correspond à une diminution de densité de l'ordre de quelques dix millièmes.

La restauration laisse intactes ces régions lacunaires; seules des régions de moindre désordre se perfectionnent par des faibles déplacements d'atomes.

Pendant la recristallisation, au contraire, il y a d'importants mouvements qui font disparaître les lacunes.

L'existence de ces grandes lacunes dans le métal écroui doit avoir une influence essentielle pour la détermination de la charge de rupture.

M. C. Crussard. — 1. A propos de la distinction faite par Dorn et ses collaborateurs entre ortho- et metarestauration, je voudrais signaler que nous avons fait des essais du même genre (au Centre des Recherches métallurgiques de l'Ecole des Mines), mais sur des éprouvettes polycristallines et monocristallines d'aluminium de haute pureté (99,99 et 99,997 %).

Dans ce cas, lorsqu'on étudie la forme des courbes de traction après le recuit de restauration et la manière dont elles prolongent la courbe de traction initiale, on ne trouve pas de limite nette entre les deux types de restauration; quand la température de recuit croît, on passe de façon continue et très graduelle du premier type de courbe (fig. IV, 1. du Rapport) au deuxième (fig. IV, 2). Pour s'en rendre compte quantitativement, nous avons utilisé la méthode d'analyse parabolique de la forme des courbes de restauration, développée dans notre laboratoire (1) et (2); la tension σ étant liée à l'allongement vrai ε par une loi parabolique de la forme

$$\sigma = \sigma_0 + a\,\varepsilon^m,$$

nos études ont montré que, dans un métal restauré, la valeur de l'exposant m était étroitement liée à la dimension des fragments (domaines de polygonisation plus ou moins parfaite) en lesquels sont décomposés les cristaux. Le résultat de cette analyse appliquée

(1) C. Crussard, *Rev. Métallurgie*, 1944, p. 111.
(2) B. Jaoul et C. Crussard, *Rev. Métallurgie*, 1950, p. 589.

au problème qui nous occupe est le suivant : l'exposant m varie de façon continue et progressive avec la température de restauration, indiquant une croissance continue de la dimension des fragments, sans que l'on puisse définir une température où le phénomène change d'allure.

Il est probable que la distinction en ortho- et metarestauration observée par Dorn est due à la présence d'impuretés, sans doute parce que les « nuages de Cottrell » formés autour des dislocations s'évaporent lorsque la température croît.

2. L'origine superficielle des germes de recristallisation dans les monocristaux faiblement écrouis, constatée par Burgers et Tiedema (p. 98 du Rapport) avait aussi été observée par nous (1). Nous avons également montré que l'astérisme des monocristaux étirés est plus fort dans les couches superficielles qu'à l'intérieur (1). Je crois que l'étude de l'orientation des germes formés dans ces conditions est d'un grand intérêt pour la théorie de la germination; nous avons en effet défini plusieurs types d'orientation des germes par rapport à celle du cristal initial (2); or, chaque cristal présente une individualité bien marquée, avec un type d'orientation des germes (ou parfois deux types, l'un près des « têtes » et l'autre près des « profils » des lignes de glissement). Ceci permet de conclure que, pour les faibles déformations, c'est le *mode d'écrouissage* qui détermine l'orientation des germes formés dans un recuit ultérieur; dans ce cas, il semble que les germes potentiels (domaines pouvant se transformer en germes) sont peu nombreux et que tous (ou un bon nombre d'entre eux) donnent des nouveaux cristaux lors du recuit.

Si l'on augmente le taux d'écrouissage préalable au recuit, le nombre de germes potentiels devient très grand et ceux qui se développent sont probablement ceux qui présentent des orientations favorables pour la croissance (selectivity of growth).

Remarquons que les cristaux « stimulés » appartiennent à la première catégorie d'expériences (faibles écrouissages) et que leur existence prouve seulement que les conditions de sélectivité de croissance ne jouent pas pour les faibles écrouissages; c'est ce que nous venons justement de montrer. Mais je ne crois pas qu'ils consti-

(1) C. Crussard, *Rev. Métallurgie*, 1944, p. 111.
(2) A. Laloeuf et C. Crussard, *Rev. Métallurgie*, 1951, p. 462.

tuent un argument général contre la sélectivité de croissance (cf. p. 128 du Rapport).

3. Il semble actuellement que l'on puisse décrire les joints entre deux cristaux de deux façons différentes :

(a) par des *parois de dislocation* comme Read et Shockley;

(b) par un réseau à deux dimensions de défauts locaux. Nous appellerons ces joints : *joints lacunaires* (misfit boundaries) (Mott, Ting-Sui-Ké).

On est d'accord pour admettre que, lorsque la désorientation entre les deux cristaux bordant le joint, θ, est faible, c'est le modèle (a) qu'il faut adopter. Pour de plus fortes valeurs de θ, la description en parois de dislocation perd son sens, et le modèle (b) semble préférable. Les valeurs critiques de θ séparant ces deux modes de description semblent être de l'ordre de 5 à 15°.

Il est bon d'insister sur deux autres propriétés qui permettent de distinguer les deux types de joint :

— au point de vue de la *mobilité*, les parois (a) ne sont mobiles que dans un sens (lorsqu'elles sont formées de dislocations identiques), et *seulement sous l'action de tensions de cisaillement*; dans ce sens, qui correspond à celui du vecteur de Burgers (J.M.) des dislocations, elles sont très mobiles. La mobilité constatée par certains auteurs au cours d'un recuit est due certainement à de petites tensions parasites (1). Les joints lacunaires, par contre, se déplacent par diffusion, soit normalement (par exemple dans la croissance des grains), soit tangentiellement (déplacement visqueux d'un grain par rapport à l'autre).

Au cours du fluage d'éprouvettes d'aluminium à haute température (1), on observe très bien une fragmentation des grains par polygonisation. Les joints de polygonisation sont d'abord du type (a) et ne se déplacent que normalement à leur place; puis, quand l'angle θ dépasse quelques degrés, ils deviennent capables de mouvements visqueux tangentiels, ce qui prouve qu'ils sont devenus du type (b).

— au point de vue de l'action sur les impuretés, les parois du type (a) drainent les atomes dissous qui sont situés dans leur voisinage, alors qu'il semble que les joints (b) les repoussent.

(1) G. Wyon et C. Crussard, *Rev. Métallurgie*, 1951, p. 121.

Il est difficile de dire s'il y a une différence de nature entre les deux types de joint, ou si, lorsque dans les parois de dislocation (a) la distance entre dislocations décroît, on ne passe pas *ipso facto* et progressivement à un joint possédant les propriétés du type (b).

Quoi qu'il en soit, il semble que la question de la germination par recristallisation puisse s'éclaircir en introduisant cette distinction entre deux types de joints, et en faisant l'hypothèse suivante : admettons, comme R.W. Cahn, que la formation de germe correspond à une polygonisation; au fur et à mesure que la polygonisation progresse, l'angle θ entre blocs voisins croît; si à un moment il peut devenir assez fort pour que la paroi du type (a) devienne un joint lacunaire du type (b), la mobilité du joint par diffusion devient beaucoup plus grande, et le germe potentiel devient germe réel capable de croître dans la matière voisine. Il semble que la germination consiste essentiellement en cette transformation du type de joint, par augmentation de la désorientation θ entre blocs voisins. On peut ainsi justifier l'hypothèse de Cahn que le temps d'incubation est inversément proportionnel à la courbure locale.

L'hypothèse que nous présentons ici s'accorde d'ailleurs en partie avec les suggestions faites par W.G. Burgers à la page 119 de son Rapport.

M. Burgers. — A la fin de sa deuxième remarque, le professeur Crussard dit : « Si l'on augmente le taux d'écrouissage préalable du recuit, le nombre de germes potentiels devient très grand et ceux qui se développent sont probablement ceux qui présentent des orientations favorables pour la croissance (selectivity of growth) ».

Selon l'avis de M. Tiedema et de moi-même, afin qu'un « germe potentiel » avec une certaine orientation puisse se développer, il est en premier lieu nécessaire qu'il puisse subir une polygonisation (cette expression prise dans le sens général de réarrangement de dislocations avec formation de parois) en avant des germes potentiels avec d'autres orientations, ainsi qu'il puisse les consumer (ce qui demande une différence assez grande entre l'orientation des domaines voisins).

Je suis d'accord avec M. Crussard que la présence des « cristaux stimulés » ne constitue pas un argument fort contre la sélectivité de croissance, vu spécialement le fait que la différence en vitesse de

croissance entre « cristal stimulant » et « cristal stimulé » est assez petit (de l'ordre de quelques pour cents, selon May (thèse Delft [1950]).

J'ai pris connaissance avec beaucoup d'intérêt de l'hypothèse concernant le mécanisme précis de la germination (cf. troisième remarque).

M. Dehlinger. — Für die Unterscheidung der verschiedenen Erscheinungen, die als Erholung und Rekristallisation bezeichnet werden, scheint mir der Gesichtspunkt der Reaktionsordnung wichtig zu sein, auch wenn man diese in festen Körpern noch nicht so genau bestimmen kann wie in Gasen. Bekanntlich versteht man unter Reaktionsordnung eines Vorgangs die Zahl der statistisch unabhängigen Ereignisse, die notwendig sind um den Vorgang hervorzururen. In unserem Fall wird es sich vielfach um die Zahl der Versetzungen handeln, die gleichzeitig aufgelöst oder bewegt werden müssen, um eine bestimmte Art der Erholung oder Rekristallisation hervorzubringen. So ist wahrscheinlich die Erholung, die nach einer reinen Schubverformung eintritt, eine Reaktion von nahezu erster Ordnung. Dagegen kommt die Polygonisation durch die gemeinsame Bewegung mehrerer Versetzungen zustande. Für die echte Rekristallisation gibt es anscheinend mindestens zwei verschiedene Arten der Keimbildung. Sie unterscheiden sich von den Erholungsvorgängen dadurch, dass sie viel seltener sind. Ihre Reaktionsordnung ist also viel höher. Es ist ja kaum zu erwarten, dass die bisher versuchte phänomenologisch-kristallographische Betrachtung der Keimbildung den kleinen Absolutwert ihrer Geschwindigkeit erklären kann. Die Berechnung der Reaktionsordnungen hängt eng zusammen mit dem Problem der Stabilität der Versetzungen in ihrer gegenseitigen Wechselwirkung, das bisher mathematisch noch wenig behandelt wurde.

M. Seitz. — Although I have not given thought to the phenomenon of recrystallisation in recent years, the clear summary of professor Burgers and the illuminating comments and additions of professors Guinier and Crussard suggest to me that a new idea is needed to complete our qualitative picture of the recrystallisation mechanism. I wonder if the sequence of events can be as follows :

1. During cold work the Frank-Read generators spin out new dislocations which generate vacancies. The vacancies lock the

dislocations and prevent them from moving spontaneously under forces they excert on one another.

2. During the heating in which polygonisation occurs, the vacancies aggregate extensively to form the low-density regions described by professor Guinier. The dislocations then become much freer to move under the action of their own forces. They form more stable configurations, corresponding to the polygonised state. Thermal fluctuations help the dislocations to move.

3. The final step, recrystallisation, involves more than the migration of dislocations, which accounts for polygonisation. I would like to propose that the critical process occurs in the boundary layer between two regions which are relatively highly disoriented relative to one another, one of which is more highly deformed than the other, that is contains a higher density of dislocations and vacancy aggregates. Such a boundary layer, according to the views of professors Smith and Frank can be regarded as a thin fluid-like « phase » possessing a high density of vacancies. This « phase » acts as a catalyst for growth of the new perfect region at the expense of its neighbours, diffusion playing a role of primary importance and being aided by the high density of vacancies.

The fluid boundary will move normal to itself as the more perfect crystal grows at the expense of the less perfect.

I believe the « fritting » agents wed in the growth and union of crystals in vacancies play a similar catalytic role.

The orientation of the recrystallised grains is determined by that of the relatively undistorted regions, which may be rotated relative to the original orientation both during cold work and polygonisation.

A minimum degree of disorientation is needed to guarantee a boundary with a relatively high density of vacancies.

The moving « fluid » boundary may aid in the annihilation of some of the dislocations it meets, particularly when it meets dislocation rings which can be regarded as vacancy sheets. Some of the dislocations may be entrapped in the new grain, however, much as dislocations are formed in crystals grown from the melt.

M. Burgers. — I was particularly interested in the final remark, according to which the orientation relationship in crystal growth is mainly determined by the conditions for rapid movement of the

boundaries. This seems to fit in well with what was said on page 119 of the Report. Again, however (see answer to Crussard), I think that nucleation in the sense of polygonization, i.e. formation of « strain-free » domains by rearrangement of dislocations in regions of high dislocation-density, is a primary factor (at least when recrystallizing a cold-worked matrix) in determining what orientations will finally develop.

M. Hollomon. — One of the basic problems of quantitatively describing the boundary motion involved in recrystallization and grain growth is an understanding of the detailed kinetics of the process. In terms of the formalism of the Eyring rate theory, the linear rate of growth G is

$$G = \lambda\,(KT/h)\,(\Delta F/RT)\ exp(-\triangle F_A/RT)$$

where γ is the thickness of the boundary ΔF is the driving free energy (strain or surface) and ΔF_A is the activation energy for the atomic process involved. Similarly the coefficient of diffusion D is given by

$$D = \lambda^2\,(KT/n)\ exp[-\Delta F'_A/KT].$$

From measurements of lattice and grain boundary diffusion in silver $\Delta F'_A$ have been calculated. From the rates of secondary recrystallization of silver, ΔF_A for grain-boundary migration can be calculated after an estimation of ΔF is made from surface energy considération (1).

The values are compared in Table I (1). It would appear that the atomic process involved in grain-boundary migration is grain-boundary diffusion. Smoluchowski (2) has recently determined the qualitative variation of grain-boundary diffusion of silver into copper as a function of orientation. He has shown this to be of the form illustrated in figure 1 (2). Thus if grain boundary diffusion is the rate determining step in grain-boundary migration, one would expect the migration rate to decrease as the disorientation decreases, as Burgers has discussed. Further quantitative measurements of grain-boundary migration and diffusion rates in silver as a function of orientation are under way in our Laboratory.

The agreement between the $\Delta F'_A$s for grain-boundary diffusion

(1) D. Turnbull, « Theory of Grain-Boundary Migration Rates » *Trans. AIME*, p. 661, 1951, and *Journal of Metals*, **3**, No. 8, August 1951.

(2) M. R. Achter and R. Smoluchowski, « Diffusion in Grain Boundaries and their Structure », *Journal of Applied Physics*, **22**, No. 10, p. 1260, October 1951.

TABLE I.

Comparison of Energy, Entropy, and Free Energy of Activation in Self-Diffusion and Grain Boundary Migration.

Substance	Strain	Grain Size, Cm	Temperature Range, °C	G_0 Cm per Sec	ΔS_A (Cal per Degree, Gram Atom)			Q (Kcal per Gram Atom)			ΔF_A (Kcal per Gram Atom)		
					$(\Delta S_A)_L$	$(\Delta S_A)_G$	$(\Delta S_A)_B$	Q_L	Q_G	Q_B	$(\Delta F_A)_L$	$(\Delta F_A)_G$	$(\Delta F_A)_B$
a) Primary Recrystallization													
Aluminium[17]	0.04		425-540	4.5×10^{7}	9.2	22.2		37.5	34.0		30.5	17.2	
Aluminium[1]	0.051		310-370	1.5×10^{16}		60.7			59.0		32.0	21.8	
Rock salt[20]	~0.1*		650-770	9×10^{11}	18.4[21]	59.0		51.4[21]	59.0		33.0	19.8	
	~0.3*		400-350	4.2×10^{8}		23			32.0		38.0	15.0	
Copper[16]	0.10		300-320	10^{13}	14.[22]	45		57.2[22]	50.0		49.0	23.8	
			340-360	10^{7}		17.4			32.0		48.8	21.1	
Silicon ferrite[10]	0.07		740-800	1.7×10^{11}	13.**	37.5		59.7**	73.0		46.2	33.8	
b) Secondary Recrystallization													
Copper[2]			900-1000	10^{11}	14.	47		57.2	73.0		40.1	15.5	
Silver[3]			433-533	2×10^{3}	9.[24]	11.8	2[24]	46.0	28.0	20.2	39.2	19.1	18.7
c) Normal Grain Growth													
Aluminium[30]		0.03	400-500	10^{31}	9.2	93		37.5	87.0		30.8	19.7	
α brass[31] (comm.purity)		0.03	450-700	10^{9}		38			60.0			27.8	
α brass[31] (high purity)		0.03	450-850	10^{4}		15			40.0			26.0	

Superscripts except exponents of ten refer to referances.
* Given data on synthetic crystal expressed as stress, Strains estimated from stress-strain curve on natural crystals.
** From data on self-diffusion on pure iron.

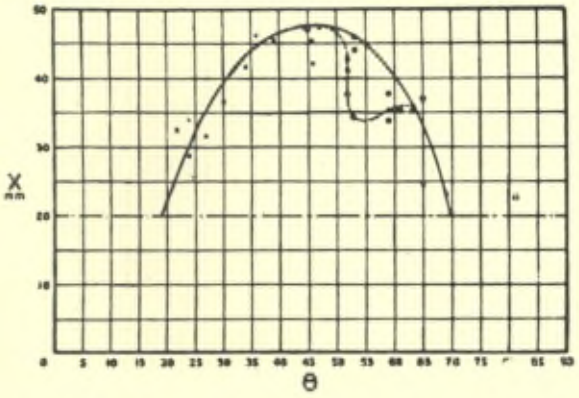

Fig. 1. — Extent of diffusion, X, *vs* orientation difference θ. 141 hours at 725 °C.
—·— Extent of volume diffusion.
——— Extent of intergranular diffusion.
× (100) directions parallel within 8°.
• (100) directions not parallel within 8°.

and migration might be surprising. Mott (1) has shown that the entropy of activation calculated from boundary migration rates is so high that he has suggested that 30 to 50 atoms might be involved in the elementary process. However, the agreement between the $\Delta F'_A$s indicates that the large entropy may simply be the result of the variation of the driving free energy with temperature because of the varying solubility of impurities. The situation probably is as illustrated in figure 2 (2) where at each temperature the driving force is different and the apparent straight line drawn through experimental points leads to too high an entropy of activation.

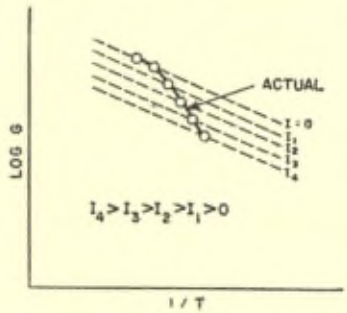

Fig. 2. — Representation of log G vs. 1/T for various degrees of dispersion (I) of inclusions at grain boundaries.

(1) N. F. Mott, *Proc. Phys. Soc.*, **60**, p. 391, 1948.
(2) D. Turbull, « Theory of Grain-Boundary Migration Rates » *Trans. AIME*, p. 661, 1951, and *Journal of Metals*, **3**, No. 8, August 1951.

Recent Work on Solid State Transformations in Sweden

by E. Rudberg

Swedish Institute for Metal Research, Stockholm

In attempting a review of recent research work in Sweden dealing with the solid state, particularly as regards transformations, one is at first a bit bewildered by the variety of problems tackled by the different groups and research institutions. Most of the pioneer work of crystal structure determinations by X-ray methods in Sweden was accomplished or inspired by Westgren at Stockholm University, beginning early in the nineteentwenties. Westgren and his pupils investigated inorganic compounds in the crystalline state, making systematic studies of existing phases, limits of solubility and type of solution in a number of alloy systems, and solving for the atomic arrangement in reasonably simple cases. The school founded by Westgren at Stockholm University is engaging in structure problems of increasing complexity under his successor, Ölander. At Upsala University, Hägg, one of Westgren's first associates, started fifteen years ago to build up a laboratory for structure studies, which soon became an active research centre in this field. In recent years a good deal of its work has been devoted to the structures of oxides of the transition elements, of the polyacids of Mo and W and their salts, and of boric acids. The results are interesting in several respects but will not be described here, since they appear to have little direct bearing on the main theme of imperfections and transformations.

METALLIC BORIDE STUDIES AT UPSALA

There is, however, one sector of the work from Hägg's laboratory which should be mentioned : the structure and properties of borides of the transition elements, as investigated by Kiessling ([1]). In many of these compounds, all of which have metallic character, the boron atoms form linear chains, the successive boron-boron links of which make angles of 120° with each other; there are also structures with

double chains, forming rows of linked hexagons, and compounds with complete hexagonal nets of boron atoms, as well as borides with three-dimensional boron frameworks. The linear chain structures with one boron per metal atom are of particular interest. They form lattices which are related to the hexagonal close-packed arrangement and could be depicted as deformed configurations of that type. All the pure metals which give rise to borides with linear chains crystallize with body-centred cubic lattices or — in the case of Mn — a lattice not so different from the body-centred arrangement. The change in the configuration of metal atoms, when the boron chains are brought in, is thus, as Kiessling shows, in the direction indicated by the electron theory of Jones, if it is assumed that each boron atom gives up one electron to the metal lattice, retaining two for its own boron-boron bonding in the chain. Kiessling also remarks that neither Ti and Zr, which have electron-rich close-packed hexagonal cells, nor Cu and Ni, with their face-centred cubic structures, give borides with boron chains. On this view, the electron transfer between boron atoms and metal atoms, when the boride is formed, is in the opposite direction to that suggested by Pauling.

CHEMICAL REACTIVITY OF SOLIDS

The possibility and importance of chemical reactions involving solid substances, where reactions in a gaseous or liquid phase are not responsible or essential for the changes observed, were emphasized many years ago, particularly by Hedvall. At Chalmers Institute of Technology in Gothenburg, Hedvall and his students have now, for more than two decades, investigated a large number of reactions, where solid substances take part. A large group of these are cases, which exhibit a marked change in reaction rate as a function of temperature at a transformation point for the solid substance involved. Examples are the oxydation of sulphur at the change rhombic/monoclinic, as well as oxydation of several metals and alloys where crystallographic changes take place, reactions between oxides, sulphates and silicates at high temperature upon passing a transformation point for one of the solid reaction partners. A number of solid catalysts for reactions in gases and liquids belong to this group. It is claimed that Curie points of ferromagnetic metals and alloys can be obtained with considerable accuracy from the change in rate of a suitable fluid phase reaction, catalysed by the metal in question,

as typified by the gaseous decomposition of CO in the presence of Ni. The work of Hedvall's laboratory, which has a number of important industrial applications, extends over a wide field of different reactions; it is still largely of an exploratory nature, a search for new reactions and new means of activating particular solids to increased reactivity, as *e.g.*, by irradiation or exposure to supersonic wave fields (2). In the former group may be cited the adsorption of organic substances from solution by a suspension of red HgS, which could be increased by almost a factor of ten, when the suspension was illuminated by a radiation strongly absorbed by the sulphide (3). No such increase could be produced with the black sulphide variety. It was pointed out that black HgS is an electronic conductor, whereas the red form has insulating properties, but exhibits photoconductivity in the spectral region where the large effect on adsorption was found. In recent years considerable interest has been given to the enhanced reactivity to lime, which is produced in alumina, silica, ferric oxide and other substances by the presence of a neutral gas like nitrogen. According to Hedvall (4) the gas dissolves to some extent in the oxide and thereby creates a disturbance, responsible for the increased reactivity. — Remarkable as these findings are, not only because of their sometimes far-reaching technical consequences, the complexity of the systems involved would seem to make definite interpretation in terms of the concepts of crystal physics a rather difficult task. Finally it must be remembered that, in all these reactions in solids, the process exhibiting a change in reaction rate occurs at the boundary of a solid phase towards a gas, a liquid or a second solid. The altered reactivity of that boundary region could well be associated with definite changes in the structure of the main body of the solid, but need not always be so.

PRECIPITATION AND ORDER-DISORDER CHANGES

In the physics department at the Royal Institute of Technology in Stockholm, systematic studies of precipitation and of order-disorder transformations in binary alloys have been in progress for some 25 years, under the direction of Borelius. The main tools for the experimental side of this work are resistivity measurements, fine structure X-ray determinations and calorimetric methods of several kinds. As the chief guide in interpreting the results obtained, as well as for planning new experiments, Borelius has been using a

thermodynamic approach, adopting as far as possible mathematically simple expressions for the thermodynamic functions involved.

Precipitation. — In discussing a binary alloy system, AB, with a solubility gap in a certain temperature range, it is customary to separate out a structural part u, s and f from the thermodynamic functions internal energy u', entropy s' and free energy f' per atom of the alloy, and consider only this part in its dependence on temperature T and atomic concentration x of one of the components, A. The structural part is here defined as

$$u = u' - xu'_A - (1-x)u'_B \tag{1}$$

where subscripts A and B refer to the pure components. The concentration dependence of the free energy

$$f = u - Ts \tag{2}$$

is then represented by a series of isotherms for different temperatures as in Fig. 1. Equilibrium phases correspond to the regions represented

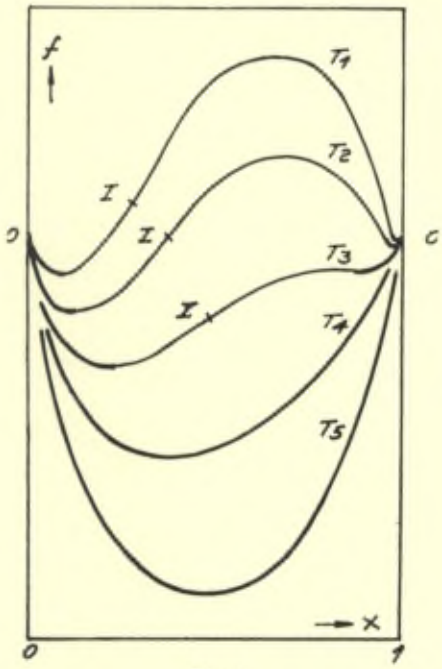

Fig. 1

by heavy lines extending inward from both ends of the entire composition range; and in the strictest sense of the classical theory, thermo-

dynamic functions would only be defined for these regions. Experimentally, however, alloy states of considerable duration can be realized in the remaining region, corresponding to supersaturation, and it is customary, as an extension, to ascribe thermodynamic functions to these by the methods of statistical thermodynamics. Thus the expression for s is generally taken simply as that for the entropy of mixing over the entire range :

$$-s/k = x \log x + (1-x) \log (1-x) \tag{3}$$

k being Boltzmann's constant. To construct the curve family of f for a given system, it remains then to find u. One method, suggested and used by Borelius (5) (6), of computing u with the aid of solubility determinations on the system in question, is the following. It is assumed that, to a sufficient approximation, u can be regarded as a function of x only, independent of T, like s. In many cases the solubility corresponds rather closely to the minimum of the f-isotherm for the temperature in question, where

$$\partial f/\partial x = du/dx - T\, ds/dx \tag{4}$$

vanishes, so that a first approximation, u_0, is obtained by neglecting $\partial f/\partial x$ for all points (T, x) along the solubility boundary in the phase diagram and taking for u_0 the integral $\int_0^x T(ds/dx)dx$ along that boundary. Insertion of $u_0 - Ts$ for f in (4) gives upon integration a second approximation for u, and so on.

For a temperature T such as T_2, where there exists a solubility gap, the ultimate equilibrium should be a state with two phases of compositions x_a and x_b determined by the common tangent to the f-curve, Fig. 2. Any supersaturated composition $x_a < x < x_b$, such as P, should in the end change into this with a total release of free energy of amount GP for each transforming atom of composition x. However, the concentration changes are considered to take place continuously, so that the first step in the precipitation is from concentration x to two adjacent concentrations x_1 and x_2 on opposite sides of x, represented by M and N. From these the process continues, and thus the precipitate x_2 may ultimately reach x_b along the f-curve. The ease with which the first step will occur depends on the sign of $\partial^2 f/\partial x^2$ at x. For $\partial^2 f/\partial x^2 < 0$, *i. e.*, where the f-curve is concave downward as in Fig. 2, this step is accompanied by a release of free energy of an amount represented

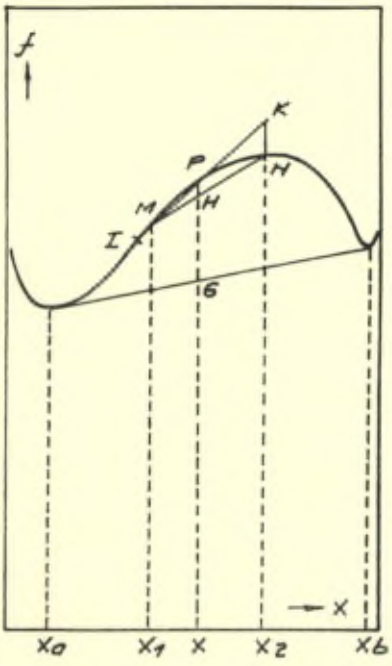

Fig. 2

by HP per decomposing atom x, or by NK per atom formed of composition x_2. If instead $\partial^2 f/\partial x^2 > 0$ for the initial composition x, Fig. 3, the first step requires that free energy of amount KN is supplied to the system per atom x_2 formed. If the x_2-atom is to be produced with a minimum of free energy expenditure, x_1 should be infinitely close to x, so that the line MP becomes tangent to the f-curve at P; in the limit then, for a finite yield of x_2, the amounts of x and x_1 would be infinite. All this is merely a consequence of the conservation of atoms of both species in the process.

Measurements by Borelius and collaborators, as well as by others, have shown that the initial rate of precipitation from a supersaturated solid solution of given composition x increases with temperature in a way which can be described by a Boltzmann factor, $e^{-A/kT}$, for low temperatures and high supersaturation. The corresponding activation energy, A, supports the view that the rate-controlling process here is diffusion ([5]). As the temperature is raised further, however, a point is reached, where the rate instead starts to decrease rapidly with further increase in temperature. For temperatures

below this point, the f-curves are such that the initial composition x falls in a region of $\partial^2 f/\partial x^2<0$. As the temperature is raised, the changing f-curves gradually move their inflexion point I closer to the composition x, Fig. 1. The onset of retarded precipitation occurs when the inflexion just passes the composition x, so that $\partial^2 f/\partial x^2$ for higher temperatures becomes positive. The retardation is described for each composition and temperature by an additional factor $e^{-F/kT}$ in the rate expression*. For a given composition x, F is zero at (and below) the temperature which just places the inflexion at x; above this temperature F increases rapidly with T.

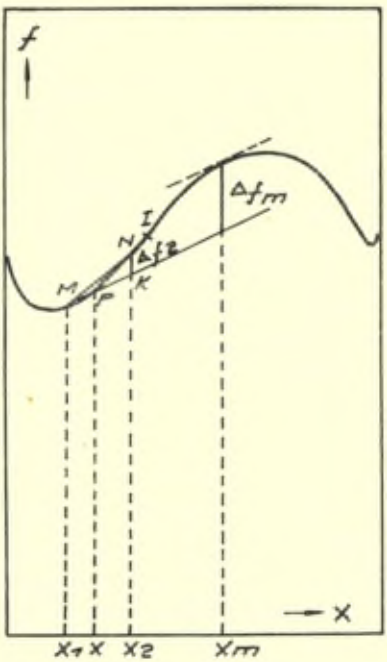

Fig. 3

The interpretation of F as a thermodynamic potential barrier, proposed by Borelius, is this. In an alloy of nominal composition x within the supersaturated region of $\partial^2 f/\partial x^2 > 0$, local fluctuations of composition and hence fluctuations of free energy will occur. The probability that a group comprised of n atoms will be found to

(*) Such a description is formally always possible, and therefore without physical significance, as long as F is left free to be any function it choses of T.

have composition x_2 and the large rest of surrounding alloy a composition x_1 very close to x, will be proportional to $e^{-n\Delta f_2/kT}$, where Δf_2 denotes the ordinate difference KN in Fig. 3. Unless this increase in concentration to x_2 is appreciable, it will require further increments of free energy to carry the group over into a stable precipitate, and the local concentration is under those circumstances likely to revert to the value x. But fluctuations large enough to change the composition to x_m, where the ordinate difference KN attains its maximum Δf_m, should be capable of growing into precipitate without further addition of free energy. It is fluctuations of this size which are considered rate determining in the region of retarded precipitation. Hence

$$n \Delta f_m = F_4 \tag{5}$$

If the family of f-curves is available, Δf_m can be computed for each temperature T and supersaturated composition x. With F known from rate measurements under the same conditions, n, the number of atoms in the fluctuation group of critical size, can then be derived.

Borelius and his students have made systematic solubility measurements, from which f-curves were then computed, and have measured precipitation rates to determine F, to which the theory just outlined was applied. Among alloy systems thus investigated are AuPt (7), PbSn (5) (8) (9), AlCu (10) and AlZn (11). In most of these experiments the progress of the precipitation reaction could be followed by the attending increase in resistivity. More recently, improved calorimetric methods have been used for such precipitation studies in Borelius' laboratory. In this way the measured total amount of heat developed in isothermal precipitation, carried to completion, should give a check on the structural internal energy u entering in the f-curve calculations. Again, the rate at which heat is liberated in the first part of isothermal precipitation provides the data from which F is derived.

Order-disorder studies. — Retardation phenomena, similar to the ones exhibited by precipitation reactions, were encountered in the early studies of order-disorder transformations for the copper-gold system in Borelius' laboratory (12). They have later been investigated in considerable detail in that laboratory by different methods. Most of the work is concerned with the alloy with equal numbers of Au

and Cu atoms. For the sake of simplicity the theoretical considerations, which at least in form are similar to the ones used for precipitation, will be reviewed with respect to this case ([13]). Starting from the fact that the completely ordered structure can be described as one where all the atoms of one kind, the B-atoms, occupy the points of an a-lattice, whilst similarly all the atoms of the other kind, the A-atoms, occupy a b-lattice set into the a-lattice, Borelius defines a certain state of disorder x as that where the composition in the a-lattice is x parts of A and $(1-x)$ parts of B. The expression in x for the disorder part of the entropy per atom for this state is then identical with the expression for the entropy of mixing, used in the case of precipitation (3). If further the disorder part of the internal energy, u, can be found as function of the « disorder composition » x,

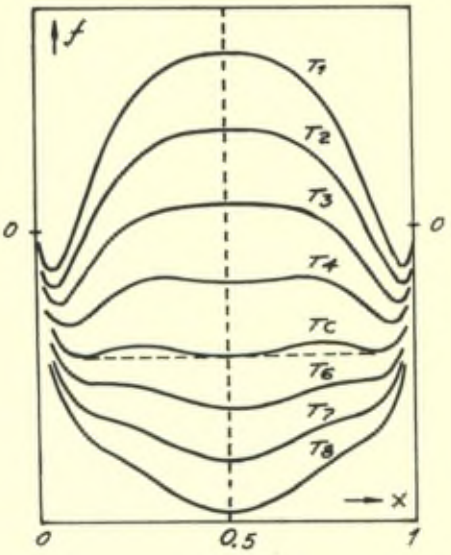

Fig. 4

the family of isotherms can be traced, which should represent the disorder part f of the free energy per atom, as a function of this disorder composition x. This is illustrated for CuAu in Fig. 4. The range from full order to complete disorder is here covered from $x = 0$ to $x = .5$, the remaining right half of the picture from $x = .5$ to $x = 1$ being obviously the mirror image of this. For temperatures higher than T_c complete disorder $x = .5$ has the lowest value of f, but for a temperature T below this critical point T_c, the minima

near the order ends — $x < .1$ and $x > .9$ — represent the stable state to which a supercooled disordered alloy, with $x = .5$, will eventually turn. The discussion of this process with the aid of such a diagram for f can be modelled very closely on the earlier treatment in the case of precipitation.

Thus if, as in Fig. 5, the supercooled state P ($x = .5$) turns into a

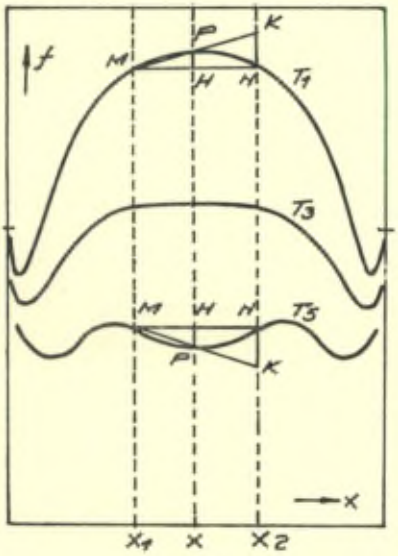

Fig. 5

state of disorder x_1, so that the concentration of A-atoms in the a-lattice drops to x_1, the concentration of A-atoms in the coexisting b-lattice must simultaneously increase to $x_2 = 1 - x_1$. In this sense the two compositions x_1 and x_2, into which the disordered composition x changes, are always symmetrically located to the vertical $x = .5$, and the line MN joining the corresponding points on the isothermal f-curve must always remain horizontal. The ordinate difference HP represents the free energy change in the process per atom of the decomposing double lattice ab, whereas NK gives the free energy change per atom of the lattice b only, of composition x_2. For a low temperature like T_1, where the f-curve has such a shape that $\partial^2 f / \partial x^2 < 0$ for the initial disordered composition x, the change will evidently be attended by a release of free energy from the very beginning. In the opposite case, when $\partial^2 f / \partial x^2 > 0$, as at the higher temperature T_5, the first part of the change towards order will require

that free energy is supplied to the system, by an amount represented by KN per atom of lattice b, or by ½ of this — HP — per atom of the decomposing double lattice ab. The shift from the first to the second case takes place at that temperature T_3 for which $\partial^2 f / \partial x^2$ vanishes at $x = .5$. For temperatures above T_3 then, the rate of the disorder-order reaction is, according to Borelius, retarded by a thermodynamic potential barrier, which is surmounted, just as in the corresponding situation for ordinary precipitation, by local fluctuations involving a group of n atoms, this time fluctuations of order, whereby the required local increase in free energy is provided.

Experimental rate determinations for the transformation in AuCu have been made in Borelius' laboratory by intensity measurement of X-ray reflexions (14), by resistivity studies (15) and by calorimetric work (15) (16). The values found for the retardation as function of temperature by all three methods are in very good agreement (15) (16).

It has not been possible to compute the disorder part of the internal energy u as a function of the variable x from equilibrium data by a method similar to the one used for ordinary precipitation, since there does not appear to be any direct way of measuring the disorder variable itself, in equilibrium at different temperatures. Borelius has adopted to represent u by a power series in $x\,(1 - x)$, here limited to the quadratic expression :

$$u/k = \alpha x(1 - x) + \beta x^2(1 - x)^2 \qquad (6)$$

The two empirical constants α and β were chosen to give the best fit with experimental data, obtained in the X-ray work (14). As a matter of fact, the simple equation : $T_3 = \frac{1}{2}\,(\alpha + \frac{1}{2}\,\beta)$ follows for the temperature where retardation should begin; a second relation for fixing the constants is obtained from the experimental value for the critical temperature T_c.

Numerical results. — In the case of precipitation in PbSn, direct measurements of the heat evolution have, for the region of low concentration and temperature, yielded values appreciably lower than those computed from the equilibrium diagram. It is believed that strain energy, stored in the lattice upon precipitation, will account for the difference. A somewhat similar effect seems to occur in the range of retarded transformation disorder-order in AuCu, where in some experiments the measured heat of reaction was only 50 — 80 % of that demanded by (6) with the constants adjusted to

fit the rate data. In recent work this point would appear to have been cleared up, since it could there be shown (16) that the evolution of heat actually takes place in two steps : the first comparatively fast, giving the low values just mentioned, the second, much slower, but making the total heat evolved come out just as calculated. These new values are, in fact, in very good agreement with the calculated ones, over the entire temperature range below the critical point. Even so, the range in x covered by these calorimetric measurements was only from 0 to .07, whilst the range which determines the potential barrier lies much nearer to .5. It would seem to be a feature of this phenomenon that the latter range remains inaccessible for direct reaction heat measurements.

Values reported for n, the number of atoms in the fluctuation group in the case of retardation, are for precipitation in PbSn 120 and in AlCu 390, for disorder-order in AuCu 2500.

SINGLE CRYSTAL CRITICAL SHEAR STRESS FOR DILUTE SOLUTIONS IN Cu

Some very recent results from a different line of research, pursued by Linde and collaborators (17) (18), also in the physics department of the Royal Institute of Technology, may be briefly mentioned here.

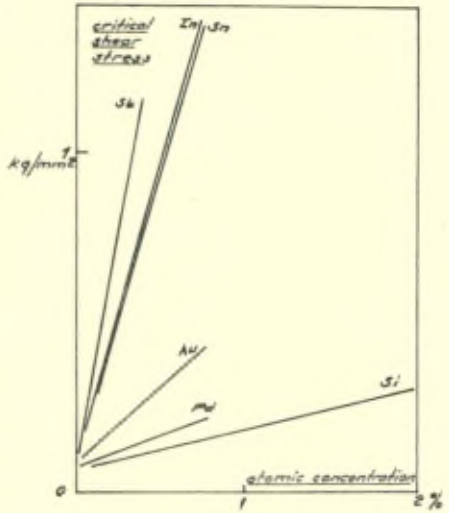

Fig. 6

Linde determines the resolved critical shear stress for the principal planes and directions of easy shear, from measurements of the yield point of single crystals of known orientation in simple tension. By a special arrangement the rate of loading is kept very constant, usually at a low value. Elongation is measured with a strain gauge method. The experiments are made at room temperature. Results have been obtained for dilute solutions in copper of Si, Pd, Au, Sn, In, Sb, in atomic concentrations downwards from .5 — 5 %. For any given solute atom, the critical shear stress increases linearly with concentration in the range studied. Fig. 6 illustrates this. As compared to the low value at infinite dilution the critical shear stress for a 1 % solution shows an increase by a factor of about 2 for Si and by more then 30 in the case of Sb. The other solute elements will be seen to arrange themselves in between these two extremes, in the order they are listed here. Linde points out that this is also essentially the order of increasing difference in atomic volume of solute and solvent.

ISOTHERMAL TRANSFORMATION OF AUSTENITE

Axel Hultgren, who heads the department of metallography at the Royal Institute of Technology, is conducting an extensive research on the different reactions which take place in austenite when held at different, in each case constant, temperatures. For the present report the studies at reaction temperatures below the eutectoid point are of particular interest. This work has been going on for the last ten years, and a number of students and some research assistants have participated. A progress report ([19]) was published and discussed in 1946. A summary of new experimental results, obtained chiefly in collaboration with K. Kuo, and a comprehensive account of the theoretical interpretation of the various effects observed, was presented by Hultgren at the discussion meeting of Jernkontoret ([20]) in May 1951.

The material used in this investigation comprises a number of alloy steels, with a carbon content usually near .50 % and a second alloying element in amount of the order of one or, in some cases, a few percent (*). Thin samples were austenitized, usually at 1300 °C, then held at the chosen reaction temperature in a lead or lead alloy bath for a series of increasing time intervals, terminated by quenching

(*) In this entire section concentrations are always referred to in *weight* percent.

in water or oil. Metal microscopy of polished and suitably etched sections served to determine the nature and relative amount of the different phases formed, as a function of time at a given temperature, and also yielded information as regards orientation relationships, particularly between neighbouring parts of the same phase. From these determinations the usual TTT-diagrams were constructed, giving time of first appearance — *i. e.*, the 1 % curve — and of 99 % completed reaction as function of temperature for the different constituents identified. These are, in all steels investigated, in the first place the phase mixtures pearlite and bainite, consisting of ferrite and cementite $(Fe,M)_3C$, and the corresponding separate phases. In a long series of special experiments, involving electrolytic separation, the carbides were isolated, their structure checked by X-ray measurements and their composition determined by chemical analysis. A further control was obtained from Curie point measurements. Of the wealth of information thus secured, a good deal will probably be found valuable for technical applications. Some of the results, which appear to have particular interest for the theory of reactions in solids, are listed in the following.

Ortho- and parareactions. — It was found by Hultgren that, if a steel is held at a temperature below the eutectoid point A_1 for a sufficiently long time, a definite distribution ratio for the alloying element in the cementite and the ferrite formed is ultimately attained. This ratio is the same, whether approached from previously formed pearlite or bainite, or from martensite after tempering. It is therefore regarded as an equilibrium ratio. For temperatures just below A_1 the following values (*) for the distribution ratio were determined after long heating :

For element :	Cu	Al	Si	P	Co	Ni	W	Mo	Mn	Cr
Conc. ratio in cementite/ferrite:	0	0	0	0	.2	.3	2	8	11	28

Whenever the phase resulting from transformation has the concentration of the alloying element, which corresponds to the ratio for complete equilibrium, Hultgren designates it as an orthophase : orthocementite, orthoferrite. Strictly, for two phases in contact at a given temperature, orthoequilibrium exists and the two phases are « ortho » with respect to each other, if their compositions are the

(*) The values quoted are weight percent ratios; from a theoretical point, ratios of atomic fractions M/(Fe + M) would appear more significant, at least for low concentrations where the use of such fractions would result in values higher than those of the present table by a factor of about 1.07.

ones arrived at when diffusion of all components is granted. Evidently, the concentration of an alloying element in an orthophase will usually differ — and widely so for elements at both ends of the list — from that in the parent austenite from which the phase was formed, directly or via an intermediate product. In contrast to the orthophase, Hultgren considers a phase formed under conditions of partial equilibrium, where the alloying element retains its concentration (relative to Fe) unaltered from the parent austenite. This is called a paraphase.

Chemical analysis shows bainite to consist of paracementite and paraferrite. The cementite formed from martensite in the early stages of tempering proves to be paracementite. In a limited number of cases cementite from pearlite has also been analysed. Thus with Ni, Co, Si and Mn the pearlite obtained consisted of paracementite and paraferrite. With Mo and Cr, the first samples that could be analysed yielded cementite compositions about half-way between ortho- and para-. More recently isolated carbide from pearlite in Cr-steel has shown definite ortho-composition.

In molybdenum steels, Hultgren has found two different forms of ferrite, distinguished, from their appearance, as *ordinary* and *wrinkled* ferrite. They can sometimes be seen in the same microspecimen. Likewise, two pearlites occur, *wrinkled* pearlite at higher temperature, containing wrinkled ferrite, and *ordinary* pearlite. The latter consists of paracementite and paraferrite, like the pearlite found in the other alloy steels. Cementite isolated from wrinkled pearlite has a Mo-content between para and ortho. The possibility is suggested that the wrinkled ferrite is ortho-; and that wrinkled pearlite starts as paracementite and orthoferrite, the cementite partly changing in the direction of ortho- during growth. In hypoeutectoid steels, propearlitic ferrite, formed before wrinkled pearlite appears, is of the wrinkled variety, whereas the ordinary pearlite and the bainite are preceded by ferrite of the ordinary type. Hultgren suggests that the wrinkled appearance is caused by an uneven distribution of Mo, in wrinkles, exposed by the etchant. This distribution is understandable from the assumed mechanism of the growth process, if the phase is an orthophase and hence requires migration of Mo; it is not to be expected in a paraphase with its Mo-atoms frozen in. The microphotograph in Fig. 7 at a magnification of 2000, for a Mo steel sample held at 625 °C reaction temperature

for 10 minutes, shows some of the constituents here mentioned. The white areas, of two types, are ferrite, ordinary and wrinkled; the regions between these are occupied by wrinkled eutectoid. In addition to the two cementitic pearlites just described, a third pearlite, containing the double carbide $Fe_{21}Mo_2C_6$, appears in the highest

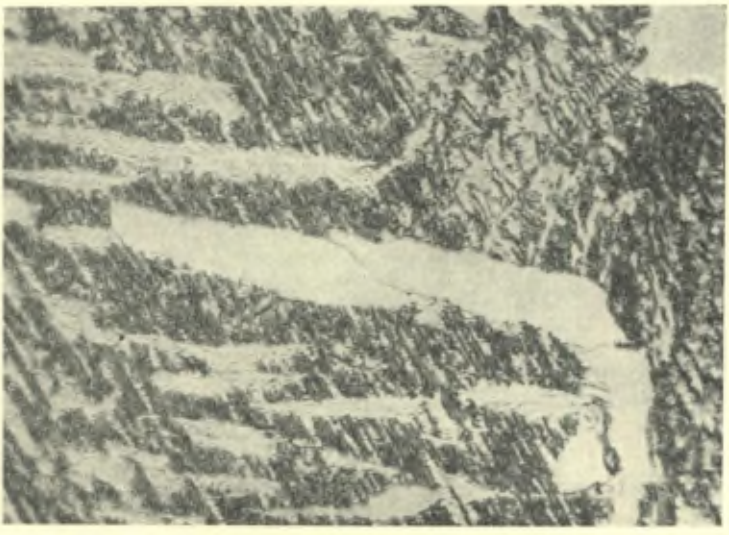

Fig. 7

temperature range immediately below A_1. Thus the complete TTT-diagram for a typical steel (C = .54 %, Mo = .54 %) investigated contains three separate pearlite curves, Fig. 8, where « 2 » denotes double-carbide-pearlite, « 1*a* » wrinkled and « 1*b* » ordinary cementite-pearlite. In this diagram ferrite curves are distinguished by unfilled circles, bainite curves by filled circles and pearlite curves by plain lines. — Similar phenomena as for Mo are observed for Cr as alloying element.

In many hypoeutectoid steels with Mo, Cr or Ni, the ferrite formed isothermally below the eutectoid point will, if the heating is sufficiently prolonged, show precipitation of carbide. This carbide is hence formed from the ferrite phase, and not directly from austenite, as the proeutectoid cementite or the pearlitic and the bainitic cementite.

Diagramatic representation. — Hultgren illustrates his theory of these phenomena, particularly the ortho- and parareactions,

by phase diagrams of the type reproduced in Fig. 9, where temperature is represented along the height of a triangular prism and composition in the base triangle. In the top of this picture is shown the projections of two isothermal sections, at T_1 and $T_2 < T_1$, on to the Fe corner of the composition triangle Fe-C-M. The Fe-C-temperature side of the prism is drawn in the lower half of the picture, with the temperature axis pointing down. The well-known equilibrium lines in the Fe-C-temperature diagram, extended without

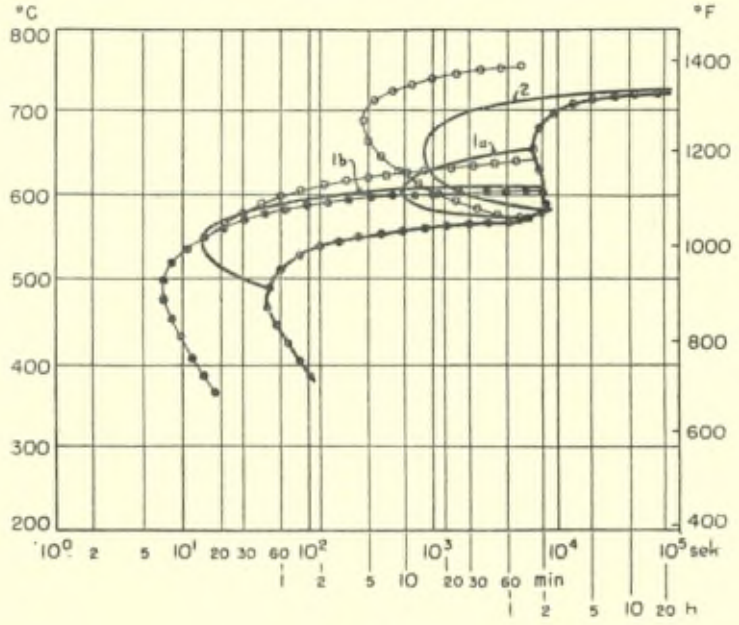

Fig. 8

break to temperatures below A_1, are the edges of the corresponding curved equilibrium surfaces in the prism. The solid curves in the top projection represent the intersections of planes T_1 and T_2 with these surfaces for orthoequilibrium; intersections with paraequilibrium surfaces are shown by dashed curves. Orthocompositions are indicated by plain letters, the corresponding letters for parastates being marked by a dash.

When, at the higher temperature T_1, austenite of composition P forms orthoferrite, the latter must have the composition F deter-

mined by the intersection with the α_{γ_1}- curve of the tie line through P pertaining to orthoequilibrium ferrite/austenite at that temperature. The austenite simultaneously adjusts itself to the composition A. If, instead, the austenite at P should decide to deposit orthocementite, the orthoequilibrium tie line through P pointing to the distant, fairly M-rich orthocementite will determine the composition B for the remaining austenite. At the lower temperature T_2, where the new phases are assumed to form without migration of component

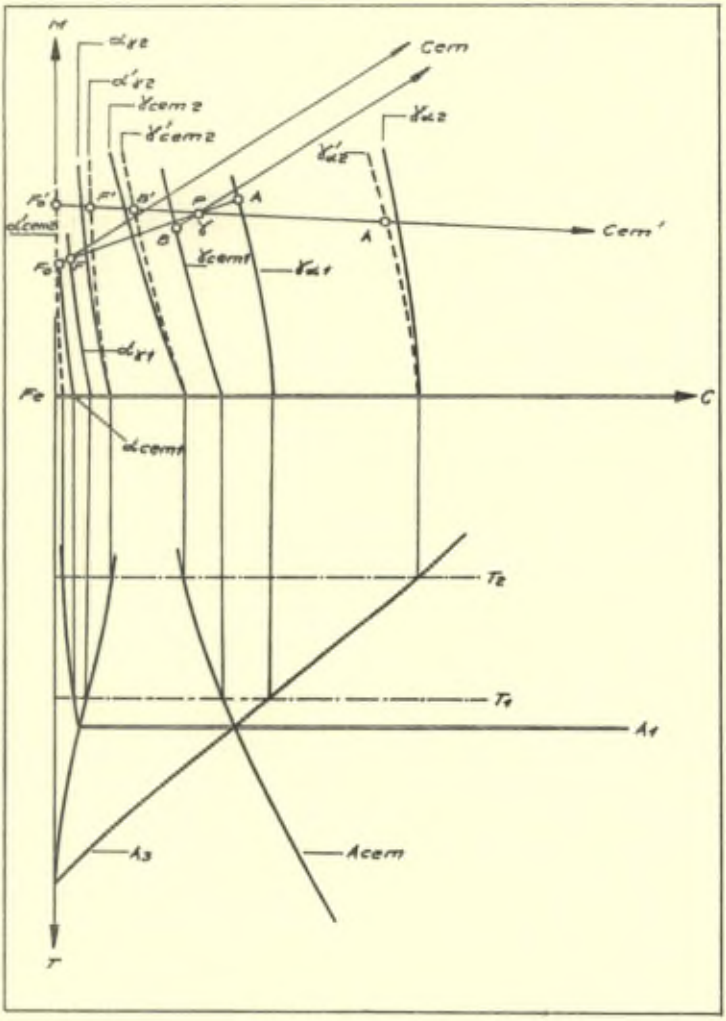

Fig. 9

M, all of them must have compositions on the straight line through P to the pure C corner, this being the locus of all combinations with constant ratio M/Fe, equal to that for P. Hence, if ferrite is formed, its composition will be given by F′, and that of the remaining austenite by (*) A′, on the intersections with the paraequilibrium curves, which, for non-vanishing M-concentrations, differ from the orthoboundaries. Likewise, austenite forming paracementite at T_2 should take on composition B′. The paraferrite at F′ is supersaturated with respect to paracementite; upon precipitation of the latter, the ferrite takes on composition F'_o. Hultgren remarks, that the experimentally verified precipitation of cementite from proeutectoid ferrite, formed below A_1, speaks for the correctness of reasoning from equilibrium lines and surfaces, extrapolated without break to temperatures below A_1, as here done. In a similar way the orthoferrite at F is not in equilibrium with orthocementite, but must change its composition to F'_o, in order to establish equilibrium with that phase.

SUGGESTED EMBRYOLOGY FOR PRECIPITATING PHASE

Hultgren's experimental results have thus clearly exemplified that isothermal formation of a new phase from a supersaturated solid solution will override obstacles, due to low mobility of components, by disregarding the ordinary equilibrium requirements as to composition. The new phase, then, is characterized primarily by its lattice structure, and less by its composition.

This view, carried back to the very first stage of precipitation, leads Hultgren ([19]) to a picture of the nucleus formation associated with these processes, which seems rather different from the one adopted by Borelius for the region of retarded precipitation in a number of binary alloys. It will be recalled that in the latter case the formation, by fluctuations, of a fairly large segregate of the correct composition for the new phase is required, consisting of some 10^2 to 10^3 atoms. Hultgren deems it unlikely, that such a high number of atoms should be involved in the fluctuation leading to a stable nucleus. Instead, he considers that fluctuations in *structure* will produce small regions, comprising only a few atoms, within

(*) The A to the right in Fig. 9 (its dash is lost).

which the structure is that of the new phase. In pure γ-iron this would seem to be the only way for the nucleation of ferrite. Some of these *embryos* (*) will grow to nuclei, aided, in carbon steels and alloy steels, by local changes of composition, as far as atom mobilities will permit.

It would seem that these two views need not be mutually incompatible, but could perhaps, in a sense, be made to appear as parts of the same picture. The segregation by fluctuation in Borelius' treatment must include the corresponding (equilibrium) structure adjustment implicitly, inasmuch as the internal energy term, used in the free energy, is calculated from equilibrium boundary data. Within that theory itself, the comparatively high number of atoms in the fluctuation group comes out as the quotient of the rather high potential barrier F from retardation measurements, divided by the computed, fairly low hump, Δf_m, to be overcome by composition changes in the free energy plane. Presumably, a higher hump might be obtained, by considering transitions in free energy space to states of the new phase, having nearly the proper structure, but composition nearer to that of the parent phase. If so, this would make the size of the critical fluctuation region come out smaller. — The inclusion of an additional free energy contribution from the surface of the embryo should operate in the same direction, increasing the denominator in the expression for n.

(*) The word « embryo » with this meaning was introduced by Hultgren [19], p. 968.

REFERENCES

(1) R. Kiessling, *Acta Chemica Scandinavica*, **4**, p. 209 (1950).

(2) J. A. Hedvall and G. Ekwall, *Arkiv f. Kemi*, **18A**, No. 11 (1944).

(3) J. A. Hedvall and S. Nord, *ZS f. Elektrochem.*, **49**, p. 467 (1943).

(4) J. A. Hedvall and T. Günther, *Arkiv f. Kemi*, **17A**, No. 1 (1943).

(5) G. Borelius, F. Larris and E. Ohlsson, *Arkiv f. mat., astr., o. fysik*, **31A**, No. 10 (1944).

(6) G. Borelius, *Arkiv f. mat., astr. o. fysik*, **32A**, No. 1 (1945).

(7) C. G. Wictorin, *Diss.*, Stockholm (1947).

(8) G. Borelius and K. M. Säfsten, *Arkiv f. mat., astr. o. fysik*, **36B**, No. 5 (1948).

(9) J. Nyström, *Arkiv f. fysik*, **1**, No. 18 (1949).

(10) G. Borelius and L. Ström, *Arkiv f. mat., astr. o. fysik*, **32A**, No. 21 (1945).

(11) G. Borelius and L. E. Larsson, *Arkiv f. mat., astr. o. fysik*, **35A**, No. 13 (1948)

(12) G. Borelius, C. H. Johansson and J. O. Linde, *Ann. d. Physik*, **86**, p. 291 (1928).

(13) G. Borelius, *Journ. Inst. of Metals*, **74**, p. 17 (1947).

(14) O. Källbäck, J. Nyström and G. Borelius, *Ing. Vet. Akad. Handl.*, No. 157, (1941).

(15) J. Nyström, *Arkiv f. fysik*, **2**, No. 16 (1950).

(16) G. Borelius, L. E. Larsson and H. Selberg, *Arkiv f. fysik*, **2**, No. 17 (1950).

(17) J. O. Linde, B. Lindell and C. H. Stade, *Arkiv f. fysik*, **2**, No. 11 (1950).

(18) J.O. Linde, Reported at 2nd Internat. Congr. of Cryst. Stockholm July 1951.

(19) A. Hultgren, *Trans. Am. Soc. Metals*, **39**, p. 915 (1947).

(20) A. Hultgren, *Jernkontorets Annaler* **135**, p. 403 (1951).

Discussion du rapport de M. Rudberg

M. G. Borelius. — I should like to emphasize that the rate of precipitation of a supercooled solid solution is dependent on two things : the rate of nucleation and the rate of growth of the nucleus. About the rate of growth we do not know very much so far from experiment. We know however that the velocity has to increase with incrasing temperature because of increased mobility of the atoms and again decrease and go to zero at the boundary of the gap of solubility. So there will be a maximum velocity at some distance from this boundary. I have tried to put into relation the rate of nucleation and the distribution of concentration fluctuations. The simple view has been that whatever the special conditions for the formation of a stable nucleus may be, a narrow distribution of fluctuations (with a very small probability for the large fluctuations which are a first general condition for nucleation) must decrease the rate of fluctuations.

As the distribution of fluctuations is dependent on the second derivative of the free energy with respect to concentration, this means that a retardation of this nucleation has to start at the spinodal, where this derivative goes from negative to positive values, when the temperature is increased. The measurements so far give a good coincidence with this idea. At the measurements one has however to be careful to measure if possible the initial rate of precipitation, as the later stages are more dependent on the rate of growth than on the rate of nucleation.

M. Dehlinger. — Die von Herrn Borelius abgeleiteten thermodynamischen Beziehungen können auch in andrer Ausdrucksweise dargestellt werden. Die Geschwindigkeit jedes irreversiblen Vorgangs bei konstant gehaltener Temperatur ist mindestens näherungsweise proportional der dabei eintretenden Abnahme der freien Energie F des Systems, also es gilt :

$$\frac{\partial \Lambda}{\partial t} = - C \exp\ (- \lambda/kT) \frac{\partial F}{\partial t}$$

wo Λ die Laufzahl der Reaktion bedeutet.

Bei Vorgängen in übersättigten Mischkristallen müssen die Atome gewisse Wege zurücklegen daher ist es anschaulich, hier mit dem Diffusions-Koeffizienten zu arbeiten. Wenn man nun die obige Gleichung zur Berechnung des Diffusions-Koeffizienten in Substitution Mischkristallen D' anwendet, erhält man exakt :

$$D' = D\, x\,(1-x)\,(\partial\, ln\, a_m/\partial x + \partial ln\, a_n/\partial x)$$

Hierin ist a_m die Aktivität der Komponents m, a_n die der Komponente n, x die Konzentration von m. D ist der Diffusions Koefficient eines idealen nicht ausscheidungsfähigen Mischkristalls.

Da die Aktivität a_m durch die Bezichung definiert ist $RT ln\, a_m = \partial F/\partial m$, und $F = (m + n) f$, wo f die von Borelius gebrauchte Grösse ist, erhält man durch Differenzieren und Beachtung der Duhem-Margulès' schen Gleichung :

$$D' = D\, \frac{x\,(1-x)}{RT}\, \frac{\partial^2 f}{\partial x^2}$$

Das bedeutet folgendes :

In Konzentrations — und Temperaturgebieten, wo $\partial^2 f/\partial x^2 > \sigma$, ist der effektive Diffusions Koeffizient $D' > 0$, und daraus folgt, das kleine Konzentrationsschwankungen, die stets durch statistische Schwankungen entstehen, immer wieder ausgeglichen werden (down hill diffusion).

Auf der « Spinodalen » ist $\partial^2 f/\partial x^2 = \sigma$, die Schwankungen bleiben bestehen, ganz ähnlich wie am kritischen Punkt der Flösigkeiten nach Van-der-Waals. Nach Überschreiten dieser Kurve wird $D' < \sigma$, kleine Schwankungen werden im Lauf der Zeit vergrössert (up hill diffusion).

Zweifellos gilt ähnliches auch für den Fall der order-disorder Umwandlung.

Es ist aber zu betonen dass diese Betrachtungen über die Geschwindigkeit von Reaktionen nur dann richtig sind, wenn das System während der Reaktion im makroskopischen Sinn homogen bleibt, d. h. wenn die Kohärenz des Gitters erhalten bleibt. Wenn inkohärente, inhomogene Zwischenzustände auftreten, ist die Reaktionsgeschwindigkeit nicht von den Differentialquotienten, sondern von den Differenzen der freien Energie abhängig und die Spinodale verliert ihre Bedeutung.

Die Bildung von Komplexen durch die oben beschriebene « up hill diffusion » ist wie die normale Diffusion ein Vorgang von erster

oder zweiter Reaktionsordnung, dagegen ist die zur Entstehung inkohärenter Gitter notwendige Keimbildung ein Vorgang horer Ordnung.

M. Köster. — The work done by Hultgren on isothermal transformation of austenite is in good agreement with the research of Max Planck-Institute für Eisenforsehung at Düsseldorf. There are only, so far as I can see, differences in the interpretation of the results in the following respect. Hultgren said formerly (1946), and this is also the opinion held at Düsseldorf to-day based on their experimental results, that the stages of pearlite-, bainite- and martensite-transformation are characterised by the extent of diffusion of the alloying elements on the one side and of carbon on the other. Nowadays he uses these differences to explain the existence of orthophases and paraphases, whereby these reactions are not identical with those going on during pearlite- and bainite-transformation.

The designation as orthophase or paraphase is based upon analysis of isolated carbides. The concentration of the corresponding mixed crystal is given by calculation. This way of determining the composition of the equilibrium phases is not quite right, if the remaining austenite changes its concentration. That this is the case when the bainite-transformation occurs, is shown by the research done at Düsseldorf. At the Max Planck-Institut für Eisenforsehung is confirmed the view as early as 1939 that the concentration of the alloying element in the cementite at a given temperature below A_1 is independent of the way by which this temperature is reached. But this fact is definitely proved only for carbide. Furthermore, is on the slope of bainite-reactions austenite remaining to a greater deal, comparison between the structure of bainite and tempered martensite is not allowed. In this case there is no difference between the nature and the composition of the constituents as well as between the percentage of carbide.

Mr. Allen. — This contribution is relevant to the views developed by Borelius and Hultgren on the nature of the primary nucleus of a precipating phase. Borelius has studied cases in which the free energy-composition curve has the form given in Fig. 1 of the paper, characterised by a change in sign of $\frac{\partial^2 f}{\partial x^2}$ in the supersaturated region.

When $\frac{\partial^2 f}{\partial x^2} < 0$, precipitation is subject to no barrier, and the rate of transformation is governed by the diffusion rate, but when $\frac{\partial^2 f}{\partial x^2} > 0$ the change is subject to a thermodynamic potential barrier which, in the cases he has studied, increases as the temperature rises, resulting in a fall of transformation rate with rising temperature.

At the National Physical Laboratory, the rate of the transformation $\alpha \rightarrow \gamma$ in iron-nickel alloys has been studied. In this case, the form of the free energy curves was determined (1) and is reproduced in Fig. A of this discussion. There are two intersecting U-shaped curves corresponding respectively to the α and γ solid solutions, and the point of intersection moves uniformly to lower nickel contents as the temperature rises. In both phases $\frac{\partial^2 f}{\partial x^2}$ is everywhere positive, so that the transformation is subject to an energy barrier, whenever a separation into two phases of different composition is required. The rate of transformation however, increases uniformly as the temperature rises and becomes too rapid to measure as soon as that temperature is reached at which transformation requires no separation into regions of different composition. An alloy with 6 per cent of nickel for exemple, X, Fig. A, initially in the α—condition changes at an imperceptibly slow rate at 327 °C or 527 °C, but begins to change slowly as the temperature 727 °C is approached, and cannot be restrained from changing as soon as 727 °C is reached. In this case the magnitude of the thermodynamic potential barrier appears to be determined principally by the difference in composition between the α phase and the γ phase which separate from it, and decreases as the temperature rises.

It has been found (2) that the rates of transformation of these alloys can be accounted for if it is assumed that the rate is proportional to the probability of the formation in the matrix of α of groups of about 300 atoms having the composition of the γ phase that should separate at the temperature in question. If the number of atoms in the group is N and X and Y are the atomic fractions of nickel in the matrix and in the group respectively this probability is given by :

$$P = {}^{N}C_{YN} X^{YN} (1-X)^{(1-Y)N} \qquad (1)$$

(1) C. Kubaschewski and C. von Goldbeck, *Trans. Faraday Soc.*, No. 322, Vol. XIV, Part 10, October 1949, p. 948.

(2) N. P Allen and C. C. Earley, *J. Iron and Steel Inst.*, December 1950, p. 261.

FIG. A

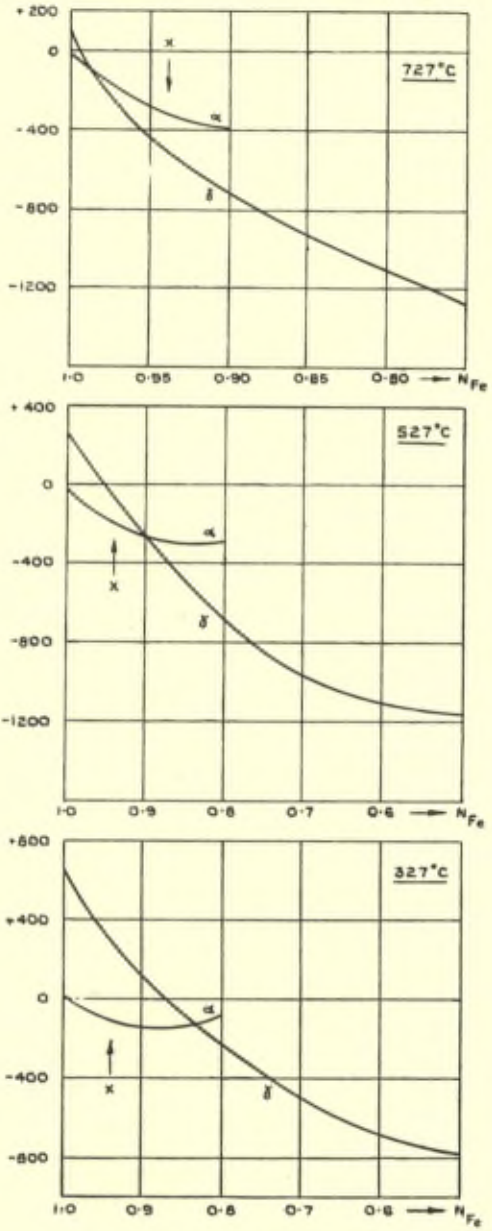
+200
0
-400
-800
-1200
x
α
β
727°C
1·0
0·95
0·90
0·85
0·80
N_{Fe}
+400
0
-400
-800
-1200
527°C
1·0
0·9
0·8
0·7
0·6
+800
+400
0
-400
-800
327°C

The relative rates of transformation at different temperatures of an alloy containing 15.3 per cent of nickel, calculated on this basis, and observed, are given in Table I.

TABLE I.

Relative Rates of Transformation of 15.3 % Nickel 84.7 % Iron Alloy.

Temp. °C	Calculated Relative Rate	Observed Relative Rate
590	1	1
600	2	1.7
610	4.2	2.6
620	6.4	5.7

The relative rates of transformation at the same temperature of alloys of different nickel content can also be derived. The concept of the transformation process that arises from these experiments is that small groups of atoms of the required composition arise by accident in the matrix of alpha crystals, and that these subsequently undergo the change from α to γ. This concept is essentially the same as that of Borelius : the agreement of the number of atoms in the group with the numbers found in some of his experiments is noteworthy.

The significance of this number may be considered further. If the nuclei of γ are considered, for the purpose of calculation, to be cubes, the minimum size of group is given by (1):

$$N\Delta G = \frac{6}{4^{2/3}} N^{2/3} a^2 \sigma, \qquad (2)$$

where ΔG is the difference of free energy per atom between the α phase and the composition of the nucleus, a is the lattice constant of the γ phase, and σ the surface energy per unit area of the surface between the alpha and gamma phases. The strain energy is neglected, because high strains cannot persist at the temperature in question. ΔG can be obtained from the work of Kubaschewski and von Goldbeck. It is less easy to assign a value to σ. According to C. S. Smith (2) the surface energies of α-iron grain boundaries at 825 °C are about 720 ergs/cm^2 and those of boundaries between α and γ in carbon steels are about three-quarters of this value. The energies of

(1) The f.c.c. lattice of γ iron has four atoms per unit cube.

(2) Preliminary Draft of paper for the Solvay Conference 1951. — « Interfaces between crystals ».

9.7 % Nickel alloy transformed at 650 °C.
× 750

15.3 % Nickel alloy transformed at 600 °C. × 750

19.7 % Nickel alloy transformed at 450 °C for 1000 hours. Reaction still incomplete. × 750

boundaries are strongly dependent upon their direction and the relative orientation of the material on either side, and it is to be assumed that if from a randomly formed group of atoms a nucleus can be formed with a favourable orientation and favourably disposed surfaces, this will be done, since energy will thereby be conserved. The measured energies of boundaries between favourably oriented crystals are about 20 per cent of the maximum energies. It is therefore reasonable to assume a surface energy of about 100 ergs/cm^2 for the boundaries between the α matrix and the γ nuclei. The nucleus that separates from an alloy containing 18 per cent of nickel at 527 °C contains 23 per cent of nickel, and the free energy change is 490 cals per gram atom. From (2) the minimum number of atoms in a stable nucleus is 745, which is of the right order of magnitude. The calculation is very sensitive to the value chosen for surface energy and free energy change, and if the effective surface energy has been seriously under-estimated, the expected nucleus size will be much greater than that which results from the experiments.

The probability that any group of 745 atoms in a matrix containing 18 per cent of nickel will contain 35 per cent of nickel is about 10^{-4}, so that 10,000 such groupe will be found in every cubic micron of the alloy. The microstructure, Fig. B, suggest that the numbers of nuclei, though large, are very much smaller than this, so that it is unlikely that every chance aggregate of atoms having the right composition becomes a transformation nucleus. As Hultgren suggests, it is quite improbable that so large a group of atoms will co-operate at once to the change from α to γ, and this may well be the reason why so few of the chance aggregates become nuclei.

In the range of temperature under consideration the isothermal transformation from γ to α is very much slower than the isothermal transformation from α to γ, and indeed, is very difficult to observe. The curves in Fig. A suggest a reason, for at 527 °C the change in free energy when a γ nucleus of the required composition (4 per cent nickel) changes to α is only 220 cals per gram atom, leading to an expected size of nucleus of 9,000 atoms. The formation of such a large nucleus so low in nickel content is very improbable indeed.

On cooling, γ changes to α by a diffusionless transformation at a temperature which for each alloy corresponds quite closely to the temperature at which the α solid solution has the same free energy

as the γ solid solution ([2]). Curiously enough, the reverse change does not occur on heating until a much higher temperature is reached. The reason is probably to be found in the geometry of the moments whereby γ is converted to α, and α to γ. The necessary shear is a natural shear mode of the γ crystal, and therefore may occur without a large activation energy : it is not a natural shear mode of the α crystal and the resistance to the movement is likely to be great.

Les défauts de périodicité dans les réseaux des solutions solides

A. Guinier

Conservatoire National des Arts et Métiers, Paris

Une solution solide homogène mais désordonnée n'est pas, à rigoureusement parler, un cristal puisque les atomes ne se correspondent pas avec une périodicité parfaite. Les perturbations du réseau ont une double origine. Supposons d'abord que les centres des ions soient répartis aux nœuds d'un réseau géométriquement parfait : néanmoins le potentiel autour de l'ion varie d'un nœud à l'autre sans régularité; le nombre et la répartition des électrons « liés » dépendent de la nature de l'ion. La seconde cause de perturbation est due aux différences de forces répulsives entre ions de nature différente, ou, plus schématiquement, aux différences de leur rayon : il se produit certainement des variations irrégulières de distances entre ions voisins.

Pour décrire la répartition réelle des atomes dans la solution solide, nous admettrons qu'elle est homogène d'après tous les moyens d'observation à notre disposition, c'est-à-dire qu'il n'existe pas de perturbations à long rayon d'action. On peut alors imaginer un réseau périodique idéal *moyen* et découper le solide, suivant la méthode de Wigner et Seitz, en autant de polyèdres réguliers qu'il contient d'atomes. L'atome qui n'est pas au centre du polyèdre a une position définie par un vecteur de déplacement $\overrightarrow{\Delta_L}$ dans la Lième cellule. Pour décrire le potentiel dans le solide, la première approximation sera d'admettre que dans chaque cellule, le potentiel ne dépend que de l'ion qui l'occupe et qu'il vaut : $V_i(\vec{r} - \overrightarrow{\Delta_L})$ si $V_i(\vec{r})$ est le potentiel caractéristique de l'ion i, au point $\vec{r}$. Evidemment, il est vraisemblable que l'influence du milieu modifie la fonction V_i. C'est ainsi que Mott admet, dans le cas de la solution d'un atome polyvalent dans un métal monovalent, qu'un ou plusieurs électrons de valence restent liés à l'atome de façon, par effet d'écran, à diminuer l'effet de la charge positive multiple. Raynor et Waldron (1949) ont même émis l'hypothèse que les éléments de transition pouvaient absorber des électrons (au lieu de contribuer au nuage des électrons libres). On peut, dans tous les cas, imaginer un atome fictif représentant la

moyenne des atomes réels. *Celui-ci, placé aux nœuds du réseau moyen, définira le cristal périodique idéal moyen* dont la solution solide dérive par de petites perturbations.

Les propriétés des solutions solides se classent en deux catégories : celles qui sont uniquement, ou pour la plus grande part, déterminées par le réseau moyen (densité par exemple) et celles qui dépendent au premier chef des perturbations. Ce second groupe contient notamment les propriétés mécaniques et électriques pour les alliages. On voit donc combien il est important pour le progrès de la physique des solides, de pouvoir définir les irrégularités dans les solutions solides. Les théoriciens sont obligés d'introduire des hypothèses qui ont besoin d'un soutien expérimental pour ne pas paraître trop arbitraires.

L'objet de ce rapport est de faire le point des résultats qui ont été acquis dans ce domaine par la méthode expérimentale la plus directe, la diffraction des rayons X. L'interprétation des données des rayons X se heurte à de nombreuses difficultés. Il y a encore assez peu d'études, mais les progrès de la technique semblent pouvoir offrir maintenant de nouvelles possibilités. Notre but principal est de discuter ces possibilités et de décrire les essais déjà effectués de façon à avoir une base de discussion avec les théoriciens pour l'établissement d'un programme de recherches sur la structure *réelle* des solutions solides.

1. LA DIFFRACTION DES RAYONS X PAR UN RÉSEAU PERTURBÉ

Le problème a été traité de nombreuses fois, les auteurs s'étant attachés à différents cas particuliers. Nous rapellerons ici les résultats généraux, en suivant à peu près la méthode de calcul de Zachariasen (1945), de façon à pouvoir classer les méthodes expérimentales possibles.

Le fait fondamental est que la diffraction des rayons X est, au premier ordre, commandé par le réseau moyen de la solution solide : c'est par exemple ce que donne le simple diagramme Debye-Scherrer. Les perturbations du réseau ne produisent que des effets secondaires : d'où les deux difficultés principales de l'étude. D'une part il faut utiliser des techniques expérimentales très perfectionnées, d'autre part, le réseau réel est souvent loin d'être entièrement déterminé à partir des données.

Nous rapporterons le solide réel au réseau moyen idéal contenant N mailles. Pour alléger l'écriture, nous ne considérerons ici que le réseau à un atome par maille. Nous précisons en outre l'origine du réseau moyen par l'une des conditions suivantes :

$$\Sigma_1^N \vec{\Delta}_L = 0$$

si les atomes sont tous identiques ou :

$$\Sigma_1^N Z_L \vec{\Delta}_L = 0$$

si l'atome de la maille L a un nombre atomique Z_L (on admet que pour tous les angles de diffraction, le facteur de diffusion est proportionnel à Z).

Suivant l'usage, appelons $\vec{S}_0$ et $\vec{S}$ les vecteurs unitaires suivant les rayons incident et diffracté, et s le vecteur $\frac{\vec{S} - \vec{S}_0}{\lambda}$. f_L est le facteur de diffusion de l'atome de la Lième maille, $\vec{A}_L$ le vecteur définissant dans l'espace cette maille, A_e et I_e sont respectivement l'amplitude et l'intensité diffusée par l'électron libre (formule de Thomson).

L'amplitude diffractée par le solide est :

$$A/A_e = \Sigma_L f_L e^{2\pi i \vec{s} \cdot (\vec{AL} + \vec{\Delta L})} = \Sigma_L f_L e^{2\pi i \vec{s} \cdot \vec{\Delta L}} \cdot e^{2\pi i \vec{s} \cdot \vec{AL}} \quad (1)$$

Ecrit sous la deuxième forme, cette expression montre que la diffraction est celle du réseau géométrique moyen dont les nœuds seraient occupés par un atome fictif de facteur de diffusion (complexe s'il est déplacé),

$$g_L = f_L e^{2\pi i \vec{s} \cdot \vec{\Delta L}} . \quad (2)$$

L'intensité diffractée est :

$$I/I_e = \Sigma_L \Sigma_{L'} g_L g^*_{L'} e^{2\pi i \vec{s} \cdot (\vec{AL} - \vec{AL'})} \quad (3)$$

On peut décomposer cette expression en deux termes dont l'un correspond à la diffraction par le réseau parfait moyen et l'autre représente la diffraction supplémentaire due aux défauts de périodicité. Il suffit à cet effet de faire intervenir la valeur moyenne de g_L dans le solide, g.

Si on pose : $g_L = g + \varphi_L$ on trouve :

$$I/I_e = |g|^2 \Sigma_L \Sigma_{L'} e^{2\pi i \vec{s} \cdot (\vec{AL} - \vec{AL'})} + \Sigma_L \Sigma_{L'} \varphi_L \varphi^*_{L'} e^{2\pi i \vec{s} \cdot (\vec{AL} - \vec{AL'})} \quad (4)$$

Le premier terme I_1 représente la diffraction par un réseau normal. Il est donc nul dès que l'on s'écarte dans l'espace réciproque des nœuds du réseau moyen. L'intensité *diffusée* en dehors de la direction de réflexion sélective est donc représentée par le second terme I_2 de (4). C'est ce terme qui est caractéristique du désordre du cristal : c'est le terme que l'on peut se borner à garder pour l'étude de la diffusion que nous allons d'abord examiner. Par contre ce mode de décomposition n'est plus valable quand on se rapproche trop des nœuds du réseau moyen, notamment pour chercher la forme et l'intensité des raies, que nous étudierons ensuite.

a) *La diffusion continue.*

Dans un solide indéfini, homogène, *sans ordre à grande distance*, on remarque que le vecteur $\overrightarrow{A_L} - \overrightarrow{A_{L'}}$ est un vecteur du réseau cristallin $\overrightarrow{A_M}$: on peut remplacer la somme double de I_2 par une somme simple :

$$I_2 = N \, \Sigma_M \, \Phi_M \, e^{2\pi i \vec{s} \cdot \overrightarrow{A_M}} \tag{5}$$

en posant :

$$\Phi_M = \frac{1}{N} \Sigma_L \, \varphi_L \, \varphi^*_{L,M} \tag{6}$$

La fonction Φ_M est l'analogue d'une fonction de Patterson pour les structures cristallines : elle représente la moyenne du produit des désordres existant dans deux mailles séparées par le vecteur $\overrightarrow{A_M}$. L'intensité diffusée correspondant à un certain point de l'espace réciproque est donc proportionnelle au coefficient du développement de Fourier de Φ_M :

$$\Phi_M = \frac{1}{N} \Sigma_p \, \psi_p \, e^{-2\pi i \vec{\tau}_p \cdot \overrightarrow{A_M}} \tag{7}$$

$\vec{\tau}_p$ étant le vecteur de l'espace réciproque. Etant donné que Φ_M n'est défini que pour les nœuds du réseau cristallin, $\vec{\tau}_p$ peut être choisi à l'intérieur de la première zone de Brillouin du réseau réciproque, car les valeurs de ψ_p sont identiques en deux points distants d'un vecteur de translation du réseau réciproque.

Le premier résultat sur lequel il convient d'insister est que l'expérience, par les diagrammes de diffusion, ne pourra donner que Φ_M et non pas les facteurs de désordre eux-mêmes. Etant donné l'irrégularité de φ_L, il sera à priori bien plus difficile d'interpréter le diagramme que les diagrammes de Patterson pour les structures cristallines. D'autre part, pour utiliser les formules générales, il est nécessaire de partir de très bonnes expériences si l'on veut obtenir un résultat significatif après les opérations de sommation de Fourier : ceci montre l'importance primordiale des techniques de mesure.

Des conclusions simples peuvent être tirées dans de nombreux cas particuliers importants. Nous rappellerons les points principaux suivants :

1. Si l'interaction entre le désordre dans des mailles voisines ne détruit pas la périodicité du réseau dans les trois dimensions simultanément, deux cas sont à considérer : *le désordre planaire* pour lequel les paramètres φ_L sont les mêmes pour tous les nœuds d'un plan réticulaire d'une certaine famille (P) et le *désordre linéaire* où φ_L est constant le long d'une rangée quelconque d'une famille donnée (R). Dans ces deux cas, la fonction Φ_M admet aussi ces périodicités à deux ou une dimension. Les facteurs ψ_p de la transformée de Φ_M ne sont donc respectivement différents de zéro que le long des rangées du réseau réciproque conjuguées des plans (P) ou des plans conjugués des rangées (R). Les diffusions anormales sont localisées sur ces rangées ou dans ces plans.

Dans le cas des désordres tridimensionnels, nous considérerons quelques cas particuliers : 1° Le *désordre thermique* par suite de l'interaction entre atomes voisins peut se résoudre en une superposition d'ondes de déformation. Chacune de ces ondes donne naissance à une diffusion limitée à un point de l'espace réciproque défini par la longueur d'onde et la direction de propagation de l'onde. Cette étude sort entièrement du cadre de notre rapport, néanmoins, elle est essentielle parce que l'agitation thermique existe dans tous les solides et son effet doit être déduit des diffusions observées pour pouvoir atteindre le désordre « statique ». Heureusement, à l'heure actuelle la question de l'agitation thermique a déjà été bien plus poussée que les études des autres désordres. Les corrections peuvent être faites à condition qu'on admette que l'agitation thermique d'un cristal perturbé est très voisine de celle du cristal moyen idéal.

2. Un cas fréquemment étudié est celui du « désordre parfait », c'est-à-dire dans lequel il n'y a aucune interaction entre les valeurs de

φ_L pour des mailles voisines. La formule générale (6) se simplifie : en effet puisque la valeur moyenne de φ_L est nulle et qu'il n'y a aucune corrélation entre φ_L et φ_{L-M} les termes Φ_M sont nuls sauf toutefois :

$$\Phi_o = \frac{1}{N} \Sigma_L \varphi_L \varphi_L^*$$

On montre que Φ_0 peut se mettre sous la forme :

$$\Phi_o = \overline{|g_L|^2} - |g|^2 \tag{8}$$

et d'après (5) :

$$I_2 = N (\overline{|g_L|^2} - |g|^2) \tag{9}$$

La diffusion ne dépend de la direction de diffusion que par l'intermédiaire de g dans lequel entrent les facteurs de diffusion des atomes et la valeur de $|s|$. Les variations de l'intensité diffusée sont lentes et ne dépendent que de l'angle de diffusion, et non de l'orientation du cristal.

Nous nous attacherons spécialement à la valeur de l'intensité diffusée pour les faibles angles de diffusion. Nous supposons donc $|s|$ petit et nous considérons aussi un solide assez peu désordonné (φ_L petit).

L'intérêt de considérer la portion de l'espace réciproque voisine du centre est que l'on peut distinguer l'effet des irrégularités de la *position* et de la *nature* des atomes.

Supposons d'abord que les atomes ne soient pas déplacés. La formule (8) n'est autre que la formule donnée par Laue (1941) pour la diffusion d'une solution solide parfaitement désordonnée. Si l'on considère le cas d'un alliage binaire formé de deux atomes A et B de facteurs de diffusion f_A et f_B, dans les proportions c et $1 - c$, on a :

$$g = c f_A + (1 - c) f_B$$

$$\overline{g_L^2} = c f_A^2 + (1 - c) f_B^2$$

et :

$$I_2 = N c (1 - c) [f_A - f_B]^2 \tag{10}$$

L'intensité diffusée est *maximum* au centre et décroît lentement avec l'angle comme les facteurs de diffusion des atomes : elle est d'autant plus forte que la solution solide est plus près de la formule AB.

Considérons ensuite le cas opposé : un solide composé d'atomes

tous identiques (facteur de diffusion f) et légèrement déplacés des nœuds du réseau théorique :

$$g_L = f\, e^{2\pi i \vec{s} \cdot \vec{\Delta}_L}$$

Quand s est petit, on développe l'exponentielle :

$$g_L = f(1 + 2\pi i \vec{s} \cdot \vec{\Delta}_L - 2\pi^2 (\vec{s} \cdot \vec{\Delta}_L)^2 + \ldots)$$

et puisque : $$\Sigma \vec{\Delta}_L = 0$$

$$\bar{g} = f(1 - \frac{2\pi^2}{N} \Sigma (\vec{s} \cdot \vec{\Delta}_L)^2 + \ldots)$$

D'autre part :

$$g_L^2 = f^2\, e^{4\pi i \vec{s} \cdot \vec{\Delta}_L}$$

et : $$\overline{g_L^2} = f^2(1 - \frac{8\pi^2}{N} \Sigma (\vec{s} \cdot \vec{\Delta}_L)^2 + \ldots)$$

on trouve finalement, d'après (9), en première approximation :

$$I_2 = N \cdot 4\pi^2 s^2 \frac{\Delta^2}{3} \qquad (11)$$

si Δ est la moyenne quadratique des déplacements des atomes hors des nœuds. La formule (11) montre que dans le cas de désordre dû aux déplacements des atomes, l'*intensité diffusée au centre tend vers zéro contrairement à ce qui se passe dans le cas où les atomes sont de nature différente* (formule 10).

Quand les deux causes de désordre se superposent, tout se passe, en première approximation, vers les très faibles angles, comme si les atomes étaient régulièrement disposés.

On voit donc que l'étude de la diffusion aux faibles angles et la comparaison de celle-ci avec la diffusion aux grands angles permet de distinguer entre les effets du désordre de position et de substitution des atomes.

La région centrale de l'espace réciproque est d'autant plus intéressante à explorer que d'autres causes de diffusion s'annulent ou deviennent très faibles : l'intensité du rayonnement Compton tend vers zéro pour les faibles angles; le diffusion thermique est régie aussi par une formule analogue à (11). Mais l'amplitude des ondes de déplacement est de la forme $\frac{K}{|s|}$, ce qui conduit à une limite finie

pour l'intensité diffusée à l'angle nul ; on trouve d'ailleurs qu'elle est très faible, en tout cas, elle est là plus faible que pour tout autre angle de diffusion.

3. Quand il y a interaction entre les désordres dans les mailles voisines, l'intensité diffusée subit des variations dans la maille de l'espace réciproque : les régions de forte diffusion correspondent aux lieux des extrémités des vecteurs $\vec{\tau}_p$ pour lesquels les coefficients du développement de Fourier sont élevés. Les grandes périodes pour la répartition du désordre correspondant à des vecteurs $\vec{\tau}_p$ très petits donc à des points groupés autour des nœuds du réseau réciproque, les très courtes périodes à des points au milieu de la maille. Dans le cas des désordres de position, il ne peut pas y avoir de brusques variations de φ_L à cause du diamètre minimum des atomes; on peut donc préciser qu'en général les périodes assez grandes seront prépondérantes dans le développement de Φ_M et la diffusion sera concentrée autour des nœuds du réseau moyen. Dans le cas des alliages semi-ordonnés, au contraire il y aura des diffusions au voisinage du milieu des deux nœuds, points qui correspondent à des périodes doubles de celle du réseau moyen (tendance à l'alternance des deux sortes d'atomes).

b) *Largeur angulaire et intensité des diffractions du réseau moyen.*

Les raies ou taches de diffraction du réseau moyen dépendent en premier lieu du terme I_1 de l'expression (4). A condition que les désordres soient faibles et surtout que les grandes périodes ne soient pas prédominantes dans le développement, le terme I_2 reste négligeable devant I_1. Comme le terme I_1 a la même structure que pour un réseau parfait, on prévoit qu'il n'y aura pas d'effet d'élargissement des raies : c'est ce qui se passe pour l'agitation thermique. Dans le cas d'un désordre de substitution sans déplacements d'atomes, le facteur de structure pour toutes les raies reste constant et égal au facteur moyen. L'intensité relative des raies des différents ordres sera donc la même que pour un réseau parfait : il n'y a donc aucun renseignement à tirer de l'étude des raies. Mais si les atomes sont déplacés (supposons qu'ils soient tous identiques), le facteur de structure moyen peut s'exprimer quand les déplacements sont petits par l'approximation :

$$\overline{g} = f\, e^{-2\pi^2 \frac{r^2 \Delta^2}{3}}$$

donc les intensités des raies seront proportionnelles à :

$$f^2 \, e^{-4\pi^2 \frac{s^2 \Delta^2}{3}}$$

C'est un facteur qui vient diminuer l'intensité des raies à mesure que l'angle de diffraction augmente et qui s'ajoute au facteur de Debye pour les effets des vibrations thermiques qui a une forme analogue. On pourra donc par la mesure de la décroissance de l'intensité des raies, déterminer la valeur quadratique moyenne du déplacement des atomes, mais cette mesure ne sera possible que si on peut comparer la solution solide à un cristal pur dans lequel les vibrations thermiques sont identiques, et si, de plus, le désordre thermique n'est pas trop grand vis-à-vis du désordre « statique ».

Il est essentiel de noter que les conclusions précédentes ne sont valables que si le terme de diffusion I_2 reste faible au voisinage de la raie de diffraction. Si, au contraire, il existe des désordres à grande périodicité, par exemple, concentration d'atomes dans une région du réseau, ou existence de volumes notables, où le paramètre de la maille a une valeur constante et légèrement différente de la moyenne, la décomposition de l'expression (4) en I_1 et I_2 n'a plus de sens. La raie de diffraction pourra devenir plus large. Plusieurs auteurs récemment [Wilson (1943), Averbach et Warren (1949), Bertaut (1950)] ont étudié la forme de la raie et ont montré comment on pouvait en déduire la répartition des tensions internes. Les calculs ont été appliqués pour des réseaux déformés par écrouissage. Il ne semble pas qu'on ait signalé d'effet d'élargissement des raies pour des cristaux mixtes sauf dans le cas d'alliages durcissants : il serait intéressant de reprendre l'étude de la largeur des raies du duralumin avec les nouvelles acquisitions tant du côté expérimental que du côté théorique pour comparer les résultats déduits de la forme des raies à ceux déduits des diffusions continues.

D'un autre point de vue, il est difficile de définir d'une manière précise l'intensité d'une réflexion. En effet, on soustrait généralement du « pic » de la raie, le fond continu. Mais suivant qu'on prolonge les mesures plus ou moins loin du centre de la raie, on englobe ou on néglige les « ailes » de la raie, c'est-à-dire qu'on compense plus ou moins la diminution de l'intensité de la raie par l'augmentation de la diffusion continue à son immédiate proximité. Ainsi s'expliquent les résultats contradictoires obtenus par différents auteurs sur les

mesures d'intensité des raies dans les réseaux déformés [Brindley et Spiers (1935) — Averbach et Warren (1949)].

En résumé, il est imprudent de ne se fier qu'à des mesures de largeur ou d'intensité des raies de diffraction sans étudier par ailleurs la répartition de l'intensité de la diffusion continue.

II. LES POSSIBILITÉS EXPÉRIMENTALES

Ayant examiné les divers effets des désordres sur les diffractions ou diffusions des rayons X, il faut déterminer ceux qui seront utilisables pour l'étude de la structure réelle du solide.

Deux difficultés se présentent : La première est que les effets sont de second ordre : la diffusion continue est d'intensité faible, la modification de l'intensité ou de la forme des raies est légère. Il faut donc des appareils puissants (tubes à grande brillance, récepteurs sensibles) et précis : la plaque photographique qui a été utilisée principalement jusqu'ici ne suffit pas pour obtenir des résultats quantitatifs et doit être remplacée par le compteur Geiger-Muller. Le deuxième obstacle est l'existence de plusieurs causes de diffusion qui se superposent à celle que l'ont veut étudier. Par des dispositifs expérimentaux, on peut en général éliminer les diffusions parasites (causées par autre chose que l'échantillon) et le rayonnement de fluorescence, mais il reste le rayonnement Compton et la diffusion thermique. Le premier peut être évalué théoriquement, le second mesuré sur des cristaux purs très analogues, et les corrections peuvent être faites par soustraction à condition que l'on ait des mesures précises. On pourrait aussi songer à opérer à basse température pour éliminer la diffusion thermique : ainsi en opérant à la température de l'air liquide on réduit de 60 % la diffusion du cuivre, Il n'y aurait aucun intérêt à opérer dans l'hélium liquide, car il y a un résidu important dû aux vibrations constituant le « zero point energy ».

III. LES ÉTUDES DE STRUCTURES DES CRISTAUX MIXTES PAR LES RAYONS X

Nous allons maintenant passer en revue les résultats qui ont été acquis par les méthodes dont le principe vient d'être exposé. Quand les études faites ne sont qu'à leur stade préliminaire, nous discuterons des possibilités dans l'état actuel de la technique.

a) Les solutions solides en équilibre thermodynamique.

Le premier problème qui se pose est la constitution des solutions solides en équilibre thermodynamique. La théorie élémentaire représente le cristal mixte comme constitué par un réseau unique aux nœuds desquels sont disposés les atomes des différentes sortes. On sait qu'il y a des distorsions puisque les solutions solides ne peuvent exister que si les diamètres des atomes ne sont pas trop différents (règle de Hume-Rothery). Voyons ce que les rayons X peuvent nous apprendre sur l'ordonnancement des atomes et leurs déplacements.

1. *Cas de solutions solides étendues.*

Pour étudier la répartition des atomes, la méthode la plus simple est la mesure de l'intensité diffusée vers les très petits angles. Si, suivant l'hypothèse la plus simple, la répartition des atomes est parfaitement irrégulière, la formule de Laue (10) donne l'intensité de la diffusion que l'on doit observer. Mais celle-ci est-elle expérimentalement décelable? Nous la mesurerons en équivalent i d'électrons libres par atome présent dans le cristal mixte. D'après (10), on a :

$$i = c\,(1-c)\,(f_A - f_B)^2.$$

Considérons une solution solide de cuivre dans l'aluminium. Si nous supposons que les deux métaux sont à l'état d'ions Cu^+ et Al^{+++} pour une concentration de 1 % :

$$i = 0{,}01\ (28\text{-}10)^2 = 3{,}2 \text{ élec./atomes.}$$

Olmer (1948) a trouvé des pouvoirs diffusants de cet ordre de grandeur dans l'étude de l'agitation thermique de l'aluminium pur dans les régions de moindre diffusion. L'effet est donc à la limite de ce qui est accessible à l'expérience. Toutefois les premiers essais que nous avons faits n'ont pas été concluants; ils ont montré qu'il est nécessaire d'opérer avec un tube plus puissant et de prendre plus de précautions pour éviter tout rayonnement parasite. De plus le cas schématique pris pour exemple, n'est pas des plus favorables. On pourrait opérer sur des solutions plus concentrées (5 à 10 %) avec des atomes de nombres atomiques très différents l'un de l'autre.

On peut donc raisonnablement considérer comme possible la mesure de la diffusion des solutions solides aux faibles angles. Que

tirera-t-on du résultat si celui-ci est différent du résultat de la formule de Laue?

1. Conservons l'hypothèse que les atomes A et B sont distribués au hasard. Nous avons admis que les nœuds étaient occupés par des ions. Mais, comme nous l'avons déjà dit, on ne connaît pas de façon certaine le nombre d'électrons effectivement liés à l'ion (Pauling, 1945). Or il est très difficile de déterminer ce nombre par des mesures ordinaires d'intensité de réflexion cristalline, car les facteurs de diffusion de l'ion et de l'atome ne sont différents que pour les faibles angles de diffraction, région où il n'y a pas, en général, de raies (fig. 1). La diffusion des solutions solides aux très faibles angles

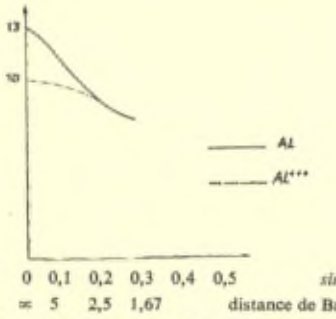

Fig. 1. — Facteur de diffusion atomique.

permettrait de déterminer le nombre d'électrons liés à l'ion. Ainsi, si au lieu des ions Cu^+ et Al^{+++} on avait des ions Cu^+ et Al^+; l'intensité de diffusion serait diminuée dans le rapport :

$$\left(\frac{28-12}{28-10}\right)^2 = \left(\frac{16}{18}\right)^2 = 0{,}8,$$

ce qui est appréciable.

2. Supposons connu l'état électronique des ions. Si l'intensité diffusée au centre est inférieure à celle que l'on attend, c'est qu'il y a tendance à répulsion entre les atomes dissous : il y a moins de couples d'atomes dissous proches voisins que ne le prévoit la distribution au hasard. Mais dans le cas de solutions étendues, la plupart des atomes dissous sont trop loin l'un de l'autre pour avoir une action : les possibilités d'arrangement sont donc peu importantes. Nous retrouverons, par contre, ce cas à propos des solutions concentrées.

Si l'intensité diffusée au centre est trop élevée, c'est qu'il y a, pour les atomes dissous, tendance à l'agglomération. Si on suppose schématiquement que tous les atomes dissous sont groupés en noyaux de m atomes et que ces groupes sont disposés au hasard dans la solution solide, l'intensité limite que l'on mesure vers l'angle nul de diffusion est m fois plus grande que l'intensité donnée par la formule (10). De plus, la variation de l'intensité avec l'angle de diffusion permet d'évaluer la dimension de l'amas d'atomes (Guinier, 1945*a*). Il est évident qu'une telle répartition d'atomes dissous n'est pas probable, étant donné que nous avons supposé que la solution solide était dans un état stable. Mais ceci peut n'être plus vrai, si le réseau cesse d'être parfait. L'énergie libre de l'ensemble peut être diminué si les atomes étrangers sont groupés dans les régions les plus désordonnées du réseau.

C'est l'hypothèse de Cottrell (1948) sur les nuages d'atomes autour des dislocations. Une simple dislocation dans un métal pur ne produit pas de diffusions au centre (Wilson, 1948). Mais elle serait « révélée » si un nombre suffisant d'atomes de nombre atomique franchement différent venaient s'y rassembler. Est-ce que l'expérience pourrait prouver l'existence des nuages de Cottrell? Dans un plan (100) d'aluminium de 1 cm^2 il y a 10^{15} atomes environ. On a souvent avancé le chiffre de 10^{12} lignes de dislocation par cm^2 comme chiffre maximum quand le métal est déformé. Si chaque dislocation rassemble 10 atomes par plan réticulaire, il y a une proportion de 1 % d'atomes étrangers rassemblés. Dans les cas favorables, cette irrégularité de répartition serait, à la rigueur, perceptible aux rayons X. Mais le phénomène ne serait interprétable que si l'on peut admettre qu'il n'y a pas d'autres défauts plus importants dans le métal écroui (lacunes par exemple) perturbant également la diffusion au centre.

En résumé, les expériences sur les diffusions aux faibles angles des solutions solides peuvent être tentées mais elles sont certainement délicates, car les effets intéressants sont à la limite des possibilités expérimentales.

En ce qui concerne la mesure des désordres de déplacement des atomes dans les solutions solides étendues, la diffusion continue n'a pas été utilisée encore. D'ailleurs, elle doit, d'après le calcul d'Huang (1947) avoir des caractères communs avec la diffusion thermique (maximum près des nœuds du réseau moyen) et être bien plus faible aux températures ordinaires. Il y a donc peu de chances

que l'on puisse résoudre ce problème expérimental dans le cas de solutions étendues. Nous verrons comment il a été abordé sur les cristaux mixtes formés d'éléments en proportion du même ordre de grandeur.

Une autre donnée importante qu'on doit rechercher expérimentalement, c'est l'état de l'atome introduit en solution solide. La structure électronique de l'ion peut être étudiée par la spectroscopie d'émission ou d'absorption des rayons X mous : peu de résultats ont encore été acquis de façon sûre (Cauchois, 1948). Nous avons déjà parlé d'une méthode de détermination du nombre d'électrons liés (p. 208). Un autre élément à évaluer est le volume de l'ion qui peut n'être pas rigoureusement le même que dans le métal pur. Ce sont les mesures précises des paramètres du réseau moyen qui peuvent donner la solution. Huang (1947), dans son calcul de la distorsion du réseau, a trouvé pour le paramètre du réseau moyen celui qui est prévu par la loi de Végard. Mais on sait que celle-ci n'est pas rigoureusement vérifiée. Jaswon, Henry et Raynor (1951), ont tenté d'expliquer cette divergence en calculant la déformation des atomes par une méthode semi-empirique. La concordance avec l'expérience n'est bonne que dans un cas (Cu-Ag) et est franchement mauvaise dans d'autres (Au-Cu).

Remarquons que si la loi de Végard est suivie, il n'y a pas addition des volumes atomiques : mais si on part de cette dernière hypothèse, le paramètre calculé concorde bien avec l'expérience dans un plus grand nombre de cas que pour le calcul de Raynor (Au-Cu — Ag-Cu) : il reste des divergences notables dans d'autres cas (Cu — Ag). On est donc encore loin de pouvoir rendre compte de façon satisfaisante du paramètre du réseau moyen et l'on ne connaît pas le rayon réel d'un atome quand il est inclus dans un cristal d'atomes différents.

2. *Cas des solutions solides concentrées.*

Quand il y a suffisamment d'atomes dissous dans une solution solide homogène, la probabilité de trouver deux atomes dissous proches voisins est notable : il y aura donc interaction entre ceux-ci et l'énergie libre de l'ensemble dépend de l'arrangement des atomes dissous aux nœuds de la solution solide. Depuis longtemps on a reconnu que dans certaines solutions solides concentrées, à une

température donnée, dite température critique, Tc, l'alliage subit une transformation entre un état désordonné et un état ordonné. Ce dernier se manifeste par l'apparition sur le diagramme de diffraction de raies de surstructure. Nous allons examiner les progrès récemment réalisés dans l'étude expérimentale de l'ordre dans les solutions solides concentrées et montrer comment les résultats trouvés s'accordent avec les dernières études théoriques.

On considérera uniquement le désordre de substitution des atomes dans leur solution solide binaire. Tant pour l'interprétation des résultats expérimentaux que pour l'élaboration des théories, on a toujours supposé les atomes aux nœuds d'un réseau parfait. Nous ne considérerons pas le cas, pourtant fréquent, où l'ordonnancement des atomes s'accompagne d'un changement de réseau.

On définit l'ordonnancement des atomes par des « paramètres d'ordre » dont nous rappelons la signification. A basse température, en état de parfait équilibre, les N nœuds du réseau sont différenciés en Na nœuds α occupés par les atomes A et Nb nœuds β par les atomes B. Dans l'état de désordre complet, les Na nœuds α ne sont occupés que par Na^2 atomes A. Un état d'ordre intermédiaire est défini par le *paramètre d'ordre à grande distance*, S, proportionnel au nombre $n_{\alpha,A}$ des nœuds α occupés, par les atomes A et choisi de façon qu'il varie de 0 à 1 quand on passe de l'ordre parfait au désordre complet. D'où la définition :

$$n_{\alpha,A} = (1-a)S + a$$

D'autre part, on définit les paramètres d'ordre à petite distance pour chaque vecteur de translation $\vec{M}$ du réseau cristallin. Si un atome B est à l'origine du vecteur M, à l'extrémité, la probabilité de trouver un atome A sera $n_{2,BA}(\vec{M})$. Pour le désordre complet, ce serait p_A, proportion des atomes A dans le réseau, le paramètre d'ordre sera défini par :

$$\alpha(\vec{M}) = 1 - \frac{n_{2,BA}(M)}{p_A}$$

α est nul pour le parfait désordre, il prend sa valeur maximum (en valeur absolue) pour l'ordre parfait : par exemple pour l'alliage Au-Cu_3 ordonné α (110) = — 1/3 et α (200) = 1.

Dès que le paramètre d'ordre à grande distance a une valeur notable, les $\alpha(\vec{M})$ sont très près de leur maximum : c'est quand S est nul, que les $\alpha(\vec{M})$ prennent de l'intérêt car ils peuvent conserver une valeur notable.

Les rayons X actuellement permettent la mesure, avec une bonne précision, des différents paramètres qui viennent d'être définis.

3. *Mesure de l'ordre à grande distance.*

Les raies de surstructure caractéristiques de l'ordre ont une intensité qui dépend uniquement de l'ordre à grande distance. Prenons par exemple le cas de la solution solide AB s'ordonnant suivant un réseau cubique centré, c'est-à-dire que les deux atomes A et B tendent à se séparer sur l'un et l'autre des deux réseaux cubiques simples. La proportion d'atomes A sur le premier est :

$$\frac{1+S}{2}$$

et sur le second :

$$\frac{1-S}{2}$$

donc le facteur de structure d'une raie de surstructure est :

$$f_A\left(\frac{1+S}{2}\right)+f_B\left(\frac{1-S}{2}\right)-f_A\left(\frac{1-S}{2}\right)-f_B\left(\frac{1+S}{2}\right)$$

soit :

$$S\,(f_A-f_B).$$

La mesure de l'intensité de la raie de surstructure donne directement S^2. Cette mesure peut être faite actuellement dans de bonnes conditions. La mesure est d'autant plus aisée qu'il y a une grande différence de facteurs de diffusion entre les deux atomes. Mais Chipman et Warren (1950) sont parvenus à mesurer l'ordre à grande distance dans le laiton β Cu-Zn en employant un monocristal et en mesurant avec un compteur le pouvoir réflecteur du plan (100).

Non seulement la radiation primaire doit être monochromatisée mais il est essentiel de prendre des précautions spéciales pour ne pas être géné par l'harmonique $\frac{\lambda}{2}$ qui est aussi réfléchi par le cristal.

(Emploi d'un double filtre : Ni et Co pour Cu Kα), La correction pour le facteur de température peut être déterminée de façon simple et précise par l'étude des réflexions normales du réseau. Les mesures sont faites à différentes températures de façon à déterminer la courbe $S = f(T)$ (fig. 2).

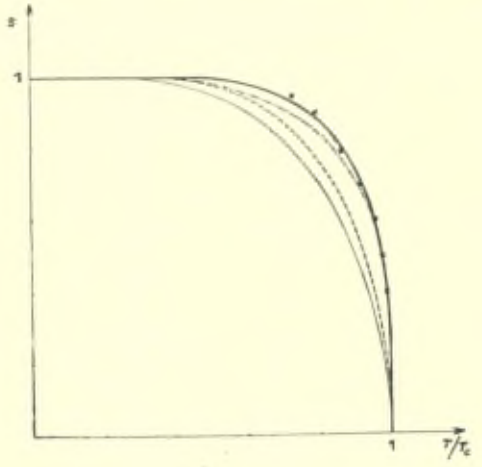

Courbes théoriques
- ——— d'après Bragg
- - - - - - - - - - - - - - - d'après Bethe
- — — - — — - — — d'après Cowley
- ——— d'après Fournet
- × × × × × × × Points expérimentaux de Chipman-Warren

Fig. 2. — Variation du degré d'ordre à grande distance avec la température.

4. *Mesure de l'ordre à petite distance.*

C'est la diffusion continue du cristal de solution solide qui permet d'atteindre les paramètres d'ordre à petite distance. En effet, dès que la solution solide n'est plus complètement désordonnée, la diffusion continue n'est plus constante (à la décroissance des facteurs de diffusion près). C'est la formule (5) qui permet de la calculer. Les paramètres Φ_M sont directement reliés aux divers paramètres d'ordre. En effet, le facteur de diffusion moyen de l'atome est :

$$g = p_A f_A + p_B f_B$$

donc Φ_L est égal à :

$$\varphi_A = p_B(f_A - f_B) \qquad \text{pour un atome A}$$

$$\varphi_B = -p_A(f_A - f_B) \qquad \text{pour un atome B}$$

Appelons $n_{2,AA}$, $n_{2,BB}$, $n_{2,AB}$, $n_{2,BA}$ les probabilités de trouver deux atomes A, deux atomes B, les atomes A et B aux extrémités du vecteur $\overrightarrow{M}$. On trouve :

$$\Phi_M = p_A\, n_{2,AA} \varphi_A^2 + (p_A\, n_{2,AB} + p_B\, n_{2,BA})\, \varphi_A\, \varphi_B + p_B\, n_{2,BB} \varphi_B^2$$

Les probabilités n_2 se déduisent simplement de α_M.

$$\begin{aligned} n_{2,AA} &= p_A + p_B\, \alpha_M \\ n_{2,AB} &= p_B\,(1 - \alpha_M) \\ n_{2,BA} &= p_A\,(1 - \alpha_M) \\ n_{2,BB} &= p_B + p_A\, \alpha_M \end{aligned}$$

On en tire :

$$\Phi_M = p_A\, p_B\, (f_A - f_B)^2\, \alpha_M$$

Donc d'après (5) :

$$I_2 = N\, p_A p_B\, (f_A - f_B)^2 \sum \alpha_M\, e^{2\pi i \vec{s} \cdot \vec{M}} \qquad (11)$$

I_2 est donc exprimé comme une série de Fourier à trois dimensions, c'est une fonction périodique dans l'espace réciproque ayant la périodicité de la maille élémentaire du réseau moyen. Il est donc possible inversement de déduire les coefficients α de la connaissance de I_2 pour tous les points de cette maille :

$$\alpha_M = \int \frac{I_2}{N\, p_A \cdot p_B\, (f_A - f_B)^2}\, e^{-2\pi i \vec{s} \cdot \vec{M}}\, \overrightarrow{ds} \qquad (12)$$

Cowley (1950*b*) puis Norman et Warren (1951) ont montré que cette méthode pouvait être appliquée avec succès. On mesure la diffusion d'un monocristal en faisant varier l'orientation des faisceaux incidents et diffractés, de façon à explorer tout le volume de la maille du réseau réciproque. (Compte tenu des symétries, le volume à explorer est évidemment inférieur à la maille.) Le rayonnement incident doit être monochromatisé, mais l'usage d'un cristal courbé permet d'avoir néanmoins une intensité suffisante. Des corrections doivent être faites pour déduire de l'intensité observée le rayonnement Compton (environ 10 %) et le rayonnement de diffusion thermique : le premier est calculé et le second déduit d'expériences à diverses températures.

Le résultat obtenu par Cowley avec l'alliage Cu_3Au à une température supérieure à la température critique est représenté pour le plan (100) du réseau réciproque dans la figure 3. Chaque point de l'espace réciproque qui est un nœud de surstructure dans la phase ordonnée est entouré d'une zone de diffusion : ces zones ont une forme particulière, elles sont aplaties, leurs faibles dimensions étant

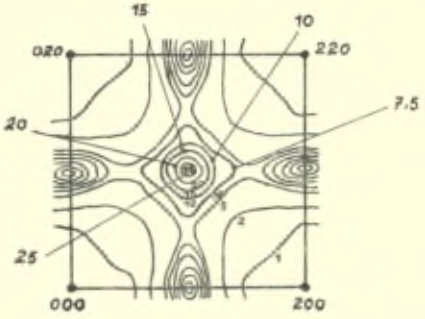

Fig. 3. — Répartition de l'intensité diffusée dans le plan (001) de l'espace réciproque de Cu^3Au à 405° C

parallèles à celui des axes [001] pour lequel l'indice du nœud a une parité différente des deux autres (par exemple, l'axe 0*z* pour 110, l'axe 0*x* pour 100, etc.). Ces résultats confirment et précisent les études antérieures faites par photographie (Guinier et Griffoul, 1948) et l'on voit sur cet exemple les rôles respectifs des deux techniques expérimentales : la photographie est un moyen d'exploration d'un phénomène et le compteur G. M. un moyen de mesure très sensible et actuellement d'une bonne précision.

Le tableau suivant donne les degrés d'ordres trouvés par Cowley pour Au-Cu_3 à 405° C : il montre que même après les premières couches, il reste encore un degré d'ordre faible certes, mais différent de 0 et franchement variable d'une couche à l'autre.

N° de la couche	Coordonnées du vecteur $\vec{M}$ dans le cristal	C_M pour l'ordre parfait	C_M pour l'alliage en équilibre à 405°
1	110	— 0,33	— 0,15
2	200	1,00	0,19
3	211	— 0,33	0,009
4	220	1,00	0,095
5	310	— 0,33	— 0,053
6	222	1,00	0,025
7	321	— 0,33	— 0,016
8	400	1,00	0,048
9	330	— 0,33	— 0,026
	411	— 0,33	0,011
10	420	1,00	0,026

L'alliage Au-Ag est intéressant parce qu'on ne le connaît pas sous une forme ordonnée. Néanmoins il existe un ordre à petite distance [Guinier, (1945*b*), Norman et Warren (1951)]. Mais le degré d'ordre

est plus faible et les diffusions sont bien moins intenses que dans le cas de Au Cu_3.

Pour Cu-Zn, la différence des facteurs de diffusion atomiques est trop faible pour que l'effet soit perceptible.

5. *Accord avec la théorie de la transformation ordre-désordre.*

Les résultats sur la répartition des atomes sont en accord général avec ce que permettent de prévoir les théories les plus poussées à l'heure actuelle. L'exposé détaillé de celles-ci est en dehors du cadre de ce rapport, mais nous en citerons quelques résultats pour montrer comment les perfectionnements des mesures expérimentales permettent de donner les points d'appui nécessaires au progrès des études théoriques.

Le calcul de l'état d'équilibre d'une solution solide concentrée à été repris de nombreuses fois [voir la revue de Nix et Shockley (1938)]. Récemment, dans des travaux encore en grande partie non publiés, Fournet (1951) a fait la synthèse des diverses approximations à partir de la théorie rigoureuse donnée par Yvon (1945). Yvon part d'hypothèses très générales : il considère un réseau parfait, rigide, indépendant du degré d'ordre et suppose connue la structure cristalline de l'alliage parfaitement ordonné. Il admet que l'énergie potentielle totale est la somme des énergies mutuelles des atomes pris deux à deux. L'énergie mutuelle d'un couple ne dépend que de la distance des atomes et de leur nature. Elle décroît avec la distance et s'annule pour de grandes distances. Ce qui intervient dans le calcul est en réalité la différence des énergies des paires semblables et dissemblables :

$$W(\vec{r}) = W_{AA}(\vec{r}) + W_{BB}(\vec{r}) - 2\,W_{AB}(\vec{r})$$

Etant donnée la structure d'un réseau, on n'a à considérer qu'une suite discontinue des distances interatomiques correspondant aux premiers, seconds, etc.. voisins, $W(r_1)$, $W(r_2)$, etc... Yvon applique la thermodynamique statistique classique pour évaluer la probabilité d'une configuration et l'énergie libre du système en fonction de son degré d'ordre.

A partir de ces hypothèses, Yvon a pu donner les équations donnant le paramètre d'ordre à grande distance, et les différents paramètres d'ordre à petite distance définis au paragraphe précédent. Ces équations se présentent sous la forme d'un développement infini. Mais

on peut diviser l'équation en termes ne faisant intervenir seulement un nœud, seulement deux nœuds, trois nœuds, etc...

$$A_1 + A_2 + A_3 + \ldots = 0;$$

à leur tour les deuxième, troisième,... termes peuvent être subdivisés en plusieurs parties : dans la première n'intervient que l'énergie entre premiers voisins $W(r_1)$, dans les secondes que $W(r_1)$ et $W(r_2)$, énergies entre premiers et seconds voisins, etc...

L'équation d'Yvon peut donc s'écrire :

$$\begin{aligned} & A_1 + A_{2,r_1} + A_{3,r_1} + \ldots\ldots \\ & \quad + A_{2,r_2} + \quad\; + \ldots\ldots \\ & \quad + A_{2,r_3} + \quad\; + \ldots\ldots \\ & \quad + \ldots\ldots\ldots\ldots\ldots\ldots = 0. \end{aligned}$$

Fournet a pu montrer que toutes les théories proposées pour le calcul de l'ordre [à l'exception de celle de Cowley (1950*a*)] sont fondées sur des équations dérivées de celles d'Yvon après différentes simplifications. Bragg et Williams (1934) avaient supposé que $W(r_1)$ était infiniment petit (mais le produit de $W(r_1)$ par le nombre des premiers voisins était fini); Bethe (1935), Fowler et Guggenheim (1936) n'avaient considéré que les premiers voisins et les termes à deux nœuds. Yvon, en négligeant $W(r_2)$ $W(r_3)$... avait considéré en plus les termes à trois et quatre nœuds, mais l'amélioration n'était pas très notable. Aussi Fournet a-t-il tenté de considérer à la fois l'énergie entre premiers et seconds voisins mais n'a conservé que les termes à deux nœuds. Dans son article récent sur les phénomènes coopératifs, R. Kikuchi (1951) a donné un nouveau mode de calcul valable pour quelques réseaux simples. Fournet a montré que ses résultats, ainsi que ceux, plus rigoureux de Oguchi, peuvent être retrouvés à partir de la théorie d'Yvon en considérant les termes faisant intervenir respectivement six et sept nœuds et en négligeant $W(r_2)$, etc.

En écrivant que l'état stable est celui de l'énergie libre minimum à une température donnée, Fournet a pu calculer la fonction :

$$S = f\left(\frac{T}{T_c}\right),$$

T_c est la température au-dessus de laquelle le seul état stable, d'après

les équations, est celui où S = 0, c'est-à-dire l'état désordonné. T_c et la forme de la courbe S dépendent de $W(r_1)$ et du rapport :

$$\frac{W(r_2)}{W(r_1)},$$

les deux paramètres étant choisis de façon que T_c soit égal à la valeur expérimentale de la température critique de désordre, on a un faisceau de courbes à comparer à la courbe expérimentale S(T).

Par exemple, pour l'alliage Cu-Zn, Fournet a trouvé une très bonne concordance avec l'expérience pour :

$$\frac{W(r_2)}{W(r_1)} = 0{,}33.$$

Le progrès sur les précédentes approximations est très notable (fig. 2). Mais le test de la théorie est de prévoir les autres propriétés de la solution solide à partir des deux seuls paramètres empiriques $W(r_1)$ et $W(r_2)$. Fournet a ainsi calculé l'anomalie de chaleur spécifique au point de transformation; il a trouvé pour la chaleur spécifique atomique :

$$C_{T_c - \varepsilon} = 5{,}80\ k$$

(k constante de Boltzman) alors que les chiffres précédents étaient : Bethe, 1,78 k, Cowley, l'infini, et que la valeur expérimentale est 5,1 k.

Puisqu'on peut calculer les paramètres d'ordre à petite distance, on peut à priori prévoir les diagrammes de diffusion des rayons X [formule (11)]. Pour le cas de Cu-Zn, le calcul est sans objet, puisqu'il n'est pas possible de le vérifier expérimentalement. Mais Fournet a fait le calcul pour $Au\text{-}Cu_3$. Il semble (1) que l'ensemble des résultats de Cowley (1950*b*) se retrouve et notamment la forme particulière des zones de diffusion entourant les nœuds de surstructure.

La conclusion qui se dégage est que la théorie peut actuellement bien rendre compte des faits expérimentaux. Cela donne confiance dans les hypothèses de départ. Cependant il ne faut pas oublier que l'on a admis la structure cristalline de la solution ordonnée et que l'on n'a pas tenu compte du désordre de position dû aux différences de volume des atomes. Les interactions ne sont décrites que par les paramètres $W(r_1)$ et $W(r_2)$ qui ne sont pas directement accessibles à l'expérience.

(1) Le calcul définitif n'est pas encore terminé.

Hume-Rothery et Powell (1935) avaient qualitativement expliqué la formation du réseau ordonné du Au-Cu_3 en cherchant comment on pouvait minimiser les déformations dues à l'introduction d'un gros atome d'or dans le réseau du cuivre dans la proportion de 1/4.

6. *Etude du désordre de position.*

Du point de vue expérimental, plusieurs des méthodes générales peuvent être employées. On pourrait étudier la diffusion continue en choisissant un alliage tel que le laiton Cu-Zn, où le désordre de substitution n'a pratiquement pas d'influence. En plus, il faudrait que l'agitation thermique n'ait pas un effet prépondérant. En fait, Cole et Warren (1950) ont étudié la diffusion d'un cristal Cu-Zn, et l'ont expliqué de façon satisfaisante par l'agitation thermique : il serait nécessaire de comparer soigneusement la diffusion à des températures voisines mais de part et d'autre de la température critique.

L'autre méthode possible est l'étude de la décroissance de l'intensité des raies en fonction de l'angle de diffraction. Cette étude n'a pas à notre connaissance été faite avec des alliages mais Wasastjerna (1945) a effectué des mesures précises d'intensité des raies de sels doubles (KCl-KBr) et (RbCl-KCl) en les comparant aux raies des cristaux purs composants. Comme les amplitudes des vibrations thermiques étaient voisines dans les deux cristaux, l'interpolation pour le cristal mixte est assez sûre. L'expérience montre que l'intensité des raies décroît nettement plus pour le cristal mixte : Wasastjerna a ainsi déterminé le déplacement quadratique moyen W et, connaissant le déplacement d'agitation thermique U_{th}, il en déduisait le déplacement V dû au désordre par la formule :

$$W^2 = U_{th}^2 + V^2.$$

Voici les résultats obtenus pour les deux sels et chacun des ions :

Cristal mixte	K Cl — KBr		K Cl — Kb Cl	
ions	K^+	Cl^-, Br^-	K^+, Rb^+	Cl^-
V^2 (Å^2)	0,027	0,008	0,003	0,002

Il faut noter, pour apprécier la valeur des données, que U_{th} est de

l'ordre de 0,07. Ce qui est frappant, c'est la différence entre le déplacement de l'ion commun et celui des ions mixtes. Wasastjerna remarque que si l'alternance des ions Cl^- et Br^- est régulière (fig. 4),

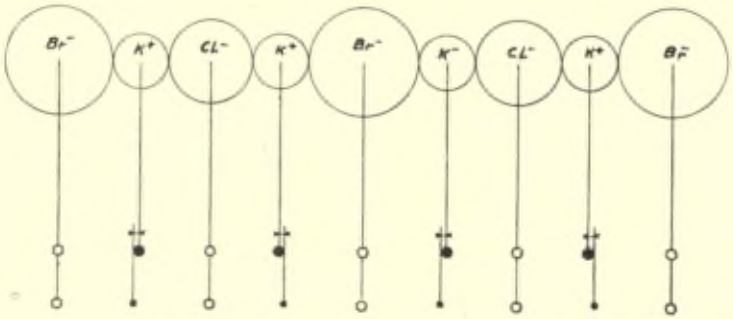

Fig. 4. — Disposition des atomes si les ions Cl^- et Br^- sont régulièrement alternés.

le déplacement de ces ions par rapport au réseau moyen est nul. Au contraire, les ions K^+ sont tous déplacés d'une quantité égale à la moitié de la différence des rayons. Si au contraire il n'y a aucun ordre dans la répartition des ions Cl^- et Br^- les déplacements sont distribués également entre les deux sortes d'ions.

Wasastjerna conclut donc que, dans les cristaux mixtes, il doit y avoir un certain degré d'ordre local, sans toutefois qu'il y ait d'ordre à grande distance parce qu'aucune raie de surstructure n'est perceptible.

L'analyse est évidemment ingénieuse mais fondée sur des résultats expérimentaux délicats. Il est certain qu'actuellement ceux-ci pourraient être beaucoup améliorés, la méthode pourrait être reprise avec plus d'efficacité et les conclusions devraient être vérifiées sur les diagrammes de diffusion.

Il semble que c'est seulement après que de nouvelles tentatives expérimentales auront été effectuées qu'il faudrait revenir sur les hypothèses admises dans la théorie d'Yvon.

b) **Solutions solides hors d'équilibre.**

A cause de la relative lenteur des réactions à l'état solide, une solution solide peut subsister dans un état qui ne correspond pas à l'énergie libre minimum. Sur la structure de telles solutions, et sur la cinétique de leur évolution vers l'état le plus stable, la théorie est

encore fort peu avancée. Donc, on a spécialement besoin des données expérimentales. De fait, c'est dans ce genre de structures désordonnées que les rayons X ont mis en évidence le plus de faits nouveaux.

Deux cas ont été surtout étudiés. Tous deux sont relatifs à une solution solide homogène désordonnée en équilibre à haute température, et ramenée brusquement à une température où l'état stable est, dans un cas, un *état ordonné*, et, dans l'autre, un *mélange de deux phases*. Si la température est assez basse, les mouvements des atomes sont assez lents pour que l'on puisse étudier à loisir les différentes phases de la réaction qui d'ailleurs peut n'être jamais complète. Les rayons X ont alors révélé des états intermédiaires à structure caractérisée par un désordre assez prononcé.

1. *Transformations désordre-ordre.*

Les expériences ont surtout porté sur l'exemple classique de l'alliage Au-Cu_3. Quand l'alliage est trempé à la température ambiante depuis une température supérieure à la température critique, l'ordre à grande distance reste nul. Cependant, il existe un ordre à petite distance donnant naissance à des diagrammes de diffusion du même type que ceux relatifs à l'alliage en équilibre à haute température (p. 187). L'alliage n'évolue pas sensiblement avec le temps à l'ambiante. L'évolution n'est perceptible que si la température est portée à 150°-200°. Sykes et Jones (1936) avaient observé que les raies de surstructure apparaissaient d'abord non seulement avec une intensité faible, mais encore qu'elles étaient floues. Maintenant par l'emploi des monocristaux, on peut faire l'étude complète de la diffusion continue dans l'espace réciproque, avec les techniques qui ont été mentionnées pour l'étude des alliages en équilibre. Le résultat est qu'on retrouve des zones de diffusion autour des nœuds de surstructure, zones plates et orientées comme pour les alliages en équilibre. La différence essentielle est que ces zones sont plus intenses et mieux délimitées. Mais, après un recuit au-dessus de 200 °C [Guinier et Griffoul (1948), Raether (1951)], les zones de diffusion ont une structure interne particulière schématisée dans la figure 5. L'intensité diffusée est concentrée sur les deux axes [100] contenus dans le plan de la zone et, de plus, concentrée en deux points de ces axes symétriques par rapport au nœud à une distance de 0,06 b, b étant le paramètre de la maille du réseau réciproque.

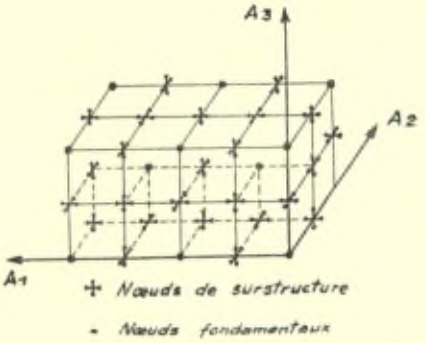

Fig. 5. — Répartition des zones de diffusion dans le réseau réciproque déduite des diagrammes monocristallins.
Cu_3Au trempé et recuit à 200 °C.

Comment interpréter ce résultat? Il est évident qu'on pourrait par la méthode décrite au paragraphe précédent, déduire du réseau réciproque, les différents coefficients d'ordre à petite distance α_1, α_2, ... Mais le calcul ne serait possible que si des mesures d'intensité venaient préciser les données qualitatives des diagrammes photographiques. Certainement, étant donnée la plus grande netteté des zones de diffusion les paramètres d'ordre seraient bien plus élevés : cela signifie qu'un nombre notable d'atomes sont entourés par des proches et même seconds, troisièmes, etc... voisins en position correcte : il y a donc des domaines ordonnés. C'était l'idée qu'avaient émise Sykes et Jones : l'état intermédiaire serait constitué par la juxtaposition de domaines parfaitement ordonnés, mais décalés l'un par rapport à l'autre (« out of step »). Sykes et Jones déduisaient les dimensions du domaine de la largeur de la raie de surstructure. Mais le calcul n'était pas correct, parce qu'il admettait que les domaines diffusaient les rayons X de façon incohérente. On a cherché ensuite si un modèle construit sur de tels domaines décalés pouvait rendre compte des diffusions observées (Wilson, 1943, Guinier et Griffoul, 1948) en tenant compte des interférences entre domaines contigus. Considérons les deux petits domaines représentés dans la figure 6, ils sont séparés par « un plan de défaut » parallèle à [100] et le long duquel un domaine a été glissé d'une translation égale à :

$$\frac{\vec{a}}{2}, \frac{\vec{a}}{2}, 0.$$

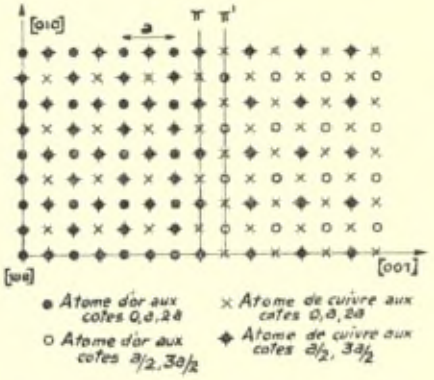

Fig. 6. — Schéma de deux blocs décalés.

Ainsi, bien que l'ordre à grande distance n'existe pas dans l'ensemble, aucun atome d'or n'a de proches voisins de même nature. Le calcul montre que ces deux domaines donnent naissance à des zones de diffusion ayant les mêmes caractéristiques que celles qui sont observées.

Quand l'ordre est très faible, la description statistique de la solution solide est seule possible. Dans le cas des états intermédiaires où l'ordre est plus poussé, la détermination des différents paramètres d'ordre est certes toujours valable et parfaitement objective. Mais l'introduction des domaines est une hypothèse justifiée. Considérer les solutions solides comme un ensemble des domaines parfaitement ordonnés, tous les désordres étant concentrés à des limites continues comme des joints de grains dans un métal recristallisé, est certainement trop simpliste. Il peut y avoir des régions très désordonnées à côté de germes ordonnés. Ce que l'expérience des rayons X suggère, c'est la présence fréquente dans les régions bien ordonnées des plans de défauts [100] et du type de décalage décrit plus haut. Ce fait, trouvé pour Au-Cu_3 est à rapprocher de l'existence dans l'alliage Au-Cu d'une phase intermédiaire se produisant avant la phase ordonnée parfaite et donnant un diagramme analogue à celui qui pour Au-Cu_3, correspond au réseau réciproque de la figure 5. La différence essentielle est que les zones de diffusion sont remplacées par des groupes de taches nettes entourant les nœuds de surstructure. Johannson et Linde (1936) ont interprété cette structure, Au-Cu II, qui, dans ce cas, est véritablement cristalline, comme formée de feuillets parallèles à [100], décalés entre eux et d'épaisseur égale à

cinq couches atomiques. Dans Au-Cu_3 la structure feuilletée a tendance à se former, mais ne parvient pas à un stade parfait.

On peut se demander si, pendant le recuit de l'alliage, les paramètres d'ordre à petite distance croissent de façon régulière et continue, ou bien si le processus n'est pas plus complexe. Il y aurait d'abord évolution vers une structure différente de la structure d'équilibre. Pour Au-Cu, sa forme parfaite est atteinte, pour Au-Cu_3, la transformation vers la forme définitive se produit avant. Mais il reste une question obscure : comment peuvent se former des structures à si grandes périodes, c'est-à-dire faisant intervenir des actions à longue distance? On les a signalées dans d'autres alliages hors d'équilibre [Hargreaves (1949)]. Peut-être est-ce là le résultat des déformations très légères qui s'ajoutent de couche en couche et qui, ayant atteint une valeur critique au bout d'un nombre donné des couches atomiques, déclenche un défaut planaire; ces défauts ainsi se trouvent régulièrement espacés.

2. *Précipitation d'une solution solide sursaturée.*

Le deuxième type d'état hors d'équilibre que nous considérerons est celui de la solution homogène dont l'énergie libre est diminuée par le rassemblement des atomes étrangers en une seconde phase : c'est le cas de la solution sursaturée qui précipite (durcissement des alliages). Si la température est trop basse, la réaction est incomplète : le précipité du diagramme d'équilibre ne se forme pas, néanmoins la solution solide ne reste pas homogène. Là encore, c'est à l'expérience que l'on demande les éléments essentiels de la connaissance des états intermédiaires. La théorie de ces phénomènes est bien plus difficile que celle de l'ordre parce qu'ici il y a, en même temps, déformation des réseaux et changement de composition de la solution solide. Etant donné la complexité et la variété des phénomènes mis en évidence, on sent qu'on est encore bien loin de pouvoir en rendre compte à priori : l'expérience est indispensable.

La meilleure méthode est l'étude de la diffusion continue. L'avantage est que, dans ce cas, celle-ci est relativement intense. Mais il existe de graves difficultés d'interprétation qui viennent du fait que les désordres de position et de substitution des atomes sont mêlés et la formule générale donnant les paramètres Φ_M (formule 8) est peu exploitable. Au surplus, tous les travaux ont été effectués avec la méthode photographique, c'est-à-dire que les résultats sont la

plupart du temps qualitatifs, il s'agit encore de premières études sur la structure des états intermédiaires.

Ces études ont abouti à des résultats que nous voudrions ici très brièvement résumer, surtout pour donner une idée du degré des connaissances que l'on a atteint dans ce domaine.

La première théorie a été celle des zones [Preston (1938), Guinier (1939)]. D'après celle-ci, le premier stade de l'évolution de l'alliage serait la ségrégation des atomes dissous en éxcès dans de petites zones — dites zones Guinier-Preston — incluses dans la matrice, les atomes étrangers restant aux nœuds de la matrice (fig. 7*a*). Quand

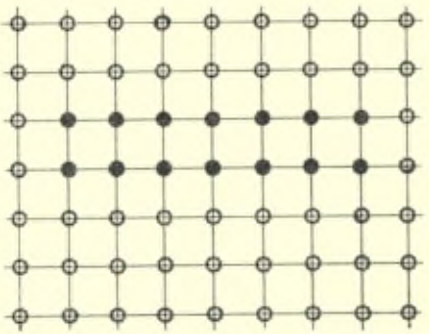

Fig. 7*a*. — Zone simple.

les zones ont atteint une certaine extension, elles ne sont plus stables et c'est le précipité véritable qui se forme.

Geisler et Hill (1949) ont montré sur des exemples qu'il était indubitable, d'après les diffusions observées sur les diagrammes de rayons X, que les atomes ségrégés ne pouvaient pas rester aux nœuds de la matrice. Ces auteurs, pour interpréter les diagrammes sont alors partis d'un autre point de vue. Il n'est pas nécessaire de considérer un état de pré-précipitation : les premières ségrégations se feraient sous forme d'un petit grain de précipité cohérent avec la matrice à cause de la similitude de leurs réseaux cristallins. A cause de la petite taille du précipité, la tache de diffraction est élargie, sa forme étant fonction de la forme du précipité. Les taches diffuses constitueraient les diffusions observées.

Nous avons examiné à nouveau (*) les données expérimentales

(*) Article devant paraître prochainement dans *Acta Crystallographica* (1952).

obtenues sur divers alliages durcissants et nous sommes arrivés à la conclusion que ni le schéma des zones simples sans perturbation, ni celui des petits précipités à réseau différent n'étaient satisfaisants. L'effet de la taille et de la forme de la ségrégation ne peut être la seule cause des diffusions observées, il y a en outre les irrégularités de structure qui jouent un rôle important. Il est vraisemblable d'admettre que dans les régions où se rassemblent les atomes dissous, il se produit de fortes perturbations des réseaux et que *progressivement* les atomes s'écartent de la structure dans les matrices pour tendre vers une autre structure (fig. 7*b*). Mais ce semble un fait très général

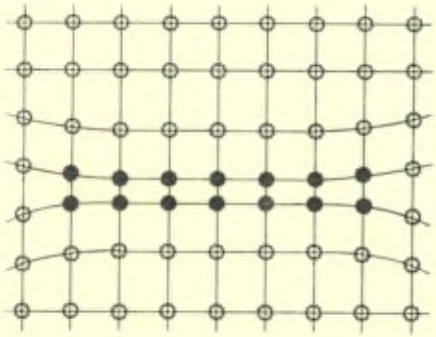

Fig. 7*b*. — Zone avec distorsion.

que cette structure imparfaitement réalisée est proche de celle de la matrice et nettement distincte de celle du ou des précipités qui se produisent ultérieurement à l'état de grains visibles au microscope. Ainsi les rayons X conduisent, comme les études des nombreuses propriétés des alliages, à l'idée de la discontinuité du processus de précipitation [Köster (1951)].

Les zones, se produisant aux premiers stades du durcissement, ont donc non seulement une teneur en éléments dissous très élevée mais aussi une structure propre. Il est évidemment équivalent de regarder celle-ci comme dérivant de la matrice où d'un précipité, puisqu'en fait c'est une structure intermédiaire. Mais ces zones ont des caractères particuliers qui les distinguent de phases ordinaires. D'abord leur structure est toujours imparfaite, ensuite elles sont très cohérentes avec la matrice, si bien qu'il n'y a pas d'interface bien définie, et l'énergie superficielle étant très faible, elles peuvent être stables à partir d'une taille très faible. Il n'y a donc pas germina-

tion comme pour une phase ordinaire et la cinétique de leur développement est différente. C'est pourquoi nous sommes d'avis de conserver l'appellation de « zones » pour les distinguer des précipités. Les zones seraient responsables du « Kaltaushärtung » et les précipités du « Warmaushärtung », les deux actes du durcissement décrite par W. Köster dans son rapport à cette conférence.

L'étude de la structure des zones repose uniquement sur les données de la diffusion continue des rayons X. Le désordre, heureusement, dans beaucoup de cas, préserve la périodicité dans une ou deux directions : désordre linéaire dans Al-Mg-Si [Lambot, (1950)], désordre planaire dans Al-Cu, [Guinier (1942)]. Malgré cet élément de simplification, les difficultés d'interprétation à priori du réseau réciproque, sont grandes : aussi est-on conduit à imaginer des modèles de structure désordonnée et à vérifier s'ils sont acceptables. Ce qui s'est produit, c'est qu'à mesure qu'on précise la détermination expérimentale du réseau réciproque, on a été obligé de compliquer le modèle de la zone et sa description devient moins précise. Ainsi, dans le cas de la solution Al-Cu, la région centrale de l'espace réciproque peut s'expliquer par la présence des amas plans de cuivre parallèle à [100] et les données de la diffusion permettent de calculer le diamètre et l'épaisseur moyenne de ces amas [Guinier (1939)], et même leur distance moyenne dans le réseau. Mais ces amas simples ne peuvent pas rendre compte de l'ensemble des diffusions observées, On doit admettre qu'à côté des amas plans, il y a des zones plus épaisses, où les plans riches en cuivre se rapprochent les uns des autres, et l'introduction de si nombreux paramètres rend une description quantitative assez arbitraire. Dans un état donné, l'alliage contient des zones de tailles variées, même si toutes les précautions ont été prises pour assurer l'uniformité du traitement thermique. Cette hétérogénéité est peut-être la conséquence du fait que les défauts du réseau de la matrice ont une influence décisive sur la formation et la croissance des zones. (On sait que l'on ne peut pas expliquer la vitesse de formation des zones à partir des coefficients normaux de diffusion : la diffusion doit être considérablement accélérée par la perturbation du réseau.)

En résumé, les rayons X ont montré que le désordre de structure était caractéristique des états intermédiaires dans le processus de précipitation. Actuellement, la répartition de la diffusion des rayons X a été étudiée dans un nombre notable d'alliages, ceux pour lesquels les phénomènes sont les plus intenses et les plus marqués. Le travail

doit se poursuivre dans plusieurs directions. D'abord on devra s'efforcer de mesurer avec précision ce qui n'a été jusqu'ici qu'évalué par des méthodes photographiques. D'autre part, on a maintenant des moyens techniques suffisants pour déceler des désordres moins importants. Ainsi on peut espérer atteindre les petits groupes d'atomes tels que les « nuclei » de Borelius (1945) ou encore les « embryos » de Turnbull (1948) qui se formeraient au début de l'hétérogénéisation de la solution solide sursaturée.

IV. CONCLUSION

De cette revue des diverses applications des rayons X à l'étude du désordre des structures se dégage l'impression que ces techniques progressent rapidement, mais qu'il reste des difficultés fondamentales qui souvent interdisent de préciser la constitution détaillée d'une solution solide sans y introduire des hypothèses ou des données extérieures aux seuls résultats des rayons X. Il ne faut pas cependant minimiser les points déjà acquis et, pour en juger la valeur, il faut les comparer avec ce qu'on peut espérer obtenir d'autres méthodes expérimentales.

Les propriétés mécaniques ou électriques du cristal mixte sont très sensibles aux perturbations du réseau. Inversement, est-il possible de déduire celles-ci des mesures mécaniques ou électriques? Dans le premier cas, la théorie est encore trop peu avancée, et toute mesure expérimentale est le résultat de bien trop de facteurs pour que l'on puisse isoler l'effet de la perturbation due aux atomes étrangers. Pour les propriétés électriques, on sait faire le calcul par exemple de la résistivité due aux vibrations thermiques des atomes. Mais le problème de la propagation des ondes électroniques dans un cristal mixte, connaissant la répartition réelle des atomes, n'a pas encore été traité. Un élément favorable dans le cas de mesures électriques, c'est qu'on peut en suivant la variation de la résistance avec la température isoler la part due aux vibrations thermiques et la résistance de l'alliage en l'absence de vibrations. Qualitativement ces mesures de résistivité servent à caractériser l'ordre d'une solution solide ou encore à suivre les étapes de la précipitation d'une solution sursaturée. Toute tentative de calcul de la structure réelle exige l'introduction de nombreuses hypothèses.

Il semble donc que, malgré leurs imperfections, ce soit les méthodes

d'analyse aux rayons X qui aient le plus de chances d'aboutir à une bonne connaissance de la structure réelle des solutions solides. Les résultats obtenus par les rayons X pourront servir à établir la théorie des effets des défauts de périodicité sur les autres propriétés des solides, qui fourniront ainsi des moyens de contrôle des structures imaginées.

Je suis heureux de remercier très vivement mon collaborateur G. Fournet dont j'ai utilisé très largement les résultats encore inédits sur la transformation ordre-désordre.

RÉFÉRENCES

Averbach et B. E. Warren, *Journ. Appl. Phys.*, **20,** p. 885 (1949).

F. Bertaut, *Acta Cryst.*, **3,** p. 14 (1950).

H. A. Bethe, *Proc. Roy. Soc.*, **150***A*, p. 552 (1935).

G. Borelius, *Ark. fur Mat. Astr. och Fys.*, **32***A*, n° 1 (1945).

W. L. Bragg et E. J. Williams, *Proc. Roy. Soc.*, **145***A*, p. 699 (1934).

Brindley et Spiers, *Phil. Mag.*, **20,** p. 882 (1935).

Y. Cauchois. « Les spectres de rayons X et la structure électronique de la matière », Gauthiers-Villars, Paris (1948).

D. Chipman et B. E. Warren, *Journ. Appl. Phys.*, **21,** p. 696 (1950).

H. Cole et B. E. Warren, « Communication à la VIII^{eme} Conférence de Pittsburgh sur la diffraction des rayons X » (novembre 1950), (1950).

A. H. Cottrell, « Report on the strenght of solids », London, Physical Society (1948).

J. M. Cowley, *Phys. Rev.*, **77,** p. 669 (1950*a*); *Jour. Appl. Phys.*, **21,** p. 24 (1950*b*).

G. Fournet, *Comp. Rend.*, **232,** p. 155 (1951).

Fowler et Guggenheim, « Statistical Thermodynamics », Cambridge University Press (1933).

A. H. Geisler et J. K. Hill, *Acta Cryst.*, **1,** p. 238 (1948).

A. Guinier, *Ann. Phys*, **12,** p. 161 (1939); *Jour. Phys.* ,VIII, p. 124 (1942), *Radiocristallographie*, Dunod Paris, p. 220 (1945*a*); *Proc. Phys*, **57,** p. 310 (1945*b*); *Comp. Rend.*, **231,** p. 655 (1950).

A. Guinier et R. Griffoul, *Rev. Met.*, XLV, p. 387 (1948).

M. E. Hargreaves, *Acta Cryst.*, **2,** p. 259 (1949).

K. Huang, *Proc. Roy. Soc.*, **190***A*, p. 102 (1947).

W. Hume-Rothery et H. M. Powel, *Zeit. für Krist.*, **91,** p. 23 (1935).

M. A. Jaswon, W. G. Henry et G. V. Raynor, *Proc. Phys. Soc.*, **64***B*, p. 177 (1951).

C. H. Johannson et J. O. Linde, *Ann. der Phys*, **52,** p. 1 (1936).

R. Kikuchi, *Phys. Rev.*, **81,** p. 988 (1951).

W. Köster, Conférence Solvay (1951).

H. Lambot, *Rev. Met.*, **45,** p. 387 (1950).

M. Von Laue, « Röntgenstrahlinterferenzen », Leipzig, Akademische Verlaggesellschaft (1941).

F. C. Nix et W. Shockley, *Rev. Mod. Phys.*, **10,** p. 2 (1938).

N. Norman et B. E. Warren, *Jour. Appl. Phys.*, **22,** p. 483 (1951).

Ph. Olmer, *Bul. Soc. Franc. Minér.*, **71,** p. 145 (1948).

L. Pauling, « The Nature of Chemical Bond », Cornell, University Press (1945).

G. D. Preston, *Proc. Roy. Soc.*, **167***A*, p. 526 (1938).

H. Raether, *Acta Cryst.*, **4,** p. 70 (1951).

G. V. Raynor et D. M. B. Waldon, *Phil. Mag.*, **40,** p. 198 (1949).

C. Sykes et F. W. Jones, *Proc. Roy. Soc.*, **157***A*, p. 213 (1936).

D. Turnbull, « Metals Technology », *Tech. Publ.*, p. 2365 (1948).

J. A. Wasastjerna, Societas Scientiarum Fennica Commentationes Physico-Mathematicae, XIII, p. 5. (1945).

A. J. C. Wilson, *Proc. Roy. Soc.*, **181***A*, p. 360 (1943); *Proc. Phys. Soc, Lon.*, **56,** p. 174 (1944); *Research*, **2,** p. 541 (1949).

J. Yvon, *Cahiers de Physique* n° 28, p. 1 (1945).

W. H. Zachariasen, « Theory of X-Ray Diffraction in Crystals », Wiley and Sons, New York (1945).

Discussion du rapport de M. A. Guinier

M. G. Borelius. — Professor Guinier has outlined theories on order-disorder phenomena by Yvon and Fournet and has made some comments on the possible approximation to experimental results from those theories in comparison with earlier theories of Bragg and Williams, Bethe and Cowley. As there is no comparison with the formulae I developed in 1934 for a 50 per cent alloy (one of the type AB), formulae which so far have given the best, and in fact a very good agreement with experimental results, I should like to have some more information about the possibilities of the formulae developed by Fournet.

With two experimental constants my formulae are capable of describing the long range order of transformations with discontinuities of the second order with any critical temperature and any value of the specific heat at the critical point, as well as transformations with discontinuities of the first order with varying transition temperatures and varying latent heats.

They have given good agreement with later determinations of the energy of transformation in CuZn by Moser and by Sykes and Wilkinson and in CuAu by my collaborators and myself. At the development of these formulae I avoided the simplifying assumption, made by all other authors so far, namely that the energy of disorder should be built up by central forces between pairs of atoms. Also two and three dimensional groups of atoms were taken into account. The great simplicity of the formulae was obtained by taking into account the symmetry between the two kinds of atoms in a 50 % alloy. The calculations of Yvon and Fournet, reported by professor Guiner, are again based on the assumption of central forces between pairs of atoms. They have with two empirical constants given a rather good agreement in the case of CuZn. I should like to know if this is the case also for instance in the case of CuAu?

M. A. Guinier. — La théorie du professeur Borelius a un point de départ complètement différent de toutes les autres (Bragg-

Williams, Bethe, Yvon, etc.). Ces dernières partent de l'analyse de la structure à l'échelle atomique, tandis que le professeur Borelius considère l'état de l'alliage sans prendre en considération la position des atomes individuels. Il est donc difficile de comparer les deux sortes de théories, sinon par leur résultat final. Remarquons que, comme le professeur Borelius, Fournet ne fait intervenir que deux paramètres W^1 et W^2, mais il leur donne une signification précise dans le modèle atomique : l'énergie d'interaction entre premiers et seconds voisins.

M. Prigogine. — En ce qui concerne votre référence aux travaux d'ailleurs fort intéressants d'Yvon, je voudrais signaler que tous ces calculs, y compris ceux d'Yvon, se basent sur le modèle d'Ising (additivité de l'énergie potentielle considérée comme une somme de termes dus aux différents couples de particules). Le problème n'a pu être traité que dans le cas à deux dimensions par Onsager (1944). Dans les autres cas, on ne dispose que de différents développements en série (Kirkwood, Yvon, Rushbroucke, Wakefield) ou de méthodes d'approximation « globales » (méthode variationnelle de Kramers-Wannier, de Kikuchi).

En général, les méthodes qui se présentent comme des développements en série sont très lentement convergentes. Ce serait un fait très remarquable s'il n'en était pas ainsi de la méthode d'Yvon.

M. A. Guinier. — Deux faits peuvent être cités pour montrer que l'on n'est pas gêné par la lenteur de la convergence du développement d'Yvon :

1) dans son étude de Cu-Zn, Fournet a retrouvé les données expérimentales en considérant seulement deux termes pour l'ordre à grande distance et un terme pour l'ordre à petite distance.

2) dans un travail qui doit bientôt être publié, Fournet a cherché à retrouver les résultats de Kikuchi à partir de la théorie générale d'Yvon : il suffit, pour arriver à l'indentité de résultats, de considérer cinq termes.

Ce qu'Yvon a apporté de nouveau pour arriver à cette convergence relativement rapide de son développement, c'est la manière de grouper les termes. Au lieu « d'ordonner les termes d'après le nombre de nœuds qu'ils font intervenir, ceux-ci pouvant être distincts ou confondus », dit Yvon « nous les grouperons d'après le nombre de nœuds distincts qu'ils font intervenir ». Ainsi l'influence

des termes ne comprenant que deux nœuds donnés se fait uniquement sentir sur un terme.

M. Bragg. — The new theoretical treatment by Yvon gives a much better fit to curve of specific heat in passage from the ordered to the disordered state.

What new physical assumption has lead to this better fit?

M. A. Guinier. — Le nouveau paramètre physique introduit est l'interaction entre *seconds* voisins.

Neuere Untersuchungen zur Frage der Aushärtung

Von Werner Köster in Stuttgart

(Aus dem Max-Planck-Institut für Metallforschung, Stuttgart)

Im vergangenen Jahrzehnt haben R. F. Mehl und L. K. Jetter (1), H. K. Hardy (2) und G. C. Smith (3) zuzammenfassende Übersichten über die Aushärtungserscheinungen und ihre Deutung gegeben. Der vorliegende Bericht kann sich also darauf beschränken, auf Grund neuerer Messungen einen Beitrag zur Klärung der Anschauungen zu liefern. Den Berichten der genannten Autoren ist ja zu entnehmen, dass der Übergang von einer übersättigten festen Lösung zum Gleichgewichtszustand ein höchst komplizierter Vorgang ist, den in einem einheitlichen Bilde zu erfassen bisher noch nicht gelungen ist.

Das Problem der Aushärtung wird im wesentlichen von drei Seiten aus behandelt. Einmal wird, ausgehend von der technologischen Fragestellung, die Kinetik der Vorgänge durch Messung der Zeit- und Temperaturabhängigkeit verschiedener Eigenschaften verfolgt. Zum andern wird mit Hilfe der Röntgenstrahlen versucht, das atomistische Bild der aufeinanderfolgenden Zustände zu erfassen. Zum dritten werden thermodynamische Betrachtungen angestellt, um Hinweise auf den möglichen energetischen Ablauf der Vorgänge zu erlangen. Jeder dieser drei Wege führt zu entscheidenden Aussagen, jeder hat aber auch seine Grenzen. Bei den kinetischen Messungen fehlt es vielfach an der Kenntnis des funktionellen Zusammenhanges zwischen der Messgrösse und dem atomistischen Vorgang. Ein Röntgeninterferenzbild lässt oft verschiedene Deutungen zu, und die Thermodynamik gibt nur ungenügenden Aufschluss über die Zwischenzustände. Es ist deshalb unerlässlich, worauf in letzter Zeit H. Auer (4) und W. Köster (5) erneut hingewiesen haben, die Ergebnisse aller drei Richtungen aufeinander abzustimmen und in Einklang zu bringen.

KINETISCHE MESSUNGEN ZUR KLÄRUNG DES GEGENSEITIGEN VERHÄLTNISSES VON KALT- UND WARMHÄRTUNG.

Ein umstrittener Punkt sind die gegenseitigen Beziehungen der Vorgänge, die zur Kalt- und Warmhärtung führen. Hierüber bestehen geteilte Auffassungen. Aus den Messungen der Kinetik der Aushärtung werden andere Folgerungen gezogen als aus den Strukturuntersuchungen. In Verfolg der grundlegenden röntgenographischen Arbeiten von G. Wassermann und J. Hengstenberg (6), A. Guinier (7) sowie G. D. Preston (8) wird im Anschluss an die Ausführungen von R. F. Mehl und L. K. Jetter (1) die Auffassung vertreten, dass ein kontinuierlicher struktureller Übergang von den ersten Ansammlungen der Atome im Wirtgitter bis zur mikroskopisch sichtbaren ausgeschiedenen Phase besteht. Nach A. H. Geisler und J. K. Hill (9) kann der Ausscheidungsvorgang bis zum frühesten Beginn des Aushärtungsvorganges zurückverfolgt werden. In dem Wirtgitter bilden sich eindimensionale Gebilde, Stäbchen (stringlets), die als Ausscheidungen aufgefasst werden. Sie wachsen sich zu Plättchen (platelets, Guinier-Preston-Zonen) aus, die ihrerseits über verschiedene Stufen zu einer kohärenten Zwischenphase und endlich zur Gleichgewichtskristallart führen. Auf dieser Basis, wo jeder Zustand in stetigem Übergang aus dem voraufgegangenen entsteht (sequence-Theorie), hat A. H. Geisler (10) auch versucht, den zeitlichen Ablauf der Eigenschaftsänderungen zu klären. Der Kalthärtungszustand ist gemäss dieser Vorstellung eine Vorbereitung der Ausscheidung; ein Zustand, der nicht einer echten Ausscheidung entspricht, wird abgelehnt.

Demgegenüber weisen die Ergebnisse der kinetischen Verfolgung physikalischer und technologischer Eigenschaften darauf hin, dass Kalt- und Warmhärtung auf zwei voneinander abweichenden atomistischen Vorgängen beruhen, die in keinem ursächlichen Zusammenhang stehen. Die Kalthärtung ist die Folge einer einphasigen Entmischung. Unter einphasiger Entmischung soll eine Komplexbildung in homogener Phase verstanden sein entsprechend Vorstellungen, die im englischen Sprachgebrauch als clusters, pre-precipitation, segregates bezeichnet werden. Die Entmischung geht im instabilen Zustand vor sich und stellt einen selbständigen Vorgang dar. Sie findet in einem unterhalb der Löslichtkeitskurve befindlichen,

nach Temperatur und Konzentration begrenzten Zustandsfeld statt. Es ist dies das Feld, in dem nach U. Dehlinger ([11]) und R. Becker ([12]) der Diffusionskoeffizient negativ ist (uphill diffusion), in dem also Anhäufungen der gelösten Atome sich verstärken anstatt sich zu zerstreuen. Unterhalb der genannten Grenztemperaturen kann sich, wie A. Durer und W. Köster ([13]) sowie H. Auer ([14]) gezeigt haben, ein bestimmter Aushärtungsgrad einstellen, dessen Betrag durch eine temperaturabhängige Gleichgewichtsbeziehung zwischen den an den Atomen des Zusatzelementes verarmten und den an ihnen angereicherten Gebieten geregelt ist. Die Zustände, die durch diese Eigenschaft-Temperatur-Kurven für eine bestimmte Legierungszusammensetzung gegeben sind, können reversibel eingestellt werden. Es handelt sich um ein dynamisches metastabiles Gleichgewicht zwischen den zur Entmischung führenden Kräften und der ihnen entgegenwirkenden thermischen Atombeweglichkeit, wie von der Einstellung einer geordneten Atomverteilung her bekannt ist. Der Kalthärtungsvorgang setzt ohne Anlaufzeit ein, der Tangens im Nullpunkt der Eigenschaftsisothermen hat einen endlichen Wert. Es liegt strukturell gesehen ein Vorgang vor, der ohne Keimbildung im Mischkristallzustand vonstatten geht, bei dem die Atome nur kurze Wegstrecken zurücklegen.

Die Warmhärtung wird durch den Austritt der überschüssig gelösten Atome aus dem Mischkristallgitter (Ausscheidung) hervorgerufen, also durch einen Vorgang, an dem mindestens zwei Phasen beteiligt sind. Es wird durch diese Ausscheidung schliesslich das stabile Gleichgewicht eingestellt. Das Gebiet der Warmhärtung ist im Zustandsbild zu höheren Temperaturen hin durch die Löslichkeitskurve begrenzt. Die Ausscheidung setzt Keimbildung voraus, die Warmhärtung beginnt demzufolge erst nach einer bestimmten Anlaufzeit; die Tangente im Nullpunkt der Eigenschaftsisothermen ist die Abszissenachse. Der Vorgang ist heterogener Art. Es ist anzunehmen, dass die Ausscheidung bevorzugt an Störstellen des Gitters wie Korn- und Mosaikgrenzen stattfindet. Hierfür spricht die stets zu beobachtende Beschleunigung der Ausscheidung durch Kaltverformung.

KINETISCHE VERFOLGUNG DER AUSHÄRTUNG VON Al-Ag-LEGIERUNGEN

Eine Übersicht über das kinetische Verhalten von Aluminium-Silber-Legierungen bei der Aushärtung, das von W. Köster gemeinsam mit F. Braumann, H. Steinert und J. Scherb[15] aufgenommen worden ist, möge den eben dargelegten Sachverhalt erläutern. Bild 1 zeigt

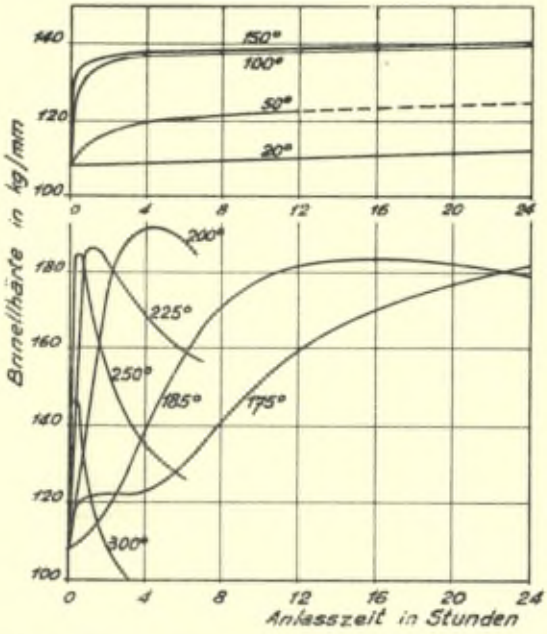

Bild 1. — Zeitliche Änderung der Härte einer Aluminium-Legierung mit 38 % Ag.

die zeitliche Änderung der Härte einer Legierung mit 38 % Ag bei verschiedenen Anlasstemperaturen nach dem Abschrecken von 550°. Bei Anlasstemperaturen unter 185° steigt die Härte rasch auf einen Wert an, der dann längere Zeit beibehalten wird; die Geschwindigkeit der Härtezunahme nimmt mit der Anlassdauer ab. Je höher die Temperatur ist, umso steiler ist der Anstieg, umso kürzer ist das Kurvenstück gleichbleibender Härte. Bei Anlasstemperaturen oberhalb 185° nimmt die Geschwindigkeit der Härtesteigerung anfänglich mit der Anlassdauer zu. Späterhin wird ein Höchstwert erreicht, an den sich ein Härteabfall anschliesst. Die Härte steigt bei 185° bei kurzen

Anlasszeiten zunächst wesentlich langsamer an als unterhalb dieser Temperatur. Bei längerem Zuwarten schliesst sich unterhalb 185° an den Kurvenast der zuerst beschriebenen Art ein Ast der zu zweit geschilderten Form an. Die Aluminium-Silber-Legierungen verhalten sich also durchaus ähnlich den Aluminium-Kupfer-Legierungen, über die M. V. Gayler ([16]) berichtet hat.

Gleicherweise verhält sich die Elastizitätsgrenze (0,01 % — Dehngrenze) der Legierungen. Das Ergebnis dieser Messreihe ist in Bild 2

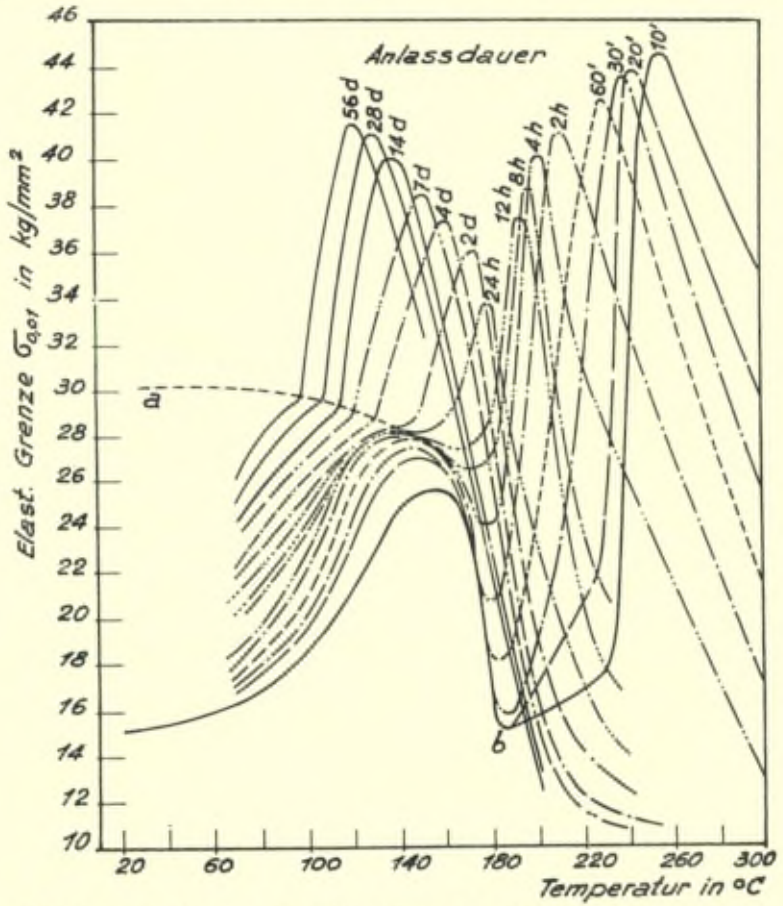

Bild 2. — Isochronen der Elastizitätsgrenze einer Aluminium-Legierung mit 38 % Ag.

wiedergegeben, in dem die Elastizitätsgrenze in Abhängigkeit von der Anlasstemperatur für verschiedene Anlasszeiten dargestellt ist. Das Isochronenschaubild zerfällt in zwei Gebiete, die durch die

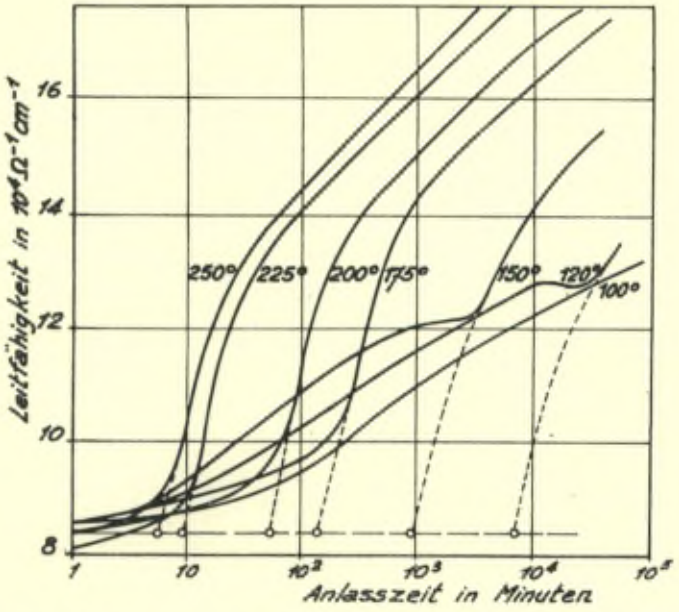

Bild 3. — Zeitliche Änderung der Leitfähigkeit einer Aluminium-Legierung mit 38 % Ag.

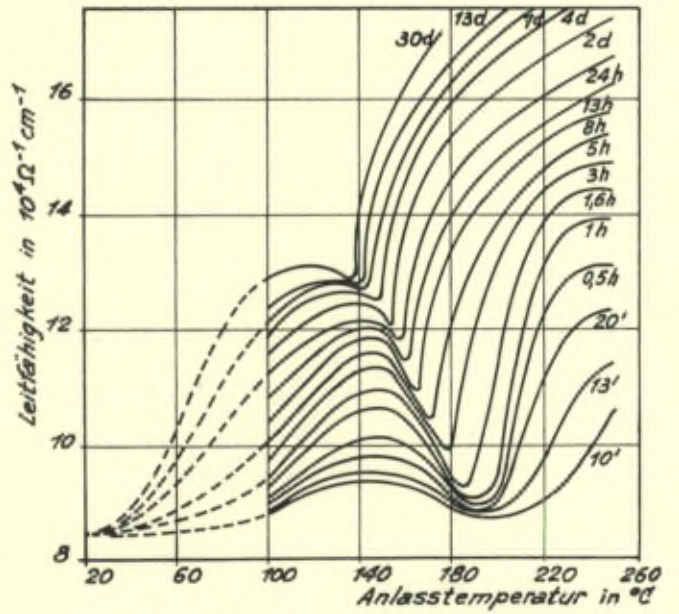

Bild 4. — Isochronen der Leitfähigkeit einer Aluminium-Legierung mit 38 % Ag.

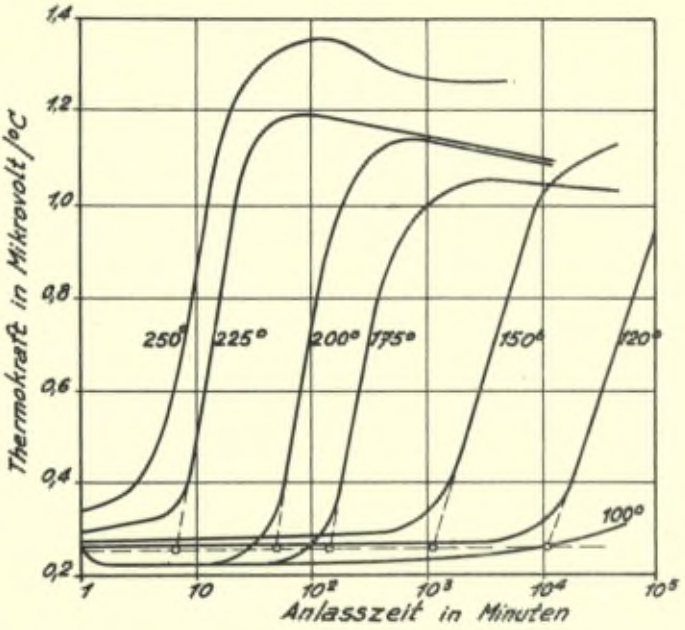

Bild 5. — Zeitliche Änderung der Thermokraft einer Aluminium-Legierung mit 38 % Ag.

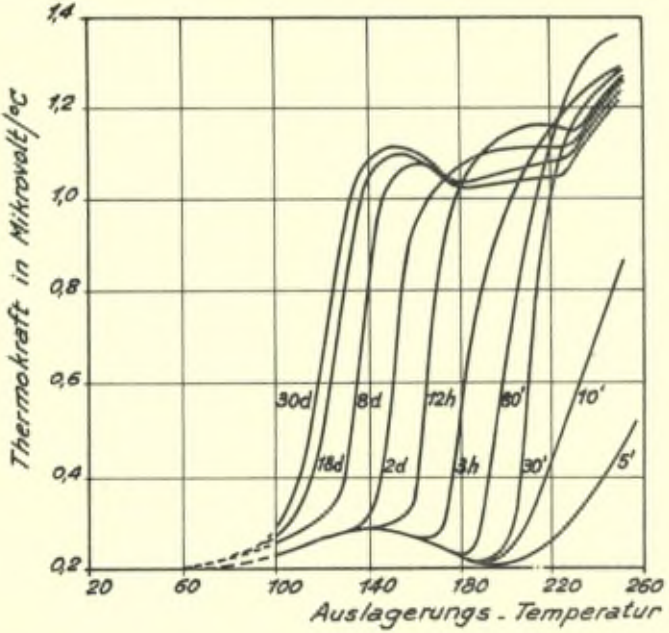

Bild 6. — Isochronen der Thermokraft einer Aluminium-Legierung mit 38 % Ag.

Linie a — b voneinander geschieden sind. Diese Linie gibt die Endwerte an, auf die die Elastizitätsgrenze im Zuge der Kalthärtung ansteigt. Sie werden umso später erreicht, je niedriger die Anlasstemperatur ist. Die Grenzkurve fällt mit steigender Anlasstemperatur zu niedrigeren Werten ab und endet bei 185°. Da der Kalthärtungszustand sich unterhalb etwa 100° nur sehr langsam voll ausbildet, durchläuft die Härte, die Elastizitätsgrenze oder eine andere Eigenschaft im Bereiche unterhalb der Kurve a — b bei mässigen Anlasszeiten einen Höchstwert in Abhängigkeit von der Anlasstemperatur. Von der Kurve a — b lösen sich die Kurven eines zweiten Anstieges der Elastizitätsgrenze ab. Die Knickpunkte liegen bei umso grösseren Anlasszeiten, je niedriger die Anlasstemperatur ist. Dieser Anstieg führt zu einem Härtehöchstwert, der mit steigender Anlassdauer zu niedrigeren Anlasstemperaturen verlagert wird.

Ein analoges Bild erhält man bei der Verfolgung der elektrischen Leitfähigkeit, wie Bild 4 zu entnehmen ist. Beachtenswert ist, dass die Leitfähigkeit im Gegensatz zu anderen Legierungssystemen im Kalthärtungsgebiet nicht ab- sondern zunimmt.

Die zeitliche Verfolgung physikalischer und mechanischer Eigenschaften lehrt somit auf das eindringlichste, dass zwei Aushärtungsvorgänge beim Anlassen abgeschreckter Aluminium-Silber-Legierungen zu unterscheiden sind. Der kinetische Vorgang bei tiefen Temperaturen setzt sofort ein, der bei höheren Temperaturen erst nach einer gewissen Anlaufzeit, wie sie für eine Keimbildung charakteristisch ist.

Im System Aluminium-Silber besteht nun eigenartigerweise die Möglichkeit, die Anlaufzeit der Ausscheidung verhältnismässig genau zu messen. Die Thermokraft spricht nämlich verschwindend wenig auf die Kalthärtung an und ändert sich erst stark, wenn die Ausscheidung erfolgt. Dieser Sachverhalt geht deutlich aus Bild 3 und 5 hervor, in dem die zeitliche Änderung der elektrischen Leitfähigkeit und der Thermokraft in logarithmischem Zeitmasstab dargestellt ist. Die Isothermen der Thermokraft und dementsprechend auch die Isochronenschar (Bild 6) spiegeln nur einen Vorgang wieder.

Man erkennt vor allem, dass der Beginn der Ausscheidung auch im Kalthärtungsgebiet, also unterhalb 185°, deutlich festzulegen ist. Die aus der Thermokraft ermittelten Anlaufzeiten stimmen hinreichend genau mit denen überein, die zich aus den Isothermen der Härte und Elastizitätsgrenze ergeben und die man aus den

Isothermen der Leitfähigkeit durch Extrapolation des geradlinigen Anstieges auf den Ordinaten-Ausgangswert gewinnt.

Die Anlaufzeiten liegen, gegen die reziproke absolute Temperatur aufgetragen, auf einer Geraden, der als Aktivierungsenergie der Ausscheidung der Wert 25.000 cal/Mol zu entnehmen ist (Bild 7).

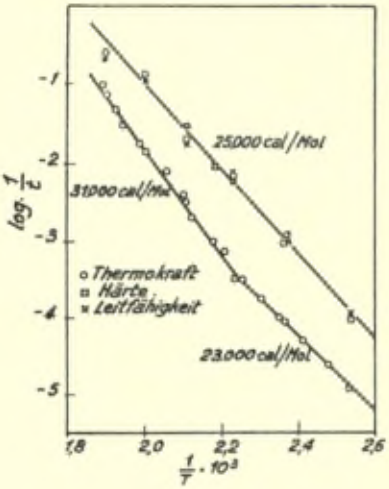

Bild 7. — Zur Bestimmung der Aktivierungsenergie.

Im System Aluminium-Silber scheint die Ausscheidung danach weitgehend unabhängig von einer voraufgegangenen Kalthärtung zu sein. Auch die Auswertung der Härtemessungen ergibt einen einheitlichen Gang der Ausscheidung, insofern als sie sich, wie an vier Legierungen mit verschiedenem Silbergehalt gefunden wurde, durch je eine Gerade im ganzen Temperaturbereich wiedergeben lassen. Dabei nimmt die Aktivierungsenergie mit zunehmendem Silbergehalt von 32.000 cal/Mol für die Diffusion des Silbers in Reinaluminium auf 24.000 cal/Mol bei 38 % Ag ab. Dagegen lassen sich die aus der Elastizitätsgrenze ermittelten Werte besser durch zwei Gerade darstellen, denen bei tieferen Temperaturen der Wert 24.000 cal/Mol, bei höherer Temperatur der Wert 32.000 cal/Mol zu entnehmen ist (Bild 7). A. H. Geisler, C. S. Barrett und R. F. Mehl ([17]) haben für die Ausscheidung einer Legierung mit 20 % Ag den Wert 23.000 cal/Mol gefunden.

RÜCKBILDUNGSVERSUCHE AN Al-Ag-LEGIERUNGEN.

Die einphasige Entmischung kann durch kurzzeitige Erwärmung auf höhere Temperaturen beseitigt werden; der Zustand des ursprünglichen Mischkristalls wird zurückgebildet. In das Zustandsbild Bild 8 sind die nach verschiedenen Verfahren bestimmten Grenztemperaturen eingezeichnet, oberhalb der der Zustand der einphasigen Entmischung nicht auftritt bzw. nicht beständig ist. Das schraffierte Gebiet stellt somit das Zustandsfeld dar, in dem die einphasige Entmischung stattfinden kann. Die Entmischungskurve läuft über ein Maximum

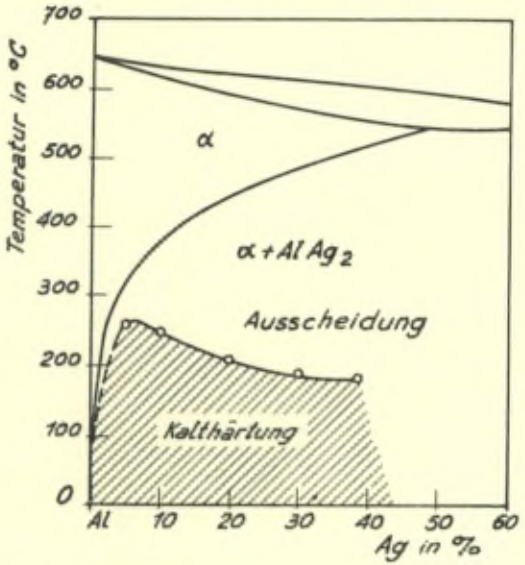

Bild 8. — Kalthärtungsgebiet im Zustandsbild Aluminium-Silber.

bei etwa 5 % Ag. Ein ähnlicher Konzentrationsverlauf ist von G. Borelius ([18]) in den Systemen des Aluminiums mit Kupfer und Zink festgestellt worden.

Die Rückbildung findet in einem Temperaturintervall statt, bei der Legierung mit 38 % Ag zwischen 130 bis 185°. Es stellt sich dabei ein bestimmter Entmischungsgrad oder Ordnungsgrad ein, dessen Betrag mit zunehmender Rückbildungstemperatur auf Null bei der Grenztemperatur abnimmt (Kurve $a - b$ in Bild 2). Er ist weitgehend unabhängig von der Vorbehandlung und kann bei einer Wärmebehandlung im Kalthärtungsgebiet bei steigender und sinkender Temperatur erreicht werden. Es liegt also eine reversible Zustandsänderung vor, deren Gang eindeutig von der Temperatur

bestimmt ist. Bild 9 und 10 belegen diese Aussage; unabhängig von der Vorbehandlung stellen sich bei jeder Temperatur dieselben Härtewerte ein. Bei jeweils 1/2-stündiger Erhitzung der abgeschreckten Legierung wird bei steigender Anlasstemperatur die Kurve fcba in Bild 10 durchlaufen. Sie führt über das Maximum bei c, weil sich unterhalb etwa 130° infolge mangelnder Atombeweglichkeit der endgültige Kalthärtungszustand innerhalb dieser kurzen Frist nicht voll ausbildet. Unterhalb des Maximums bei c würden sich bei hinreichend langer Anlassdauer die Werte des Kurvenstückes c e einstellen (vgl. Bild 2). Geht man nun stufenweise, wie Bild 9 zeigt, von Punkt a, 175°, zu tieferen Temperaturen über, so steigt die Härte

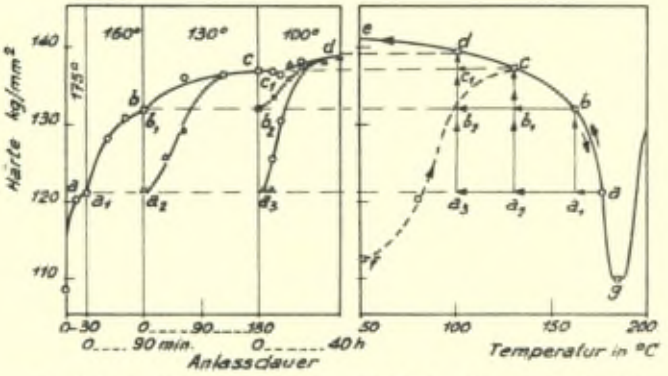

Bild 9. — Zeitliche Änderung der Härte bei stufenweiser Erniedrigung der Anlasstemperatur.

Bild 10. — Die gemäss Bild 9 erreichte Endhärte in Abheingigheit von der Anlasstemperatur.

Bild 9 und 10. — Wärmebehandlung im Kalthärtungsbereich.

jeweils auf den durch den Gleichgewichtszustand gegebenen Wert an. Dabei ist es einerlei, ob der Weg von a unmittelbar nach b, c oder d führt (a a_1 b, a a_2 c, a a_3 d) oder mittelbar (a a_1 b b_1 c, a a_1 b b_1 c c_1 d, a a_1 b b_2 d). Ähnliche Ergebnisse wurden auch bei Leitfähigkeitsmessungen erhalten. Da die elektrische Leitfähigkeit sowohl bei einphasiger Entmischung wie auch bei der Ausscheidung ansteigt, bedurfte es eines Kriteriums, dass keine Ausscheidung stattgefunden hatte. Dieses lieferte die Messung der Thermokraft, die bei den Aluminium-Silber-Legierungen nur durch echte Ausscheidung erhöht wird. Bei den beschriebenen Vorgängen blieb der Wert der Thermokraft praktisch unverändert.

Bild 11 gibt eine Messreihe von A. Durer und G. Baer [19] wieder. Als Mass für den Entmischungsgrad dient hier die Thermokraft,

die bei den Aluminium-Kupfer-Legierungen wie bei den Aluminium-Magnesium-Zink-Legierungen ([13]) durch Kalthärtung verändert wird. Sie zeigt mit aller Deutlichkeit die Einstellung eines temperaturabhängigen Gleichgewichtszustandes zwischen 100 und 220° an,

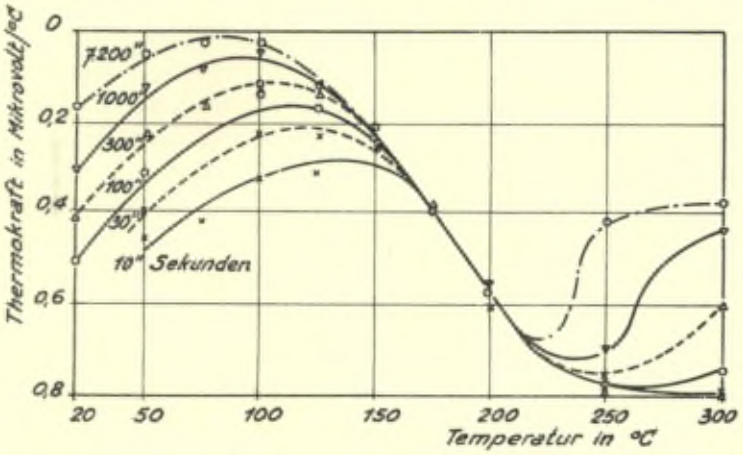

Bild 11. — Isochronen der Thermokraft einer Aluminium-Legierung mit 5 % Cu.

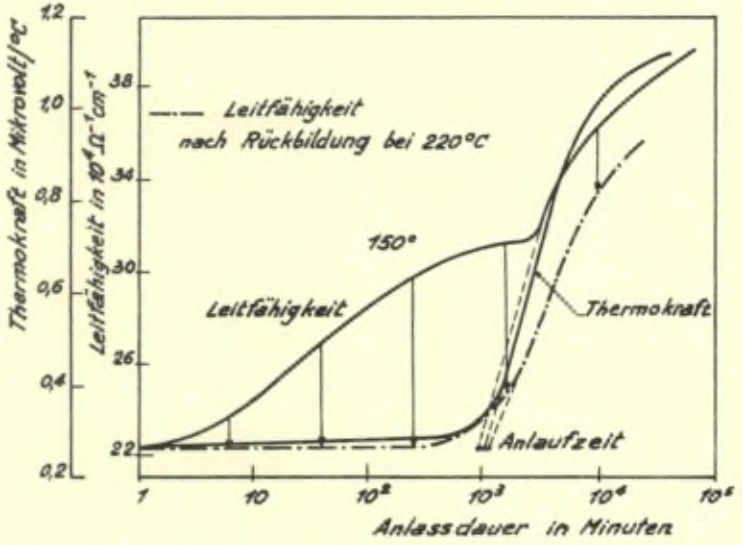

Bild 12. — Bestimmung der Anlaufzeit durch Rückbildungsversuche.

der über einen längeren Zeitraum hinweg konstant erhalten bleibt.

Durch Rückbildungsbehandlung von Proben, die verschieden lange bei bestimmten Temperaturen ausgelagert worden sind, lässt

sich die zeitliche Änderung des Anteiles der einphasigen Entmischung an der Zustandsänderung von dem der Ausscheidung trennen. Ein Beispiel gibt Bild 12, das die zeitliche Änderung der Leitfähigkeit und Thermokraft der Aluminium-Silber-Legierung durch Anlassen bei 150° zeigt und ausserdem in der gestrichelten Kurve die Leitfähigkeitswerte enthält, die nach verschieden langer Vorlagerung bei 150° sich ergeben, wenn die Probe zur Rückbildung der Kalthärtung kurzfristig auf 220° erhitzt und von dort abgeschreckt worden ist. Man sieht, dass die Leitfähigkeitszunahme bis etwa 16 1/2 Stdn. Anlassdauer völlig, darüber hinaus dann in stetig abnehmendem Masse rückgängig gemacht wird. Die Zeiten, die man aus den Rückbildungsisothermen durch Extrapolation des geradlinigen Anstieges auf den Ordinatenausgangswert erhält, sind als die Anlaufzeiten der Ausscheidung zu betrachten, sie stimmen gut mit denen aus der Thermokraft ermittelten überein. Auch auf diese Weise ergibt sich für das System Aluminium-Silber, dass der Ausscheidungsverlauf in dem ganzen untersuchten Temperaturbereich ein geschlossener Vorgang ist.

Die kinetischen Messungen zeigen somit eindeutig, dass die einphasige Entmischung einen besonderen Zustand darstellt, der sich unterhalb der Löslichkeitslinie aus dem übersättigten Mischkristall heraus bildet. Sie ist demzufolge nicht eine Vorbereitungsstufe für die Ausscheidung, sondern sie stellt, wie H. Auer (14) sich ausgedrückt hat, eine Sackgasse auf dem Wege zum Gleichgewichtszustand dar.

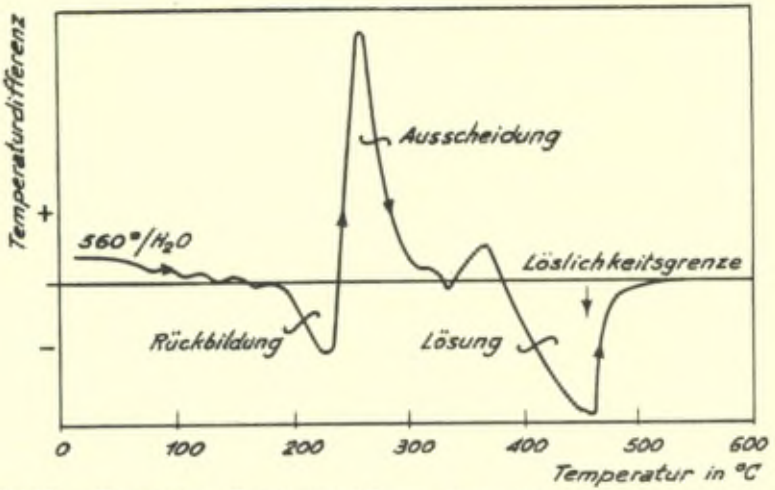

Bild 13. — Temperatur - Temperaturdifferenz - Kurve einer Aluminium-Legierung mit 20 % Ag.

Thermochemisch betrachtet, kann von einer stufenweisen Reaktion gesprochen werden, wenn jeder Schritt von einer Wärmeentbindung begleitet wird. Eine solche einsinnige Entwicklung liegt beim Anlassen des Martensit in der Folge tetragonaler Martensit → kubischer Martensit → α — Fe + Fe_3C vor. Auf der Erhitzungskurve einer kaltgehärteten Aluminium-Legierung wird dagegen zunächst ein Wärme verbrauchender Vorgang registriert, nämlich die Wiederauflösung der zunächst gebildeten an Zusatzmetall angereicherten Bezirke. Dann folgt als Wärme abgebender Vorgang die Ausscheidung. Schliesslich ist in Bild 13, das die Temperatur-Temperaturdifferenz-Kurve einer Legierung mit 20 % Ag während der Erhitzung wiedergibt, noch die Wiederauflösung der heterogenen Ausscheidung infolge der zunehmenden Lösungsfähigkeit des Mischkristalls bis zur Überschreitung der Löslichkeitsgrenze zu erkennen, die wieder unter Wärmeaufnahme erfolgt. Die einphasige Entmischung ist also auch thermodynamisch nicht als Vorstufe der Ausscheidung aufzufassen.

UNTERSUCHUNG VON Al-Ag-EINKRISTALLEN.

Eine vollgültige Koordinierung der widerstreitenden Ansichten über die Beziehung zwischen Kalt- und Warmhärtung kann nur durch röntgenographische Verfolgung der Strukturwandlung und den Vergleich mit den Ergebnissen der Messung verschiedener Eigenschaften an ein und derselben Probe erreicht werden. Von besonderer Wichtigkeit werden dabei die Ergebnisse einer Rückbildungsbehandlung sein. Zu diesem Zweck sind Versuche an Aluminium-Silber-Einkristallen eingeleitet worden. Die röntgenographischen Aufnahmen wurden im Institut von R. Glocker und G. Ziegler nach dem Schiebold-Sauter-Verfahren hergestellt. Bild 14 zeigt die Aufnahme eines Einkristalles nach 10-stündigem Erhitzen auf 150°. Die Flecke sind Interferenzpunkte der (100)-Ebene des Aluminium-Gitters. Unmittelbar nach dem Abschrecken sind sie allein sichtbar. Nach der Anlassbehandlung werden dagegen diffuse Verlängerungen der Reflexe beobachtet, die ganz bestimmten kristallographischen Richtungen entsprechen. Bei längerem Anlassen, Bild 15, schliessen sich die Ansatzstreifen zu Linien zusammen, die die (100)-Interferenzpunkte verbinden. Die Linien entsprechen (111)-Gitterstäben im reziproken Gitter. Es treten dazuhin scharf begrenzte Interferenzpunkte der sich ausscheidenden hexagonalen Phase Ag_2Al auf. Sie liegen genau auf den Streifen.

Es handelt sich um Reflexe der Basisebene der hexagonalen Kristallart, die, wie aus Untersuchungen von C. S. Barrett, A. H. Geisler und R. F. Mehl ([17]) bekannt ist, parallel zur Oktaederebene des Wirtgitters liegt. Durch weiteres Anlassen wird die Intensität der Ag_2Al-Reflexe verstärkt, die der Streifen vermindert.

Das erste Ergebnis von Rückbildungsversuchen an den Einkristallen ist in Tabelle 1 zusammengefasst. Danach wurde die elektrische Leitfähigkeit zyklisch durch Anlassen bei 150° infolge Ausbildung des Kalthärtungszustandes erhöht und durch Abschrecken von 260° infolge seiner Rückbildung praktisch wieder auf den Ausgangswert erniedrigt. Im abgeschreckten Zustand zeigte der Kristall nur die

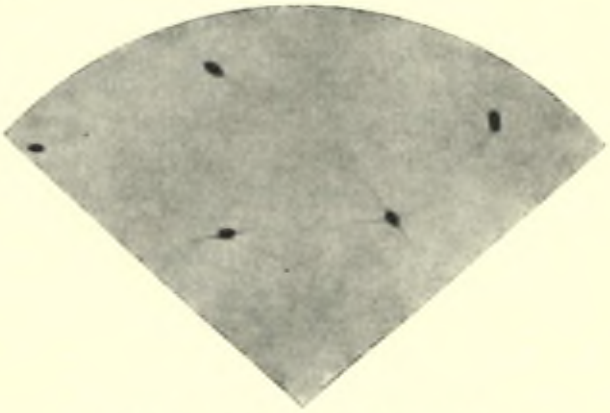

Bild 14 — 10 Stdn. bei 150° angelassen.

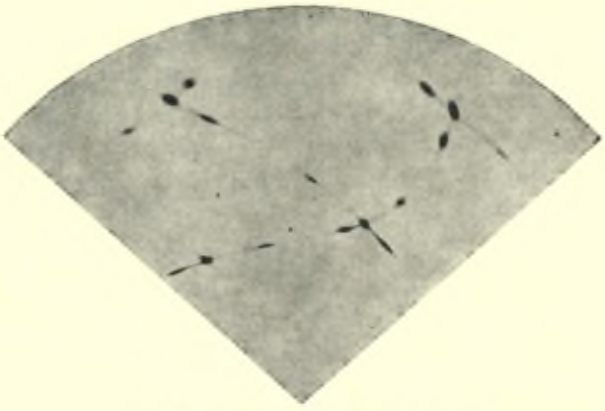

Bild 15 — 6 Tage bei 150° angelassen

Bild 14 und 15 — Schiebold-Sauter-Aufnahmen eines Aluminium-Einkristalles mit 38 % Ag.

kubischen Reflexe, beim ersten Anlassen auf 150° entstanden streifige Verlängerungen (Bild 14), die dann unabhängig vor der weiteren Wärmebehandlung bestehen blieben. Daraus ist zu schliessen, dass die auf den Schiebold-Sautter-Aufnahmen sichtbar werdenden Streifen keine Symptome der Kalthärtung sind. Sie sind vielmehr den Warmhärtungsvorgang zuzuschreiben und spiegeln das Anfangsstadium der Ausscheidung wieder. Diese Zuordnung besagt, dass die Ausscheidung unabhängig von einer etwa gleichzeitig stattfindenden Kalthärtung vorbereitet wird. Sie verträgt sich bestens mit den Ergebnissen der kinetischen Verfolgung der physikalischen Eigenschaften, insbesondere der Thermokraft. Erst nach dem Abschrecken von der Homogenisierungstemperatur treten die Streifen nicht mehr auf, war also der ursprüngliche Zustand des Kristalls wieder voll hergestellt.

Dieser neue Befund über das Verhältnis von Kalt- zur Warmhärtung wird dazu beitragen, manche Widersprüche aufzuhellen. Die von A. H. Geisler und J. K. Hill (9) aus ihren röntgenographischen Untersuchungen abgeleitete Strukturfolge ist aller Wahrscheinlichkeit nach der Warmhärtung zuzuordnen und stellt die verschiedenen Stadien der Ausscheidung dar. Unzutreffend ist, diese Ergebnisse mit den zur Kalthärtung führenden Vorgängen in Verbindung zu bringen. Als kennzeichnende Merkmale der Kalthärtung im Röntgenbild sind Änderungen der Intensität der Interferenzen und der Diagramme bei der Kleinwinkelstreuung zu erwarten.

TABELLE 1.

Leitfähigkeitsmessungen und röntgenographischer Befund an einem Aluminium-Silber-Einkristall nach verschiedener Wärmebehandlung.

Wärmebehandlung	Leitfähigkeit in 10^{-4} Ohm^{-1} cm^{-1}	Röntgenographischer Befund
Von 545° abgeschreckt . .	8,30	keine Streifen
6 h bei 150° angelassen . .	11,44	Streifen
30 sec. auf 260° erhitzt abgeschreckt	8,47	Streifen
3 h bei 150° angelassen . .	11,09	Streifen
30 sec. auf 260° erhitzt abgeschreckt	8,63	Streifen
von 545° abgeschreckt . .	7,76	keine Streifen

WEITERE BEMERKUNGEN ZUM VERHÄLTNIS VON KALT- ZU WARMHÄRTUNG.

Im Zustandsfeld der Kalthärtung geht die einphasige Entmischung unvermeidlich der Ausscheidung zeitlich voran. Diese zeitliche Aufeinanderfolge kann sich in der Kinetik und der strukturellen Entwicklung der Ausscheidung auswirken. Denn die Ausscheidung findet nunmehr aus einem anderen Zustand des Mischkristalls heraus als vordem statt. Man könnte dann in der Kurve der Abhängigkeit des Logarithmus der Geschwindigkeit einer Eigenschaftsänderung von der reziproken absoluten Temperatur zwei in ihrer Neigung voneinander unterschiedene Kurventeile erwarten. Im System Aluminium-Silber liegen für einen derartigen Einfluss keine sicheren Anzeichen vor. Aus den Bestimmungen der Anlaufzeit und der Härte ergibt sich ein ungebrochener Kurvenverlauf. Nur aus der Streckgrenzenmessung folgt eine zweiteilige Kurve, wobei die Aktivierungsenergie im Gebiet niederer Temperaturen kleiner als im Bereich höherer ist. Nach Untersuchungen von G. Wassermann mit J. Ch. Lankes ([20]) über die Längenänderung von Aluminium-Kupfer-Legierungen und mit W. Gruhl ([21]) über die Leitfähigkeit von Kupfer-Beryllium-Legierungen setzen die Geschwindigkeit-Temperatur-Kurven sich aus zwei Geraden zusammen, deren Schnittpunkt bei der Grenztemperatur der einphasigen Entmischung liegt (Bild 16). In diesen Fällen ist die Aktivierungsenergie im Gebiet

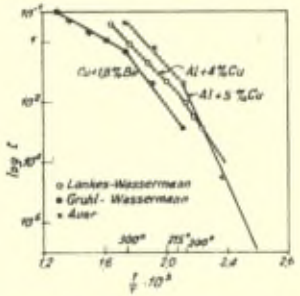

Bild 16. — Zur Bestimmung der Aktivierungsenergie der Aushärtung.

reiner Ausscheidung kleiner als nach voraufgegangener Kalthärtung. M. V. Gayler und R. Parkhouse ([16]) sowie K. L. Hardy ([22]) erhalten bei der Auswertung ihrer Härtemessungen im System Aluminium-Kupfer ebenfalls eine Unstetigkeit oberhalb 200°, wobei nicht ganz klar zu erkennen ist, ob die Aktivierungsenergie ab- oder zunimmt. So

wird es also noch weiterer Messungen bedürfen, um den Einfluss der Kalthärtung auf die Kinetik der Warmhärtung mit aller Sicherheit festzulegen.

In welchem Masse eine voraufgegangene Kalthärtung das atomistische Bild der Ausscheidung beeinflusst, ist die zweite Frage. Auf alle Fälle ist es notwendig, die Ergebnisse der röntgenographischen und kinetischen Forschungsrichtung kritisch miteinander zu verbinden und aus den möglichen Deutungen eines Röntgeninterferenzbildes die auszuwählen, die mit den Befunden der kinetischen Untersuchungen übereinstimmt. In diesem Sinne sei auf eine Auswertung der an Aluminium-Kupfer-Legierungen erhaltenen Röntgenbilder durch H. Jagodzinski und F. Laves ([23]) hingewiesen, die unter Beachtung der dynamischen Tatsachen auf eine von der bisherigen Deutung etwas abweichenden Auffassung über die ersten Stufen der einphasigen Entmischung gekommen sind. Auf Grund der Daten über das Diffusionsverhalten errechnen sie, dass die Anreicherung bei tiefen Temperaturen nicht den bisher angenommenen Umfang erreichen kann. Ihrer Ansicht nach finden sich nur wenige Atome unter Verrückung um einige wenige Atomabstände im Gitter unter Verzerrung des Wirtgitters zusammen. Aus Überlegungen über die Struktur der θ'- und θ-Phase schliessen sie, dass der Aluminium-Kupfer-Bindung eine grosse Bedeutung zukommt, und dass diese sich bereits bei der einphasigen Entmischung dadurch bemerkbar macht, dass die Kupferatome aus dem Wirtgitter austreten und sich in dessen oktaedrische Lücken einbauen. Durch die Bindungskräfte entsteht eine Verzerrung des Aluminiumgitters. Da die Ausbildung einer unmittelbar benachbarten zweiten kupferreichen Netzebene ausgeschlossen ist, weil dann die Aluminium-Kupfer-Bindung wieder zugunsten der Kupfer-Kupfer-Bindung zurückgedrängt würde, sind die Entmischungsgebiete für den Bereich der Guinier-Preston-Zonen wahrscheinlich zweidimensional. Ein Modell dieser Art, von dem Bild 17 einen Eindruck vermitteln möge, ist in der Lage,

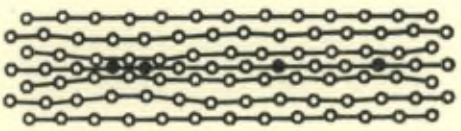

Bild 17. — Vorstellung über die Bildung der Guinier-Preston-Zone bei einer Aluminium-Kupfer-Legierung nach H. Jagodzinski und F. Laves.

die beobachteten Röntgenbeugungsbilder zu erklären. Es berücksichtigt die durch die Verspannungen bedingten Gitterstörungen.

Da die Kräfte, die zur Bildung der auszuscheidenen Phase führen würden, auch im Gebiete der einphasigen Entmischung wirksam sind, kann die Anordnung der Atome in der Endphase auch bei der Atomansammlung innerhalb des Mischkristalls schon angedeutet sein. Darauf wurde bereits eben bei der Besprechung des Versuches einer Beschreibung des atomistischen Zustandes der ersten Stufe der einphasigen Entmischung durch H. Jagodzinski und F. Laves [23] hingewiesen. Besonders offensichtlich ist dieser Zusammenhang im System Kupfer-Beryllium. Nach A. Guinier [24] sammeln sich die Beryllium-Atome zunächst zweidimensional auf Würfelflächen an. Auf eine Berylliumschicht folgt beidseitig eine Kupferschicht. Damit ist die abwechselnde Atomlage in der raumzentrierten γ-Endphase mit geordneter Atomverteilung vorgebildet. Aus diesem Zustand heraus entsteht unterhalb 325°, der oberen Temperaturgrenze für die einphasige Entmischung in einer Legierung mit 1,82 % Be, nach W. Gruhl und G. Wassermann [21] eine Phase mit tetragonal-raumzentriertem Gitter und Überstruktur. Sie ist an neuen Interferenzen auf Debye-Scherrer-Diagrammen zu erkennen. Sie wandelt sich mit der Zeit in die stabile γ-Phase um. Die γ' -Phase bildet sich nur im Anschluss an die einphasige Entmischung aus. Oberhalb ihres Existenzgebietes scheidet sich sofort die stabile γ-Phase aus. Es hat so den Anschein, dass in besonders einfach gelagerten Fällen ein schrittweiser Übergang einzelner Guinier-Preston-Zonen über eine Zwischenphase zur Gleichgewichtsphase möglich ist. Der γ'-Zustand stellt sich gleichermassen als ein an Beryllium bis zur Konzentration Cu-Be angereicherter Mischkristall mit geordneter Atomverteilung oder als tetragonal verzerrte γ-Phase dar. Es liegt also eine enge kristallographisch-geometrische Verwandtschaft vor, die die Ursache einer strukturellen Kontinuität sein könnte.

In dem wesentlich verwickelteren System Aluminium-Kupfer bilden sich im Kalthärtungsbereich dagegen je nach der Anlasstemperatur unterschiedliche Zwischenzustände aus. Eine festgelegte Reihenfolge im Sinne der sequence-Theorie besteht nicht. Auch die Deutung der Röntgenbefunde belässt den einzelnen Aushärtungszuständen vielmehr eine gewisse Selbständigkeit, wie A. Guinier [25] auf Grund einer zusammenfassenden Beurteilung seiner experimentellen Ergebnisse dargelegt hat. Die Aufeinanderfolge der einzelnen strukturellen Zustände, so sagt er, könne nicht als ein kontinuier-

liches Wachsen aufgefasst werden, weil die zuerst entstandenen Komplexe einzelner Strukturen sich nicht durch einfache Atombewegungen auseinander ableiten lassen. Es sei vielmehr eine Wiederauflösung der ihrer Struktur nach instabilen Ansammlungen oder Phasen zu beobachten und damit eine diskontinuierliche Entwicklung anzunehmen.

In diesem Zusammenhang sei auch darauf verwiesen, dass die mehrfach vertretene Ansicht, wonach die gleichartige Orientierung der Guinier-Preston-Zonen und der Ausscheidungen ein Beweis für den kontinuierlichen Übergang von der Anreicherung der Atome im Mischkristall zur ausgeschiedenen Phase sei, nicht haltbar ist, weil sie die Stabilität der einzelnen Aushärtungszustände ausser acht lässt.

EINFLUSS VON ABSCHRECKSPANNUNGEN AUF DIE KINETIK DER AUSHÄRTUNG

Die beim Abschrecken in den Legierungen entstehenden Spannungen wirken sich in verschiedener Weise aus. Ein geringer anfänglicher Härteabfall ([15]) oder eine anfängliche Ausdehnung beim Anlassen ([20]) sind z. B. auf ihre Auslösung zurückzuführen. Um ihren Einfluss auf die Kinetik der Aushärtung zu erfassen, wurde die zeitliche Änderung der Härte der Aluminium-Legierung mit, 38 % Ag nach Beseitigung der inneren Spannungen durch kurzzeitige stossweise Erhitzung auf 220° verfolgt. Dabei ergab sich, dass die Abschreckspannungen nur die Geschwindigkeit der Kalthärtung erhöhen. Auf die Warmhärtung hatte die zusätzliche Massnahme keinen Einfluss. Verständlicherweise ist der Geschwindigkeitsunterschied umso geringer, je höher die Anlasstemperatur ist, weil bei den höheren Temperaturen neben der Kalthärtung gleichzeitig der Abbau der Spannungen einhergeht. Auf diesen Einfluss ist die mehrfach beschriebene Tatsache zurückzuführen, dass die im Anschluss an eine Rückbildungsbehandlung bei Raumtemperatur durchgeführte Kalthärtung langsamer vonstatten geht als unmittelbar nach dem Abschrecken ([26]).

RÜCKBILDUNG DER AUSSCHEIDUNG

Während die Rückbildbarkeit der Kalthärtung frühzeitig erkannt und beachtet worden ist — wurde W. Fraenkel ([27]) doch nicht zuletzt durch diese Erscheinung zu der klaren Trennung der Aus-

härtungsvorgänge in Kalt- und Warmhärtung veranlasst —, wurde der Frage, ob auch Ausscheidungen gemäss den Überlegungen von A. Volmer ([28]), wonach hinreichend kleine Keime bei Temperaturen, die über ihrer Bildungstemperatur liegen, instabil sind, rückgebildet werden können, geringere Aufmerksamkeit geschenkt. Messungen von G.Masing und L. Koch ([29]) an Duralumin sprachen für eine Wiederauflösung auch heterogener Ausscheidungen. Wurde die Aushärtung nämlich bei einer Temperatur vorgenommen, bei der der Widerstand infolge einphasiger Entmischung anstieg, so sank er nach einer Rückbildungsbehandlung. Wurde sie dagegen bei höherer Temperatur durchgeführt, bei der der Widerstand infolge Ausscheidung abfiel, so stieg er wieder nach stossweiser Erhitzung auf eine noch höhere Temperatur an. Diese Methode hat W. Gruhl ([30]) auf Kupfer-Beryllium-Legierungen angewandt. Bild 18 zeigt das Ergebnis einer Messreihe. Der Widerstand, der durch Ausscheidung der γ-Phase nach 1100-stündiger Vorlagerung bei 200° um einen gewissen Betrag gesunken war, steigt infolge der Erhitzung auf 420° fast auf den Ausgangswert an. Dann erst sinkt er auf Grund vermehrter Ausscheidung ab.

In diesem Falle konnte der Vorgang röntgenographisch nachgewiesen werden. Der Strukturbefund ist an die Kurve in Bild 18 an-

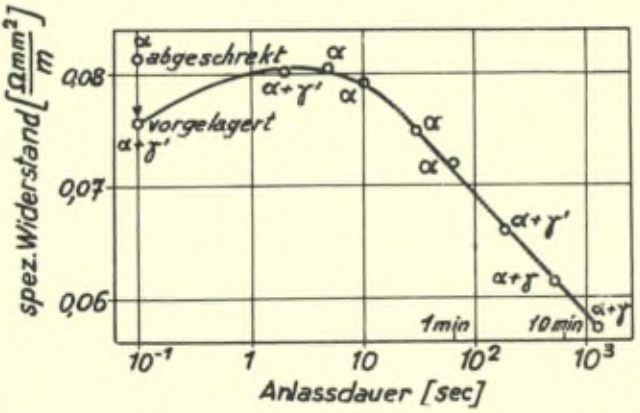

Bild 18. — Rückbildung bei 420° nach 1100-stündiger Vorlagerung bei 200° einer Kupfer-Legierung mit 1,82 % Be.

geschrieben worden. Neben dem Gitte- des α-Mischkristalls liegt zunächst das der γ'-Zwischenphase vor. Diese verschwindet bei der Erhitzung während des Zeitraumes, in dem der Widerstand ansteigt.

Späterhin erscheinen dann die Interferenzen der stabilen γ-Phase, nachdem vorher noch einmal die der γ′-Form schwach sichtbar geworden waren.

Auch aus den Längenänderungsmessungen von J. Ch. Lankes and G. Wassermann ([20]) an Aluminium-Kupfer-Legierungen kann auf eine Rückbildbarkeit der Ausscheidungen geschlossen werden. Während einer Wärmebehandlung bei 200°, die nach verschieden langer Vorlagerung bei 150° durchgeführt wurde, trat zuerst eine Verlängerung auf infolge der Rückbildung des Kalthärtungszustandes, dessen Entstehung mit einer Verkürzung verknüpft ist. Bei längerer Vorlagerungsdauer folgte darauf eine Verkürzung; es wurde die infolge der θ′-Bildung eingetretene Verlängerung teilweise rückgängig gemacht.

Auch das Verhalten der Eisen-Kohlenstoff-Legierungen führt zu dem gleichen Schluss. Durch die Dämpfungsmessungen von L. J. Dijkstra ([31]) ist erwiesen, dass ihre Aushärtung auf der Ausscheidung des Eisenkarbides beruht. W. Geller und H. Kuntze ([32]) sowie W. Gruhl ([33]) haben nun durch Messung der Härte und der elektrischen Leitfähigkeit nachgewiesen, dass die nach dem Abschrecken vorhandenen Eigenschaftswerte durch eine zweckmässige Wärmebehandlung bei einer unterhalb der Löslichkeitskurve gelegenen Temperatur wiederhergestellt werden können. Die über die Keimbildungsvorgänge entwickelten Vorstellungen sind somit auch im Bereiche der Ausscheidung aus übersättigter fester Lösung bestens gestützt worden.

DIE AUSSCHEIDUNG IM SYSTEM KALIUMCHLORID-NATRIUMCHLORID

Die Konstitutionsbedingung für die Aushärtung ist auch in Systemen von Salzen vorhanden. Bei ihnen besteht die Möglichkeit, optische Messgrössen zur Aufklärung der Erscheinungen heranzuziehen. Ein geeignetes System ist das Salzpaar Kaliumchlorid-Natriumchlorid, das zu einer Reihe lückenloser Mischkristalle erstarrt und im festen Zustand ein Entmischungsgebiet aufweist. E. Scheil und H. Stadelmaier ([34]) haben an Kaliumchlorid-Natriumchlorid-Einkristallen die Kinetik der Ausscheidung durch optische Messung der die Entmischung begleitenden Trübung der Kristalle verfolgt. Die Extinktion des durch den Kristall gestrahlten Lichtes ist proportional zur Menge der ausgeschiedenen Phase.

Die Messergebnisse sind in Bild 19 in der üblichen Weise so dargestellt, dass der reziproke Wert der Halbwertszeit der Entmischung gegen den reziproken Wert der absoluten Temperatur auf-

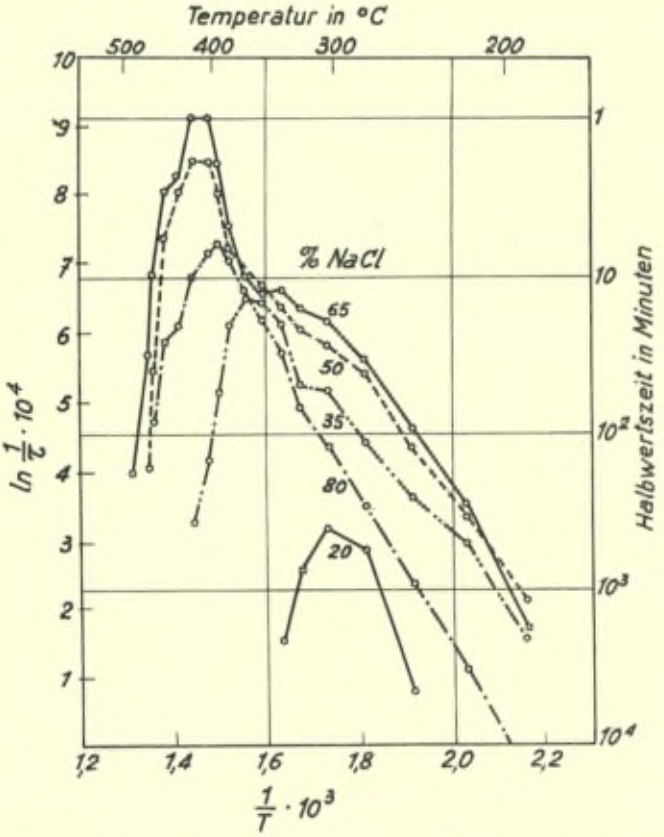

Bild 19. — Temperaturabhängigkeit der Halbwertszeit.

getragen ist. Die Kurven steigen von niedrigen Temperaturen ausgehend zu einem Höchstwert an und fallen bei der Annäherung an die Gleichgewichtskurve wieder ab. Dieser Verlauf ist für einen auf Keimbildung beruhenden Vorgang charakteristisch, insofern als die mit abnehmender Temperatur zunehmende Instabilität des Ausgangszustandes zu einer Steigerung der Zerfallsgeschwindigkeit führt, der jedoch die damit ebenfalls verbundenen wachsenden Diffusionsschwierigkeiten entgegenwirken. In Bild 20 sind die Linien gleicher Ausscheidungsgeschwindigkeit oder genauer gleicher Halb-

wertzeit im Temperatur-Konzentration-Diagramm eingezeichnet. In dieser Darstellung tritt die Kurve maximaler Entmischungsgeschwindigkeit sehr deutlich hervor. Sie zeigt zumindest in diesem

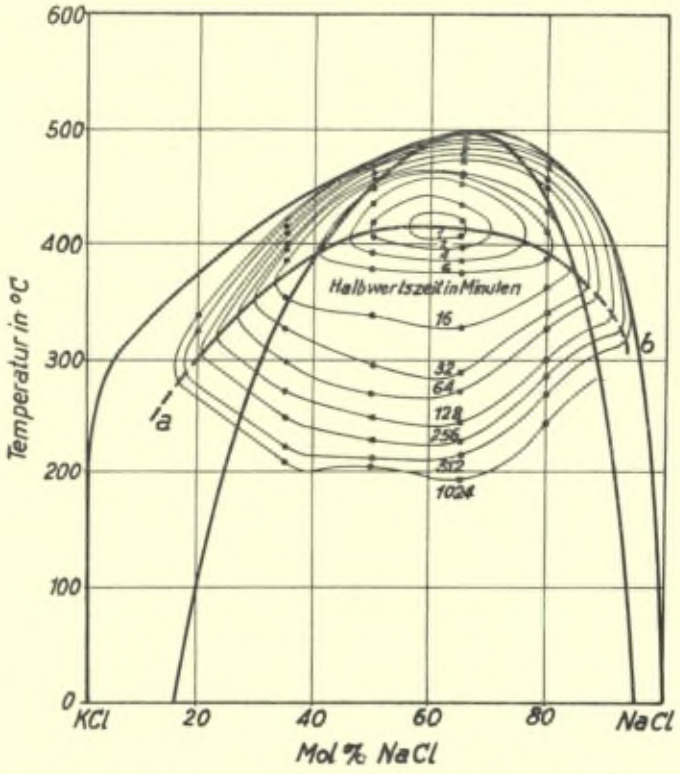

Bild 20. — Kurven gleicher Ausscheidungsgeschwindigkeit.

System keine engere Beziehung zur Spinodalen, die aus der Entmischungskurve berechnet worden und in Bild 20 eingezeichnet ist. Wie weit in anderen Systemen, z. B. dem von C. Wiktorin ([35]) untersuchten System Gold-Platin die Punkte maximaler Entmischungsgeschwindigkeit als experimentelle Grundlage zur Festlegung der Spinodalen herangezogen werden können, bleibe dahingestellt.

Unter der Voraussetzung isothermer Behandlung der Proben hat die Halbwertszeit ihren niedrigsten Wert ungefähr bei der Konzentration des kritischen Punktes der Entmischungskurve. In dieser Hinsicht verhält sich das Salzpaar demnach analog dem Metall-

system Gold-Nickel nach den Angaben von W. Köster und W. Dannöhl ([36]).

Aus dem geradlinigen Kurventeil in Bild 19 ergib sich für die Entmischung der Chloride eine für alle Konzentrationen etwa gleiche Aktivierungsenergie von 22.000 cal/Mol. Dieser Wert entspricht dem der strukturempfindlichen Ionenleitfähigkeit, bei der die Diffusion über Gitterleer- und Gitterstörstellen erfolgt. Wenn ein Platzwechselvorgang im ungestörten Gitter vorliegen würde, müsste die Aktivierungsenergie nach A. Smekal ([37]) 47.300 cal/Mol betragen. Bei den Salzkristallen besteht somit die experimentelle Möglichkeit, über Art und Weise der Diffusion Näheres auszusagen, die bei den Metallen nicht ohne weiteres gegeben ist. Das Ergebnis lautet, dass die Ausscheidung offenbar bevorzugt an Gitterstörstellen stattfindet.

Im ganzen gesehen, scheint es möglich zu sein, Salze als Modellsubstanz für Ausscheidungsvorgänge in Metallen zu benutzen. Es ist damit eine Handhabe gegeben, mit anderen Grössen, als es bei Metallen durchführbar ist, z. B. mit Hilfe der Dielektrizitätskonstante oder der Absorption des Lichtes, diese Erscheinungen messend zu verfolgen. Umgekehrt ist es nicht ausgeschlossen, dass die Übertragung der an Metallen gewonnenen Erkenntnisse für die Salzchemie von Bedeutung sein kann.

VERFOLGUNG DER EIGENSPANNUNGEN WÄHREND DER AUSHÄRTUNG

Der Zerfall eines übersättigten Mischkristalls führt zur Entstehung innerer Spannungen; sie gelten als Ursache der Härtung. An ferromagnetischen Legierungen können sie ihrer Grösse nach überschlägig ermittelt werden. Bekanntlich sind verschiedene magnetische Eigenschaften von der Richtungsverteilung der spezifischen Magnetisierung abhängig. Für sie sind Beziehungen zu Stoffkonstanten wie der Sättigungsmagnetisierung und der Sättigungsmagnetostriktion aufgestellt worden, in denen als Proportionalitätsfaktor die Spannungsgrösse σ_i vorkommt, die von den inneren Spannungen hergeleitet wird ([38]). W. Köster und G. Krüger ([39]) haben die Änderung dieser Grösse

bei der Aushärtung einer Nickel-Beryllium-Legierung mit 1,9 % Be durch Messung der Anfangspermabilität

$$\left(\chi a = \frac{2}{9}\frac{\mathcal{J}_s^2}{\lambda_5 \sigma_i}\right)$$

und der Remanenzänderung unter Zug

$$\left(\frac{d\mathcal{J}a}{d\sigma} = \frac{1}{4}\frac{\mathcal{J}s}{\sigma_i}\right)$$

gemessen.

Die Zunahme der aus der Remanenzänderung berechneten inneren Spannungen vollzieht sich gleichlaufend mit der Härtesteigerung. Sie ist also mit dem Zerfall des übersättigten Mischkristalls in die Gleichgewichtsphasen verbunden. Zwischen der Änderung der Härte und der der Eigenspannungen besteht angenäherte Proportionalität; einer Härtezunahme von 100 kg/mm² entspricht eine Spannungssteigerung von rund 3 kg/mm². Sowohl aus der Remanenzänderung unter Zug als auch der Anfangssuszeptibilität berechnen sich Maximalspannungen von 16 kg/mm². Die Suszeptibilitätswerte hinken etwas hinter den Remanenzwerten einher.

Die Aktivierungsenergie der Ausscheidung, ermittelt aus der Kinetik der verschiedenen Eigenschaften, ist gleichermassen 40.000 cal/Mol. In einer Darstellung, in der der Logarithmus des reziproken Wertes der Zeit, in der ein Höchstwert einer Eigenschaft erreicht wird, gegen die reziproke absolute Temperatur aufgetragen ist, sind die Geraden parallel zueinander verschoben. Es ändert sich also die Aktionskonstante $1/t_0$ oder, anders ausgedrückt, der Elementarschritt, der durch Diffusion vollzogen werden muss, um eine Eigenschaft zu beeinflussen, wächst in der Reihenfolge Härte, Eigenspannung aus $\frac{d\mathcal{J}_R}{d\sigma}$, Eigenspannung aus χ_a, Koerzitivkraft. Dieses Ergebnis steht in Übereinstimmung mit gleichlautenden Beobachtungen am System Eisen-Kohlenstoff (40) und Eisen-Gold (41).

LITERATURVERZEICHNIS

(1) R. F. Mehl und L. K. Jetter, « Age Hardening of Metals Symposium » of the American Society for Metals, S. 342 (1939).
(2) H. K. Hardy, *J. Inst. Metals* **75**, S. 707 (1949).
(3) G. C. Smith « Progress in Metal Physics » *Butterworths Scientific Publications* (London I), S. 163 (1949).
(4) H. Auer, *Z. Naturforschg.*, **40**, S. 533 (1949).
(5) W. Köster, *Z. Metallkde*, **41**, S. 71 (1950).
(6) G. Wassermann und J. Hengstenberg, *Z. Metallkde*, **23**, S. 114 (1931).
(7) A. Guinier, *C. R.*, **206**, S. 164 (1938); *Arm. Physique*, **12**, S. 161 (1939).
(8) G. D. Preston, *Proc. Roy. Soc., A* **167**, S. 526 (1938).
(9) A. H. Geisler und J. K. Hill, *Acta Cryst.*, **1**, S. 238 (1948).
(10) A. H. Geisler, *A. I. M. E., Techn. Publ.*, S. 2436 (1948).
(11) U. Dehlinger, *Z. Phys.*, **102**, S. 633 (1936).
(12) R. Becker, *Z. Metallkde*, **29**, S. 245 (1937).
(13) A. Durer und W. Köster, *Z. Metallkde*, **30**, S. 311 (1938).
(14) H. Auer, *Z. Metallkde* **30**, H. V. 48 (1938);
H. Auer und H. Schröder, *Ann. Phys.*, **37**, S. 137 (1940).
(15) W. Köster, F. Braumann, H. Steinert und J. Scherb, *Z. Metallkde*, demnächst.
(16) M. V. Gayler, *J. Inst. Met.*, **60**, S. 249 (1937);
M. V. Gayler und R. Parkhouse, *J. Inst. Met.*, **66**, S. 67 (1940).
(17) C. S. Barrett, A. H. Geisler und R. F. Mehl, *Trans. A. I. M. E.*, **143**, S. 134 (1941).
(18) G. Borelius, *J. Metals*, **3**, S. 477 (1951);
G. Borelius, J. Anderson und K. Gullberg, *Ingeniörsakademiens Handl.*, Nr. 169 (1943).
(19) A. Durer und G. Baer, *Z. Metallkde*, demnächst.
(20) J. Ch. Lankes und G. Wassermann, *Z. Metallkde*, **41**, S. 381 (1950).
(21) W. Gruhl und G. Wassermann, *Metall*, **5**, SS. 93, 141 (1951).
(22) K. L. Hardy, *J. Inst. Met.*, **78**, S. 321 (1951).
(23) H. Jagodzinski und F. Laves, *Z. Metallkde*, **40**, S. 296 (1949).
(24) A. Guinier, *Rev. Mét.*, **16**, S. 1 (1944).
(25) A. Guinier, *C. R.*, **231**, S. 655 (1950).
(26) A. Dreyer, *Z. Metallkde*, **31**, S. 147 (1939).
(27) W. Fraenkel und L. Marx, *Z. Metallkde*, **21**, S. 2 (1929);
H. Meyer, *Z. Phys.*, **76**, S. 268 (1932).
(28) A. Volmer und N. Weber, *Z. Phys. Chem.*, **19**, S. 277 (1926).
(29) G. Masing und L. Koch, *Z. Metallkde*, **25**, SS. 137, 160 (1933).
(30) W. Gruhl, *Metall*, **5**, S. 231 (1951).
(31) L. J. Dijkstra, *J. Metals*, **1**, S. 252 (1949).
(32) W. Geller und H. Kuntze, *Z. Metallkde*, **40**, S. 16 (1949).
(33) W. Gruhl, *Z. Metallkde*, **41**, S. 171 (1950).
(34) E. Scheil und H. Stadelmaier, *Z. Metallkde*, demnächst.
(35) C. G. Wiktorin, *Ann. Phys.*, (5), **33**, S. 509 (1938).
(36) W. Köster und W. Dannöhl, *Z. Metallkde*, **28**, S. 248 (1936).
(37) A. Smekal, *Handbuch der Physik* XXIV/2, 5 Ziff. 18.
(38) R. Becker und W. Döring, « Ferromagnetismus », J. Springer-Verlag, Berlin (1939).
(39) W. Köster und G. Krüger, *Z. Metallkde*, demnächst.
(40) W. Köster, *Arch. Eisenhüttenwes.*, **21**, S. 305 (1950).
(41) W. Köster und E. Braun, *Z. Metallkde*, **41**, S. 238 (1950).

Discussion du rapport de M. Köster

M. G.A. Homès. — Vous avez parlé d'une température limite du « Kalthärtung » comme s'il s'agissait d'une constante physique pour un alliage de composition donnée.

Dois-je comprendre que la relation entre la composition et la température critique serait réellement univoque?

Il me semble que la déformation plastique doit influencer cette température. Le degré d'écrouissage mécanique est peut-être toujours petit devant le degré d'écrouissage d'origine chimique, ce qui expliquerait les choses.

M. Köster. — Nous avons opéré sur des alliages recuits, dépourvus de tout écrouissage mécanique, mais, nous ne savons pas ce que devient la relation si cet écrouissage intervient.

M. Seitz. — If the Kalthärtung were the result of the precipitation of the solute atoms at dislocations, one might expect to enhance the effect by cold working the material first to obtain more dislocations for precipitation. Actually the interpretation in terms of precipitation at dislocations seems to be highly unlikely. I understand from professors Borelius and Dehlinger that about half of the heat of precipitation is released in Kaltaushärtung and that this is of the order of 100 cal. per mol of precipitate. This could mean that about 1 cal. or more is released per cubic centimetre in the Kaltaushärtung stage. Since no more than 10^{17} atoms should lie along dislocation lines per cubic centimetre, one would expect the heat of precipitation at dislocations in the Koehler-Cottrell manner to be no more than about 0.01 cal. per cubic centimetre and probably much less.

M. Borelius. — A main subject of the report of professor Köster is the equilibrium conditions and the kinetics of what he calls « die einphasige Entmischung » (or the sub-microscopic formation of the Guinier-Preston aggregates) as compared with and distinguished

from the usual microscopic precipitation. I should like to sum up what according to my own experiences seems to be the most characteristic features of this sub-microscopic precipitation or shortly sub-precipitation.

1. The range of this phenomenon in the phase diagram has an upper limit within the two-phase boundary. We have in our laboratory determined this limit in the systems Al-Cu and Al-Zn and also to some extent in Al-Ag, where it has now been determined in a more elaborate way by professor Köster.

2. The sub-precipitate has to dissolve before the atoms belonging to it can go over into the stable precipitate, as was first made probable in 1938 by the calorimetric work of Swindells and Sykes.

3. Though the sub-precipitate is only metastable it can to a certain extent be treated as a new phase according to the rules of heterogeneous equilibrium. Its heat of solubility was in Al-Cu computed to some 60 per cent of that of the stable phase.

4. The limit of the range of sub-precipitation in the phase diagram is not related to the spinodal. This becomes quite clear in the system Al-Ag, where the range of sub-precipitation is well available for measurements on both sides of the spinodal. I therefore do not understand why professor Köster connects the sub-precipitation with so-called « negative diffusion ». The use of this conception of negative or uphill diffusion is somewhat varying, but as it was once derived by professor Dehlinger, it was bound to negative values of the second derivative of the free energy with respect to concentration and thus should occur only on the side of the spinodal, towards higher concentration.

5. The rate-curve, for instance the power of evolution of heat as a function of time, has no observable maximum and decreases in a hyperbolic way, whereas in usual precipitation the rate-curve has a maximum and a more or less exponential tail.

6. The rate of sub-precipitation is mainly a function of the concentration of foreign atoms still in solution and, at least at low concentrations, independent of the amount of precipitate. I made this conclusion from our earlier calorimetric measurements on Al-Cu alloys and have now found further evidence from new unpublished resistometric measurements on Al-Ag alloys.

7. These characteristic features of the kinetics of the sub-preci-

pitation can be understood by the simple assumption that the aggregates cannot grow beyond a limited size, the reason being for instance internal stresses. The continuation of the precipitation process therefore presupposes continued formation of new aggregates, and the probability for this formation of aggregates through fluctuation is chiefly dependent on the concentration of foreign atoms in solution. I have the impression from the papers of professor Köster that he is unwilling or reluctant to accept this simple view, but I am not sure of his reasons.

M. Köster. — Die experimentallen Ergebnisse über die ich berichtet habe, sind phänomenologisch in bester Übereinstimmung mit denen von professor Borelius. Auch in der Deutung, glaube ich, gehen wir nicht weit auseinander. Ich kann mich dabei auf die Ausführungen von professor Dehlinger, Vortrag von professor Rudberg und der Diskussionsbemerking von professor Hollomon beziehen.

M. Bragg. — Professor Köster has given us a very dear account of the cogent reasons for supposing that the phenomenon of « cold » and « hot » age hardening has a different physical origin, and proceed independently in the crystal. If I may make an analogy, the behaviour of a metal from which all hardening has been removed by annealing is like that of an area of forest which has been denuded of trees. A « second growth » of wood springs up of a different nature to the permanent forest in equilibrium given time; however, the long-lived permanent trees establish themselves and once more dominate the forest. The cold hardening is due to an aggregation of platelets, or an opalescence of the metal due to negative diffusion.

The warm hardening is produced by a slow nucleation of a new phase, which starts concurrently and independently, and which finally drains the regions which produced the cold hardening and produces separate crystals of the new phase. I would like to ask how these two processes are correlated with X-ray diffraction phenomenon of the kind first studied by Guinier and Preston.

M. Köster. — Preston hat bei Laue- und Drehkristal laufnahmen bei langdauernder Exposition Schwärzungsstreifen beobachtet, die von einzelnen Interferenzpunkten ausgehen und unter Umständen

sich von einem Punkt zum anderen erstrecken. Guinier hat ausserdem Veränderungen im Interferenzbild in unmittelbarer Umgebung des primären Strahlenbündels festgestellt. Die erste Art von Interferenzerscheinungen werden als Guinier-Preston-Streifen bezeichnet. Preston gibt an, dass bei einer Aluminium-Kupfer-Legierung mit 4 % Cu eine bei 20° ausgehärtete Legierung Streifen zeigte, die nach kurzer Glühung bei 200° verschwanden und nach weiterer Glühung bei 200° wieder erschienen. An der Aluminium-Silber-Legierung mit 38 % Ag haben wir beobachtet, dass die Streifen nicht mit dem Vorgang der Kalt- sondern der Warmhärtung verknüpft sind. Mit Kleinwinkelstreuung haben wir selbst nicht gearbeitet. Insgesamt sieht es so aus, als ob die Auffassungen der Röntgenologen und der Kinetiker leichter auf einen Nenner gebracht werden können, als es von einigen Seiten her angenommen wurde. So entspricht die Auslegung, die Guinier in der seinem Konferenzbericht beigefügten Arbeit seinen Röntgenbefunden gibt, durchaus den Folgerungen, die aus kinetischen Messungen zu ziehen sind.

Eines sei indessen noch bemerkt. Die Aushärtungserscheinungen sind sehr vielseitig und wechseln von System zu System. Es kommt sehr darauf an, ob aus dem Grundmetall sich das hinzulegierte Metall oder eine intermediäre Kristallart ausscheidet, ob diese ein dem Grundmetall sehr verwandtes und in gewissen Abmessungen ähnliches Gitter hat, ob sich instabile Zwischenphasen bilden können oder nicht, ob es sich um Substitutions- oder Einlagerungsmischkristalle handelt. Ergebnisse an einer Legierungsreihe sind also nicht ohne weiteres auf eine zweite zu übertragen.

M. A. Guinier. — 1. Il est, je crois, important de signaler que l'accord entre les études de structure des alliages durcis par les rayons X et les études de cinétique, est actuellement bien meilleur qu'il est indiqué au début du mémoire du professeur Köster. Cela provient des modifications qui ont été apportées à l'interprétation des premières études auxquelles l'auteur fait référence dans les premières pages.

Ainsi, les conclusions tirées des diagrammes de rayons X auxquelles nous arrivons dans l'article sous presse dans *Acta Crystallographica* sont tout à fait conformes à l'idée fondamentale du mémoire du professeur Köster : la distinction entre deux processus « Kalt » et « Warm Aushärtung ». Le premier est caractérisé par les zones et le second par une phase précipitée véritable. Dans la plupart

des cas, la structure atomique de la zone est différente de celle du précipité, si bien que l'idée de discontinuité s'impose naturellement.

2. L'apparition des zones ou des précipités dépend de l'état de perfection du réseau de la matrice. Ainsi il est possible d'observer des petits précipités dans des régions particulièrement perturbées du réseau (sous-limites entre grains polygonisés, bandes de glissement, etc.), à une température très inférieure à la température de stabilité de la phase. Ces précipités observés au microscope électronique sont très rares et n'ont probablement pas d'influence sur les propriétés moyennes du métal.

M. Orowan. — What is the first stage in hardening? It seems there are two models, either an uphill diffusion which produces a statistical cloudiness, or is it a lot of small plates or rods, limited in size for some reason? It is not possible that the elastic energy limits the size of coherent precipitates?

M. Guinier. — En ce qui concerne l'hypothèse du professeur Orowan, dans l'alliage Al-Ag, il n'y a pas d'évidence pour que la zone soit plate ou longue. Dans les photographies du professeur Köster, les stries ne sont pas en relation avec la forme des zones, mais probablement avec des irrégularités de structure des précipités qui se forment par passage du réseau cubique à faces centrées au réseau hexagonal (stacking disorder). Les zones initiales se manifestent aux rayons X par d'autres phénomènes : diffusion aux petits angles en forme d'anneau.

M. Rudberg. — Professor Köster has shown that the « Kaltaushärtung » process, which does reveal itself through an altered resistivity, is attended by no change of thermoelectric force in the Al-Ag case, but involves some change in the case of the Al-Cu alloy. In other respects the process has the appearance of a segregation of solute atoms in regions of the metal which exhibit a temperature dependent saturation, as remarked particularly by Borelius and Guinier. A process of this kind would be the accumulation of solute atoms into atmospheres of increased density around dislocations, envisaged by Cottrell. If this is what happens, the effect on the main body of the alloy, outside these atmospheres, might be expected to be chiefly a decrease in solute concentration. The thermoelectric force ought to be governed by the thermodynamic

potential of the electrons in this main body. Is it possible that the behaviour formulated by professor Köster means that the relative change in concentration in the main body of the alloy is really small in the case of the Ag rich alloy, but becomes appreciable for the Cu alloy, where the supply of solute atoms available is smaller by a factor of seven?

M. A. Crussard. — Les expériences du professeur Köster sur les alliages Al-Ag, en dehors de leur intérêt capital pour l'étude du durcissement structural et de la précipitation, présentent un grand intérêt pour l'étude thermoélectrique des alliages.

Nous avons en effet étudié l'influence de divers éléments d'alliage sur le pouvoir thermoélectrique de l'aluminium. Cet effet ω, est tantôt positif, tantôt négatif, selon l'élément d'alliage. Au cours d'une précipitation par formation d'amas cohérents, cet effet ω subit une variation $\Delta\omega$, parfois très importante. En étudiant divers éléments d'alliages, nous avons établi que le signe de $\Delta\omega$ dépend, non du signe de ω, mais de la grosseur relative des atomes dissous et de ceux d'aluminium. Si l'atome dissous est plus gros, $\Delta\omega$ est positif; s'il est plus petit, $\Delta\omega$ est négatif. Une analyse semi-théorique du phénomène nous a montré que la variation était liée aux tensions internes produites aux environs des amas (probablement la composante hydrostatique de ces tensions).

Les expériences du professeur Köster viennent compléter magnifiquement les nôtres, puisque, pour l'argent, $\Delta\omega$ est nul, alors que les deux atomes Al et Ag ont un même diamètre, et donc que les tensions internes sont pratiquement nulles.

Cette absence de tensions internes est probablement l'explication du fait signalé par le professeur Köster, que la formation d'amas riches en argent abaisse la résistivité, au lieu de l'élever comme pour les autres alliages.

L'égalité des rayons atomiques d'Al et d'Ag explique aussi qu'un écrouissage préalable n'accélère pas la précipitation (Warmaushärtung), puisque l'interaction élastique entre dislocations et atomes d'Ag dissous est nulle. En effet, dans les autres alliages, l'accélération de la précipitation à chaud est due à un accroissement de la vitesse de germination, les dislocations drainant les atomes à elles et augmentant les chances de germination dans les zones de concentration ainsi formées. Cet effet n'existe pas pour les alliages Al-Ag.

Il faut préciser que, pour ces alliages Al-Ag, c'est seulement

l'interaction élastique *à longue distance* entre dislocations et atomes d'Ag qui est absente. Il existe certainement une interaction à petite distance, sans quoi l'alliage ne durcirait pas au cours de la précipitation cohérente (à moins que les atomes d'Ag n'interviennent de façon dynamique, par leur masse, sur la propagation des dislocations). Ceci prouve, soit dit en passant, que le durcissement par formation d'amas cohérents n'est pas dû (au moins entièrement) aux tensions internes.

M. Cottrel. — The question has been raised about whether cold-hardening might be due to segregration of solute atoms to dislocations. Previously I had always dismissed this possibility because the X-ray evidence seemed to point clearly in a quite different direction. Now that the X-ray effects observed during cold-hardening have been re-interpreted, it may be useful to re-open the question of segregation to dislocations.

I wish to point out that this process could explain two of the observations about cold-hardening. First, the fact that the change comes to a stop while the solution is still supersaturated; this would be due to the saturation of dislocations with solute. Second, the cold-hardening process begins without an induction period and develops parabolically with time; Bilby and I showed that the segregation of solute atoms to dislocations should behave in this way, the amount of solute transferred to dislocations increasing as the two-thirds power of the time of ageing.

Dr. Hollomon asked whether, on the dislocations theory, one would expect the segregates to evaporate from the dislocations at temperatures of around 100 °C. I replied that there always will be a temperature of evaporation, but I cannot say that this would be to any given system without making detailed calculations.

Professor Seitz pointed out to me privately during this discussion that the release of energy during cold-hardening is almost certainly too large to be accounted for by the comparatively small amount of solute that can be transferred to dislocations in an unworked crystal. In my opinion this is a convincing argument against the hypothesis that cold-hardening is caused by the segregation of solute to dislocations.

M. Hollomon. — In general, the precipitate from a supersaturated solid solution will have a different structure and a different

composition from that of the solvent phase. At the temperature of the solvus the rate of reaction will be zero since the driving free energy is zero. As the temperature is gradually lowered, a precipitate of the equilibrium structure and composition can form. If the temperature is further lowered, however, the rate of this process will decrease both because of the decrease in the rate of nucleation and the decrease in the rate of diffusion. At a temperature sufficiently removed from the solvus temperature there is sufficient free energy available for the formation of a phase elastically deformed to be coherent with that of the matrix and hence, having a lower interfacial energy with the matrix. Thus, even though the driving force for the precipitation is decreased by the formation of the non-equilibrium phase, the rate of the process may be enhanced since the rate of nucleation is increased. There will, however, be a critical temperature at which the strained coherent phase has the same free energy as the matrix phase. Essentially, this is the solvus temperature for the precipitation of an elastically distorted precipitate. Figure 1 is a schematic diagram illustrating

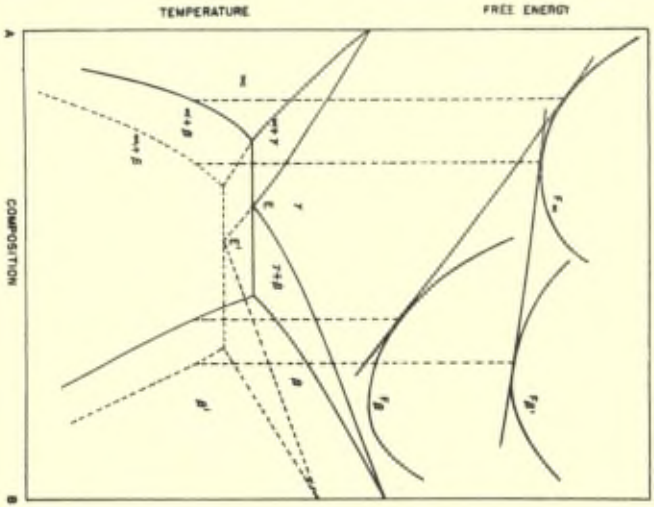

the equilibrium conditions for both the unstrained and strained precipitate. Thus, from solid solutions there can occur two types of precipitates; at an elevated temperature an incoherent precipitate can form and below some definite temperature, a coherent phase can precipitate. If the temperature is further decreased, the rate of formation of both the coherent and incoherent precipitate will

become negligibly small and finally a temperature will be reached at which a phase may form having the structure of the precipitating phase (possibly distorted) but having the composition of the solution from which it forms. This transformation can occur without long-range diffusion and will occur at a still faster rate than ordinary precipitation. There will, however, be a definite temperature above which this transformation cannot occur. This latter transformation is called a Martensite transformation. It is, of course, possible that there can be several coherent precipitates in which the degree of distortion and the amount of reduction in the interfacial energies are different. It is conceivable that some of the several hardness peaks observed upon precipitation from the solid solution may be accounted for by the formation of several of these precipitates.

M. Dehlinger. — Vielleicht ist es nicht überflüssig zu sagen, dass die von Herrn Hollomon berechnete elastische Spannungsenergie sowie etwaige Änderungen der Entropie in folge der Komplexbildung zu der von Herrn Borelius dargestellten freien Energie zu addieren sind, die zunächst aus der Wärmetönung der Gleichgewichtszustände berechnet wird. Dadurch ändert sich die durch $d^2f/dx^2 = O$ bestimmte Grenzkurve. Im allgemeinen wird sie nach tieferen Temperaturen verlagert werden, es ist dabei noch zu untersuchen, ob sie sich auch teilweise nach höheren Temperaturen verschieben kann.

Wenn die Spannungsenergie pro Atom von der Grösse der kohärenten Komplexe abhängt, tritt ein weiterer Effekt ein. Die Komplexe können nicht beliebig weiterwachsen und kleinere Nachbar-Komplexe aufzehren sondern es stellt sich ein von der Temperatur abhängender metastabiler Gleichgewichtszustand ein. Wie aus dem Bericht von Köster hervorgeht, ist durch Widerstands- und Härtemessungen bei der Kaltaushärtung von Al-Cu und Al-Ag ein solches Gleichgewicht gefunden worden.

M. Smith. — An alloy of Cu, Ni and Mn (80/20/20) when annealed at about 450 °C for long periods of time hardens considerably (1) though this has been incompletely studied, it seems to be by a mechanism analogous to « cold-hardening » and is not followed by a second stage of precipitation. The rate of hardening

(1) See, e. g., paper by M. Cook and W. O. Alexander, *J. Inst. Metals*, **72**, p. 381 (1946).

is not greatly influenced by prior deformation, which seems to indicate that in this case at least dislocations are not involved in the hardening mechanism. It may be a sort of short-range ordering phenomenon involving two constituents in a lattice of the third. Similar effects are observed in the ternary system copper-silver-palladium where, although there is some hardness increase on ordering in the binary copper-palladium alloys, the hardness occurring in the ternary alloys is very much greater (1).

(1) E. M. Wise, *Metals Handbook* (A. S. M.), 1948, 1128.

Sur l'élasticité du milieu cristallin

par Jean Laval

INTRODUCTION

APERCU HISTORIQUE. LES FORCES CENTRALES

La première théorie de l'élasticité cristalline est due à Cauchy (*) qui, d'emblée, a défini les vingt et une constantes élastiques estimées jusqu'ici suffisantes pour déterminer les tensions et l'énergie nécessaires à la production de toutes les déformations conformes à la loi de Hooke. Le grand géomètre envisage un réseau de particules identiques s'attirant les unes les autres suivant les droites qui les joignent : l'attraction entre deux d'entre elles est entièrement déterminée par leur distance, elle décroît vite si la distance augmente et devient négligeable si la distance excède un rayon d'action sensible. Puis Voigt (**) a développé systématiquement la théorie de Cauchy. Il l'a confirmée par des expériences nombreuses et précises, surtout il l'a renouvelée entièrement par l'invention des tenseurs. Mais Voigt, à l'encontre de Cauchy, ne se réfère plus à la structure réticulaire. Il applique au milieu cristallin les lois de l'élasticité classique. Il admet de la sorte que ce milieu est homogène à toute échelle; car la théorie classique de l'élasticité exige une homogénéité absolue.

C'est Born (***) qui a réédifié l'élasticité cristalline sur la structure atomique. Il rejoint toutes les conclusions de Voigt. Mais pour y parvenir, il fait appel aux forces centrales : il pose que deux atomes exercent l'un sur l'autre une force dirigée suivant la droite qui les réunit, déterminée uniquement par leur distance. C'est tenir les atomes engagés dans les cristaux pour des sphères rigides impénétrables; et c'est encore leur attribuer une densité électronique invariable, douée d'une symétrie exactement sphérique.

Or ces atomes ne sont pas limités par des surfaces indéformables

(*) *Mémoires de l'Académie des Sciences*, IX, p. 114; X, p. 293; XVIII, p. 153.
(**) *Lehrbuch der Kristallphysik*, Teubner, Berlin 1910.
(***) *Dynamik der Krystallgitter*, Teubner, Berlin, 1915.

et séparés par des espaces vides. Ils ne sont pas même individualisés. Le milieu cristallin est continu : nulle part sa densité électronique tombe à zéro. Néanmoins, nous pouvons distinguer dans un cristal des ions positifs sensiblement sphériques et rigides, qui baignent dans une sorte de milieu fluide, constitué par les électrons liés faiblement, de valence ou de conductibilité. Quand le cristal subit une déformation, les ions positifs conservent sensiblement leur forme et leur densité électronique, mais alentour le milieu fluide est nécessairement déformé : les fonctions propres de ses électrons sont modifiées, sa densité électronique varie.

Les ions positifs forment presque toute la masse du cristal, et les forces prises en compte par l'élasticité sont celles qui leur sont appliquées. L'un exerce sur l'autre une force de rappel qui se réduit, en première approximation, à deux composantes. La première est produite par le déplacement relatif des deux ions. Elle existerait seule si le milieu fluide était supprimé, le cristal réduit aux ions positifs, séparés par le vide. Comme les ions positifs gardent une densité électronique sensiblement sphérique cette première composante est sensiblement centrale. Mais les deux ions réagissent encore l'un sur l'autre par l'intermédiaire du milieu électronique qui les entoure. La force de rappel développée par cette réaction n'obéit plus aux lois des forces centrales. De beaux travaux (*) ont été consacrés, pendant ces dernières années, aux calculs des constantes élastiques. Mais, la déformation du milieu électronique autour des ions positifs, n'a jamais, que je sache, été prise systématiquement en compte. Pourtant si les électrons, de valence et de conductibilité, ne conservent pas la même fonction d'onde ils ne conservent pas la même énergie globale : leur énergie de corrélation varie, comme leur énergie d'échange avec les électrons incorporés dans les ions positifs, et surtout l'énergie prise par chacun d'eux, supposé seul dans le champ de force créé par les ions positifs; l'énergie de Fermi même est changée.

La force de rappel entre deux ions positifs se différencie d'autant plus d'une force centrale que cette seconde composante est plus importante par rapport à la première. Chez les cristaux ioniques, du type sel gemme, elle est la plus faible, chez les cristaux métalliques,

(*) Bardeen, *Journ. of Chem. Phys.*, **6**, p. 367 (1938);
Fuchs, *Proc. Roy. Soc.*, **151**, p. 585 (1935); **153**, p. 622 (1935); **157**, p. 444 (1936).
Grüneisen, *Handbuch der Physik*, Vol. X.
Landshoff, *Z. Physik*, **102**, p. 201 (1936); *Phys. Rev.*, **52**, p. 246 (1937).

la plus forte. En conséquence, les constantes élastiques des cristaux ioniques sont, à peu près, dans les rapports prévus par Cauchy, celles des cristaux métalliques, dans des rapports fort différents.

Ainsi, les forces de rappel appliquées aux atomes du milieu cristallin ne se confondent point avec des forces centrales, sauf chez quelques cristaux ioniques, encore est-ce approximativement, et dans un bref intervalle de température. Il convient donc de reprendre la théorie atomique de l'élasticité cristalline en excluant l'hypothèse des forces centrales. C'est l'objet de cette étude. Elle est restreinte aux déformations qui développent des forces de rappel sensiblement proportionnelles aux déplacements. Les déformations purement élastiques, strictement conformes à la loi de Hooke, appartiennent au domaine de l'idéal. La loi de Hooke est une approximation; mais l'écart à cette loi est infime si la déformation est légère.

SYMBOLISME ET HYPOTHÈSES

La position d'un atome, mj, situé dans le motif cristallin m en position j, sera définie par trois translations :

$$\vec{m} + \vec{j} + \vec{u}_j^m$$

La première part du nœud (000), pris pour origine, aboutit au nœud (m_1, m_2, m_3), contenu dans le motif cristallin m qui renferme l'atome. Si $\vec{l}_1, \vec{l}_2, \vec{l}_3$, sont les périodes du milieu cristallin :

$$\vec{m} = m_1\vec{l}_1 + m_2\vec{l}_2 + m_3\vec{l}_3$$

$$m_1,\ m_2,\ m_3 = \ldots; -2; -1; 0; 1; 2; \ldots$$

La seconde translation $\vec{j}$, transporte le nœud (m_1, m_2, m_3) sur la position moyenne de l'atome :

$$\vec{j} = j_1\vec{l}_1 + j_2\vec{l}_2 + j_3\vec{l}_3$$

et :

$$|j_1|, |j_2|, |j_3| \leqslant 1$$

La dernière translation $\vec{u}_j^m$ est une élongation : elle va de la position moyenne à la position instantanée.

De même, un autre atome, pk, se trouve dans le motif cristallin p, en position k, à l'extrémité d'un vecteur.

$$\vec{p} + \vec{k} + \vec{u}_k^p$$

mené de l'origine : $\vec{p}$, comme $\vec{m}$, est une translation du réseau cristallin; et $\vec{k}$, comme $\vec{j}$, indique la position moyenne de l'atome à l'intérieur de la maille.

Le déplacement de l'atome mj par rapport à l'atome pk s'exprime de cette façon :

$$\vec{u}_{j\ k}^{m-p} = \vec{u}_j^m - \vec{u}_k^p$$

La masse du motif cristallin sera représentée par μ, son volume (celui de la maille élémentaire) par v, la masse spécifique du cristal, μ/v, par ρ, la masse d'un atome en position j par μ_j, le nombre des atomes formant le motif cristallin par g; c'est aussi celui des vecteurs j, et celui des vecteurs k; de sorte que dans les sommations, j et k seront aussi pris comme indices courants de 1 à g; et de même, m et p, comme indices affectés à chaque motif cristallin.

Je me référerai souvent au réseau polaire, ou réseau de Fourier, de périodes : $\vec{L}_1$, $\vec{L}_2$, $\vec{L}_3$, telles que :

$$\vec{L}_\alpha \vec{l}_\beta = \delta_{\alpha\beta} \qquad (1)$$

Une translation de ce réseau sera représentée par :

$$\vec{M} = M_1 \vec{L}_1 + M_2 \vec{L}_2 + M_3 \vec{L}_3$$

$$M_1, M_2, M_3 = \ldots; -2; -1; 0; 1; 2; \ldots$$

Enfin, je ferai usage de coordonnées rectangulaires, et représenterai par V_α la projection orthogonale de tout vecteur $\vec{V}$ sur l'axe de coordonnées Ox_α : $\alpha = 1.2.3$.

Le champ de force qui règne à l'intérieur du milieu cristallin est extrêmement complexe. Il a été le sujet d'innombrables travaux. Pourtant il recèle encore de nombreuses inconnues. En conséquence je ne ferai pas intervenir la nature des forces de rappel appliquées aux atomes. Je supposerai seulement ces forces déterminées entièrement par leurs déplacements relatifs :

$$\vec{u}_{j\ k}^{m-p}$$

Je prendrai en compte les atomes 2 à 2, et exprimerai par un tenseur la force de rappel exercée par l'un sur l'autre. C'est exprimer par ses trois composantes, dirigées suivant les trois axes de coordonnées, la force de rappel :

$$\vec{f}_{j\ k}^{m-p}$$

exercée sur l'atome mj par l'atome pk :

$$f^{m-p}_{\substack{j\\ \alpha}\ \substack{k}} = -\sum_{\beta} C^{m-p}_{\substack{j\\ \alpha}\ \substack{k\\ \beta}}\, u^{m-p}_{\substack{j\\ \beta}} \qquad (2)$$

Le tenseur $\left(C^{m-p}_{\substack{j\\ \alpha}\ \substack{k\\ \beta}}\right)$ est déterminé par la nature et la position des deux atomes : soit par les trois composantes $m_\alpha - p_\alpha + j_\alpha - k_\alpha + u^{m-p}_{\substack{j\\ \alpha}\ \substack{k}}$, du vecteur $\overrightarrow{m-p+j-k+u^{m-p}_{j\ k}}$. Mais, admettons la loi de Hooke, je pose le tenseur $\left(C^{m-p}_{\substack{j\\ \alpha}\ \substack{k\\ \beta}}\right)$ constant, et le définis seulement par les trois composantes, constantes, $m_\alpha - p_\alpha + j_\alpha - k_\alpha$, du vecteur $\overrightarrow{m-p+j-k}$. J'utilise de la sorte les coordonnées de Lagrange. Le calcul tensoriel rigoureux exige les coordonnées d'Euler. Mais les déformations considérées sont faibles : les rapports $u^{m-p}_{\substack{j\\ \alpha}\ \substack{k}}/(m_\alpha - p_\alpha + j_\alpha - k_\alpha)$ inférieurs au millième. Dans ces conditions, l'erreur introduite par les coordonnées de Lagrange, l'erreur inhérente à la loi de Hooke, est infime.

La tenseur $\left(C^{m-p}_{\substack{j\\ \alpha}\ \substack{k\\ \beta}}\right)$ est covariant, symétrique, en α et β. En outre :

$$C^{p-m}_{\substack{k\\ \alpha}\ \substack{j\\ \beta}} = C^{m-p}_{\substack{j\\ \alpha}\ \substack{k\\ \beta}} \qquad (3)$$

car :

$$\overrightarrow{f^{p-m}_{k\ j}} = -\overrightarrow{f^{m-p}_{j\ k}} \text{ et } \overrightarrow{u^{p-m}_{k\ j}} = -\overrightarrow{u^{m-p}_{j\ k}}$$

Le problème est posé de la sorte sans restriction : car la force de rappel entre deux atomes pourra toujours être exprimée par un tenseur, quelles que soient sa nature et sa forme.

Le tenseur $\left(C^{m-p}_{\substack{j\\ \alpha}\ \substack{k\\ \beta}}\right)$ bien qu'attaché à l'atome mj, concerne aussi l'atome pk, au total deux atomes. Pour éviter toute restriction dans les sommations ultérieures, je définirai des tenseurs $\left(C^{v}_{\substack{j\ j\\ \alpha\beta}}\right)$, tels que :

$$\sum_{pk}\ C^{m-p}_{\substack{j\\ \alpha}\ \substack{k\\ \beta}} = 0 \qquad (4)$$

c'est-à-dire :

$$C^{v}_{\substack{j\ j\\ \alpha\beta}} = -\sum_{pk}\ C^{m-p}_{\substack{j\\ \alpha}\ \substack{k\\ \beta}},$$

l'atome mj exclu de la sommation.

Ainsi la force de rappel globale, $\overrightarrow{F^m_j}$, appliquée à l'atome mj, se formule simplement :

$$\left.\begin{aligned} F^{m}_{\substack{j\\ \alpha}} &= -\sum_{pk\beta} C^{m-p}_{\substack{j\\ \alpha}\ \substack{k\\ \beta}}\ u^{m-p}_{\substack{j\\ \beta}} \\ &= \sum_{pk\beta} C^{m-p}_{\substack{j\\ \alpha}\ \substack{k\\ \beta}}\ u^{p}_{\substack{k\\ \beta}} \end{aligned}\right\} \qquad (5)$$

Le tenseur $\left(C^{\circ}_{\substack{jj \\ \alpha\beta}}\right)$ exprime la force de rappel $\vec{F}_{0j}^{m}$ exercée sur l'atome *mj*, seul écarté de sa position moyenne :

$$F_{0\,\alpha j}^{m} = \sum_{\beta} C^{\circ}_{\substack{jj \\ \alpha\beta}} u_{\beta j}^{m}$$

Cette force s'oppose au déplacement; de sorte que les coefficients $C^{\circ}_{\substack{jj \\ \alpha\alpha}}$ sont tous négatifs, de l'ordre de 10^{-7} dynes par *u*.X.(10^{-3} Å). Par contre les coefficients $C^{m-p}_{\substack{jk \\ \alpha\beta}}$, afférents à deux atomes, sont en majorité positifs, généralement plus faibles.

SUR LES FORCES DE RAPPEL INTERATOMIQUES

Les neuf coefficients $C^{m-p}_{\substack{jk \\ \alpha\beta}}$ ($\alpha, \beta = 1.2.3$) sont égaux aux dérivées secondes, par rapport à $u^{m-p}_{\alpha jk}$, $u^{m-p}_{\beta jk}$, de l'énergie potentielle mutuelle V^{m-p}_{jk}, prise dans le milieu cristallin par les deux atomes *mj* et *pk* :

$$C^{m-p}_{\substack{jk \\ \alpha\beta}} = \left(\frac{\partial^2 V^{m-p}_{jk}}{\partial u^{m-p}_{\alpha jk}\, \partial u^{m-p}_{\beta jk}} \right) u^{m-p}_{\alpha jk} = u^{m-p}_{\beta jk} = 0$$

Quand la distance :

$$r = \left| \vec{m} - \vec{p} + \vec{j} - \vec{k} \right|$$

augmente, la composante coulombienne du coefficient $C^{m-p}_{\substack{jk \\ \alpha\beta}}$ décroit comme $1/r^3$, la composante de Van der Wals sensiblement comme $1/r^8$, celle de répulsion mutuelle sensiblement comme $e^{-r/\rho}$, où ρ est de l'ordre de l'angström...; donc le coefficient $C^{m-p}_{\substack{jk \\ \alpha\beta}}$ tombe rapidement vers zéro. Au contraire, le déplacement relatif des atomes $\vec{u}^{m-p}_{jk}$ est une fonction de *r* lentement variable : l'oscillation du rapport $\left|\vec{u}^{m-p}_{jk}\right|/r$, reste faible; car le milieu cristallin est, par nature, triplement périodique; il supporte seulement de petits écarts à la triple périodicité; au-delà il se rompt ou se disloque. Ainsi la force de rappel (2) entre deux atomes diminue vite quand leur distance, *r*, augmente. Pour des déformations uniformes, ou proches de l'uniformité, telles les déformations produites par les ondes élastiques, les termes :

$$- C^{m-p}_{\substack{jk \\ \alpha\beta}} u^{m-p}_{\beta jk}$$

classés par distance r croissante, forment une série qui converge rapidement, car outre que les termes décroissent vite, ils changent de signe. La somme $\underset{\alpha}{F_j^m}$ (5) de cette série illimitée, étendue aux atomes d'un cristal sans limites, et la somme $\underset{\alpha}{F_j^m} \pm \varepsilon$, de la même série tronquée, réduite à ses n premiers termes, restreinte aux atomes voisins de l'atome mj, présentent une différence relative $\varepsilon / \underset{\alpha}{F_j^m}$ négligeable, inférieure au millième, dès que n dépasse quelques milliers, donc quand r excède un rayon R d'action sensible, égal à quelques dizaines d'angströms, tout au plus à quelques centaines. La force de rappel $\vec{F}_j^m$ (5), appliquée à l'atome mj est exercée presque intégralement, par ses voisins immédiats, contenus dans une sphère de rayon R, dont il occupe le centre.

Au cours des déformations, sensiblement conformes à la loi de Hooke, les atomes peuvent être portés, hors de leurs positions moyennes, à des distances $\vec{u}_j^m$, $\vec{u}_k^p$, très grandes par rapport aux périodes du milieu cristallin; mais leurs déplacements relatifs $\vec{u}_j^{m-p}{}_k$, restent toujours minimes auprès des distances qui les séparent. De sorte que la formule (5) exprime toujours correctement les forces de rappel développées par de telles déformations, si grands que soient les déplacements absolus $\vec{u}_j^m$, $\vec{u}_k^p$ imposés aux atomes.

LES ONDES ÉLASTIQUES ET LA MATRICE DE FOURIER

PROPRIÉTÉS DES ONDES ÉLASTIQUES

J'étudierai en premier lieu les déformations produites par les ondes élastiques. C'est décrire les oscillations accomplies par les atomes. Les unes, inhérentes au milieu cristallin, forment l'agitation thermique; les autres, provoquées par des impulsions extérieures, font l'objet de l'élasticité classique. Toutes ont lieu dans le même champ de force, obéissent aux mêmes lois.

Le milieu cristallin est continu; ses atomes — je crois l'avoir montré — ne peuvent se déplacer indépendamment. Leurs oscillations se transmettent de l'un à l'autre, constituent des trains d'ondes élastiques. Je considèrerai uniquement des ondes planes, soit un milieu cristallin illimité.

L'oscillation globale d'agitation thermique, accomplie par un atome, est presque périodique : décomposable en oscillations harmoniques $\vec{a}^m_j$, transportées par des ondes planes :

$$a^m_{j\,\alpha} = \frac{\zeta^j_\alpha}{\sqrt{\mu_j}}\, e^{i2\pi\,[\nu t - \vec{S}\,(\vec{m}+\vec{j})]} \tag{6}$$

Le vecteur d'onde $\vec{S}$ est constant, le « vecteur propre » $\vec{\zeta}^j$ de l'oscillation généralement complexe :

$$\zeta^j_\alpha = u^j_\alpha\, e^{i\varphi^j_\alpha} \tag{7}$$

Les oscillations $\vec{a}^m_j$: $j = 1, 2, \ldots g$, se propagent toutes à la même vitesse, mais présentent entre elles des différences de phases égales à :

$$-2\pi\vec{S}\left(\vec{j}-\vec{k}\right) + \varphi^j_\alpha - \varphi^k_\alpha$$

et non à :

$$-2\pi\vec{S}\left(\vec{j}-\vec{k}\right)$$

Le propagation est uniforme au travers du réseau cristallin, d'un nœud à l'autre; en général, elle ne le reste plus au travers d'un motif cristallin, d'un atome à l'autre. Les différences de phases :

$$\varphi^j_\alpha - \varphi^k_\alpha$$

tiennent compte de ce fait.

Souvent, on fait seulement état de la propagation uniforme. C'est poser :

$$\xi^j_\alpha = \zeta^j_\alpha\, e^{-i2\pi\vec{S}\vec{j}} \tag{8}$$

et exprimer les élongations :

$$a^m_{j\,\alpha} = \frac{\xi^j_\alpha}{\sqrt{\mu_j}}\, e^{i2\pi(\nu t - \vec{S}\vec{m})} \tag{9}$$

Le corps de chaque atome, l'ensemble constitué par le noyau et les électrons fortement liés, oscille sans déformation sensible, tel un bloc rigide. L'oscillation ne se propage donc point à travers ce corps, seulement d'un corps à l'autre. C'est pourquoi nous pouvons la représenter par celle d'un seul point, le centre de gravité. Les atomes en position j forment un réseau, les atomes en position k en forment un autre... Ces réseaux, en même nombre, g, que les atomes du motif

cristallin, sont tous égaux et orientés de même. Ce sont les oscillations accomplies par leurs nœuds que nous prenons en compte. Cette discontinuité de la propagation, dans un milieu triplement périodique, confère aux ondes élastiques une propriété remarquable. Reportons nous à la seconde expression des oscillations (9); ajoutons au vecteur d'onde $\vec{S}$ une translation $\vec{M}$, du réseau polaire. Compte tenu de (1) :

$$\vec{M}\ \vec{m} = \ldots; -2; -1; 0; 1; 2; \ldots$$

donc :
$$e^{-i2\pi(\vec{S}+\vec{M})\vec{m}} = e^{-i2\pi\vec{S}\vec{m}} \qquad (10)$$

Nous retombons sur la même oscillation. Les translations du réseau polaire sont en nombre infini. La même oscillation harmonique forme une multitude de trains d'ondes planes qui se propagent suivant des directions $\vec{S} + \vec{M}$ différentes, avec des vitesses et des longueurs d'ondes différentes.

LA MATRICE DE FOURIER (*)

Appliquons le principe de d'Alembert aux oscillations harmoniques (6), pilotées par le même vecteur d'onde $\vec{S}$. Compte tenu de (5), où nous prenons :

$$u_{j\,\alpha}^{m} = a_{j\,\alpha}^{m}$$

nous trouvons que les composantes ζ_{α}^{j} des vecteurs propres $\vec{\zeta}_j$, sont les racines de $3g$ équations linéaires et homogènes :

$$\left.\begin{aligned} &\omega^2\,\zeta_{\alpha}^{j} + \sum_{k\beta}\gamma_{\alpha\beta}^{j\,k}\,\zeta_{\beta}^{k} = 0 \\ &j,k = 1,2\ldots g; \quad \alpha,\beta = 1,2,3 \end{aligned}\right\} \qquad (11)$$

$\omega = 2\pi\nu$ est la pulsation des oscillations, $(\gamma_{\alpha\beta}^{j\,k})$ un tenseur covariant et symétrique en α et β :

$$\gamma_{\alpha\beta}^{j\,k} = e^{i2\pi\vec{S}(\vec{j}-\vec{k})} \sum_{b} \frac{C_{j\,k}^{b}{}_{\alpha\beta}}{\sqrt{\mu_j \mu_k}}\ e^{i2\pi\vec{S}\vec{b}} \qquad (12)$$

et
$$\vec{b} = \vec{m} - \vec{p}$$

(*) Max Born, *Atomtheorie des Festen Zustandes*, Teubner, Berlin 1923, p. 574. Ivar Waller, *Zeits. f. Phys.*, **17-6**, p. 398 (1923); *Ann. der Phys.*, **83-10**, p. 153 (1927).

Nous conserverons toujours le même système de référence, les coefficients $\gamma_{\alpha\beta}^{jk}$ restent donc constants, et peuvent être envisagés comme les éléments d'une matrice γ, d'ordre $3g \times 3g$, qui est hermitienne (3), et que j'appellerai matrice de Fourier. Dans les mêmes conditions, les $3g$ composantes ζ_α^j des vecteurs propres, forment une matrice à une colonne (d'ordre $3g \times 1$). De la sorte les $3g$ équations linéaires (11) se formulent simplement :

$$\omega^2 \zeta + \gamma \zeta = 0$$

Elles admettent seulement des racines ζ_α^j différentes de zéro si :

$$|\gamma + \omega^2 \mathrm{I}| = 0$$

(I = matrice unité) (13)

C'est là une équation, en ω^2, de degré $3g$.

Si le milieu cristallin est stable, toutes ses racines

$$\omega_n^2 \; ; \; n = 1, 2 \ldots 3g \tag{14}$$

sont réelles et positives. A chacune correspond une fréquence :

$$\nu_n = \frac{\omega_n}{2\pi} \tag{14 \textit{bis}}$$

et, par (11), un système de g vecteurs propres $\vec{\zeta}^j$, donc une oscillation harmonique des atomes (6). Ainsi, le même vecteur d'onde $\vec{S}$, pilote $3g$ oscillations harmoniques.

La matrice γ (12) se rapporte à l'expression (6) des oscillations, celle qui fait état de la propagation fine, au travers du motif cristallin. Si l'on considère seulement la propagation uniforme au travers du réseau cristallin, c'est-à-dire si l'on adopte la seconde expression (9) des oscillations, on obtient une variante γ' de la matrice de Fourier, plus simple :

$$\gamma'^{jk}_{\alpha\beta} = \sum_b \frac{C^{bjk}_{\alpha\beta}}{\sqrt{\mu_j \mu_k}} e^{i 2\pi \vec{S} \vec{b}} \tag{15}$$

A vecteur d'onde $\vec{S}$ égal, la matrice γ' prend les mêmes valeurs propres ω_n^2 (14) que la matrice γ. Et les racines ξ_α^j des 3 g équations linéaires, homogènes :

$$\omega^2 \xi + \gamma' \xi = 0$$

sont liés aux racines ζ_α^j des équations (11), par la relation (8).

Que l'on prenne en compte la matrice γ ou la matrice γ', on aboutit au même résultat.

La seconde, γ' (15), est, d'après (10), une fonction triplement périodique du vecteur d'onde S; elle a les mêmes périodes que le réseau polaire. En conséquence, la fréquence des oscillations harmoniques et leurs vecteurs propres sont aussi des fonctions triplement périodiques du vecteur d'onde, et leurs périodes sont aussi celles du réseau polaire. Si l'on remplace le vecteur $\vec{S}$ par son égal et opposé $-\vec{S}$, la fréquence ν (14*bis*) des oscillations, et les rapports u_α^j/u_α^k (7), reprennent la même valeur. Ce sont des fonctions paires du vecteur d'onde. Par contre, les différences de phase $\varphi_\alpha^j - \varphi_\alpha^k$ (7) sont des fonctions impaires de la même variable. A chaque oscillation pilotée par le vecteur d'onde $\vec{S}$, correspond donc une oscillation de même fréquence, pilotée par le vecteur d'onde $-\vec{S}$. Si ces deux oscillations sont rectilignes, leurs élongations sont parallèles; si elles sont elliptiques, elles ont lieu suivant deux ellipses semblables dans des plans parallèles; mais l'une des ellipses est parcourure dans le sens direct, l'autre est parcourue dans le sens opposé.

Une oscillation harmonique est de la sorte, par sa fréquence et son vecteur propre, une fonction du vecteur d'onde à déterminations multiples : $\vec{S} + \vec{M}$. Désormais, nous ne retiendrons que les plus petites déterminations. Ce sont les vecteurs d'onde inscriptibles dans une première zone de Léon Brillouin, leur origine au centre. Et nous adopterons comme variables, au lieu du vecteur d'onde $\vec{S}$, le nombre d'onde σ sur la longueur 2π, et le vecteur unitaire $\vec{q}$ normal au plan d'onde :

$$\sigma\vec{q} = 2\pi\vec{S}$$

CLASSIFICATION DES OSCILLATIONS

Le vecteur $\vec{q}$ conservant la même direction, nous nous proposons de rechercher comment le carré de la pulsation ω^2, varie avec σ. Ce carré, fonction paire du vecteur d'onde, peut être développé en série suivant les puissances paires de σ :

$$\omega^2 = \Omega_0 + \Omega_2\sigma^2 + \Omega_4\sigma^4 + \ldots \qquad (16)$$

Le problème se ramène à la détermination des coefficients $\Omega_0, \Omega_2, \ldots$ Il requiert le développement en série de la matrice de Fourier suivant les puissances entières et positives de σ :

$$\gamma = \gamma_0 + \gamma_1 \sigma + \gamma_2 \sigma^2 + \ldots \tag{17}$$

Les matrices γ_0, γ_2, ... sont réelles et symétriques, les matrices γ_1, γ_3, ... imaginaires pures et antisymétriques, et la matrice γ_0 est seulement de rang $3(g-1)$ car, compte tenu de (4),

$$\sum_j \sqrt{\mu_j}\, \gamma_{0\alpha\beta}^{jk} = \sum_k \sqrt{\mu_k}\, \gamma_{0\alpha\beta}^{jk} = 0 \tag{18}$$

Explicitons l'équation caractéristique (13) :

$$\left|\gamma + \omega^2 \mathrm{I}\right| = \omega^{2r} + \tau_1\, \omega^{2(r-1)} + \ldots + \tau_{r-1}\, \omega^2 + \tau_r = 0 \tag{19}$$
$$r = 3g$$

τ_n est la somme des mineurs principaux d'ordre n pris dans le déterminant $|\gamma|$

$$n = 1, 2 \ldots, 3g$$

Puisque la matrice de Fourier est hermitienne, tout coefficient τ_n est une fonction paire de σ :

$$\tau_n = \tau_{0n} + \tau_{2n}\, \sigma^2 + \tau_{4n}\, \sigma^4 + \ldots \tag{20}$$

Et, compte tenu de (18) :

$$\tau_{0r} = \tau_{0r-1} = \tau_{0r-2} = 0 \tag{21}$$

$$\left.\begin{aligned} \tau_{2r} = \tau_{2r-1} = 0 \\ \tau_{4r} = 0 \end{aligned}\right\} \tag{22}$$

Portons les expressions (16) de ω^2, et (20) de τ_n, dans l'équation caractéristique (19). Elle devient :

$$c_0 + c_2 \sigma^2 + c_4 \sigma^4 + \ldots = 0 \tag{23}$$

La variable σ prend des valeurs qui forment une suite continue; donc :

$$c_0 = c_2 = c_4 = \ldots = 0$$

Compte tenu de (17) et de (21) :

$$c_0 = \left|\gamma_0 + \Omega_0 \mathrm{I}\right| = (\Omega_0^{r-3} + \tau_{01}\, \Omega_0^{r-4} + \ldots \tau_{0r-3})\, \Omega_0^3 = 0$$

Trois racines, Ω_0, de cette équation sont nulles, les $3(g-1)$ autres déterminent des fréquences toujours élevées :

$$\nu_0 = \sqrt{\Omega_0}/2\pi$$

de 10^{12} à 10^{13} par seconde.

Le même vecteur d'onde, pilote $3g$ oscillations harmoniques. Quand σ tend vers zéro, 3 d'entre elles ont une fréquence qui s'annule. Ce sont les « oscillations acoustiques ». Dans la série (16), qui exprime le carré de leur pulsation, le terme constant Ω_0 disparaît :

$$\omega^2 = \Omega_2 \sigma^2 + \Omega_4 \sigma^4 + \ldots \qquad (24)$$

Les $3(g-1)$ oscillations restantes conservent, au contraire, une haute fréquence quand σ tombe à zéro.

Prenons en compte, dans l'équation caractéristique (19), le carré de la pulsation, ω^2 (24), des oscillations acoustiques. D'après les égalités (21-22), Ω_0 nul, les coefficients c_0, c_2, c_4 disparaissent de l'équation (23). Il reste :

$$c_6 \sigma^6 + c_8 \sigma^8 + c_{10} \sigma^{10} + \ldots = 0 \qquad (25)$$

et

$$c_6 = \tau_{0\,r-3}\, \Omega_2^3 + \tau_{2\,r-2}\, \Omega_2^2 + \tau_{4\,r-1}\, \Omega_2 + \tau_{6^r} = 0$$

ou, puisque $\tau_{0\,r-3}$ est toujours différent de zéro,

$$\Omega_2^3 + \frac{\tau_{2^{r-2}}}{\tau_{0^{r-3}}} \Omega_2^2 + \frac{\tau_{4^{r-1}}}{\tau_{0^{r-2}}} \Omega_2 + \frac{\tau_{6^r}}{\tau_{0^{r-3}}} = 0 \qquad (26)$$

C'est une équation du troisième degré en Ω_2, qui admet, si le milieu cristallin est stable, trois racines réelles et positives :

$$\Omega_2^1,\ \Omega_2^2,\ \Omega_2^3$$

Remplaçons, dans l'expression de c_8 (25), Ω_2 par l'une d'elles, Ω_2^1 par exemple. L'égalité,

$$c_8 = 0,$$

devient une équation du premier degré en Ω_4 ; la résolvant nous obtenons le coefficient Ω_4^1 correspondant à Ω_2^1. Puis, remplaçons, dans l'expression de c_{10} (25), Ω_2 et Ω_4 par Ω_2^1 et Ω_4^1. L'égalité,

$$c_{10} = 0,$$

devient, de même, une équation du premier degré en Ω_6, d'où nous déduisons le coefficient Ω_6^1 ; et ainsi de suite.

La courbe de dispersion, celle qui représente la fonction $\nu = f(\sigma)$, comporte de la sorte, 3 « branches acoustiques », une par racine Ω_2 de l'équation (26). Donc le même vecteur d'onde pilote toujours trois oscillations acoustiques qui, d'après la formule (24), se propagent avec une vitesse :

$$V = \frac{\omega}{\sigma} = \Omega_2^{\frac{1}{2}} \left(1 + \frac{\Omega_4}{\Omega_2} \sigma^2 + \ldots\right)^{\frac{1}{2}} \qquad (27)$$

LES OSCILLATIONS ACOUSTIQUES DE BASSE FRÉQUENCE

L'APPROXIMATION DE L'ÉLASTICITÉ CLASSIQUE

En élasticité classique on considère seulement les oscillations acoustiques de basse fréquence. Et l'on trouve, que dans le milieu cristallin, peuvent se propager, suivant toute direction, trois de ces oscillations, rectilignes, orthogonales. Soient : $\vec{u}$ le vecteur propre de l'une d'elles ($\vec{u}$ est la direction de l'élongation) et V sa vitesse de propagation, les trois composantes u_α, du vecteur $\vec{u}$ sont les racines de trois équations linéaires et homogènes :

$$\begin{gathered} V^2 u_\alpha + \sum_\beta A_{\alpha\beta} u_\beta = 0 \\ \alpha, \beta = 1, 2, 3 \end{gathered} \tag{28}$$

ou

$$V^2 u + A u = 0$$

u est la matrice à une colonne, formée par les trois composantes u_α, A la matrice, d'ordre 3×3, formée par les coefficients $A_{\alpha\beta}$.

Cette matrice A est déterminée par la direction $\vec{q}$ du vecteur d'onde et par les coefficients d'élasticité statiques ou coefficients de Voigt :

$$\begin{gathered} A_{\alpha\beta} = -\frac{1}{\rho} \sum_{\gamma\delta} c_{\alpha\gamma,\,\beta\delta}\, q_\gamma\, q_\delta \\ \gamma, \delta = 1, 2, 3 \end{gathered} \tag{29}$$

La matrice de Fourier γ (12) est fonction du nombre d'onde σ; la matrice A n'en dépend plus. Pour la même direction de propagation $\vec{q}$, elle détermine, par son équation caractéristique :

$$| A + V^2 I | = 0 \tag{30}$$

des vitesses V constantes.

Tenir la vitesse de propagation constante, c'est d'après la formule (27), restreindre la série (24) à son premier terme, c'est poser :

$$\omega = \Omega_2^{\frac{1}{2}}\, \sigma \text{ et } V = \Omega_2^{\frac{1}{2}} \tag{31}$$

L'erreur est infime, car tant que la fréquence reste basse le vecteur d'onde reste extrêmement petit par rapport aux périodes du réseau polaire. A cette approximation, l'équation (26) détermine, comme

l'équation caractéristique (30), la vitesse des ondes élastiques. Or cette équation (26) provient de la matrice de Fourier par l'intermédiaire d'une matrice B, d'ordre 3 × 3, dont elle est précisément l'équation caractéristique. Je vais d'abord démontrer que cette matrice B est entièrement déterminée par la matrice de Fourier, ensuite qu'elle définit la direction des oscillations acoustiques de basse fréquence. Comme elle définit déjà leur vitesse de propagation par son équation caractéristique (26), la preuve sera faite qu'elle se rapporte exactement aux oscillations considérées par l'élasticité classique. Enfin, je la comparerai à la matrice classique A (28).

LA MATRICE ATOMIQUE DES OSCILLATIONS DE BASSE FRÉQUENCE ET LES COEFFICIENTS D'ÉLASTICITÉ QUI RÉGISSENT CES OSCILLATIONS

On tire la matrice B de la matrice de Fourier par des calculs sans difficulté, mais longs. J'en donnerai seulement l'essentiel. Il convient de prendre en compte, non la matrice γ même (12), mais une variante Γ :

$$\left.\begin{aligned} \Gamma_{\alpha\beta}^{jk} &= e^{i\sigma\vec{q}(\vec{j}-\vec{k})} \sum_{b} C_{\substack{jk \\ \alpha\beta}}^{b} e^{i\sigma\vec{q}\vec{b}} \\ &= \Gamma_{0\,\alpha\beta}^{jk} + \Gamma_{1\,\alpha\beta}^{jk}\,\sigma + \Gamma_{2\,\alpha\beta}^{jk}\,\sigma^2 + \dots \end{aligned}\right\} \qquad (32)$$

Les mineurs principaux du déterminant $|\Gamma|$ s'obtiennent par des calculs simples; ceux du déterminant $|\gamma|$ s'en déduisent aussitôt. Au moyen des opérations classiques, addition de lignes et de colonnes, multipliées par des facteurs constants, on transforme le déterminant $|\Gamma|$, en un autre, de même valeur, bordé : à droite, par trois colonnes où les éléments ne contiennent plus de termes constants, ni du premier degré en σ; en bas, par trois lignes où les éléments ne renferment plus de termes constants. L'opération achevée, les coefficients de σ^2 qui figurent dans les éléments inscrits à l'intersection des trois dernières lignes et des trois dernières colonnes sont, au facteur $1/\mu$ près, les éléments de la matrice B :

$$\mu\, B_{\alpha\beta} = i \sum_{jk\varepsilon} \Gamma_{1\,\alpha\varepsilon}^{jk}\, y_{\varepsilon,\beta}^{k} + \sum_{jk} \Gamma_{2\,\alpha\beta}^{jk} \qquad (33)$$

Les nombres réels $y_{\varepsilon,\beta}^{k}$ sont les racines de $3g$ équations linéaires :

$$\sum_{k\varepsilon} \Gamma_{0\,\alpha\varepsilon}^{jk}\, y_{\varepsilon,\beta}^{k} = i \sum_{k} \Gamma_{1\,\alpha\beta}^{jk} \qquad (34)$$

$j, k = 1,2, \dots g$; $\alpha, \varepsilon = 1,2,3$; β constant.

Compte tenu de la condition (4) :

$$\sum_j \Gamma_0 \, {}^{j\,k}_{\alpha\beta} = \sum_k \Gamma_0 \, {}^{j\,k}_{\alpha\beta} = 0 \qquad (35)$$

Mais la matrice Γ_1 est antisymétrique :

$$\sum_{j\,k} \Gamma_1 \, {}^{j\,k}_{\alpha\beta} = 0 \qquad (36)$$

Donc les équations (34) sont compatibles; toutefois, d'après les relations (35), la matrice Γ_0 est seulement de rang $3(g-1)$: trois racines :

$$y_{\varepsilon,\,\beta}^{\,k}; \; \varepsilon = 1,\ 2,\ 3,$$

peuvent être choisies arbitrairement. Les différences :

$$\delta \, {}^{k-n}_{\varepsilon,\,\beta} = y^{k}_{\varepsilon,\,\beta} - y^{n}_{\varepsilon,\,\beta} \quad (k,\, n = 1,\, 2,\, \ldots\, g \quad ;\; \varepsilon = 1,\, 2,\, 3) \qquad (37)$$

sont seules déterminées. De la seconde condition (35) nous tirons :

$$\sum_k \Gamma_0 \, {}^{j\,k}_{\alpha\beta} = - \, \Gamma_0 \, {}^{j\,n}_{\alpha\beta}$$

$$k = 1,\ \ldots,\ n-1,\ n+1,\ \ldots,\ g$$

d'où :

$$\sum_{k\,\varepsilon} \Gamma_0 \, {}^{j\,k}_{\alpha\varepsilon} \, y^{\,k}_{\varepsilon,\,\beta} = \sum_{k\,\varepsilon} \Gamma_0 \, {}^{j\,k}_{\alpha\varepsilon} \, \delta \, {}^{k-n}_{\varepsilon,\,\beta}$$

Les $3(g-1)$ différences $\delta^{k-n}_{\varepsilon,\,\beta}$, prises par rapport à $y^{n}_{\varepsilon,\,\beta}$, n constant, sont de la sorte les racines des $3(g-1)$ équations linéaires,

$$\sum_{k\,\varepsilon} \Gamma_0 \, {}^{j\,k}_{\alpha\varepsilon} \, \delta \, {}^{k-n}_{\varepsilon,\,\beta} = i \sum_k \Gamma_1 \, {}^{j\,k}_{\alpha\beta}$$

$$j = 1,\ \ldots,\ n-1,\ n+1,\ \ldots\ g$$

$$\alpha = 1,2,3;\ \beta \text{ constant}$$

où les coefficients des inconnues forment une matrice Γ_0^n seulement d'ordre $3(g-1)$. $3(g-1)$. C'est la matrice obtenue en supprimant dans la matrice Γ_0 les trois lignes et les trois colonnes $n\varepsilon$ ($\varepsilon = 1,2,3$). Quel que soit n, elle admet une matrice réciproque $\underset{n}{G}$.

Posons :

$$\mathscr{L}^{\,j}_{\alpha\beta,\,\delta} = \frac{1}{v} \sum_{bk} C^{\,b}_{j\,k\;\alpha\beta} \, (b_\delta + j_\delta - k_\delta) \qquad (38)$$

$$\delta = 1,2,3$$

Nous avons :

$$i \sum_{k} \Gamma_{1\zeta\beta}^{jk} = - v \sum_{\delta} \mathscr{L}^{j}_{\zeta\beta,\,\delta}\, q_{\delta};$$

$$\zeta = 1,2,3;$$

et :

$$\delta^{k-n}_{\varepsilon,\,\beta} = - v \sum_{\delta} \left(\sum_{j\zeta} \underset{n}{G}{}^{kj}_{\varepsilon\zeta}\, \mathscr{L}^{j}_{\zeta\beta,\,\delta} \right) q_{\delta} \qquad (39)$$

$$j = 1, \ldots n{-}1, n{+}1 \ldots g.$$

Compte tenu de (37) et (36) :

$$\sum_{jk\varepsilon} \Gamma_{1\alpha\varepsilon}^{jk}\, y^{k}_{\varepsilon,\,\beta} = \sum_{jk\varepsilon} \Gamma_{1\alpha\varepsilon}^{jk} \left(\delta^{k-n}_{\varepsilon,\,\beta} + y^{n}_{\varepsilon,\,\beta}\right)$$

$$= \sum_{jk\varepsilon} \Gamma_{1\alpha\varepsilon}^{jk}\, \delta^{k-n}_{\varepsilon,\,\beta} \qquad (40)$$

Cette somme est formée par les différences $\delta^{k-n}_{\varepsilon,\,\beta}$ rapportées à $y^{n}_{\varepsilon,\,\beta}$. Prenons en compte un autre système de différences $\delta^{k-n'}_{\varepsilon,\,\beta}$, n' différant de n. Nous avons encore, d'après (36) :

$$\sum_{jk\varepsilon} \Gamma_{1\alpha\varepsilon}^{jk}\, y^{k}_{\varepsilon,\,\beta} = \sum_{jk\varepsilon} \Gamma_{1\alpha\varepsilon}^{jk}\, \delta^{k-n'}_{\varepsilon,\,\beta}$$

$$= \sum_{jk\varepsilon} \Gamma_{1\alpha\varepsilon}^{jk} \left(\delta^{k-n}_{\varepsilon,\,\beta} + \delta^{n-n'}_{\varepsilon,\,\beta}\right)$$

$$= \sum_{jk\varepsilon} \Gamma_{1\alpha\varepsilon}^{jk}\, \delta^{k-n}_{\varepsilon,\,\beta}$$

La somme est constante : indépendante du système de différences adopté, donc de la matrice Γ_0^n utilisée.

D'autre part, puisque la matrice Γ_1 est antisymétrique,

$$i \sum_{j} \Gamma_{1\alpha\varepsilon}^{jk} = - i \sum_{j} \Gamma_{1\alpha\varepsilon}^{kj} = v \sum_{\gamma} \mathscr{L}^{k}_{\alpha\varepsilon,\,\gamma}\, q_{\gamma}\,; \quad \gamma = 1,\, 2,\, 3.$$

D'où, compte tenu de (40) et de (39),

$$i \sum_{jk\varepsilon} \Gamma_{1\alpha\varepsilon}^{jk}\, y^{k}_{\varepsilon,\,\beta} = - v \sum_{\gamma\delta} \left[v \sum_{jk\varepsilon\zeta} \mathscr{L}^{k}_{\alpha\varepsilon,\,\gamma}\, \underset{n}{G}{}^{kj}_{\varepsilon\zeta}\, \mathscr{L}^{j}_{\zeta\beta,\,\delta} \right] q_{\gamma}\, q_{\delta}$$

$$= - v \sum_{\gamma\delta} \mathfrak{M}_{1\alpha\gamma,\,\beta\delta}\, q_{\gamma}\, q_{\delta}; \qquad (41)$$

et :

$$\mathfrak{M}_{1\alpha\gamma,\,\beta\delta} = v \sum_{jk\varepsilon\zeta} \mathscr{L}^{k}_{\alpha\varepsilon,\,\gamma}\, \underset{n}{G}{}^{kj}_{\varepsilon\zeta}\, \mathscr{L}^{j}_{\zeta\beta,\,\delta} \qquad (42)$$

L'indice n est exclu de la sommation sur j et k. Nous rappelons cette restriction par la lettre n inscrite au dessous du symbole $G^{kj}_{\varepsilon\zeta}$.

$(\mathscr{L}^{j}_{\alpha\beta,\delta})$ (38) est une densité tensorielle covariante et symétrique en α et β, contrevariante en δ. La sommation sur les indices ε et ζ, dans la formule (42) produit une contraction tensorielle qui porte sur un indice covariant de chaque coefficient $\mathscr{L}$. En conséquence :

$$(\mathfrak{M}_{1\alpha\gamma,\,\beta\delta})$$

est une densité tensorielle covariante en α et β, contrevariante en γ et δ. La matrice Γ_0 (32) est symétrique, toute matrice Γ^{n}_{0} l'est aussi, et, de même, toute matrice $\underset{n}{G}$. La densité tensorielle $(\mathfrak{M}_{1\,\alpha\gamma,\,\beta\delta})$ est de la sorte symétrique en $\alpha\gamma$ et $\beta\delta$.

Posons :

$$\mathfrak{M}_{2\alpha\gamma,\,\beta\delta} = \frac{1}{2v} \sum_{b\,j\,k} C^{b}_{\substack{j\,k \\ \alpha\beta}} (b_\gamma + j_\gamma - k_\gamma)(b_\delta + j_\delta - k_\delta) \qquad (43)$$

Nous avons :

$$\sum_{j\,k} \Gamma_{2\substack{j\,k \\ \alpha\beta}} = -v \sum_{\gamma\delta} \mathfrak{M}_{2\alpha\gamma,\,\beta\delta}\, q_\gamma\, q_\delta \qquad (44)$$

$(\mathfrak{M}_{2\,\alpha\gamma,\,\beta\delta})$ est aussi une densité tensorielle covariante en α et β, contrevariante en γ et δ, mais elle est symétrique en α et β, et en γ et δ. Pour un cristal triclinique, ses composantes, au nombre de 81, prennent 36 valeurs distinctes.

Posons enfin :

$$\mathfrak{N}_{\alpha\gamma,\,\beta\delta} = \mathfrak{M}_{1\alpha\gamma,\,\beta\delta} + \mathfrak{M}_{2\alpha\gamma,\,\beta\delta} \qquad (45)$$

Compte tenu de (33), (41), (44) et (45) :

$$B_{\alpha\beta} = -\frac{1}{\rho} \sum_{\gamma\delta} \mathfrak{N}_{\alpha\gamma,\,\beta\delta}\; q_\gamma\; q_\delta \qquad (46)$$

$(\mathfrak{N}_{\alpha\gamma,\,\beta\delta})$ est aussi une densité tensorielle covariante en α et β, contrevariante en γ et δ. Sa symétrie est celle de son terme le moins symétrique $\mathfrak{M}_1$ (42); seuls peuvent être permutés les deux couples d'indices $\alpha\ \gamma$ et $\beta\ \delta$ (forces centrales exclues). Ainsi, les 81 coefficients $\mathfrak{N}\alpha\gamma,\,\beta\delta$ prennent en général, c'est-à-dire si le cristal est triclinique, 45 valeurs différentes. Pour le voir aisément, il convient de remplacer les deux couples d'indices $\alpha\gamma$ et $\beta\delta$ par deux indices seulement ε et ζ :

$$\begin{aligned} \alpha\gamma,\,\beta\delta &= 11,\ 22,\ 33,\ 23,\ 31,\ 12,\ 32,\ 13,\ 21 \\ \varepsilon,\,\zeta &= \ 1,\ \ 2,\ \ 3,\ \ 4,\ \ 5,\ \ 6,\ \ 7,\ \ 8,\ \ 9 \end{aligned}$$

$(\mathfrak{N}_{\varepsilon\zeta})$ est une densité tensorielle symétrique dans un espace à neuf dimensions. Elle compte bien 45 composantes distinctes.

Mais les coefficients $\mathfrak{N}_{\alpha\gamma,\,\beta\delta}$ sont assujettis à la symétrie cristalline par les règles du calcul tensoriel. Cette symétrie réduit leur nombre, comme celui de leurs valeurs distinctes. Si le cristal est cubique, le nombre des coefficients tombe à 21, celui de leurs valeurs à 4, à 3 même si la position moyenne de chaque atome coïncide avec un centre de symétrie du milieu cristallin.

Enfin, puisque : $\mathfrak{N}_{\beta\delta,\,\alpha\gamma} = \mathfrak{N}_{\alpha\gamma,\,\beta\delta}$

la matrice B (46) est symétrique.

Les expressions (38), (42), (43) des coefficients $\mathfrak{N}$ (45) renferment les coordonnées j_α, k_α ... des atomes à l'intérieur de la maille, car elles proviennent de la matrice de Fourier γ (12), celle qui fait état de la propagation des oscillations à l'intérieur du motif cristallin. Déduits de la matrice de Fourier γ' (15) les coefficients (45) revêtent une forme plus simple. Pour définir cette forme, il convient de prendre en compte au lieu de la matrice γ' une de ses variantes Γ' :

$$\begin{aligned}\Gamma' &= \sum_b C^{\,b}_{\substack{\gamma k\\ \alpha\beta}}\, e^{i\sigma\overrightarrow{q}\overrightarrow{b}} \\ &= \Gamma'^{\,j\,k}_{0\alpha\beta} + \Gamma'^{\,j\,k}_{1\alpha\beta}\,\sigma + \Gamma'^{\,i\,k}_{2\alpha\beta}\,\sigma^2 + \dots\end{aligned} \tag{47}$$

On trouve :

$$\mu\, B_{\alpha\beta} = i \sum_{j\,k\,\varepsilon} \Gamma'^{\,j\,k}_{1\alpha\varepsilon}\; y'^{\,k}_{\varepsilon,\,\beta} + \sum_{j\,k} \Gamma'^{\,j\,k}_{2\alpha\beta} \tag{48}$$

Les nombres $y'^{\,k}_{\varepsilon,\,\beta}$ sont les racines des $3g$ équations linéaires :

$$\sum_{k\,\varepsilon} \Gamma'^{\,j\,k}_{0\alpha\varepsilon}\; y'^{\,k}_{\varepsilon,\,\beta} = i \sum_{k} \Gamma'^{\,j\,k}_{1\alpha\beta}, \tag{49}$$

$j, k = 1,2 \dots g$; $\alpha,\varepsilon = 1,2,3$; β constant.

On obtient les coefficients :

$$\mathscr{L}'^{\,j}_{\alpha\beta,\,\delta} = \frac{1}{v} \sum_{b\,k} C^{\,b}_{\substack{j\,k\\ \alpha\beta}}\, b_\delta \qquad (\delta = 1, 2, 3);$$

$$\mathfrak{M}'_{1\alpha\gamma,\,\beta\delta} = v \sum_{j\,k\,\varepsilon\zeta} \mathscr{L}'^{\,k}_{\alpha\varepsilon,\,\gamma}\, G^{k\,l}_{n\,\varepsilon\zeta}\, \mathscr{L}'^{\,j}_{\zeta\beta,\,\delta} \qquad (\zeta = 1, 2, 3);$$

puis,

$$\mathfrak{M}'_{2\alpha\gamma,\,\beta\delta} = \frac{1}{2v} \sum_{b\,j\,k} C^{\,b}_{\substack{j\,k\\ \alpha\beta}}\, b_\gamma\, b_\delta \qquad (\gamma = 1, 2, 3)$$

enfin,

$$B_{\alpha\beta} = -\frac{1}{\rho} \sum_{\gamma\delta} (\mathfrak{M}'_{1\alpha\gamma,\,\beta\delta} + \mathfrak{M}'_{2\alpha\gamma,\,\beta\delta})\, q_\gamma\, q_\delta$$

donc :

$$\mathfrak{N}_{\alpha\gamma,\,\beta\delta} = \mathfrak{M}'_{1\alpha\gamma,\,\beta\delta} + \mathfrak{M}'_{2\alpha\gamma,\,\beta\delta}$$

La vérification de ce résultat est immédiate :

Posons :

$$\mathscr{L}''^{\,j}_{\alpha\beta,\,\delta} = \frac{1}{v} \sum_{bk} C^{b}_{\substack{jk \\ \alpha\beta}} (j_\delta - k_\delta) = -\frac{1}{v} \sum_{k} \Gamma_{0\,\alpha\beta}^{jk}\, k_\delta$$

de sorte que :

$$\mathscr{L}^{j}_{\alpha\beta,\,\delta} = \mathscr{L}'^{\,j}_{\alpha\beta,\,\delta} + \mathscr{L}''^{\,j}_{\alpha\beta,\,\delta}$$

Remplaçons les coefficients $\mathscr{L}$ par cette expression dans la formule (42). Nous avons :

$$\sum_{j\zeta} \frac{G^{kj}_{\varepsilon\zeta}}{n}\, \Gamma_{0\,\zeta\beta}^{jk'} = \delta_{kk'}\, \delta_{\varepsilon\beta}$$

$$\sum_{k\varepsilon} \Gamma_{0\,\alpha\varepsilon}^{j'k}\, \frac{G^{kj}_{\varepsilon\zeta}}{n} = \delta_{jj'}\, \delta_{\alpha\zeta}$$

d'où :

$$\mathfrak{M}_{1\,\alpha\gamma,\,\beta\delta} = \mathfrak{M}'_{1\,\alpha\gamma,\,\beta\delta} - \frac{1}{v} \sum_{bjk} C^{b}_{\substack{jk \\ \alpha\beta}} (b_\gamma\, j_\delta + b_\delta\, j_\gamma - j_\gamma\, k_\delta)$$

d'autre part :

$$\mathfrak{M}_{2\alpha\gamma,\,\beta\delta} = \mathfrak{M}'_{2\,\alpha\gamma,\,\beta\delta} + \frac{1}{v} \sum_{bjk} C^{b}_{\substack{jk \\ \alpha\beta}} (b_\gamma\, j_\delta + b_\delta\, j_\gamma - j_\gamma\, k_\delta)$$

donc :

$$\mathfrak{M}'_{1\,\alpha\gamma,\,\beta\delta} + \mathfrak{M}'_{2\,\alpha\gamma,\,\beta\delta} = \mathfrak{M}_{1\,\alpha\gamma,\,\beta\delta} + \mathfrak{M}_{2\alpha\gamma,\,\beta\delta}$$

Les coefficients d'élasticité $\mathfrak{N}$ sont fonctions seulement des périodes du milieu cristallin et des tenseurs $(C^{b}_{\substack{jk \\ \alpha\beta}})$ qui expriment les forces de rappel entre deux atomes.

Ainsi la matrice de Fourier, quelle que soit sa forme, détermine une matrice B et une seule.

LA MATRICE ATOMIQUE DÉTERMINE LES DIRECTIONS DES OSCILLATIONS

Cette matrice B, définit, par son équation caractéristique (26), les vitesses de propagation ($V = \Omega^{1/2}$) des oscillations macroscopiquement observables, les oscillations acoustiques de basse fréquence. Reste à démontrer qu'elle définit aussi les directions des mêmes oscillations.

Pour y parvenir, je suivrai la méthode de Born (*).

La matrice Γ (32) est obtenue en exprimant les oscillations harmoniques (6) (7) :

$$a^m_{j\,\alpha} = \eta^j_\alpha \; e^{i\,[\omega t - \sigma \vec{q}\,(\vec{m} + \vec{j})]} \tag{50}$$

$$\eta^j_\alpha = \frac{\gamma^j_\alpha}{\sqrt{\mu_j}}$$

Le vecteur propre $\vec{\eta}_j$ est une fonction de σ, paire par son module, impaire par son argument :

$$\eta^j_\alpha = (u^j_\alpha + v^j_\alpha \, \sigma^2 + \ldots) \, e^{i(\theta^j_\alpha \sigma + \ldots)}$$

Revenons aux oscillations acoustiques de basse fréquence et faisons derechef l'approximation de l'élasticité classique.

La longueur σ reste fort petite par rapport aux périodes du réseau polaire, nous pouvons prendre :

$$\eta^j_\alpha = u_\alpha + i u_\alpha \, \theta^j_\alpha \, \sigma + (v^j_\alpha - \frac{\theta^{2\,j}_\alpha}{2} \, u_\alpha) \, \sigma^2 \tag{51}$$

$\vec{u}$ est le vecteur propre (la direction) de l'élongation observable, celle qui est accomplie par le motif cristallin pris en bloc, Le principe de d'Alembert, appliqué aux oscillations (50) donne :

$$\mu_j \, \omega^2 \, \eta^j_\alpha + \sum_{k\beta} \Gamma^{\,j\,k}_{\alpha\beta} \, \eta^k_\beta = 0$$

Remplaçons cans cette équation ω^2 par $V^2 \, \sigma^2$, et η^j_α par la série (51); puis développons l'expression obtenue suivant les puissances entières et positives de σ, et arrêtons nous aux termes du second degré. L'équation devient :

$$c_0 + c_1 \, \sigma + c_2 \, \sigma^2 = 0$$

(*) Born, *Atomtheorie des Festen Zustandes*, Teubner, Berlin, p. 582 (1923).

Et, comme σ est une variable continue :

$$c_0 = c_1 = c_2 = 0$$

Nous avons :

1° $$c_0 = \sum_{k\beta} \Gamma_{0\,\alpha\beta}^{j\,k}\, u_\beta = 0,$$

égalité toujours satisfaite d'après (35).

2° $$c_1 = \sum_{k\beta} (i\,\Gamma_{0\,\alpha\beta}^{j\,k}\, \theta_\beta^k + \Gamma_{1\,\alpha\beta}^{j\,k})\, u_\beta = 0$$

ou, puisque β est un indice muet,

$$i \sum_{k\varepsilon} \Gamma_{0\,\alpha\varepsilon}^{j\,k}\, \theta_\varepsilon^k\, u_\varepsilon + \sum_{k\beta} \Gamma_{1\,\alpha\beta}^{j\,k}\, u_\beta = 0,$$

condition remplie, d'après (34), par :

$$\theta_\varepsilon^k = \sum_\beta y_{\varepsilon,\beta}^k\, \frac{u_\beta}{u_\varepsilon} \qquad (52)$$

Ainsi, au facteur $\dfrac{u_\beta}{u_\varepsilon}$ près, les nombres $y_{\varepsilon,\beta}^k$ (33) expriment des phases. En général, la propagation de l'oscillation n'est pas uniforme au travers du motif cristallin. Les différences :

$$\theta_\varepsilon^k - \theta_\varepsilon^n = \sum_\beta \delta_{\varepsilon,\beta}^{k-n}\, \frac{u_\beta}{u_\varepsilon} \quad (k, n = 1, 2, \ldots g)$$

indiquent, à l'approximation faite, l'écart entre la propagation véritable et la propagation uniforme. C'est pourquoi les différences (37)

$$\delta_{\varepsilon,\beta}^{k-n} = y_{\varepsilon,\beta}^k - y_{\varepsilon,\beta}^n$$

sont seules déterminées et non les nombres $y_{\varepsilon,\beta}^k$

3° $$c_2 = \mu_j\, \nabla^2 u_\alpha + \sum_{k\beta} [\Gamma_{0\,\alpha\beta}^{j\,k}\, v_\beta^k + (-\Gamma_{0\,\alpha\beta}^{j\,k}\, \frac{\theta^2{}_\beta^k}{2} + i\,\Gamma_{1\,\alpha\beta}^{j\,k}\, \theta_\beta^k + \Gamma_{2\,\alpha\beta}^{j\,k})\, u_\beta] = 0$$

d'où :

$$\sum_{k\beta} \Gamma_{0\,\alpha\beta}^{j\,k} v_\beta^k = -\mu_j \, V^2 u_\alpha - \sum_{k\beta} \left(-\Gamma_{0\,\alpha\beta}^{j\,k} \frac{\theta^{2\,k}_\beta}{2} \right.$$

$$\left. + i\,\Gamma_{1\,\alpha\beta}^{j\,k}\,\theta_\beta^k + \Gamma_{2\,\alpha\beta}^{j\,k} \right) u_\beta \qquad (53)$$

$$j = 1,2 \ldots g;\ \alpha = 1,2,3$$

Ce sont $3g$ équations linéaires dont les inconnues sont v_β^k. Compte tenu de (35), leur compatibilité exige :

$$\sum_j \left[\mu_j \, V^2 u_\alpha + \sum_{k\beta} \left(-\Gamma_{0\,\alpha\beta}^{j\,k} \frac{\theta^{2\,k}_\beta}{2} + i\,\Gamma_{1\,\alpha\beta}^{j\,k}\,\theta_\beta^k + \Gamma_{2\,\alpha\beta}^{j\,k} \right) u_\beta \right] = 0$$

ou compte tenu encore de (35), puis de (52) :

$$\mu \, V^2 u_\alpha + \sum_\beta \left(\sum_{jk\varepsilon} i\,\Gamma_{1\,\alpha\varepsilon}^{j\,k}\, y_{\varepsilon,\beta}^k + \sum_{jk} \Gamma_{2\,\alpha\beta}^{j\,k} \right) u_\beta = 0$$

ou enfin, d'après (33 et (46) :

$$V^2 u_\alpha + \sum_\beta B_{\alpha\beta}\, u_\beta = 0 \qquad (54)$$

La matrice B a toujours trois valeurs propres réelles et positives : elle détermine toujours trois vitesses de propagation, et, par suite, trois oscillations rectilignes et orthogonales. Nous retombons sur les conclusions de l'élasticité classique. Mais le dernier résultat (54), est déduit de la condition requise par la solution des équations (53). Or les racines v_β^k, exactement leurs différences $(v_\beta^j - v_\beta^k)$, seules définies par les équations (53), ne figurent pas dans les équations (54), déterminées de la sorte par l'existence d'inconnues, dont elles ne dépendent point, et qui expriment un déplacement correctif, inobservable à l'échelle macroscopique. Notre raisonnement prêterait à critique si nous ne découvrions le sens de cette singularité.

Prenons en compte la matrice de Fourier Γ' (47). C'est exprimer les oscillations acoustiques de basse fréquence :

$$\left.\begin{aligned} a_{j\,\alpha}^m &= \lambda_\alpha^j \, e^{i(\omega t - \sigma \vec{q}\vec{m})}, \\ \lambda_\alpha^j &= u_\alpha + i u_\alpha \theta'^j_\alpha \sigma + (v_\alpha^j - \frac{\theta'^{2\,j}_\alpha}{2} u_\alpha) \sigma^2 \end{aligned}\right\} \qquad (55)$$

(par comparaison avec (9) : $\lambda_\alpha^j = \dfrac{\xi_\alpha^j}{\sqrt{\mu_j}}$)

Sur l'atome mj, effectuant l'oscillation (55), est appliquée une force de rappel $\vec{F}^m_j$, qui se formule compte tenu de (5) :

$$\underset{\alpha}{F^m_j} = \psi \sum_{k\beta} \Gamma'^{\,jk}_{\alpha\beta}\, \lambda^k_\beta ;$$

$$\psi = e^{i(\omega t - \sigma \vec{q}\,\vec{m})} \tag{56}$$

Développons cette expression de la force suivant les puissances entières et positives de σ, jusqu'aux termes du second degré. Nous obtenons :

$$\underset{\alpha}{F^m_j} = \psi \sum_{k\beta} \{ \Gamma'^{\,jk}_{0\alpha\beta}\, u_\beta + (i\, \Gamma'^{\,jk}_{0\alpha\beta}\, \theta'^k_\beta + \Gamma'^{\,jk}_{1\alpha\beta})\, u_\beta\, \sigma$$

$$+ [\Gamma'^{\,jk}_{0\alpha\beta}\, v^k_\beta + (-\Gamma'^{\,jk}_{0\alpha\beta} \frac{\theta'^{2k}_\beta}{2} + i\, \Gamma'^{\,jk}_{1\alpha\beta}\, \theta'^k_\beta + \Gamma'^{\,jk}_{2\alpha\beta})\, u_\beta]\, \sigma^2 \}$$

Compte tenu de (4), nous avons :

$$\sum_k \Gamma'^{\,jk}_{0\alpha\beta} = 0 \tag{57}$$

donc :

$$\sum_{k\beta} \Gamma'^{\,jk}_{0\alpha\beta}\, u_\beta = 0$$

D'autre part, la fréquence d'une oscillation est une fonction paire de σ. Donc la force de rappel développée par une oscillation est aussi une fonction paire de la même variable. A l'approximation faite, celle de l'élasticité classique, la force $\vec{F}^m_j$ est proportionnelle à σ^2. Cela exige :

$$\sum_{k\beta} (i\, \Gamma'^{\,jk}_{0\alpha\beta}\, \theta'^k_\beta + \Gamma'^{\,jk}_{1\alpha\beta})\, u_\beta = 0, \tag{58}$$

ou, puisque β est un indice muet,

$$i \sum_{k\varepsilon} \Gamma'^{\,jk}_{0\alpha\varepsilon}\, \theta'^k_\varepsilon\, u_\varepsilon + \sum_{k\beta} \Gamma'^{\,jk}_{1\alpha\beta}\, u_\beta = 0,$$

condition satisfaite, d'après (49), par :

$$\theta'^k_\varepsilon = \sum_\beta y'^k_{\varepsilon,\beta} \frac{u_\beta}{u_\varepsilon} \tag{59}$$

En conséquence :

$$\underset{\alpha}{F^m_j} = \psi \sum_{k\beta} [\Gamma'^{\,jk}_{0\alpha\beta}\, v^k_\beta + (-\Gamma'^{\,jk}_{0\alpha\beta} \frac{\theta'^{2k}_\beta}{2} + i\, \Gamma'^{\,jk}_{1\alpha\beta}\, \theta'^k_\beta + \Gamma'^{\,jk}_{2\alpha\beta})\, u_\beta]\, \sigma^2$$

La force de rappel, appliquée à chaque atome est bien fonction des déplacements complémentaires $\vec{v}^k$, comme des différences de phases $(\theta'^j_\beta - \theta'^k_\beta)$ (et non des phases mêmes comme le porte la formule précédente par suite de l'approximation faite). Mais la force de rappel $\vec{R}_m$ appliquée au motif cristallin, tout entier, ne dépend plus des déplacements $\vec{v}^k$ ni des phases θ'^k_β. Car d'après (57) et (58) :

$$R^m_\alpha = \sum_j F^m_{j\,\alpha} = \psi\sigma^2 \sum_{jk\beta} (i\Gamma'^{\,jk}_{1\,\alpha\beta}\,\theta'^k_\beta + \Gamma'^{\,jk}_{2\,\alpha\beta})\,u_\beta$$

et compte tenu de (59) :

$$R^m_\alpha = \psi\sigma^2 \sum_\beta \Big(\sum_{jk\varepsilon} i\Gamma'^{\,jk}_{1\,\alpha\varepsilon}\,y'^k_{\varepsilon,\beta} + \sum_{jk}\Gamma'^{\,jk}_{2\,\alpha\beta}\Big)\,u_\beta$$

enfin, d'après (48) :

$$R^m_\alpha = \mu\psi\sigma^2 \sum_\beta B_{\alpha\beta}\,u_\beta \qquad (60)$$

L'oscillation observable est l'oscillation accomplie par le motif cristallin, pris en bloc; c'est d'après (55) :

$$a^m_\alpha = u_\alpha\, e^{i(\omega t - \sigma \vec{q}\vec{m})}$$

Appliquons le principe de d'Alembert à cette oscillation :

$$\mu\,\ddot{a}^m_\alpha = R^m_\alpha$$

ou compte tenu de (56) :

$$-\mu\omega^2\psi\,u_\alpha = R^m_\alpha$$

Remplaçons ω par $V\sigma$, compte tenu de (60); nous retombons sur les équations (54.)

Remarque.

Si la position moyenne de chaque atome coïncide avec un centre de symétrie du milieu cristallin, la matrice de Fourier Γ (32) est réelle; la matrice Γ_1 est nulle, et par suite toutes les différences de phases $\theta^{k-n}_{\varepsilon,\beta}$ (34)(37)(52); la propagation des oscillations est uniforme au travers du motif cristallin. D'autre part, tout coefficient $\mathscr{L}^j_{\alpha\beta,\delta}$(38) est nul, et, par conséquent tout coefficient $\mathfrak{M}_{1\alpha\gamma,\beta\delta}$(42). Le coefficient d'élasticité $\mathfrak{N}_{\alpha\gamma,\beta\delta}$ (45) se réduit à sa composante $\mathfrak{M}_{2\alpha\gamma,\beta\delta}$ (43). L'autre composante, $\mathfrak{M}_{1\alpha\gamma,\beta\delta}$ est de la sorte, liée à la propagation non uniforme de l'oscillation au travers du motif cristallin.

Si le motif cristallin est monoatomique toutes les oscillations sont du type acoustique. On peut les exprimer :

$$a_\alpha^m = \frac{u_\alpha}{\mu} e^{i\,\sigma\,\vec{q}\,\vec{m}}$$

L'équation de d'Alembert (11) se réduit à :

$$\omega^2 u_\alpha = -\frac{1}{\mu} \sum_{b\beta} C_{\alpha\beta}^{b}\, u_\beta \cos.\, \sigma\,\vec{q}\,\vec{b}$$

$$= \frac{2}{\mu} \sum_{b\beta} C_{\alpha\beta}^{b}\, u_\beta \sin.^2 \frac{\sigma}{2}\,\vec{q}\,\vec{b}$$

Pour les oscillations de basse fréquence σ est minime par rapport aux périodes du réseau polaire. L'approximation de l'élasticité classique donne :

$$\omega^2\, u_\alpha = \frac{\sigma^2}{2\mu} \sum_{\beta} \left(\sum_{b} C_{\alpha\beta}^{b}\,\vec{q}\,\vec{b}\right) u_\beta$$

$$= \frac{\sigma^2}{\rho} \sum_{\beta} \left(\sum_{\gamma\delta} \mathfrak{M}_{2\alpha\gamma,\,\beta\delta}\, q_\gamma\, q_\delta\right) u_\beta$$

et, après division par σ^2,

$$V^2\, u_\alpha + \sum_{\beta} B_{\alpha\beta}\, u_\beta = 0$$

où

$$B_{\alpha\beta} = -\frac{1}{\rho} \sum_{\gamma\delta} \mathfrak{M}_{2\alpha\gamma,\,\beta\delta}\, q_\gamma\, q_\delta$$

CONCLUSION
COMPARAISON DE LA MATRICE CLASSIQUE ET DE LA MATRICE ATOMIQUE

Comme la matrice A (29), la matrice atomique B (46), détermine la vitesse de propagation, et les directions des oscillations acoustiques de basse fréquence. Elle a la même forme que la matrice classique. Et dans l'une et l'autre les coefficients d'élasticité entrent en même nombre. Mais ce ne sont pas les mêmes. Les coefficients de Voigt, $c_{\alpha\gamma,\beta\delta}$, tels qu'ils ont été définis par l'élasticité classique, sont contrevariants par rapport à leurs quatre indices, symétriques en $\alpha\ \gamma$ et $\beta\ \delta$, en α et γ, et en β et δ. Les coefficients atomiques $\mathfrak{N}_{\alpha\gamma,\beta\delta}$ (45)

sont covariants en α et β, contrevariants en γ et δ, symétriques seulement en α γ et β δ (forces centrales exclues). Bien qu'en même nombre que les coefficients de Voigt, ils prennent donc, en général, davantage de valeurs distinctes, quarante cinq si le cristal est triclinique au lieu de vingt et une.

Pour retrouver les vingt et une constantes élastiques de Cauchy, je ferai appel aux déformations linéaires du milieu cristallin.

LES DÉFORMATIONS LINÉAIRES DU MILIEU CRISTALLIN

Caratères généraux des déformations statiques. — Energie nécessaire pour les produire.

Une onde élastique fait osciller les atomes; elle ne déplace pas leurs positions moyennes, ne modifie pas le réseau cristallin. Son étude peut être faite dans un système de référence constant, car elle laisse le réseau cristallin constant.

Au contraire, une tension, lentement variable, déplace les positions moyennes des atomes. Quand elle devient constante, le réseau cristallin reste constant, mais il est changé. La déformation statique est celle du réseau cristallin. Son étude est celle de l'équilibre des atomes sous des tensions constantes. Pour être rigoureuse, cette étude exige un système de référence variable qui subit la même déformation que le réseau cristallin.

Ainsi, les déformations statiques sont essentiellement différentes des déformations produites par les ondes élastiques; elles ne peuvent être régies par les mêmes lois.

Il convient d'envisager la production d'une déformation statique en trois étapes :

1° L'agitation thermique est éteinte : chaque atome rejoint sa position moyenne. L'opération libère l'énergie de l'agitation thermique, W_1, dans l'état initial (avant la déformation).

2° Le cristal subit la déformation; les atomes sont portés sur de nouvelles positions d'équilibre, le réseau cristallin prend une autre forme. L'opération exige une énergie W'.

3° L'agitation thermique est régénérée, le cristal reprend sa température première. Cette dernière opération absorbe l'énergie de l'agitation thermique, W_2, dans le cristal déformé.

Le bilan énergétique de la transformation globale se solde par une dépense :

$$W = W' + W_2 - W_1$$

W est l'énergie nécessaire pour produire la déformation.

Toute déformation statique change les distances entre les positions moyennes des atomes, et modifie, par là, le champ de force qui règne dans le milieu cristallin; en particulier, elle modifie les tenseurs $\begin{pmatrix} C_{j\ \alpha}^{m-p\ \beta} \\ k \end{pmatrix}$ (2); elle fait donc varier l'énergie de l'agitation thermique. En général W_2 diffère de W_1, et W diffère de W'.

Je supposerai, qu'avant la déformation, le milieu cristallin est stable, libre de toute tension, à température uniforme. Je considèrerai seulement des déformations légères, conformes sensiblement à la loi de Hooke. Pour de telles déformations la différence relative $\frac{W - W'}{W}$ reste fort petite auprès de l'unité. Dans ces conditions je confondrai W avec W', et ne ferai point état de l'énergie superficielle, envisageant un cristal infiniment grand. Enfin, je représenterai par $\overrightarrow{u_j^m}$ et $\overrightarrow{u_k^p}$, non plus les élongations des atomes, mais le déplacement de leurs positions moyennes.

Les déformations linéaires.

J'appelle déformation linéaire, et non déformation homogène, celle qui conserve la triple périodicité du milieu cristallin.

Son tenseur $(t_{\alpha\gamma})$ est constant,

$$t_{\alpha\gamma} = \frac{\partial u_\alpha}{\partial x_\gamma}\ ;\ \alpha,\ \gamma = 1,\ 2,\ 3 \qquad (61)$$

Elle communique aux atomes des déplacements $\overrightarrow{u_j^m}$ tels que :

$$u_{j\ \alpha}^{m} = d_\alpha^j + \sum_\gamma t_{\alpha\gamma}\ (m_\gamma + j_\gamma) \qquad (62)$$

En conséquence :

$$u_{j\ \alpha}^{m-p}{}_{k} = u_{j\ \alpha}^{m} - u_{k\ \alpha}^{p} = d^{j-k}{}_\alpha + \sum_\gamma t_{\alpha\gamma}\ (b_\gamma + j_\gamma - k_\gamma) \qquad (63)$$

$$d^{j-k}{}_\alpha = d_\alpha^j - d_\alpha^k \text{ et } b_\gamma = m_\gamma - p_\gamma$$

L'appellation déformation homogène engendre la confusion entre le milieu cristallin et le milieu homogène, le milieu idéal considéré

par les théoriciens de l'élasticité classique. Seul un milieu homogène à toute échelle peut être le siège d'une déformation homogène : se reproduisant identiquement dans tout élément si petit soit-il. Or le milieu cristallin est un assemblage d'atomes. Il est par là hétérogène et ne peut être le siège d'une déformation homogène à l'échelle atomique, surtout à échelle moindre. Quand le cristal est soumis à des tensions, les atomes se déplacent les uns par rapport aux autres. Ils subissent une déformation, mais elle est minime, restreinte à leur périphérie, et porte sur une masse infime auprès de la masse totale. Seule varie la densité des électrons faiblement liés, mais le corps des atomes garde sa configuration première.

Condition d'équilibre du milieu cristallin.

La méthode suivie pour calculer les coefficients d'élasticité s'étend sans difficultés au calcul des tensions $T_{\alpha\gamma}$ appliquées sur les plans réticulaires. Elle donne :

$$T_{\alpha\gamma} = \sum_{\beta\delta} \mathfrak{N}_{\alpha\gamma,\,\beta\delta}\, t_{\beta\delta} \qquad (64)$$

Je prends encore en compte des tenseurs $(C_{j\ k}^{m-p})$ constants qui ne font pas intervenir les déplacements relatifs $\overleftarrow{u}_{j\ k}^{m-p}$, et je les confonds avec ceux qui déterminent les forces de rappel développées par les oscillations (5). Car l'agitation thermique éteinte, $\overleftarrow{u}_{j\ k}^{m-p}$ représente comme auparavant, le déplacement de l'atome *mj* par rapport à l'atome *pk*. Bref, je fais encore l'approximation inhérente à la loi de Hooke et conserve les coordonnées de Lagrange. Ainsi, mon étude des déformations linéaires sera cohérente avec l'étude précédente des ondes élastiques.

L'équilibre du milieu cristallin exige :

$$T_{\alpha\gamma} = T_{\gamma\alpha}$$

Soit, compte tenu de (64) :

$$\sum_{\beta\delta} (\mathfrak{N}_{\alpha\gamma,\,\beta\delta} - \mathfrak{N}_{\gamma\alpha,\,\beta\delta})\, t_{\beta\delta} = 0;\ \alpha, \gamma = 1, 2, 3 \qquad (65)$$

Ces trois conditions déterminent trois composantes du tenseur $(t_{\beta\delta})$ [ou $(t_{\alpha\gamma})$] en fonction des six autres.

Posons, comme en élasticité classique :

$$\tau_{\alpha\gamma} = \tau_{\gamma\alpha} = \frac{t_{\alpha\gamma} + t_{\gamma\alpha}}{2}$$

et :

$$\bar{\omega}_{\alpha\gamma} = \tau_{\alpha\gamma} - t_{\alpha\gamma} \tag{66}$$

Le tenseur $(\tau_{\alpha\gamma})$ est symétrique, le tenseur $(\bar{\omega}_{\alpha\gamma})$ antisymétrique. La condition d'équilibre (65) s'exprime encore :

$$\sum_{\beta\delta} (\mathfrak{N}_{\gamma\alpha,\beta\delta} - \mathfrak{N}_{\alpha\gamma,\beta\delta})\, \bar{\omega}_{\beta\delta} = \sum_{\beta\delta} (\mathfrak{N}_{\alpha\gamma,\beta\delta} - \mathfrak{N}_{\gamma\alpha,\beta\delta})\, \tau_{\beta\delta} \tag{67}$$

$$\alpha, \beta = 1, 2, 3;$$

d'où l'on tire les trois rotations $|\bar{\omega}_{\beta\delta}|$, qui représentent l'écart entre la déformation véritable et la déformation pure (ou irrotationnelle).

La déformation est pure quand les six composantes du tenseur $(\tau_{\beta\delta})$ vérifient les trois relations linéaires :

$$\sum_{\beta\delta} (\mathfrak{N}_{\alpha\gamma,\beta\delta} - \mathfrak{N}_{\gamma\alpha,\beta\delta})\, \tau_{\beta\delta} = 0 \tag{67 \textit{bis}}$$

$$\alpha, \gamma = 1, 2, 3$$

Ces trois relations définissent trois composantes $\tau_{\beta\delta}$ en fonction des trois autres, et, par conséquent, trois tensions $T_{\alpha\gamma}$ (64) en fonction des trois restantes.

Ainsi, dans le cas général, celui du cristal triclinique, les tensions qui produisent une déformation pure sont liées par trois relations linéaires. Quand la symétrie du milieu cristallin s'élève, le nombre de ces relations diminue, et tombe à zéro pour les cristaux cubiques : de la sorte la déformation des cristaux cubiques est toujours irrotationnelle.

Déplacements relatifs subis par les réseaux d'atomes (*) au cours d'une déformation linéaire.

Désormais nous prendrons uniquement en compte les déformations qui satisfont aux conditions d'équilibre (65) (67). Dans le cristal déformé linéairement, chaque atome supposé au repos, est en équilibre stable. Les tensions qu'il supporte ont une résultante nulle, et de même les forces de rappel $\vec{f}^{m-p}_{j\ k}$ (2) qui lui sont appliquées par tous les autres atomes, développées par les déplacements relatifs $\vec{u}^{m-p}_{j\ k}$ (63). En conséquence, compte tenu de (5),

$$\sum_{p\,k} f^{m-p}_{j\ k\ \alpha} = \sum_{p\,k\beta} C^{m-p}_{j\ k\ \alpha\ \beta}\, u^{p}_{k\ \beta} = 0$$

(*) Max Born, *Atomtheorie des Festen Zustandes*; Teubner, Berlin, p. 562 (1923).

c'est-à-dire, compte tenu de (62) (32) (38) :

$$\sum_{k\beta} \Gamma_{0\,\alpha\beta}^{j\,k}\, d_\beta^k = v \sum_{\beta\delta} \mathscr{L}^j_{\alpha\beta,\,\delta}\, t_{\beta\delta} \tag{68}$$

ou, puisque β est un indice muet :

$$\sum_{k\varepsilon} \Gamma_{0\,\alpha\varepsilon}^{j\,k}\, d_\varepsilon^k = v \sum_{\beta\delta} \mathscr{L}^j_{\alpha\beta,\,\delta}\, t_{\beta\delta}$$

condition satisfaite, d'après (34) par :

$$d_\varepsilon^k = -\sum_\beta y^k_{\varepsilon,\,\beta}\, \frac{t_{\beta\delta}}{q_\delta} \tag{69}$$

ou, d'après (39) par :

$$d^{k-n}_\varepsilon = v \sum_{\delta\beta} \Big(\sum_{j\zeta} G^{k\,j}_{n\,\varepsilon\zeta}\, \mathscr{L}^j_{\zeta\beta,\,\delta} \Big)\, t_{\beta\delta} \tag{70}$$

$$k,\ n = 1,2\ \ldots\ g;\ \zeta = 1,2,3$$

Ainsi, les déplacements relatifs d^{k-n} subis par les réseaux d'atomes correspondent à la propagation non uniforme des oscillations au travers du motif cristallin.

Si la position moyenne de chaque atome coïncide avec un centre de symétrie du milieu cristallin, tous les coefficients $\mathscr{L}^j_{\alpha\beta,\,\delta}$ sont nuls, et, par conséquent, aussi tous les déplacements relatifs d^{k-n}. Après la déformation, toute position moyenne se trouve sur un centre de symétrie comme avant. C'est ce qui a lieu dans le sel gemme. (Les déplacements relatifs imposés aux réseaux d'atomes, interviennent dans l'effet piézoélectrique. Et l'effet piézoélectrique influe sur les coefficients d'élasticité. Je me restreins au cas où cette influence est négligeable; je ne la prendrai donc point en compte).

Les coefficients d'élasticité statiques.

L'énergie nécessaire pour produire une déformation linéaire a pour densité, par volume unitaire :

$$\mathcal{E} = \frac{1}{4v} \sum_{p\,j\,k\,\alpha\beta} C^{m-p\ \ p}_{j\ \ k\ \ \alpha\ \ \beta}\, u^{m-p}_{j\ \ \alpha}\, u^{m-p}_{j\ \ \beta} \tag{71}$$

Soit, compte tenu de (63) (32) (35) (38) (43) :

$$\mathcal{E} = -\frac{1}{2v} \sum_{j\,k\,\alpha\beta} \Gamma_{0\,\alpha\beta}^{j\,k}\, d^j_\alpha\, d^k_\beta + \sum_{j\,\alpha\beta\delta} \mathscr{L}^j_{\alpha\beta,\,\delta}\, d^j_\alpha\, t_{\beta\delta}$$
$$+ \frac{1}{2} \sum_{\alpha\beta\gamma\delta} \mathfrak{M}_{2\alpha\gamma,\,\beta\delta}\, t_{\alpha\gamma}\, t_{\beta\delta}$$

et d'après (68),

$$\mathcal{E} = \frac{1}{2} \sum_{j\alpha\beta\delta} \mathscr{L}^{j}_{\alpha\beta,\ \delta}\, d^{j}_{\alpha}\, t_{\beta\delta} + \frac{1}{2} \sum_{\alpha\beta\gamma\delta} \mathfrak{M}_{2\,\alpha\gamma,\ \beta\delta}\, t_{\alpha\gamma}\, t_{\beta\delta}$$

enfin, d'après (70) (40)(69) (41) (45),

$$\mathcal{E} = \frac{1}{2} \sum_{\alpha\beta\gamma\delta} \mathfrak{N}_{\alpha\gamma,\ \beta\delta}\, t_{\alpha\gamma}\, t_{\beta\delta} \tag{72}$$

ou compte tenu de (66),

$$\mathcal{E} = \frac{1}{2} \sum_{\alpha\beta\gamma\delta} \mathfrak{N}_{\alpha\gamma,\ \beta\delta}\, \tau_{\alpha\gamma}\, \tau_{\beta\delta}$$

$$+ \frac{1}{2} \sum_{\alpha\beta\gamma\delta} \mathfrak{N}_{\alpha\gamma,\ \beta\delta} (\tau_{\alpha\gamma}\, \bar{\omega}_{\beta\delta} + \tau_{\beta\delta}\, \bar{\omega}_{\alpha\gamma} + \bar{\omega}_{\alpha\gamma}\, \bar{\omega}_{\beta\delta}) \tag{73}$$

Nous avons :

$$\mathrm{T}_{\alpha\gamma} = \frac{\partial \mathcal{E}}{\partial t_{\alpha\gamma}}$$

Ainsi, nous retombons sur la formule (64), laquelle, obtenue en évaluant seulement les tensions exercées sur les plans réticulaires, définit donc les tensions appliquées sur n'importe quel plan.

D'autre part, d'après (65) (67),

$$\mathrm{T}_{\alpha\gamma} = \mathrm{T}_{\gamma\alpha} = \frac{1}{2} \left(\frac{\partial \mathcal{E}}{\partial t_{\alpha\gamma}} + \frac{\partial \mathcal{E}}{\partial t_{\gamma\alpha}} \right) \tag{74}$$

Les tensions $\mathrm{T}_{\alpha\gamma}$, sommes de deux composantes dissymétriques du tenseur :

$$\frac{1}{2} \left(\frac{\partial \mathcal{E}}{\partial t_{\alpha\gamma}} \right)$$

ne forment plus elles-mêmes un tenseur.

Supposons la déformation pure, c'est-à-dire $\bar{\omega}_{\alpha\gamma} = \bar{\omega}_{\beta\delta} = 0$, d'après (73),

$$\mathcal{E} = \frac{1}{2} \sum_{\alpha\beta\gamma\delta} \mathfrak{N}_{\alpha\gamma,\ \beta\delta}\, \tau_{\alpha\gamma}\, \tau_{\beta\delta}$$

Posons :

$$\Lambda_{\alpha\gamma,\ \beta\delta} = \frac{1}{4} (\mathfrak{N}_{\alpha\gamma,\ \beta\delta} + \mathfrak{N}_{\gamma\alpha,\ \beta\delta} + \mathfrak{N}_{\alpha\gamma,\ \delta\beta} + \mathfrak{N}_{\gamma\alpha,\ \delta\beta}) \tag{75}$$

Nous avons :

$$\mathcal{E} = \frac{1}{2} \sum_{\alpha\beta\gamma\delta} \Lambda_{\alpha\gamma,\,\beta\delta}\, \tau_{\alpha\gamma}\, \tau_{\beta\delta} \tag{76}$$

et :

$$T_{\alpha\gamma} = T_{\gamma\alpha} = \sum_{\beta\delta} \Lambda_{\alpha\gamma,\,\beta\delta}\, \tau_{\beta\delta} \tag{77}$$

Les coefficients d'élasticité statiques $\Lambda_{\alpha\gamma,\beta\delta}$ (75) sont symétriques en $\alpha\gamma$ et $\beta\ \delta$, en α et γ, et en β et δ. Ils ont donc la même symétrie que les coefficients de Voigt, et prennent les mêmes valeurs. Nous retrouvons de la sorte les vingt et une constantes élastiques de Cauchy. Remarquons toutefois que les coefficients Λ, sommes de quatre composantes dissymétriques de la densité tensorielle $(\mathfrak{N}_{\alpha\gamma,\beta\delta})$ ne constituent plus, au sens propre du terme, une densité tensorielle, et diffèrent par là, des coefficients de Voigt qui forment, eux, une densité tensorielle quatre fois contrevariante.

Les coefficients Λ et les formules (76) (77) se rapportent aux déformations pures. Si les déformations ne sont plus irrotationnelles, si $t_{\gamma\alpha}$ diffère de $t_{\alpha\gamma}$, les coefficients $\mathfrak{N}_{\alpha\gamma,\beta\delta}$ entrent en compte individuellement (72) (73), le nombre des constantes élastiques s'élève à 45; et, il devient impossible de définir exactement les tensions par la formule (77). Si l'on applique quand même cette formule aux mesures, on obtiendra des coefficients Λ variables, dont l'oscillation croîtra avec les rotations $|\,\bar{\omega}_{\alpha\gamma}\,|$, et, comme nous le verrons plus loin, avec l'écart entre les forces de rappel véritables et les forces centrales. Pourtant, cette oscillation reste sans doute minime car, il est à présumer que le second terme de la formule (73) :

$$\frac{1}{2} \sum_{\alpha\beta\gamma\delta} \mathfrak{N}_{\alpha\gamma,\,\beta\delta}\, (\tau_{\alpha\gamma}\, \bar{\omega}_{\beta\delta} + \tau_{\beta\delta}\, \bar{\omega}_{\alpha\gamma} + \bar{\omega}_{\alpha\gamma}\, \bar{\omega}_{\beta\delta})$$

reste toujours très petit par rapport au premier :

$$\frac{1}{2} \sum_{\alpha\beta\gamma\delta} \mathfrak{N}_{\alpha\gamma,\,\beta\delta}\, \tau_{\alpha\gamma}\, \tau_{\beta\delta}$$

Cas des forces centrales.

L'élasticité d'un milieu cristallin assujetti à des forces centrales, a été traitée, par Max Born, en deux mémoires admirables (*). Il serait téméraire de reprendre le sujet.

(*) *Dynamik der Krystallgitter*, Teubner, Berlin, pp. 17 et 40 (1915); *Atomtheorie des Festen Zustandes*, Teubner, Berlin, pp. 536 et 548, (1923).

J'appliquerai directement à mon étude les conclusions de l'illustre physicien.

Supposons donc les atomes soumis à des forces centrales et le milieu cristallin stable; soient $V_j^{m-p}{}_k$ l'énergie potentielle, mutuelle, des deux atomes *mj* et *pk*, et $\vec{r}$ le vecteur qui part du second, *pk*, et aboutit au premier, *mj*.

Posons :

$$\chi_j^{m-p}{}_k = \left(\frac{1}{r}\frac{d\,V_j^{m-p}{}_k}{dr}\right) r = |\vec{m} - \vec{p} + \vec{j} - \vec{k}| \tag{78}$$

$$\psi_j^{m-p}{}_k = \left\{\frac{1}{r}\left[\frac{d}{dr}\left(\frac{1}{r}\frac{d\,V_j^{m-p}{}_k}{dr}\right)\right]\right\} r = |\vec{m} - \vec{p} + \vec{j} - \vec{k}| \tag{79}$$

Selon Born :

$$\sum_{p\,k} \chi_j^{m-p}{}_k\,(m_\alpha - p_\alpha + j_\alpha - k_\alpha) = 0$$

et :

$$\sum_{p\,j\,k} \chi_j^{m-p}{}_k\,(m_\alpha - p_\alpha + j_\alpha - k_\alpha)(m_\beta - p_\beta + j_\beta - k_k) = 0\,;$$

en conséquence :

$$\mathscr{P}^{j}_{\alpha\beta,\,\delta} = \frac{1}{v}\sum_{p\,k} \psi_j^{m-p}{}_k\,(m_\alpha - p_\alpha + j_\alpha - k_\alpha)(m_\beta - p_\beta + j_\beta - k_\beta) \times (m_\delta - p_\delta + j_\delta - k_\delta) \tag{80}$$

$$\mathfrak{M}_{2\alpha\gamma,\,\beta\delta} = \frac{1}{2v}\sum_{p\,j\,k} \psi_j^{m-p}{}_k\,(m_\alpha - p_\alpha + j_\alpha - k_\alpha) \times (m \quad - p_\beta + j_\beta - k_\beta)(m_\gamma - p_\gamma + j_\gamma - k_\gamma) \times (m_\delta - p_\delta + j_\delta - k_\delta) \tag{81}$$

Ainsi, les coefficients $\mathfrak{M}_{2\alpha\gamma,\,\beta\delta}$ deviennent symétriques en α, γ, β et δ; les coefficients $\mathscr{P}^{j}_{\alpha\beta,\,\delta}$ symétriques en α, β, et δ*; et les coefficients $\mathfrak{N}_{\alpha\gamma,\,\beta\delta}$ (45) prennent de la sorte la même symétrie que les coefficients de Voigt, et peuvent être confondus avec eux. Deux cas se présentent :

1° La position moyenne de chaque atome coïncide avec un centre de symétrie du milieu cristallin : les coefficients $\mathfrak{N}_{\alpha\gamma,\,\beta\delta}$ se réduisent à leur composante $\mathfrak{M}_{2\alpha\gamma,\,\beta\delta}$; étant symétriques par rapport à leurs quatre indices, ils satisfont aux relations de Cauchy.

(*) Les cœfficients $\mathfrak{N}_{1\alpha\gamma,\,\beta\delta}$ symétriques en $\alpha\gamma$ et $\beta\delta$, en α et γ et en β et δ.

2° Si les positions moyennes des atomes ne se trouvent pas toutes sur des centres de symétrie, les coefficients ne sont plus, d'après (42), symétriques par rapport à leurs quatre indices, seulement en $\alpha\gamma$ et $\beta\delta$, en α et γ, et en β et δ.

D'autre part, les conditions d'équilibre du milieu cristallin (65) sont satisfaites par n'importe quelle déformation linéaire; les neuf composantes du tenseur $(t_{\beta\delta})$ ne sont plus assujetties à aucune relation; toutes peuvent être choisies arbitrairement. En particulier, les conditions d'équilibre sont satisfaites par les déformations pures, prises en compte par les théoriciens de l'élasticité classique.

CONCLUSION

Dans cette étude, la force est covariante, le tenseur $(C^{m-p}_{j\ k\ \alpha\ \beta})$ (2), qui exprime la force de rappel entre deux atomes est deux fois covariant, le tenseur des déformations $t_{\alpha\gamma}$ (61) contrevariant en α, covariant en γ, la densité tensorielle formée par les coefficients $\mathfrak{N}_{\alpha\gamma,\beta\delta}$, deux fois covariante et deux fois contrevariante. Quant aux tensions $T_{\alpha\gamma}$ (74) et aux coefficients d'élasticité statique $\Lambda_{\alpha\gamma,\beta\delta}$ (75), ils ont été rendus symétriques par combinaison de composantes dissymétriques prises dans un autre tenseur : les tensions $T_{\alpha\gamma}$ sont symétriques par rapport à leurs deux indices, et les coefficients $\Lambda_{\alpha\gamma,\beta\delta}$ ont la même symétrie que les coefficients de Voigt.

En élasticité classique (*) les grandeurs sont d'une autre nature. C'est la longueur du déplacement qui est prise comme donnée première. Elle est posée invariante, d'où découle un tenseur des déformations deux fois covariant, des tensions $T_{\alpha\gamma}$ deux fois contrevariantes, des coefficients d'élasticité $c_{\alpha\gamma,\,\beta\delta}$ quatre fois contrevariants. De la sorte, le tenseur (2) qui définit la force de rappel entre deux atomes serait deux fois contrevariant; contradiction irréductible avec la covariance de cette force de rappel comme avec l'invariance de l'énergie prise par la déformation (71). La théorie classique de l'élasticité est donc seulement applicable au milieu absolument homogène; elle ne s'accorde pas avec la structure cristalline, mais elle ne se préoccupe point des déformations dans le

(*) Léon Brillouin, *Les tenseurs en Mécanique et en Elasticité*, Paris, p. 212 (1946). Aristotle Michal, *Matrix and Tensor Calculus*, John Wiley & Sons, Inc., New-York, p. 75 (1948).

détail atomique, seulement à grande dimension. Et, une fois écartée la contradiction fondamentale sur la nature des forces de rappel interatomiques, elle s'adapte au milieu cristallin assujetti à des forces centrales. Car, si la longueur est posée invariante, les fonctions $\chi_{j\ k}^{m-p}$ (78) et $\psi_{j\ k}^{m-p}$ (79) sont invariantes, et les coefficients d'élasticité $\mathfrak{N}_{\alpha\gamma,\ \beta\delta}$ deviennent bien, d'après les expressions (80) (81), quatre fois contrevariants comme les coefficients de Voigt.

On aboutit à la même conclusion par une autre voie.

Soit un milieu absolument homogène, parcouru par un train d'ondes élastiques, et dans ce milieu, un élément, en forme de parallélipipède rectangle, les arêtes parallèles aux axes de coordonnées à l'état de repos. A l'intérieur de cet élément la déformation varie, au même instant, d'un point à l'autre. Mais le milieu étant homogène à toute échelle, les arêtes de l'élément peuvent être réduites indéfiniment, raccourcies suffisamment pour que les déformations $t_{\alpha\gamma}$ et $t'_{\alpha\gamma}$ en deux points intérieurs, quelconques, présentent une différence relative :

$$\frac{2\,(t'_{\alpha\gamma} - t_{\alpha\gamma})}{t'_{\alpha\gamma} + t_{\alpha\gamma}},$$

moindre que tout nombre ε, si petit soit-il. Quand l'élément devient de plus en plus petit, la déformation dont il est le siège, tend vers une déformation linéaire, l'énergie requise pour le déformer tend vers la densité :

$$\mathcal{E} = \frac{1}{2} \sum_{\alpha\beta\gamma\delta} c_{\alpha\gamma,\ \beta\delta}\ \tau_{\alpha\gamma}\ \tau_{\beta\delta} \tag{82}$$

et les tensions appliquées sur ses faces vers (*) :

$$T_{\alpha\gamma} = \frac{\partial \mathcal{E}}{\partial t_{\alpha\gamma}} = \sum_{\beta\delta} c_{\alpha\gamma,\ \beta\delta}\ t_{\beta\delta} \tag{83}$$

Ces deux formules impliquent la loi de Hooke. A la même approximation :

$$\tau_{\alpha\gamma} = \frac{t_{\alpha\gamma} + t_{\gamma\alpha}}{2}$$

(*) Pour plus de détails, voir Léon Brillouin : *Les tenseurs en Mécanique et en Elasticité*, Paris, pp. 246-255 (1945).

Nous pouvons de la sorte définir les tensions en un point : elles sont égales à la limite (83) vers laquelle tendent les tensions $T_{\alpha\gamma}$, appliquées sur les faces d'un élément centré sur ce point, quand le volume de l'élément tombe à zéro.

Envisageons derechef un élément du même milieu, d'arêtes $\vec{dx_1}$, $\vec{dx_2}$, $\vec{dx_3}$, le centre au point de coordonnées (x_1, x_2, x_3). Les tensions appliquées sur ses faces ont une résultante $\vec{df}$, telle que :

$$df_\alpha = \left[\sum_\gamma \frac{\partial}{\partial x_\gamma}\left(\frac{\partial \mathcal{E}}{\partial t_{\alpha\gamma}}\right)\right] dv$$

$$dv = dx_1\, dx_2\, dx_3$$

Comme l'élément a des dimensions infiniment petites, tous ses points accomplissent sensiblement la même oscillation que son centre :

$$a_\alpha = u_\alpha\, e^{i(\omega t - \sigma \sum_\gamma q_\gamma x_\gamma)} \tag{84}$$

Si ρ est la masse spécifique du milieu homogène :

$$\rho\, \ddot{a}_\alpha = \sum_\gamma \frac{\partial}{\partial x_\gamma}\left(\frac{\partial \mathcal{E}}{\partial t_{\alpha\gamma}}\right)$$

Nous avons :

$$t_{\alpha\gamma} = \frac{\partial a_\alpha}{\partial x_\gamma}$$

et si V est la vitesse de l'onde élastique, compte tenu de (83) (84).

$$V^2\, u_\alpha = \frac{1}{\rho} \sum_\beta \left(\sum_{\gamma\delta} c_{\alpha\gamma,\,\beta\delta}\, q_\gamma\, q_\delta\right) u_\beta \tag{85}$$

$$\alpha, \beta, \gamma, \delta, = 1, 2, 3\ ;$$

Nous obtenons de la sorte la matrice classique des oscillations (28) (29).

Au temps où il était permis de tenir le milieu cristallin homogène, en 1877, E. B. Christoffel (*) étendit les équations classiques (85) aux cristaux. Puis, quand Voigt eut défini les coefficients d'élasticité statiques du milieu cristallin, les théoriciens de l'élasticité portèrent ses coefficients dans la matrice classique à la place des coefficients d'élasticité, propres au milieu homogène. Ainsi, de proche en proche, les équations classiques des oscillations ont été appliquées au milieu cristallin.

(*) *Annali di Matematica*, série II, Tome VIII, p. 193 (1877).

Or la formule fondamentale (83) de la théorie classique des oscillations, celle qui définit les tensions en un point, est atteinte par un passage à la limite, possible seulement dans un milieu absolument homogène, impossible dans un cristal. Car la déformation du milieu cristallin, tout au moins la déformation sensiblement conforme à la loi de Hooke, c'est essentiellement le déplacement des atomes les uns par rapport aux autres. De sorte que le plus petit élément cristallin où nous puissions définir la déformation contient nécessairement des atomes nombreux : ses dimensions sont bornées inférieurement par les périodes du cristal. Si les atomes contenus dans cet élément oscillent, ils sont soumis à des forces de rappel. Donc la déformation de l'élément n'est pas linéaire. Car si elle l'était, chaque atome serait porté par la déformation dans une nouvelle position d'équilibre : il n'oscillerait point, il n'existerait pas d'onde élastique. Nulle part, dans un cristal dont les atomes oscillent, la déformation est strictement linéaire. La matrice classique A implique une telle déformation, elle ne peut donc s'appliquer au milieu cristallin; l'étendre à ce milieu c'est confondre dynamique et statique.

Mais si les forces de rappel entre les atomes devenaient centrales, les coefficients d'élasticité $\mathfrak{A}_{\alpha\gamma,\,\beta\delta}$ se confondraient avec ceux de Voigt, $c_{\alpha\gamma,\,\beta\delta}$; et le milieu cristallin, bien qu'hétérogène à l'échelle atomique, obéirait aux lois qui règlent l'élasticité d'un milieu homogène à toute échelle. L'écart entre les coefficients $\mathfrak{A}_{\alpha\gamma,\,\beta\delta}$ et les coefficients de Voigt, $c_{\alpha\gamma,\,\beta\delta}$, comme entre la matrice atomique B et la matrice classique A, est donc déterminé par l'écart entre les forces de rappel véritables et les forces centrales.

La matrice classique des oscillations A (29), est incompatible avec la structure atomique du milieu cristallin; elle est fondée sur les propriétés des déformations linéaires; et de telles déformations ne peuvent être produites par une onde élastique.

D'autre part, les théoriciens de l'élasticité classique considèrent uniquement les déformations linéaires qui sont pures (ou irrotationnelles). Limitons nous à ces déformations. Elles sont régies par les coefficients d'élasticité atomiques $\Lambda_{\alpha\gamma,\,\beta\delta}$ (75) qui ont la même symétrie que les coefficients de Voigt, et prennent les mêmes valeurs, rapportée au même système de référence. De la sorte les coefficients $\Lambda_{\alpha\gamma,\,\beta\delta}$ peuvent être pris en compte dans la matrice classique au lieu des coefficients de Voigt : après substitution, la matrice classique détermine les mêmes oscillations qu'avant. Or, la matrice atomique des oscillations, B (46), est fonction des coefficients d'élasticité

$\mathfrak{N}_{\alpha\gamma,\,\beta\delta}$ (45), qui diffèrent, en général, des coefficients $\Lambda_{\alpha\gamma,\,\beta\delta}$ (75). Donc la matrice atomique B diffère, en général, de la matrice classique A.

Reportons nous aux cristaux cubiques : leurs déformations linéaires sont pures, et, suivant la règle générale, leurs coefficients d'élasticité $\mathfrak{N}_{\alpha\gamma,\,\beta\delta}$ et $\Lambda_{\alpha\gamma,\,\beta\delta}$ sont en même nombre : 21.

Les premiers, $\mathfrak{N}_{\alpha\gamma,\,\beta\delta}$ prennent en général quatre valeurs distinctes :

$$1) \qquad \mathfrak{N}_{11,\,11} = \mathfrak{N}_{22,\,22} = \mathfrak{N}_{33,\,33};$$

$$2) \qquad \mathfrak{N}_{23,\,23} = \mathfrak{N}_{31,\,31} = \mathfrak{N}_{12,\,12} = \mathfrak{N}_{32,\,32} = \mathfrak{N}_{13,\,13} = \mathfrak{N}_{21,\,21};$$

$$3) \qquad \mathfrak{N}_{22,\,33} = \mathfrak{N}_{33,\,11} = \mathfrak{N}_{11,\,22} = \mathfrak{N}_{33,\,22} = \mathfrak{N}_{11,\,33} = \mathfrak{N}_{22,\,11};$$

$$4) \qquad \mathfrak{N}_{32,\,23} = \mathfrak{N}_{13,\,31} = \mathfrak{N}_{21,\,12} = \mathfrak{N}_{23,\,32} = \mathfrak{N}_{31,\,13} = \mathfrak{N}_{12,\,21};$$

Mais, si la position moyenne de chaque atome coïncide avec un centre de symétrie du milieu cristallin, les valeurs prises par les coefficients $\mathfrak{N}_{\alpha\gamma,\,\beta\delta}$ tombent à trois :

$$\mathfrak{N}_{32,\,23} = \mathfrak{N}_{22,\,33}$$

Les coefficients $\Lambda_{\alpha\gamma,\,\beta\delta}$, propres aux mêmes cristaux, n'ont, dans tous les cas, que trois valeurs distinctes :

$\Lambda_{11,\,11} = \mathfrak{N}_{11,\,11}$, correspondant au coefficient $c_{11,\,11}$ (*ou* c_{11}) de Voigt;
$\Lambda_{22,\,33} = \mathfrak{N}_{22,\,33}$, » » $c_{22,\,33}$ (*ou* c_{23}) »

$\Lambda_{23,\,23} = \dfrac{\mathfrak{N}_{23,\,23} + \mathfrak{N}_{32,\,23}}{2}$ correspondant au coefficient $c_{23,\,23}$ (*ou* c_{44}) de Voigt,

Donc $\Lambda_{23,\,23}$ diffère toujours de $\mathfrak{N}_{23,\,23}$ et de $\mathfrak{N}_{32,\,23}$.

Ainsi, même pour les cristaux cubiques, les coefficients d'élasticité $\mathfrak{N}_{\alpha\gamma,\,\beta\delta}$ et $\Lambda_{\alpha\gamma,\,\beta\delta}$ ne se confondent pas tous; et les deux matrices, classique A, et atomique B, sont différentes.

Bien entendu, cette différence tient à l'écart entre les forces de rappel véritables et les forces centrales. Si cet écart s'annulait, les coefficients $\mathfrak{N}_{23,\,23}$ et $\mathfrak{N}_{32,\,23}$ prendraient la même valeur, donc les coefficients $\mathfrak{N}$ et Λ deviendraient égaux, et les deux matrices

identiques. En outre, si la position moyenne de chaque atome coïncidait avec un centre de symétrie, les coefficients $\mathfrak{N}$ et Λ ne conserveraient plus que deux valeurs distinctes :

1) $\Lambda_{11,\,11} = \mathfrak{N}_{11,\,11}$ correspondant au coefficient c_{11} de Voigt;

2) $\Lambda_{23,\,23} = \Lambda_{22,\,33} = \mathfrak{N}_{23,\,23} = \mathfrak{N}_{22,\,33}$, ou $c_{44} = c_{23}$ (Cauchy),

Discussion du rapport de M. Laval

M. Bragg. — Mr. Laval's paper makes considerable demand on our courage! The theory of crystalline elasticity seemed formidable enough when we believed there were 21 coefficients in the general case. We know now that we must envisage 45. Nevertheless he deals with a very practical point which must be taken into consideration when we consider the stresses and strains of a distorted crystal. In a very simple case, Mr. Lomer and I encountered this feature when examining quantitatively the elastic behaviour of the bubble model. The analysis was made by Mr. Lomer. We had shown that in a two-dimensional array of bubbles, of diameter about one millimetre, the forces of attraction and repulsion closely followed those between metal atoms. It is not sufficient to regard the force between two bubbles as depending on the distance between centres alone; if one does so, one arrives at incorrect values of the shear and compressibility modulus and the Poisson's ratio. The force between two bubbles A and B depends on the positions of other bubbles touching A and B as well as are their distances of separation. This I understand to be equivalent to Laval's statement that the forces are not « central ». The effect is quite marked; for instance, Poissons ratio would be 0.5 on the simple assumption, whereas the full theory gives a value of about 0.65 which is borne out by experiment.

Crystal Growth and Dislocations

by F. C. Frank

1. THE THEORY OF CRYSTAL GROWTH

Introduction.

The history of the theory of crystal growth divides into two parts. One is the theory of the growth of ideally perfect crystals, starting with Willard Gibbs (1878), and then developed between 1920 and 1948 by various workers, notably Volmer (1920 onwards), Kossel, Stranski, Becker and Döring, Frenkel, and Burton and Cabrera. The second is the theory of the growth of imperfect crystals, commencing with Burton, Cabrera and Frank (1949). The second makes use of the results of the first : basic to both is some understanding of the atomic nature of a crystal surface in equilibrium. In the early work this point is disposed of by tacit assumption, and its theoretical study has only recently been undertaken (Burton and Cabrera 1949, 1951).

2. THE EQUILIBRIUM STATE OF A CRYSTAL SURFACE

It has usually been assumed that the faces of low index of a perfect crystal, when in equilibrium with its vapour (or solution) are atomically smooth, with the exception of small numbers of absorbed molecules, and of surface vacancies, and of successively smaller numbers of pairs, triads, etc., of these. Provided these numbers are small, it is not difficult to make some calculation of their magnitude. In particular the proportion of surface sites occupied by single adsorbed molecules (or surface vacancies) is expressed approximately by :

$$n_s = \exp(-W_s/kT) \qquad (1)$$

where W_s is about half the total evaporation energy W. To derive such a result, we neglect interactions between these surface singu-

larities. This becomes less justifiable as their number increases, and the problem must then be treated as a « cooperative » one. This has been undertaken by Burton and Cabrera, who arrive at the conclusion that for every rational face of a crystal there is a critical temperature, at which its surface roughness on the atomic scale increases rapidly with increase of temperature. This may be called a surface melting temperature. These temperatures have the same order of magnitude as the ordinary melting point, but are lower in the faces of higher index. It appears probable that most crystals retain some faces which have not « melted » in this sense, up to the ordinary melting point, when they are in contact with their vapours. They probably also retain some « unmelted » faces, in contact with their dilute saturated solutions in reasonably efficient solvents (since in such cases the temperatures as well as the surface energies are lower). This is probably not always the case when crystals are in contact with their own melts : such cases must be distinguished from the rest in the theory of crystal growth, and we shall return to their consideration later.

At all temperatures below which there exists, in the given environment, a set of « unmelted » faces capable of enclosing a geometrical solid, any other possible face of the crystal may be described as one of these principal faces, modified by « steps », one or more lattice spacing in height.

Steps of any orientation in a given face can in turn be described in terms of steps in certain principal directions in the face, modified by « kinks », which make a sideways displacement of the step by one lattice spacing. There is no critical temperature for the « melting » of a monolayer step. As was shown by Frenkel (1945) and Burton and Cabrera (1949), if n_+ and n_- is the number of kinks of opposite sign per atomic spacing measured along the nearest principal direction :

$$n_+ \, n_- = \exp(-2\, w/kT) \tag{2}$$

where for close-packed crystals with homopolar binding w is of the order of magnitude of 1/12 of the evaporation energy. The angle between the mean direction of the step and the nearest principal direction is given essentially by :

$$\tan \theta = n_+ - n_- \tag{3}$$

so that the mean kink density is :

$$n_+ + n_- = [4 \exp(-2\, w/kT) + \tan^2 \theta]^{1/2} \tag{4}$$

This is usually quite a high density : the lowest temperature at which one is likely to grow a crystal from its vapour is, let us say, that at which its vapour pressure is 10^{-10} atmospheres. W/kT is then 23, and w/kT therefore about 2. Then, even in the closest packed direction of a step, kinks occur every three of four atoms apart. Under the same conditions the fraction of surface lattice sites occupied by single molecules or surface vacancies is only about 10^{-5}. These considerations apply to crystals whose vapour is monatomic, or consists of molecules which have rotational freedom in the solid at its melting point. The kink density corresponding to a given vapour pressure will be smaller when the vapour molecules possess rotational degrees of freedom not present in surface molecules of the solid : similarly, it will be higher for ionic crystals, but it will never be zero, or negligibly small.

One other important consideration about the state of the crystal surface first emphasized by Volmer is the ease of surface diffusion. The most important measure of this is the mean distance x_s diffused by a molecule between arrival from the vapour and re-evaporation. This is given by the interatomic spacing a, multiplied by the square root of the frequency of jumping to neighboring positions divided by the frequency of jumping off into the vapour, and essentially by :

$$x_s = a \exp [W_s' - U_s)/2kT] \qquad (5)$$

where W_s' is the work of desorption (say about half the evaporation energy W — we have the exact equation $W = W_s + W_s'$) and U_s is the activation energy for surface migration (estimated to be about W/20). x_s/a is several hundred under the simple conditions considered above.

It follows from this that the rate of direct arrival of molecules from the vapour at any particular point on a crystal surface is generally small compared with the rate of indirect arrival by way of surface migration. The particular points of greatest importance are the kinks in the steps. The addition of one molecule at a kink constitutes Kossel's « *wiederholbare Schritt* » of crystal growth. The total energy released in bringing a molecule from the vapour to this point is precisely the evaporation energy. In equilibrium vapour, molecules join and leave these points with equal frequency. The rate of departure depends only on temperature, while the rate of arrival is proportional to vapour concentration (or more precisely, to the local concentration of absorbed molecules). Hence in super-

saturated vapour more molecules join the kinks than leave them and so the step advances. The formation of kinks in a step is an easy process, and we may assume as a good approximation that the kink density in a step of given orientation retains its equilibrium value whether growth is proceeding or not. We may not make this assumption for the step density, which at equilibrium is zero in a principal face. On a perfect crystal the growth process removes all steps initially present to the boundaries of the principal faces, i. e., to the crystal edges.

3. SURFACE NUCLEATION : THE THEORY OF GROWTH OF PERFECT CRYSTALS

Further growth of a perfect crystal, beyond the polyhedron of principal faces circumscribed to the initial shape, requires the initiation of new layers of the crystal. As was first appreciated by Gibbs (1878) this is a nucleation process, essentially like the nucleation of droplets from a vapour. Any island monolayer on the crystal surface, of finite size, has a higher vapour pressure than the infinite crystal. This increase may be attributed to the specific edge free energy of the monolayer. Burton and Cabrera (1951) have shown that when the ambient vapour pressure exceeds that in equilibrium with the infinite crystal by a factor α, the shape and size of the island monolayer in equilibrium with the vapour is given by the formula :

$$h(\theta) = s_0 \gamma(\theta)/kT \ln \alpha \qquad (6)$$

where $h(\theta)$ is the distance from the origin of a tangent, of orientation θ, to the boundary of the island, s_0 is the area per molecule in the layer, and $\gamma(\theta)$ is the specific free energy of the boundary at orientation θ. This result generalizes both the Gibbs-Thomson formula and the Wulff theorem, in two dimensions. In particular, at points where a circle (of radius r) centred on the origin touches the boundary, we have :

$$r = s_0 \gamma/kT \ln \alpha = a \Phi/2kT \ln \alpha \qquad (7)$$

We shall refer to this, loosely, as the radius of the critical nucleus, and sometimes disregard the fact that it is not circular. $s_0 \gamma$ has been replaced by $\frac{1}{2} a \Phi$, where Φ is an energy which in the simplest approximation is the neighour-neighbour binding energy in the crystal — say about 1/6 of the evaporation energy per molecule.

Any smaller island than is specified by (6) has a much higher

probability of evaporating than of growing larger. Any larger one has a much higher probability of growing than of shrinking. The island specified by (6) is referred to as the critical nucleus. The formation of a new layer thus depends on improbable fluctuations among aggregates of adsorbed molecules ultimately producing a critical nucleus. The probability of this occurrence is proportional to $\exp(-A_0/kT)$ where A_0 is half the total edge free energy of the critical nucleus. Apart from a numerical factor which can be calculated, and is close to one (it must for example lie between $\pi/4$ and 1 on a surface of fourfold symmetry), this « activation energy for nucleation » is given by :

$$A_0 = \Phi^2/kT \; ln \; \alpha \tag{8}$$

The rate of formation of critical nuclei is given essentially by

$$Z \, (S/s_0) \exp(-A_0/kT) \tag{9}$$

A formula of this type was first surmised by Volmer, and derived by Becker and Döring (1935) with the assumption of rectangular nuclei, within which restriction they could show that nuclei departing significantly from square shape were unimportant. S is the surface area of the crystal face under consideration. Z is essentially the rate of arrival of fresh molecules at single surface lattice sites. Even in a dense environment it cannot exceed about 10^{13}. On a crystal of millimetre dimensions the whole factor outside the exponential must be less than 10^{27} : in fact it is commonly around 10^{22}. For an appreciable growth rate of 10^{-3} layers per sec. (about 1 micron per month) it follows that $ln \; \alpha$ must be at least $(\Phi/kT)^2/90$, which with a typical value of (Φ/kT) signifies a supersaturation not less than 25 %. Fifty per cent or more is commonly necessary.

The nucleation rate is an extremely sensitive function of supersaturation. For a small change of the latter, it changes from a quite negligible value, to one which imposes no significant hindrance to growth whatever.

Volmer and Schultze (1931), thinking to verify this result, found a very different one. They studied the growth rate of individual iodine crystals in slightly supersaturated vapour at 0 °C. For supersaturations above 1 % the growth rate was a proportional to supersaturation. Only below this degree of supersaturation did it fall below proportionality, and then not abruptly.

On the other hand, the observations of Haward (1939) correspond strikingly to the expectations of surface nucleation theory. He

studied the deposition of various sublimable solids on a metal surface, coated with a previous deposit of the same substance, held at a fixed temperature and subjected to a vapour « beam » of controlled intensity. He used a weighing technique which measured the mean overall rate of deposition and would have been insensitive to the growth of a small proportion of crystals on the target. Fig. 1 is plotted from his data for Hg I_2 at 22.9 °C. As the figure shows, there is no appreciable growth or evaporation unless the beam intensity corresponds to more than about 40 % supersaturation, or 40 % subsaturation, and the rate of deposition or evaporation is equal to the excess or deficit from these critical values. (These figures are rough, since I_{eq} is an extrapolated figure, and also contains all the calibration errors of the apparatus. The ration of the critical intensities is more reliable). The ratio between the critical values increases slowly with decrease of temperature. This result is in astonishingly straightforward agreement with the theory of surface nucleation. In suggests, surprisingly, that most of the crystals in the compact deposit have perfect crystal surfaces, and are able in some way to protect each other's edges.

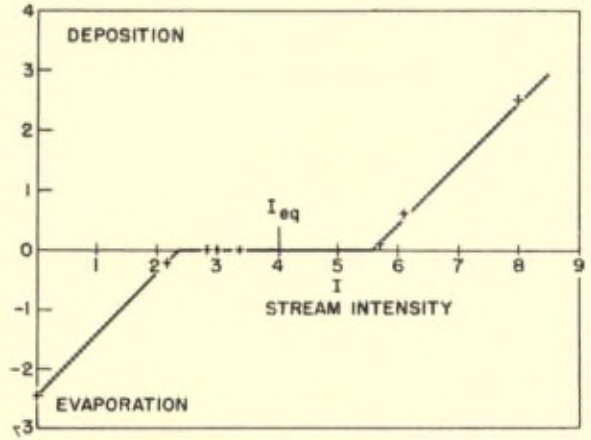

Fig. 1. — Rate of deposition, D, (and evaporation, —D) at HgI_2 surface at 22.9 °C, vs. vapour stream intensity I. I_{eq}^2 is the rate at which molecules from saturated vapour would strike the surface. D and I are in the same arbitrary units. Plotted from data of Haward (1939).

Similar observations were made with anthracene, the ratio of the two critical intensities being nearer to three.

There are no other observations of this kind. It is the general

experience that *those crystals which do grow* do so at rates proportional to supersaturation down to supersaturations much lower than the theoretical critical supersaturation of surface nucleation theory.

4. THE GROWTH OF IMPERFECT CRYSTALS

General Theory.

X-ray diffraction studies show that most real crystals are imperfect. Studies of the mechanical behaviour of crystalline solids have led to the recognition that some of the imperfections present are dislocations. A principal crystal face which contains the end of a screw dislocation will appear essentially like Fig. 2 : i. e., it will have a step, one of whose terminations is not at the boundary, but at the end of the dislocation. In this case growth of the crystal does not eliminate the step. The same is true for any dislocation whose Burgers vector has a component normal to the face in which the dislocation ends. Unlike the ideal crystal of n layers, this dislocated crystal consists of one layer only, in the form of a helicoid. When the dislocation is of multiple strength, we have a crystal of several interleaved helicoidal layers. When it contains several dislocations, it consists of a number (possibly one) of similar interleaved « Expanded Riemann surfaces ».

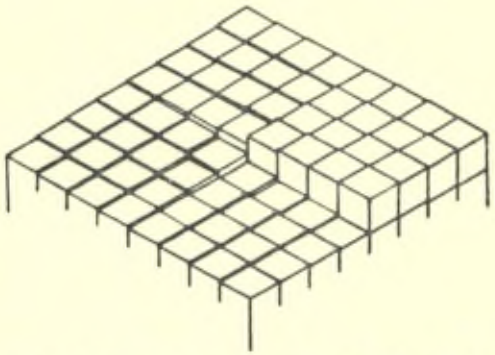

Fig. 2. — The end of a screw dislocation in a building-block crystal model. Each cube represents a molecule.

In general, the emergence of screw dislocations in a crystal face eliminates the need for surface nucleation on that face, provided only that the distance between pairs of dislocations, or between a dislocation and the boundary, exceeds the diameter of the critical

nucleus of surface nucleation theory. Suitably dislocated crystals are thus able to grow at arbitrarily low values of the supersaturation. The limiting case is a crystal whose faces are only twice as wide as the critical nucleus, which can just grow with a dislocation. This is the size of the critical nucleus in the theory of three-dimensional nucleation (Becker and Döring, 1935).

The theory of growth kinetics for dislocated crystals has been developed by Burton, Cabrera, and Frank (1949, 1951). The main principles of the theory are outlined below.

The step in a crystal face containing the end of only one screw dislocation will run to the boundary, nearly in a straight line, when the environment is just saturated. If supersaturation is now brought about, the step will advance. It can be shown fairly easily that the rate of advance of a « straight » step is :

$$v_0 = 2 (\alpha - 1) x_s Z_v \beta \qquad (10)$$

Where Z_v is the frequency with which molecules from the equilibrium vapour strike a lattice site in the surface, and β is a factor which is unity in simple cases, but may be less than unity if kinks are not close together compared with x_s, or if molecules do not always adhere to the kinks which they reach (*e. g.* if it is also necessary for them to arrive in the proper orientation).

Now, a curved step, whose shape corresponds to an arc of the boundary of the critical nucleus for the local supersaturation, will have a rate of advance zero. In the approximation that the critical nucleus is circular, of radius ρ_c, given by equation (7), the rate of advance of a step with radius of curvature ρ may be shown to be :

$$v = v_0 (1 - \rho_c/\rho) \qquad (11)$$

Hence, the step, initially straight, advances parallel with itself, with constant velocity v_0, over the greater part of its length, but in the neighbourhood of the dislocation end, where such advance would produce a sharp corner, it advances more slowly in such a way that its curvature is everywhere less than ρ_c^{-1}. This causes it to wind up into a spiral, centered on the dislocation end, with a spacing of approximately 20 ρ_c between turns. The final stationary form of this

rotating spiral, satisfying the differential equation (11) is given to a close approximation by :

$$r/\rho_c + ln\,(1 + 3^{-\frac{1}{2}}\, r/\rho_c) = 2\,(1+3^{-\frac{1}{2}})\,[\theta - v_0 t/2\,\rho_c\,(1+3^{-\frac{1}{2}})] > 0 \quad (12)$$

An approximation sufficient for most purposes is :

$$r/\rho_c = 2\,(\theta - v_0 t/2\,\rho_c) > 0 \quad (13)$$

The most important quantity to know is the number of turns of the spiral passing a fixed point in unit time, $v_0/4\,\pi\,\rho_c\,(1 + 3^{-\frac{1}{2}})$ since this quantity, multiplied by the step height, is the rate of growth of the crystal surface. Since v_0 is proportional to, and ρ_c inversely proportional to, the supersaturation $\alpha - 1$ (when this amounts to a few percent or less), the steady state growth rate is proportional to the square of the supersaturation.

This result is derived on the assumption that turns of the spiral are so far apart that they do not compete with each other for molecules from the vapour. This is no longer true, if they are closer together than twice the surface diffusion distance x_s : a further increase in step density beyond this scarcely contributes to the increase in growth rate, so that the latter now becomes proportional to the first power of the supersaturation. The full expression for growth rate, assuming a sufficient kink density in the steps is :

$$R = \beta\, d\, Z_v\, (\alpha - 1)\, (x_s/10\,\rho_c)\, \tanh\,(10\,\rho_c/x_s) \quad (14)$$

$$= \beta\, d\, Z_v\, (\sigma^2/\sigma_1)\, \tanh\,(\sigma_1/\sigma) \quad (15)$$

where :

$$\sigma = (\alpha - 1) \sim ln\,\alpha$$

and :

$$\sigma_1 = (10\,\rho_c/x_s)\, ln\,\alpha = 10\,\gamma\, s_0/x_s kT$$

This gives a transition from the parabolic law $R = \sigma d Z_v \sigma^2/\sigma_1$, at low values, to the linear law $R = \beta d Z_v \sigma$ at high values of the supersaturation, σ.

Crude theoretical estimates of γ and x_s for iodine at 0° C, by the methods of paragraph (2) make $\gamma\, a \sim 4\, kT$ and $x_s \sim 400\, a$, whence $\sigma_1 \sim 0.1$ The resulting curve is in reasonably satisfactory agreement with the observations of Volmer and Schultze (Fig. 3). Their non-observance of departures from the linear law with phospho-

rus and naphthalene suggest that for these substances $x_s > 10^4 a$, which is not improbable.

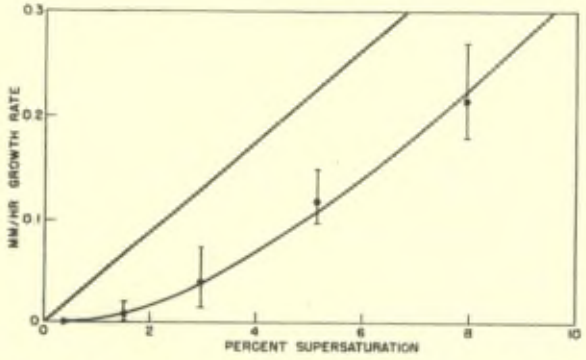

Fig. 3. — Growth rate of I_2 crystals from vapour at 0 °C (Volmer and Schultze, 1931). Mean value and range of scatter shown for 7 crystal faces, omitting one anomalously-slow-growing face, 2 (II).
Straight line : Hertz law, $\beta = 0.4$.
Curve : Equation (15), $\beta = 0.4$, $\sigma_1 = 0.1$.

5. THE SHAPES OF GROWTH SPIRALS

The growth spiral has « circular symmetry » (a paradoxical phrase which we shall re-examine presently) unless the factor β of equation (10) varies with orientation in the crystal face. An obvious source of variation is that when the step is parallel to certain close-packed directions, it may be relatively free from kinks. However, equations (4) and (5) and the accompanying estimates of energy parameters show that in general, when a crystal is growing from its vapour, the surface diffusion distance x_s will largely exceed the distance between kinks even in the step of closest-packed orientation. In this case the rate of advance of a step should not be appreciably dependent on orientation. (The molecule which misses a kink on its first approach to the step will still have several chances to find one before evaporating).

When a crystal grows from solution, x_s probably loses its significance, and is replaced by δ, the thickness of the effectively unstirred boundary layer of solution at the crystal surface. At low temperature the distance between kinks in a close-packed step may exceed this, the rate of advance of steps in this orientation will be reduced, and polygonal spirals will result.

The segments of the polygon will only be straight at the limit of very low temperatures; in general, they will be curved convexly, but the corners will be macroscopically sharp, having essentially the same curvature as the boundary of a critical nucleus.

The « stationary » shape of a polygonal growth spiral is defined by a variant of the Wulff construction.

All « corresponding » corners of the polygonal spiral are in line with one side of a polygon, which we may call the conjugate polygon : and the normal distances of a pair of straight segments of the spiral meeting at such a corner, from any point in the corresponding side of the polygon are in the ratio of their velocities of advance.

The rotational symmetry of a growth spiral may now be defined as the rotational symmetry of its conjugate polygon. It must possess at least the rotational symmetry of the crystal face, assuming a symmetrical environment.

The spacing between successive turns of a growth spiral is equal to the diameter of the critical nucleus multiplied by a numerical factor. It is, therefore, essentially inversely proportional to the supersaturation. The numerical factor is $2\pi(1+3^{-\frac{1}{2}})$ for spirals of circular symmetry according to equation (12) [or 2π according to the approximate equation (13)]. It takes other values of the same order of magnitude for various polygonal spirals, e. g., four for a square spiral. 2π will serve as a representative approximate figure for all cases.

A circular or polygonal spiral step on the crystal face will appear, macroscopically, as a low cone or pyramid of vicinal faces. The slope of its faces is inversely proportional to the spacing between turns and, therefore, proportional to the supersaturation. In order of magnitude, it is about 1 minute of arc per 1 % of supersaturation. We expect in general growth cones when a crystal grows from its vapour and growth pyramids when it grows from solution, with less curvature in the pyramid faces the lower the temperature.

6. INTERACTIONS OF GROWTH SPIRALS

The theory presented above assumes only one dislocation, or two of opposite sign, to be present. The presence of more makes remarkably little difference. Two dislocations separated by a distance large compared with $2\pi\rho_c$ can be the centers of two independent growth spirals so that the crystal face is divided into two regions, whose

growth steps radiate from the two centers. The growth rate is everywhere the same as if only one dislocation were present, but examination of the vicinal faces will reveal two growth hills. However, if the supersaturation at the center of one is slightly greater than that at the center of the other, the territory of the second will continually shrink and, if the conditions remain constant, ultimately only one growth hill will be visible. We say that one dislocation is dominating the other. If two dislocations of the same sense are closer together than $2\pi\rho_c$, they generate a pair of non-intersecting growth spirals, thus behaving like a dislocation of double strength. They are now said to be cooperating. A cooperating pair sends out growth steps twice as fast as a single dislocation. The growth rate in the regime of low supersaturation, which gives a parabolic law, is thus doubled; this chiefly means that the regime of the linear law is reached sooner, since it is difficult to make accurate observation in the regime of the parabolic law anyway.

The chief inferences are : (*a*) that observations of crystal growth rate alone tell us little more about the dislocation density than whether or not there is one screw dislocation emergent in each crystal face (*b*) that examination of vicinal pyramids on crystal faces does not necessarily show us all the screw dislocations emergent in the face. If we can eliminate the possibility that they are centered on specks of dirt which have settled on the face during growth, the number of pyramid apices gives a lower limit to the number of screw dislocations emergent. Only when techniques are available that make monomolecular steps in the crystal surface visible are we in a position to count all the screw dislocations emergent. As a rule, edge dislocations (meaning, in this context, those whose Burgers vectors lie in the plane of the crystal face) will still be invisible.

7. OBSERVATIONAL EXAMPLES

Growth pyramids of vicinal faces have long been recognized, and were so named by Miers (1903-1904). His studies and others, mainly qualitative, show general conformance to the theoretical expectations outlined above.

Growth pyramids are well seen on the major rhombohedral face of almost any quartz crystal. The number in a face varies from one to thousands, and their size from 15 cms to fractions of a millimeter. There is a specimen in the Field Museum in Chicago, in which a single

vicinal pyramid, with very flat faces, occupies the whole crystal face, about 15 cm across; in some natural crystals, and almost all artificial quartz crystals, the growth pyramids are numerous, and have distinctly curved faces.

Much more information can be obtained when we can see the edges of crystal monolayers. The first to do so knowingly was L. J. Griffin (1950), who studied surfaces of natural beryl crystals, by ordinary microscopy (later using phase contrast microscopy with advantage). In this case the step height is only 8 A, and the visibility of the step is probably due to localized natural etching of some kind. (Fig. 4).

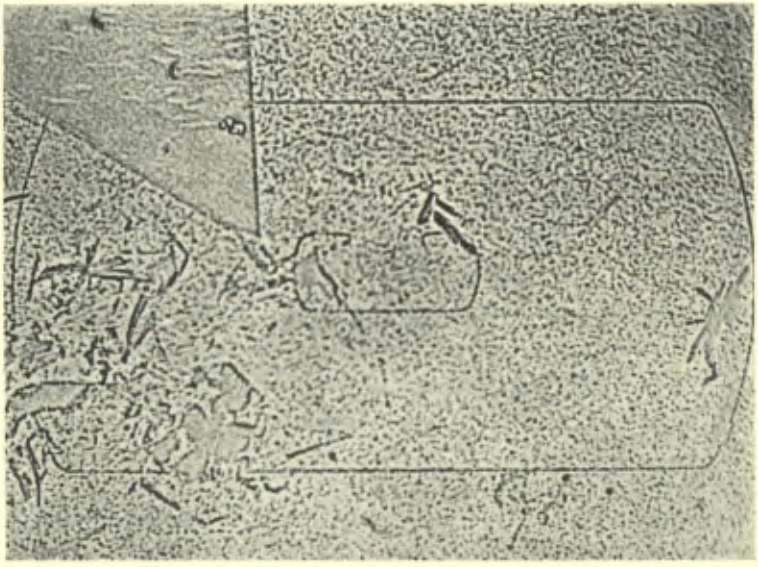

Fig. 4. — Growth steps on Beryl : $Be_3\ Al_2\ Si_6\ O_{18}$ (Griffin).

A much simpler case is provided by the long chain paraffin crystals ($C_{36}H_{74}$) grown from solution in light petroleum, studied by Dawson and Vand (1951). (Fig. 5 and 6). As the step height for a monolayer of these crystals is about 50 A., it is easily visible by direct electron microscopy after metal shadowing. The examples shown are selected for their simplicity. Other crystals with larger numbers of dislocations are also seen.

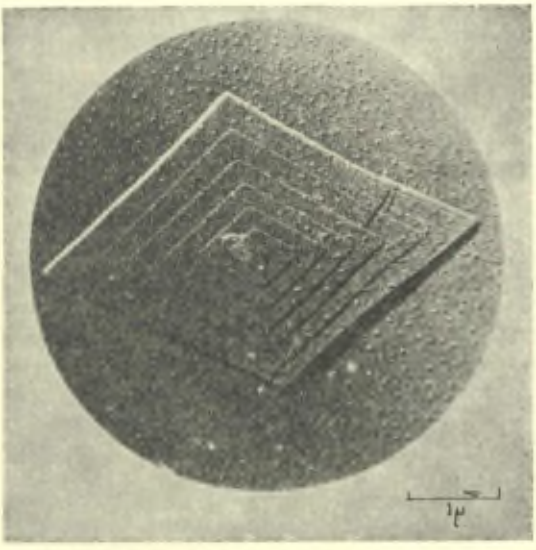

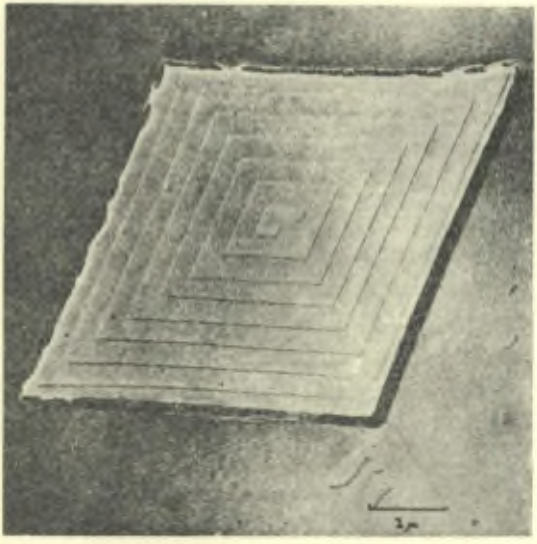

Figs. 5, 6. — Growth steps on long chain paraffin crystals : n — $C_{36}H_{74}$ (Dawson and Vand).

Silicon carbide provides another convenient case for observation. Spiral markings which may be seen with a low power magnifier, or the naked eye, have been known for some time (Menzies and Sloat, 1929). These often represent steps several hundred Angstrom units high. Verma (1951) and also Amelinckx (1951) have recently found that much smaller steps can be made visible by phase contrast microscopy on lightly silvered SiC surfaces, and that these correspond to the unit cell thickness, which is 15 A. for the common variety. The examples shown (Fig. 7 - 10) illustrate various points in the theory described above — a detailed discussion of them has been given by Frank (1951*a*). A point of particular interest is that the dislocations in SiC are often visibly hollow. This can be generally expected with a dislocation of Burgers vector exceeding about 10 A (Frank 1951*b*) unless it can easily dissociate into partial dislocations. Another is that the remarkable polytypism of carborundum (which has variant structures with repeating lattice units of up to 198 layers) is immediately comprehensible when we learn that the crystals frequently grow upon dislocations groups of large total strength.

Crystal growth based on dislocation groups of multiple strength, producing large growth steps (of height 80 A. upwards), but otherwise essentially similar to any other kind of crystal growth based on dislocations, can be followed while in progress by techniques developed by Forty (1951). He has made studies of CdI_2 and PbI_2 growing from aqueous solution. In favorable cases the step height can be measured with a precision of about 1 A, by use of interference fringes formed between the front and back surfaces of a thin crystal. A notable observation is that dislocations penetrating the basal plane are commonly absent initially in PbI_2 crystals, and are formed in a catastrophic event after considerable lateral growth has occurred. Until then the crystal grows as an extending plate with no increase of thickness whatever. The most probable explanation is that non-uniform distribution of impurties stresses the thin plate to its true yield limit, when it gives way by buckling and shearing to produce dislocation groups usually of large total Burgers vector.

Fig. 7

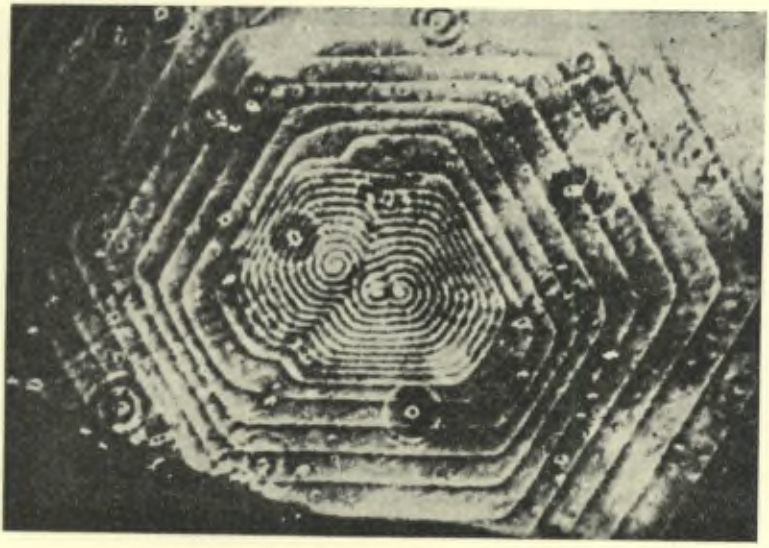

Fig. 8

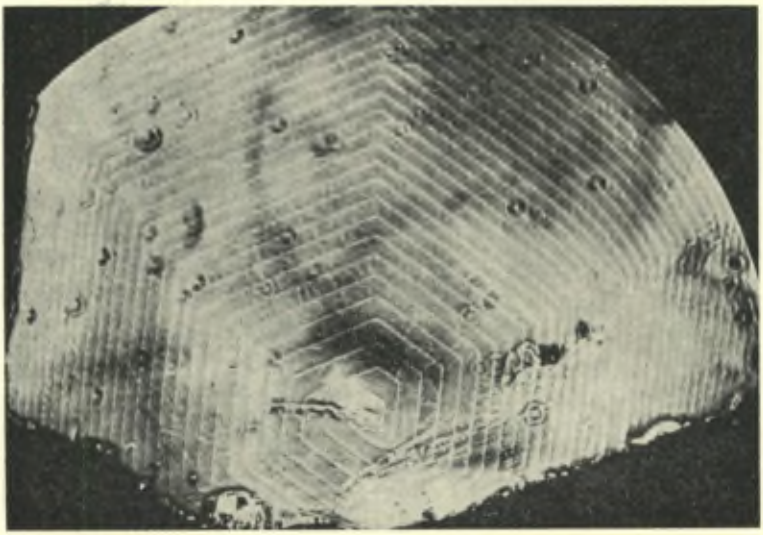

Fig. 9

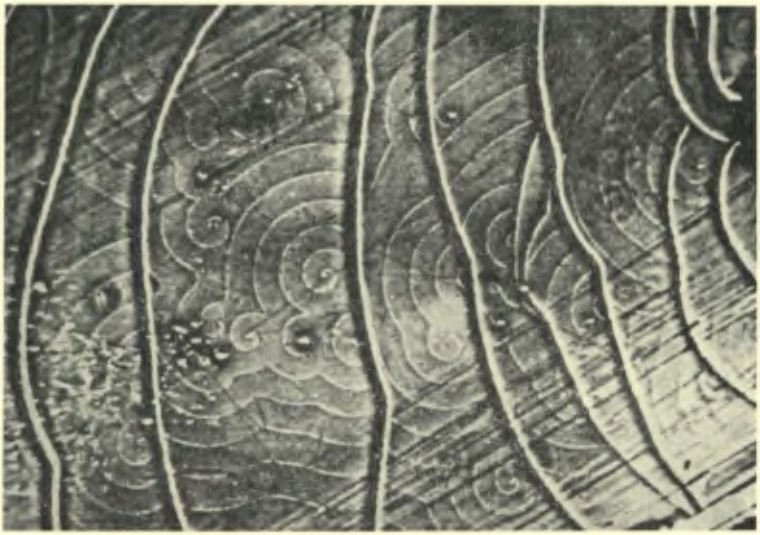

Figs. 7-10. — Growth steps on Carborundum, SiC (Verma).

8. THE ORIGIN OF DISLOCATIONS IN CRYSTAL GROWTH

The origin of the initial dislocations in a crystal presents no great problem. Either the crystal begins to grow on a foreign solid, which may be dislocated already, or its nucleation occurs at a very high supersaturation, which need only be a little higher to nucleate a dislocated crystal instead of a perfect one. Or, if dislocations are not created immediately, the probable mode of early growth is dendritic, and when the dendritic arms unite they are likely to do so in imperfect registration with each other, so producing dislocations. If growth then continues at low supersaturation, there is a natural selection of suitably dislocated crystals.

This, however, accounts only for one or a few dislocations emergent near the center of each growing face. Elsewhere, such crystals would be substantially perfect. While such crystals apparently exist, observations suggest that in the majority of crystals dislocations occur more or less throughout their volume. The writer is inclined to attribute this principally to deformations caused by impurities. Space will not permit a full discussion of such phenomena, but we may sketch an approach to the subject.

(*a*) If a solution contains two components capable of forming a mixed crystal, and $G_L(x)$, $G_S(x)$ are the free energies of liquid and solid as a function of molar fraction x, then if the tangent to $G_L(x)$ at the actual liquid composition x_L cuts the curve $G_S(x)$ at two points deposition can occur on crystal seeds within a finite range of compositions. The decrease of free energy is greatest for a composition x_S^* defined by :

$$G_S'(x_S^*) = G_L'(x_L) \tag{16}$$

where primes signify differentiation with respect to x. If there is only one seed of composition x_0, and the temperature is adjusted so that the deposition just occurs, the composition of the deposit, x_D is given by :

$$\frac{x_D - x_0}{x_S^* - x_0} = \frac{\alpha}{\alpha - \beta} \tag{17}$$

where :

$$\alpha = G_S''. \tag{18}$$

(higher derivatives being neglected) and :

$$\beta = 2\,a'\,VE/(1 - \nu) \tag{19}$$

a' is the derivative of lattice parameter with respect to x, V is molar

volume, E Young's modulus and ν Poisson's ratio. β is typically 10^{12} ergs. An order of magnitude for α is obtained by supposing it to arise only from entropy of mixing whence :

$$\alpha = RT/x(1 - x) \qquad (20)$$

so that α is 10^{13} ergs when $x = 1/4000$. α also contains temperature independent contributions. With decrease of temperature it can approach zero and become negative. The mixed crystal is then unstable, and will segregate if solid diffusion can occur ; but the composition of the deposit from solution is stably defined so long as $(\alpha + \beta)$ remains positive.

(*b*) If the substrate crystal is not homogeneous [and it cannot remain so during growth according to (*a*)] the appropriate value of x_0 is some mean value defined by the lattice parameter at the surface. Its determination involves the solution of an elastic problem. In general, it is not the same at all points of the crystal surface.

(*c*) With appropriate variation of composition, it is possible to have curved crystal lattices, free from dislocations, and as free from elastic stress as is possible in any kind of mixed crystal (i. e. when the local stress fields around individual atoms are averaged out). For example, the curved lattice generated by geometrical inversion of the simple cubic lattice, in which all lattice planes become spheres passing through the origin, still has almost perfectly cubic unit cells (with angular errors equal to lattice parameter divided by local radius of curvature). The lattice parameter is proportional to the square of the distance from the origin, so that this curved lattice can be occupied in a mixed crystal system allowing 5 % variation of lattice parameter throughout a spherical shell whose thickness is $2\frac{1}{2}$ % of its radius, or 5 % of the radius of curvature of the most highly curved lattice surfaces. A crystal bounded by lattice surfaces would show, qualitatively, the kind of curvature commonly observed in crystals of dolomite (Ca, Mg) CO_3. Non-cubic systems allow a greater variety of curved lattice than we have described here.

(*d*) When α is small compared with β, the crystal which deposits from solution will approximate to one of the unstressed curved forms mentioned under (*c*) and will be not much less stable in one of these than in the rectilinear lattice. It will grow on in the extrapolation of whatever curved lattice it has to begin with. However, it is characteristic of curved lattices that, since there is a limit to the variation of lattice parameter, the region in which they can be occupied is bounded. To grow outside this region the crystal must degenerate

into a « lineage structure » of roughly parallel overgrowths upon the curved core, or alternatively, undergo plastic deformation of the core. In the first case, the junctions of the overgrowths are the sites of dislocations.

(*e*) Plastic deformation of the core may proceed by displacement of dislocations already present. Unpublished observations by Griffin suggest that this may have occurred in the growth of Beryl crystals. Crystals which grow initially as very thin plates (CdI_2, PbI_2, hypothetically SiC) make a special case in that this deformation can occur in a catastrophic manner by buckling, so producing the very large dislocation groups and high growth steps which are observed.

(f) Much has been omitted from this account. An important point is that the composition of the liquid continually changes during deposition. What matters here is the composition of the liquid in contact with the crystal, which will become constant if there is no stirring. This agrees with the observation that crystals grown upwards from a melt are in general much more free from lineage structure than those grown downwards. Solid recrystallization eliminates stirring in the highest degree and is known to produce crystals which preserve lattice parallelism over great distances.

REFERENCES

J. W. Gibbs, 1878, *Collected Works*, p. 325 (1928), footnote.

M. Volmer, « Kinetik der Phasenbildung », Dresden und Leipzig : Steinkopff (1939).

W. Kossel, *Nachr. Ges. Wiss.* (Göttingen), p. 135 (1927).

I. N. Stranski, *Z. Phys. Chem.*, **136**, p. 259 (1928).

R. Becker and W. Döring, *Ann. Physik*, **24**, p. 719 (1935).

J. Frenkel, « Kinetic Theory of Liquids » Oxford : Clarendon Press (1946).

W. K. Burton and N. Cabrera, *Disc. Faraday Soc.*, **5**, pp. 33, 40 (1949).

W. K. Burton, N. Cabrera and F. C. Frank, *Nature*, **163**, p. 398 (1949).

W. K. Burton and N. Cabrera, *Phil. Trans. Roy. Soc.*, A **243**, 334 (1951).

W. K. Burton, N. Cabrera and F. C. Frank, *Phil. Trans. Roy. Soc.*, A **243**, 299 (1951).

J. Frenkel, *J. Phys. U. S. S. R.*, **9**, p. 392 (1945).

M. Volmer and W. Schultze, *Z. Phys. Chem.*, (A), **156**, p. 1 (1931).

R. N. Haward, *Trrans. Faraday Soc.*, **35**, p. 1401 (1939).

Sir H. A. Miers, *Proc. Roy. Soc.*, **71**, p. 439 (1903); *Phil. Trans. Roy. Soc.* (A), **202**, p. 459 (1904).

L. J. Griffin, *Phil. Mag.*, **41**, p. 196 (1950).

A. W. C. Menzies and C. A. Sloat, *Nature*, **123**, p. 348 (1929).

A. R. Verma, *Nature*, **167**, p. 939 (1951), *Phil. Mag.*, [1] **42**, 1005 (1951)

S. Amelinckx, *Nature*, **167**, p. 939 (1951).

F. C. Frank, *Phil. Mag.*, [1] **42**, 1014 (1951*a*).

F. C. Frank, *Acta Cryst.* **4**, 497 (1951*b*).

A. J. Forty, [1] **42**, 670 (1951).

Discussion du rapport de M. Frank

M. Bragg. — The very elegant treatment of crystal growth which Frank has given us depends upon the advancing step unit of molecular dimensions. Many of the exemples he has shown us, however, have steps of a thousand Angström, many molecular in thickness. Such steps are effective new crystal faces. How is it that the same laws of spiral growth apply?

M. Frank. — I think it is true that the « riser » of the step does sometimes come to be a new close-packed face of the crystal, or very nearly. But this face makes a re-entrant angle with the lower « land », in which new atoms can be preferentially attached, initiating a new monolayer on the rising face by which the step as a whole advances. At the same time it may initiate a new monolayer on the lower land. If the riser and the lower land are crystallographically equivalent faces, this will cause the multilayer step to dissociate into monolayer steps, unless (*a*) there is a stacking fault at the bottom of the multilayer, making its lowest monolayer naturally slow growing, or (*b*) impurities absorbed on the lower land, which has been exposed for a relatively long time, impede the advance of a new monolayer on it.

M. Bragg. — I think Frank's exposition here needs more clarification. The curve of free energy against composition only has a meaning for a homogeneous crystal. How can such a curve be drawn when the crystal is strained because it is not homogeneous? I do not see what the abscissa means in such a case.

M. Frank. — Let $G_s(x_1)$ be the free energy of the crystalline substance of composition x_1, forming part of a large homogeneous crystal. This corresponds to a point on the usual curve we draw for the dependence of the free energy of a crystalline substance on composition. Now let a slice of this crystalline substance be deformed elastically, doing an amount of work $W(x_1, x_2)$ against elastic forces,

until its surface lattice spacings correspond to those of a crystal of composition x_2. Let the slice now be united with a much thicker slice of crystal of composition x_2 : since the latter is much thicker, the combined body will now be in elastic equilibrium. The free energy of crystalline material of composition x_1 deposited on the substrate of composition x_2 is therefore $G_s(x_1) + W(x_1, x_2)$ which exceeds $G_s(x_1)$ unless $x_1 = x_2$. The curve of free energy against composition, for deposition on one given seed crystal, therefore rises above the curve for deposition in each case on the optimum seed crystal, which is usually plotted, and only touches this latter curve at one point.

M. Seitz. — Crystals of the rock salt type, such as the alkali and silver halides play an exceedingly important role in fundamental research with non-metals. I wonder if you would express your views on the mechanisms of growth in these cases, particularly when grown from solution or by vapor deposition.

M. Franck. — I think that under low supersaturation these crystals also grow by the mechanism I have described. I find, however, that I can best interpret the form of the Ag-Br crystals shown by Trivelli and Sheppard in their book « The Silver Bromide Frain of Photographic Emulsions » (Eastman Kodak Research Monograph No. 1 : New York : Van Nostrand Co. 1921) by supposing they grew by surface nucleation at their corners. So they may be free from dislocations.

It has been pointed out to me by Dr. J. W. Mitchell, however, that despite the title of the book, these are not typical photographic emulsion grains. The latter are, speaking broadly, crystals of Ag-Br grown on nuclei of AgI, and the resulting faults are probably essential to their photograph sensitivity.

M. Shockley. — If I understand Dr. Frank's remarks concerning silicon carbide correctly, they seem to me to be worthy of special emphasis. In some of the structures of Si - C the repeat distance may be thousands of lattice constants. These distances seem wholly unreasonable on the basis of any scheme of action at a distance. They now find a natural explanation in terms of Frank's picture, not of a repeating structure, but instead of a single structure simply overlaying itself after time. I should like to ask if the resulting struc-

Bild 1. — Eutektikum Zn + 3% Mg

Bild 2. — Eutektikum Zn + 3% Mg

tures are to be thought of simply as randomly arranged Si — and C - planes which are then repeated according to the accidental nature of the screw displacement on which they grow?

Very nearly : except that we need to understand why, when the pitch of the screw does not correspond to $6n$ layers, producing the common 6-layer hexagonal modification of Si-C, it most frequently corresponds to $(6n + 5)$ layers.

M. Bragg. — I feel that this paper of Frank is of fundamental importance, and that it marks a big advance in our understanding of crystal growth. The vital feature, which seems to me so important, is that the whole crystal consists of one and not of a series of superposed sheeds. A mistake in the stacking of molecular planes, once it has occurred, is thus perpetuated at completely regular intervals. We have been shown that it explains the case of silicon carbide in an elegant way, and I can think of other cases when this explanation may well be given by envisaging some such method of growth as that pictured by Frank.

M. Köster. — Zunächst lege ich zwei Gefügebilder von spiralartiger Ausbildung eines Eutektikums vor, die im System Zink-Magnesium beobachtet werden kann. (Bild 1 und 2).

Alsdann verweise ich auf Untersuchungen von L. Graf über das Wachstum von Kristallen aus der Schmelze, die in unseren Institut durchgeführt worden sind. Ich gebe das Ergebnis seiner Beobachtungen, deren Deutung in der Richtung eines soeben von Professor Orowan vortgetragenen Hinweises liegt, in der Form bekannt, wie sie Professor Graf zusammenfassend gegeben hat. Es handelt sich un mikrokopische Feststellungen über das lamellare Wachstum der Kristalle.

Bild 3 zeigt z. B. die Lamellenstruktur eines vielkristallinen Zinkgusstückes, Bild 4 einen Ausschnitt eines lamellierten Golddendriten. Diese Lamellenstruktur von Kristallen tritt auch bei sehr rasch erstarrten Metallen und Salzen unabhängig von der Kristallsymmetrie in ausgeprägter Form auf. Auch die in ihrer Schmelze gewachsenen vergröberten Dendriten hochsymmetrischer Salze und Metalle weisen eine ausgeprägte Lamellierung parallel zu den dichtest besetzten Netzebenen auf und bauen sich somit aus mehreren, unter verschie-

150 ×

Bild 3. — Oberfläche von rasch erstarrtem, vielkristallinem Zink-Guss, ungeätzt. Lamellarer Aufbau der Kristallite parallel zur hexagonalen Basisebene.

600 ×

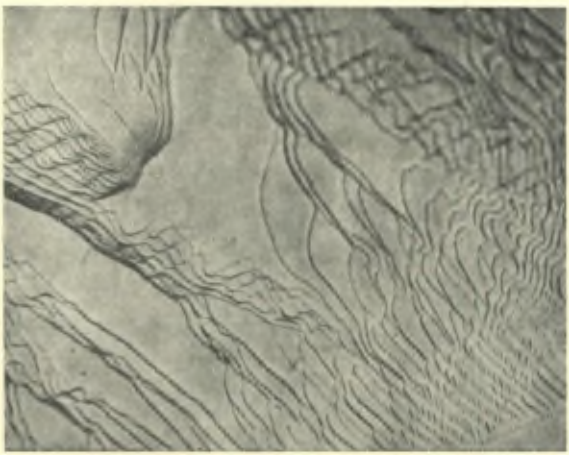

Bild 4. — Lamellenausbildung auf der rasch erstarrten Oberflächen eines Gold Kristalliten.

denen Winkeln zu einander geneigten Lamellensystemen auf. Bild 5 zeigt die Spitze eines Steinsalzdendriten mit Lamellierung parallel

160 ×

Bild 5. — Spitze eines in seiner Schmelze gewachsenen NaCl-Dendriten; Lamellenbildung parallel zur Würfelebene, Wachstumsrichtung des Dendriten parallel zur Würfelflächen-Diagonalen.

zu der an der Spitze ausgebildeten Würfelebene und Bild 6 die Spitze eines Kupferdendriten mit Lamellen parallel zur Oktaederebene. Diese Versuchsergebnisse stützen die Auffassung, dass es sich bei

300 ×

Bild 6. — Seitenansicht der Spitze eines in seiner Schmelze gewaschsenen Cu-Dendriten. Lamellenbildung auf den Oktaederebenen, Wachstumsrichtung des Dendriten parallel zur Würfelkante.

der Lamellenstruktur um eine grundsätzliche, mit dem Wachtsumsmechanismus der Kristalle verbundene Erscheinung handelt. Eine Bestätigung dieser Auffassung wird darin gesehen, dass die beobachtete Lamellendicke non 10^{-4} bis 10^{-5} cm bei Gold aus der Grenzflächenspannung zwischen festem und flüssingem Gold einerseits und der kritischen Schubspannung am Schmelzpunkt andereseits in bester Übereinstimmung berechnet werden konnte. Dies weist darauf hin, dass die bisher bei der Erklärung des Kristallwachstums unberücksichtigt gelassene Grenzflächenergie offensichtlich eine sehr wesentliche Rolle spielt.

Eine Berücksichtigung der Grenzflächenenergie führt zu der Erkenntnis, dass der wachsende Keim in seiner Schmelze zunächst kugelförmige Gestalt annimmt und nicht, wie bisher vorausgesetzt wurde, von ebenen, kristallographisch definierten Flächen niederer Indizierung begrenzt ist. Erst wenn nach Erreichen einer bestimmten, durch das Verhältnis von Grenzflächenspannung zur Schubfestigkeit zu berechnenden Grösse des Kugelkristalls der Einfluss der Grenzflächenspannung überwunden ist, kann der Kristall in eine andere Gestalt hineinwachsen.

Die Art des weiteren Auswachsens des Kugelkristalls hängt nunmehr davon ab, ob das Wachstum sehr nahe am Phasengleichgewicht und damit extrem langsam, oder sehr fern von Gleichgewicht und damit extrem schnell erfolgt. Im ersten Fall wird tangentiales Flächenwachstum stattfinden und damit die Therie von W. Kossel und I. N. S. Stranski Gültigkeit besitzen : aus der Kugel bildet sich ein ebenflächig begrenzter Kristall. Im zweiten Fall herrschen jedoch infolge vertikalen Flächenwachstums ganz andere Anlagerungsbedingungen, und aus der Kugel bildet sich je nach der Symmetrie des betreffenden Kristallsystems eine Lamelle oder ein Dendrit, wobei die Dicke der Lamelle bzw. der Äste des Dendriten durch den Kugeldurchmesser bestimmt wird.

Das weitere Wachstum der Kristalle fern vom Phasengleichgewicht erfolgt in der Weise, dass sich auf einer vorhandenen Lamelle, ähnlich wie in der Schmelze, ebenfalls ein räumlicher Keim bildet, der in Kugelform auswächst und anschliessend wieder in lamellares Wachstun übergeht, wobei dieses durch die Unterlage katalytisch beschleunigt wird, sodass auch hochsymmetrische Kugelkristalle lamellar auswachsen.

Bei hochsymmetrischen Kristallen tritt lamellares Wachstum erst

auf, wenn sich aus den dünnen Ästen und Zweigen durch Zusammenwaschen derselben ein vergröberter Dendrit gebildet hat, an dem die dichtest belegten Netzebenen mehr und mehr in Erscheinung treten. Die Paraboloid-ähnliche Form der Spitzen sowie der Abstand der Seitenäste des vergröberten Dendriten sind durch die Wärmeableitungsverhältnisse in der Schmelze bedingt.

Mit grosser Wahrscheinlichkeit ist die Wachstumslamellenstruktur identisch mit der sogenannten « Mosaikstruktur » des gegossenen, d.h. in seiner Schmelze gewachsenen Kristalls, womit diese Fehlstruktur auf den Wachstumsmechanismus der Kristalle zurückgeführt wird.

M. Guinier. — Est-ce que les spirales ont été observées sur des cristaux plastiques? Peut-on avoir l'espoir de se servir des figures pour révéler le comportement des dislocations pendant la déformation plastique?

M. Frank. — The paraffin crystals are plastic. Some of the electronmicrographs of these show, in addition to the growth pattern, markings which we attribute to slip induced by crumpling of the supporting film. These are rather complex, however, and it seems rather difficult to stress crystals of electron-microscopic size in a controlled manner.

Remarkably enough, however, we have evidence of past slip in natural beryl crystals. Griffin will shortly be publishing photographs in which the observed pattern is uninterpretable by growth alone, but can be interpreted when we suppose that in addition the dislocations have moved, by a distance commonly of the order of magnitude 10 microns, usually following the trace of the basal plane. There is also evidence of limited slip bands, comprising a number of dislocations, both on basal planes and prim planes of the crystal.

We have not yet been able to make observations on metals, but have hopes of doing so.

Etude des interférences des ondes d'agitation thermique dans les cristaux : application à l'activation des transformations

par C. Crussard

I. INTRODUCTION

Les modifications de structure à l'état solide sont déclenchées, ou, — pour employer le mot propre — activées, par l'agitation thermique. Certains phénomènes, tels que la diffusion, ne font appel qu'à des mouvements d'atomes individuels, ou, à la rigueur, de quelques atomes; par contre, la plupart des transformations ne peuvent être provoquées que par des mouvements synchrones d'un certain nombre d'atomes, constituant un embryon (*), et se déplaçant tous dans le même sens. Nous appellerons dans la suite *volume embryonnaire* le volume V_e contenant ces atomes, et *mouvements coopératifs* des mouvements de ce genre. Les exemples de transformations abondent, qui sont susceptibles d'être déclenchés par des mouvements coopératifs : transformation allotropiques (sauf celles qui débutent par une précipitation cohérente ou amas de Guinier-Preston), comme l'a montré P. Laurent ([2]); transformations martensitiques; naissance des glissements plastiques et formation de dislocations (**) (nous prenons ici le mot « transformation » dans un sens large); macles mécaniques. Dans tous ces cas, la transformation peut être amorcée par un basculement ou glissement d'un petit volume embryonnaire, dans une direction cristallographique bien définie, suivi

(*) Nous adoptons ici la terminologie proposée par Fisher, Hollomon et Turnbull pour l'étude de la germination transitoire (1).

(**) L'impossibilité où l'on était jusqu'ici d'évaluer les probabilités de tels mouvements coopératifs a incité beaucoup d'auteurs à admettre que les embryons de martensite et les dislocations sont des défauts congénitaux des cristaux métalliques, formés au cours de leur croissance. Nous reviendrons sur ce point plus loin.

parfois de réajustements locaux. Nous ne parlerons pas dans ce qui suit des mouvements d'extension locale, qui peuvent amorcer les ruptures.

Or l'agitation thermique des atomes d'un cristal n'est pas désordonnée; on sait qu'elle se produit par ondes planes. Il est tout naturel d'imaginer que les mouvements coopératifs de glissement sont activés par une *onde transverse* d'amplitude exceptionnelle, et d'essayer de calculer la probabilité d'un tel phénomène par la statistique de ces ondes. C'est là un problème d'interférence : il se peut qu'à un certain moment un certain nombre d'ondes soient en phase, en sorte que leurs amplitudes s'ajoutent, et non leurs énergies, ce qui peut produire de fortes amplitudes résultantes.

Dans un premier essai (3), j'avais obtenu une formule peu satisfaisante, car elle reposait sur des hypothèses un peu arbitraires, et de plus elle avait un grave défaut : lorsqu'on faisait tendre le volume embryonnaire vers celui d'un atome, on ne retrouvait pas la formule de Boltzmann classique, ce qui indiquait évidemment une erreur.

La présente communication a pour but d'exposer une méthode qui semble plus satisfaisante. Mais auparavant, passons sommairement en revue dans la littérature scientifique la question de l'activation des transformations à l'état solide.

Tout d'abord, la mécanique statistique nous apprend que la probabilité pour que l'*énergie libre* de l'ensemble d'un solide s'élève d'une quantité ΔG au-dessus de sa valeur moyenne est proportionnelle à :

$$\pi_1 = \nu e^{-\frac{\Delta G}{kT}} \qquad (1)$$

où υ représente un facteur de fréquence.

On a parfois utilisé une extension de la formule (1) par des raisonnements qui se ramènent tous à celui-ci : on considère *a priori* un petit volume V_e égal au volume embryonnaire et, d'après (1) on y calcule la probabilité d'avoir un excès d'*énergie* ΔU (4). Celle-ci est proportionnelle à :

$$\pi_2 \div e^{-\frac{\Delta U}{kT}} \qquad (2)$$

à un facteur d'entropie près. Mais la grosse difficulté, à la fois pratique et théorique, vient précisément de ce terme d'entropie : en réalité, la définition même de l'entropie devient très délicate lorsque le nombre d'atomes du système envisagé diminue. En outre, on n'a

pas le droit d'isoler ainsi par la pensée le volume V_e, car s'il produit dans ce volume une concentration d'énergie thermique, c'est en général au détriment des zones avoisinantes.

On a envisagé de tourner la difficulté en appliquant au cas qui nous intéresse les théories de cinétique chimique développées par Eyring, et dans lesquelles on considère un équilibre entre des « complexes activés » et des molécules non activées. Une transposition de ces théories a été faite à la formation des dislocations ([5]); on y envisage un mouvement coopératif de cinq atomes dans un très petit volume embryonnaire, que l'on assimile à une molécule. Cette assimilation n'est pas du tout justifiée; en outre, les volumes embryonnaires considérés sont trop petits, et lorsqu'on en considère de plus grands, les probabilités données par cette théorie sont beaucoup trop faibles.

Toutes ces théories négligent la nature fondamentale de l'agitation thermique, qui est de se produire par ondes élastiques planes, et ne sont par conséquent pas rigoureuses, — sauf évidemment la formule (1), qui est fondamentale. En analysant les fluctuations d'énergie que l'on peut déduire de cette dernière, Léon Brillouin a envisagé ([6]) le cas d'un corps noir à température T, où les ondes (électromagnétiques) de fréquence ν, à $d\nu$ près, possèdent une énergie :

$$E = V. \frac{8 \pi h \nu^3}{c^3} \frac{1}{e^{\frac{h\nu}{kT}} - 1} d\nu \qquad (3)$$

(V est le volume du corps noir et c la vitesse de la lumière); il a calculé la valeur quadratique moyenne des fluctuations d'énergie pour ce groupe d'ondes; nous modifierons légèrement sa formule originale pour l'écrire :

$$\overline{\Delta E^2} = h \nu E \left(1 + \frac{1}{e^{\frac{h\nu}{kT}} - 1} \right) \qquad (4)$$

Le premier terme de cette somme correspond évidemment aux fluctuations sur le *nombre de quantums* (ici de photons) par onde, alors que le second est dû aux *interférences* entre ondes. On voit donc apparaître ici le terme d'interfèrences que nous cherchons; on peut donc songer à transporter ce calcul dans le cas des ondes d'agitation thermique d'un solide. Malheureusement, les fluctuations que l'on obtient ainsi sont relatives à l'*ensemble* du volume. Or, ce qui nous intéresse, c'est de savoir si *localement* les interférences ne peuvent pas produire un supplément d'énergie dans un petit volume,

même *sans changement de l'énergie totale*, en concentrant l'énergie des ondes dans le volume embryonnaire, au détriment des zones avoisinantes.

Il faut donc considérer le problème local des interférences.

Polanyi et Wigner (7) ont esquissé le calcul, pour les ondes d'un réseau linéaire, à une dimension. Le calcul donne bien un certain facteur de fréquence, qui joue le même rôle que le facteur ν de la formule (1), mais ne donne aucun renseignement nouveau pour le facteur exponentiel, pour lequel les auteurs supposent la forme (2), sans démonstration complète. En outre ce calcul suppose, tout-à-fait gratuitement, qu'à un moment donné toutes les ondes sont en phase. Enfin l'extension faite par les auteurs au problème tridimensionnel ne semble pas valable.

Une théorie cinétique beaucoup plus intéressante et complète a été faite par Slater (8) pour les réactions monomoléculaires. Elle échappe aux critiques que nous venons de faire. On pourrait songer à la transposer aux transformations des solides, en considérant ceux-ci comme une juxtaposition de petits volumes embryonnaires, dont chacun serait assimilé à une molécule. Malheureusement, cette assimilation ne semble pas très justifiée, car les molècules sont indépendantes, et échangent leurs énergies par chocs, ce qui n'est pas le cas pour les volumes embryonnaires. D'autre part, le calcul de Slater suppose que les fréquences propres sont *linéairement indépendantes*, ce qui n'est pas le cas dans les cristaux cubiques, où les nombres d'onde sont multiples entiers d'une même quantité; il en résulte que toutes les ondes ayant à peu près même direction et même fréquence (donc même vitesse) sont *linéairement dépendantes*. Pour résoudre le problème qui nous préoccupe, nous ne pouvons pas procéder par analogie, et nous sommes donc forcés de construire la théorie depuis le début.

II. CALCUL DE LA PROBABILITÉ DES MOUVEMENTS COOPÉRATIFS

Nous considérerons dans cette section un cristal indéfini, à structure idéale, dépourvue de défauts, dans lequel nous étudierons un volume V contenant N atomes, et satisfaisant aux conditions cycliques de Born; c'est ce que Olmer appelle une « maille cinétique » (9). Ces légères restrictions ne nuisent en rien à la généralité de la solu-

tion; elles évitent simplement d'avoir à étudier les perturbations introduites par des conditions aux limites compliquées, qui rendent quasi-impossible toute description mathématique de l'agitation thermique. Nous indiquerons qualitativement comment ces perturbations peuvent modifier le résultat.

Dans ces conditions, les vibrations propres indépendantes de ce volume correspondent à 3N ondes planes dont N longitudinales et 2 N transverses. Chaque onde de fréquence ν possède une *énergie moyenne* :

$$\mathcal{E} = h\nu \left(\frac{1}{2} + \frac{1}{e^{\frac{h\nu}{kT}} - 1} \right) \qquad (5)$$

$h\nu$ représente l'énergie de chaque quantum, et le terme entre parenthèses le nombre moyen de quanta par onde. Ce nombre est sujet à fluctuations.

Le premier terme de l'expression (5), le demi-quantum $\frac{h\nu}{2}$, mérite quelques explications. Il représente l'énergie de l'onde au zéro absolu. Cette énergie provient de l'application du principe d'Heisenberg à un solide cristallin : la notion même de « solide » implique que l'on fixe la position des atomes, sinon rigoureusement, du moins dans les limites étroites; il en résulte que la vitesse de ceux-ci est indéterminée, autrement dit, peut osciller, entre des valeurs extrêmes définies par la relation d'Heisenberg. Or d'après un calcul classique, l'énergie ou zéro absolu d'un oscillateur harmonique est égal à un demi-quantum. Ce résultat s'applique aux vibrations propres du cristal que nous supposons rester dans le domaine élastique; leur énergie au zéro absolu est donc $\frac{h\nu}{2}$.

Le point important, au point de vue de l'activation, est qu'au zéro absolu le nombre de quantums par onde est fixe, et ne subit aucune fluctuation. Une accumulation locale d'énergie, ne peut donc provenir que d'un phénomène d'interférence, qui est probablement susceptible de produire une activation même au zéro absolu.

Le deuxième terme de l'équation (5) représente la part proprement « thermique » de l'agitation, due à l'équilibre thermique avec le milieu ambiant et à l'équipartition de l'énergie entre les vibrations propres du solide et l'énergie des molécules ou photons qui viennent cogner sa surface. Cette équipartition se produit par l'inter-

médiaire d'un système d'ondes superficielles, que l'on peut assimiler à des ondes capillaires ([10]); mais en profondeur, on peut admettre que seules subsistent les fréquences propres de la maille cinétique.

La répartition des fréquences des vibrations propres a été calculée théoriquement ([11]) ([12]). Mais, à ces évaluations assez approximatives, il est préférable de substituer la très belle détermination expérimentale directe qui en a été faite par Olmer dans le cas d'un métal comme l'aluminium ([9]), et dont les vérifications quantitatives sont nombreuses. Si N (ν) est le nombre de vibrations propres possédant la fréquence ν à $d\nu$ près, nous admettrons donc que $\frac{N(\nu)}{N}$ est représenté par une courbe analogue à celle de la figure 1, extraite du travail d'Olmer (cette courbe a été tracée en prenant pour intervalle $d\nu = 10^{11}$ sec^{-1}; il est probable qu'en prenant un intervalle plus petit, on ait des pointes encore plus aiguës). Dans cette figure, la courbe qui

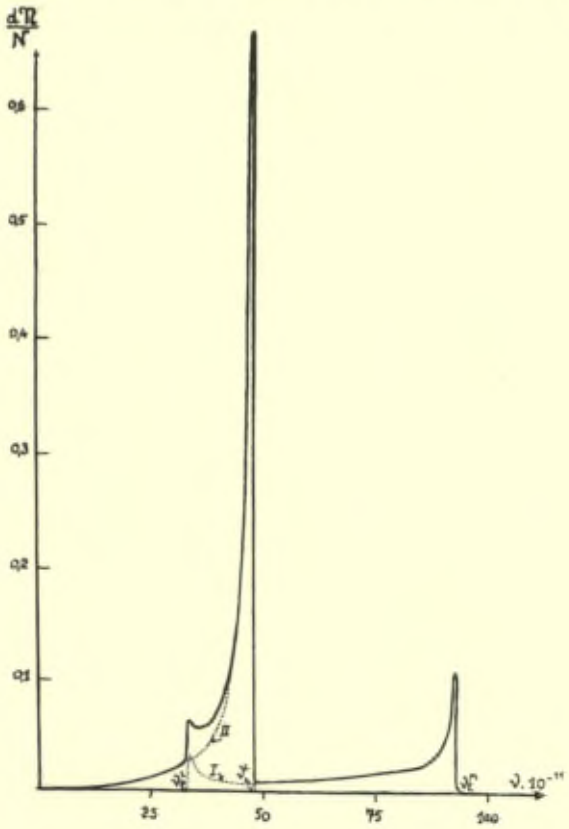

nous intéresse, est la courbe II, relative aux ondes transversales. On peut admettre une courbe analogue pour tous les cristaux de métaux purs, formés d'une seule sorte d'atomes, dont nous nous occupons ici. Dans la suite N (ν) représentera la densité de répartition des ondes transversales seules.

Un mouvement coopératif de l'espèce que nous étudions, est déclenché par une onde de glissement, ou onde transversale parallèle à un plan réticulaire donné, et à une direction donnée de ce plan. Les ondes qui y contribuent ont donc un vecteur de propagation de direction déterminée, perpendiculaire au plan de glissement dans les cas les plus simples. Pour chaque vecteur de propagation, il y a deux ondes transverses; on peut toujours choisir l'une d'elles dans la direction de glissement, et l'autre perpendiculaire; de sorte que, pour chaque vecteur, il y a toujours une et une seule onde contribuant au glissement considéré. Il n'est pas nécessaire que le plan de l'onde soit rigoureusement parallèle au plan de glissement; des plans qui s'en écartent légèrement peuvent également contribuer au mouvement, en sorte que les vecteurs de propagations intéressants sont compris dans un petit angle solide $d\omega$. En outre, le volume embryonnaire ayant dans presque tous les cas la forme d'une lentille aplatie, l'épaisseur de cette lentille doit être de l'ordre de la demi-longueur d'onde, en sorte que seules les ondes d'une certaine fréquence ν, à $\Delta\nu$ près, contribuent au mouvement. Comme le sens de propagation des ondes n'a pas d'importance, qu'on peut admettre que la densité de répartition est pratiquement isotrope, et qu'une onde transversale sur deux seulement intervient, le nombre total d'ondes contribuant au mouvement coopératif est :

$$n = \frac{1}{2} \cdot \frac{d\omega}{2\pi} \cdot N(\nu)\,\Delta\nu = \chi N \qquad (6)$$

où $N(\nu)\,\Delta\nu$ est la densité de répartition des ondes transversales (courbe II de la figure 1), et N le nombre d'atomes du volume V considéré. Cette égalité définit le *coefficient χ d'utilisation* des ondes.

A chaque type de transformation, donc d'embryon, correspond un certain $d\omega$ ou un certain $\Delta\nu$, donc un certain coefficient χ. Nous reviendrons plus loin sur la détermination de ces quantités, à propos d'exemples concrets.

Pour l'instant, nous nous proposons de résoudre le problème suivant : étant donné ces n ondes, comment interfèrent-elles en un

point quelconque O, qui sera le centre du volume embryonnaire éventuel ? En O, l'équation de chaque onde est :

$$x_i = A(\nu) \cos(2 n \nu t + \varphi_i) \tag{7}$$

l'amplitude A (ν) étant reliée à la fréquence par la relation évidente :

$$\varepsilon = 2\pi^2 m \, N. \, A^2(\nu) \, . \, \nu^2 \tag{8}$$

où m est la masse de l'atome.

On ne sait rien sur les phases φ_i; il faut donc admettre qu'elles sont réparties au hasard.

Le problème statistique comprend donc deux variables aléatoires indépendantes pour chaque onde : son nombre de quanta, et sa phase.

Dans un cristal parfait, tel que nous l'avons supposé, il n'y a pas de diffusion des ondes par des défauts internes, et les fluctuations du nombre de quanta provient des fluctuations dans les chocs superficiels. A l'intérieur du cristal, les fluctuations d'énergie qui en résultent sont indépendantes de celles dues aux interférences. On peut donc n'en pas tenir compte; elles ne feraient d'ailleurs qu'augmenter les probabilités que nous calculerons dans la suite. Nous supposerons donc le nombre de quanta égal à la moyenne donnée par (5).

Reste la phase. En représentant les ondes dans le plan complexe, le problème statistique revient à ceci : étant donné n vecteurs de même longueur A (ν), mais d'orientation répartie au hasard, quelle est la probabilité pour que leur somme (qui représente l'amplitude résultante) ait un module égal à une grandeur donnée α, à $d\alpha$ près. Un problème analogue a été traité par Lord Rayleigh, et généralisé par Chandrasekar ([13]); on trouve pour la probabilité cherchée :

$$W(\alpha) \, d\alpha = \frac{2\alpha}{n A^2(\nu)} \cdot e^{-\frac{\alpha^2}{n A^2(\nu)}} d\alpha \tag{9}$$

d'où l'on déduit par intégration la probabilité pour que le module de la somme soit supérieur ou égal à α :

$$W(\alpha) = e^{-\frac{2\alpha}{n A^2(\nu)}} \tag{10}$$

Comment utiliser pratiquement cette formule?

Le glissement unitaire (ou distorsion) correspondant à une onde

d'amplitude A et de l'ongueur d'onde λ est maximum au nœud de l'onde, où il vaut :

$$\delta = A \cdot \frac{\pi}{2} \cdot \frac{4}{\lambda} = \frac{2\pi A.\nu}{C} \tag{11}$$

en appelant C la vitesse *de phase* de l'onde.

La valeur moyenne du glissement correspondant au groupe des n ondes que nous considérons est donc :

$$\Delta = \frac{2\pi A(\nu)\sqrt{n}.\nu}{C} \tag{12}$$

on a aussi, d'après (8) :

$$\Delta^2 = \frac{2n\varepsilon}{m C^2 N} = 2\chi \frac{\varepsilon}{m C^2} \tag{13}$$

La probabilité pour qu'au point O le cisaillement local dû aux n ondes considérées soit égal ou supérieur à une certaine valeur δ est donc, d'après (10) et (13) :

$$W(\delta) = e^{-\frac{\delta^2}{\Delta^2}} = e^{-\frac{mc^2}{2\varepsilon} \cdot \frac{\delta^2}{\chi}} \tag{14}$$

Il suffit, pour chaque type de transformation, de connaître la valeur critique, δ_c, du glissement, au-delà de laquelle la transformation de l'embryon se poursuit et s'achève toute seule : cette valeur δ_c correspond en somme au seuil d'énergie de distorsion qu'il faut franchir pour activer la transformation. La formule (14) donne alors la probabilité de cette activation.

III. REMARQUES COMPLÉMENTAIRES

A. Forme du volume embryonnaire.

Cherchons le *volume d'interférence* dans lequel le calcul d'interférence ci-dessus est applicable. Soit OX la direction de glissement, *xoy* le plan de glissement, et *oz* la normale à ce plan. Les plans des n ondes considérés sont voisins de *xoy*; leur normale est comprise dans un petit cône d'angle solide $d\omega$ et d'axe *oz*. Supposons pour

simplifier, que ce petit cône soit à section carrée, c'est-à-dire que les ondes considérées sont définies par les conditions suivantes :

$$\begin{cases} \text{angle de la normale avec } yoz,\ \xi, \text{ compris entre } -\theta \text{ et } +\theta \\ \text{angle de la normale avec } xoz,\ \eta, \text{ compris entre } -\theta \text{ et } +\theta \end{cases} \quad (15)$$

auquel cas, si θ est petit :

$$d\omega = 4\,\theta^2 \quad (16)$$

Considérons un point M (x, y) dans le plan xoy. Pour une onde d'orientation (ξ, η) la différence de phase entre ce point et l'origine O est évidemment :

$$\psi = 2n\,\frac{x\,\xi + y\,\eta}{\lambda} \quad (17)$$

L'amplitude résultant des n ondes au point M sera donc

$$\sum_n \cdot A(\nu) \cos\left(2\pi\,\nu t + \varphi_i + 2\pi\,\frac{x\,\xi + y\,\eta}{\lambda}\right) \quad (18)$$

Le nombre n est assez grand pour que l'on puisse décomposer l'intervalle total de variation de ξ et η en éléments $d\xi$ et $d\eta$ où l'on peut répéter le raisonnement statistique qui nous a conduits aux formules (9) et (10). Autrement dit l'amplitude au point M est égale à l'amplitude au point O multipliée par un facteur :

$$I = \frac{1}{4\,\theta^2} \iint_{(-\theta,+\theta)} \cos\left(2\pi\,\frac{x\,\xi + y\,\eta}{\lambda}\right) d\xi\,d\eta \quad (19)$$

En développant le cosinus, on peut intégrer séparément en et l'on trouve :

$$I = \frac{\lambda^2 \sin\left(\frac{2\pi x}{\lambda}\,\theta\right) \times \sin\left(\frac{2\pi y}{\lambda}\,\theta\right)}{4\,\pi^2\,xy\,\theta^2} \quad (20)$$

En O, le facteur est égal à 1 ; sur ox et oy, il s'annule en des points d'abscisse $\pm\frac{\lambda}{2\,\theta}$; aux points d'abscisses $\pm\frac{\lambda}{4\,\theta}$, il vaut encore $\frac{2}{\pi}$. Sur les bissectrices, I atteint la même valeur à très peu près à la même distance. On peut donc dire que, dans le plan xoy, à l'intérieur d'un contour à peu près circulaire (intermédiaire entre un cercle et un carré) de rayon $\frac{\lambda}{4\,\theta}$, le coefficient I varie entre 1 et $\frac{2}{\pi} = 0{,}63$; à

l'intérieur du contour, les amplitudes s'ajoutent, par interférence, selon la loi calculée plus haut.

Comment se limite ce volume d'interférence dans le sens *oz*? Les *n* ondes considérées constituent un train d'onde (en réalité il y a deux trains d'ondes se propageant en sens opposé, mais cela ne change rien aux résultats ci-dessous), en forme de *signal carré* dont les fréquences sont comprises entre :

$$\nu - \frac{\Delta \nu}{2} \text{ et } \nu + \frac{\Delta \nu}{2}$$

Par transformation de Fourier, cela revient au même qu'une onde porteuse modulée de telle façon que le passage du train d'ondes dure un temps $\tau = \frac{2}{\Delta \nu}$, ou, ce qui revient au même, que le train d'onde comporte un nombre d'oscillations égal à $2 \frac{\nu}{\Delta \nu}$. Dans le sens *oz*, la longueur du volume d'interférence vaut donc $2 \lambda \frac{\nu}{\Delta \nu}$

Le volume d'interférence est donc un cylindre, s'appuyant sur le contour défini ci-dessus dans le plan *xoy*, et de hauteur $\pm \lambda \frac{\nu}{\Delta \nu}$ de part et d'autre de *o* le long de *oz*.

Quant au volume embryonnaire, il ne constitue qu'une fraction de ce volume d'interférence, car c'est seulement dans des tranches d'épaisseur $\frac{\lambda}{2}$ que le cisaillement garde le même sens. C'est une de ces tranches (en général la tranche centrale, où l'amplitude du mouvement est maxima) qui joue le rôle de volume embryonnaire. Celui-ci est donc un cylindre aplati, de hauteur $\frac{\lambda}{2}$ et dont la base sensiblement circulaire, à un rayon égal à $\frac{\lambda}{4\theta}$

Dans ces conditions, que devient l'énergie de toute la portion du volume d'interférence situé en dehors du volume embryonnaire? Au moment où l'embryon se forme, par rupture de liaisons interatomiques dans le volume embryonnaire, ce dernier devient une zone de discontinuité, qui diffuse les ondes d'agitation thermique et empêche leur transmission à travers l'embryon. En regardant la question de près, on voit que les nouvelles liaisons établies dans le volume embryonnaire subissent des vibrations en opposition de phase avec

celles qu'elles prendraient sous l'effet du reste des ondes thermiques, et de ce fait dérivent le flux d'énergie de celles-ci vers la périphérie de l'embryon. Cet effet est très difficile à calculer, mais nous admettrons, en première approximation, que la moitié de l'énergie du train d'onde sert ainsi à étendre le volume embryonnaire par les bords.

Le volume embryonnaire réel est donc un disque de même hauteur que celui calculé précédemment, $\frac{\lambda}{2}$, et de rayon $K_1 \frac{\lambda}{4\theta}$, où K_1 est un coefficient de l'ordre de :

$$K_1 = \frac{\nu}{\Delta\nu} \qquad (21)$$

Nous ne nous dissimulons pas ce que ce mécanisme d'extension latéral du volume embryonnaire a d'imprécis, mais il est certain que l'énergie du train d'onde doit passer quelque part, et il est vraisemblable que, une fois la transformation amorcée, cette énergie sert à augmenter celle de l'embryon, soit en étendant son volume, soit par un autre processus que nous suggérons ici en note (*).

Du point de vue pratique, il reste à évaluer les facteurs K_1 et χ, donc à choisir $\Delta\nu$ et θ (ou $d\omega$).

B. Ondes voisines de la fréquence limite.

La pointe très aiguë que l'on constate sur la figure 1 aux environs de la fréquence limite ($48{,}1.10^{11}$) suggère que les ondes correspondantes, qui sont en grand nombre, vont jouer un rôle privilégié. De fait, on voit qu'un très grand nombre d'ondes se concentre entre les fréquences 46 et 48.10^{11}, et que la courbe de répartition correspondante est assimilable à un triangle de base $\Delta\nu = 2.10^{11}$, et de hauteur $N(\nu) = 0{,}7$ N.; ce triangle a effectivement même largeur à mi-hauteur (10^{11}) que la pointe de la figure 1. Ce groupe d'ondes ayant

(*) On peut aussi penser à un autre processus : le cisaillement du volume embryonnaire ne serait pas suffisant pour déclencher d'un bloc toute la transformation, mais l'énergie de distorsion serait, par exemple K_1 fois plus petite que l'énergie correspondant au cisaillement critique. Cependant, comme les $(3N - n)$ ondes qui ne participent pas aux trains d'ondes considérés introduisent un certain désordre dans les atomes, certaines liaisons atomiques pourront être rompues dans le volume embryonnaire. Celui-ci devient absorbant pour le reste du train d'ondes, en sorte que l'énergie locale s'augmente à chaque période, et finit par atteindre la valeur de l'énergie de cisaillement critique. Ce raisonnement conduit à la même probabilité que le premier, avec un θ qui serait $\sqrt{K_1}$ fois plus petit, donc un χ qui serait K_1 fois plus petit, mais un δ^2 qui serait aussi K_1 fois plus petit, ce qui ne change rien à la formule (14).

des fréquences très voisines, représente une fraction importante des ondes d'agitation thermique; il doit donc jouer un rôle particulier. Il est équivalent à un train d'ondes à signal triangulaire (et non plus carré); dans ce cas, la durée de passage du train d'ondes est $\tau = \frac{4^*}{\Delta \nu}$, le coefficient K_1 vaut $2\,\frac{\nu}{\Delta \nu}$, soit ici environ 50. D'autre part le coefficient χ de la formule (6) vaut.

$$\chi = \frac{n}{N} = 0{,}7\,\frac{d\omega}{4\pi} = 0{,}7\ 0^2 \qquad (22)$$

Il faut remarquer que, dans ce cas, $\frac{\lambda}{2}$ est égal à la distance interatomique a.

C. Facteurs correctifs.

Nous n'avons pas tenu compte dans ce qui précède de certains facteurs correctifs.

1. *Facteur d'anharmonicité.* — Lorsque les amplitudes des ondes sont grandes, elles ne sont plus harmoniques, et le module élastique diminue. L'amplitude réelle est donc plus grande que celle obtenue par la simple sommation des ondes en phase, en sorte que, si l'on veut appliquer la formule (14) il faut multiplier le δ critique par un *facteur d'anharmonicité* < 1 (pour un module à variation sinusoïdale, ce facteur est de l'ordre de $\frac{2}{\pi}$).

2. *Facteur d'anisotropie.* — En établissant la courbe de la figure 1, Olmer a supposé les ondes isotropes, ou, si l'on veut, la première zone de Brillouin sphérique. En réalité, c'est un cuboctaèdre. Il s'ensuit une correction, qui n'est sensible qu'au voisinage de la fréquence limite : la pointe de la fréquence limite est un peu étalée; par contre, pour les ondes d'orientation voisines de (111), qui correspondent aux points de la zone les plus proches de l'origine, il y a une forte diminution de la dispersion des ondes (comme toujours

(*) Il faut remarquer que les vitesses de groupe des ondes,

$$U = \frac{\Delta \nu}{\Delta s}$$

(où s est le nombre d'ondes) est ici à peu près nulle et tend vers 0 quand ν tend vers la fréquence limite. Autrement dit les ondes considérées sont quasi stationnaires; leur vitesse moyenne vaut 2 % de la vitesse du son.

lorsqu'on s'approche d'une limite de zone), et par conséquent la densité de répartition des ondes doit être fortement accrue. Au total, il faut multiplier χ et K_1 par des *facteurs d'anisotropie* certainement > 1, et peut être assez forts, ce qui augmentera toutes les probabilités dont il sera question dans la suite.

D. Agitation thermique d'un atome.

En faisant croître θ et $\Delta\nu$ de façon à englober toutes les ondes de toutes les directions et toutes les longueurs d'onde, le volume d'interférence se réduit progressivement à celui d'un atome, ou plus exactement à celui qui occupe une liaison entre deux atomes.

Pour traiter le problème, la méthode normale consisterait à considérer tous les groupes d'ondes ($\Delta\nu$, $d\omega$), et à chercher la probabilité composée correspondant à l'ensemble de ces groupes. La loi de probabilité de chaque groupe est une loi appelée « loi de χ^2 » en calcul de probabilité. En faisant la composition de ces lois élémentaires, on trouve une « loi de χ^2 » dont le degré tend vers l'infini (nous ne détaillerons pas les calculs). Il est connu qu'une telle loi tend vers une loi de Laplace-Gauss, de sorte qu'au total, la loi de probabilité composée sera de la forme $W \div e^{-\frac{\alpha^2}{\alpha_o^2}}$. Mais le calcul de la valeur moyenne α_o est inextricable.

On peut conduire le calcul de façon approchée, mais plus simple. Alors que nous avons appliqué jusqu'ici la formule de Chandrasekar pour des groupes de vecteurs ($\Delta\nu$, $d\omega$) ayant tous la même longueur dans chaque groupe, nous allons utiliser le remarque, que cette formule peut s'appliquer dans certaines conditions à la valeur moyenne (quadratique) d'un ensemble de vecteurs de longueurs variées.

Pour calculer la probabilité d'activation par glissement dans une direction donnée OX, et parallèlement à un plan donné, *xoz*, il faut calculer la composante de l'amplitude de chaque onde selon *ox* (en tenant compte des ondes longitudinales). En utilisant les coordonnées polaires, par rapport à *ox* : β (angle avec *ox*), et γ (angle avec *oz* de la projection sur *yoz*), on trouve pour ces composantes :

$$u_e = \frac{1}{\pi\nu}\sqrt{\frac{\varepsilon}{2Nm}} \cdot \sin\beta\cos\beta\cos\gamma \qquad (23)$$

pour une onde longitudinale, et :

$$u_t = \frac{1}{\pi\nu}\sqrt{\frac{\varepsilon}{2Nm}}\sin^2\beta\cos\gamma \qquad (24)$$

pour une onde transversale (on sait qu'il ne faut en considérer qu'une sur deux).

Calculons maintenant la valeur quadratique moyenne de toutes ces composantes pour toutes les valeurs possibles de β, γ et ν (β variant de 0 à π, γ de $-\frac{\pi}{2}$ à $+\frac{\pi}{2}$, et de ν de 0 à la fréquence maxima ν_m). Les intégrations pouvant se faire séparément, on trouve les valeurs quadratiques moyennes suivantes :

$$\left.\begin{array}{l}\text{pour } \sin\beta\cos\beta\cos\gamma : \dfrac{2}{\sqrt{15}} \\ \text{pour } \sin\beta\cos\gamma \quad\quad : \dfrac{1}{\sqrt{3}}\end{array}\right\} \text{ pour l'ensemble } \sqrt{\frac{3}{5}} \qquad (25)$$

pour $\frac{\sqrt{\varepsilon}}{\nu}$: N B (T), où B (T) est une fonction de la température ayant les dimensions d'une énergie, et définie par :

$$B^2(T) = \int_o^{\nu_m} \frac{N^2(\nu)}{N^2\nu_m^2}\cdot\frac{h}{\nu}\left(\frac{1}{2}+\frac{1}{e^{\frac{h\nu}{kT}}-1}\right)d\nu \qquad (26)$$

Il en résulte que la probabilité d'un déplacement d'amplitude $\geqslant\alpha$ est, d'après (10) :

$$W(\alpha) = e^{-\left[2\pi^2\nu_m^2\cdot\frac{5m}{3}\cdot\frac{\alpha^2}{B^2(T)}\right]} \qquad (27)$$

On remarque que $2\pi m^2\nu_m^2\alpha^2$ est l'énergie d'activation E pour une fréquence égale à la fréquence maxima, d'où :

$$W(\alpha) = e^{-\frac{5}{3}\frac{E}{B^2(T)}} \qquad (28)$$

La fonction B (T) a une valeur finie pour T = 0, et pour T très grand est proportionnelle à T. On voit donc que la probabilité tend, pour les grandes valeurs de T, vers une valeur tout-à-fait analogue à celle que donne la formule de Boltzmann, à une constante près pour l'énergie d'activation. Par contre elle reste finie quand T tend vers 0.

IV. APPLICATIONS

Dans toute application à un problème particulier, il faut se fixer une certaine probabilité d'apparition d'un embryon, par unité de volume, correspondant aux conditions dans lesquelles s'effectue la transformation; d'autre part, il faut évaluer la valeur critique du glissement unitaire δ, et la longueur d'onde utile λ, qui vaut le double de l'épaisseur de l'embryon (*). Dans ces conditions, la formule (14) définit le coefficient χ, d'où $d\omega$ et θ, qui (avec λ) définit la *forme et les dimensions de l'embryon probable*.

D'autre part, dans toute transformation, il existe une dimension critique des embryons, définie par l'équilibre entre les forces qui tendent à le faire grandir, et celles qui tendent à le réduire (énergie superficielle) On peut calculer cette dimension critique. Dès que la dimension probable calculée plus haut est supérieure à la dimension critique, la germination a lieu. Comme ces deux grandeurs, ou au moins l'une, sont en général fonction de la température, cette égalité définit en général une température à laquelle la germination peut commencer.

A. Théorie des dislocations.

On peut se demander si la théorie que nous venons de développer fournit une probabilité raisonnable pour qu'une dislocation se forme, sous l'action d'une tension σ, au sein d'un cristal parfait.

Les ondes qui interviennent ici sont celles voisines de la fréquence limite des ondes transversales; c'est un cas où s'appliquent les considérations que nous avons développées au paragraphe (III B). La longueur d'onde correspondante est $\lambda = 2a$ (a = distance interatomique). Le temps que dure le passage du signal éventuel est de l'ordre de 10^{-11} sec, en sorte que la fréquence possible du phénomène est 10^{11}. Fixons-nous comme condition que la probabilité soit de l'ordre de une activation par seconde et par cm^3 (on pourrait prendre 10 ou 100, cela ne changerait presque pas le résultat comme on le voit par la suite), et étudions le cas de l'aluminium à l'ambiante. Dans

(*) Il y a là un certain arbitraire, mais on peut aussi parfois déterminer à priori la forme de l'embryon, en calculant d'abord les dimensions critiques du germe, et en choisissant pour λ le double de l'épaisseur de ce germe. Nous verrons plus loin, dans deux cas différents, comment l'on peut chosir $\Delta\nu$.

un cm³, il y a 10^{24} nœuds, qui peuvent tous être centrés d'embryons éventuels, en sorte que, dans un cm³, la probabilité est 10^{24} W (α).

Le facteur exponentiel sera donc défini par l'équation :

$$W = 10^{11} \cdot 10^{24}\, e^{-\frac{mc^2}{2\varepsilon} \cdot \frac{\delta^2}{\chi}} = 1 \qquad (28)$$

En prenant pour c la valeur 2.000 mm/sec trouvée par Olmer (9), on a $\frac{mc^2}{\varepsilon} = 25$ d'où :

$$\frac{\delta^2}{\chi} = 3{,}2 \qquad (29)$$

Le glissement unitaire critique est difficile à estimer; et il doit y avoir un fort effet d'anélasticité dans ce cas. On peut néanmoins utiliser un calcul de Frenkel (15), d'après lequel la résistance au glissement en bloc d'un cristal atteint son maximum quand le glissement atteint 0,1. Le maximum de l'énergie doit être atteint à peu près pour un glissement double, en sorte que l'on peut prendre pour δ la valeur 0,2.

On a donc :

$$\chi = \frac{1}{100} = \theta^2 \times 0{,}7 \qquad (30)$$

d'où :

$$\theta = \frac{1}{8} \qquad (31)$$

et, pour le rayon de l'embryon probable :

$$r_p = 12\sqrt{K_1} \cdot \mathring{A} = 100\ \mathring{A} \qquad (32)$$

le *rayon probable* de l'embryon, en forme de disque très plat, d'épaisseur a, est donc de l'ordre de 100 A. Calculons maintenant le *rayon critique*.

L'énergie d'une boucle circulaire de dislocation de rayon r est très sensiblement $\frac{G\, a^2\, r}{2} \operatorname{Log} \frac{r}{a}$ (G module de Coulomb) (*). D'autre part le travail des forces extérieures (qui tendent à développer la

(*) La forme de moindre énergie n'est sûrement pas une boucle circulaire, mais ovale, car les parties en dislocation —vis ont une énergie moindre que celles en dislocation — coin. Mais cela ne peut pas changer beaucoup le résultat.

boucle) est très sensiblement $\pi\sigma a r^2$. La variation d'énergie totale par création d'une boucle de rayon est donc :

$$U = \frac{G\, a^2 r}{2} \log \frac{r}{a} - \pi\sigma a r^2 \qquad (33)$$

Le rayon critique est atteint quand $\frac{dU}{dr}$ s'annule, ce qui donne :

$$r_c = a \cdot \frac{G}{4\pi\sigma} \left(1 + \text{Log } \frac{r_c}{a}\right) \qquad (34)$$

équation qu'il faut résoudre par approximations successives. Pour $\sigma = 100$ gr/mm^2, valeur de la limite élastique des cristaux d'aluminium, on trouve que r_c est de l'ordre de 100.000 Å.

Il y a donc un écart considérable entre le rayon probable et le rayon critique; c'est dire qu'une boucle de dislocation ne peut naître au sein d'un cristal parfait. On peut essayer de réduire cet écart en tenant compte de divers facteurs :

— facteur d'anélasticité,
— facteur d'anisotropie,
— existence de défauts de structure, abaissant la cohésion du métal en certains points, et pouvant y multiplier la tension par un facteur d'entaille.

Néanmoins, il semble peu probable qu'on arrive à combler l'écart considérable que nous venons de trouver.

Examinons par contre la naissance de dislocations à la surface d'un cristal. Evidemment, notre théorie ne s'y applique plus rigoureusement, car elle est construite pour étudier l'agitation thermique au sein d'un cristal. D'une part, les ondes superficielles vont brouiller les interférences; d'autre part, l'agitation thermique moyenne doit être un peu plus forte aux endroits où se produit une diffusion des ondes. L'un compensant l'autre, admettons que la probabilité est du même ordre de grandeur. Mais les dimensions critiques d'une dislocation sont certainement beaucoup plus petites, car elles peuvent apparaître sous forme d'une demi-boucle de très faible courbure. Le calcul est très difficile dans ce cas, mais on arrive vraisemblablement à combler l'écart entre dimensions probables et critiques des embryons, en considérant des embryons semi-elliptiques à grand axe parallèle à la surface du cristal, et à forte execntricité. Pour les

polycristaux, il est possible que les joints intergranulaires jouent le même rôle, si la structure y est assez lacunaire.

Il n'est donc pas du tout certain qu'on soit forcé d'admettre que les dislocations sont des défauts congénitaux des cristaux, apparaissant au moment de leur formation.

Certes, on est sûr que dans les cristaux formés par solidification, il y a de nombreuses dislocations, dont l'existence a été prouvée expérimentalement dans le cas du cuivre par Nowick, par mesure de frottement interne. Mais Guinier a montré que de tels cristaux étaient très imparfaits en orientation; ils présentent toujours la « lineage structure » de Buerger, qui suppose la présence de dislocations. Le mécanisme de croissance en spirale de Franck, peut aussi expliquer la présence de dislocations.

Par contre, les cristaux formés par recristallisation après écrouissage critique sont, d'après Guinier, quasi parfaits en orientation. On ne voit d'ailleurs pas très bien comment des dislocations y apparaîtraient en cours de croissance. En outre, les expériences de Dehlinger et Gisen (14), dont la figure 2 représente quelques résultats,

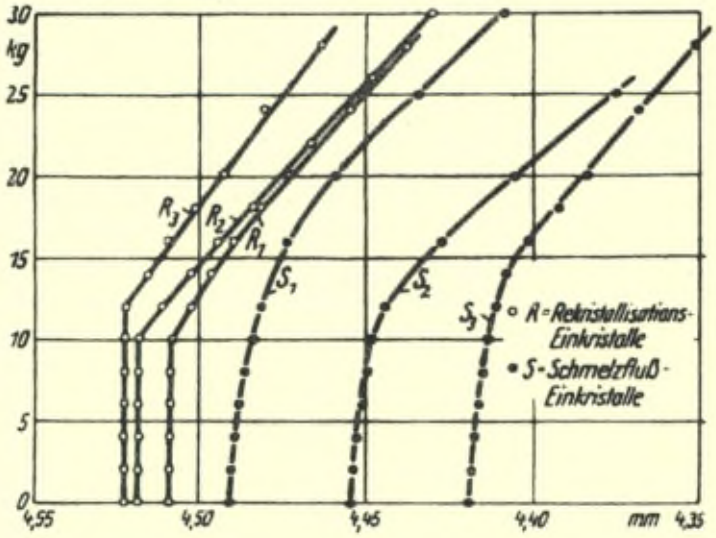

montrent que ces cristaux ont une limite élastique beaucoup plus marquée et moins dispersée que les cristaux de solidification, comme si l'apparition de glissements plastiques faisait appel ici à un phénomène intrinsèque, et non à un phénomène « sensible de structure ».

D'ailleurs, en comparant diverses valeurs de limite élastique de cristaux d'Al de titres supérieurs à 99,95 obtenus par recristallisation, on trouve les résultats suivants :

Auteur	Titre	Limite élastique
Dehlinger et Gisen . .	99,998 %	70-80 gr/mm^2
Crussard	99,996 %	80 gr/mm^2
	99,99 %	70 gr/mm^2
Miller et Milligan. . .	99,95 %	60 gr/mm^2

La dispersion de ces valeurs est faible, bien que la teneur en impuretés varie dans le rapport de 1 à 25. Il ne semble donc pas que l'apparition des glissements plastiques puisse être commandé par un facteur aussi variable d'un métal à l'autre que la répartition ou la forme de dislocations préexistantes.

Du point de vue expérimental, on peut encore faire une remarque intéressante, à propos de l'influence de la température sur la limite élastique des monocristaux. D'après la formule (2), elle devrait varier comme $A - B\sqrt{T}$, c'est-à-dire que la variation serait très rapide aux basses températures. Or ce ne semble pas être le cas : Koehler ([16]) a trouvé même limite élastique pour le cuivre à 20 °C et à — 190 °C. Même pour des métaux plus fusibles, comme le Zn, il semble, d'après les résultats de Schmidt ([17]), que la limite élastique varie peu en-dessous de — 200 °C. Un tel comportement s'explique bien par notre théorie : en effet, que l'on admette que les dislocations sont créées sous l'action de la tension, ou bien que l'on admette que des dislocations préexistantes sont arrachées d'une position correspondant à un minimum d'énergie, dans les deux cas, il s'agit d'un mouvement coopératif, auquel s'applique la formule (14). La température y intervient par la quantité ε, qui précisément varie peu aux très basses températures, tout en conservant une valeur finie.

B. Transformation martensitique.

Dans le cas de la transformation martensitique, il faut choisir pour la probabilité W une valeur plus élevée que dans le cas précédent : pour expliquer par exemple qu'une vitesse de refroidissement de l'ordre de 10.000 °/sec n'abaisse pas sensiblement le point M_s d'un acier (à 1° près), il faut admettre que W est de l'ordre de l'unité

en 10^{-4} sec. En raisonnant comme précédemment, on trouve ainsi :

$$\frac{\delta^2}{\chi} = 1{,}4 \tag{35}$$

Le choix du cisaillement critique est, ici aussi, délicat. Si l'on adopte l'interprétation de la transformation martensitique donnée par Greninger et Troaino ([19]), le cisaillement principal est de 0,17 environ. Bien que l'on ne sache pas grand chose sur la variation de l'énergie des liaisons interatomiques au cours du cisaillement, il semble raisonnable d'admettre que le seuil d'énergie est atteint à mi-chemin, c'est-à-dire pour un ciasillement critique d'environ 0,08,

Ceci fixe le coefficient d'utilisation à une valeur $\chi = 0{,}004$.

Il faut maintenant se fixer ν et $\Delta\nu$. Nous verrons que l'épaisseur critique de l'embryon est d'environ 5 Å. Ce qui nous intéresse donc, ce sont les ondes de longueur $\lambda = 10$ Å $= 2\lambda_m$, ce qui correspond à une fréquence ν sensiblement moitié de la fréquence ν_m. On pourrait prendre pour $\Delta\nu$ une valeur arbitraire de part et d'autre de ν; une erreur sur $\Delta\nu$ serait compensée par une erreur en sens inverse sur le coefficient K_1. Mais ici, il est évident que toutes les ondes de longueur d'onde $> \lambda$ sont utiles, ainsi que celles comprises entre λ et une limite inferieure de l'ordre de $3/2\ \lambda_m$; nous considérons donc toutes ces ondes comme comprises dans l'intervalle utile $\Delta\nu$. L'application de la formule (14) n'est plus rigoureuse, car les fréquences varient dans de larges limites, et il faudrait faire intervenir une moyenne analogue à celle de la formule (26). Nous nous contenterons d'appliquer la formule (14) en prenant pour N (ν) une valeur moyenne dans l'intervalle $\Delta\nu\left(0, \frac{2}{3}\ \nu_m\right)$. En utilisant les valeurs numériques de la figure 1 et en supposant la formule de Debye valable pour ces basses fréquences on trouve ici : N (ν). $\Delta\nu = 0{,}32$ N, d'où :

$$\chi = 0{,}004 = 0{,}32\ \theta^2 \tag{36}$$

et $\theta = 0{,}11$, ce qui, avec la valeur de λ choisie, donne pour rayons probable de l'embryon

$$r_c = 25\ \text{Å} \tag{37}$$

Calculons maintenant le rayon critique.

Soit ΔF la variation d'énergie libre par unité de volume transformé en martensite à la température considérée ($\Delta F < 0$), h l'épaisseur de

l'embryon, r son rayon, et σ la tension interfaciale austénite-martensite.

En nous inspirant d'un calcul de Fisher, Hollomon et Turbnull ([18]), écrivons la variation d'énergie par formation de cet embryon :

$$\Delta U = 2 \pi r^2 \sigma + w + \frac{\pi r^2 h}{\lambda} \Delta F \qquad (38)$$

où w représente l'énergie des tensions élastiques dues à la transformation (*). Ce terme n'a jamais été calculé de façon satisfaisante. Nous l'évaluerons en l'assimilant à l'énergie d'un ensemble de n boucles de dislocations concentriques, dans le plan de l'embryon, et de rayons :

$$\frac{r}{n}, \frac{2r}{n}, \ldots \frac{n-1}{n} r, r$$

Le nombre n doit être calculé de façon que le déplacement relatif des deux lèvres de la boutonnière que constitue l'embryon, soit 0,17 h (au centre) soit égal à n fois le déplacement d'une dislocation, soit na (**).

d'où :

$$n = \frac{h}{6a} \qquad (39)$$

Pour calculer l'énergie w, il ne faut pas oublier l'énergie d'interaction des dislocations prises deux à deux. En supposant que cette énergie n'existe, pour chaque paire, que dans la zone distordue par la plus petite, on trouve (en négligeant la variation de $\log \frac{r}{a}$):

$$\begin{aligned} w &= \frac{G a^2}{2} \log \frac{r}{a} \cdot \frac{r}{n} [n^2 + (n-1)^2 + \ldots + 1] \\ &= \frac{G a^2}{12} (n+1)(2n+1) r \log \frac{r}{a} = \frac{G}{50} r h^2 \end{aligned} \qquad (40)$$

d'où :

$$\Delta U = 2 \pi r^2 \sigma + \frac{G}{50} r h^2 + \frac{\pi r^2 h}{2} \Delta F \qquad (41)$$

(*) En toute rigueur, il n'est pas certain que ΔF ait la même valeur pour des plaquettes de martensite visibles au microscope et pour des embryons aussi petits que ceux dont nous parlons.

(**) Le plan de l'embryon n'est pas un plan normal de glissement de l'austénite. Mais cela n'a pas d'importance, car nous passons par l'intermédiaire des dislocations simplement pour nous rattacher à un problème d'élasticité plus simple, déjà résolu, et dont la solution classique est donnée sans tenir compte de l'anisotropie cristalline.

En cherchant la forme d'embryon qui correspond au minimum de Δ U, pour un volume donné, on trouve :

$$\frac{h^2}{r} = \frac{70\sigma}{G} \tag{42}$$

Pour les embryons de cette forme :

$$\Delta U = \frac{G^2}{4900\,\sigma^2}\,(7{,}76\,h^4 + 1{,}6\,\Delta F\,h^5) \tag{43}$$

Δ U passe par un maximum pour :

$$h_c = 3{,}9\frac{\sigma}{\Delta F} = 5\ \text{Å} \tag{44}$$

Prenons pour σ la valeur 20 erg/cm^2 ([18]) et pour Δ F, la valeur au point M*s* : 290 cal/mol = 1,6.10^9 ergs/cm^3.

d'où le rayon critique :

$$r_c = 44\ \text{Å} \tag{45}$$

Le rayon probable est donc légèrement inférieur au rayon critique. L'écart pourrait être comblé en raffinant les calculs, en tenant compte de la correction d'anharmonicité, et aussi de ce que l'embryon peut être un peu plus renflé que la forme d'équilibre donnée par (42).

Mais, dans l'état actuel des connaissances sur la transformation martensitique ([20]), il semble que la transformation s'amorce près de défauts de structure, de dislocations en particulier, qui créent des tensions élastiques capables de diminuer le terme *w* de l'équation (38). Il faut remarquer que les tensions s'amortissent rapidement quand on s'éloigne des dislocations, et ne peuvent conserver la valeur correspondante au cisaillement critique à des distances de la dislocation de l'ordre de 40 Å. Le rôle principal reste à l'agitation thermique, par le mécanisme que nous venons d'étudier; les tensions internes (ou autres défauts de structure) n'apportent que l'appoint nécessaire à combler l'écart entre rayon probable et rayon critique (s'il existe!).

On arrive ainsi à faire une synthèse des théories classiques selon lesquelles la martensite se forme par pure agitation thermique (Scheil, Dehlinger, etc.) et de celles, plus récentes, qui voient l'origine de la martensite uniquement dans des défauts préexistants. Il est possible que le point M*s* auquel conduit notre calcul corresponde en réalité au point M*b* découvert récemment par Cohen et ses collaborateurs.

V. CONCLUSION

En analysant les interférences des ondes d'agitation thermiques dans un cristal, on montre qu'elles peuvent produire des glissements (ou distorsions) locaux dans des volumes appréciables, contenant jusqu'à 1.000 atomes ou plus. De tels mouvements coopératifs peuvent expliquer la germination dans beaucoup de transformations à l'état solide, ou la formation de dislocation.

L'agitation thermique, dans ce cas, se manifeste sous la forme d'un train d'ondes d'amplitude exceptionnelle. Une fois la transformation amorcée localement, le flux du reste du train d'ondes doit contribuer à en étendre le domaine. C'est là, il faut le reconnaître, un des points les plus incertains de la théorie proposée ici, mais qui doit jouer un rôle.

En appliquant cette théorie au problème de la naissance des dislocations, on démontre qu'une dislocation ne peut prendre naissance par simple agitation thermique à l'intérieur d'un cristal parfait que sous des tensions considérables, de l'ordre de 10 à 100 kg/mm^2, beaucoup plus élevées que la limite élastique des cristaux métalliques. Par contre il semble qu'une dislocation puisse prendre naissance à la surface, bien qu'ici notre calcul ne soit pas assez précis.

Dans le domaine de la transformation martensitique la même théorie permet de faire une synthèse des théories proposées jusqu'ici.

Un fait remarquable est que, dans la formule donnant la probabilité d'activation, la température intervient par une fonction qui reste finie au zéro absolu, en sorte que la probabilité ne s'y annule pas.

RÉFÉRENCES BIBLIOGRAPHIQUES

(1) J. C. Fisher, J. H. Hollomon et D. Turnbull, *J. Appl. Phys.*, **19**, p. 775 (1948).
(2) P. Laurent, *Revue de Métallurgie*, p. 835 (1950).
(3) C. Crussard, *Physica*, **46**, p. 61 (1949).
(4) R. Becker, *Z. Tech. Phys.*, **7**, p. 347 (1926).
(5) A. S. Nowick et E. S. Machlin, *J. Appl. Phys.*, **18**, p. 79 (1947).
(6) L. Brillouin, « Les Statistiques quantiques et leurs applications ». Ed. Presses Universitaires, 1930.
(7) M. Polanyi et E. Wigner, *Z. f. Physical Chem.*, **139**, p. 439 (1928).
(8) N. B. Slater, *Proc. Roy. Soc.*, **194**, p. 112 (1948).
(9) P. Olmer, *Bull. Soc. Franç. Minéral.*, **71**, p. 145 (1948).
(10) L. Brillouin, *C. R. Acad. Sci.* (Paris), **180**, p. 1248 (1925).
(11) Debye, *Ann. d. Phys.*, **39**, p. 789 (1912).
(12) M. Blackmann, *Proc. Phys. Soc.* A, **148**, p. 365 (1938).
(13) S. Chandrasekar, *Rev. Mod. Physics.*, **15**, p. 1 (1943).
(14) F. Gisen, *Z. Metallkunde*, **27**, p. 256 (1935).
(15) J. Frenkel, *Z. Physik*, **37**, p. 572 (1926).
(16) P. W. Neurath et J. S. Koehler, *J. Appl. Phys.*, **22**, p. 621 (1951).
(17) E. Schmid et W. Boas, *Kristallplastizitpt*, J. Springer, **135**, p. 153.
(18) J. C. Fisher, J. H. Hollomon, et D. Turnbull, *J. Metals*, p. 691 (1949).
(19) A. B. Greninger et A. R. Troiano AIME, *Metals Technology*, juin 1941, T. P. n° 1338.
(20) M. Cohen, E. S. Machlin et V. G. Paranjpe, *Trans. A. S. M.*, p. 242 (1950).

Discussion du rapport de M. Crussard

M. Bragg. — 1) Professor Crussard's paper raises an extremely important question : Has classical application of thermodynamic principles led in the past to no law or estimate of the energy available in a localised region for enabling an energy barrier to be surmounted? Does his alternative approach in considering the interference of waves lead actually to higher estimates?

There must be a definite answer, yes or no, on theoretical grounds, and it is very desirable to have this point cleared up.

2) I am no expert in statistical mechanics, but I believed that in principle local fluctuations from the average were absent at absolute zero, although zero point energy exists.

M. Seitz. — It is perhaps worth pointing out that there is a very great difference between the states attainable by thermal fluctuation and by zero-point fluctuations. The energy of a crystal can vary over many states as a result of thermal fluctuations. For example, it may be found in a state in which a large dislocation ring has been generated because of these fluctuations. Such generation is probably very important in determining the plasticity of liquids, glasses and metals at elevated temperature. On the other hand, the fluctuations associated with zero point oscillations are intimate by associated with the process of measurement and express the unavoidable influence of the measuring apparatus upon the crystal when one is measuring the position of the atoms. A crystal left to itself at absolute zero of temperature will automatically jump to higher energy states, such as those containing large dislocation rings. If the cristal is placed under shearing stress, and if a state of lower (or equal) energy can be achieved by generation of dislocation ring, assuming one does not exist first, such a ring could be generated, much as electrons and holes are generated in pairs in insulators when a strong electrostatic field is present by the Oppenheimer-Zener mechanism. Since states with dislocation rings have an energy higher than those without rings by several electron-volts in the

absence of an applied shearing stress, one would expect such generation in the presence of a field, only when the field is near the theoritical value for the rigid displacement of crystalline planes past one another, that is for the field near 10^{11} dynes per cm^2.

M. Frank. — The uranium nucleus is a system in which things hapen at absolute zero.

M. Seitz. — The uranium nucleus regarded as an isolated system, does not change its energy when it emits an alpha particle or undergoes spontaneous fission.

M. Shockley. — In connection with the effect of zero point vibrations, it may be appropriate to mention the case in metal physics in which zero point vibration may play the largest role. This is the case of the diffusion of protons in palladium on iron at absolute zero. As will be shown, this effect may be large enough to be observable.

This case occurred to me during the discussion at a meeting of the American Physical Society of a paper by Yü-Chang Hsieh and I. Bloch, *Phys. Rev.* **83,** 228, 1951. These authors propose that tunneling may have an appreciable influence upon the diffusion of vacancies in metals.

Since tunneling through a barrier of potential energy V and width W is given approximately by the penetration factor

$$\exp - 4\pi \, W \, (2m \, V/h^2)^{1/2}$$

where h is Planck's constant and m is the mass, it is evident that tunneling is most favorable for small masses. For hydrogen in iron, the activation energy for diffusion is about 0.1 ev (Hollomon, personal communication) and thus corresponds to a wavelength (the reciprocal of the square root above) of about

$$\lambda = h/(2mV)^{1/2}$$
$$= 0.1 \text{ Å}.$$

If we assume the barrier is 1 A wide, the penetration factor is

$$P = \exp(-4\pi) \doteq 4 \times 10^{-6}$$

The diffusion constant for protons at absolute zero should thus be about

$$D = \nu \, d^2 \, P \doteq 10^{-6} \text{ cm}^2/\text{sec}$$

if we use reasonable values for ν and d. This value will lead to a diffusion distance of about 0.3 cm in one day. This suggests an experiment in which an attempt should be made to observe the redistribution of hydrogen in a sample cooled to liquid helium temperatures.

M. Seitz. — In Shockley's example of diffusion of hydrogen in palladium by tunneling the system does not alter, its energy as a result of the migration from one equivalent interstitial position to another. Such a process does not represent a jump from a low energy state to a higher one. Hence it can occur at absolute zero in an undisturbed system.

M. Prigogine. — Il n'y a en principe aucune difficulté à calculer les fluctuations de l'énergie dans tout l'élément de volume de dimensions microscopiques ou macroscopiques qui fait partie d'un système plus grand caractérisé par une température T. Toutes les formules nécessaires sont bien connues et découlent de la théorie des ensembles canoniques de Gibbs.

Un calcul basé sur le modèle de Debye ne peut en tout cas s'appliquer qu'à des volumes suffisamment grands pour être traités sur une base macroscopique. Dans ces conditions, on peut appliquer la distribution canonique sous sa forme la plus simple ($P \sim \exp [-\Delta F/kT]$). Il suffit s'y remplacer F par sa valeur calculée pour le modèle de Debye en fonction des variables énergie et volume pour avoir automatiquement les fluctuations. Lorsque l'on s'approche du zéro absolu, le système tout entier tend vers son état quantique le plus bas et on ne comprend pas de quelles fluctuations il pourrait être question alors.

M. Crussard. — Je crois que les fluctuations dont parle M. Prigogine concernent l'énergie d'ensemble du volume macroscopique qu'il considère. Je suis tout à fait d'accord que ces fluctuations s'annulent au 0 absolu. Mais les fluctuations que je considère (pour en prouver éventuellement l'existence) sont des fluctuations à échelle submicroscopique, *qui ne s'accompagnent pas forcément d'une variation de l'énergie de l'ensemble du volume*; elles sont dues seulement à des interférences qui modifient la répartition de l'énergie dans un élément de volume microscopique, pour la concentrer en son centre au détriment des zones périphériques.

Dans ce calcul, je ne fais aucune hypothèse sur la fluctuation de l'énergie de l'ensemble du volume. Léon Brillouin a montré qu'une fluctuation de cette énergie d'ensemble s'accompagnait toujours d'une fluctuation dus à un phénomène d'interférence (qui est responsable d'une partie de la fluctuation d'ensemble). Mais la réciproque n'est pas démontrée à ma connaissance. Sans avoir fait le calcul complet, je crois que le genre d'interférence que j'ai étudié ici n'entraîne pas de variation de l'énergie totale.

M. Dehlinger. — Innächst möchte ich betonen dass wir bisher noch keine konsequente Berechnung von Übergangswahrscheinlichkeiten im Kristall besitzen, so dass die Rechnungen von Herrn Crussard sehr wertvoll sind. Jedoch scheint folgendes nicht beachtet zu sein : Jede Statistik muss Elemente benützen, die mechanisch mindestens näherungsweise unabhängig von einander sind, d. h. Eigenbewegungen des Gitters. Nun sind aber die von Herrn Crussard betrachteten einseitigen Atombewegungen keine Eigenbewegungen. Wenn sie nach der berechneten Formel entstehen, wird ihre Energie sofort nach der Seite abfliessen. Sie entsprehen also keinem zeitlich beständigen Zustand, und die Formel kannnicht in Analogie zur Boltsmannschen angewandt werden.

In einer demnächst erscheinenden Arbeit hat Seeger in Stuttgart für das lineare Modell von Frenkel gezeigt, dass ein durch eine positive und eine negative Verzetsung gebildetes Paar aus einem Wellenpaket entstehen kann. Lauft nun dieses Paar ein in Gebiet, in dem ein Gradient der Schubspannung (d. h. eine Kerbstelle) besteht, zo wird die positive von der negativen Versetzung getrennt. So wird es demnächst wenigstens in linearen Fall möglich sein, die Wahrscheinlichkeit zu berechnen, dass durch thermische Schwingungen Verzetungen gebildet werden.

M. Crussard. — Je crois que les mouvements que j'ai considérés sont bien des fréquences propres, indépendantes : les glissements d'atomes que je considère ne sont pas unidirectionnels (« einseitig »), mais bien symétriques par rapport à la position d'équilibre. Si mon texte peut donner l'impression contraire, c'est que j'ai décrit le déplacement d'une couche d'atome par rapport à sa voisine; mais il s'agit seulement de déplacements *relatifs*.

M. Orowan. — The result obtained by Crussard depends on the

exclusion of all waves except those whose normals lie in a narrow cone. To what extent is the neglect of these other waves permissible?

M. Crussard. — La question soulevée par le Dr Orowan est très intéressante, et mérite d'être regardée de près. Les ondes dont les vecteurs de propagation sont extérieurs au cône que j'ai défini (que j'appellerai par abréviation *ondes extérieures*), produisent en effet pour les atomes du volume embryonnaire des mouvements quasi-désordonnés autour de leur position moyenne. L'effet des « ondes intérieures » est de superposer à ces mouvements un déplacement d'ensemble (glissement) de ces positions moyennes, dans tout le volume embryonnaire; le fait qu'il y ait simple superposition est dû à l'hypothèse d'indépendance des ondes, que j'ai faite au début.

On peut objecter que ce glissement d'ensemble est indéterminé, puisque le choix de l'angle au sommet du cône est arbitraire. Il faut en réalité raisonner ainsi : étant donné une transformation possible, nécessitant un glissement déterminé dans un volume embryonnaire déterminé, celui-ci ne peut être produit que par un groupe d'ondes dont les normales sont contenues dans un cône déterminé; si pour ce groupe la probabilité de glissement est appréciable, il y a activation, quels que soient les mouvements désordonnés dûs aux ondes extérieures. On pourrait dire que le volume embryonnaire « choisit » les ondes qui lui sont utiles. La notion de « rayon probable » que j'ai introduite est un intermédiaire commode, mais qui n'a pas de sens physique rigoureux.

Le point délicat de cette partie du calcul est en réalité l'extension latérale du volume embryonnaire et l'introduction du coefficient K_1.

M. Rudberg. — In the interesting theory presented by Professor Crussard the remarkable result that there should still exist quite considerable fluctuations, giving high local shear strains in small regions, at the absolute zero of temperature, would seem to be due to two circumstances. The first is the existence of the zero point energy $1/2h\nu$ in each wave of the normal modes of vibration by which the state of the crystal is described. The second is the assumption that the phases of these separate waves distribute themselves completely at random. This randomness enables the waves to meet occasionally under conditions where the individual waves re-inforce each other and build up a wave packet of considerable amplitude. The description by a set of waves is useful when the forces on the

crystal atoms are truly harmonic, for then the wave equation is separable in a set of coordinates corresponding to such standing waves. These waves are strictly independent of each other as long as the potential energy contains only harmonic stress. The absolute zero of temperature being a limiting situation, is it not possible that the neglect, for a real crystal, of anharmonic energy terms, which is justified for finite temperatures, where these terms are small compared with the unit energy of temperature fluctuation kT, is no longer legitimate in the limit? Inclusion of anharmonicity will produce a coupling between the different waves. Is it not conceivable that, on the detailed picture of Professor Crussard with individual waves pilling up in a classical sense over local regions of space, such a coupling would actually reveal itself by phase relations between interfering waves, which, as T approaches zero, would lock them into a definite pattern where bunching of amplitudes is avoided?

M. Crussard. — L'hypothèse de couplage des phases au 0 absolu, proposée par le Dr Rudberg, est très intéressante. Mais si elle intervient, j'ai l'impression que ce serait plutôt dû à des conditions aux limites mal précisées qu'aux termes d'anharmonicité. Toute cette question est en relation avec l'effet tunnel des électrons; je ne sais pas si on a étudié les fluctuations qui en résultent.

On peut suggérer la possibilité d'activation au 0 absolu d'une autre façon, moins rigoureuse, mais plus parlante. Si l'on considère l'agitation thermique individuelle des atomes, on sait que les rayons X, par la mesure du facteur de Debye, permettent de déterminer le déplacement quadratique moyen. Pour l'aluminium à 293° K, par exemple, il est de 0,10 Å. Si on admet que la variation de l'agitation thermique des atomes en fonction de la température suit la loi (5) du texte, la température caractéristique de Debye de l'aluminium étant 398° K, on trouve qu'au 0 absolu le déplacement quadratique moyen doit être 0,077 Å, ce qui correspond à un glissement unitaire moyen de 0,067. Comme les mouvements des atomes voisins ont de fortes chances d'être plus ou moins couplés, on voit que même au 0 absolu des glissements locaux de l'ordre de 0,07 sont très probables, ce qui n'est pas très loin des valeurs nécessaires à certaines transformations, notamment martensitiques.

On the Generation of Vacancies by Moving Dislocations

by Frederick Seitz

University of Illinois, Urbana, Ill.

ABSTRACT

New experiments of Molenaar and Aarts, Blewitt and others seem to confirm the view of the author, previously based only on the experiments of Gyulai and Hartly and Stepanow on sodium chloride, that vacant lattice sites, and possibly interstitial atoms, are generated during plastic flow in ductile cristals, most particularly in metals. It is pointed out that the average temperatures near a moving dislocation are probably not sufficiently high to evaporate vacant lattice sites or interstitial atoms as a result of thermal effects alone. Instead one apparently must conlude that the imperfections are generated either by purely geometrical means during the looping of dislocations about appropriate obstacles, as the result of dynamical instability in the motion of a dislocation, possibly near a jog, or in the very high thermal pulses or « spikes » which are generated either in the zone where two dislocations of opposite sign annihilate one another or near impediments where dislocations are strongly curved. It is pointed out that a pair of vacancies is probably stable near room temperature and may diffuse more rapidly than a single vacancy. Is is also proposed that vacancies retained during quenching of Al-Cu alloys and those generated by cold work play an important role in the precipitation process. The origin of work hardening in single crystals is discussed and several alternative interpretations, which involve the impediment of Frank-Read generators either directly or indirectly as a consequence of the generation of vacancies, are presented. The importance of prismatic dislocations formed by condensation of vacancies is restated. The role that vacancies formed by cold work may play in determining the stored energy, and decrease

in density and in affecting processes such as creep and the hardening of latent slip planes is also discussed. Finally a number of experiments, typical of those which could prove decisive in isolating the influence of vacancies, are proposed.

1. INTRODUCTION

In a recent paper, the writer (1) has pointed out that experiments of Gyulai and Hartly (2) and Stepanow (3) on the influence of plastic flow upon the electrical conductivity of sodium chloride seem to imply that vacant lattice sites are generated within the crystal when dislocations move, as during ordinary « static » experiments in the range of stress where plastic strain occurs. More recent experiments on metals by Molenaar and Aarts (4), working at Druyvesteyn's Laboratory at Delft, which will be described briefly below, appear to support the same conclusion. There is enough ambiguity in the interpretation of the existing experimental work that the writer's point of view cannot be regarded as proved. Nevertheless, the implications of the viewpoint appear to be sufficiently far reaching if it is sustained by further research that additional discussion appears justified.

The first part of the paper will deal with an analysis of the experiments. Following this some speculative comments on the implications of the viewpoint will be made, with ample emphasis on the subjunctive mood.

The writer is indebted to Dr. T. Blewitt of Oak Ridge National Laboratory for calling his attention to the work of Molenaar and Aarts. Blewitt had similar experiments in progress at the time the work of the Netherlands group appeared. He had observed the increase in resistivity of polycrystalline copper with cold work at low temperatures to be described in the next section.

2. EXPERIMENTAL OBSERVATIONS : THE DENSITY OF VACANCIES GENERATED

A. Experiments of Molenaar and Aarts.

Molenaar and Aarts extended polycrystaline specimens of copper, silver and aluminium in tension by about 10 percent of strain at liquid air temperature and measured the change in electrical resistivity

which accompanies the strain (see Fig. 1). The specimens were then warmed to room temperature for various periods of time and cooled

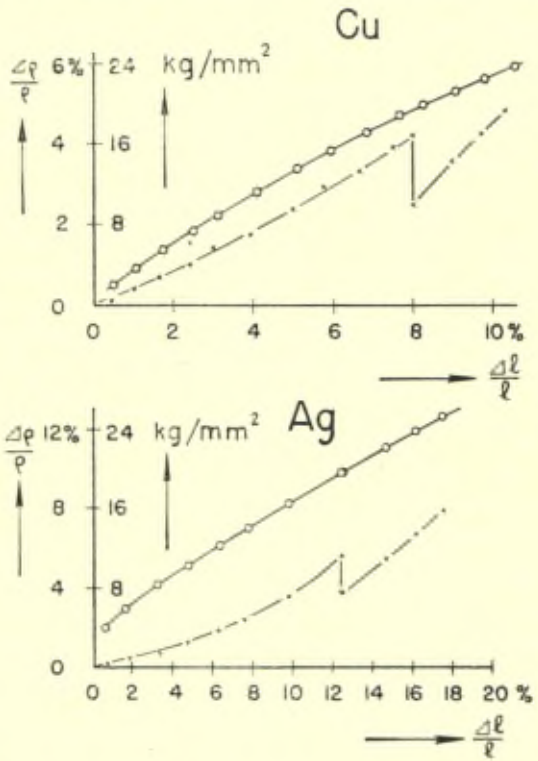

Fig. 1. — The stress-strain curves and increment in resistivity versus strain for copper and silver (after Molenaar and Aarts). The specimens were deformed at liquid air temperature and all resistivity measurements were made there. The discontinuities in the resistivity curves are the result of an « anneal » at room temperature. The anneal is complete in the case of aluminium, which is not shown. Blewitt and investigators at North American Aviation Company have found that the annealing process takes place at a measurable rate in copper at —80 °C.

to liquid air temperature again. Measurements of electrical resistivity were continued along with further plastic flow. The principal qualitative results were : *a)* The increase in electrical resistivity produced during the initial flow is at least partly eliminated by warming to room temperature. That is, the resistivity is lower when the specimen has regained liquid air temperature than it was after plastic flow, just prior to being warmed. Most of this annealing is achieved in ten minutes at room temperature. Practically all the resistance

imparted to aluminium by the cold work is annealed at room temperature, whereas only a fraction disappears in copper and silver. *b)* The stress-strain curve does not appear to be altered by warming to room temperature. That is, the curve obtained when plastic flow is continued at low temperatures after the specimen has been annealed at room temperature, joins smoothly on to that obtained previously. Thus the curve showing electrical resistivity versus strain at liquid air temperature shows a discontinuity at the point where the strain was interrupted and the specimen was annealed at room temperature, whereas the stress-strain curve does not.

Blewitt (see Section 1) has found that the recovery of electrical conductivity is apparent even at -80° C in copper.

From the viewpoint the writer presented previously ([1]), these results may be interpreted by stating that vacant lattice sites, and possibly other lattice defects, such as interstital atoms, are generated during plastic flow and increase the electrical resistivity because they introduce centers which scatter the conduction electrons. We shall usually refer to the imperfections as vacancies for brevity, since the experiments on NaCl imply that a substantial fraction are of this type. More detailed work may show that interstitial atoms are as important. The vacancies are immobile at liquid air temperature, but have enough mobility at room temperature, and in fact even at dry ice temperature, that they form aggregates which are sufficiently large to produce less scattering than the isolated vacancies formed at low temperatures. This aggregation proceeds farther in aluminium than in copper or silver, since vacancies are more mobile in aluminium. The clusters may be in the form of planar sheets probably nucleated at imperfections which are the equivalent of dislocation rings. The linear dimensions of the « rings » may be small initially.

If this interpretation is accepted as a tentative working hypothesis, it is possible to estimate the density of vacancies which are generated, at least to order of magnitude. Attention will be focussed on copper, although the conclusions drawn seem to be equally valid for silver and aluminium.

When the specimen of copper is loaded to 24 kg per mm^2 ($2.4.10^9$ ergs per cm^3) the strain achieved is ten percent. Since the stress-strain curve is nearly linear, the work done is about $1.2.10^8$ ergs per cm^3.

During the strain, the resistivity is altered by about 6 % (Fig. 1), or rather would have been if the specimen were not annealed at room temperature. Since the resistivity of pure copper at liquid air

temperatures is $0.322.10^{-6}$ ohm-cm, the change $\Delta\rho$ in resistivity is about $0.019.10^{-6}$ ohm-cm. Now Linde [5] has determined the influence of various alloying elements upon the resistivity of copper and has found that the change varies linearly with the amount of a substitutional alloying agent added, as long as the amount of the alloying agent is not more than a few percent. Moreover, the change in resistivity per atom percent of solute varies with the nature of solute, being smaller for elements which resemble copper and larger for those which lie farther away in the given row of the periodic chart. The range of $\Delta\rho$ extend from zero to 10.10^{-6} ohm-cm per atom percent of addition depending on the solute. We shall assume that a vacancy (or an interstitial atom) produces a relatively radical change in the lattice and assume that one atom percent of vacancies would change the resistivity by $10 \cdot 10^{-6}$ ohm-cm. It follows from this assumption that ten percent of strain induces about 0.0019 atom percent of vacancies, or about $1.6 \cdot 10^{18}$ vacancies per cc.

Since the energy expended in straining the lattice is $1.2 \cdot 10^{8}$ ergs per cm^3, it follows that one vacancy is produced for each $7.5\ 10^{-11}$ ergs, or for each 47 ev. If we employ the rough rule[6] that half of the energy of activation for self-diffusion in metals is associated with generation of vacancies and half with migration, we conclude that about 1.1 ev is required to generate a vacant lattice site in copper under conditions of thermal equilibrium since the best value for the activation energy for diffusion is 48 kg cal per mol (2.1 ev per atom). Hence about two percent of the energy of cold-work is expended in producing vacant lattice sites, if the picture presented here is consistent. Taylor and Quinney [7] have found that between five and ten percent of the energy of cold-work is stored in copper during cold-work. The present work suggests that an appreciable fraction of this, that is a fifth or more, resides in the form of vacant lattice sites or interstitial atoms. In fact, it is possible that the majority of the stored energy resides in the form of vacancies. This may be particularly true when single crystals are deformed in a manner approaching pure shear for which asterism is very small.

There is another profitable way of viewing the foregoing results. A strain of ten percent can be generated by having one dislocation move across every tenth plane, Since there are about $5 \cdot 10^{7}$ parallel planes per cm^3 in copper, it follows that in moving unit distance a dislocation produces $5 \cdot 3 \cdot 10^{11}$ vacancies per unit length. Or it produces one vacancy in each plane of a set parallel to the slip vector in moving 7,000 atom distances.

B. Experimental of Gyulai and Hartley.

Gyulai and Hartley ([2]) observed that the electrolytic conductivity of NaCl was raised by a factor of 100 or more when a specimen was loaded in compression by 2.5 kg per mm^2 ($2.5 \cdot 10^8$ ergs per cm^3). The specimen was strained by almost exactly 10 %, so that the energy expended was about $2.5 \cdot 10^7$ ergs per cc.

If the writer assumes that the natural specimens of rock salt employed by these investigators contained one part per million of divalent impurity, which is a common value ([8]) for « pure » rock salt, the increase in conductivity implies that the plastic flow raised the density of positive ion vacancies to about 1 per 10^4 sodium ions, or raised the density to about 2.10^{18} per cc. It is possible ([9]) that the specimen was ten times purer, in which case the density of vacancies would be nearer $2 \cdot 10^{17}$. In the first case the energy expended per vacancy would be 6 ev, whereas it would be 60 ev in the second case. Wagner and Hantelmann ([10]) have found that the equilibrium value of the energy of formation of a pair of positive- and negative-ion vacancies is 2.1 ev. Evidently the second value of 60 ev per vacancy during plastic flow is more reasonable than the first, for otherwise we would conclude that most of the energy of cold-work is stored.

In any case, it would seem to be highly desirable to have the experiment of Gyulai and Hartley duplicated, under conditions in which the results are specified more compltely so that this relatively large ambiguity may be removed.

C. The Experiments of Masima and Sachs.

Masima and Sachs ([11]) have measured the change of electrical resistivity of single crystals of brass (Cu 70 Zn 30) with plastic flow and have correlated the changes with those in hardness and density. The relationships were also investigated during annealing stages at various temperatures. Although these experiments are exactly of the type that is needed to extend the topic under discussion in this paper and provide a test of the speculations, it is unfortunate that the metal chosen is the alloy brass. For single crystals of brass exhibit a number of irregularities, such as the Bauschinger effect, which are not observed generally in crystals. There is a strong probability that the effects observed in brass are somewhat atypical.

The outstanding results of the measurements seem to be the following :

1) The electrical resistivity of the single crystals increases during plastic flow, the increase being of the order of 1 % of the room temperature value during the first few percent of plastic flow. The crystals were strained at room temperature, so that the results cannot readily be compared with those of Molenaar and Aarts, who deformed the materials at lower temperatures. The increment in resistivity was found to be independent of the temperature of measurement at any temperature where annealing did not occur. Since the resistivity of brass at room temperature is about 50 times larger than that of copper at liquid air temperature, it follows that the change in resistivity of brass during the first ten percent of strain is about 50 % of the resistivity of copper at liquid air temperature. In other words, the increment in resistivity is several times larger than the change observed in polycrystalline copper for comparable deformation.

2) The increment in electrical resistivity produced in brass by cold-work does not rise with the stress-strain curve, but appears to saturate after about ten percent of plastic flow. However the resistivity rises again when the specimens, which were deformed in tension, begin to neck. The stress-strain curve rises during the entire process of plastic flow.

3) The increase in electrical resistivity could be removed by annealing at a lower temperature than is required to resoften the specimens. For example, most of the increase in resistivity could be removed by annealing at 200 °C for one half hour, whereas an anneal near 500 °C was required to produce resoftening in a comparable period of time.

4) The measurements of the change of density of deformed single crystals show that a decrease of the order of 0.06 % can be obtained by a strain near unity. This would correspond to a generation of about $5 \cdot 10^{19}$ vacancies per cc, if we were to ascribe all of the change to the generation of vacant sites. Actually most of the change in density occurs only after double slip has begun to take place within the specimens; it is less than 0.006 percent during the first ten percent of strain.

5) The decrease in density starts to anneal with the same ease as the increase in electrical resistivity. Thus the two processes appear to be closely correlated. Actually the manner in which the density

anneals is somewhat peculiar : The change in density of the cold-worked specimen with annealing temperature, for a half-hour anneal, rises as this temperature increases to about 200 °C. It then falls in the range between 200 °C and 400 °C and rises again at higher temperatures. The investigators associate this second rise, which begins at about 400 °C, with the onset of recrystallization. However the original density does not appear to be regained even if the specimen is heated as high as 700 °C, where dezincification begins. In other words, it does not seem likely that the annealing process consists merely in the coagulation of vacant lattice sites into larger and larger aggregates in the range below 500 °C before resoftening and recrystallization occurs.

Although the effects observed in these measurements are closely associated with those described in the preceding paragraphs of this section, it is evident that there probably are important side effects which may arise from the fact that brass is an alloy or that it is a highly anisotropic material. The alloy character may have a strong influence upon the events which occur during plastic flow, for the degree of short range order may decrease, as the relatively large change in resistivity with cold-work implies is the case. In addition it is possible that vacant lattice sites are entrained in the lattice by inhomogeneities associated with fluctuations in composition.

The observation that the density decreases relatively rapidly when double slip begins suggests, at least vaguely, that the dislocations produce vacancies more readily when they encounter major obstacles than when they move through the nearly perfect lattice; however, it seems unwise to push this conclusion very far.

It would be desirable to have the experiments of Masima and Sachs repeated on single crystals of pure metals, particularly if the strain was carried out a low temperatures. The decrease in the amount of recovery of density which occurs as the annealing temperature is increased from 200 °C to 400 °C is a highly interesting effect. It would be valuable to know if it is a general phenomenon.

D. Experiments of Tammannand Coworkers.

Tammann and Dreyer ([12]) have carried out a series of somewhat unrefined measurements on the annealing of the increase in electrical resisitivity and hardness induced by cold-work somewhat similar to those of Masima and Sachs. They subject copper, silver, gold,

palladium and platinum to a series of temperature anneals at room temperature and above. The specimens had been cold rolled or drawn by amounts varying from 10 to 98 %. In the case of copper, silver and gold it was found that the increase in hardness and resistivity of a given specimen decreased in nearly the same manner as the annealing temperature was raised, whereas the annealing or hardness required a relatively higher temperature in the case of palladium and platinum. Results similar to that for palladium and platinum were obtained in iron and nickel by Tammann and Moritz [12]. The initial increase in resistance was in the same range in all cases.

Apparently the effect observed by Molenaar and Aarts and Blewitt could not be observed by Tammann and Dreyer in copper, silver and gold because the temperature at which their experiments started was sufficiently high that they had complete recovery from the effects the writer has associated with the production and coagulation of dispersed vacancies before measurements were started. Presumably their experiments on these metals are concerned primarily with the annealing of the effects arising from dislocations. The latter may be the dislocations responsible for plastic flow and for the generation of vacancies, or may be dislocations formed by precipitation of the vacancies generated during plastic flow, which may act as impediments to motion of the original dislocations (see later sections).

On the other hand, the experiments on palladium, platinum, iron and nickel suggest that vacancies do not coagulate at room temperature in these metals and that one must heat well above room temperature in order to obtain the type of condensation observed in copper, silver and aluminium near room temperature or below, As we shall see later, it is possible that impurities present in these metals prevent the vacancies from coagulating by acting as traps which retain them in widely dispersed form.

Tammann, Dreyer, and Coglioti [12] have also investigated the influence of annealing on the recovery of electrical resistivity and hardness of alloys. The fractional increase in resistance may either increase or decrease with rising concentration of solute. However, the temperatures required to produce a given amount of annealing always increases with rising concentration of solute. It seems to be a general rule that the increase in electrical resistance of the alloys may be annealed more easily than the increase in hardness.

The experiments on the effect of cold-work on the alloys may be more difficult to interpret than those on the relatively pure metals

for reasons discussed in C. A part of the recovery of resistance and hardness may be related to the reestablishment of local order and hence be related only indirectly to the influence of vacant lattice sites.

3. THE MODE OF GENERATION OF VACANT SITES

There seem to be four methods by which vacant lattice sites could conceivably be generated during plastic flow :

1) By local heating of the lattice in the immediate vicinity of the dislocation as it moves through the lattice and absorbs energy from the applied stress field.

2) By purely geometrical means in which dislocations of opposite sign moving in neighboring planes annihilate one another and produce a row of vacancies.

3) As a result of instability of the in-phase motion of atoms during passage of a dislocation. For example, it is possible that incipient vacancies are occasionally torn loose from a jog in a dislocation because of a local disturbance in the lattice.

4) As a result of large, transient thermal pulses in regions where dislocations annihilate one another and produce a large lattice disturbance.

We shall consider these processes individually.

A. Local Heating.

It seems very unlikely that local heating over the entire length of the moving dislocation can be the agent effective in producing vacancies by evaporation, for the average temperature is probably very low. In order to proceed with a calculation of this temperature, we shall make several assumptions. First, we shall assume that the moving dislocation achieves velocities near that of sound ([13]) in the medium, but somewhat lower. Leibfried ([14]) and the writer ([15]) pointed out independently that a moving dislocation should dissipate the energy which it receives from the stresses field at an appreciable rate. It appears to be very difficult to evaluate this loss precisely, but seems safe to say that the velocity of a dislocation becomes no larger than a value of the order of ten percent of sonic velocity. Leibfried has focussed attention on the dissipation which arises from the interaction of the moving dislocation with thermal waves, whereas

the writer has considered the influence of anharmonic forces, which will cause dissipation even in an ideal, quiescent lattice, that is, even at a « classical » absolute zero of temperature. Actually the argument of interest to us at the moment is not critically dependent upon the question of whether or not the dislocation actually may achieve sonic velocity, but this matter will be important in later discussions of this section.

The rate at which a unit length of a dislocation receives energy from the stress field is given by :

$$s = \sigma a v \tag{1}$$

where σ is the component of the stress field effective in inducing motion, a is the slip distance, which for simplicity we shall take to be the interatomic distance, as if the lattice were simple cubic, and v is the velocity of the dislocation ([16]). If all this energy is transformed into thermal energy at the immediate vinicity of the dislocation line, the dislocation will act like a moving line source of thermal energy. We shall estimate the temperature distribution under steady-state conditions by the simple expedient of treating the dislocation as if it were a stationary line source and as if the medium had a simple thermal conductivity $\varkappa$, whose value will be discussed below. The thermal field is then symmetrically distributed about the dislocation line. This simplified procedure probably leads to an underestimate of the temperature near the dislocation because its speed approximates that of sound. We shall attempt to compensate for this effect, which would be very difficult to treat rigorously, by underestimating the value of $\varkappa$.

Undea these assumptions, the temperature T at a distance r from the dislocation (r is the radial variable in cylindrical coordinates in which the axis of the cylinder is coincident with the dislocation line) is

$$T = (s/2\pi\varkappa) \log (R/r) + T_a \tag{2}$$

in which s is the rate of dissipation of energy, given by (1), and R is the distance at which the temperature may be regarded as having the ambient value, T_a. R may conceivably be as large as the linear dimensions of the specimen, but its value it not critical for this discussion.

Let us consider a case in which σ has a value of 1×10^9 dynes/cm^2 as during the initial deformation in copper, a is 2×10^{-8} cm, and v is 10^5 cm/sec (the velocity of compressional waves in a metal such as

copper is 3.9×10^5 cm per sec). Hence s is 2×10^6 ergs per cm/sec. If $\varkappa$ is chosen to be as small as 10^{-3} cal/(cm^2/sec) (deg/cm), or 4.2×10^4 ergs/(cm^2-sec) (deg/cm), the temperature rise in the vicinity of the dislocation attains a value :

$$\Delta T = 8 \log (R/a) \ (^{\circ}C) \tag{3}$$

in which r has been replaced by the interatomic spacing. Since $\log(R/a)$ should be less than 20, ΔT is less than 200 °C. Actually we may anticipate much lower values if the assumption that the temperature field has rotational symmetry about the axis of the dislocation line is not grossly in error, for we have given all of the parameters values which would provide an upper limit for ΔT. For example, $\varkappa$ should be nearer unity than 10^{-3} cal/(cm^2-sec) (deg/cm) in a good metal, and is actually larger than this at low temperatures. The value is 1.3 in conventional units in copper at 80° K. Even if use of the lower value of $\varkappa$ is justified in the immediate vicinity of the dislocation, where there is a high degree of lattice distortion, it would not be justified at somewhat larger distance, of the order of 10^{-7} cm, so that the value of 20 selected for log (R/r) is artificially large, by a factor of 5 or more.

The larger value of $\varkappa$ is more appropriate for salts, at least in the vicinity of room temperature. For example $\varkappa$ is 0.021 cal/(cm^2-sec) (deg-cm) at room temperature for NaCl. However ΔT has been grossly overestimated even in this case. To consider one point, the stresses required to produce ten percent of strain in NaCl under the conditions employed by Gyulai and Hartly are almost exactly ten times smaller than those employed by Molenaar and Aarts for copper, which served as the basis for the preceding estimate. Hence a more appropriate value of s would be ten times smaller in the case of NaCl, that is nearer 2×10^5 ergs/cm-sec.

We may expect vacancies to evaporate from a given atomic site on the edge of a dislocation at a rate :

$$v = v_0 \exp(-\varepsilon/kT) \tag{4}$$

as a result of temperature alone. Here ε is the energy required to form a vacancy under equilibrium conditions and v_o is of the order of 10^{13} sec^{-1}. If we set $\varepsilon = 1.1$ ev, for the cases of NaCl and Cu, and assume that T is 500° K, that is, is about 200° above room temperature as a result of local heating, the rate of evaporation is about 10^2 sec^{-1}. Since a dislocation moves unit distance in about 10^{-5} sec

under the conditions we have assumed, the rate of evaporation, arising purely from temperature, is found to be negligible small, that is the dislocation would have to migrate of the order of 10 meters to evaporate one vacancy in a given plane of atoms normal to the axis of the dislocation, instead of a distance of the order of 10^{-4} cm. Since this calculation is based on the highest value of ΔT which we have estimated, namely 200° K, it seems very unlikely that the local heating of the dislocation is the important effect either in sodium chloride or in copper.

H. Brooks (private communication) has pointed out to the writer that temperature much higher than the average may be generated at special places along the dislocation line, where it is held up temporarily by an impediment and then moves on as a result of the concentration of applied stress through curving of the dislocation in the direction of motion [Mott and Nabarro, Bristol Conference, reference ([16])]. Two factors may contribute to the enhancement : First, after the stuck dislocation has been placed in motion, it may move for a distance in a stress field associated with the impediment, which is much higher than the applied field; second, the curved dislocation may shorten its length after it has been freed from the restraint, and thereby release some of the energy stored during lengthening. Both of these processes will be localized in relatively specialized regions; however, these regions may vary during the course of plastic flow. For example, the impediments may be dislocations associated with a slip system not parallel to the family to which the dislocation under consideration belongs and which change positions during plastic flow.

Of the two factors contributing to the enhancement of temperature, that arising from shortening of the dislocation line is presumably the most interesting, for the region in which the shortening takes place could be outside the region in which the impediment occurs, that is, where the crystal is relatively perfect, Actually we shall see that the temperatures are significant only within ten atom distance or so of the impediment.

The conditions under which appreciably higher temperatures may be generated in this way can be envisioned from the following argument. If a dislocation moves one atomic distance a in simple cubic lattice, the energy transferred to it from an applied stress field of intensity σ is σa^3 per atomic spacing along the length of the dislocation. On the other hand, if a dislocation line which is bent into a

half-circle of radius R straightens itself to length 2R, the energy released is $(\pi-2)R\varepsilon_0$ in which ε_0 is the energy per unit length of the dislocation line. If this energy is spread uniformly over the area $\pi R^2/2$ the energy transmitted per atom is $2(\pi-2)\varepsilon_0 a/\pi(R/a) = 0.73\ \varepsilon_0 a/(R/a)$. When σ is 10^9 ergs/cm^3, σa^3 is about 0.01 ev in a typical case. Since ε_0 a is presumably at least 1 ev in a typical solid, the energy transmitted per atom in the two cases is about equal when $R/a = 100$. Thus R/a must be of the order of 10 if the energy released per atom in this way is to be an order of magnitude larger than that released by a stress field of 10^9 dynes/cm^2. The same result may be obtained in the following way. The stress field required to maintain a segment of a dislocation line curved into an arc with radius of curvature R is $\mu a/R$, where μ is the shear modulus. Since μ is of the order of 10^{11} dynes per cm^2, the effective stress field causing the dislocation to straighten is 10^9 dynes per cm^2 when R/a is about 100.

To summarize, temperatures of the order of 1.000° K or higher can be expected only if R/a is small compared with 10. Thus the effect described by Brooks becomes important principally when the dislocation is held up by impediments which produce a very high local curvature, that is, by impediments in which the stress opposing the motion of the dislocation is at least 10^{10} dynes per cm^2. The high temperatures are then realized only within ten atom distances or so of the impediment. The most important instance of this might be that in which impurity atoms are distributed throughout the lattice and cause large local curvature of dislocations.

B. Geometrical Means.

It is evident that there are many purely geometrical methods by which dislocations can generate vacancies or interstitial atoms. One such method is sufficient for consideration. Let us assume that a screw, or Burgers, dislocation meets another screw dislocation which extends in a direction oblique to the plane in which the first screw dislocation is moving (Fig. 2). We may assume that the slip vector for the second dislocation is not in the same direction as that of the moving direction, so that it can be regarded as stationary. The moving dislocation will be restrained by the stationary dislocation in the region where the latter intersects the slip plane of the former and will, as a result, loop around it and eventually pinch off a segment which encircles the stationary dislocation. During the process of

looping, the portions of the moving dislocation which are extended parallel to the direction of motion become, in effect, lenghts of edge, or Taylor-Orowan, dislocations. Portions of the loop on opposite sides of the stationary screw dislocation will be edge dislocations of opposite sign so that they will attract one another. However, they will be moving in neighboring atomic planes because of the screw character given to the slip planes by the stationary screw dislocation. Hence when the edge-type segments of the moving dislocation meet they will annihilate during the process of pinching-off, but will leave either a row of vacant lattice sites or a row of interstitial atoms, depending upon the relative orientation of the Burgers vectors associated with the two dislocations. If we postulate that a row of vacant sites produced in this way will break up into component

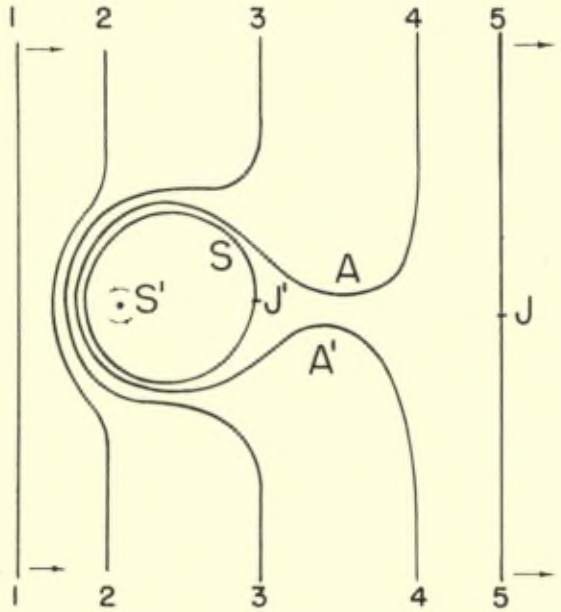

Fig. 2. — Generation of vacancies or interstitial atoms by interaction of two dislocations (schematic). S′ represents the intersection of a stationary screw dislocation with the slip plane in which another dislocation is moving. The line of the second, moving dislocation is indicated at successive positions during motion by 1, 2, 3, 4, 5. Initially the moving line lies entirely in a single slip plane. However, after looping around the stationary screw dislocation and leaving a closed segment behind, it possesses a jog J, on either side of which it lies in different slip planes. The ring left behind will also have a jog, J'. The segments A and A′, which are shown just before combining, move in neighboring slip planes and have the character of Taylor dislocations if the moving dislocation is initially of screw type (stage 1). Hence a row of vacancies or interstitial atoms will be generated when A and A′ meet, depending upon the sign of the dislocation involved in the collision.

vacancies and disperse sowewhat as a result of the local temperature engendered during the annihilation of the edge dislocation (see paragraph 4 below), we obtain a feasible, essentially geometrical method of generating vacant sites.

Since the density of dislocations which may be generated in this way, or in similar, purely geometrical ways, depends very strongly upon the entire pattern of dislocations present in the lattice, it is difficult to estimate the density which can be achieved. Speaking very roughly, we might expect a given dislocation to produce 10^4 vacant lattice sites or interstitial atoms in moving a distance of the order of the linear dimensions of mosaic blocks, namely about 10^4 atomic distances. For we might expect the line of the moving dislocation to undergo major distortion in moving from one mosaic region to another and hence to produce an aggregate extra length of the order of 10^4 atom distances, at least part of which will be annihilated in the manner described above. Hence a given dislocation would generate one vacancy per atomic plane normal to the axis of the dislocation in moving about 10^4 atomic distances. This number corresponds very closely with the observed value, as estimated in Sect. 2. However it is difficult to place much confidence in the estimate since we are relatively ignorant about the general distribution of dislocations.

C. Dynamical Instability.

The passage of a dislocation through a crystalline lattice at a speed approaching that of sound requires detailed coordination of the positions of the atoms of the lattice under conditions in which inertial forces are high. As the dislocation approaches a given atom, the atom is accelerated, attains a maximum velocity when it is at the center of the dislocation, and then comes to rest again by a more or less symmetrical process of deceleration. The local strain near the center of the dislocation is of the order of 0.1, so that the forces between atoms are no longer harmonic. It is conceivable that dynamical instabilities happen along the dislocation line at the high velocities which probably occur and that vacant lattice sites are produced as a result of this instability. This might occur with particular ease at a point where a dislocation jogs from one slip plane to a parallel one which is separated by one atomic distance. Such jogs are the seat of what the writer has termed (1) incipient vacant lattice sites. These sites are particularly easy to visualize when one is dealing with

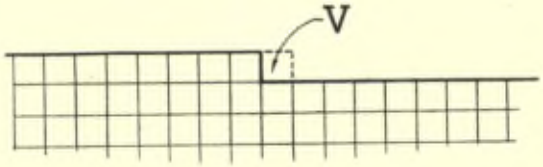

Fig. 3. — Lateral view of the « extra plane » in a Taylor dislocation and position of incipient vacancy V. The heavy line represents the Taylor dislocation when viewed in a plane normal to the slip plane and normal to the slip direction. The squares represent atomic cells. The Taylor dislocation possesses a jog and the incipient vacancy V occurs at the jog (dashed square).

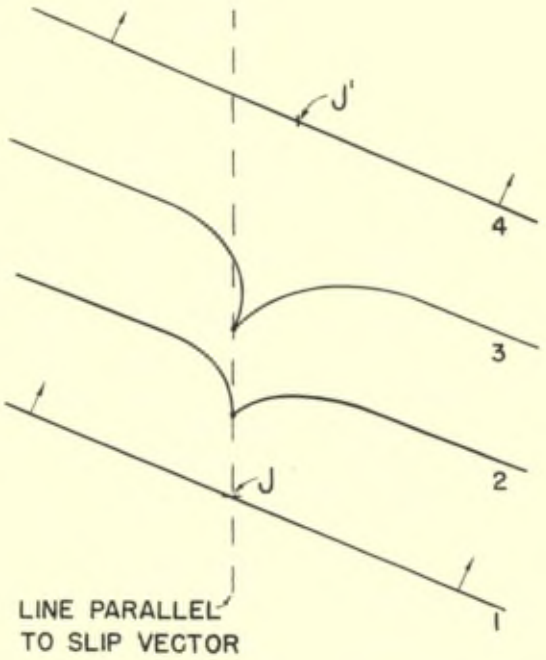

Fig. 4. — Generation of vacancies or interstitial atoms from a jog in a dislocation by geometrical means. The dislocation of mixed direction indicated by the arrows, the jog becomes caught (lines 2 and 3), and the line loops around the impediment. After the loops meet, the jog is at position J' and is displaced relative to the rows of atoms in the direction of the Burgers vector (dashed line). A row of lattice vacancies or interstitial atoms, equivalent to the distance between J. and J' normal to the dashed line, is generated in this process. The sign of the imperfections generated depends upon the sign of the jog.

Taylor dislocations, so that the dislocation can be regarded as formed by the introduction of an extra plane into the lattice in a direction normal to the slip vector. The jog then corresponds to a position where the extra plane has a step and the incipient vacancy occupies the vacant site at the step (Fig. 3). It is geometrically possible for a step of this type to move in the direction of the Burgers, or slip, vector along with the remainder of the dislocation. However, it is possible that instabilities develop and that the atom which is to move into the position of the incipient vacancy occasionally fails to do so. The vacancy would thereby be left behind. Since the energy required to free the incipient vacancy and make a normal vacancy of it is large, of the order of 1.1 ev in copper or sodium chloride, it follows that this instability would require the cooperative action of a number of atoms in the neighborhood of the jog, which would share in some communal manner the energy required. One might expect vacancies to be produced preferentially, if this mechanism prevails, in any crystal in which the energy required to generate a vacancy is appreciably less than that required to generate an interstitial atom.

It is also possible ([17]) that the instability arises from the fact that the jog becomes caught in the lattice and is brought to rest, or nearly to rest. The adjacent part of the dislocation may then loop around the restrained area and, as in the case of a dislocation that has looped around a static screw dislocation discusses in (2) above, generate a row of vacant sites or interstitial atoms (Fig. 4). In the present case the jog furnishes the differences in position of the slip planes on which the annihilating segments of the dislocation move, so that the screw character of the stationary Burgers dislocation is not required. Evidently this method of generating vacancies passes into a purely geometrical method when the dislocation is stopped by a rigid impediment in the region near the jog. It differs from the case discussed in paragraph (2) (Fig. 2), only in the means by which the displacement of two parts of the dislocation to neighboring slip planes occurs.

D. Influence of Transient Thermal Pulses.

A large amount of stored energy is released whenever two dislocations moving in the same or closely neighboring, parallel slip planes unite by annihilation. Since the energy per atomic length of a dislocation is of the order of 1 ev or more, the energy released is of this magnitude per atomic plane normal to the dislocation line.

Hence the line at which the dislocations combine becomes the seat of a very large source of thermal energy which raises the local temperature to the neigborhood of 10,000 degrees.

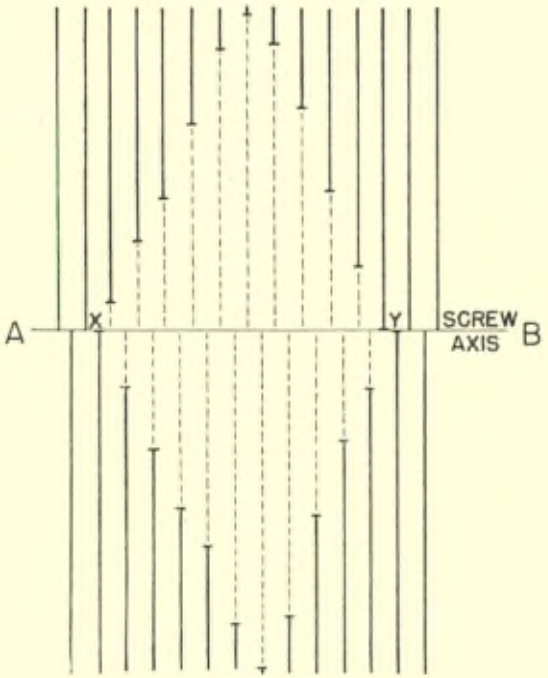

Fig. 5. — Schematic view of vacancy pattern in a spiral prismatic dislocation, formed by precipitation of vacancies. The horizontal line AB represents the line of a screw dislocation for wich the Burgers vector is in the direction AB. The vertical lines represent the intersection, with the plane of the paper, of atomic planes which are transformed into a spiral sheet as a result of the presence of the screw dislocation AB. The lines jog at AB because the screw is centered on this line. The full segments of the vertical lines are sections of the planes which are complete, whereas the dashed segments are portions of the plane on which vacancies have precipitated and «eaten» a hole. In three dimensions, the dotted portion is enclosed in a double « cone » formed by abutting the bases of two cones. The short horizontal bars outline the intersection this double cone makes with the plane of the paper. The common axis of the cones is the line AB. In practice the planes will collapse in the direction AB in order to eliminate the void represented by the dashed segments. Successive planes will be displaced by a relative distance equal to the Burgers vector for new dislocations. This is assumed to be an allowed translational vector of the lattice and need not be the same as the Burgers vector for the screw dislocation. The terminal points between the full and dashed lines (designated by horizontal bars) then become the loci of a spiral dislocation which winds about the double cone, starting at X and ending at Y.

The thermal surges pointed out by Brooks (paragr. A), which occur when a dislocation line having sufficiently large curvature is straight ened, are genetically related to the surges produced during annihilation since the total length of dislocation line is diminished in both cases. It is easy to imagine situations in which it is difficult to distinguish between the two effects.

The large burst in temperature will have subsided by the time the energy has migrated a distance of the order of 30 atomic spacings from the line of annihilation, since the energy of annihilation per atomic length along the pair of lines will be diluted over about 1,000 atoms. The average energy per atom will be of the order of 10^{-3} ev when this has occurred. The time required for this migration of heat is given by :

$$t_{30} \cong r^2/4D \tag{5}$$

in which r is the distance corresponding to 30 atomic spacings and D is the appropriate diffusion coefficient. If we assume that, under the conditions of great agitation which prevail immediately after annihilation, each atom passes its energy on to the next in the characteristic oscillational time T of 10^{-13} sec, and that $D = a^2/T$, where a is the interatomic spacing, we find that :

$$t_{30} = 2.5 \cdot 10^{-11} \text{ sec} \tag{6}$$

The time will be slightly shorter in a metal because the electrons may contribute to the diffusion; however, their mean free path should be of the order of atomic dimensions during the period when the temperature is high, hence this effect should not decrease the time by an order of magnitude. In addition the equilibrium between conduction electrons and lattice vibrations is established sufficiently slowly that the lattice vibrations retain most of the energy until the temperature has retrogressed to an uninteresting level.

There is little doubt that temperature « spikes » of this type, which are highly reminiscent of those which occur [18] when heavy particles such as alpha particles pass through matter, will promote the dispersal of rows of vacant lattice sites or interstitial atoms which are generated during the annihilation by purely geometrical effects of the type described in (2) and (3) above. The instantaneous temperatures are sufficiently high that the Boltzmann factor occuring in the expression for the diffusion coefficient of vacant sites or interstitial atoms should be close to unity. As a result, these entities

should diffuse nearly as rapidly as the thermal energy, at least for a distance of about five atomic spacings. Hence, the lines of vacancies of interstitial atoms that would be formed under ideal geometrical conditions, in which two Taylor dislocations having opposite sign and moving in planes separated by one atomic spacing annihilate one another so slowly that the temperature retains the ambient value, are broken up and partly dispersed.

It is more questionable whether stable pairs of vacancies and interstitial atoms are generated in the regions where these bursts of energy appear. The calculations of Huntington ([19]) and the writer indicate that about 10 ev is required to create such pairs in metallic copper. Even if the energy of annihilation per atomic length along a pair of dislocations is comparable to this, it is probable that the peak temperature attained is somewhat lower, when expressed in units of ev, for the annihilation energy will be liberated over the distance, of the order of five atomic spacings, for which the strain in a dislocation is large. Hence the Boltzmann factor in the expression giving the rate of generation of vacancy-instertitial pairs should be somewhat less than unity, perhaps of the order of 10^{-2}. In addition, the members of a pair will exert a very strong attractive force on one another because they produce lattice strains which are both large and of opposite sign. The energy of interaction falls off as the third power ([20]) of the distance for sufficiently large distances of separation and probably maintains this mathematical form to distances of the order of a few atomic spacings. Hence pairs which are separated by a few atomic distances, which is as far as they can be separated during the time the thermal pulse endures, will probably migrate together and recombine. This is certain to be the case if the ambient temperature is sufficiently high to allow the vacancy or interstitial atom some degree of mobility as is true near room temperature in sodium chloride and copper, for jumps which bring the two closer together should be much more probable than those which separate them, as long as they are separated by no more than a few atomic distances.

To summarize, the thermal bursts accompanying the annihilation of dislocations should make it possible for rows of defects of a given kind that are generated as a result of the geometry of annihilation to disperse by a few atomic distances. A few pairs of vacancy-interstitial atoms may be formed in the thermal burst; however, it probably is necessary to maintain the crystal at very low temperatures to prevent them from recombining as a consequence of the strong attractive forces.

4. THE MOBILITY OF VACANCIES AND PAIRS

A. Alkali Halides.

The study of ionic conductivity in the alkali halides has contributed a substantial amount of information concerning the ability of these units to migrate. It is known ([21]), for example, that the positive-ion vacancy is much more mobile than the negative-ion vacancy. The ratio of the jump frequencies ([22]) is about 10^5 at room temperature in KCl, and the value is probably close to this in NaCl. The activation energy for migration of the positive-ion vacancies is ([24]) about 0.85 ev in KCl. Hence the jump frequency is found to be near 1 sec^{-1} near room temperature, if the values obtained at higher temperatures are extrapolated to lower temperature. This value is supported by the observation that processes involving ionic migration actually occur at room temperature.

Essentially nothing is known about the behaviour of interstitial ions in the alkali halides. On the other hand, interstitial silver ions are ([25]) very mobile in the silver halides. It is probable that interstitial alkali metal ions would possess a mobility comparable to that of the positive-ion vacancies; however the energy required to generate interstitial ions in the alkali halides is larger than that required to generate vacancies.

Vacancies of opposite sign should have an association energy of the order of 1 ev in the alkali halides. In fact calculations by Reitz and Gammel ([26]) have led to a value of 0.89 ev in the case of NaCl. It seems very likely that the coupled pair of vacancies ([22]) possesses a relatively high mobility, perhaps higher than that of the positive-ion vacancy. Dienes ([27]) has estimated that the activation energy for migration of this pair is near 0.4 ev in KCl, in contrast with a value nearly twice this for the positive-ion vacancy.

B. Copper.

The precise value of the activation energy for migration of vacancies in copper is not known. However it is probably close to 1.0 ev, since the entire energy required ([28]) to form a vacancy and permit it to diffuse is only 2.1 ev and it seems reasonable, in light of the calculations of Huntington and the writer, to take the viewpoint that the activation energy for migration is about half this total. On the assumption that the jump frequency is determined by an expression

of the form (4), it is readily found that this frequency is 10^{-4} at room temperature and 10^{-21} at 100° K. Thus isolated vacancies should possess some degree of mobility at room temperature, but be frozen into position at liquid air temperature.

It is interesting to speculate on the question of the energy of association of vacancies in metals. There is little doubt that vacancies have a short-range attractive force since any degree of clustering should diminish the ratio of surface to volume of the void formed by the vacancy. For example, the average kinetic energy associated with the wave functions of the conduction electrons should diminish if the electrons are compelled to avoid only the cavity associated with a coupled pair of vacancies instead of the two voids associated with two isolated vacancies. It is possible, however, that the vacancies repel one another at large distances because they produce identical elastic distortion in the lattice. It would be highly interesting to know the general form of the interaction potential, but until this question has been studied in some detail, we can only guess the results.

It is perhaps not unreasonable to suppose that the energy of association of a pair of vacancies is close to 1.0 ev, so that nearly half the energy of about 2.0 ev associated with the pair of vacancies when they are separated is regained by combination. If this is the case, the total activation energy required to separate a pair should be near 2.0 ev, since the total activation energy would be roughly the sum of the activation energy required for migration of an isolated vacancy plus the energy of association. The time required for the pair to dissociate under thermal fluctuations at room temperature would then be infinite for all practical purpose. A direct theoretical value, obtained with the use of an equation of the form of (4) is 10^{20} sec.

There is no reason to suppose that the energy of association of a pair of vacancies actually is quite as large, or larger, than the energy of formation of a single vacancy. However, if this situation actually did occur, the energy required to form a pair of vacancies would be equal to or less than the energy required to form a single vacancy. In this case, pairs would probably be formed in preference to single vacancies by normal thermal means since the entropy increase associated with the presence of a pair is probably larger than the entropy increase associated with a single vacancy. As Brooks has pointed out to the writer (private communication), a crystal

in which pairs are formed in preference to single vacancies could exhibit remarkable properties. For example, if diffusion takes place by means of vacancies, the activation energy for self diffusion might be markedly lower in such a crystal than in a comparable one in which single vacancies are prefered, for, as we shall see below it is not unreasonable to suppose that pairs of vacancies diffuse more rapidly than single vacancies.

As in the case of the salts ([27]), we should expect the pair to be very mobile, for the number of repulsive bonds, arising from closed-shell interation that must be overcome is reduced. If we assume that the activation energy for migration of the pair is near 0.5 ev in copper, the jump frequency at room temperature is about 10^5 sec.$^{-1}$, whereas that at 200° K is about 1 sec.$^{-1}$. The jump frequency at 100° K is of the order of 10^{-10}/sec., which is negligible small. It is evident that pairs of this type may play a very important role in coagulation affected by migration of vacant lattice sites at room temperature, and even at 200° K. In fact, it is natural to suggest, at this very incomplete stage of our knowledge, that the diminution of resistivity observed in the experiments of Molenaar and Aarts, when the specimens deformed at liquid air temperature are annealed at room temperature, is the result of coagulation of vacancies by diffusion of pairs, or possibly larger aggregates which also possess a relatively high mobility.

Although the calculations of Huntington and the writer indicate that the energy required to form an interstitial atom in copper is much larger than that required to form a vacancy, the results also suggest that the activation energy for diffusion of the interstitial atom by replacement of neighbors, that is by the interstitialcy([6]) mechanism, is of the same magnitude as that for migration of vacancies. Hence interstitial atoms should have some mobility at room temperature. However, even if pairs of interstitial atoms become bonded, we should not expect such pairs to diffuse faster than single interstitial atoms. For the situation is presumably just the opposite of that around a pair of vacancies in the sense that the pair of interstitial atoms will compress the immediate neighborhood in which they are situated and make migration more difficult. It seems unlikely that the migration of interstitial atoms plays an important role in copper and similar metals in the vicinity of room temperature.

Diffusion in aluminium will be considered in the next section.

5. INFLUENCE OF COLD-WORK ON THE RATE OF PRECIPITATION

A. Experiments.

It appears to be well established ([30]) that cold-work increases the rate at which copper precipitates in aluminium containing a few percent of copper. This effect has been investigated most carefully by Gayler ([30]) whose observations may be summarized as follows.

1) The measurements show that the logarithm of the time required to achieve a given state of precipitation, such as the time t_m required to achieve the second, or maximum, peak in hardness, varies linearly with 1/T, where T is the absolute temperature. Gayler has found that this line is displaced parallel to itself by cold-work produced during rolling. The investigations were made for reduction in area lying between zero and 90 percent and for temperatures between 100 °C and 187 °C. This result suggests that the activation energy for the process determining precipitation is not altered by cold-work. Instead, the rate process is enhanced by a factor which is essentially independent of temperature. If we assume that diffusion is the limiting process, the result supports the view that the coefficient of the Boltzmann factor in the conventional expression for the diffusion constant, and not the activation energy, is altered by cold-work.

2) The rate of aging at a given temperature is a continuous function of cold-work. Gayler has shown that the curve giving the relation between the reduction of cross section and the logarithm of time required to achieve the secondary maximum of hardening is approximately linear for reduction to about 80 %. The curve then flattens near 100 % reduction when plotted in this manner. The result might have been plotted in other ways which would have been more revealing. The writer has attempted to transcribe Gayler's result in such a way that $1/t_m$ is represented as a function of the strain $\varepsilon = -\log(1-R)$, in which R is the fractional reduction in cross section. The resulting curve is nearly linear for the entire range of R. Thus, within the precision that this transcription of Gayler's data allows, one may say that the increase in rate of precipitation varies linearly with the strain to strains of the order of 3.2 (96 % reduction).

B. Vacancy Diffusion

Gayler's results may be explained on the assumption that diffusion of the copper atoms responsible for precipitation occurs with the use of vacancies in the manner proposed by Johnson and Wagner [31] and that the vacancies produced during cold-working are able to assist in the process. The precipitation rate is determined by the density of vacancies. From the slope of the log t_m versus 1/T curves given by Gayler, which is available for three decades of t_m, one may estimate that the activation energy for diffusion of copper is about 28,000 cal per mol. This is smaller than the experimental values [32] of the diffusion coefficient of copper determined by various investigators, which range between 33,900 and 41,900. These values are determined from diffusion data obtained at higher temperatures than those of interest in normal precipitation studies; moreover, the range of temperature employed is sufficiently small that the diffusion coefficient varies only by a factor of ten, which does not permit very accurate evaluation of the activation energy. We should expect the activation energy for precipitation after cold-work to be lower than that for diffusion a higher temperature, for the vacancies will presumably be at thermal equilibrium at elevated temperature and the energy required to form a vacancy near a copper atom will appear in the activation energy for diffusion whereas this is not the case if vacancies are formed during deformation. It is very interesting to note, however, that the activation energy for precipitation in the range below 200 °C in the absence of cold-work is the same as that after cold-work. From the present point of view, this is to be explained on the assumption that the density of vacancies is higher than the equilibrium value during precipitation, There would appear to be two possible explanations of this fact :

1) Some of the vacancies formed at elevated temperatures are captured by copper atoms during the quenching step and succeed in coming more nearly to complete equilibrium only after the precipitation process has taken place. Before being bound into dislocations or other stable clusters they succeed in helping the copper atoms to precipitate. An argument to be given in a later paragraph of this section indicates that the density of vacancies retained in Gayler's undeformed specimens is of the order of 3×10^{16} per cc, that is of the order of one per million aluminium atoms. This is the density which would be at equilibrium at about 500 °C, that is at a temperature

somewhat above those employed in Gayler's experiments. If this interpretation is valid, the activation energy involved in precipitation should increase at temperatures somewhat higher than those employed in Gayler's experiments because the density of vacancies will correspond to the equilibrium value. Moreover, the temperature at wich the equilibrium value is attained should increase with increased cold-work because the density of vacancies arising from cold-work increases.

2) The vacancies which are responsible for precipitation in the undeformed alloys are generated during precipitation because of localized plastic flow which accompanies the process. Presumably the stresses engendered during precipitation will be relieved, at least in part, by the motion of dislocations in regions about the precipitates. One might expect vacancies to be produced during this process and enter into the diffusion process until they are recaptured by a dislocation, or cluster together. This explanation can be valid only if the density of vacancies formed during precipitation is independent of the rate of precipitation. For if the alloys in which precipitation is rapid have a higher density of vacancies than those in which it is slow, one would not expect the rate of precipitation to be proportional to the value for a cold-worked specimen, which presumably starts with a fixed density of vacancies, over the entire range of temperature.

On the whole, the first of these two possibilities appears to be more reasonable than the second, although available experimental material is not sufficient to distinguish between tho two.

C. Nabarro's Viewpoint.

Nabarro ([33]) has suggested that the increase in rate of precipitation with cold-work, without a change in activation energy for the process, is related to an increase in the density of nucleating centers for the precipitation process. It would be very interesting to test the relative merits of this proposal with that given above by comparing the size of the precipitate particles in a deformed and an undeformed specimen, for this size should vary inversely as the density of nuclei, and hence be strongly dependent on cold-work, if Nabarro's proposal is correct.

The specimens employed by Gayler contained 4 % of copper. Since the density of vacancies in cold-worked specimens should be

less than this even when the reduction in area is 96 %, corresponding to a strain of about 3.2, it is evident that the vacancies must act in the manner of catalysts, if we are correct in assuming that the Johnson-Wagner mechanism prevails. Presumably the vacancies deposit a copper atom at the site of a precipitate and then wander away to assist another, somewhat in the manner in which positive-ion vacancies presumably catalyse the coagulation of F-centers in colored alkali halides ([22]). Again, it is quite possible that the vacancies migrate as pairs or larger clusters during the process. The activation energy for self-diffusion in aluminium is apparently unknown, but is probably in the vicinity of 35,000 cal per mol. If we assume that the activation energy for diffusion of a single vacancy is about half of this, the jump frequency should be about 10^3 at 100 °C. This rough value is sufficiently large that we cannot exclude the possibility that the vacancies act as single units instead of pairs or clusters. Moreover, it is sufficiently large to suggest that the vacancies generated in aluminium during cold-work are able to migrate more than a few atomic distances at temperatures near room temperature, in agreement with the observation of Molenaar and Aarts that the increase in electrical resistivity induced in aluminium during cold-work at low temperatures anneals completely at room temperature in a time of the order of a few minutes.

D. Density of Retained Vacancies

There is one additional matter of interest that may be gleaned from Gayler's measurements. The rate of precipitation of copper is about 1,000 times faster in the specimen which has been reduced by 96 % than in the material which has been subject to quenching without cold-work. If we assume that the first specimen has been strained by 3,2 and that the density of vacancies is proportional to the strain, we may conclude that the cold-worked specimen contains about 3×10^{19} vacancies per cc. It follows that the quenched specimen, which was not cold-worked, must have contained about 3×10^{16} vacancies per cc, or somewhat less than one vacancy per million normal sites. This would not be sufficiently large to determine by measurements of density and lattice spacing, even if the complication of distortion as a result of the formation of precipitates did not exist.

E. Rohner's Theory.

In surveying the literature on precipitation in the aluminium-copper system, the writer noted the paper of Rohner ([34]) with interest. This investigator has suggested that vacancies play an important role in the precipitation and hardening process, however his views do not appear to follow the conventional pattern of current thought. He proposes, in effect, that the copper atoms migrate interstitially and that at least a part of the hardness of the alloy is a result of the formation of vacant sites as a consequence of the transfer of copper atoms from normal to interstitial positions. The evidence presented in the foregoing paragraphs suggests that the vacancies produced in the way envisaged by Rohner would coagulate in a few minutes at the temperatures where precipitation is observed, so that they should not have an influence on hardening. In justice to Rohner, one must admit that something akin to Frenkel disorder may occur in aluminium and that interstitial diffusion may be an important process. Our present knowledge of diffusion in the aluminium system does not preclude this possibility.

FOOTNOTES

(1) F. Seitz, *Phys. Rev.*, **80**, p. 239 (1950).
(2) Z. Gyulai and D. Hartley, *Zeits. f. Phys.*, **51**, p. 378 (1928).
(3) A. W. Stepanow, *Zeits. f. Phys.*, **81**, p. 560 (1933).
(4) J. Molenaar and W. H. Aarts, *Nature*, **166**, p. 690 (1950).
(5) J. O. Linde, *Ann. d. Phys.*, **15**, p. 219 (1950).
(6) See, for example, the discussion by the writer, *Acta Crystallographica*, **3**, p. 355 (1950).
(7) G. I. Taylor and H. Quinney, *Proc. Roy. Soc.*, **143**, p. 307 (1934); **163**, p. 157 (1937).
(8) See, for example, H. W. Etzel and R. J. Maurer, *Jour. Chem. Phys.*, **18**, p. 1003 (1950).
(9) See note added in proof, reference 1.
(10) C. Wagner and P. Hantelmann, *J. Chem. Phys.*, **18**, p. 72 (1950).
(11) M. Masima and G. Sachs, *Zeits f Phys.*, **51**, p. 321 (1928); **54**, p. 666 (1929).
(12) G. Tammann and K. L. Dryeer, *Ann. d. Phys.*, **16**, p. 111 (1933);
G. Tammann and G. Bandel, *ibid.* p. 120;
G. Tammann and K. L. Dreyer, *ibid.*, p. 657;
G. Tammann and G. Moritz, *ibid.*, p. 677;
G. Tammann and V. Caglioti, *ibid.*, p. 680.
This work includes measurements of the change in thermoelectric potential as a result of cold-work. Transient effects resemble sowewhat those observed by Gyulai and Hartly are described for a number of metals and alloys. I am indebted to Professor N. F. Mott for calling my attention to these papers.
(13) The possibility that dislocations move at a velocity close to that of sound was first exploited by F. C. Frank, Bristol Conference on the Strength of Solids (Proceedings of the Physical Society of London, p. 46, 1948), who attempted to employ this property to achieve dynamic multiplication of dislocations. The dynamics of such motion has been investigated by J. D. Eshelby, *Proc. Phys., Soc.*, **62**, p. 307 (1949) under the assumption that the medium is continuous. Eshelby has demonstrated in a very elegant way that the energy varies with velocity in a manner resembling the variation of energy of a particle in the special theory of relativity.
(14) G. Leibfried, *Zeits. f. Phys.*, **127**, p. 344 (1949);
See also F. R. N. Nabarro, *Phil. Mag.*, **41**, p. 1270 (1950).
(15) F. Seitz, *Pittsburgh Symposium of the Plastic Deformation of Crystalline Solids* (Naval Research Laboratory, p. 1 1950).
(16) For a review of dislocation theory see, for example, Bristol Conference on the Strength of Solids (reference 13); Pittsburgh Symposium on the Plastic Deformation of Crystalline Solids (reference 15); A. H. Cottrell, *Progress in Metal Physics* (Interscience Press, New York, 1949); W. T. Read and W. Shockley, *Phys. Rev.*, **78**, p. 275 (1950).
(17) This possibility was suggested independently by W. T. Read (Private Communication), on the basis of a viewpoint developed by Read and Shockley and to be published in the reports of the Pocono Conference on Imperfect Crystals.
(18) See, for example, the paper by the writer, Discussions of the Faraday Society, No. 5, p. 271 (1949) and that by S. Siegel, *Phys. Rev.*, **75**, p. 1823 (1949).
(19) H. B. Huntington and F. Seitz, *Phys. Rev.*, **61**, p. 315 (1942); H. B. Huntington *ibid.*, p. 325.
(20) See F. Seitz and T. A. Read, *Journ. App. Phys.*, **12**, p. 182 (1941);
A. E. H. Love, *Mathematical Theory of Elasticity* (Cambridge University Press, 1927).

(21) C. Tubandt, « Handbuch der Experimental Physik », Vol. XII, part I.
(22) See, for example, the review by the writer, *Rev. Mod. Phys.*, **18**, p. 384 (1946).
(23) H. W. Etzel and R. J. Maurer, *Journ. Chem. Phys.*, **18**, p. 1003 (1950);
D. E. Mapother, H. N. Crooks and R. J. Maurer, *Jour. Chem. Phys., ibid.*, p. 1231.
(24) H. Kelting and H. Witt, *Zeits. f. Phys.*, **126**, p. 697 (1949).
(25) J. Teltow, *Ann. d. Phys.*, **5**, pp. 63, 71 (1949); *Zeits. Phys. Chem.*, pp. 195, 197, 213 (1950).
(26) J. R. Reitz and J. L. Gammel, (As yet unpublished work).
(27) G. J. Dienes, *Journ. Chem. Phys.*, **16**, p. 620 (1948).
(28) The writer accepts the measured value of M. S. Maier and H. R. Nelson, *Trans. A. I. M. E.*, **147**, p. 39 (1942), as the most reliable one. (See reference 8).
(29) The writer is indebted to N. F. Mott for calling his attention to this aspect of the influence of cold-work on the properties of metals.
(30) M. L. V. Gayler, *Jour. Instit. of Metals*, **72**, p. 243, 543 (1946). See also the review by G. C. Smith in *Progress in Metal Physics* (Butterworth Scientific Publications, 1949) and the book, *Age Hardening of Metals* (American Society for Metals, Cleveland, 1939).
(31) R. P. Johnson, *Phys. Rev.*, **56**, p. 814 (1939);
C. Wagner, *Zeits. Phys. Chem.*, **38***B*, p. 325 (1937).
(32) See, for example, C. J. Smithells, *Metals Reference Book* (Butterworth Scientific Publications, London, 1949);
R. F. Mehl, F. N. Rhines and K. A. von den Steinen, *Metals and Alloys*, **13**, p. 41 (1941);
H. Hückel, *Zeits. f. Elek.*, **49**, p. 238 (1943);
A. H. Bierwald, *Zeits. f. Elek.*, **45**, p. 789 (1939).
(33) F. R. N. Nabarro, « Symposium on Internal Stresses in Metals » (Institute of Metals, London, 1948), p. 237.
(34) F. Rohner, *Jour. Inst. Metals*, **73**, p. 285 (1947).

Discussion du rapport de M. Seitz

M. Mott. — 1) If we are to attribute all the effect of cold work on the rate of age-hardening to the increase of number of vacancies in the metal, would we expect any change in the distribution of precipitates? Can Mr. Guinier say whether any change of distribution, which might indicate an effect of cold work on nucleation of Preston-Guinier zones, can be observed by X rays?

2) Has anyone calculated the effect of an increased diffusion rate on the distribution of precipitates?

M. Guinier. — Pour les précipités, le microscope électronique montre que les premiers précipités apparaissent dans les régions perturbées du cristal (lignes de glissement, sous-limites). Pour ce qui est des zones, j'ai observé sur l'alliage Al-Zn un accroissement de la vitesse de croissance avec l'écrouissage. Des expériences plus systématiques et plus précises vont être entreprises sur cette question.

Il semble qu'outre les expériences de Gayler, deux faits pourraient

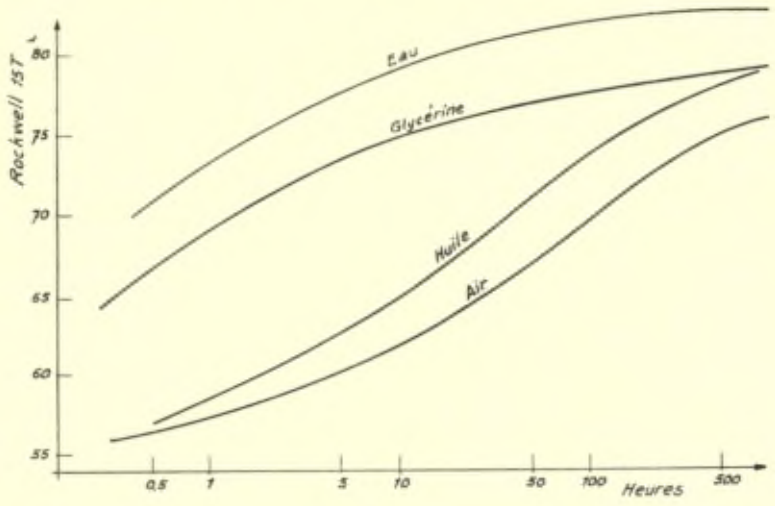

Fig. 1

être cités en faveur de la théorie exposée dans le rapport en discussion.

1) On sait que le durcissement à froid d'un alliage Al-Cu c'est-à-dire en formation d'amas est d'autant plus rapide que la trempe est plus brutale (fig. 1). Généralement, on dit que le fait est la conséquence des tensions de trempe. Mais nous avons remarqué que la déformation du cristal par la trempe à l'eau est faible et qu'une déformation de cet ordre appliquée sur un cristal trempé à l'air a une influence faible sur la vitesse de durcissement.

On pourrait donc imaginer que les lacunes en équilibre à haute température n'ont pas le temps de disparaître comme dans la trempe à l'air et constituent des amorces pour les amas d'atomes de cuivre.

2) Quand un alliage Al-Cu durci à froid est soumis pendant un temps très court (4 minutes) à la température de 200°, le durcissement disparaît parce que les amas d'atomes se dissolvent et que la phase précipitée n'a pas le temps de se développer (Phénomène de réversion — Rückbildung). De nouveau laissé à la température ordinaire, l'alliage durcit de nouveau, mais bien plus lentement (fig. 2). Dans ce cas encore, l'alliage étant trempé seulement depuis 200°, il n'y a pas de lacunes pour servir d'amorces à la formation de nouveaux amas.

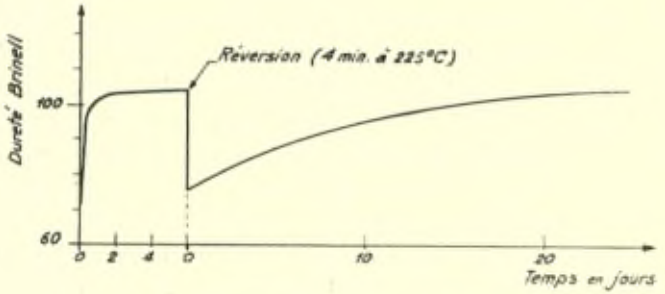

Variation de la dureté du duralumin avant et après réversion.

Fig. 2

Mais il faut remarquer que les mêmes raisonnements dans les deux cas cités pourraient être faits avec d'autres défauts que des lacunes (par exemple des embryons dus aux fluctuations thermiques).

M. Mott. — Both the experiments quoted by Guignier show that frozen-in vacancies contribute to diffusion and accelerate hardening.

They do not show, however, whether the effect of cold-work on age-hardening is by creating vacancies and so accelerating precipitation, or by creating favourable spots for the nucleation process. In the latter case one would expect a higher concentration of smaller precipitates with cold-work than without.

M. Seitz. — I agree that one has an alternative choice of explaining the existing experimental information by assuming that there is an acceleration in the rate of nucleation. Presumably an extension of the present experiments is necessary to decide between the two choices. I wish to emphasize that the viewpoint I have taken is consistent with wath we know at the present.

M. Kramers. — What is an incipient vacancy?

M. Seitz. — An incipient vacancy is a point along a dislocation at which a vacancy may be generated or annihilated in the crystal lattice with essentially the same energy that would be resquired if it were generated or annihilated at the surface of the crystal. The simplest case to consider is that in which the dislocation is of the pure Taylor type. In this case, the dislocation can be visualized geometrically by assuming that the crystal contains an extra half plane. The dislocation line then runs along the edge of the extra half plane. Imagine that there is a partially completed row of atoms on the edge of the extra plane as if the edge had a jog. The point where the jog occurs represents the site of the incipient vacancy. One may generate a vacancy by taking an atom from a neighboring portion of the lattice and moving it to the end of the incompleted row thereby extending this row by one atom and generating a vacant site in the lattice. The lattice is under tension in the region where the atom has been added so that it has some of the characteristics of a vacancy. One can regard the vacancy as being produced by « evaporation » from this position.

M. Bragg. — Can we please have explained to us the geometry of a jog?

M. Orowan. — The jog could be called elementary errors-slip.

M. Frank. — The jog is precisely equivalent to Kossel's reproducible point at the surface of crystal, and the formation of a vacancy at it is equivalent to Kossel's « wiederholbare Schritt », occurring however in the interior of a crystal. I should like to call it an interior Kossel point.

M. Hollomon. — Concerning the Kirkendall Effect, it should be pointed out that in diffusion couples in which the Kirkendall Effect is observed and the specimen is carefully examined, porosity can be observed on the side of the couple in which vacancies must condense. Recent experiments by Alexander and his colleagues at Sylvania Electric Company indicate that the quantitative conclusions of da Silva and Mehl (*) may have to be somewhat re-evaluated because of this porosity. Furthermore, during the motion of inert markers, even if one side of the couple is a single crystal, recrystallization and motion of grain boundaries take place during the diffusion and thus it is difficult to assess the contributions of grain boundaries as sources and sinks of vacancies.

There seems to be much confusion about the effect of deformation on the rate and amount of precipitation from solid solution. Specimens of supersaturated alloys are usually deformed and the rate of hardening determined. The change in hardness as a function of time and temperature is then compared with the change in hardness of an undeformed specimen without super-imposing upon that specimen the comparable deformation. Thus the specimens are not compared with equivalent deformations. Secondly, if a supersaturated solution is deformed and then hardened, part of the hardness change will certainly be caused by strain aging which is associated with precipitation and under other circumstances recovery and recrystallization. The meaning of experiments in which the rate of hardening due to precipitation of deformed specimens has been determined is difficult to ascertain. Lubahn, of the General Electric Research Laboratory, has performed experiments on specimens of an 61S alloy. In these experiments one specimen was deformed at —190° before aging at room temperature and another specimen was aged at room temperature and then deformed an equal amount at —190 °C. The subsequent deformation behavior of the two

(*) L. C. C. da Silva, R. F. Mehl, « Interface in Diffusion in Solid Solutions » *Journal of Metals*, **188**, October 1950.

specimens was the same. Admittedly for this alloy the precipitation was of the « cold-hardening » type; i. e., it took place at low temperatures.

It was concluded from these results that the deformation accelerates precipitation along slip bands but that general precipitation where subsequent slip must take place is not accelerated by deformation.

M. Mott. — In these experiments it appears that the dislocations have accelerated the nucleation, rather than that there has been a general increase in the rate of precipitation.

M. Guinier. — Dans l'influence de l'écrouissage sur le durcissement, il faut bien distinguer deux effets :

1) la nucléation de précipités (caractéristiques du Warmaushärtung) est facilitée par le désordre du réseau; il apparaît donc des précipités sur les bandes de glissement, mais ces précipités très rares ne doivent pas avoir d'influence sur les propriétés mécaniques;

2) Si la cinétique du durcissement varie, c'est que la vitesse de formation de zones est modifiée (Kaltaushärtung).

Mais les observations sur la présence de précipités ne donnent aucun renseignement sur ce second phénomène. Ce sont les rayonsX qui permettent de suivre le développement des zones.

M. Crussard. — Lorsqu'on parle d'influence de l'écrouissage sur la vitesse de précipitation, il est essentiel de distinguer la précipitation cohérente (Kaltaushärtung) de la précipitation avec germination (Warmaushärtung). Des expériences récentes de P. Lacombe et de notre laboratoire montrent que sur un alliage Al-Cu à 4 %, l'écrouissage par traction diminue la précipitation du premier type. Au contraire, pour la précipitation du deuxième type, de nombreuses expériences montrent que l'écrouissage l'accélère; dans ce cas, des essais de Jolivet sur l'influence de l'écrouissage sur la vitesse de décomposition isotherme de l'austénite, ont prouvé que la *vitesse de germination* seule était accrue, mais que la vitesse de croissance était peu affectée.

Il faut remarquer que les lacunes réticulaires produites par écrouissage, selon le mécanisme suggéré par Seitz, ne peuvent accélérer la diffusion que si elles sont isolées ou en tout petits groupes, c'est-à-dire aux très basses températures. Aux températures voisines de l'ambiante, les lacunes doivent être déjà drainées par les dislocations ou coales-

cées en trous. Ce qui expliquait l'absence d'influence de l'écrouissage à chaud sur la vitesse de croissance, mise en évidence par Jolivet.

M. Bragg. — The bubble model often shows multiple vacancies, of a regular geometrical form. A number of examples are shown in the paper by Mr. Nye and myself on the model. Such multiple vacancies are very mobile and must be in constant Brownian movement, may they not be mainly responsible for many changes in the solid state such as diffusion and allotropic change. Their small number is compensated by their mobility.

M. Seitz. — Yes, this is probably so according to calculation on properties of double vacancies in sodium chloride.

M. Orowan. — The large changes in density observed in some experiments may be due to the formation of large cavities such as those known as « Rose Channels », which are results of twinning or slip on incompatible planes.

M. Seitz. — This is very true and all experiments on this subject should be done under conditions of single slip, as has been done at Stuttgart.

M. Guinier. — La décroissance de la résistivité est associée à la coalescence des lacunes qui sont donc moins effectives à l'état d'amas que des lacunes isolées. Au contraire, dans le durcissement des alliages, le rassemblement des atomes dissous accroît la résistivité. Comment expliquer la différence?

M. Seitz. — When atoms coagulate in a lattice during precipitation, the imperfection they produce grows as precipitation proceeds and, in a sense, the irregularity endures as a permanent irregularity. When vacancies precipitate they may form a dislocation ring or may add to an existing dislocation. If the ring is sufficiently large, the disturbance of the lattice will be less than if one had the corresponding number of vacancies distributed as individuals in the lattice. The atoms on either side of the surface bounded by the ring can be in register so that all of the imperfection is at the perimeter of the ring. If the vacancies add to an existing dislocation then of course the imperfection is no worse than it was to begin with. The main point is that vacancies have the means, which foreign atoms do not, to leave the lattice in a much more nearly perfect condition as they precipitate.

Diskussionsbeitrag zur Theorie der Versetzungen

U. Dehlinger

Eine der zentralen Fragen in der Theorie der Versetzungen ist die nach der Existenz und Höhe einer Aktivierungsenergie für die Auflösung von Versetzungen, d. h. die Erholung von der Verfestigung, die nach unseren Messungen proportional der Zahl der durch das Gitter gewanderten Versetzungen ist. In einer Dissertation von P. Fischer wurde daher mit der Peierls' -schen Integralgleichung in einem endlichen Gitter mit zwei glatten Rändern die Energie einer geraden Versetzungslinie als Funktion des Abstandes von den Rändern berechnet. Dabei ergab sich, dass zum Herstellen der Versetzung am Rande zunächst 1 eV und zum Eindringen in das Innere nochmals etwa 2 eV nötig sind. Am anderen Rand ergibt sich zunächst keine weitere Energieschwelle, was im Gegensatz zu den empirischen Befunden, vor allem den Erholungsmessungen von Masing, Kuhlmann und Raffelsieper steht. Man kann also eine Mosaikgrenze nicht als freie Oberfläche behandeln. Denkt man sich statt dessen in den Mosaikgrenzen festliegende Versetzungen, so erhöht deren Spannungsfeld die Energie der in ihre Nähe kommenden wandernden Versetzungen, wirkt also näherungsweise wie eine Vergrösserung der elastischen Moduln in der Nähe der Grenze. Man erhält so für die Energie einer Versetzung als Funktion ihres Ortes im Mosaikblock die Abb. 1, die eine Grundlage für das Verständnis der Erholung und wohl auch der Verfestigung bilden kann.

Eine genauere Berechnung wurde von A. Seeger in Stuttgart in folgender Weise durchgeführt :

Das Schubspannungsfeld des von Read und Shockley (1) u. a. vorgeschlagenen Versetzungsmodells der Korngrenzen ist im ein-

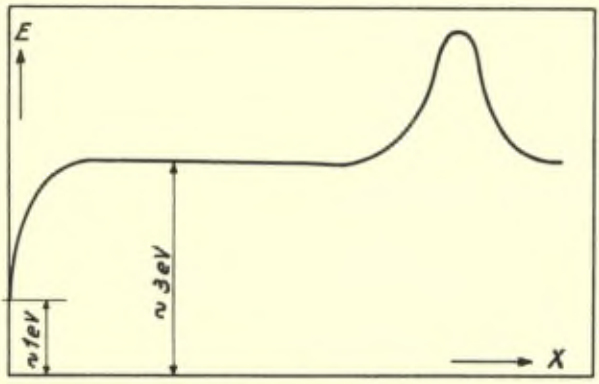

Abb. 1

fachsten Fall (isotropes Medium, einfach kubischer Kristall, Korngrenze [$x = 0$] senkrecht zur Gleitrichtung [x — Richtung])

$$\tau_{xy}(x,y) = -\frac{G\,a}{2\pi(1-\nu)}\left(\frac{\pi}{D}\right)^2 \times \frac{\sin^2\frac{\pi y}{D}\cosh^2\frac{\pi x}{D} - \cos^2\frac{\pi y}{D}\sinh^2\frac{\pi x}{D}}{\left[\sin^2\frac{\pi y}{D}+\sinh^2\frac{\pi x}{D}\right]^2}$$

(G = Schubmodul, ν = Poissonsche Zahl, a = Gitterkonstante, D = Versetzungsabstand in der Korngrenze). Gl. (1) gilt in elastizitätstheoretischer zweidimensionaler Näherung für $+y$—Versetzungen (1) in der Korngrenze; in gleicher Näherung ist die Kraft pro Netzebene auf eine $+y$—Versetzung gegeben durch (2).

$$K_x = a^2\,\tau_{xy}(x,y)$$

Die potentielle Energie pro Netzebene einer Versetzung (abzüglich ihrer Eigenenergie) in einem Punkt x, y ist :

$$U(x,y) = -a^2\int_{-\infty}^{x}\tau_{xy}(\xi,y)d\xi = \frac{Ga^3}{2\pi(1-\nu)}\left[\frac{x\pi}{D}\frac{\sinh^2\frac{\pi x}{D}}{\cosh^2\frac{\pi x}{D}-\cos^2\frac{\pi y}{D}}\right.$$

$$\left. -\frac{1}{2}\ln\left[2\left(\cosh\frac{2\pi x}{D}-\cos\frac{2\pi y}{D}\right)\right]\right]$$

Die Energiefläche U (x, y) ist symmetrisch zu $x = 0$ und periodisch in y-Richtung. Ihre Schnitte $y = \text{const.}$ besitzen längs der in Abb. 2 mit Kreizen bezeichneten Linien :

$$\left(x = 0 \text{ und } tg^2 \frac{\pi y}{D} = tgh^2 \frac{\pi x}{D}\right)$$

Mulden bzw. Kämme; in gleichschschraffierten Gebieten hat τ_{xy} das gleiche Vorzeichen. Man erkennt sofort, dass die Versetzungsanord-

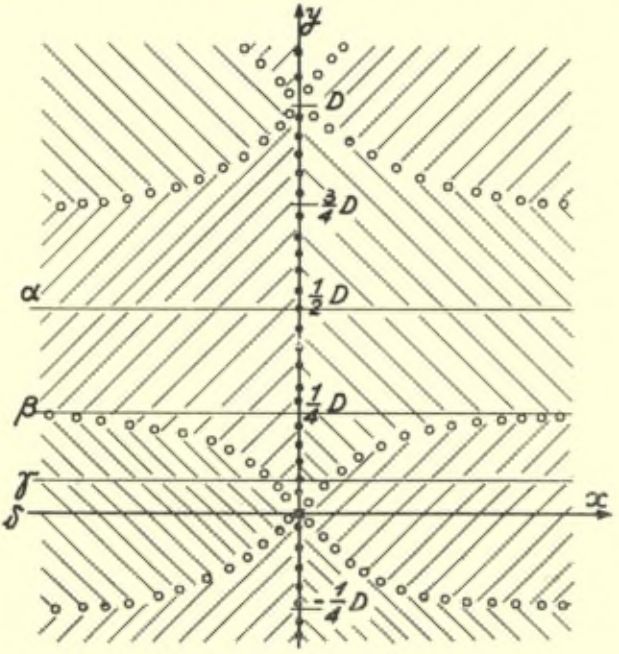

Abb. 2. — Das Spannungsfeld in der Umgebung der Korngrenze. In entgegengesetzt schaffierten Bereichen hat τ_{xy} entgegengesetztes Vorzeichen.

nung in der Korngrenze stabil ist, da eine herausgegriffene Versetzung durch das Spannungsfeld aller übrigen an ihrem Ort festgehalten wird. Abb. 3 gibt Schnitte der U—Fläche längs der in Abb. 2 gestrichelt gezeichneten Geraden α — δ wieder; Abb. 4 stellt die Maxima und Minima der Schnitte $y = \text{const.}$ als Funktion von y dar. Die Abbildungen sind für eine $+ y$ — Versetzung im Punkt (x, y) gezeichnet; für $- y$ — Versetzungen ist die U-Achse umzukehren.

Die Einheit für U in den Abb. 3 und 4 ist im Falle von Cu ($G = 4{,}53, 10^{11}$ dyn cm $^{-2}$, $\nu = 0{,}340$, $a = 2{,}552$ Å) 11,4 eV. Die auftre-

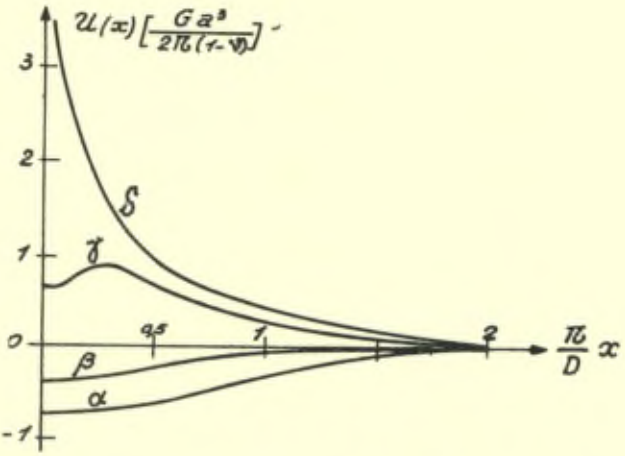

Abb. 3. — Schnitte y = const. durch die U-Fläche längs der in Abb. 2 gestrichelt gezeichneten Geraden α ($y = D/2$), β ($y = D/4$), γ ($y = D/12$) und δ ($y = 0$).

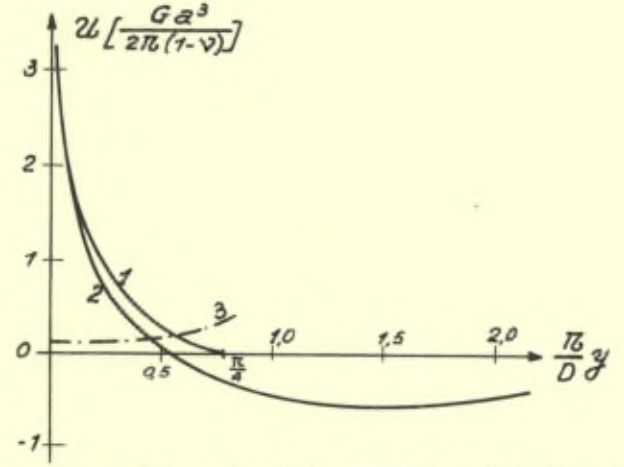

Abb. 4. — Maxima (Kurve 1) und Minima (Kurve 2) der Schnitte y = const. als Funktion von y. Die strichpunktierte Kurve 3 gibt die Differenz der Kurven 1 und 2, also die eigentliche Energieschwelle wieder.

tenden Energieschwellen haben also gerade die Grössenordnung der Auflösungs- bzw. Bildungsenergieschwellen, wie die Analyse der experimentellen Ergebnisse nach Kochendörfer [3] fordert (2—3*e*V). Im vorliegenden Bild erfolgt die Auflösung von Versetzungen durch die Vereinigung ungleichnamiger Versetzungen über die Korngrenze

hinweg, oder noch wahrscheinlicher durch Diffusionsbewegungen zwischen weiter entfernten ungleichnamigen Versetzungen, während die Bildung von Versetzungspaaren durch das (unabhängig voneinander) von Crussard (4) und Seeger (5) vorgeschlagene Zusammenwirken von Schubspannungen mit günstig interferierenden thermischen Schwingungen zustande kommt. Dies ist möglich in der Nähe der Korngrenzenversetzungen, da dort die U—Kurven (Abb. 2) drei Extrema besitzen und deshalb ungleichnamige Versetzungen bei genügender Separation stabil sein können.

(1) W. T. Read and W. Shockley : *Phys. Rev.*, **78,** S. 275 (1950).

(2) G. Leibfried : *Z. Phys.*, **126,** S. 781 (1949).

(3) A. Kochendörfer : *Plastische Eigenschaften von Kristallen und metallischen Werkstoffen*, Springer, Berlin 1941 und *Z. Phys.*, **126,** S. 548 (1949).

(4) C. Crussard : Solvay-Conf. 1951.

(5) A. Seeger, Dissertation Stuttgart 1951 (Veröffentlichung in *Z. Phys.* vorgesehen).

Discussion du rapport de M. Dehlinger

M. Frank. — Professor Dehlinger's calculation shows an activation energy of 2 e. V. per atomic plane for the penetration of a dislocation wall by a free dislocation. We cannot think of taking one atomic unit of length of dislocation line through by itself : we must at least take through a short loop of say 10 atomic lengths at one time. This would make the activation energy 20 e.V., which is too large.

M. Bragg. — It is not quite clear how we can consider one dislocation as free, and those in the wall as bound and quite immobile.

M. Dehlinger. — Die Versetzungen der Wände halten sich gegenseitig im Gleichgewicht, während die die Verformung tragenden Versetzungen einzeln durch das Gitter wandern. Wie weit die Versetzungen der Wände trotz ihrer Vernetzung unter den Einfluss von Schubspannungen sich verschieben können, wird von Dr. Shockley besprochen werden. Auf alle Fälle ist diese Verschiebung geringer als bei den Einzelversetzungen.

M. Crussard. — Suite à la question de Sir L. Bragg (pourquoi les dislocations de la paroi sont elles stables, alors que les autres se propagent?) :

On peut admettre que les dislocations de la paroi, qui sont là depuis un certain temps, ont drainé à elles les impuretés et atomes dissous, qui ont deux effets :

— ancrer les dislocations de la paroi,

— abaisser les tensions internes aux environs des dislocations de la paroi, ce qui abaisse les énergies d'activation calculées par le professeur Dehlinger.

M. Frank. — It seems that however much we may modify and refine the calculation of the activation energy for a single dislocation

to pass through an array, we shall always arrive at a very high result. A more likely physical process for the penetration of such barriers by dislocations is that many dislocations pile up on one slip plane and so produce a very large stress concentration sufficient to achieve the results without the aid of thermal activation.

M. Dehlinger. — Das von Herrn Frank erwähnte Problem des Zusammenwirkens einer ganzen Reihe von Versetzungen ist experimentell dadurch klar definiert, dass nach Kuhlmann die Aktivierungsenergie von der Verfestigung, d. h. der Zahl der gebildeten Versetzungen abhängt. Rechnungen in dieser Richtung sind in Vorbereitung.

M. Cottrell. — Professor Dehlinger has discussed a model in which a moving dislocation tries to pass through a mosaic wall the dislocations of which are parallel to the moving dislocation. This model leads to difficulties; the activation energy appears to be very large and there is uncertainty about the effect of the applied stress on the dislocations in the wall. I want to suggest an alternative model which is easier to discuss and leads to a reasonable activation energy. Suppose that the moving dislocation runs up against a mosaic wall the dislocations of which are perpendicular to the slip plane of the moving dislocation. When the Burgers vector of the wall dislocations is perpendicular to that of the moving dislocation, there is no elastic interaction and the moving dislocation will « hang up » against the row of wall dislocations, taking a form rather like that of a string slung loosely across a horizontal row of rods. To move the dislocation through the wall, it must cut through the wall dislocations, and whenever such a cut occurs a jog will be formed on the dislocation line. The energy of formation of such a jog can be supplied partly by the applied stress and partly by thermal fluctuations. The energy of a jog is of order μb^3(μ is shear modulus, b is lattice spacing), let us say of order 1eV. The activation energy for the unit step in cutting through the wall can never be larger than this value, and such a value as this is within the range of accomplishment by thermal fluctuations at room temperature. When an applied stress is present the activation energy may be reduced further. Let the spacing of the dislocations in the wall be L and the applied shear stress be σ. To cut through one wall dislocation, a length L of the moving dislocations moves a distance of order b.

The work done is then $\sigma\ Lb^3$. Hence the activation energy is of order $\mu b^3 - \sigma L b^2$. This is zero when $\sigma/\mu = L/b$.

M. Bragg. — It seems as though the effect of a dislocation wall might be rather like a piece of polaroid, only permitting dislocations lying on lines perpendicular to those in the wall to pass easily through.

M. Crussard. — In a face centred cubic lattice there are no sets of dislocations with Burger's vectors normal to each other.

M. Cottrell. — That is true. However the angles between the dislocation lines themselves and between their Burger's vectors can both be large; in such cases the force in the slip direction due to the elastic interactions of these dislocations is always small and in certain orientations may vanish altogether.

M. Shockley. — The blocking action of dislocations cutting through each other can be analyzed semiquantitatively by considering the energy required to offset two planes to be approximately $G\ b^3$ where G is the rigidity and b the Burgers vector. Since this cutting requires a relative motion of the dislocations over a distance several Burgers vectors in length, the force required for cutting is of the order of

$$F = G\ b^2$$

This force is of the same order as the linear tension of the core of a dislocation. Consequently, if two dislocations are forced together, they will make a relatively sharp angle before they cut through each other. It is interesting to note that this mechanism leads to a hardening formula that depends on dislocation density in the same way as does that of Taylor. (For a more complete discussion see Heidenvich and Shockley (1948), referred to in my report.)

Additionnal Comment.

The model of a cold worked metal as a sort of froth of dislocations receives support from the observations of B. E. Warren (reported in « Imperfections in Nearly Perfect Crystals », John Wiley, N.Y. 1952). Warren has studied the dependence of mean squared stress $<\sigma_0^2>$ in cold worked materials as a function of the length L of a column of

atoms over which the stress is averaged. I shall quote a comment (*) prepared in collaboration with W. T. Reach that brings out the relationships.

It is possible to obtain from dislocation theory a rough quantitative prediction of the relation between the root mean square average stress $<\sigma_0^2>^{1/2}$ at L = 0 and the distance over which the stress is substantially uniform. If D is the average spacing between dislocations, the root mean square stress is approximately

$$<\sigma_0^2>^{1/2} = (Gb/\pi D)\,(ln\ D/2b)^{1/2}, \qquad (D.1)$$

where $b \doteq 2.5$ Å is the slip distance and G is the shear modulus. To investigate theoretically the dependence of root mean square stress on orientation in an anisotropic material such as alpha brass, it would be necessary to use anisotropic elasticity and to carry out a much more involved analysis than is attempted here. We shall therefore take

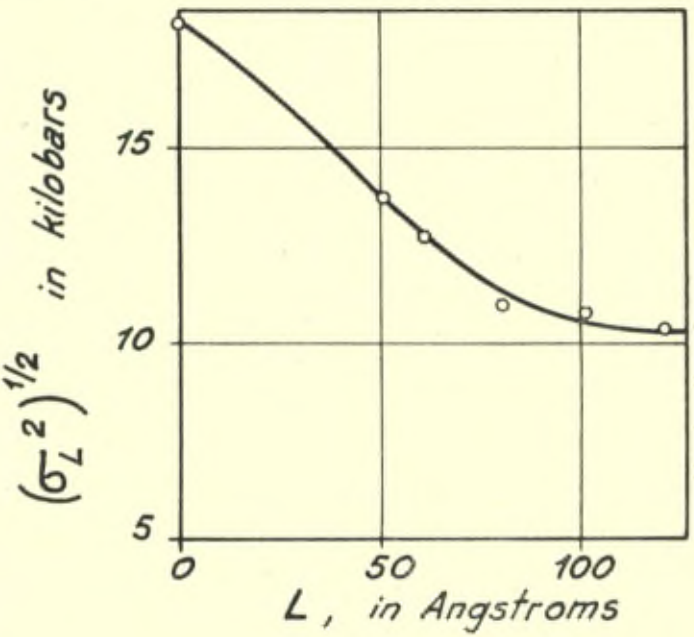

Fig. 1. — Root mean square values of stress averaged over distances L for cold-worked (70 — 30) α-brass.

(*) Quoted from « Imperfections in nearly perfect crystals », John Wiley, New York 1952.

$G = c_{44} = 720$ kilobars. From the curve of fig. 1, $<\sigma_0^2>^{1/2} = 18$ kilobars. Substituting in the foregoing equation gives $D = 50$ Å. If the dislocations are spaced 50 Å apart, it would be expected that the stress would be uniform for regions less than 50 Å in extent but would decrease for regions larger than 50 Å, a prediction in agreement with the curve of fig. 1, which shows an appreciably decay for ordinates larger than 50 Å. Thus the dislocation density calculated from the peak of the curve agrees with the spacing of centers of disturbance as indicated by the rate of decay of the root mean square average stress with distance of averaging.

It should be emphasized that the general agreement between the value of D deduced from $<\sigma_0^2>^{1/2}$ and the value of L at which $<\sigma_L^2>^{1/2}$ begins to decrease would not necessarily be obtained for other models of the cold-worked metal. For example, the alloy might be considered to consist of large blocks, perfect except for elastic deformation, fitted together at grain boundaries in such a way as to be alternately under compression and tension. Under these conditions, the strain would be homogeneous over regions whose size was large compared to D deduced above. It should thus be regarded as a gratifying, but not surprising, confirmation of dislocation theory that the values of L and D do turn out to be comparable in magnitude.

Because of the atomic nature of the material studied, it follows that the stress cannot vary appreciably for distances less than one or two atomic diameters. Consequently, $<\sigma_L^2>^{1/2}$ must have a value independent of L as L approaches zero and must, therefore, have a vanishing derivative at $L = 0$. The curve of fig. 1 should, accordingly, be drawn with a zero slope at $L = 0$; this is entirely consistent with the experimental points.

M. Burgers. — How definitely can we say the block model of a crystal's imperfections is of no use?

M. Seitz. — Warren used filings in his experiments. Hirsch has found in Cambridge that less severely worked metals show a structure much more like the usual one of blocks.

M. Frank. — Suppose we consider two like parallel dislocation lines, a distance D apart, and locked at points a distance D apart along their length. Then we may calculate the radius of curvature

by which the dislocation lines will bow out, on account of their mutual elastic repulsion. When D is of the order of magnitude 1 micron (this enters in a logarithmic factor), the radius of curvature is about 20 D. I interpret this in the sense that the line-tension property of dislocations predominates over their action-at-a-distance: so that to a first approximation I expect the structure of a random collection of dislocations in an annealed metal to correspond to a three-dimensional network in tensile equilibrium, with dislocations joining at nodes according to the rule that the sum of the Burgers vectors of the dislocations meeting at a node, as seen from the node, is zero.

This applies when there is no large excess of dislocations all of one kind. When there is such an excess, e.g. in a region of uniform bending or torsion, their actions-at-a-distance will cooperate, predominate over the tensile forces, and gather them into girds, as is seen in polygonisation. Thus the picture of a block-like mosaic structure, and the other extreme pictures of a random three-dimensional network of dislocations, may either of them be appropriate in various cases.

Calorimetric Studies of Isothermal Recovery

by G. Borelius

In the physical laboratory of the Technical University of Stockholm we have by the method of isothermal calorimetry made measurements on the heat evolved during recovery at raised temperatures after cold-working at room temperature. The measurements have only gone on for a short time and the results are preliminary.

Al and Cu rolled at 23° C and immediately after rolling measured at 60° C gave a power-time curve (P. t curve), the first part of which can be given by

$$P = \frac{a}{t} - b$$

where a and b are constants, Fig. 1 shows P as a function of t and of $1/t$.

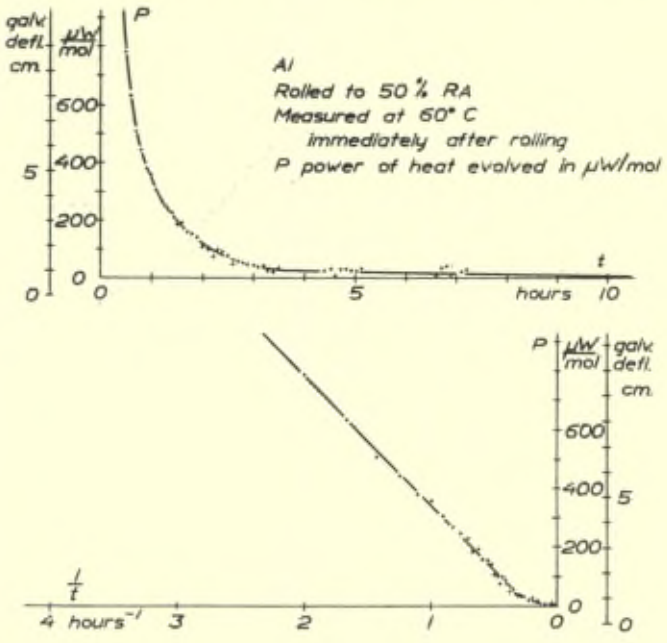

Fig. 1.

For samples of Al and Cu which after the rolling were aged for some time at room temperature and then measured at 60° C, the curves take on the form

$$P = \frac{a}{t + t_0} - b.$$

Fig 2 shows curves obtained for a sample of pure Cu, which had been aged for a day at room temperature. The three curves give P as a function of t, $1/t$ and $1/(t + t_0)$, where t_0 is found to be 0.25 hours. This probably means that the state of recovery reached after 24 hours at 24° C, is reached after 15 minutes at 60° C.

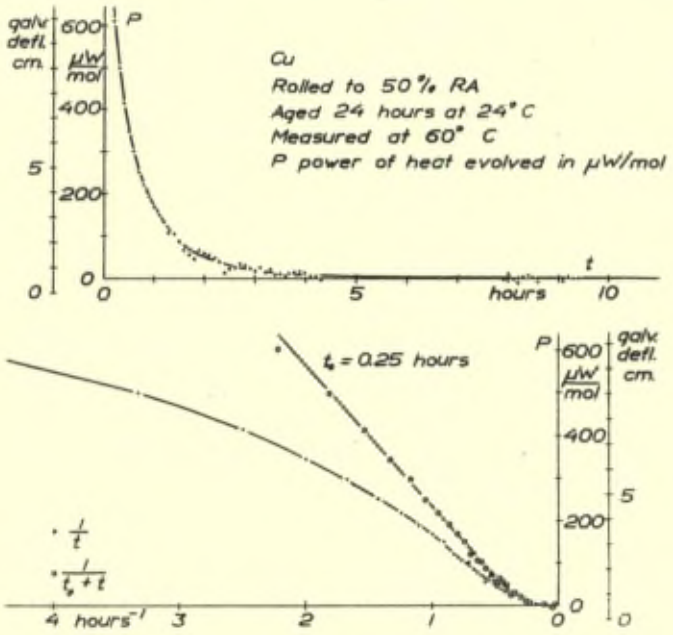

Fig. 2.

Discussion du rapport de M. Borelius

M. Kramers. — In your expression $P \sim \frac{1}{t + t_0}$, does the t_0 arise from a mathematical approximation and would a more exact treatment give the « tail » of the curve?

M. Borelius. — The expression $P = \frac{1}{t + t_0}$ is in accordance with the differential equation

$$P = -\frac{dQ}{dt} = Q\ c\ \exp\left(\frac{-E - nQ}{RT}\right)$$

where Q is the heat per mol still to be given off, t the time variable, c a constant, which according to van Liempt should be of the order of magnitude of the Debye frequency of vibrations of the atoms, E the activation energy per mol for the place change of atoms in the undisturbed lattice, n a constant number, R the gas constant and T the absolute temperature. This equation is a slight modification of formulae given by Kuhlmann, which in turn are modifications of the formulae of van Liempt. The colorimetric measurements give the values of the constant n which are of the order of 2,000 — 4,000. For the tail there seems so far to be no theoretical treatment.

M. Dehlinger. — Die während und kurz nach der Verformung eintretenden Vorgänge können am besten aus Messungen der Härte oder der kritischen Schubspannung entnommen werden. Daher ist es wichtig zu wissen, wie die gemessene Wärmeentwicklung mit dem zeitlichen Verlauf der Härte usw. korrespondiert.

M. Orowan. — The rest period after working and before the experiments seems to be an avoidable complication. A means of continuous testing with X-rays at the exit side of a wire drawing die suggests a method of attack.

Dislocation Models of Grain Boundaries *

W. Shockley

Bell Telephone Laboratories, Inc.

Murray Hill, N. J., U. S. A.

1. INTRODUCTION

The suggestion that an array of dislocations constitutes the interface between two crystal grains was discussed about ten years ago by W. L. Bragg (1940) and J. M. Burgers (1940). For boundaries between crystals of very small orientation difference, such a model for the boundary seems as natural as do dislocations themselves as one form of imperfection in nearly perfect crystals. Such a boundary is illustrated in Figure 1 (b).

In the late 1940's, a number of workers gave consideration to the energetic consequences of this model. The most striking conclusion is that if other quantities are held constant E, the energy per unit area of grain boundary, should vary with θ, the orientation difference, according to the law :

$$E = E_0 \theta[A - \ln \theta] \qquad (1.1)$$

where E_0 and A are independent of θ. This formula was apparently derived independently at several places, including Cambridge University and the University of Bristol and was first published by Read and Shockley (1949).

The formula (1.1) occupies a unique position in the field of dislocation theory. The reason is that only in the case of a grain boundary and in the case of a crystal growing by the Frank mechanism (reported elsewhere in this volume) is there reason to believe that

(*) This report is based largely on two previous publications by W. T. Read and W. Shockley, *Phys. Rev.*, **78**, p. 275 (1950) and a paper in Imperfections in Nearly Perfect Crystals, John Wiley, New York, 1952. The author is indebted to the two publishers for permitting the reproduction of some of the figures and text from each article.

we know what the dislocation pattern is in detail. Of these two cases only the grain boundary has properties determined directly by the energies of the dislocations. The crystal growth case is concerned with geometry rather than energy. Thus the grain boundary case is, at present, the one in which direct comparisons between theoretical and experimental energies may best be made.

These comparisons are aided by the fact that E_0 and A depend on different aspects of the energy of the dislocations. The quantity E_0 is independent of the « core energy » of the dislocation which arises in part from broken interatomic bonds. It may be calculated, by means described in Sections 2 and 3, in terms of the geometry of the dislocation array and elasticity theory. Thus it may be possible from experimental measurements of E_0, as discussed in Sections 5 and 6, to establish that a grain boundary consists of some particular array of dislocations. Beyond this it may be possible to determine just what part of A is due to local distortions at the core of the dislocation. The way in which theory and experiment could be compared for core energies is discussed in Section 2.

In addition to being static energy systems, grain boundaries are dynamic and will move under applied stresses. The possible mechanisms of motion for a small angle boundary are discussed in Section 7 and the extensions of the considerations to large angle boundaries, in Section 8. The treatment of large angle boundaries as layers of liquid metal suggests a model of a molten metal as a solid with a high density of dislocations. This point is pursued to a limited extent in Appendix A4.

Formula (1.1) has been found to fit the experimental data surprisingly well over a large range of angles. This agreement has been criticized as possibly accidental or spurious in discussion at the Solvay conference prior to the presentation and final preparation of this report. These points are discussed and to some degree disposed of at the end of Section 5.

2. ON THE ORIGIN OF GRAIN BOUNDARY ENERGY

In order to illustrate the principles involved in determining grain boundary energies for small angle boundaries, we shall consider the simple example shown in Figure 1 (b). For the determination of the constant E_0, only one result is required from anisotropic elasticity theory. The expression for the component τ of shearing

stress in the slip direction and on the slip plane of a single dislocation. Letting r be the perpendicular distance from the dislocation axis, assumed to be an infinite straight line, it may be shown that τ may be expanded in the form :

$$\tau = \tau_0 b/r + \tau_1 (b/r)^2 + \ldots + \tau_n (b/r)^n + \ldots \qquad (2.1)$$

where τ_0 is uniquely determined by the slip vector, whose length is b, and the elastic constants of the anisotropic material, and the coefficients $\tau_1 \ldots \tau_n \ldots$ are determined by the interaction of the elastically strained material with the disordered material near the dislocation

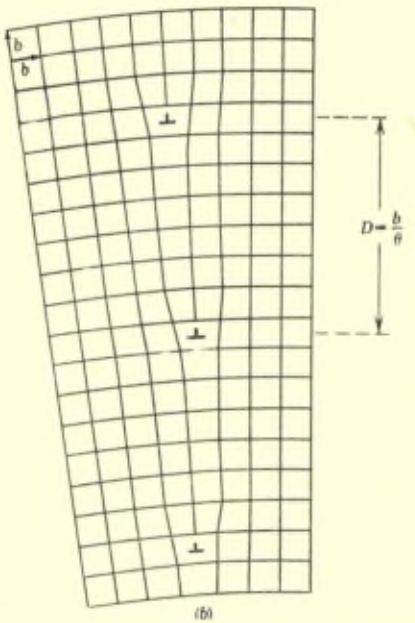

Fig. 1. A dislocation model of a small-angle grain boundary in a two-dimensional square lattice.

axis, where (2.1) does not apply. If we are interested in the stress only at distances of many atomic spacings from the dislocation, then only the first term in (2.1) need be considered. Also the first term is the only one which contributes to the dependence of the energy on the size of the crystal; or, when many dislocations are present having stress fields which cancel at large distances, the first

term in (2.1) is the only one which gives an energy dependence on the size of the stressed region. In contrast the other terms in (2.1) represent a localized elastic energy, which may be added to the inelastic energy of the dislocation core to give a total concentrated energy per dislocation depending on atomic misfit.

The dislocation model of the grain boundary in Figure 1 consists of a vertical row of edge dislocations, as indicated in the figure by the symbol $\perp$. Due to the symmetry of the boundary, only a single type of dislocation is required. To calculate the energy, we could sum the stress fields due to an infinite vertical row of dislocations, and integrate the stress energy over the entire domain. So far as the value of E_o is concerned a much simpler procedure is possible based on the following physical reasoning.

Let us consider *the energy per dislocation per unit length along the dislocations* as the sum of three energies E_I, E_{II} and E_{III} associated with the regions shown in Figure 2 (a). E_I is the energy inside of a

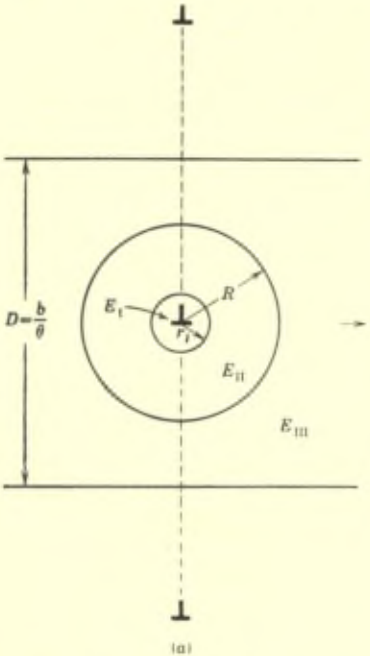

Fig. 2. Origin of energy in the grain boundary.
(a) The 3 types of energy, E_I, E_{II} and E_{III}, in the grain boundary of Fig. 1.

circle of radius r_l which is several times b such that for $r > r_l$ Hooke's law and linear elasticity theory are valid. E_{II} is the energy in the region of elastic distortion between the circle of radius r_l and a circle of radius $R \gg b$, where R is proportional to but sufficiently smaller than D that inside of R the stress can be assumed to be due entirely to the included dislocation. We shall introduce the symbol K to define this proportionality :

$$R = K D ; \tag{2.2}$$

as the angle θ of the grain boundary varies, K is held constant, E_{III} is the elastic energy in the remainder of the strip. Since the array of dislocations represents an alternating stress field with period D, and since the stress vanishes at large distances from the array, the stress falls off as $\exp(-2\pi r/D)$ along region III and consequently the energy in III is localized near the grain boundary.

Since the length of dislocation line per unit area is $1/D$, the energy per unit area of grain boundary is :

$$E = (E_I + E_{II} + E_{III})/D. \tag{2.3}$$

We shall next consider how the individual energy terms depend upon θ, r_l and K.

Inside r_l, the energy arises entirely from the encircles dislocation.

Thus
$$E_I = E_I(r_l) \tag{2.4}$$

is independent of θ unless θ becomes so large that the $R = KD < r_l$ so that stress fields of adjoining dislocations contribute appreciably inside r_l.

The energy E_{III} is also independent of θ. This is due to the cancellation of two effects produced by decreasing θ and increasing R:(1) Corresponding elements of area vary as R^2 in Fig. 2; (2) the energy density at corresponding points varies as $1/R^2$. To prove (2), consider that all the linear dimensions, including b, increase in proportion to R; the energy density would then remain the same at corresponding distances from the dislocation; that is, the whole picture would simply be photographically enlarged. The effect of increasing b in proportion to R is to increase the energy density proportionally to R^2 since both stress and strain are proportional to b. Thus, for constant b, the energy density must vary as $1/R^2$. Hence E_{III} is independent of θ. It does, however, depend on K so that we may write :

$$E_{III} = E_{III}(K) . \tag{2.5}$$

The energy E_{II} depends on r_l, θ and K. The dependence on θ is readily calculated with the aid of the construction shown in Figure 2 (b). In this ring the distortion is elastic and the stress, by hypothesis, can be considered to be due entirely to the included dislocation, hence the energy is readily calculated if the elastic stress field around a single dislocation is known. The following simple calculation involves knowing only the shearing stress τ, (2.1). The

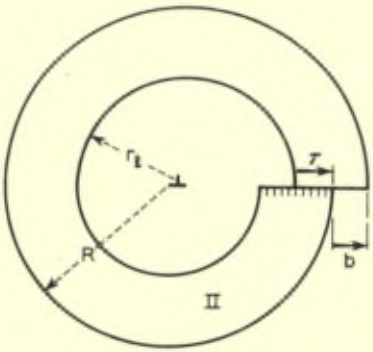

Fig. 2. Origin of energy in the grain boundary.
(b) Method of calculating the energy in region II.

energy in the ring is equal to the work done on the boundary in the virtual (equilibrium) process of forming the dislocation, and thus is equal to one-half the product of surface stress and displacement integrated over the complete boundary, which includes, not only the two circles, but also the connecting section of slip plane. From dislocation theory we know that the stress varies as r^{-1} and the displacement, except for a rigid body translation of each circle, is independent of r; hence the integrated product of stress and displacement is equal and opposite on the two circles except for the contribution of the rigid body displacement, which can be seen to vanish since the net force on each circle necessarily vanishes. Thus the energy E_{II} in the ring is equal to simply one-half the force $\int \tau dr$, Figure 2, times the slip distance b, and we have :

$$E_{II} = (b/2) \int \tau dr \qquad (2.6)$$

the integral extending from r_l to Kb/θ. Substituting (2.1), in (2.6) and neglecting for the moment higher order terms in b/r in (2.1), the expression (2.6) becomes :

$$E_{II} = (1/2)\tau_0 b^2 \int dr/r = (1/2)\tau_0 b^2 \ln(K\, b/r_l\, \theta) \; . \qquad (2.7)$$

The expressions just considered can be substituted in (2.3) leading to :

$$E(\theta) = [E_I(r_l) + E_{III}(K) + \frac{1}{2}\tau_o b^2 \ln(Kb/r_l) - \frac{1}{2}\tau_o b^2 \ln\theta] (\theta/b)$$

$$= E_o\theta(A - \ln\theta)$$

$$= E_o\theta[1 - \ln(\theta/\theta_m)] \qquad (2.8)$$

where :

$$A \equiv [E_I(r_l) + E_{III}(K) + \frac{1}{2}\tau_o b^2 \ln(Kb/r_l)]/bE_o \qquad (2.9)$$

$$E_o \equiv b\tau_o/2 \qquad (2.10)$$

$$\theta_m \equiv \exp(A-1), \qquad A = 1 + \ln\theta_m . \qquad (2.11)$$

The quantity E_o is thus seen to be defined uniquely in terms of the Burger's vector and the elastic constants of the material.. It has been emphasized that this unique dependence of E_o upon the dislocation model affords one of the best opportunites for checking quantitative predictions of dislocation theory. If E_o/θ is plotted as a function of $\ln\theta$, as is done C. S. Smiths's report in this volume, then the slope of the resulting straight line is E_o.

It is of interest to point out that E/θ is simply related to

$$\text{the energy per unit length of dislocation} = bE/\theta \qquad (2.12)$$

for the simple boundary of Figure 1. Thus plots of E/θ versus $\ln\theta$ show how the energy per dislocation decreases with increasing angle due to the decrease in the surrounding volume of elastically strained material. This interpretation also makes it clear why the slope should depend only on elasticity theory since in E/θ the core energy contributes a constant term.

Once E_o has been determined from the data the value of A may be found. This may be done graphically by extrapolating the line to $E/\theta = 0$, thus obtaining an angle θ_o. The value of A is :

$$A = \ln\theta_o . \qquad (2.13)$$

Alternatively, if E is plotted versus θ, the maximum value of E occurs for $\theta = \theta_m$ and A may then be determined from θ_m. This latter

method has the disadvantage of putting emphasis on high angle data, where the theory may be extended beyond its range of validity. The best procedure is thus to use the small angle data to determine A, by extrapolating to θ_0 for example.

Once A is known, the sum (2.9) can be evaluated to find $E_I(r_l)$, the energy at the core of the dislocation. Thus calculation involves the additional step of evaluating $E_{III}(K)$ which requires a more detailed working out of dislocation theory than is involved in finding E_0. With E_{III} regarded as known, (2.9) can be expressed in the form:

$$E_I(r_l) - \frac{1}{2} b^2 \tau_0 \ln (r_l/b) =$$

$$bE^0A + E_{III}(K) + \frac{1}{2} b^2 \tau_0 \ln (K) . \qquad (2.14)$$

The right side is actually independent of K, since varying K within the range allowed by its definition [see discussion near eq. (2.2)], simply exchanges energy between E_{II} and E_{III}. In a similar way, the choice of r_l does not affect the left side. (A specific value of E_{III} is discused in (2.17) below.)

The fact that an experimental determination of E_0 and A leads to definite value of

$$E_I(r_l) - \frac{1}{2} \tau_0 b^2 \ln(r_l/b) \qquad (2.15)$$

reflects the fact that $E_I(r_l)$ is arbitrary in its dependence upon r_l. In other words, the « core energy » of a dislocation is not uniquely defined and depends upon the amount of elastically strained material that is included with it. Mathematically, the role of r_l and the core energy can be eliminated at one stroke by introducing a new parameter r_0. The radius r_0 is defined to satisfy the equation :

$$E_I(r_0) =$$

$$bE_0 A + E_{III}(K) + \frac{1}{2} b^2 \tau_0 \ln(Kr_0/b) = 0 ; \qquad (2.16)$$

this definition has the physical interpretation that r_0 is the radius such that the elastic energy between r_0 and r_l, assuming Hooke's law is valid for $r \geq r_0$, is equal to the true energy of the dislocation inside r_l including core energy and energy in the range where Hooke's law fails. This interpretation leads automatically to $E_I(r_c) = 0$, since (2.16) results in attributing all of the energy to elastic energy.

Furthermore, from this interpretation, we can make a rough estimate of r_o.

A rough estimate of r_o can be made by the following reasoning : If r_o is allowed to approach zero, then the energy in region II increases logarithmically to infinity as $(b^2\tau_o/2)\ \ln(b/r_o)$. This is physically unreasonable because for $r_o < b$, the energy would correspond to deforming a part of an atom. Evidently the elastic energy cannot by any stretch of imagination be considered to exist on a scale much smaller than $r_o = b$. The atomic nuclei surrounding the dislocation lie on circle of radius about b/2 and it would be reasonable to suppose that the neglect of the energy of broken bonds inside $r = b/2$ would be approximately offset by the overestimate of elastic energy for $r_1 > r > b/2$ where Hooke's law fails. Thus a value of b/2 for r_o is not unreasonable.

In order to consider the effect of the assumed value of $r_o = b/2$ upon the grain boundary energy curve, we must introduce the value of E_{III}. For the grain boundary model of Figure 1 treated by isotropic elasticity theory, it is found that (Read and Shockley [1950]) :

$$\tau_o = G/2\pi\,(1-\sigma) \tag{2.17a}$$

$$G = \text{rigidity modulus} \tag{2.17b}$$

$$\sigma = \text{Poisson's ratio} \tag{2.17c}$$

$$E_{III} = (\tau_o b^2/2)\,[1 - \ln\,(K/2\pi)] \tag{2.17d}$$

$$E_o = b\tau_o/2 = Gb/4\pi\,(1-\sigma) \tag{2.17e}$$

and this leads to :

$$A = 1 + \ln\,(b/2\pi r_o) \tag{2.18a}$$

$$\theta_m = b/2\pi r_o \tag{2.18b}$$

for $r_o = b/2$. $A = -0.15$ and $\theta_m = 1/\pi = 18^o$. This value is in the general range observed and discussed in Sections 5 and 6 below.

Actually the calculation does not proceed by calculating E_{III} but instead by calculating $E(\theta)$ directly in terms r_o and the elastic constants. From the resulting expression, the value of E_{III} can be determined by comparison with eq. (2.8).

In carrying out the calculations described above, the higher terms of (2.1) were neglected. These terms arise from the fact that the stress field near the dislocation is far from ideal. The bubble model pictures presented by W. M. Lomer show that across the slip

plane of the dislocation the strain exceeds the linear range for a region 8 to 10 lattice constants wide whereas the material on either side of the slip plane is strained only slightly. Also we see that the region of the dislocation represents a local expansion since the opening up of a gap on the slip plane as well as a shearing displacement is produced by the dislocation. Both of these departures from the ideal dislocation strain, which is so defined that it corresponds to no net expansion or contraction inside r_l, give rise to additional terms in (2.1). The contribution of these higher order terms converges as $r \to \infty$ so that they contribute a finite elastic energy E'_{II} to E_{II}. This energy is independent of θ for small θ and probably comparable to but smaller than $E_I(r_l)$, for $r_l = 5b$ for example. Their energy contributions can be included with those of the broken bonds and the non-linear region by a suitable choice of r_o.

If an exact calculation is ever made on the basis of atomic theory of the energy inside r_l, and of the energy $E'_{II}(r_l)$ outside of r_l, then the energy of the boundary will be :

$$E = [E_I(r_l) + E'_{II}(r_l) + E_{II}(\theta, r_l, K) + E_{III}(K)]/D. \qquad (2.19)$$

For the case of isotropic elasticity discussed above, E_{III} and E_{II} are given in terms of (2.7) and (2.17) so that :

$$A = 1 + \ln (b/2\pi\, r_l)$$

$$+ 2[E_I(r_l) + E'_{II}(r_l)]/b^2\tau_o \qquad (2.20)$$

$$E_o = Gb/4\pi\,(1-\sigma)\ .$$

These equations or their generalizations to the anisotropic case would furnish a basis for compating the « atomic » calculation of dislocation core energy with experimental values of grain boundary energies.

At the time of writing, calculations of E_{III} have been carried out only for isotropic elasticity theory and for particularly simple boundaries. The results are quoted in Appendix A1. The calculations are tedious but can be carried out for any case likely to be of interest. Thus experimenters should not be discouraged from attempting to obtain absolute values for grain boundary energies for fear of a lack of interpretation of the results.

It should be pointed out that the energy calculations just discussed correspond to the absolute zero of temperature since the effect of

the dislocations upon the energy rather than the free energy is evaluated. The difference is unimportant for small angle boundaries as may be seen by the following argument. The free energy at the elevated temperatures, at which the grain boundaries come to equilibrium configurations in the experiments, may be taken as the sum of the energy at absolute zero U_0 plus a sum of free energies of the form :

$$kT \ln [1 - \exp(-h\nu/kT)]$$

one from each mode of vibration. The energy U_0 is increased by the energies of the grain boundaries calculated at absolute zero. In addition the presence of dislocations affects the frequency of the normal modes. This effect can be estimated by thinking in terms of an Einstein model in which each atom is imagined to have its own frequency. For such a model we would expect appreciable changes in frequency to occur only for the atoms in the regions in which Hooke's law fails. As a rough estimate we shall assume that for each lattice constant of length along a dislocation, six atoms have a change in frequency of 15%. This will contribute a change in free energy at high temperatures, $h\nu/kT \ll 1$, of $6kT \ln 1.15 \doteq kT$ per unit length of dislocation. This free energy change will contribute additively to E_I, however, and will therefore not affect comparisons with experiment in regard to E_0; physically this is because E_0 arises from regions which are deformed elastically so that the change in their free energy may be determined from the elastic energy calculated from their isothermal elastic constants.

The contribution to E_I due to the change in frequency may be appreciable, as may be seen from the rough estimate given above and also by a more intuitive argument. For a large angle boundary, the energies E_{II} and E_{III} are small compared to E_I since the E_I regions are in contact or overlapping. Hence the free energy due to E_I per unit length of dislocation will be of the order of $E_m 2b$ since dislocations will be only a few atomic distances apart. This leads to free energies per lattice constant length of dislocation of the order of $500 \cdot 2 \cdot b^2 = 4 \times 10^{-13}$ ergs. At 1000° K the lattice frequency term estimated above would be 1.30×10^{-13} ergs and would be comparable. Another way of suggesting the importance of the free energy terms is to compare the added free energy of a large angle boundary with the free energy required to melt a layer of metal two atomic planes thick; it is then found that those energies are

comparable suggesting that the disorder at a large angle grain boundary is comparable to that in a liquid. At the melting point, of course, changes in entropy and energy make equal contributions to the free energy. This argument thus leads to the conclusion that entropy effects will be comparable to energy effects in the term E_I and will be of such a sign as to decrease the free energy.

Another phenomenon which may affect the term E_I is that of the formation near the dislocations of concentration gradients in alloys. It appears probable that an argument, similar to that presented above for vibrational free energy, can be applied to these atmospheres. For example, in a very dilute alloy, an appreciable concentration of the solute atoms close to an isolated dislocation line can occur. The presence of these atoms will produce local variations in the stress field that will contribute terms in $(b/R)^n$ with $n > 1$ in (2.1). For small angle boundaries, r_l can be taken large enough so that overlap of these terms from one dislocation to another can be neglected and hence they can be considered as simply adding to E_I. At large distances, the effect of stress on concentration will produce only linear effects and the energy E_{II} may be calculated as before; the elastic constants employed, however, should be those corresponding to isothermal processes in which diffusion effects are allowed to come to equilibrium. This reasoning suggests that the methods used in this paper for calculating grain boundary energies can be employed for alloys as well; however, a far more thorough analysis than we have carried out would be necessary to establish the conclusion rigorously.

3. EXTENSION TO THE GENERAL CASE

The grain boundary in the last section was a particularly simple one having but a single degree of freedom. Actually, an arbitrary grain boundary has five degrees of freedom; three degrees of freedom of relative rotation of the adjoining grains, and two degrees of freedom of rotation of the boundary with respect to the two grains. Read and Shockley (1950) have treated the case of a two degree of freedom boundary in which the grains have a common crystal axis, and the plane of the boundary is allowed to rotate about the common axis. Frank (1950) has given a formula for the dislocation content of an arbitrary, five degree of freedom, grain boundary. Van de

Merwe (1950) has treated a somewhat more general case in which there is « twist » or a relative rotation of the grains about the normal to the grain boundary. When the misfit is small Frank's formula can be readily derived by the following simple physical reasoning : Let the arbitrary misfit between two grains A and B be defined by a relative rotation of magnitude θ about an axis parallel to the unit vector $\vec{l}$. Now choose an arbitrary vector $\vec{r}$ lying in the grain boundary and define the vector $\vec{r}'$ having the same crystallographic indices in crystal B that $\vec{r}$ has in A. For small θ, the vectors $\vec{r}$ and $\vec{r}'$ are related by $\vec{r}' = \vec{r} + \vec{l} \times \vec{r}\,\theta$; that is, the relative rotation $\theta\vec{l}$ which brings the two grains into perfect register will bring $\vec{r}$ and $\vec{r}'$ into coincidence. We can therefore construct, a C-loop, or loop which would close in a perfect crystal, (see for example F. C. Frank 1951) connecting the end points of the vectors $\vec{r}$ and $\vec{r}'$ and passing through the grain boundary at their common origin. The closure failure $\vec{r} - \vec{r}'$ is equal to the sum of the Burgers vectors of the dislocation lines enclosed by the loop, i. e. cut by $\vec{r}$. Thus we have the theorem that the sum $\vec{S}$ of the Burgers vectors of the dislocation lines cut by arbitrary vector $\vec{r}$ lying in the grain boundary is :

$$\vec{S} = \vec{l} \times \vec{r}\,\theta \tag{3.1}$$

By making two different choices of $\vec{r}$ in (3.1) the complete dislocation content of the boundary can be determined. Clearly, if the axis of relative rotation $\vec{l}$ lies in the grain boundary, the dislocation lines will all be parallel to $\vec{l}$. When the misfit has a twist component, the dislocation lines form a crossed grid.

If there are more than 3 possible Burgers vectors, several different dislocation arrays can be constructed, each of which satisfies the condition (3.1) for the resultant dislocation content. The best model is then taken to be the one giving the lowest grain boundary energy.

From (3.1) we see that the dislocation densities are proportional to θ. We shall accordingly introduce a dislocation density for each type of dislocation :

$$\begin{aligned} &\text{Density of Dislocations of type } i \\ &= N_i\theta = \text{length of dislocation per} \\ &\qquad \text{unit area of surface.} \end{aligned} \tag{3.2}$$

The quantity $N_i\theta$ is analogous to $1/D = \theta/b$ discussed in the previous section; $N_i\theta$ may also be defined as the number of dislocation lines per unit length measured perpendicular to the dislocation axis.

The argument presented for the simple boundary can be extended to calculate the energy for the general case. Once more the space is divided into regions of three types : I(i) regions surrounding dislocations of type « i » extending to the radius r_{Ii} at which Hooke's law holds; II(i) regions extending from r_{Ii} to $K_i\, b_i/\theta$ in which the stress arises predominantly from the enclosed dislocations; and regions III which lie outside. As θ increases, the scale of each individual region III decreases as $1/\theta$ and the total number of regions per unit area of grain boundary, for the general case of a crossed grid, increase as $(1/\theta)^2$. The energy of each region increases as θ^2 because of increasing strain and decreases as $(1/\theta)^3$ because of decreased volume. The dependence of E_{III} per unit area upon θ is thus of the form

$$[\text{Energy of individual region}] \times [\text{Regions per unit area}]$$

$$\propto [\theta^2/\theta^3] \times [\theta^2] \propto \theta \qquad (3.3)$$

Thus in general regions III contribute a term proportional to θ. It is obviously true that regions I also contribute proportional to θ. Regions II may be treated individually.

Each unit length of dislocation of type « i » contributes an energy :

$$(\tau_{oi}\, b_i^2/2) \ln (K_i\theta/\, br_{Ii}) \qquad (3.4)$$

and there are $N_i\theta$ units of length per unit area of grain boundary. Summing up the various energy terms leads to :

$$E = E_0\, \theta\, [A - \ln \theta] = E_0\, \theta\, [1 - \ln \theta/\theta_m] \qquad (3.5)$$

$$A = 1 + \ln \theta_m; \qquad \theta = \exp (A-1)$$

with :

$$E_0 = (1/2)\, \Sigma\, N_i\, b_i^2\, \tau_{oi} \qquad (3.6)$$

the sum being taken over all dislocation types. For each type, the corresponding τ_{oi} is determined from elasticity theory in terms of the elastic constants and the relative orientation of the slip vector and dislocation axis.

Thus the two parameter formula, derived for the simple grain boundary, applies in the general case of a boundary with five degrees of freedom, both the calculable parameter E_0 and also the unknown

parameter A varying with the orientation of the grain boundary and axis of relative rotation.

The above derivation assumes that the dislocation model of the grain boundary consists entirely of complete, or perfect, dislocations, In a f.c.c. metal, it is possible that a boundary containing dislocation lines lying on (111) type planes might lower its energy by dissociating into two boundaries consisting of half-dislocations (Heidenreich and Shockley 1948) and connected by stacking faults. Even in an arbitrary boundary, some dislocations might lower their energies by making a zig-zag course running alternately along different (111) type planes and dissociating into half-dislocations on each plane, the half-dislocations coming together whenever there is a shift from one plane to another, as discussed by Read and Shockley (1952). In the special case of a pure twist boundary on a (111) type plane, the boundary could be made up entirely of half dislocations and stacking faults. These possibilities constitute an interesting field for investigation, in which comparison of theoretical and experimental results might lead to a better understanding of the role played by half-dislocations in metals. In the present paper, however, only boundaries containing complete dislocations will be considered.

4. READ'S FORMULA FOR COLD WORKED METAL

Read (1951) has shown that the same reasoning as that used in the last section may be used to estimate the dependence of energy upon dislocation density in a cold worked metal. If we assume that different degrees of cold work result in geometrically similar arrays of dislocations simply arranged on a different scale, then the same division into regions I, II and III is possible. The variable θ must now be correlated with some measure of the scale of the array; for example, if l is the average distance between a point on a dislocation axis and the nearest dislocation, we may define θ by :

$$\theta = a/l \tag{4.1}$$

where a is a lattice constant of the crystal. The average energy density in regions of type III is proportional to $l/l^2 \propto \theta^2$. Since the same fraction of space is occupied by these regions regardless of θ, the contribution of III to the energy density varies as θ^2.

The length of dislocation axis per unit volume varies as θ^2. So far

as regions I are concerned, this dependence of length on θ again gives a contribution to the energy density proportional to θ^2. The E_{II} regions give logarithmic terms, per unit length and thus contribute proportionally to $\theta^2 \ln (\theta'/\theta)$ where θ' is a constant depending on the nature of the array.

Combining these contributions, Read finds that the energy density varies as :

$$E' \text{ (energy/volume)} = E'_0\theta^2(1-\ln \theta/\theta_m) \qquad (4.2)$$

a form similar to the grain boundary except for an extra factor of θ. The proportionality constant E'_0 should be of the order $G/4\pi(1-\sigma)$ and θ' should probably be of the same order as θ_m for a grain boundary. As for the discussion of the last section, E'_0 can be calculated relatively simply for any assumed dislocation array.

5. COMPARISON WITH EXPERIMENTAL MEASUREMENTS OF RELATIVE ENERGIES

The quantities E_0 and A vary with the orientation of the grain boundary. Read and Shockley (1950) estimate that A varies by about $\pm$ 0.15 for a two degree of freedom boundary as the plane of the boundary rotates about the common crystal axis of the adjoining grains. If the dislocations are all of the same type crystallographically, then E_0 will vary with grain boundary orientation in proportion to the total density of dislocations, since in (3.2) E_0 multiplies the term representing the constant localized energy per dislocation. For the particular two degrees of freedom boundary considered by Read and Shockley, E_0 is proportional to $(\sin \varphi + \cos \varphi)$, where φ lies between 0 and 90° and represents the angle between the grain boundary and the average (100) axis of the adjoing grains.

Thus, experimental measurements of grain boundary energy vs. θ would be expected to show some scatter if the orientation of both the grain boundary and the axis of relative rotation were not kept constant. However, by taking a large number of points, an average experimental curve could be obtained to compare with the theory.

Recently Dunn and Lionetti (1949) measured grain boundary energies in silicon ferrite (about 3.5 weight percent silicon, b.c.c.) on a relative scale as a function of the angle of misfit θ. These experiments were especially well suited for comparison with the theory,

since the orientation of the axis of relative rotation was held constant, in one set of measurements along a (110) direction, in another set along a (100) direction. The grain boundary therefore had only two degrees of freedom. The orientation of the boundary plane about the common axis was not measured and varied at random. Using a similar experimental technique, Aust and Chalmers (1950) and Chalmers (1951) measured relative grain boundary energies in tin and lead.

All four sets of measurements, which are tabulated and discussed by Fisher and Dunn (1952), were well fitted with curves of the form (1.1). Since all the measurements were on a relative scale, the values of E_0 were unknown, and therefore can not be compared with the numerical predictions of the theory. However, by putting (1.1) in the dimensionless form :

$$E/E_m = (\theta/\theta_m)\,[1 - \ln(\theta/\theta_m)]\,, \tag{4.1}$$

where :

$$E_m = E_0\,\theta_m\,, \tag{4.2}$$

the form of the theoretical curve can be checked. If the measured relative energies are plotted as (E/E_m) vs. (θ/θ_m), where θ_m is obtained from the maximum of the best fit curve for each set of measurements,

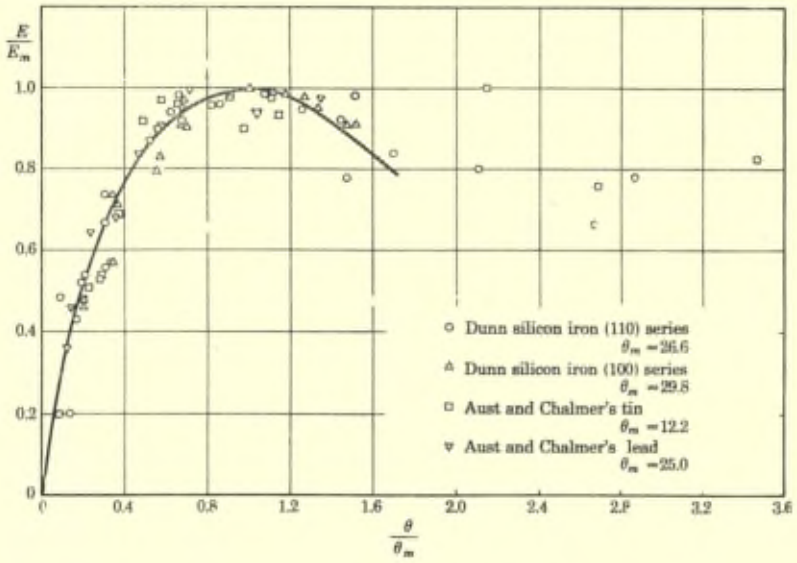

Fig. 3. Comparison of experimental energies with the :
$E/E_m = (\theta/\theta_m\ (1 - \ln \theta/\theta_m)$
form.

then the theory predicts that all the points should be represented by the single formula (4.1). Figure 3 is a plot of the experimental points together with the equation (1.1). The values of θ_m for the four sets of measurements are listed on the figure.

It is seen that the theoretical curve fits the data over a much larger range of angles than would be expected from the assumptions made in the derivation. This is probably due to a fortunate cancellation of errors, as well as to the fact that θ_m, which is important at large angles, is arbitrary in the theory, and is chosen to make the curve fit at large angles (*).

Figure 4 presents some additional measurements, by A.P. Gree-

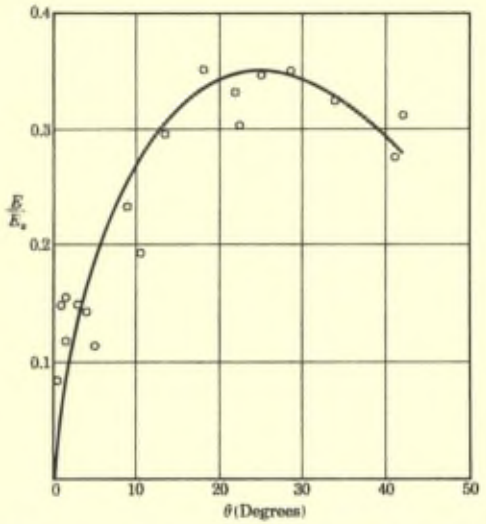

Fig. 4. Ratio of grain boundary energy to surface energy in silver.

nough (1950) on silver. Greenough measured the groove where grain boundaries met the external surface and calculated the ratio of grain boundary energy to surface energy E_s by equilabrating tensions. The specimens were bicrystals so grown that the axis of

(*) Recently van der Merwe (1950), has given a more detailed mathematical analysis of inter-crystalline boundary energies, making use of a number of approximate assumptions regarding interatomic forces, including a sine law of stress and strain for planes of atoms on the boundary. The resulting energy vs. θ curve agrees with the present one at small angles, but has no maximum and consequently gives a poor fit to the data at large angles. This may perhaps be explained in part on the basis of recent criticisms of the sine law by W. M. Lomer (1949).

relative rotation of the grains lay in the grain boundary, but was not a simple crystal axis and was not the same in all specimens. The groove angles were measured in all cases by several methods. Figure 4 is a plot of E/E_s vs θ each values of E/E_s being obtained from the average of the several determinations of groove angle. Although the scatter here is somewhat greater than in Figure 3, the data appear to be well fitted by the theoretical curve with $\theta_m = 25°$, in agreement with the θ_m value for lead.

The fact that the form of the theoretical curve is followed up to the maximum energy suggests that the theoretical value of the maximum energy $E_m = E_o\ \theta_m$ may give a good approximation to the relatively constant energy in the flat part of the curve at large angles. The energy level of this part of the curve is important because a grain boundary, picked at random, is more likely to have an energy in this range than in any other. In order for the boundary to have an energy appreciably less than the maximum, all three of the angles which specify the relative orientation of the grains must be small, and this is improbable except in a controlled boundary. A statistical analysis by C. S. Smith (1948) is in agreement with the view that random grain boundaries have approximately the same energies.

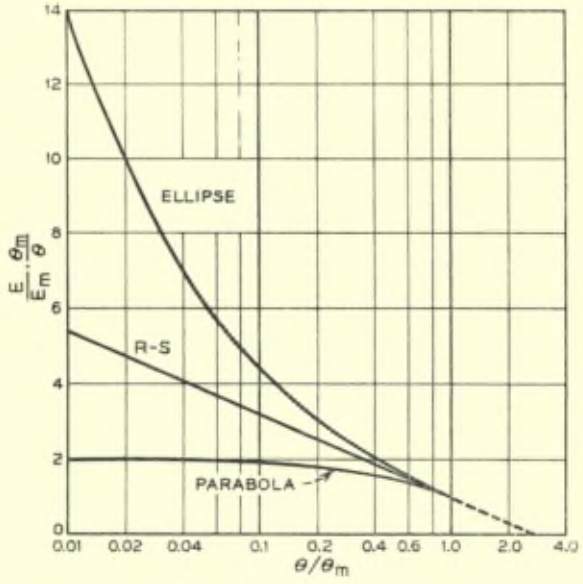

Fig. 5. Test of significance of the fit of E/θ versus $\ln \theta$ plot.

The absolute values of measured grain boundary energy in copper discussed by Fisher and Dunn (1952) apply to a random grain boundary and consequently can be compared with the theoretical values of $E_m = E_o\,\theta_m$. In Appendix A1, we quote values of E_o for

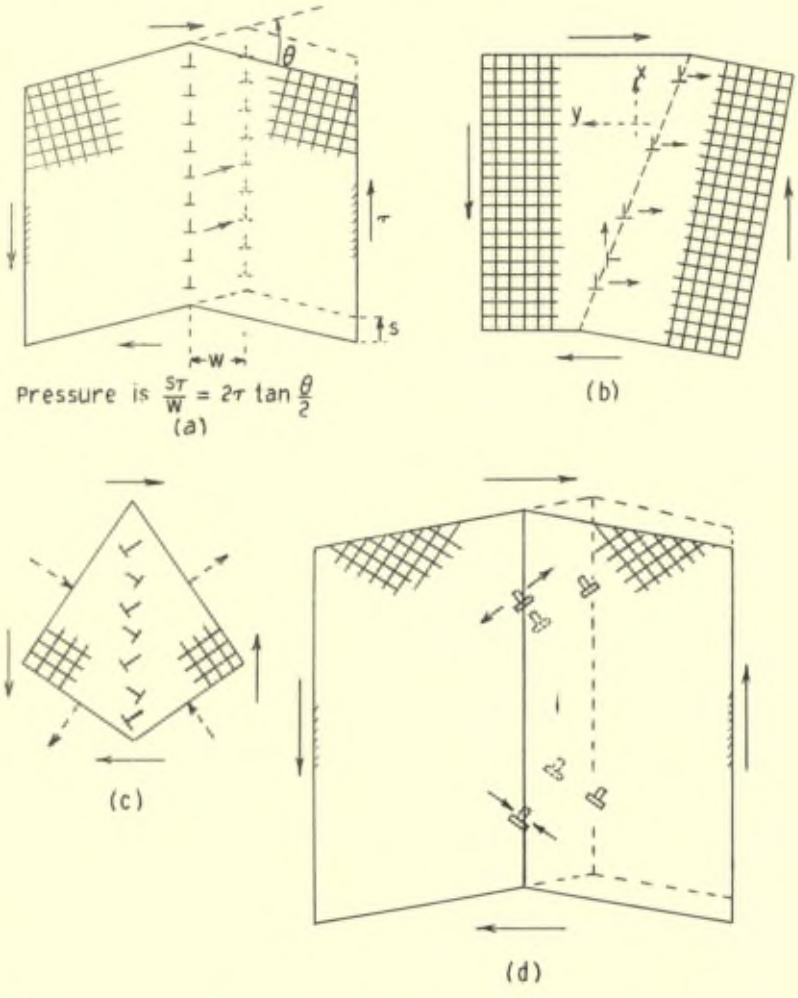

Fig. 6. Mechanism for slip across a grain boundary. (a) Yielding of a symmetrical bicrystal with $\varphi=0$ grain boundary to external shear by sidewise motion of boundary. (b) Separation of x and y arrays on an unsymmetrical boundary by applied shear. (c) Stress applied to bicrystal with 45° grain boundary resulting in (d) sidewise displacement of grain boundary by motion perpendicular to slip planes of dislocations, permitting crystal of yield to applied stress.

several boundaries, using anisotropic elasticity. In Section 6, the calculations are compared with the experimental measurements, thus providing a quantitive check on the theory.

Is the fit accidental? One question that has been raised in a previous discussion by Professor Orowan is whether the data really gives an adequate test of the θ (A — ln θ) formula. It has been suggested, for example, that since in any event the energy must go to zero at small angles, almost any curve of reasonable shape would fit the data equally well. In order to test the validity of this criticism Figure 5 has been prepared. Figure 5 shows the deviation that would be produced in a E/θ versus ln θ plot if $E(\theta)$ were in one case a parabolic curve in Figure 3 and in other case a quarter of an ellipse. The θ (A — ln θ) expression is, of course, a straight line. On the scale of this Figure, the data quoted by C. S. Smith extends in the report of this volume down to $\theta/\theta_m = 0.14$ for his Figure 6, and $\theta/\theta_m = 0.11$ for Pb and 0.2 for Sn for Figure 7.

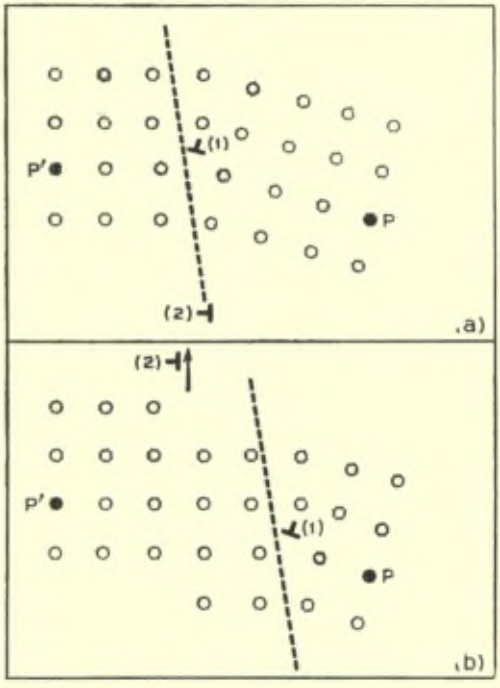

Fig. 7. Compensating effects in grain boundary motion in a square lattice.

Inspection of these figures shows that the scatter of the data is less than the spread of the curves of Figure 5. Hence, we conclude that the present data is adequate to support the θ (A — ln θ) form as opposed to the other two approximations.

In his discussion of C. S. Smith's report, W. M. Lomer shows experiments with the bubble model that indicate that strong interactions between the dislocations occur for grain boundary angles larger than a few degrees. If this same effect occurs in metals, it should produce serious deviations in the θ (A — ln θ) formula in the range of most interest, say from 4 to 20 degrees, and we would be forced to conclude that the slope on the ln θ plot was not truly E_o but included the influences of some compensating effects that happened to result in a straight line. The writer questions the validity of the bubble model conclusions and attempts to analyse how they may be erroneous in Appendix A5.

6. COMPARISON WITH EXPERIMENT FOR ABSOLUTE ENERGIES

In Section 5 it was shown that the form of the theoretical curve of E vs. θ agrees very well with experimental measurements, even at relatively large angles, where the assumptions made in the derivation are no longer valid. If the theoretical curve of energy vs. angle of misfit is assumed to hold up to $\theta = \theta_m$, then the maximum energy can be calculated from :

$$E_m = E_o\, \theta_m\, [1—\ln(\theta_m/\theta_m)] = E_o\theta_m \qquad (6.1)$$

where E_o is evaluated by elasticity theory, as derived in Appendix -A1, and θ_m is determined from an experimental curve of the type obtained by Dunn and Lionetti and Aust and Chalmers. As mentioned in Section 5, a random grain boundary will have an energy near the maximum. Consequently the calculated E_m can be compared with the measurement of the energy of a random grain boundary. The only absolute measurements of grain boundary energy recorded by C. S. Smith in his report in this volume are for random boundaries in copper and iron.

Copper.

Three independent determinations for copper give a mean of 550 ergs/cm^2. (See Smith, Table III). The value of θ_m is not known

for copper. However, as the best available estimate, we shall take $\theta_m = 25^o$ obtained for lead, and silver which have the same lattice structure, f.c.c., as copper. The quantity E_o for an arbitrary boundary depends on the four variables specifying the orientation of the boundary and axis of relative rotation. In Appendix I, we give formula for a boundary containing the [001] axis containing dislocations with Burgers vectors of (a/2) [110] and (a/2) [1-10] and having arbitrary orientation of the boundary about the [001] axis. If we average E_o over all the allowed directions (i. e. values of φ' in Appendix I), we obtain :

$$<E_o> = (a/2^{1/2}\pi^2)\,(c_{11} + c_{12})$$

$$x[c_{44}(c_{11} - c_{12})/c_{11}(c_{11} + c_{11} + 2c_{44})]^{1/2} \qquad (6.2)$$

Using $c_{11} = 17.0$, $c_{12} = 12.3$ and $c_{44} = 7.52 \times 10^{11}$ dynes/cm^2, and $a = 3.61 \times 10^{-8}$ cm, we obtain.

$$<E_o> = 1600 \text{ ergs/cm}^2.$$

For $\theta_m = 25^o = 0.436$ radians this gives :

$$E_m = <E_o>\,\theta_m = 700 \text{ ergs/cm}^2.$$

This is 30% higher than the mean of the measured values. The discrepancy might be somewhat reduced by using a model involving extended dislocations. In view of the other limitations, however, such as the necessity of averaging, it has not seemed worthwhile to improve the calculation. The agreement within a factor of 1.30 is to be regarded as encouraging.

Iron.

The same approximate treatment can be applied to the b.c.c. α — iron specimen provided we assume that the Burgers vectors are a[100] and a[010], which is one possible choice for the model. The value of $<E_o>$ is :

$$<E_o> = (a/\pi^2)/(c_{11} + c_{12}) \qquad (6.3)$$

$$x[c_{44}(c_{11} - c_{12})/c_{11}(c_{11} + c_{12} + 2c_{44})]^{1/2}$$

Using $c_{11} = 23.7$, $c_{12} = 14.1$ and $c_{44} = 11.6 \times 10^{11}$ dynes/cm^2 and $a = 2.86 \times 10^{-8}$ cm, we obtain :

$$<E^o> = 2950 \text{ ergs/cm}^2.$$

The value of θ_m found for α-iron grain boundaries in Figure 3 is about 27° or 0.47 radians. This leads :

$$E_m = \langle E^o \rangle \theta_m = 1400 \text{ ergs/cm}^2, \qquad (6.4)$$

a value larger by a factor of 1.9 than that obtained by Van Vlack and quoted in Table III of C. S. Smith's report in this volume.

This discrepancy is quite striking and there appears at present to be no explanation. The presence of a solute atoms, 3.5% silicon in Figure 3, would be expected to reduce the core energy rather than raise it so that the value of θ_m in Figure 3 should be not larger than the value for pure iron. It would appear that the resolution of this discrepancy must await the establishment of an absolute scale of energy for the small angle boundaries.

Silver.

An additional comparison between theory and experiment can be made using Greenough's data for silver. The data in Figure 4 are not sufficiently accurate at low angles to permit determination of E_o from the slope of an E/θ vs. $\ln \theta$ plot at small angles. The curve of Figure 4 corresponds to $E_m = .35\ E_s$. Using the value $E_s = 1180$ from Fisher and Dunn (1952), this gives $E_m = 413$ ergs/cm². Calculating E_m from the theory by the procedure used for copper gives $E_m = 516$ ergs/cm². Thus the calculated value is high by 25%. Again this degree of agreement is considered encouraging.

A crucial experimental check of the theory would be provided by an accurate measurement of absolute grain boundary energies for small angles of misfit. In this case the unknown parameter $A = 1 + \ln\theta_m$ would be small in comparison with $\ln\theta$ and only the part of the theory which depends on elasticity theory and the dislocation model would be involved in the quantitative theoretical predictions. An agreement between theory and experiment in this area would constitute very strong evidence for the dislocation model.

7. MOTION OF SMALL ANGLE GRAIN BOUNDARY

One of the well known features of grain boundaries is their effect upon the elastic properties of polycrystalline materials. Investigation carried out by Kê (1947) as part of the research program on internal friction in metals at the Institute for the Study of Metals indicate

that the effect of the grain boundaries can be interpreted as a viscous flow at the boundary. Kê, furthermore, concludes that for aluminium the viscosity decreases with increasing temperature as though controlled by an activation energy of 34,000 calories per mol the same as that for self diffusion. If Kê attributes the flow to a layer one lattice constant thick at the grain boundary, he can compute a viscosity for material constituting the grain boundary. On extrapolating this viscosity to the melting point, he finds that it is nearly equal to that for the molten metal at the melting point. This suggests the view that the grain boundary may be regarded as a super-cooled liquid.

The boundaries studied from the point of view of internal friction are large angle boundaries to which the small angle theory discussed above should not apply in detail. In this section we shall discuss some idea about the motion of small angle grain boundaries and shall return below to consideration of large angle boundaries and make some suggestions as to how a model may be proposed which relates the small angle theory to large angle theory and to Kê's results.

The problem of grain boundary motion, even for small angle grain boundaries, poses considerable difficulties in geometrical visualization. [The author has found that his views as to the ability of a grain boundary to yield to shear have oscillated from one point of view to another several times; even at a late stage in preparing this manuscript, he has discussed and added inequality (7.3)]. It now appears probable that most small angle grain boundaries will be able to yield to varying extents by slipping motions of the dislocations upon their slip planes. In the following portions of this section we shall consider several types of processes which may contribute to the motion of grain boundaries. These are not thought to be exaustive and are intended to be suggestive and stimulating. It is to be hoped that more experimental data on the points raised in this section will become available and as a result it will be worthwhile to carry out more detailed consideration of specific geometries.

« *Single-Type* » *Boundary Motion.* — In Figure 7 (a) we show the simplest type of grain boundary motion. In this case the grain boundary consists of a *single type* of dislocation. This dislocation array is shown dividing the crystal into two parts with an orientation difference θ. If shearing stresses are applied to the boundaries as indicated by the arrows, then the dislocations will tend to slide on their slip planes. As a result the grain boundary will move in the

crystal and the external shape of the crystal will become distorted in such a way that it yields to the applied shearing stress. The dynamics of the process can be viewed from the point of view of the forces acting on the individual dislocation. This force given by the customary formula :

$$F = b\tau \tag{7.1}$$

where τ is the component parallel to $\vec{b}$ of the shear stress in the slip plaine. The force on the boundary can equally well be considered from the point of view of the yielding of the crystal macroscopically. This yielding corresponds to an offset of :

$$\text{offset} = 2w \tan(\theta/2) \tag{7.2}$$

This offset permits the external forces to do work upon the crystal and thus leads to a pressure on the grain boundary. For a small angle grain boundary this pressure corresponds to a force per dislocation which is identical with that calculated from equation (7.1).

« *Mixed-Type* » *Blocking.* — In general the application of forces to a grain boundary in a two-dimensional, rectangular crystal lattice, such as the simple square lattice represented in Figure 6, will not result in any motion of the grain boundary. Figure 6(b) illustrates the reason for this lack of motion. For this boundary the application of external stresses tends to drive the two types of dislocations in opposite directions. Mathematical considerations show that the two forces precisely cancel so that there is no net force tending to drive the grain boundary. This conclusion may also be established by showing that if the grain boundary is moved then no offset of the crystal is produced. Figure 7 is intended to illustrate how this cancellation of motion arises. If the grain boundary moves to the right, dislocation (1) moves on its slip plane producing a bending of the crystal like that discussed in connection with Figure 6(a) and moving P upwards in respect to P'. At the same time, however, dislocation (2) moves upwards in the crystal thus producing an offset in the vertical direction as it cuts through the horizontal planes and moves P downwards in respect to P'. It can be shown that for a square lattice these two effects exactly cancel so that motion of the grain boundary does not produce any offset of the right half of the crystal in respect to the left. Consequently, the external forces will do no work as the boundary moves and there will, therefore, be no force to drive the boundary. The effects described appear to be valid

for small angle boundaries thus the orientation of the boundary φ is greater than this misfit angle θ. The orientation φ is defined for a square lattice as follows : imagine a perfect crystal is cut into two parts by a plane containing [001] and making an angle φ with [100]. Then rotate the parts by $\theta/2$ in opposite directions and rejoin them on the plane at angle φ. If θ is not very small and in particular if $\theta/2$ is greater than φ, or (φ — 90°) in Figure 7, then the slope of the grain boundary will lie on the opposite side of the vertical rows of Figure 7 and dislocations of type (2) will move down instead of up. This leads to the conclusion that mixed-type blocking will occur only if :

$$| \varphi | > | \theta/2 | . \qquad (7.3)$$

For smaller values of φ, the boundary can move much like a single-type boundary.

Purification by Slip. — If a boundary like that of Figure 7(b) is present in a small specimen so that it runs entirely across the specimen, then it is possible that the application of external stresses will tend to drive the minority dislocations to the edge of the specimen. As a result a portion of boundary of one dislocation type only will be left near one side and this boundary will tend to move subject to the applied stress. The detailed way in which the forces will act on the dislocations to accomplish this result is not easy to see in detail. However, it is evident that the process illustrated in Figure 8 will result in a yielding of the crystals to the applied stress and will thus

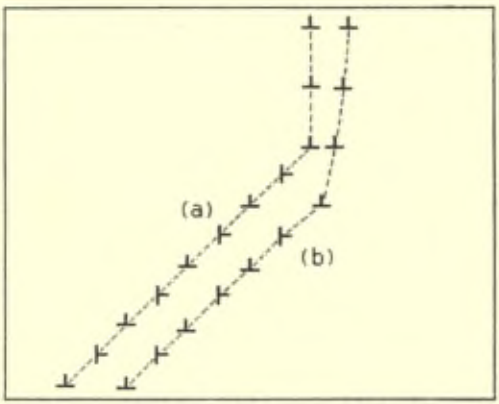

Fig. 8. Purification by slip. The boundary in position (a) can tend to lose dislocations of one type when forced by applied stresses to position (b).

exert a force tending to drive the minority dislocations out of the bottom of the crystal.

It should be emphasized that the process of Figure 8 does not result directly in a displacement of one part of the crystal to another. The slipping motion illustrated for the mixed boundary in Figure 8 leaves the relative orientation of the right and left halves of the crystal unaltered. If a stress is present, however, the portion of the dislocation line of single type will be bent by the applied stress and will thus produce a « elastic » yielding of the crystal. This displacement of the boundary will set up a stress field which will try to drive the minority dislocations out of the crystal so that the yielding of the upper boundary will be increased. This will result finally in the single-type boundary extending through the crystal so that slipping motion can occur.

« *Oblique-lattices* ». — If the Burgers vectors of the two dislocations are not perpendicular then a slipping motion of the dislocation will in general result in a translation across the grain boundary. In other words there will not be the exact cancellation of the two effects discussed in Figure 7. We treat this problem in Appendix II in which it is shown that the formula :

$$\text{offset} \cong W\theta \tag{7.4}$$

should be corrected by a factor. If the angles made by the planes of the oblique-lattice with the normal to the grain boundary are α and β, then the offset is :

$$\text{offset} \cong W\theta\,(1 - \tan\alpha \tan\beta). \tag{7.5}$$

For the case of a square lattice the product of the two tangents is unity so that there is no offset, as was discussed in connection with Figure 7. If the angle is not 90°, however, the correction factor will not vanish and in general there will be a force tending to move the grain boundary.

Slip by diffusion. — We shall next consider how atomic diffusion may result in displacement of grain boundaries in which the slipping motion is blocked as discussed above. For this purpose we return to Figure 6. If a shearing stress is applied to (b), the dislocations try to slip as shown by the arrows. As a result the x and y sets pull apart until the increasing elastic energy of the material between them balances the applied stress. If the angle φ is small, this will result

in curvature of the dense line of dislocations and resultant high stress values.

The processes which may follow the development of the stressed situation in (b) are illustrated in a simpler form in (c) and (d). Here we show a $\varphi = 45^{\circ}$ boundary with a shearing stress system which develops no shear in the slip planes. The shear stress system is equivalent to a normal stress system shown as dotted arrows. These stresses tend to squeeze out (or pull in) the extra half-planes of atoms. The mechanism whereby this may be accomplished will be discussed below; however, if we assume that the squeezing out actually occurs, then the motion of the dislocations will be as shown in (d). Here we consider two dislocations on a grain boundary which divides the specimen in two; actually there will be many dislocations on the boundary. The normal stresses on the half-planes cause one to shorten and the other to lengthen, moving the dislocations to the dotted positions. The dotted positions, however, correspond to a relative motion of the arrays of the two types of dislocations; and in order to keep the grain boundary in a minimum energy condition, the dislocations will slip in their own planes so as to move to positions in the dotted grain boundary which are at the same height as their original positions. These combined motions produce a net horizontal motion of the grain boundary in which no dislocations cut the (110) planes which are parallel to the top and bottom of the figure. The result is thus a yielding to the shear of amount $S = W2 \tan \theta/2$ as for Figure 6(a).

The process which can produce motion perpendicular to the slip plane is shown in Figure 9, which corresponds to 6(d) turned through 45°. We suppose vacancy diffusion takes place, the process being initiated by jump (1) in the figure which permits the half-plane to grow by one atom, a vacancy being produced next to the advancing edge. This vacancy diffuses until it is filled by jump 7 which shortens the other dislocation by one atom on the leading edge of the half-plane.

In Appendix A3 we consider quantitatively the consequences of this diffusion model and find that the viscosity of the grain boundary should be given approximately by the formula :

$$\eta \text{ (Diffusion)} \doteq (kT/\theta\nu a^3) \exp (Q/kT) \qquad (7.6)$$

where ν is the frequency of atomic vibration, a is the lattice constant and Q is the activation energy or self diffusion, it being assumed

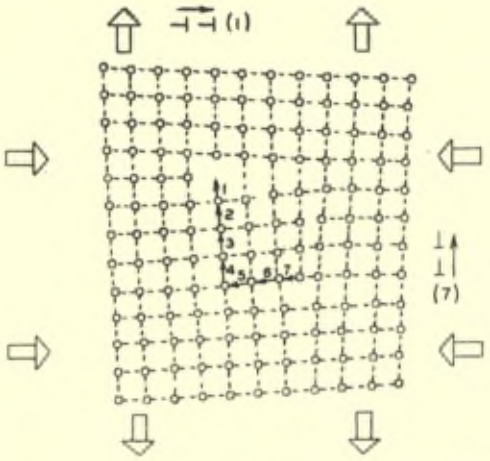

Fig. 9. Motion of dislocations perpendicular to slip planes produced by diffusion of atoms.

for the purposes of this discussion that self diffusion takes place by the mechanism of vacancies. This gives rise to the dependence of diffusion of viscosity upon the temperature reported by Kê. It gives a viscosity very much greater than the observed viscosity of molten metals near the melting point, however, and thus disagrees with Kê's value in absolute magnitude. As we shall discuss in the section on large angle boundaries, the viscosity of a molten metal at the melting point is approximately :

$$\eta \text{ (molten metal)} \doteq E_B / va^3 \qquad (7.7)$$

where E_B is the binding energy of the metal. At the melting point E_B is approximately 100 x kT for a typical metal. On the other hand the activation energy for self diffusion is about 20 x kT at the melting point; this corresponds to a value of about 10^8 for the exponential in equation (7.6). As a result the viscosity estimated by the diffusion mechanism is about 10^6 times larger than the viscosity corresponding to a molten metal. It thus appears probable that the viscosity reported by Kê arises largely from slipping motions.

« *Blocking and Cutting* ». — As was remarked by Cottrell and Shockley in the discussion of Dehlinger's report in this volume, dislocations can interfere with each other if the dislocation axes

cross during the slipping motion. In general the dislocations in a grain boundary will form a grid and as the grain boundary moves they will cross one another. This crossing will tend to block the motion of the dislocation. It seems probable that the blocking can be relieved by diffusive motions in many cases. If this is true it will explain why the yielding of the grain boundaries may be as great as that of a molten metal and still be governed by the diffusion process. The mechanism might be somewhat as follows : Under the influence of an applied stress large portions of the boundary will tend to move by pure slipping motion, however, this slip may be stopped at a few points where it is necessary for dislocations to cross. At these points there will be a large driving force tending to produce motion of the blocking point by diffusion. Under these circumstances it seems probable that the rate of motion produced by diffusion will be very much greater than that calculated for the uniform boundary and quoted above. A more detailed investigation would, however, be necessary to show that a model of this sort could account for the discrepancy of the factor of 10^6 mentioned above.

Recent Experimental Results.

It is understood that Professor Parker at the University of California has in special crystals observed a slipping motion of precisely the form discussed in connection with Figure 6(a). It is to be hoped that data will be available in time for insertion in galley proof of this report.

8. ON THE NATURE OF LARGE ANGLE GRAIN BOUNDARIES

When the angle between two crystal grains becomes large, the description of the grain boundary in terms of dislocations becomes difficult and ambiguous. The dislocations are then very close together and, furthermore, several different arrays of dislocations may appear to be equally satisfactory means for joining the crystals toegether. As discussed at the beginning of Section 7, Kê's measurements of internal friction suggest that the interface between the grain boundaries should be regarded as a layer of liquid about one lattice constant thick. We shall refer to this view of the grain boundary as the « liquid-boundary model ».

On the other hand Mott (1948) has described the grain boundary as being a region of alternating areas of good fit and bad fit between the two crystallites. By considering how these areas may change he has been able to give a theory for some of the properties of grain boundaries. We shall refer to this as the « fit-misfit model ».

Both of these descriptions are quite different from those given to small angle grain boundaries in terms of dislocations. In this section we shall by showing that to some degree all three views may be reconciled. Although the way in which the grain boundary is to be specified in terms of dislocation may not be definite, nevertheless, if we consider a large grain boundary to be a densely packed array of dislocations, we can see how it represents a natural extension of the small angle boundary and also how this description is equivalent to those discussed above. Consequently, we shall consider the third description : The grain boundary consists of a dense array of dislocations. We shall refer to this as the « dense-array model ».

As a starting point for this description we shall consider an interesting result established by Andrade (1937). Andrade has pointed out that the viscosity of liquid metals just above the melting point can be computed from a simple formula, involving ν the fequency of vibration of the atoms in the crystal, m their mass, σ the mean distance between molecules :

$$\eta = 4\nu m/3\sigma \qquad (8.1)$$

Andrade obtains this formula by analogy with the theory of viscosity in gases. We shall show that the same formula can be obtained by a consideration of the motion of dislocation. For this purpose we shall regard the liquid as being a solid densely packed with dislocations

In Figure 10 we illustrate the situation which we presume to prevail in the liquid. We suppose that on each slip plane there are dislocations spaced on the average a distance $n_s a$ apart, where a is the interatomic. We suppose that the width of each of these dislocations is $n_w a$. (We discuss the measuring of this width more fully below.) When a shearing stress is applied to this model, the crystal is assumed to be elastically deformed and this tends to move the dislocation. We suppose that in the molten liquid each dislocation relaxes the strain acting upon it in a period corresponding to a vibration in the solid. Under these conditions we find, as shown

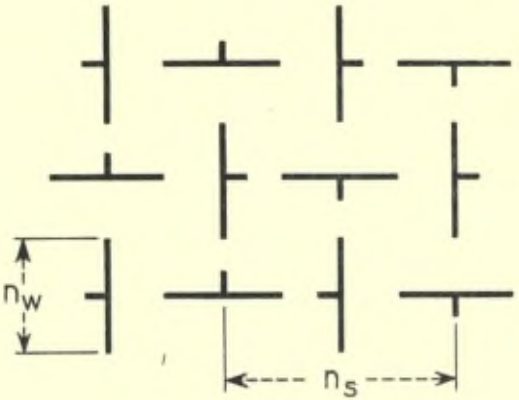

Fig. 10. The meaning of parameters n_s and n_w in a dense distribution of dislocations.

in Appendix A4, that the viscosity of the liquid is given the by formula :

$$\eta \doteq (m\nu/a)\, 2\eta\, F(n_s, n_w) \tag{8.2}$$

This formula is similar to that given by Andrade except that the expression $(4/3\sigma)$ is replaced by the coefficient involving the n's and 1/2.

Andrade finds that a large group of metals have their viscosity correctly given by this formula using the constant value 4/3 for the coefficient. In making the comparison he does not calculate ν directly but instead uses Lindemann's expression for the frequency in terms of the melting point T_m, the atomic volume V and the atomic weight A. Lindemann's formula may be written in the form, see Mott and Jones (1936),

$$\theta_D = C(T_m/AV^{2/3})^{1/2} \tag{8.3}$$

where the value of C varies from 115 to 142 for a typical group of monovalent metals. In terms of the Lindemann relation the expression for viscosity derived by Andrade becomes :

$$\eta = 5.1 \times 10^{-4}\, (AT_m)^{1/2} V^{2/3}. \tag{8.4}$$

Andrade finds that this formula fits a particular group of metals with an accuracy of about $\pm$ 10%.

Our interpretation of this result in terms of the dislocation model is simply that the density of dislocation is approximately the same in all molten metals at the melting point. This is consistent with the result that the entropy of melting does not vary greatly from one metal to another.

From this point of view it is evident that the description of the grain boundary as a layer of liquid is equivalent to its description as an array of dislocations.

It is also evident that this description is substantially equivalent to that of Mott in which he defines the grain boundary as region of good fit alternating with regions of poor fit. The ratio of good fit to poor fit can be estimated roughly by letting $a = \sigma$ and setting.

$$4/3 = 2\pi F(n_s, n_w) \tag{8.5}$$

which leads to $n_w \doteq n_s$ as discussed in Appendix A4. A typical definition of n_w would be as follows : at the center of dislocations the atom in the extra plane that is exactly midway between the correct positions is at a position of maximum misfit. At a distance of (1/4) $n_w a$ from this position the atom is approximately half-way between a good position and a bad position. According to this definition the atoms are half-way to maximum misfits over a distance of (1/2) $n_w a$ for each dislocation. This would lead us to conclude that in a molten metal at the melting point in any plane approximately 1/2 of the atoms are more than half-way out of optimum position in respect to the atoms in an adjoining plane and about half are in a good position.

In Appendix A4 we present some direct comparisons between this theory and the viscosity of molten metals.

Experimental Evidence for the Nature of Large Angle Grain Boundaries

We shall next consider experimental evidence obtained both in real crystals and in the bubble model for the nature of large angle grain boundaries.

Bubble Model Data. — W. M. Lomer has shown in his discussion of C. S. Smith's report that as the grain boundary angle becomes large, a description of the grain boundary in terms of dislocations is no longer applicable. Instead the grain boundary becomes a rather open region with occasional contacts between the bubbles. This would suggest that the large angle grain boundary is decidedly

different from a small angle grain boundary. The writer is inclined to the view that the conclusions reached from these bubble model photographs are misleading. From a quantitative point of view the writer doubts that such large spacings as are indicated by Mr. Lomer's pictures actually occur in metals. This point is discussed more fully in Appendix A 5.

At somewhat smaller angles the bubble model photographs show a tendency for the region on the tension side of the boundary to be pulled apart. I believe that this effect does occur to a somewhat smaller but significant extent in metals and that is has an important bearing on the results obtained for diffusion along grain boundaries.

Data for Diffusion Along Grain Boundaries. — Achter and Smoluchowski (1951) have studied diffusion along grain boundaries in copper. They found that grain boundaries in which the angle θ wass less than 20° showed a negligible contribution to the diffusion of silver in copper. The diffusion along gtrain boundaries increased rapidly with greater angles reaching a maximum for a difference in orientation of 45°. The grain studied had a common cubic axis and had relative rotation about this axis. The diffusion studied was parallel to the axis. It was found in the course of these experiments that the diffusion perpendicular to the axis was small. Achter and Smoluchowski explained their results in terms of islands of fit surrounded by regions of misfit in which the diffusion may take place much more readily. They point out the analogy between this description and the description of columnar edge dislocations running parallel to the common cube edge. They report an abrupt change between angles of about 25° and angles of 45° and this suggests an abrupt change of grain boundary type from a dislocation model to another model of a greater degree of misfit.

We are inclined to believe that the suggestion of an abrupt change is to some extent influenced by experimental conditions. We also believe that an effect, observed in Lomer's model for moderately large angles, plays an important role. As the grain boundary angle is increased the period in the crystal over which compression and tension change along the grain boundary becomes smaller and as a result the average absolute magnitude of stress along the boundary is greater. Since solids are more extensible than compressible due to the non-linearity of atomic forces, there will be a tendency for extra stretching to occur and this will be most pronounced as the grain boundary angle becomes higher. This is in agreement with

the result observed by Lomer in the bubble model. As this stretching increases more space will open up in the region opposite the extra plane in an edge type dislocation. This opening up should proceed continuously with increasing grain-boundary angle. The increasing space will produce a continuous decrease in activation energy for the process of diffusion. Our interpretation of Achter's and Smoluchowski's data is simply that under their conditions of measurement the decrease in activation energy became sufficiently large at an angle of about 20° so that the phenomenon of diffusion was brought prominently into play under their experimental conditions. We predict that if grain boundaries of controlled orientation in respect to the crystal axis are made and the angle is varied, a continuous increase in diffusion constant will occur. As Achter and Smoluchowski point out, the fact that they observe small diffusion in a transverse direction is strong evidence for a coherent dislocation pattern.

Activation energy for self-diffusion along grain boundaries. — The self-diffusion of silver has been observed in polycrystalline specimens by Hoffmann and Turnbull (1950). They find that the activation energy for diffusion along the grain boundary is 20.2 kilocalories per gram atom while the activation energy for diffusion in the body of the crystal is 49.5 kilogram calories per gram atom. The value for self-diffusion in the lattice stands in the same ratio to the melting temperature and binding energy as has been previously observed and reported for copper, gold and lead; for convenience of reference we repeat a previously presented table including the data of Hoffmann and Turnbull. The grain boundaries studied by Hoffmann and Turnbull were in general large angle boundaries where misfits should be large. The reduction in activation energy by a factor of about 2.5 would appear to be reasonable on the basis of almost any way of looking at the state of affairs along the grain boundary for large angle boundaries.

Grain boundary motion in recrystallization. — Turnbull (1951) has also studied the data on the migration of crystal grain boundaries in recrystallizing materials. The data used for calculating the recrystallization of silver is that of Rossi and Alexander. Turnbull finds that the activation energy for the grain boundary migration is 18.7 kilo-calories per gram atom. This is equal within experimental accuracy to the value obtained for self-diffusion along grain bounda-

TABLE I

SUMMARY OF DATA FOR SELF-DIFFUSION

Metal	A $cm^2/sec.$	Q Kcal./ Mole	Tm Melting Point °K	E Binding Energy Kcal./Mole	$\frac{Q}{Tm}$	$\frac{Q}{E}$	Ref- erence
Cu	11	57.2	1356	81.2	42	0.70	α 1
Cu	0.9	51.0	»	»	38	.63	β 2
Cu	47	61.4	»	»	45	.76	α 3
Ag	0.895	45.95	1233	68	37.2	0.68	α 4
Au	2.1	51	1336	92	38	.55	α 5
Au	410	62.9	»	»	47	.68	α 6
Pb	6.66	28.05	600	47.5	47	.59	α 7
Bi ||c	10^{-3}	31	544	47.8	57	.65	α 8
⊥c	2.4×10^{46}	140	»	»	257	2.92	α 8

α A and Q determined from plot of log D vs. $1/T°K$.
β A and Q determined from Langmuir-Dushman equation for A.

REFERENCES OF TABLES

1. Steigman, Shockley and Nix, *Phys. Rev.*, **56**, p. 13 (1939).
2. F. R. Rhines and R. F. Mehl, *Trans. A.I M.M.E.*, **128**, p. 185 (1938).
3. B. V. Rollin, *Phys. Rev.*, **55**, p. 231, (1939).
4. R. E. Hoffmann and D. Turnbull, *J. App. Phys.*, **22**, p. 634 (1951).
5. H. A. C. McKay, *Trans. Faraday Soc.*, **34**, p. 845 (1938).
6. A. Sagrubskij, *Physik. Zeits. Sowjetunion*, **12**, p. 118 (1937).
7. G. v. Hevesy, W. Seith and A. Keil, *Zeits. f. Physik*, **79**, p. 197 (1932).
8. W. Seith, *Zeits. f. Elektrochem.*, **39**, p. 538 (1933).

ries. This result appears to be reasonable on the basis of the « dense array model » or the « liquid boundary model ». For this case we can imagine that the process of migration which gives rise to the self-diffusion also serves to carry atoms from one side of the crystal to the other. It is not quite so clear that this same explanation will apply to the picture in terms of regions of fit and misfit. If the regions of fit happen to be regions in which the fit is accomplished by twinning, then it is not at all evident that these regions can be moved by a diffusion process of the same sort that produces diffusion along the grain boundary.

In concluding the section on large angle grain boundaries perhaps the comment of most significance is that at the present time from a theoretical point of view it would be advantageous to endeavor to work on small angle grain boundaries for which the theory is much better developped and much more capable of being further developed

as needed. After the small angle grain boundaries and their effects are better understood, it may be relatively easy to extrapolate the results to large angle grain boundaries.

Appendix A.1 Calculation of E^{o}.

To evaluate E_0 for most actual metals, it is necessary to use anisotropic elasticity in calculating τ_0 for the various dislocation types required. For almost isotropic crystals, such as aluminium and tungsten, isotropic elasticity is a good approximation, and involves considerably less computation, especially when the dislocation axis is not parallel to a simple crystallographic direction. We shall briefly review the general isotropic case, and then consider a few simple grain boundaries in anisotropic crystals.

For a pure edge dislocation, see Cottrell (1949),

$$\tau_0 = \frac{G}{2\pi(1-\sigma)},$$

where G is the shear modulus and σ, Poisson's ratio. For a pure screw,

$$\tau_0 = \frac{G}{2\pi}.$$

In all cases it is to be remembered that b τ_0/R is the component of shearing stress on the slip plane and in the slip direction (Section 2). In the general case where the dislocation axis makes an angle α with the slip vector, the slip vector may be resolved into edge and screw components leading to :

$$\tau_0 = \frac{G}{2\pi}\left[\frac{\sin\alpha}{1-\alpha} + \cos\alpha\right] \qquad \text{(A1.1)}$$

from which the shear stress in the slip direction can be obtained for any orientation of the dislocation axis (*).

In an anisotropic crystal, the shear stress in the slip direction depends on the orientation of the dislocation axis, not only in respect to the slip vector [as in (A1.1)], but also in respect to the crystal

(*) The slip plane is the plane containing both the slip vector and the dislocation axis; when these coincide, that is, for a pure screw dislocation, the slip plane is arbitrary, and in the isotropic case, the shear stress is found to be the same on all planes containing the dislocation axis.

axes. Eshelby (1949) has treated the case of edge dislocations in anisotropic materials, the orientation of the dislocation axis being arbitrary in the plane normal to the slip vector. In most cases, however, it is necessary to consider also screw components. When the dislocation axis is normal to a plane of crystal symmetry, the screw components can be treated separately and added to the edge components. If the dislocation axis is parallel to one of the crystal axes of a cubic crystal, then the shearing stress associated with the screw component is given by the same formula as in the isotropic case, taking $G = c_{44}$.

For an edge dislocation in a cubic crystal with the dislocation axis [001], as in Figure 1, and the slip vector [100], Eshelby's results give :

$$\tau_0 = \frac{c_{11} + c_{12}}{2\pi} \sqrt{\frac{c_{44}\, c'_{44}}{c_{11}\, c'_{11}}}, \tag{A1.2}$$

where the primed quantities are the elastic constants referred to the set of axes [110], [$1\bar{1}0$], [001], and are given in terms of c_{11}, c_{12} and c_{44} by :

$$\begin{aligned} c'_{11} + c'_{12} &= c_{11} + c_{12} \\ c'_{44} &= \frac{c_{11} - c_{12}}{2} \\ c'_{11} &= \frac{c_{11} + c_{12} + 2\, c_{44}}{2} \end{aligned} \tag{A1.3}$$

Clearly τ_0 is the same for both [100] and [110] Burgers vectors when the dislocation axis is [001].

In this section, we shall consider, as an example, a grain boundary between two f.c.c. crystallites having a common [001] axis and an angle of misfit θ, as in Figure 1, but now we introduce another degree of freedom by letting the boundary rotate about [001] making an angle φ with the mean of the [100] directions in the two grains. Taking $\vec{r}$ in (3.1) parallel to the axis of relative rotation [001], gives $\vec{S} = 0$ which means that the dislocation lines run parallel to [001]. Taking $\vec{r}$ in (3.1) as a unit vector at right angles to the [001] axis, we obtain :

$$\vec{S} = [\theta \sin \varphi, -\theta \cos \varphi, 0] \tag{A1.4}$$

We can now choose either of two physically reasonable dislocation

models, both of which satisfy condition (A1.4) for the resultant dislocation content of the boundary.

Model (1) consists of two sets of dislocations with Burgers vectors $\left(\frac{b}{\sqrt{2}}\right)$ [110] and $\left(\frac{b}{\sqrt{2}}\right)$ [1$\bar{1}$0] respectively, where $\sqrt{2}$ b is the lattice constant. For both set τ_0 is given by (A1.3). To determine the dislocation densities we refer the vector $\vec{S}$, to the [110], [1$\bar{1}$0] axes by replacing φ in (A1.4) by $\varphi' = \varphi \pm 45^\circ$, the sign of 45° being chosen so that both φ and φ' lie between 0 and 90°. The densities of the two sets per unit θ are then readily found; their sum is :

$$\Sigma N_i = \frac{\cos \varphi' + \sin \varphi'}{b} \qquad \text{(A1.5)}$$

Substituting (A1.3) and (A1.5) into (3.6) we have :

$$E_0 = \frac{(\cos \varphi' + \sin \varphi')}{4\pi} \, b(c_{11} + c_{12}) \sqrt{\frac{c_{44}\, c'_{44}}{c_{11}\, c'_{11}}} \qquad \text{(A1.6)}$$

Model (2) consists of four sets of dislocations all of which are screw and half edge. One set has slip vectors $\left(\frac{b}{\sqrt{2}}\right)$ [101] and alternates with another set having $\left(\frac{b}{\sqrt{2}}\right)$ [10$\bar{1}$]. The other two sets have slip vectors $\left(\frac{b}{\sqrt{2}}\right)$ [011] and $\left(\frac{b}{\sqrt{2}}\right)$ [01$\bar{1}$] respectively, and also alternate. We thus have two sets of edge components; the screw components associated with each set alternate in sign so that the screws give no contribution to the resultant dislocation content, as required by (A1.4).

It is convenient to treat the screw and edge components separately. The τ_0's are the same for all the edge components and also for all screw components. From (A1.4) the total dislocation density per unit θ is readily found to be :

$$\Sigma N_i = \frac{(\sin \varphi + \cos \varphi)}{b} \sqrt{2} \, .$$

Multiplying this by the sum of the τ_0's for the screw and edge components we have :

$$E_0 = \frac{(\sin \varphi + \cos \varphi)}{4\pi} \frac{b}{\sqrt{2}} \left[c_{44} + (c_{11} + c_{12}) \sqrt{\frac{c_{44}\, c'_{44}}{c_{11}\, c'_{11}}} \right] \qquad \text{(A1.7)}$$

Using the elastic constants for the f.c.c. metals aluminium, copper, lead, gold and silver, it is found that model (1) gives a lower energy except when the plane of the grain boundary is so close to a(100) type plane in gold that φ is less than 20′. For $\varphi = 45$, corresponding to a (110) boundary, model (2) has about twice the energy of model (1).

The same analysis could be carried out for b.c.c. crystals using several different models for each boundary; for example, it could be determined under what conditions a boundary consisting of dislocations with [100] Burger vectors would be better than one having [111] vectors.

A Value of A (φ)

The necessary calculations leading to the dependence of E_0 and A upon grain boundary orientation have been carried out for a model like that of Figure 6. For this case φ is the angle between the grain boundary and the slip planes. For Figure 1, for example, $\varphi = 0$. The results for an isotropic solid, published by Read and Shockley (1950), are :

$$E_0 = G\, b\, (\cos\varphi + \sin\varphi) / 4\pi\,(1-\sigma) \qquad \text{(A1.8)}$$

$$A_0 = 1 + \ln (a/2\pi r_0) \qquad \text{(A1.9)}$$

$$A - A_0 = -(1/2)\sin 2\varphi \qquad \text{(A1.10)}$$

$$- [\sin\varphi \ln(\sin\varphi) + \cos\varphi \ln(\cos\varphi)]/(\sin\varphi + \cos\varphi).$$

A2. Grain Boundary Motion in an Oblique Lattice.

In this appendix we shall derive the relationship given in equation (7.5). This result shows that if a grain boundary moves by the slipping of the dislocations upon their slip planes, there will be a net shear of the two parts of the bicrystal across the boundary. We shall not derive the results in full generality but shall, instead, consider one particular model. This will suffice to establish the conclusion that, in general, slipping motion does produce relative shear.

The example we treat is shown in Figure A.1, which is similar to Figure 6(b) except that the two slip vectors are not perpendicular. We introduce the following terminology :

A — set; these dislocations have Burgers vectors $\vec{a}$ and slide along

the lines that make angles α' and α in respect to the grain boundary normal.

B — set; similarly defined in terms of $\vec{b}$, β' and β.

The spacing A; this is the spacing between. A-lines in the oblique lattice. Evidently :

$$A = |\vec{b}| \sin(\alpha + \beta) = b \sin(\alpha + \beta) \qquad \text{(A2.1a)}$$

$$b = A \csc(\alpha + \beta) \qquad \text{(A2.1b)}$$

and similarly :

$$B = |\vec{a}| \sin(\alpha + \beta) = a \sin(\alpha + \beta) \qquad \text{(A2.2a)}$$

$$a = B \csc(\alpha + \beta) \qquad \text{(A2.2b)}$$

The density of B-dislocations is readily calculated in terms of the flux of A-lines or the grain boundary from each side; wherever an A-line from the right fails to join an A-line from the left, there

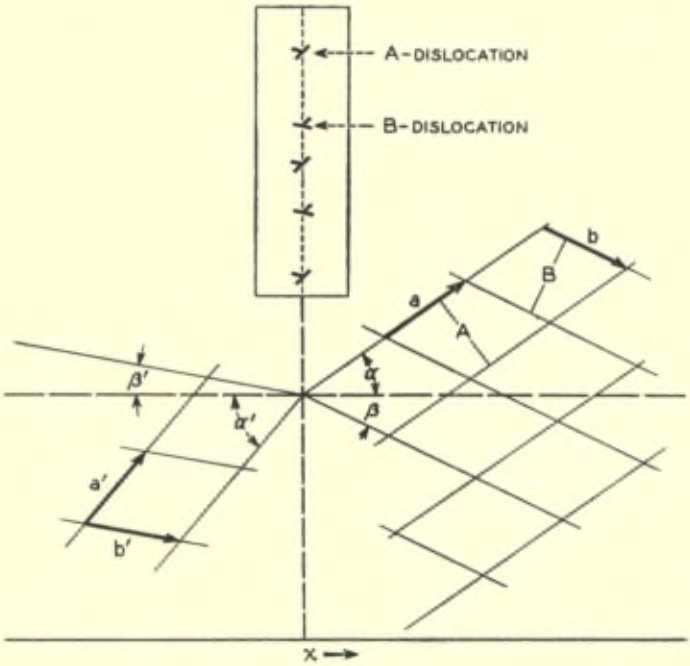

Fig. A1. A grain boundary in an oblique lattice.

is evidently a B-dislocation. This leads to a density of B-dislocations of :

$$1/D_B = (1/A)\,(\cos\alpha - \cos\alpha') \tag{A2.3}$$

and to :

$$1/D_A = (1/B)\,(\cos\beta' - \cos\beta). \tag{A2.4}$$

where the D's are the spacings between dislocations on the boundary.

We imagine that the slipping motion is produced by sliding the A-dislocations to the right slightly in advance of the B-dislocations so that the A-lines on which they slide are subsequently cut by B-dislocation slipping down and to the right on Figure A.1. The result will be slightly different if the B-set moves in advance. It is evident that after the motion the density of dislocations along the boundary will be the same since the density of dislocations on the boundary is unaltered. (This may be seen by noting that the A-density is clearly unaltered from the point of view of the crystal on the right and B-density similarly from the left.)

Now suppose the slip proceeds a distance such that each A-dislocation moves a distance W, that is the extra plane of each A-dislocation becomes a plane which was n_w planes further along, where :

$$n_w a = W \tag{A2.5}$$

In order to determine the motion produced, we consider the left grain to be fixed and consider the change in position of a point P in the right grain just at the final position of the boundary. This change is found by considering the alteration in path required to go to P from a point P', initially just to the left of the boundary and on the same A plane. Initially this path consisted of n_w steps with x and y components of :

$$X = n_w\, a \cos\alpha \tag{A2.6a}$$

$$Y = n_w\, a \sin\alpha \tag{A2.6b}$$

Afterward the motion the A-line lies in a direction α'; and in addition a number of B-dislocations have cut across it resulting in an offset of P' in respect to P of :

$$n_B \vec{b}' \tag{A2.6}$$

where n_B is the number of B-dislocations that cut across the A-plane.

It is tedious but straight forward to calculated n_B. In the calculation allowance must be made for the effect of the A-dislocations

passing in front of the B-dislocations and thus shifting them upwards in respect to the A-line and reducing the number cutting the A-line by a factor :

$$(\cos \beta / \cos \beta'). \tag{A2.7}$$

The result is that :

$$n_B = W (\cos \alpha - \cos \alpha') \sin (\alpha + \beta)/A \cos \beta'. \tag{A2.8}$$

leading to an offset by cutting of magnitude :

$$W (\cos \alpha - \cos \alpha')/\cos \beta' \tag{A2.9}$$

in a direction $-\vec{b}'$ on Figure A.1. The combination of this offset with the change in direction of W from α to α' leads to a net motion of P' given by :

$$\Delta x = 0 \tag{A2.10}$$

$$\Delta y = W \sin \theta \cos \alpha' (1 - \tan \alpha' \tan \beta') + W (\sin \alpha' + \cos \alpha' \tan \beta') (1 - \cos \theta). \tag{A2.11}$$

The result $\Delta x = 0$ is, of course, a necessity in a correct calculation since otherwise there would be an accumulation of matter on the grain boundary. For small values of θ, the first term of (A2.11) shows the proportionality to :

$$(1 - \tan \alpha' \tan \beta')$$

which is zero for a square lattice in which α and β differ by 90°.

The lack of symmetry between α' and β' results from the choice of moving one set first. The difference between moving one set first as compared to moving the other set is equivalent to making A and B dislocations rotate about each other in pairs and as shown in Figure A.2 this is equivalent to a diffusive motion of the same sort as that shown in Figure 9, which results in a net shear across the boundary.

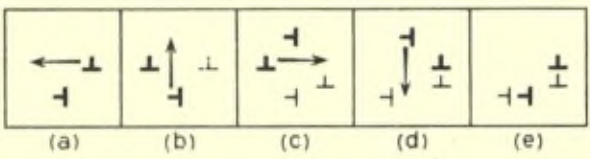

Fig. A2. The circulation of two dislocations about each other is equivalent to diffusion. (The light dislocation symbols indicate the relative positions of the old slip planes of the dislocations.)

A3. Vacancy Diffusion as a Mechanism of Slip on Grain Boundaries.

In this Appendix we shall treat the viscous flow of the grain boundary of Figure 6(d) that is produced by the process described in Figure 9. Due to jogs, or the « incipient vacancies » discussed by Seitz in his report, each dislocation tends to bring to equilibrium the vacancy density surrounding it.

If the stress is τ in Figure A.3 then the added activation energy for the creation of a vacancy is evidently :

$$\tau \, a^3 \qquad \text{(A3.1)}$$

where a^3 is the volume of one atom since the creation of a vacancy

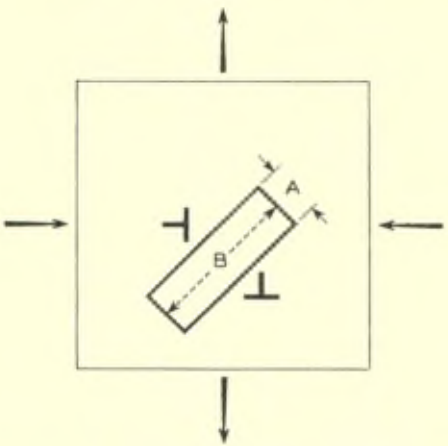

Fig. A3. Diagram used for discussing diffusion of holes from one dislocation to another.

leads to the growth of the extra plane of the dislocation by one atomic volume. Thus the stress will increase the vacancy density around one dislocation and decreases it around the other by factors of

$$\exp\,(\pm\, \tau\, a^3/kT) \qquad \text{(A3.2)}$$

and a diffusion current will flow as a result.

We shall next consider the vacancy atmosphere around an isolated dislocation. Because of the variation of stress around a dislocation, the energy of a vacancy depends on its position. This potential energy V may estimated by the reasoning used by Cottrell (1948)

in treating atmospheres around dislocations. It may be written in the form :

$$V = \delta v \, Ga \, (1 + \sigma) \, (\cos \beta)/\pi(1 - \sigma) \, R \qquad (A3.3)$$

where $-\delta v$ is the decrease in volume of a region a crystal containing a vacancy, G is the rigidity modulus, a the Burger's vector, R the distance from the dislocation axis and β the angle about the axis measured from the extra half-plane and σ is Poisson's ratio. If we let :

$$-\delta v = f \, a^3 \qquad (A3.4)$$

where f is probably between 0.05 and 0.2, this leads to an energy of :

$$V \cong - f \, G \, a^3 \, (a/R) \cos \beta \qquad (A3.5)$$

This becomes approximately :

$$V \cong - f \, G \, a^3 \doteq - E_B/10 \qquad (A.3.6)$$

for a vacancy at the edge of the extra half-plane where E_B is the binding energy of the metal. At the melting temperature this gives :

$$\exp (-V/kT) \cong \exp 3 = 20. \qquad (A3.7)$$

Hence the concentration of vacanties at the dislocation edge is 20 times c_v, the concentration in the volume of the crystal. Since vacancies can probably jump into edge positions and disappear as easily as they can jump in the normal diffusion processes, it seems reasonable to suppose that the exchange at the edge will maintain the equilibrium concentration at the edge of the extra plane at a value of about :

$$20 \, c_v \exp (\pm \tau a^3/kT_m) \qquad (A3.8)$$

when the two dislocations of Figure A.3 interact; under these conditions the limitation of diffusion probably arises from the interdislocation region.

The major portion of the vacancy flow will occur across the rectangle shown in Figure A.3. We shall take the rectangle to have dimensions A and B as shown. We shall also assume that the source and sink strengths of the dislocations are so strong that the long edges of the rectangle are in equilibrium with the sources. (This crude approximation obviates the necessity of dealing with the vacancy diffusion equation in the combined potential fields of the

form (A3.3), which incidentally cancel on points equidistant to the two dislocations.)

We, therefore, consider the diffusion due to a concentration gradient of :

$$c_v\,[\exp(\tau a^3/kT) - \exp(-\tau a^3/kT)]/A$$

$$\doteq 2\,c_v\,\tau a^3/kT\,A \qquad \text{(A3.9)}$$

acting over an area B wide and a deep. Across this the flow of vacancies is :

$$F = D_v\,aB\,2\,c_v\,\tau a^3/kT\,A\ . \qquad \text{(A3.10)}$$

Each vacancy results in a step a of the edges of the extra planes. This will produce a shear velocity approximately equal to θ times the velocity of motion of the dislocations by diffusion. Interpreting this as the viscosity of a layer a thick gives.

$$\text{shear velocity} \doteq \theta F\,a = a\,\tau/\eta \qquad \text{(A3.11)}$$

which leads to :

$$\eta = \tau/\theta F = kT(A/2B)/D_v c_v a^4\,\theta$$

$$\doteq (kT/4a\theta)/(D_v c_v a^3) = kT/4a\,D\,\theta \qquad \text{(A3.12)}$$

where we have set $A/2B = 1/4$ and D is the coefficient of self diffusion, which on the basis of the theory of diffusion by vacancies is D_v times the fraction of sites vacant, which fraction is $c_v a^3$.

Since the value of D is approximately :

$$D = a^2\nu \exp(-Q/kT), \qquad \text{(A3.13)}$$

the value of η is :

$$\eta \doteq (kT/\theta\,\nu a^3) \exp(Q/kT), \qquad \text{(A3.14)}$$

which is the expression quoted in equation (7.6).

A4. Derivation of Andrade's Formula in Terms of Dislocations.

In this appendix we consider a liquid as being a solid with a high density of dislocations. There is some support for this view in from the X-ray evidence concerning the structure of liquids. These show that each atom surrounded by neighbors almost as well as it is in a solid. If we assume, as indicated in Figure 10, that the liquid contains dislocations on every plane so close that they almost overlap, then the neighbors of an atom will vary from correct distance to the

distance at the misfit point of a dislocation. This degree of disorder may well be comparable to that in a liquid; it would be an interesting project to see how close the correspondence actually is.

The principal aim this appendix is to estimate the rate of shear in the liquid due to an applied stress. First we compare the amplitude of thermal vibration with the atomic displacement required to move a dislocation. At the center of a dislocation the atoms on opposite sides of the slip plane are relatively displaced by a/2 where a is the interatomic distance, the displacement compared to correct positions being a/4 for each atom. If the dislocation is n_w atoms wide, then the change in displacement from one atom to the next is approximately $a/4n_w$. In a solid at the melting point the atomic vibrations are larger than this. Hence thermal vibrations are large enough to cause the dislocation to move in a diffusive fashion.

Next we examine the effect of a stress τ applied across the slip plane, considering initially the effect at absolute zero. Under these conditions τ will produce a shear displacement of one plane of atoms in respect to the other of about :

$$\Delta x = a\tau/AG \qquad \text{(A4.1)}$$

where A is a factor less than unity that accounts for the fact that the rigidity is reduced in the region of the dislocation (even for very small strains that do not move it). Under the influence of the stress the relative motion of atoms at the center of the dislocation is equal to that produced by moving the dislocation by Δn units of a where :

$$\Delta x = (a/2)\ \Delta n\ (n_w/2); \qquad \text{(A4.2)}$$

the reasoning is that if the dislocation moves $n_w/2$ units of a, a relative displacement of a/2 is produced.

The decrease in rigidity A may be estimated roughly from the shearing stress necessary to move a dislocation. According to Nabarro (1947) this stress may be less than G by a facor of 10^{-3} to 10^{-7} depending upon the width of the dislocation. If we assume that the critical stress is :

$$\tau_c(n_w), \qquad \text{(A4.3)}$$

then we may estimate the reduction in rigidity as follows : When τ_c is applied, this dislocation will be deformed elastically to $\Delta n \doteq 1/4$ since this is probably the position of maximum restoring force.

This gives a relationship between Δx and τ_c from (A4.1) and Δx and Δn from (A4.2) :

$$\Delta x = a\tau_c/G' = a/4n_w$$

where G' is the rigidity at the center of the dislocation. From this we find :

$$G' = 4n_w\tau_c \qquad \text{(A4.4)}$$

For $n_w \doteq 5$, $\tau_c = G/2000$ and $G' = 10^{-2}\ G$. If we assume that this value G' extends over a distance n_w, then the value of A is :

$$A = [(n_s - n_w) + n_w(G'/G)]/n_s$$

$$\doteq 1 - 0.99\ (n_w/n_s) \qquad \text{(A4.5)}$$

for values of $n_s > n_w$.

We next combine the conclusion about the amplitude of thermal agitation with that about Δn. We assume that the shearing stress τ is transmitted elastically and produces a local elastic shear. This means that at any instant the equilibrium, absolute zero position of the dislocation is Δn beyond its position as given by the instantaneous average position of the atoms. In one half the period of vibration, the atoms will oscillate so as to be equally offside the other way. We thus conclude that in a time $(1/2\nu)$ the atoms will have vibrated so as to move the dislocation $2\Delta n$. Thus the dislocation moves with a velocity :

$$dn/dt = 4\ \nu\ \Delta n. \qquad \text{(A4.6)}$$

Each time the dislocation moves a distance n_s, unit shear is produced; hence the rate of shear is :

$$d\varepsilon/dt = (dn/dt)\ n_s\ . \qquad \text{(A4.7)}$$

This leads to a viscosity of :

$$\eta = (G/\nu)\ An_s/4n_w \qquad \text{(A4.8)}$$

For later use in comparison with experiment we write this in the form :

$$\eta = \eta_0\ F(n_s, n_w) \qquad \text{(A4.9)}$$

where :

$$\eta_0 = 2G/\pi\nu \qquad \text{(A4.10)}$$

$$F = \pi An_s/8n_w \qquad \text{(A4.11)}$$

The term η_0 is essentially the viscosity which would result from a material of stiffness G which relaxed its stress in a time $2/\pi\nu$. The

factor F, which may be greater or less than unity, represents the control exerted by the dislocation pattern over the relaxation process. For the approximation (A4.5).

$$F = (\pi/8)\,[n_s/n_w) - 0.99]. \qquad \text{(A4.12)}$$

We shall use this expression to estimate values of n_n/n_w.

The expression (A4.8) can be put in a form suitable for comparison with Andrade's by taking for ν the highest frequency of a transverse wave obtaining approximately :

$$G = \pi^2\, m\, \nu^2/a\,. \qquad \text{(A4.13)}$$

This expression leads to :

$$\eta = (m\nu/a)\, 2\pi F(n_s,n_w) \qquad \text{(A4.14)}$$

which is that quoted in the text.

Fur purposes of comparison with experiment we shall use (A4.13) to eliminate ν in (A4.10). Since rigidity moduli are not available for many metals we shall also make the approximation :

$$G = 1/2\,\varkappa \qquad \text{(A4.15)}$$

where $\varkappa$ is the compressibility. We also take the volume per atom to be $4\pi\, r_0^3/3$ and $a = 2r_0$. This leads to :

$$\eta_0 = (m/\varkappa r_0)^{1/2} \qquad \text{(A4.16)}$$

In Table A4.1 we tabulate η_0 together with Andrade's measured viscosities at the melting point. The ratio :

$$\eta\ (\text{exp})\ \eta_0 = F = (\pi/8)[(n_s/n_w) - 0.99)] \qquad \text{(A4.17)}$$

gives an estimate of the density of dislocations according to the relationship :

$$n_s/n_w = 1 \quad , 1.5 \ , 2 \quad , 4$$

$$F = 0.0039,\ 0.20,\ 0.40,\ 1.19$$

From Table A4.1 we see that values of n_s/n_w varying from about 1.7 to 2.5 are required.

The values of F are not as constant as Andrade's coefficient 4/3. The reason is probably that Andrade makes his comparison using the Lindemann relation involving T_m. Thus he makes use of one empirical quantity related to melting. In our calculation, only quantities determined by low temperature properties are involved.

The variation of F in terms of disorder due to the density of dislocations finds support from the entropy of melting. There is seen to be a strong correlation between low F values and high entropy values, both corresponding to high disorder. Bismuth and antimony do not fit into this scheme and their fusion is probably abnormal — bismuth appears to contract on melting.

This appendix, which started as a justification for thinking of large angle grain boundaries as regions of high dislocation density, has deviated towards a theory of liquids. The findings presented in Table A4.1 give encouragement that a theory may be developped along the lines discussed here. Further support is furnished by very crude entropy estimates (not presented here) which indicate that a large part of the entropy of fusion may be accounted for by the randomness of the arrangement of the dislocations.

Table A4.1 The Dislocation Model of Liquids

	1 χ	2 r_o	3 m	4 η_o	5 η	6 F	7 $\frac{\Delta V}{V}$	8 $\frac{\Delta S}{R}$	9
Na	15.8	2.10	3.82	10.7	6.9	.64	2.3	0.85	bcc
K	33	2.61	6.5	8.7	5.4	.62	2.5	0.86	bcc
Cu	0.75	1.41	10.6	100	38	.38	6.0	1.2	fcc
Ga	2.1	1.67	11.5	57	20	.35	—	—	»
Sn	1.91	1.86	19.7	74	20	.27	2.7	1.68	Tetra
Sb	2.7	1.93	20.3	62	24	.39	—	2.66	Trig.
Hg	1.76	3.8	34.2	71	21	.30	3.6	1.08	Trig.
Pb	1.93	2.30	34.4	88	28	.32	3.2	1.08	fcc
Bi	2.03	2.97	34.8	58	23	.40	—5.7	2.43	Trig.

Footnotes :

(1) 10^{12} compressibility in cm^2/dyne. From compilation in Mott and Jones, *Properties of Metals and Alloys*, Oxford 1936, Appendix II.

(2) Radius of atom in Å, from Mott and Jones, Appendix II.

(3) 10^{23} m in grams.

(4) 1000 $[(3)/(1)(2)]^{1/2}$ in dyne sec/cm^2.

(5) Measured values of 10^3 η just above the melting point from Andrade loc. cit.

(6) (5)/(4).

(7) Expansion in percent on melting deduced from data in 29th edition, *Handbook of Chemistry and Physics*.

(8) Deduced from data in Bichowsky and Rossini, *Thermochemistry of Chemical Substances*, Reinhold, New York (1936).

(9) The crystal structure in solid state.

A5. A Discussion of Bubble Models of Grain Boundaries.

The contention of this appendix is that the results deduced from the bubble model and used as criticisms of the grain boundary energy formula are misleading. The argument has three aspects : (1) Even if the size of the dislocations is seen to change somewhat, the energy will be only slightly affected. (2) The dislocations shown in the bubble model are too big because the law of force across a slip plane deviates about three times as much as it should from a sine wave. (3) The Burger's vector is too large in the bubble model and this also results in unrealistically large dislocations. These effects are thought to be large enough to explain why Lomer'sobservations are not applicable to a real metal.

First of all we note that the distortion at the dislocation core adjusts itself so as to miniminze E_I. This means that a change in dislocation width has in the first order no effect on the energy. A quantitative analysis would be necessary to find just what effect a given change in size would have, but this observation indicates that changes which appear striking in the bubble photographs may represent quite small changes in energy.

One of the striking conclusions of the bubble model experiments, Lomer (1949) Figure 3, is that the law of force between two rows of bubbles that are sliding past each other differs markedly from a sine wave. This deviation is largely responsible for the fact that the dislocation widths obtained by the bubbles are in general larger than those predicted from theory, by Nabarro (1947), for example.

We shall next consider how Lomer's Force-Displacement wave should be altered in order to predict the maximum shearing stress for a displacement resulting in a half-dislocation Burger's vector (*). For the case measured by Lomer, a bubble in the upper row varies its distance from a neighbor in the lower row from one bubble diameter d to :

$$d\sqrt{2} \doteq 1.42\, d$$

when it is at the dead-center position. Lomer's results show that at this increased separation, the force of the separated bubble pair has dropped to a very small value. His curve suggests, however, that

(*) I am indebted to W. T. Read for calling my attention to this important point.

the force is linear in displacement out to 15% of this distance and reaches its maximum at 25%. Thus we have :

Restoring force linear to	1.06 d.
Maximum at	1.10 d.

This behavior leads to great deviations from the sinusoidal curve since it gives its maximum at only 25% of the « dead-center » displacement instead of 50%.

It would appear that this situation would be radically changed for a half-dislocation motion. For this motion the dead-center position corresponds to an increase of distance to :

$$d(2)^{1/2}(3/4)^{1/2} = 1.22\ d.$$

The sinusoidal approximation would require the maximum force to occur at about 1.11 d which is where Lomer's experiment puts it for a pair of bubbles. These conclusions suggest that the shortening-up of the motion will substantially eliminate the large non-sinusoidal region in the middle of Lomer's curve.

By attempting to synthesize Lomer's curve by adding curves for pairs of bubbles, I obtain a ratio of force constants at equilibrium and dead-center of —1.75 compared to —4.5 for Lomer's displacement; for a sine wave the ratio would be —1.0. This leads to a ratio of maximum restoring force compared to sine wave of 0.85 whereas Lomer's displacement gives 0.48 The energy stored across the slip plane for the same dislocation based on the sine wave, my estimate of the half-dislocation force curve, and Lomer's force curve would be approximately in the ratio of 1 : 0.8 : 0.45.

This analysis indicates that the bubble model deviates by about twice as much from the correct form as does the sine approximation and in the opposite direction.

The Burger's vector in a bubble model dislocation is one bubble diameter d. The Burger's vector for a half-dislocation on the other hand is $d/3^{1/2} = 0.58\ d$. This means that the bubble model exaggerates the extent of the stress field and for this reason produces mutual interactions between the dislocations much larger than would actually occur in a metal.

These three effects may well mean that the interactions of dislocations do not produce important changes in core energies up to angles of 10° or 20°.

REFERENCES

(1) Achter, M. R. and Smoluchowski, R., *Phys. Rev.*, **83,** p. 163 (1951).

(2) da C. Andrade, E. N., *Inst. Metals. Jl.*, **60,** p. 427 (1937).

(3) Aust, K. T. and Chalmers, B., *Proc. Roy. Soc.*, *A***201, 210** and *A***204**, p. 359 (1950).

(4) Bragg, W. L., *Proc. Phys. Soc.*, **52,** p. 54 (1940).

(5) Burgers, J. M., *Proc. Phys. Soc.*, **52,** p. 53 (1940); *Proc. Kon. Ned. Akad. V. Wet.*, Amsterdam. **42,** p. 293 (1939); see also W. G. Burgers, *Proc. Kon. Ned. V. Wet.*, Amsterdam, **50,** p. 595 (1947).

(6) Cottrell, A. H., *Report of a Conference on the Strength of Solids*, the Physical Society, London, p. 30 (1948).

(7) Cottrell, A. H., Chapter II, *Progress in Metal Physics*, Vol. I, editor Bruce Chalmers, London, Butterworth Scientfic Pub., New York, Interscience Pub. Inc. (1949).

(8) Dunn, C. G. and Lionetti, F., *Trans. A.I.M.E.*, **185,** p. 125 (1949) (includes only [110] series [100] and more of [110] series to be published).

(9) Eshelby, J. D., *Phil. Mag.*, **40,** p. 903 (1949).

(10) Fisher, J. C. and Dunn, C. G., *Imperfections in Nearly Perfect Crystals*, N. Y. John Wiley (1952).

(11) Frank, F. C., Carnegie Inst. of Tech. Conference on the Plastic Deformation of Crystalline Solids, Discussion of paper by Read and Shockley (1950), (to be published.)

(12) Frank, F. C., *Phil. Mag.*, **42,** p. 809 (1951).

(13) Greenough, A. P., 1950, Royal Aircraft Establishment Farnborough Report No. Met. 50 (May 1950).

(14) Heidenreich, R. D., and Shockley, W., Report of a Conference on the Strengt of Solids, **57** (1948). (The Physical Society, London.)

(15) Hoffman, R. E., and Turnbull, D., *J. App. Phys.*, **22,** p. 634 (1950).

(16) Kê, T. S., *Phys. Rev.* **71,** p. 533 (1947). See also C. Zener, Elasticity and Anelasticity of Metals (University of Chicago Press, Chicago, 1948); T. S. Kê, *J. App. Phys.*, **20,** p. 274 (1949).

(17) Lower, W. M., *Proc. Roy. Soc.*, *A***196,** p. 182 (1949).

(18) Lower, W. M., *Proc. Roy. Soc.*, *A***196,** p. 182 (1949).

(19) Mott, N. F., and Jones, H., The Properties of Metals and Alloys, Oxford (1936).

(20) Mott, N. F., *Proc. Phys. Soc.*, London. **60,** p. 391 (1948).

(21) Nabarro, F. R. N., *Proc. Phys. Soc.*, **59,** p. 256 (1947).

(22) Read, W. T., (1951), personnal communication.

(23) Read, W. T., and Shockley, W., *Phys. Rev.*, **78,** p. 275 (1950); see also a preliminary report, **75,** p. 692 (1949).

(24) Read, W. T. and Shockley, W., Paper 2 in *Imperfections in Nearly Perfect Crystals*, John Wiley, New York (1952).

(25) Rossi, F. D. and Alexander, B. H., *Trans. A.I.M.E.*, **188,** p. 1217 (1950).

(26) Smith, C. S., *Trans. A.I.M.E.*, **178,** p. 15 (1948).

(27) Turnbull, David, Report RL-522, G. E. Res. Lab. (1951).

(28) van der Merwe, J. H., *Proc. Phys. Soc.*, London, *A***63,** p. 6, 616 (1950).

Discussion du rapport de M. Shockley

M. Burgers. — You have considered only a very special type of boundary in your paper and have tried to generalise it with the addition of cusps. Is there any evidence for the existence of a dependence of just this kind on the exact value of the disorientation?

M. Shockley. — Read and I have nothing further to add on the question of cusps discussed in our earlier papers. We believe that the analysis is correct and there should be pronounced changes in grain boundary energy with orientation of the boundary. These will be relatively small compared to the dependence on orientation difference however and it may be extremely hard to bring them out experimentally.

M. Bragg. — Any theory of grain boundary energy must account for the fact that, provided the misfit is bad enough, the energy is almost independent of disorientation. Is it fair to say that when there is bad misfit, some atoms fit as well as is possible and others as badly as possible. in such a way that always the same proportions are in a given state of misfit, but as we can alter the disorientation, therefore, there will be only a variation in the periodicity with which successive regions of good fit occur and the mean energy of misfit will remain unchanged.

M. Guinier. — Il semble, d'après ce rapport — comme d'après les nombreuses discussions que nous avons eues sur le sujet, qu'on peut établir une distinction assez nette entre les limites entre grains peu désorientés et les limites entre réseaux très désorientés : c'est d'une part, une suite *discontinue* de dislocations, de l'autre une région de désordre *continu*.

On pourrait établir un parallèle avec les limites entre *matrices* et *zones* et entre *matrice* et *phase précipitée*. Dans le premier cas il y a une suite de défauts nettement séparés les uns des autres, dans le second une couche continue d'atomes désordonnés. De là découleraient les propriétés très différenciées du « einphasige Entmischung » et du « Entscheidung ».

The Yield Point in Single Crystal and Polycrystalline Metals

by A. H. Cottrell,

Metallurgy Department, University of Birmingham.

June, 1951

SYNOPSIS

The purpose of this report is to review recent experimental and theoretical work on the yield phenomenon. In section **1** experiments are described which show that single crystals of various metals possess yield points when they contain certain impurities in solution, mainly carbon and nitrogen. The yield phenomenon of iron is more pronounced in polycrystals than in single crystals, a problem that is discussed in section **3** in detail. This section, together with paragraph **2**, reviews the dislocation theory which explains the yield point in terms of the segregation of solute atoms to dislocations. It is proposed in section **3** that the observed upper yield point is not the theoretical stress required to release a dislocation from its atmosphere of solute atoms. Dislocations begin to break away in regions of high stress concentration while the applied load is still small, and the observed yield point is the macroscopic stress at which yielding failure can spread from these centres into the rest of the specimen. Finally, section **4** describes recent experiments that have been made on the kinetics of the strain ageing process in order to test certain predictions of the dislocation theory.

1. Experiments on the Yield Phenomenon.

When they contain small quantities of certain impurities some metals show a peculiar feature in the stress-strain curve, known as the *yield phenomenon*. This has three main features :

1. *The yield point*; plastic flow begins abruptly at a critical stress

(upper yield stress) and can then be continued, either at the same stress or, more usually, at a lower stress (lower yield stress).

3. *Overstraining*; once a specimen has yielded it will not show another yield point, but a smooth stress-strain curve, if it is immediately retested.

3. *Strain ageing*; the specimen regains its ability to show a yield point if it is rested or annealed after overstraining.

An example of these effects is shown in Figute 1.

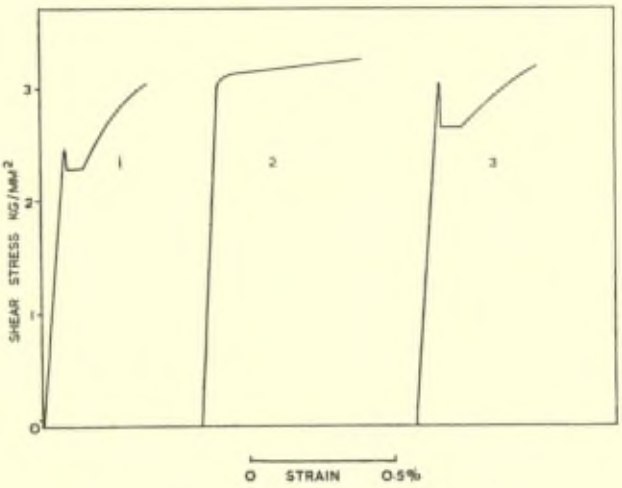

Fig. 1. — *Yielding in a single crystal of beta-brass* (after Ardley, 7.)
1. first test,
2. immediately reloaded,
3. after strain-ageing for 2 hours at 250 °C

Claims have been made at various times for the observations of yield points in several metals and alloys, but so far the yield phenomenon has been fully demonstrated only in iron, molybdenum, cadmium, zinc, and beta-brass. Soft polycrystalline iron or mild steel is the classic example, and in this case there is ample evidence that the yield phenomenon is caused by small amounts of carbon and nitrogen in the metal (1), (2), (3). Túry and Krausz (4) showed that polycrystalline molybdenum behaves very similarly to iron when it contains nitrogen. Recent work at Birmingham has shown that single crystals of cadmium (5), zinc (6), and beta-brass (7), have well-marked yield points when they contain nitrogen; Gibbons (5)

was the first to show that the phenomenon of « thermal hardening », observed by Orowan ([8]) in zinc, and by Smith ([9]) in cadmium, is the same as the yield phenomenon, and depends on the presence of certain impurities in these crystals. Figures 1 and 2 show examples of yield points in beta-brass and zinc crystals.

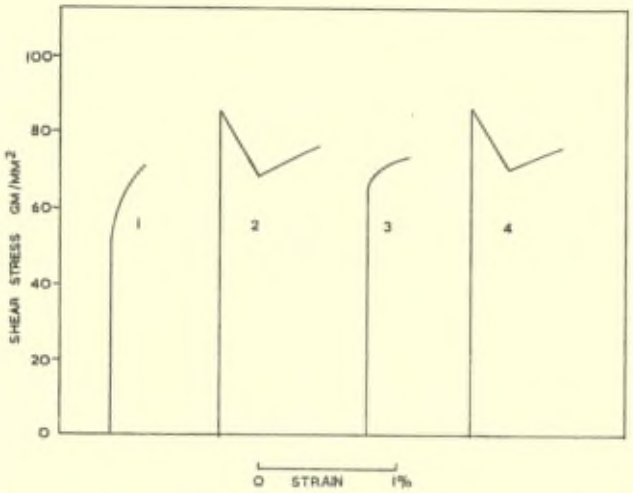

Fig. 2. — *Yielding in a single crystal of zinc* (after Wain and Cottrell, 6).
1. First test.
2. After three strain ageing treatments, each consisting of 0.3 % extension followed by 40 minutes at 180 °C.
3. Taken immediately after curve 2.
4. After seven strain ageing treatments.

There is a widely held view that single crystals of iron do not show yield points. However, this is based on early work which used crystals that had been cleaned of carbon and nitrogen by treatment in hydrogen. Three investigations have been made recently in which small amounts of carbon or nitrogen were deliberately introduced into single iron crystals in an attempt to produce the yield phenomenon. Of those, Schwartzbart and Low ([10]), and Churchman and Cottrell ([11]), observed yield points, but Holden and Hollomon ([12]) did not, or at least, not until after strain ageing their crystals ([13]). Figure 3 shows the yield behaviour of iron crystals containing about 0.02 weight per cent of carbon. This diagram shows a well-known feature of the yield phenomenon : the yield point is more marked, and occurs at considerably higher stresses, at low temperatures.

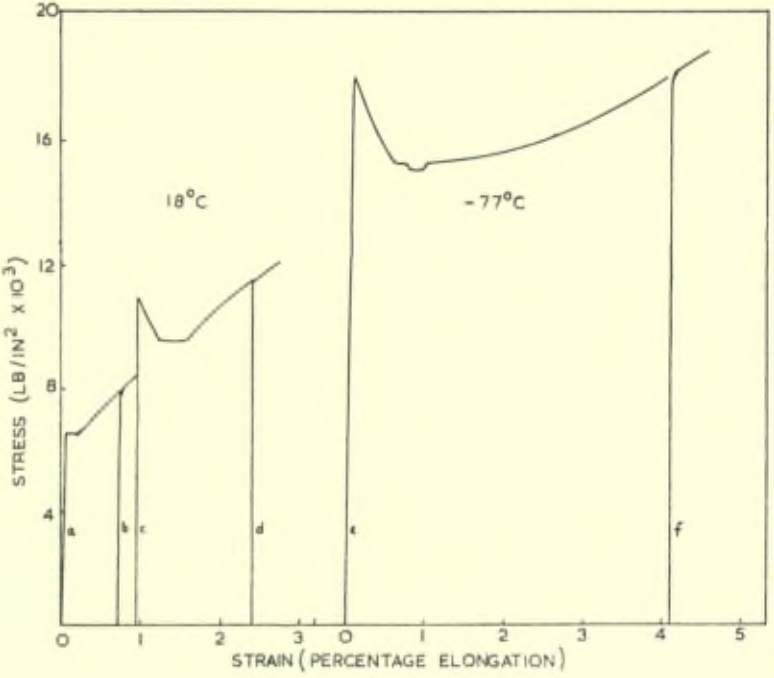

Fig. 3. — *Yielding in single crystals of Armco iron* (after Churchman and Cottrell, 11).

18 °C { *a*. First test. *b*. Immediately reloaded. *c*. After ageing for 18 hours at 18 °C. *d*. Immediately reloaded.

— 77 °C { *e*. First test. *f*. Immediately reloaded.

Figure 4 shows a yield in polycrystalline iron ([14]). Comparison of this with Figure 3 illustrates another feature of the yield phenomenon; yield points in single crystals (and coarse polycrystals) of iron are small compared with those in (fine grained) polycrystalline iron. Because they are small, yield points in single crystals can easily remain undetected unless care is taken regarding straightness of the specimen, axial loading, and absence of stress concentrations. These precautions are particularly important if a yield point is to be observed during the first loading of the specimen. This is because the deformation is almost purely elastic until yielding begins, so that sources of stress concentrations act with full intensity at the upper yield point. On the other hand, once the specimen deforms plastically, the stress concentrations become smoothed out and do not greatly affect the

subsequent plastic behaviour. Thus the yield point shows more strongly and prominently in a strain aged specimen than in an untreated one. Extreme examples of this effect are observed in very soft crystals of cadmium and zinc, which usually do not show yield points until some strain ageing treatments have been given (see Figure 2). On the other hand harder single crystals, such as iron and beta-bras,s usually show yield points during the first test (Figures 1 and 3).

2. Dislocation Theory of the Yield Phenomenon.

In this section we shall recapitulate briefly the dislocation theory of these effects, substantially in the form in which it was developed three to four years ago ([15]), ([16]), ([17]). The main points are as follows :

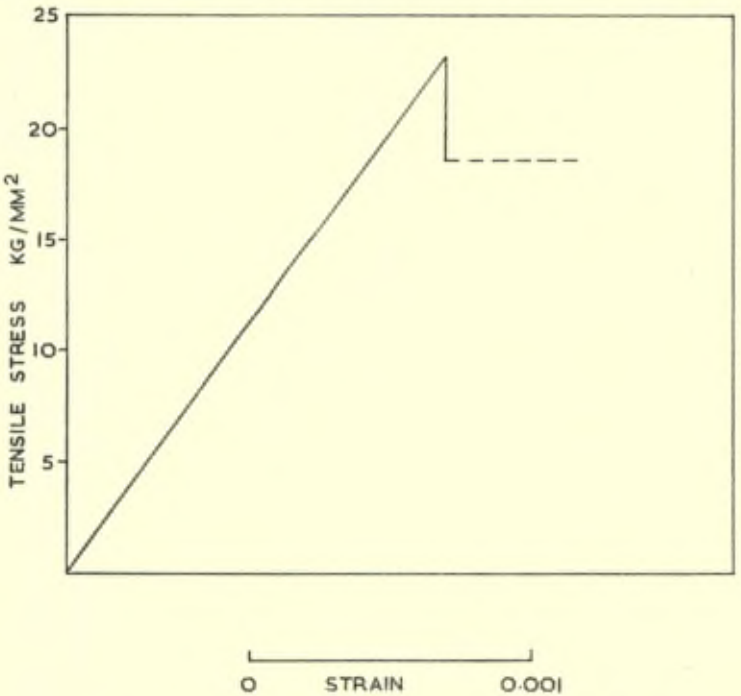

Fig. 4. — *Yielding in polycristalline iron* (after Leak, 14).

(i) *Binding of solute atoms to dislocations.* The stresses round a dislocation can be relieved by a suitable arrangement of nearby

solute atoms. We shall consider the relief of hydrostatic stress. If the elastic dilatation of the lattice at some point is θ, and the change in volume caused by a solute atom is Δv, the atom is bound to this point by an energy :

$$u = -K\theta\Delta v, \tag{1}$$

where K is the bulk modulus. When the elastic field is that of a positive edge dislocation, this becomes :

$$u = A \sin \alpha/r, \tag{2}$$

where r and α are the poler co-ordinates of the solute atom, measured from the dislocation, and A is a constant that depends on K, Δv, and the strength of the dislocation. Equation (2) breaks down at the centre of the dislocation and it is expected that (for the case where Δv is positive) the solute atom is most strongly bound at the position $\alpha = 3\pi/2$ and $r\ (= r_0) \simeq 2 \times 10^{-8}$ cm. For carbon and nitrogen in iron one obtains $A \simeq 3 \times 10^{-20}$ dyne cm^{-2}, and a binding energy $u_{max} \simeq 1$eV, at this point of strongest binding ([17]). Although correct in order of magnitude, these values are almost certainly too high because they are obtained by using linear elasticity theory, and this is not valid at the centre of a dislocation, where the strains are large.

An approximate experimental value can be deduced from Dijkstra's measurements at Chicago ([18]). Using the Snoek damping method ([19]) and a Kê pendulum ([20]), he determined the solubility of nitrogen in the iron lattice when numerous dislocations were present (introduced by cold working). At 300 °C the solubility was 0.0025 weight present, and, at 400 °C, 0.006 per cent. The corresponding values for unworked iron (which give the solubility of nitrogen in the presence of Fe^4N particles) were 0.012 per cent at 300 °C, and 0.025 per cent at 400 °C. These results show that nitrogen atoms are more firmly bound in dislocations than in iron nitride particles, i. e. $U_{max} > U_{Fe^4N}$. The difference in solubility is numerically consistent with $U_{max} - U_{Fe^4N} = 0.08\ eV$. Dijkstra gives $U_{Fe^4N} \simeq 0.35\ eV$ so that we expect $N_{max} \simeq 0.43\ eV$. In this case $A \simeq 1.4 \times 10^{-20}$ dyne. cm^{-2}.

Carbon and nitrogen not only expand the lattice of body-centred cubic iron; they also distort it to a body-centred tetragonal structure. Because of this they interact with both the shear and hydrostatic components of a stress field. This effect has been discussed by Nabarro ([16]) and Crussard ([12]). It is important because it enables

these atoms to interact strongly with screw dislocations in iron, as well as with edge dislocations.

(ii) *Segregation of solute atoms to dislocations.* The interaction described above causes a segregation of solute atoms round dislocations. In equilibrium the concentration c of solute atoms at a point where the binding energy is U is :

$$c = c_0 \exp(-u/kT), \tag{3}$$

where c_0 is the average concentration. This expression is valid provided c is small enough for the volume change caused by the segregation to be small compared with that caused by the stress field, i. e. provided $(c-c_0)\,\Delta v \ll \theta$. In the case of carbon and nitrogen in iron $U_{max} \gg kT$ at room temperature and the « atmosphere » becomes saturated at the centre of the dislocation in the sense that $(c-c_0)\Delta v \simeq \theta$. It is expected that the segregation consists in this case of a single line of carbon or nitrogen atoms lying along the dislocation line and situated at a distance $r_0 \simeq 2 \times 10^{-8}$ cm from the axis (17). The calculation of Bhatia (22) showed that carbon atoms segregated into these lines would make a smaller contribution to the electrical resistance than if these atoms were distributed at random, and an experimental confirmation of this effect was obtained by Cottrell and Churchman (23). Lacombe and Berghezan (24), Castaing and Guinier (25), and Crussard (21), have recently obtained evidence for the segregation of substitutional solute atoms (Zn, Cu and Mg) to dislocations in aluminium; the attraction of solute atoms to sub-grain boundaries was clearly demonstrated by metallographic methods (24), (25).

(iii) *The anchoring force.* When solute atoms are segregated round dislocations a larger force is needed to pull these dislocations away from their initial positions than to keep them in motion afterwards. This causes the structure to give way suddenly, and soften, at the beginning of plastic flow, thus showing a yield point. A freshly overstrained structure shows no yield point because it contains free dislocations, but the yield point returns on ageing as the solute atoms migrate to the dislocations and anchor them once more.

A detailed theory has been worked out for the case where carbon or nitrogen atoms in iron segregate into lines along the dislocations (17). Using equation (2), and denoting by x the displacement of the dislo-

cation in the slip direction from the line of solute atoms, the energy binding the dislocation to this line is :

$$U(x) = -A\, r_0/(x^2 + r_0^2), \tag{4}$$

where A and r_0 are defined as above. This corresponding force per atom plane on the dislocation is :

$$F(x) = 2A\, r_0\, x/(x^2 + r_0^2)^2. \tag{5}$$

This has a maximum (at $x = r_0/\sqrt{3}$) equal to the force due to a tensile stress,

$$\sigma_0 \simeq A/b^2 r_0^2 \text{ dyne cm}^{-2} \tag{6}$$

on the specimen, where b is the atomic spacing. Substituting numerical values appropriate to iron gives $\sigma_0 \simeq 6 \times 10^{10}$ dyne cm^{-2}. This value, about thirty times smaller than Young's modulus for iron, is probably an overestimate. Extrapolation of observed yield strengths ([26]) to 0 °K gives the value 1.25×10^{10} dyne cm^{-2} ([17]).

(iv) *The effect of temperature.* The observed yield stress at room temperature is only one-tenth of that obtained by extrapolating to 0° K. This unusually large dependence on temperature is explained in terms of the short-range character of the binding force. Because the energy trough $U(x)$ is very narrow, a small loop in the dislocation line, formed by moving a section a few atoms long forward by a distance of a few atoms, can grow in the presence of an applied stress of the order $\sigma_0/10$, and cause the whole dislocation line to break away. The small activation energy needed to make such a loop is within the range of thermal fluctuations at room temperature.

3. Propagation of Yielding, and the Grain Size Effect.

The yield stress of fine grained iron is typically four times greater than that of a single crystal. The main purpose of this section is to consider how this may be explained.

It has often been suggested that a honeycomb structure causes the yield point in polycrystalline iron ([27]), ([28]), ([29]), ([30]). The honeycomb, usually considered to be a film of carbide round the grain boundaries, is supposed to have the following properties : (*a*) it is continuous and completely envelops the grains; (*b*) it is strong and brittle; (*c*) before it breaks it carries a large part of the applied load. The upper yield point is reached when the honeycomb breaks. The

ferrite grains cannot support the extra load that is then placed on them and plastic flow takes place at a lower stress.

This theory can be criticised as follows ([15]), ([31]). The stress usually falls by 10—50 % at the yield point. To produce such a large change, when they break, the films of the honeycomb would need to have supported a load comparable with that supported by the grains. But the cross-sectional area occupied by the films is very small, only about 1 % of the total in a 0.01 % carbon iron. It follows that the films would have to be stressed to a level of about 10^{12} dyne cm^{-2}. Even supposing that they were as strong as this, which is hardly feasible, they would be strained elastically at the upper yield point by at least 10 %. Thus the specimen as a whole would be strained by this amount before yielding started. But in practice, as Figure 4 shows, the observed strain at the start of yielding is only about 0.1 %, which is no more than the value expected if the ferrite grains supported all the load and deformed purely elastically with the usual value of Young's modulus (2×10^{12} dyne cm^{-2}).

The continuation of the elastic line to the upper yield point, without sensible deviation, in Figure 4 shows that the deformation in practically every grain is purely elastic until the upper yield stress is reached. If ρ dislocations per unit area were to break away and each of them moved an average distance L to the nearest grain boundary, before the upper yield point was reached, a tensile plastic strain of about $\rho bL/4$ would occur. Taking $\rho = 10^8$ cm^{-2}, $L = 10^{-3}$ cm and $b = 2.5 \times 10^{-8}$ cm, this is about 6×10^{-4}, which is as large as the elastic strain at the upper yield point. If these dislocations were to multiply as they moved, or if the grain size were larger, an even larger plastic strain would occur. We conclude from this that, until the upper yield point is reached, the applied stress is smaller than the break-away stress of the dislocations anchored in the grains. In fact, it is expected that the observed upper yield stress, even in fine grained iron, is smaller than the theoretical break-away stress of an anchored dislocation ([34]). This is suggested by the following considerations : (*a*) it is wellknown that the observed upper yield stress of a specimen can be raised to well above its usual value (e. g. to twice the lower yield stress) by taking great care to remove sources of stress concentration ([32]), ([33]); (*b*) using equation (6), and allowing a factor of 10 for the effect of thermal fluctuations, the theoretical break-away stress at room temperature is $\sigma_0/10 \simeq 6 \times 10^9$ dyne cm^{-2}; this is

2-3 times larger than the usually observed upper yield stress of a polycrystal, and 10 times larger than that of a single crystal.

We are thus faced with the familiar problem of a material which should deform elastically up to a certain stress, the « theoretical strength », and then fail, but which in practice fails at some lower stress, the « observed strength ». The particular process of failure in this case is the conversion of the material, through the release of anchored dislocations, into the soft overstrained condition. We follow the customary explanation and suppose that the failure is nucleated at some place of high stress concentration and then spreads through the material. Evidence that yielding spreads in this way is provided by the observed surface markings known as *Lüders' bands*, or *stretcher strains*. These appear, usually at obvious places of stress concentration such as the shoulders of the specimen, when the upper yield point is reached, and spread through the specimen at the lower yield point. Their boundaries are the surfaces that divide those parts that have yielded from those that have not yielded. Certain macroscopic features of the propagation of yielding failure, in particular the preferential growth of Lüder's bands along lines at 45° C to the principal stresses, and the fact that Mohr's criterion of failure under combined stress is obeyed instead of that of V. Mises, have been shown by Taylor ([35]) to be consequences of the inability of the overstrained material to support a large shear stress.

On a microscopic scale, the propagation takes place by the continual release of anchered dislocations in the highly stressed zone just beyond the perimeter of the yielded region. The condition for releasing such a dislocation is :

$$q\,\sigma \geqslant \sigma_0/s, \tag{7}$$

where $q\,\sigma$ is the stress acting on it when the applied stress is σ, and s is the factor by which the break-away stress is reduced through thermal fluctuations. The important thing to consider now is q, which measures the amount by which the applied stress is magnified in the vicinity of the dislocation. This can be resolved to a fair approximation into two separate factors :

$$q = q_1\,(l) \times q_2\,(l), \tag{8}$$

each of which is a function of l, the distance to the end of the yielded region from the point where yielding starts (Figure 5). The first

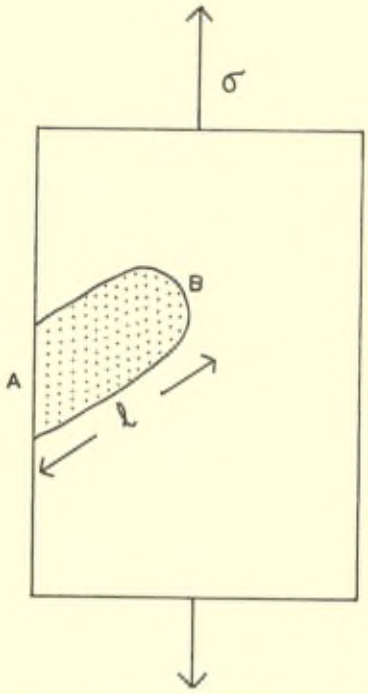

Fig. 5. — *The growth of a yielded region.* Yielding started at A and has spread to B. The applied stress σ is increased to $q\,\sigma$ at B, where q is a function of l, the length of the region.

factor, q_1, measures the original distribution of stress across the section before yielding starts, Clearly, it is largest at $l = o$ and decreases as l increases, i. e. as yielding moves away from the original source of stress concentration (Figure 6). The low yield strength of single crystals requires that $q_1\ (o) \geqslant 10$. The second factor, q_2, measures the new stress concentration caused by the transference of part of the applied load from the yielding material to the unyielded material at its perimeter. Clearly, $q_2\ (o) = 1$ and $q_2\ (l)$ increases with l.

There is thus a critical length, l_c, of the yielded region for which q is a minimum, q_c. The applied stress needed to continue yielding at this stage is the upper yield stress of the specimen, $\sigma_c = \sigma_o/sq_c$. As the growing region increases beyond this size, q increases and yielding can be propagated across the section under a decreasing load.

Several experimental observations can be explained qualitatively with this theory. If the initial stress concentration has a very short-range action, so that q_1 falls to unity while l is still small, then q_c

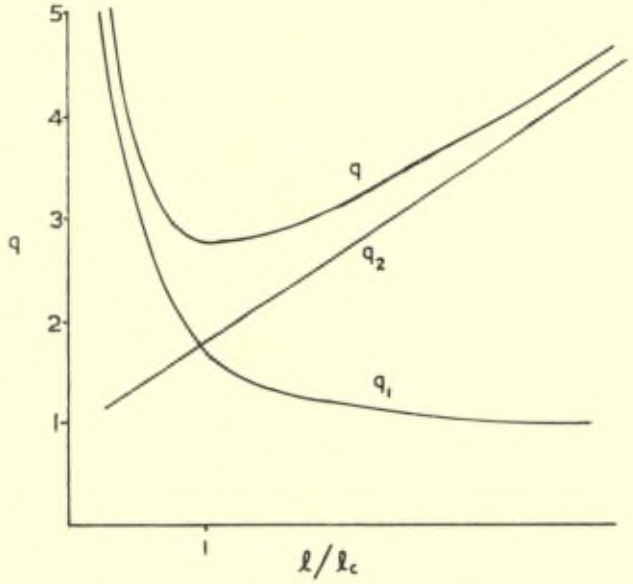

(*a*)

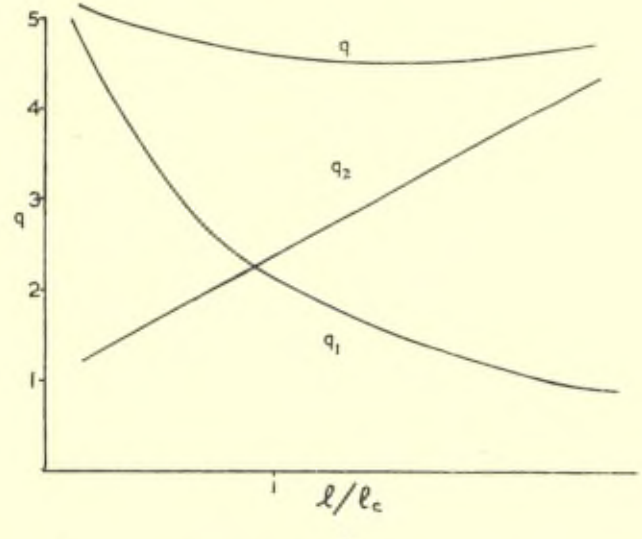

(*b*)

Fig. 6. — *Suggested variation of stress concentration factors as yielding propagates* : (*a*) giving a large upper yield point, (*b*) giving a small upper yield point.

is small and a large upper yield stress will be observed (Figure 6*a*); this corresponds with the observation that a sharp, light scratch does not greatly affect the upper yield point of fine grained iron ([33]). Alternatively, if the initial stress concentration has a long-range action, reaching over many grains in a polycrystal, q_c is large and a small upper yield point will be observed (Figure 6*b*); it is well-known that macroscopic stress concentration, such as are caused by non-axial loading and change of section at the shoulders of a specimen, reduce the upper yield point substantially.

We can now consider the effect of grain size on the yield point. We shall propose that the role of the grain boundaries is to hold up mobile dislocations in the yielded region and thereby prevent the latter from pushing against anchored dislocations at the perimeter of the region; in other words, that the grain boundaries prevent $q_2\ (l)$ from increasing so rapidly with l. The effect on q_c is the same as if the initial stress concentration $q_1\ (l)$ were changed into a shorter range function of l. Thus the same $q_1\ (l)$ could give rise to the case represented by Figure 6*b* if it existed in a single crystal or a coarse polycrystal, and yet only to that of Figure 6*a* if it existed in a fine polycrystal. This means that reducing the grain size increases the observed upper yield stress; also that the upper yield stress of a single crystal or a coarse polycrystal is affected more by light scratches, and similar sources of short-range stress concentrations, than is that of a fine polycrystal. Thus a more careful experimental technique is needed to obtain a fall in stress at the yield point in a single crystal than in a polycrystal. This agrees with the observations noted at the end of section 1.

4. Recent Experiments on Strain Ageing in Iron.

Two things have encouraged experiments to be made recently on strain ageing. The first is Snoek's demonstration that internal friction can be produced by the interstial diffusion of carbon and nitrogen atoms in body-centred cubic iron ([19]). This has been developed at Chicago into a powerful method for measuring the amounts of these elements in solution at any given time, and also their rates of diffusion ([18]), ([20]), ([36]). The kinetics of ageing processes involving the removal of these elements from random interstitial solution can thus be studied quantitatively. The method has been applied to strain ageing by Harper ([37]).

The second is the dislocation theory, which has made predictions about strain ageing that can be tested experimentaly. Starting from the theory described in section 2, Cottrell and Bilby [17] showed that, during the early stages of ageing, the number of solute atoms which segregate to unit length of a dislocation in time t is :

$$n(t) = \alpha\, n_0\, (ADt/kT)^{2/3}, \tag{8}$$

where n_0 is the number of atoms in solution in unit volume, D is the diffusion coefficient, A is the parameter of section 2 which measures the attraction between a solute atom and a dislocation, and α is a numerical factor nearly equal to 3. Introducing ρ, the density of dislocations, this may be rewritten as :

$$f = \alpha\, \rho\, (ADt/kT)^{2/3}, \tag{9}$$

where f is the fraction of the original solute that has segregated to dislocations during the time t. This expression is not applicable to the later stages of ageing becauses it does take account of the « saturation » of dislocations with solute atoms. However, Harper [37] has proposed a simple generalization to include this effect, which assumes that the rate of segregation is decreased in proportion with the amount already segregated. This gives :

$$f = 1 - \exp\,[-\alpha\, \rho\, (ADt/kT)^{2/3}], \tag{10}$$

which, of course, reduces to (9) when the exponent is small.

Figure 7, taken from Harper's experimental results, shows that $\log (1 - f)$ varies linearly with $t^{2/3}$, as is required by the theory. The slopes of the lines at different temperatures show that the activation energy for the strain-ageing process is 20,000 cal/mol. This agrees with earlier estimates [16], [23] and with the measured activation energy for the diffusion of carbon in ferrite, [2], [38], [39], [40]. Taking the value of A given in paragraph 2, and using the measured value for D [39], [40], Harper used equation (10) to determine the density of dislocations in his specimens. The values he obtained (e. g. 2.5×10^{11} lines per sq. cm after 10 % plastic extension) agree well with those obtained earlier by Cottrell and Churchman [23], who used an electrical resistance method.

These experiments by Harper, and by Cottrell and Churchman, show that the amount of carbon (or nitrogen) transferred to dislocations during strain ageing is of the order of 10^{-2} to 10^{-3} weight per cent. However, the solubility of these elements in iron at room

temperature, in equilibrium with their respective precipitates, is much smaller, of the order of 10^{-7} weight per cent for carbon and 10^{-5} weight per cent for nitrogen, according to Wert's extrapolated values ([41]). How then do the dislocations obtain all the solute that

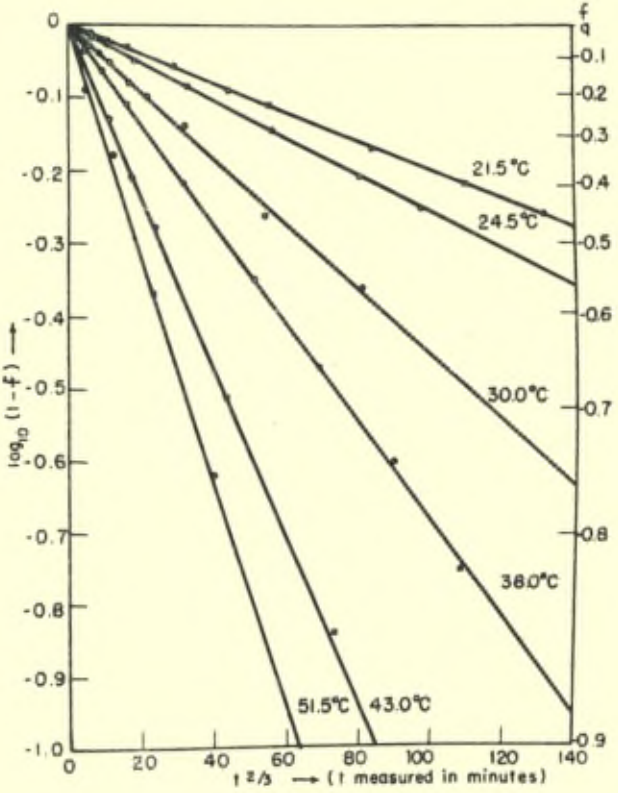

Fig. 7. — The effect of temperature on the rate of strain ageing of iron containing carbon. (After Harper 37).

they require? Evidently the metal must either be supersaturated with carbon or nitrogen when the straining and ageing experiments are made, or the dislocations must induce carbide and nitride precipitates to redissolve in order to supply the necessary amount of solute. It is likely that both of these effects operate in practice. Dijkstra ([18]) and Wert ([41]) showed that precipitation from supersaturated solution in *unworked* iron becomes extremely slow when the amount remaining in solution has been reduced to about 10^{-2}

weight per cent, and that the metal remains supersaturated to this extent after one month at room temperature. Furthermore, the experiments of Dijkstra mentioned in section 2 have shown that the binding energy of these solute atoms in dislocations is greater than that in carbide or nitride precipitates, so that particles of the latter ought to redissolve in the presence of unsaturated dislocations.

A study of these effects is now being made at Birmingham by Leak ([14]). He has shown that heat-treatments designed to make it difficult for dislocations to obtain carbon or nitrogen (e. g. prolonged ageing, *before* straining, in order to reduce the degree of supersaturation and to make the precipitates as coarse as possible) can reduce the rate at which the metal will strain age, in a subsequent experiment, by a factor of about ten. This result, amongst others, shows that our knowledge of the behaviour of carbon and nitrogen in iron has, through the systematic use of the Snoek damping method by the Chicago school and through the application of the theory of dislocations, reached the level where we can begin to exert control over some of the processes involved.

ACKNOWLEDGEMENTS

It is a pleasure to acknowledge the help I have received from stimulating discussions with Mr. F. R. N. Nabarro and Dr. B. A. Bilby during the preparation of this report; also to thank Dr. S. Harper, Dr. A. T. Churchman, Dr. G. M. Leak, and Mr. G. Ardley, for allowing me to make reference to their unpublished work.

REFERENCES

(1) C. A. Edwards, D. L. Phililps and H. N. Jones, *J. Iron and Steel Institute*, **142,** p. 199 (1940).

(2) J. L. Snoek, *Physica*, **8,** p. 734 (1941).

(3) J. R. Low and M. Gensamer, *Trans. Amer. Inst. Min. Met. Eng.*, **158,** p. 207 (1944).

(4) P. Túry and S. Krausz, *Nature*, **138,** p. 331 (1936); **139,** p. 30 (1937).

(5) A. H. Cottrell and D. F. Gibbons, *Nature*, **162,** p. 488 (1948).

(6) H. L. Wain and A. H. Cottrell, *Proc. Phys. Soc.*, **63***B*, p. 339 (1950).

(7) G. Ardley, unpublished.

(8) E. Orowan, *Z. Phys.*, **89,** p. 634 (1934); *Proc. Phys. Soc.*, **52,** p. 14 (1940).

(9) G. L. Smith, *Nature*, **160,** p. 466 (1947).

(10) H. Schwartzbart and J. R. Low, *J. Metals*, **1,** p. 637 (1949).

(11) A. T. Churchman and A. H. Cottrell, *J. Metals*, **1,** p. 877 (1949); *Nature*, in press (1951).

(12) A. N. Holden and J. H. Hollomon, *J. Metals*, **1,** p. 179 (1949).

(13) A. N. Holden and J. H. Hollomon, *J. Metals*, **1,** p.879 (1949).

(14) G. M. Leak, unpublished.

(15) A. H. Cottrell, « Report on the Strength of Solids » (London : Physical Society), **30** (1948).

(16) F. R. N. Nabarro, « Report on the Strength of Solids » (London : Physical Society), **38** (1948).

(17) A. H. Cottrell and B. A. Bilby, *Proc. Phys. Soc.*, **62***A*, p. 49 (1949).

(18) L. J. Dijkstra, *J. Metals*, **1,** p. 252 (1949).

(19) J. L. Snoek, *Physica*, **8,** p. 711 (1941).

(20) T. S. Kê, *Phys. Rev.*, **71,** p. 533 (1947).

(21) C. Crussard, *Métaux et Corrosion*, **25,** p. 203 (1950).

(22) A. B. Bhatia, *Proc. Phys. Soc.*, **62***B*, p. 229 (1949).

(23) A. H. Cottrell and A. T. Churchman, *J. Iron and Steel Inst.*, (July 1949).

(24) P. Lacombe and A. Berghezan, *C. R. Acad. Sci.*, Paris, **228,** p. 95 (1949); *Métaux et Corrosion*, **281,** p. 1 (1949).

(25) A. Castaing and A. Guinier, *C. R. Acad. Sci.*, Paris, **228,** p. 2033 (1949).

(26) D. J. McAdam and R. W. Mebs, *Trans. Amer. Soc. Test. Mat.*, **43,** p. 661 (1943).

(27) W. E. Dalby, *Proc. Roy. Soc.*, **3***A*, p. 281 (1913).

(28) A. Nadai, *Z. tech. Phys.*, **5,** p. 371 (1924).

(29) P. Ludwik, *Z. Ver. Deut. Ing.*, **70,** p. 379 (1926).

(30) M. Kuroda, *Sci. Pap. Inst. Phys. Chem. Res.*, Tokyo, **34,** p. 1528 (1938).

(31) B. A. Bilby, *Sheet Metal Indnstries*, August, p. 707 (1950).

(32) J. G. Docherty and F. W. Thorne, *Engineering*, **132,** p. 295 (1931).

(33) E. O. Hall, Private communication.

(34) A. H. Cottrell, « Conference on Plastic Deformation of Crystalline Solids » (Pittsburgh : Carnegie Institute of Technology), p. 60 (1950).

(35) G. I. Taylor, *Proc. Roy. Soc.*, **145***A*, p. 1 (1934).

(36) C. Wert, « A. S. M. Symposium on Thermodynamics in Physical Metallurgy », Cleveland (1949).

(37) S. Harper, *Phys. Rev.*, **83,** p. 709 (1951).

(38) D. Polder, *Phil. Res. Rep.*, **1,** p. 1 (1945).

(39) C. Werd and C. Zener, *Phys. Rev.*, **76,** p. 1169 (1949).

(40) J. K. Stanley, *Trans. A. I. M. E.*, **185,** p. 752 (1949).

(41) C. Wert, *J. Appl. Phys.*, **20,** p. 943 (1949).

Discussion du rapport de M. Cottrell

M. Mott. — I understand you now think that it is the locking of dislocations in the body of the crystals, and not those in the grain boundaries, which is important for the yielding, and that it is the piling up of released dislocations against the boundary which makes a stress concentration sufficient to trigger off dislocations in the next crystal.

M. Hollomon. — Even though it appears from Cottrell's present point of view that the presence or absence of a definite yield point in single crystals is not critical to the theoretical understanding of the yielding of iron, it is important, I think, to definitely establish whether or not such yield points do occur in single crystals. As Cottrell points out, such yield points have been observed in experiments in his laboratory and in experiments reported by Swartzbart and Low. Recently, however, Low and Holden at General Electric have performed experiments on carefully aligned and handled single crystals of iron containung small amounts of carbon. In no case did these single crystals, without prior plastic deformation and aging, exhibit a definite yield point. We now conclude that the yield points observed by Cottrell and by Low and Swartzbart must have arisen from small amounts of plastic deformation accidently introduced into the sample prior to testing for the yield point. A typical curve (*) for a carefully aligned single crystal is illustrated in fig. 1.

Another observation recently made in our Laboratory is that the return of the yield point after straining is a very sensitive function of the kind and type of prior deformation. For exemple, if a single crystal containing carbon is first deformed by rolling and then subsequently heated to 100 °C, its yield point will return in a time 1,000 times longer than does the yield point return upon aging a single crystal deformed the same amount in tension. Holden has interpreted these results (*) in terms of the cataclismic setting off of other

(*) A. N. Holden, « Dislocation Collision and the Yield Point of Iron » (to be published).

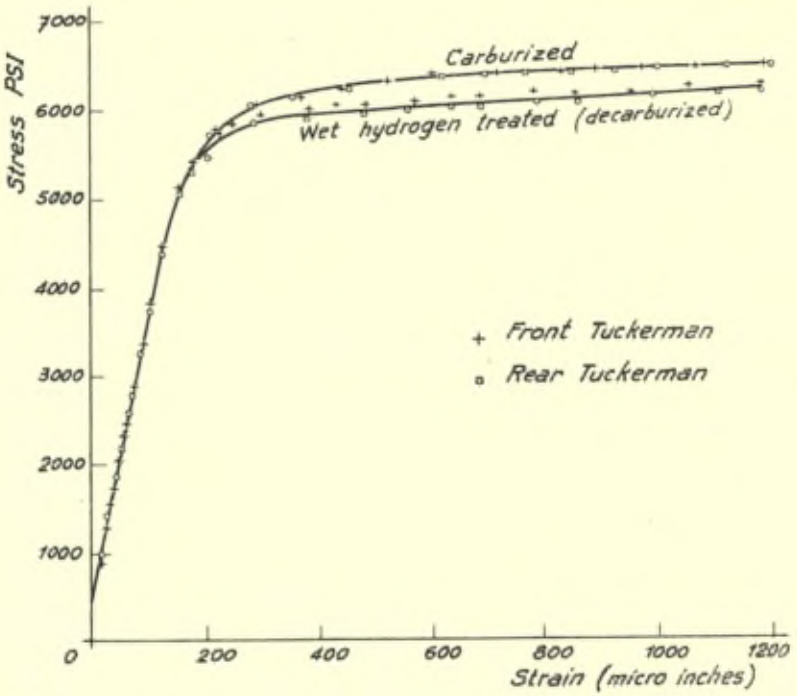

Fig. 1. — Yielding of accurate by aligned identical iron crystals with and without carbon.

Frank-Read sources by dislocations emanating from one Frank-Read source. Such an interaction between sources will take place when the dislocations created by the first deformation are anchored by carbon atoms and deformation takes place on the same planes as in the original deformation but not when the prior deformation takes place on another set of planes.

M. Koster. — Die Deutung der Entstehung eines ausgeprägten Fliessbereiches durch Professor Cottrell hat meine lebhafte Anteilnahme erweckt, zumal ich mich vor rund 25 Jahren mit dieser Erscheinung eingehend beschäftigt habe. Seine Vorstellungen dürfen heute in ihren Grundzügen als gesicherter Erkenntnisstand angesprochen werden. Es ist nun unsere Aufgabe, die Gesamtheit der Erscheinungen in das so einleuchtende Bild einzuordnen.

Bild 1 zeigt den Einfluss des Abschreckens unterhalb A_1 auf die Ausbildung des Fliessbereiches von kohlenstoffarmen Stahl.

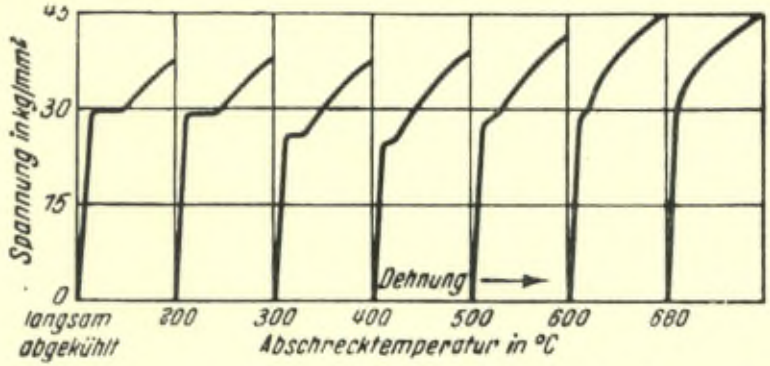

Bild 1. — Einfluss des Abschreckens auf die Ausbildung des Knickes an der Streckgrenze.

Von etwa 300° an aufwärts wird der Fliessbereich kürzer, um 600° herum ist er als Wendepunkt auf der Spannung-Dehung-Kurve anzusprechen und dicht unterhalb A_1 ist er in der Regel nicht mehr vorhanden. Bei der Aushärtung bei Raumtemperatur bildet sich keine neue Streckgrenze aus. Der Fliessbereich erscheint erst wieder beim Anlassen des abgeschreckten Stahles, wenn die Aushärtungswirkung rückgängig gemacht wird, wie Bild 2 zu entnehmen ist. Ich habe daraus seinerzeit den Schluss gezogen, dass der aus dem α -Eisen unterhalb A_1 sich an den Korngrenzen und im Innern der

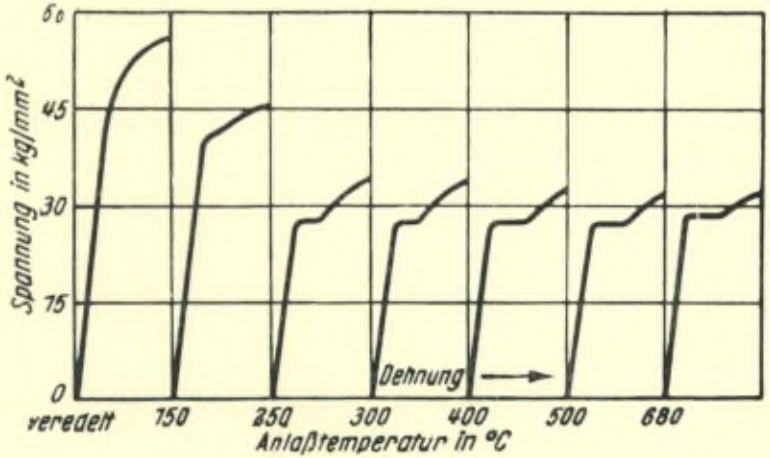

Bild 2. — Einfluss des Anlassens auf die Ausbildung des Knickes an der Streckgrenze.

Körner ausscheidende Zementit, also der tertiäre Zementit, für die Entstehung eines ausgeprägten Fliessbereiches verantwortlich sei. Es war durchaus folgerichtig anzunehmen, dass die Streckgrenze verschwindet, wenn der tertiäre Zementit gelöst wird, und dass er wieder erscheint, wenn er erneut ausgeschieden wird. Aber wenn zwei Erscheinungen parallel nebeneinander herlaufen, so ist damit nicht immer gesagt, dass sie tatsächlich miteinander verknüpft sind. Heute haben wir den tertiären Zementit durch die Anreicherung der Kohlenstoffatome um die Versetzungen, die Ausscheidung durch eine besondere Art der einphasigen Entmischung zu ersetzen. Die Wirkung einer Wärmebehandlung unterhalb A_1 ist dann nach wie vor auf die temperaturbedingte Lösungsfähigkeit des α -Eisens für Kohlenstoff zurückzuführen. Es tritt jedoch an die Stelle der Phasenänderung, Lösung und Ausscheidung von Zementit, die Einstellung eines reversiblen Gleichgewichtes zwischen Wolkenbildung und statistischer Atomverteilung. In Analogie zu den Vorgängen bei der Aushärtung können wir von einer Rückbildung sprechen, wenn wir die Auswirkung des Abschreckens von steigenden Temperaturen betrachten.

In dieser Hinsicht bereitet mir nur eine Tatsache bei der Erklärung Schwierigkeiten. Wie kommt es, dass der Knick nicht beim Lagern abgeschreckten Stahles bei Raumtemperatur wiedererscheint? Die Aushärtung beruht doch auf der Diffusion des Kohlenstoffs im α -Eisen. Nach den Untersuchungen in Chicago bildet sich dabei sogar feinstverteilter Zementit. Weshalb lagert sich der Kohlenstoff nicht an die versetzungsartigen Gitterstörungen an, wo doch alle Voraussetzungen dazu gegeben zu sein scheinen? Bei vorgerecktem Stahl ist dieses doch der Fall; der durch das Recken beseitigte Fliessbereich kehrt wieder zurück.

Die neue Auffassung vom Wesen der Streckgrenze hat noch eine Folgerung, auf die hier nur kurz hingewiesen werden soll. Die Änderung aller Eigenschaften, also auch der physikalischen wie etwa der elektrischen Leitfähigkeit, bei einer Wärmebehandlung unterhalb A_1, ist nicht wie früher angenommen, allein auf die temperaturabhängige Löslichkeit des Zementits zurückzurufen, sondern auch auf den ebenfalls temperaturbedingten Entmischungsgrad der gelösten Kohlenstoffatome. Wir haben es gewissermassen mit einem Dreistoffsystem Eisen-Kohlenstoff-Versetzungen zu tun, in dem nicht nur die Bindungsenergie zwischen Eisen und Kohlenstoff sondern auch die zwischen Versetzung und Kohlenstoff zu berücksichtigen ist.

Weil ich seinerzeit der Meinung war, dass der tertiäre Zementit den ausgeprägten Fliessbereich verursache und seine Auflösung ihn beseitige, habe ich an Stahl mit besonders langem Fliessbereich, wie er durch Reck- und Rekristallisationsbehandlung erzeugt werden kann, nachgeprüft, ob er durch Abschrecken dicht unterhalb A_1 verschwindet. Dabei hat sich herausgestellt, dass dieses keineswegs der Fall ist. Anscheinend darf eine bestimmte Fliessbereichslänge nicht überschritten werden, andernfalls wohl eine Verkürzung nicht aber eine Beseitigung der Streckgrenze erfolgt. Aus diesen Versuchen kann man schliessen, dass eben nicht der tertiäre Zementit den Knick hervorruft, sondern dass der von den Versetzungen gebundene Kohlenstoff wesentlich zur Sättigung des α -Eisen an Kohlenstoff bei Temperaturerhöhung beiträgt. Sieht man in der Länge des Fliessbereiches ein Mass für die Menge an gebundenem Kohlenstoff, so kann man feststellen, dass etwa soviel Kohlenstoff in Lösung gehen kann, als einer Dehnung van 1.5 — 2 % entspricht.

Bei den eben geschilderten Versuchen wurde beobachtet, dass der längste Fliessbereich verschwindet, sobald der Stahl in den Bereich der Perlitumsetzung eingetreten ist und nur einige wenige Zementitkörner sich mit dem α -Eisen zu Austenit umgesetzt haben. Bild 3 zeigt einmal die Verkürzung des Fliessbereiches durch Abschre-

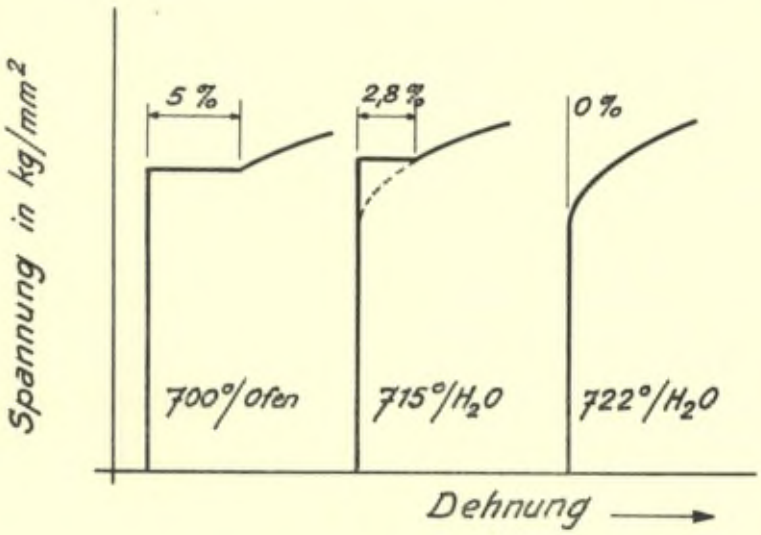

Bild 3

Bild 4*a*. — Gefrize nach Abschrecken von 715°

Bild 4*b*. — Gefrize nach Abschrecken von 822°

cken unterhalb A_1 (715°) von 5 auf 3 % und dann seine Unterdrückung durch Abschrecken aus dem Umwandlungsbereich (722°). Die beiden Dehnungskurven decken sich praktisch im übrigen Verlauf. Das Gefüge beider Zustände ist in Bild 4 *a* und *b* wiedergegeben.

Letztlich ein Wort zum Verschwinden des Knickes bei Warmzerreissversuchen. Die Streckgrenze fällt bekanntlich stetig ab und tritt oberhalb einer Grenztemperatur nicht mehr auf. Diese Temperatur hängt von der Korngrösse ab, und schwankt zwischen 300 und 500°. Man könnte meinen, dass oberhalp der Grenztemperatur aller Kohlenstoff gelöst ist. Dem widerspricht aber der Befund an den vorhin mitgeteilten Abschreckversuchen. So wird man zur Erklärung an Relaxationswirkungen denken müssen, die sich aus dem Zusammenspiel von Verformungsgeschwindigkeit und Diffusionsgeschwindigkeit ergeben und sich in der Beeinflussung der Grenztemperatur durch die Verformungsgeschwindigkeit äussern.

M. Allen. — Professor Cottrell disposes, section 3, of a theory of the action of undissolved carbides in producing the yield point in iron, but does not thereby eliminate the possibility that the undissolved carbides may be responsible for the effect for some other reason.

His alternative suggestion that the yield point is due to the action of the carbon in solution in the ferrite, though graceful in its theoretical form, does not really account for the phenomena that are observed. In order to criticise the theory effectively it is necessary to know the density of dislocations in the ferrite and the amount of dissolved carbon — both of which are difficult to measure. However some estimates of the density of dislocations are given in the paper, the figure of 10^8 dislocations per sq. cm being given for unworked material, and 2.5×10^{11} per sq. cm for material having 10 % of cold deformation, and progress can be made by considering the behaviour of samples with very small contents of carbon (and nitrogen) of which it can at least be said that the amount of carbon dissolved in the ferrite is not greater than the total carbon content of the sample.

According to the theory, no yield point is to be expected if unanchored dislocations are present in the specimen, but if all the dislocations are anchored to carbon atoms a yield point is to be expected.

Equation 6 giving the stress necessary to tear the dislocation from the carbon atoms, contains no term involving the number of dislocations or the carbon content of the metal, so that, other things being equal the stress at the yield point would be expected to be fairly constant.

In an unworked material containing 10^8 dislocation lines per sq. cm, a yield point will be expected in all materials containing more than about .000002 % of carbon if the carbon atoms have had opportunity to become anchored. In a worked material containing 2.5×10^{11} dislocations no yield point is to be expected if the carbon content is less than about .006 % whether the carbon atoms are anchored to dislocations or not. Materials containing between .000002 % and .006 % of carbon should show yield points when unworked, but no yield point after straining and ageing. The reverse actually happens. Irons with about .0005 to .003 % of carbon show no yield point when unworked, but a yield point can be detected if they are strained and aged. The appearance of a yield point in strained and aged irons containing much less than .006 % of carbon constitutes a difficulty if the estimate of the number of dislocations in strained iron is correct. Professor Cottrell appears to agree that between 10^{-2} and 10^{-3} per cent of carbon is necessary for the production of a yield point in strain-aged iron, since on page 501 he finds reasons why this amount of carbon might be in solution in spite of the probability that the solid solubility of carbon in ferrite at room temperature is of the order of 10^{-5} or 10^{-7} per cent.

Yield points may also be absent from unworked materials containing substantially more than .000002 per cent of carbon. An iron containing .006 per cent of carbon showed no yield point in the normalised condition, and one with .028 per cent of carbon showed none when quenched from 950 °C in water. According to fig. 7 at least 50 per cent of any carbon in solid solution should have been anchored by dislocations, so that the carbon in the former alloy might have anchored some 10^{11} dislocations per cm^2 and that in the latter alloy substantially more. Yet there is no reason to suppose that these samples contained substantially more dislocations than any other unworked sample.

The stresses at which plastic deformation begins do not encourage the idea that the initial yield stress is substantially constant when the dislocations are all anchored. The following figures were obtained on a series of pure irons with low carbon contents :

	% C	Yield stress (tons/sq. in.)
Furnace Cooled	.0096	6
	.028	7
	.044	7 1/2
Normalised	.0025	8
	.006	12
	.0096	10
	.0024	11
	.0044	11
Water Quenched	.0096	13
	.028	23
	.044	19

From this it is clear that the yield stress is least when the cooling is slowest — that is, when the carbon atoms have the greatest opportunity to become bound to dislocations. But slow cooling also gives the greatest opportunity for dissolved carbides to come out of solution, and it is very possible from the results in the table that the stress at the yield is determined principally by the amount of carbide remaining in solid solution.

M. Cottrell. — Dr. Hollomon, professor Köster and Dr. Allen, have all produced specimens of iron treated so that the dislocations in them ought to be anchored by carbon atoms, but which have not shown yield points on testing. As a step towards the explanation of these results I want to point out that the anchoring of dislocations by solute atoms is regarded as a necessary condition for observing a yield point, but not as a sufficient one. Before the yield point can be observed various other conditions must be satisfied. To take a simple example, one would not expect a yield point if the metal contained dispersed carbide particles, in such numbers that the stress required to drive a free dislocation through the field of these particles were greater than was required to break it away from its line of solute atoms.

The extraordinary sensitivity of the upper yield point to axiality of loading and to the shape of the specimen suggests that the most common cause of the absence of yield points is the presence of stress concentrations, produced either by imperfections in the testing

technique, or by such things as, for example, slag inclusions or quenching stresses in the material. According to the theory I have proposed these stress concentrations can be rendered fairly harmless, so far as observing an upper yield point is concerned, by introducing partitions (e.g. grain boundaries or deformation bands) into the material. These partitions act as barriers to dislocations that have become freed from their solute atoms and thereby « isolate » from the rest of the specimen those regions where yielding has begun prematurely because of high stress concentrations. This serves to explain why plastic straining and ageing is so effective for converting a specimen from a state in which the yield point is only latent to one in which it is actually observed.

Diffusion, Work-hardening, Recovery and Creep

by N. F. Mott

University of Bristol

1. INTRODUCTION

The purpose of this report is to summarise some of our present theoretical ideas on work-hardening, recovery and creep.

Tentative conclusions are reached as follows : — within crystals there exist sources of dislocation rings, of the type postulated by Frank and Read (1). For each source there is a critical stress which has to be applied for it to act. When this stress is applied to the crystal, the source generates a series of rings. These give rise to slip bands. In cubic crystals rings generated on parallel planes join up to give a single ring; this is the origin of cross slip, as described by the present author (2) in his Guthrie lecture. In cubic crystals moreover, the origin of hardening is normally, we believe, to be found in a phenomenon described alternatively as deformation or kink bands; dislocations coming from opposite directions interact with each other, and by so doing build up a planar obstacle which opposes both their own motion and that of further dislocations from the same and other sources.

It is suggested tentatively that :

(a) The reason why a pair of edge dislocations approaching each other can stick, or jam, and form an obstacle is connected with cross slip which has occurred before they meet; in hexagonal crystals, if there is no cross slip, this does not occur. The arguments on this point are given in the author's Guthrie lecture.

(b) The mechanism for stabilising deformation bands, so that they do not disappear when the stress is removed, always involves slip on one of the other sets of planes, not the ones on which the primary slip bands are formed. This was first suggested by Lomer (3) and

represents a viewpoint differing from that put forward in the author's Guthrie lecture.

(c) Deformation bands will only form if, at a given point early in the deformation, the density of moving dislocations is high enough for the proposed jamming to occur. This is most likely to be the case if the stress applied varies from point to point. If the stress is uniform, one would expect only a few Frank-Read sources to operate, namely those for which the critical shear stress is lowest. We thus expect that the onset of work hardening for single crystals by this mechanism would be delayed and would depend rather critically on the experimental conditions, such as the method of applying the stress and the state of the surface. Experiments by Kochendörfer and Röhm (4) and by Andrade (5) suggest that this may be so.

(d) It is possible that another slower mechanism of hardening exists also, which takes over when deformation bands are not formed, as in single crystals of hexagonal metals and in cubic crystals under specially controlled conditions. Some speculations about this point are given.

Turning now to recovery and creep, the hypothesis made in this report is that this is connected with self-diffusion, which we assume to take place trough the movement of vacancies. An edge dislocation is capable of moving out of its slip plane by giving off or absorbing vacancies. The activation energy for such a process is normally rather greater than that for self-diffusion, but in the regions of very high stress within a deformation band it may be somewhat less. This is assumed to be the cause of the drop in the activation energy for recovery and creep that, according to some authorities, accompanies increased cold-work, or increased stress. At low temperatures, however, a certain amount of transient creep can occur without the intervention of moving vacancies. In this case, the relation between strain and time is logarithmic.

We shall begin this report with a review of the information relating to the interaction of dislocations and vacancies; we shall then discuss some of the problems concerned with work-hardening, in particular

(i) The effect of the surface on the observed form of the slip bands.

(ii) The stability of deformation bands.

(iii) The temperature-dependence of work-hardening.

And finally we shall develop somewhat the considerations given in the author's Guthrie lecture on recovery and creep.

2. VACANCIES AND DISLOCATIONS

The concept of vacant lattice sites seems first to have been introduced into physics by Frenkel and by Schottky to account for electrolytic conduction in solid polar crystals (alkali halides, etc.). There can be little doubt that this explanation is correct. It is also likely that diffusion and self-diffusion are frequently, but not always, due to vacancies, an atom only changing its place in the lattice when a vacancy is next to it.

The most direct evidence that diffusion in solids, and particularly in metals, is due to vacancies is :

(a) The Kirkendall effect; an account of this is given below.

(b) A recent observation of Nowick ([6]) on internal damping in an alloy of the series AgZn in the α-phase. He separates a component in the damping due to the exchange of Zn and Ag atoms, and shows that after a quench this component is greatly increased, and then slowly dies away. This he ascribes to the freezing-in of vacancies on quenching, which slowly condense on dislocations or grain boundaries.

There is one special case of interest, discussed by Smolochowski and Burgess ([7]), where diffusion is certainly due to vacancies. This is the case of the alloys NiAl and CoAl. According to Bradley et. al. ([8], [9]) an intermetallic compound is formed at the 50-50 composition with the body-centred (CsCl) structure, and is able to take up excesses of the two elements. On the nickel-rich side the extra nickel atoms can replace aluminium in the lattice, but on the other side the extra atoms of aluminium cannot replace the much smaller atom of nickel, so that vacant nickel sites are formed. According to Smoluchowski and Burgess these cause no increase in the self-diffusion coefficient of nickel, because Al atoms are too big to move into the vacancies, and the nearest nickel atoms, at one cube edge away, are too far away to jump into the vacancy with reasonable activation energy. Self-diffusion of Ni will only occur through the presence of vacancies in the aluminium lattice, into which the nickel atoms can jump. The presence of excess nickel, however, which in the main replaces aluminium, will increase the number of Al vacancies. This is because the number of *thermal* Ni vacancies in the 50-50 alloy is expected greatly to exceed the number of Al vacancies; therefore for the nickel rich alloy many of the excess nickel atoms will go into these holes.

On the other hand, we do not wish to imply that diffusion is always due to vacancies. This will certainly not be the case for interstitial impurities. Zener ([10]) and Paneth ([11]) have suggested that self-diffusion in body-centred structures may be due to the direct exchange of pairs or of rings containing four atoms or more. It would be of great interest, therefore, to investigate the Kirkendall effect for such materials. Dienes ([12]) has suggested that, at any rate near the melting point, diffusion is a co-operative phenomenon involving a number of atoms; this would mean that the factor D_0 in the expression for the diffusion coefficient :

$$D = D_0 \, e^{-Q/RT}$$

would be bigger than νa^2, being increased by an entropy factor. His considerations are similar to those of Mott ([13]) in this theory of grain boundary slip. We would like here to suggest that an alternative mechanism of diffusion may be the disordering or melting of some unknown number n of atoms. The free energy F for such a process must approach zero at the melting point T_M, and so may be written :

$$F = n\,L\left(1 - \frac{T}{T_M}\right)$$

where L is the latent heat of fusion. The coefficient of self-diffusion would thus be of the form :

$$\nu\, a^3 \exp\,(nL/kT_M) \qquad \exp(-nL/kT)$$

If nL is greater than the activation energy for the vacancy mechanism, we should expect this mechanism to take over at high temperatures. We should, therefore, expect the logarithmic plot of the diffusion coefficient to show a kink, as in fig. 1.

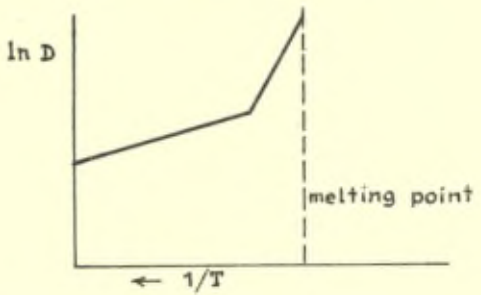

Fig. 1
Suggested dependence on temperature of the diffusion coefficient.

3. KIRKENDALL EFFECT

We shall now discuss the evidence presented by the Kirkendall effect, both for the vacancy mechanism of diffusion, and for the absorption and emission of vacancies by dislocations. We do not know of any elementary published discussion of the theory of this effect, and so give one here.

The effect was first observed by Smigelskas and Kirkendall ([14]) and has been investigated further by Correa and Mehl ([15]).

Essentially the problem is as follows : the diffusion is studied which occurs when an alloy, such as brass, is placed between two plates of one of the constituents, for exemple copper. Markers are placed at the boundaries (e. g. A, B in fig. 2), and it is found

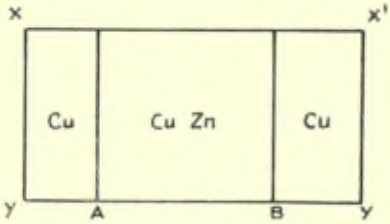

Fig. 2
Kirkendall effect.

that the markers move towards each other as the diffusion progresses and that the displacement is proportional to the square root of the time.

If diffusion is due to an interchange of atoms it is clear that no movement of the markers can occur. For the materials investigated, therefore, this mechanism is ruled out. If, however, diffusion takes place through the movement of vacancies (or through the movement of interstital atoms), a mass flow of matter out of AB will be possible. An anlysis may be made somewhat as follows. Consider two planes of atoms distant a apart; let the proportions of zinc atoms on the two planes be c, $c + a(\partial c/\partial x)$. Consider now a vacancy in either of these planes; we may suppose that it changes place more easily with a zinc than a copper atom. Let the chance per unit time that it changes place with a copper atom be P_A and with a zinc atom P_B.

The vacancy will then drift in the direction of excess zinc concentration with velocity

$$(P_B - P_A) \frac{\partial c}{\partial x} a^2$$

If, then, the proportion of vacancies is c_V (itself a function of c), and a^3 is the atomic volume, there is a mass drift of matter in the direction zinc-copper of amount

$$(P_B - P_A)\, c_V \frac{\partial c}{\partial x}\, a^4 \text{ cm}^3/\text{sec.}$$

It will be seen that the diffusion coefficient of the zinc relative to the lattice is

$$P_B\, c_V\, a^2$$

and that of the copper

$$P_A\, c_V\, a^2;$$

the mass drift thus depends in a simple way on the inequality of the diffusion coefficients of the two constituents.

For an explanation of the Kirkendall effect, however, it is not sufficient to find a mechanism — such as the vacancy mechanism — which allows for the transport of matter across a plane fixed in the lattice; one needs also a mechanism for the absorption of an unlimited number of vacancies in the central region. One possible mechanism is that the vacancies condense into plates, which then collapse, leaving dislocation rings. This mechanism would, however, gradually fill the material up with dislocations and so work-harden it, unless recrystallisation took place; there is no evidence that this occurs. A more probable explanation is that vacancies are absorbed by dislocations or grain boundaries.

One would think at first sight that edge dislocations would give a limited capacity for absorbing vacancies; when a whole half plane had been removed, the dislocation would disappear, so that the process would end when all the dislocations had been removed. If anything like this occurred, the Kirkendall effect would be a mechanism for producing the perfect crystal.

To avoid this dilemna, we may assume a spiral mechanism similar to that first proposed by Frank and Read for the sources of dislocations and by Frank for crystal growth. Except that we are dealing with the motion of dislocations perpendicular to their normal slip

planes, the process is exactly the same. It allows the subtraction (or the addition) of an unlimited number of planes *within* the crystal, by just the same mechanism as they are normally added or subtracted from the surface in the theory of crystal growth.

In order fully to explain the Kirkendall effect, one needs a mechanism for the formation as well as for the destruction of vacancies. It is, of course, possible a priori that the vacancies are all formed at the outer surface of the copper (XY, X'Y' in fig. 2). This would mean that the concentration of vacancies in the CuZn had the value appropriate to copper, much less than for brass; the diffusion coefficient in the brass would then be abnormally small. There is no evidence that this is the case. Therefore vacancies must be created in the boundary region between copper and brass. This is possible only by the second of the two mechanisms suggested, above, or at grain boundaries.

Seitz [16] considers that the density of dislocations — and particularly of dislocation kinks — should be sufficient to keep the number of vacancies at its equilibrium value. The analysis appropriate to this problem is as follows :

We may suppose that each jog in a dislocation emits and absorbs per unit time a number of vacancies of order

$$D_V/a^2$$

where D_V is the diffusion coefficient for a vacancy and a the lattice parameter. The maximum number of vacancies that the dislocations can supply is thus of order, per unit volume and unit time,

$$ND_V/a^2,$$

where N is the number of dislocation jogs per unit volume. The net flow of material out of a given volume in the Kirkendall effect, if the number of vacancies is kept in equilibrium, will be of order

$$(D_A - D_B) \frac{\partial^2 c}{\partial x^2} \frac{1}{a^3}$$

where c is the proportion of sites occupied by B atoms. Assuming $c \sim 0.5$ and $\partial^2 c/\partial x^2 \sim 1/L^2$, where L is the linear size of the specimen, and that the diffusion coefficients are all of the same order, we see that the dislocation kinks will be able to maintain equlibrium if

$$N \gg 1/a\, L^2.$$

If L is of order 1 cm, this is the case if $N \gg 10^8$ cm^{-3}. This should certainly be satisfied even in an annealed material.

Probably grain boundaries would be sufficient, even in the absence of dislocations. The writer understands that experiments are in progress in the U. S. A. which suggest that it is grain boundaries rather than dislocations which act as sources and sinks. In this connection we would like to make the following remark. As already emphasized, if dislocations are to act as sources or sinks to any considerable extent, they must do so by a spiral mechanism — i. e. by just the same mechanism as that by which a dislocation multiplies in a Frank-Read source. Now a certain stress S, of the order of the yield-stress of the material, is necessary to make a Frank-Read source operate. In the same way, a certain degree of supersaturation of vacanties, easily seen to be of order $\exp(Sa^3/kT) - 1$, is necessary if dislocation rings are to be formed by the condensation of vacancies. Calculations to see whether such degrees of supersaturation would occur would be of interest.

4. VACANCIE CREEP

Certain types of creep, occurring at high temperatures and low stresses, give further evidence on whether or not dislocations can absorb or generate vacancies. Nabarro (17) was the first to show how the movement of vacancies (or interstitial atoms) can lead to plastic deformation without the movement of dislocations. His argument is as follows. Consider first a perfect crystal without either dislocations or grain boundaries. The vacancies can only be formed at the surface. Let us apply a shear stress p to the crystal as shown. Then the work required to form a vacancy at the surfaces AB, CD (fig. 3a) is increased by pV, and decreased by the same amount at the surfaces AD, BC. V is the volume change on producing a vacancy. Thus if **c** ist he concentration of vacancies in the absence of the stress, the concentration is increased by a factor $\exp(p\mathrm{V}/k\mathrm{T})$ at the surfaces AD, BC, and decreased by the same factor at the other surfaces. There is thus a diffusion of holes in the direction shown by the arrows, the number of holes crossing area per unit time being

$$\frac{\sinh(2p\mathrm{V}/k\mathrm{T})}{\mathrm{L}} \quad \frac{\mathrm{D}}{\mathrm{V}}$$

where D is the coefficient of self-diffusion. The creep rate of strain is obtained by multiplying by V/L and is thus

$$\frac{D}{L^2} \sinh \frac{2pV}{kT} \sec^{-1}.$$

For moderate stresses the sinh can be replaced by its argument; the creep rate is thus proportional to the stress p, but depends on the linear dimension of the specimen. The material shows an apparent viscosity η given by

$$\frac{1}{\eta} = \text{const} \frac{DV}{L^2 kT}$$

where the constant is of order unity and depends on the shape of the specimen. It will be noticed that η depends on L, the size of the specimen.

It is doubtful whether this analysis applies to any real case, since real materials probably contain dislocations even at high temperatures. We give below an analysis, similar to that given for the Kirkendall effect, of how creep can occur when dislocations can act as sources and skins.

We suppose that there are per unit volume N points on dislocations from which vacancies can evaporate. Of these about half will be of the type P in fig. 3(b), about half of the type Q. Thus the vapour

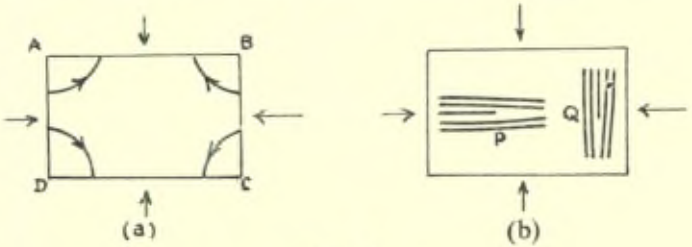

Fig. 3
Showing creep by the diffusion mechanism.

pressure of sources P is increased by $\exp(pV/kT)$, that of sources Q decreased by the same amount. The sources will thus absorb or create vacancies at a rate given by

$$(D/a^2) \{ 1 - \exp(\pm pa^3/kT) \}.$$

The creep rate is thus given by

$$NaD \sinh \frac{Pa^3}{kT}$$

where D is the coefficient of self-diffusion. It will be noticed that N is itself strongly temperature sensitive.

Such an analysis is probably valid only for very small strains. Conyers Herring [18] points out that in a material at high temperatures the dislocations are bound to take up positions — e. g. at mosaic boundaries or boundaries of polygonised elements — where they are stable against small displacements both in their slip planes and perpendicular to them. Thus under a small applied stress the dislocations, moving in the latter directions through vacancy diffusion as described above, would soon come to rest in new equilibrium positions. We have already emphasized this point in connection with the Kirkendall effect, Herring, following Nabarro, suggests that grain boundaries may act as sources and sinks of dislocations of the type required. He works out effective viscosity coefficients for various assumptions. For example, for quasi-spherical grains and tangential stress relaxed at the boundaries, he finds

$$\frac{1}{\eta} = \frac{5}{2}\left(\frac{32\,\pi}{3}\right)^{2/3} \cdot \left(\frac{DV}{kT}\right)\frac{1}{L^2}$$

where L is now the grain diameter.

Herring applies these formulae to creep rates at high temperatures measured by Udin, Shaler and Wulff [19] for copper and Alexander, Kuczynski and Dawson [20] for gold. In these experiments, low stresses of the order 1 to 100 gramme/mm^2 were used, extensions of the order 10^{-3} to 10^{-2} observed. It seems reasonable to assume that creep here is due to the above mechanism. Herring uses the experimental results to calculate L, the apparent grain size. The results for wires of radius R are

Metal	Cu	Cu	Au
T°C	1000	1000	1050
R (microns)	36	64	14
D (assumed in calculations)	2.5×10^{-9}	2.5×10^{-9}	8×10^{-9}
η (obs)	4.4×10^{12}	3.2×10^{12}	1.4×10^{12} initial 2.4×10^{12} final
L/R (calc)	1.0	0.24	9.6 to 16
L/R (obs)	4	2	2

The values suggest at any rate that the grain size is the determining, factor, rather than a much smaller distance between dislocations.

In conclusion, then, there does not seem to be any definite evidence at present that vacancies can evaporate or condense on dislocations. But in this connection we emphasize

(i) As already stated, a degree of supersaturation of vacancies of order $\exp(Sa^3/kT) - 1$ (S = yield stress) would normally be necessary for this to occur.

(ii) Vacancies can only condense on jogs, and for extended dislocations [Heidenreich and Shockely ([21])] the energies of such dislocations would be considerable. The number present due to temperature agitation may be small — and those present on dislocation rings which have cut screw dislocations in the process of formation (Mott ([2]), Guthrie lecture) will soon be used up.

5. PLASTIC DEFORMATION AND WORK-HARDENING

5. 1. Temperature dependence.

The process of work-hardening, under conditions such that deformation bands are formed, is to be envisaged as follows. There will be, scattered throughout the material, a number of Frank-Read sources. If x is the distance between the anchoring points of any one of these sources, it will start to generate dislocation rings if a stress S greater than about Gx/b is applied ([22]). b is here the Burgers vector. When, then, a stress is applied great enough to set these sources in action, they will continue to generate rings until the process is stopped — e. g. by the formation of deformation bands.

The yield point of a single crystal of pure material thus depends on the length x of the longest of these sources. We have, as far as I know, no theory of the way in which this distance depends on annealing, purity, etc. To obtain such an estimate, both for single crystals and polycrystals, is one of the most important tasks with which the theory is faced.

In impure materials, the yield atress will depend both on x and on the locking effect of impurities. These can act in two ways :

(a) by forming atmospheres on or near the dislocation line, as in Cottrell's work on the yield point of iron;

(b) by giving rise to internal strains not directly related to the

position of the dislocation, as in solid solutions and age-hardened materials [Mott and Nabarro (23)].

It is a definite consequence of the theory that for pure materials, and impure materials in case (b), the yield point should be almost independent of temperature — or if there is no recognisable yield point, the stress-strain curve in its early stages. This is because [of Mott and Nabarro (23)] strain is due to the movement of comparatively large dislocation loops. The activation energy for the case of pure materials is

$$c\, Gbx^2 \left(1 - \frac{S}{S_0}\right)^{3/2}$$

where S is the applied stress, $S_0 = Gx/b$ (the critical stress without the influence of temperature), and c a numerical constant of order 0.2. If, say, $\sim 0.9\ S_0$, this gives

$$0.006\ Gb^3\ (G/S)^2,$$

and for reasonable values of G/S this will be very large compared with kT. All these conclusions are subject to the condition that the temperature is low enough to prevent diffusion of vacancies — i. e. too low for steady-state creep.

It is satisfactory to find that recent measurements of the yield points of pure vacuum-annealed single crystals of copper made by Neurath and Koehler (24) show that the yield point is sensibly the same at — 190° C and 21° C, being equal to 200 gm/mm².

The yield-point due to locking in the Cottrell sense is on the other and, very temperature sensitive (25). This is because, if impurities segregate along a dislocation, the stress field which results is extremely local. Thus if a very small length of dislocation is enabled, by the influence of thermal vibrations, to escape from its atmosphere, the stress will drag the rest away.

Now it is of great interest that the flow stress of cold-worked specimens is very temperature-sensitive. This is illustrated in fig. 4, which shows some results due to Dr. Kennedy (*). The experiments were carried out with lead containing 0.05 % silver. The wires were 1 mm in diameter, annealed at 200° C. Curve A shows the stress-strain relationship for a wire at liquid air temperature : curve B shows the stress-strain relationship at room temperature up to the point

(*) Unpublished; I am grateful to Professor E. N. da C. Andrade for making these available to me.

marked, when the wire was immersed in liquid air. Where two points are shown at the same stress, the one to the right expresses the reading taken two minutes after loading, so that the difference between the two is due to creep.

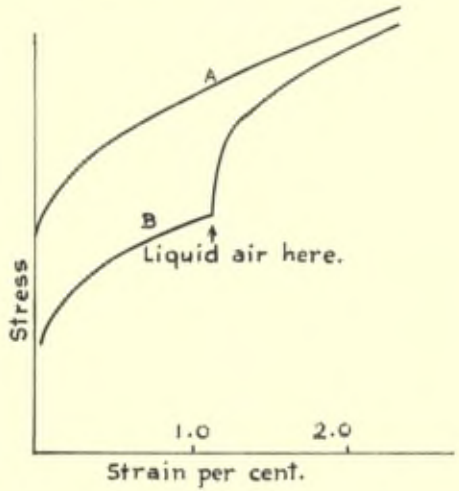

Fig. 4

Stress-Strain curves for lead (0.05% Ag) at liquid air temperature (A) and at room temperature followed by liquid air (B).

It will be seen that on cooling to liquid air temperature the flow stress increases. It follows, as far as one can see, that the obstacles to the motion of dislocations must be very localised.

The only picture of the process consistent with these facts which the writer can suggest at the present time is provisional and quite unquantitative; it is as follows. Edge dislocations which are zig-zags, as a result of cross slip, meet each other and form obstacles as described in the author's Guthrie lecture (fig. 14). Other dislocations from the same sources pile up against them.

In polycrystalline materials pile-up against grain boundaries may be the determining factor. Locally, in the resulting kink band, very strong stresses are therefore set up. These stresses will bring into operation neighbouring Frank-Read sources on other planes, which will generate dislocations. As shown by Lomer [3], these dislocations will join with a few of those on the original planes to form sessile dislocations, thus providing a locking mechanism.

The blocking effect proposed by the author will *not*, however, be uniformly distributed along the length of a dislocation, which is jagged as a result of cross slip. Such a dislocation will be blocked on some parts of its length, and free to proceed on others. It will thus, viewed in its own slip plane, tend to take up the form shown in fig. 5. Pieces of edge dislocation such as AB, blocked by this

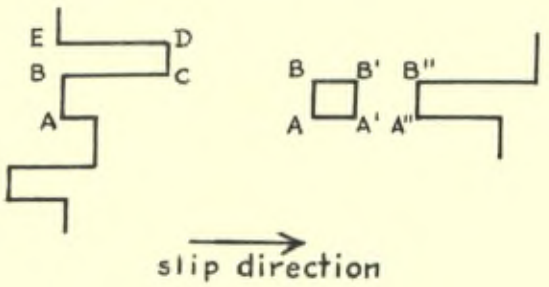

Fig. 5
Dislocations in their own slip plane.

mechanism, will be separated by lengths of screw dislocation BC from pieces CD of edge form which have been allowed to go on. If, now, some of these elements AB, CD are made sessible by joining with dislocations from another plane, we do arrive at a blocking mechanism which is

(a) capable of holding the deformation band in place, and

(b) doing it by means of obstacles of small spatial extent, thus allowing a temperature effect. Possibly sessile loops such as ABD'C' in fig. 5 (b) are formed.

We picture the process of work-hardening, then, as the pushing of dislocations into the deformation band through a gradually increasing number of such obstacles. Part of the stress required — the temperature dependent part — will be that required to overcome these obstacles; some — essentially independent of temperature — to pile up more dislocations in the band.

It must be emphasized that these considerations are quite qualitative, and not based on any mathematical analysis.

5. 2. Recovery and creep.

Since the flow stress is temperature-dependent, we must anticipate that both creep and recovery can take place, to some extent, simply by the motion of dislocations in their slip planes. As regards creep, we follow Orowan ([26]) in considering that creep under these conditions is very similar to the slow extension of a specimen under gradually increasing stress, thermal fluctuations taking the place of stress increase. The only difference is, as we have already seen, that thermal fluctuations will not bring in new sources, while a stress increase will do so. An analysis (Mott, Guthrie lecture, § 11) shows that for this type of creep one expects a relation between strain s and time of the type

$$s = A + B \ln t.$$

We have not attempted an analysis of the contribution of a process of this type to recovery.

In the author's Guthrie lecture it was suggested that the movement of vacancies is essentially connected with recovery at higher temperatures, with the polygonisation of deformation bands, with steady state creep, and with transient creep in which the strains are at all considerable.

The observed polygonisation of deformation bands provides actually the only direct evidence that edge dislocations can move out of their slip planes (« climb ») by absorbing or giving off vacancies. In our earlier discussion we have emphasized the high energy of jogs — the points on a dislocation where this can occur, with the consequence that in annealed materials there may be very few of them; but in a deformation band, with its high internal stresses and jagged dislocations, the number may be much greater.

The process of the steady-state creep we picture as follows :—

If obstacles as in fig. 5 (b) are formed, these can clearly be removed by the diffusion of vacancies, and we may expect this to occur. Also we have to remove the dislocations out of their slip bands in order to make room for more. This will occur by the diffusion process, the dislocations being pushed away by the stress set up (fig. 6). When polygonisation is complete — i. e. when a row of dislocations stretches from one active slip plane to the next, we may expect a steady rate of creep, the strength of the polygonised band increasing continually. The reason why we should expect a steady state under

these conditions is that each dislocation escaping from a slip plane must go, on the average, half the distance between the slip planes. Transient creep will occur before polygonisation is complete, when the dislocations have less far to go.

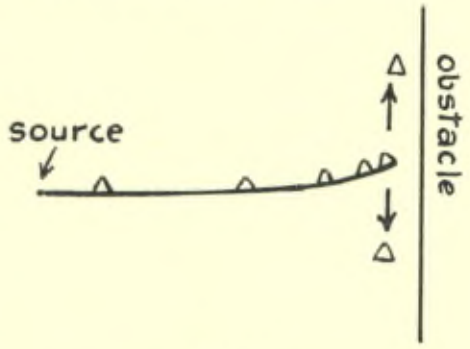

Fig. 6
Dislocations piling up against a boundary and diffussing away.

It has, of course, been maintained by various authors [e.g. Beck, Sperry and Hsun Hu ([27])] that the movement of grain boundaries will normally involve the diffusion of vacancies along the boundary. Since grain boundaries can be resolved into dislocations, and movements of the dislocations in their slip planes will not normally suffice to move the boundary, this is another aspect of the hypothesis presented here.

6. SURFACE CONDITIONS

One of the observations of Heidenreich and Shockley ([21]), of Brown ([28]), and others is that the elementary slip lines occur in clusters at a spacing of c. 200 A. We suggest that the cause of this is as follows. After slip on a single slip plane has proceeded for a considerable distance, there will be a notch on the surface (fig. 7).

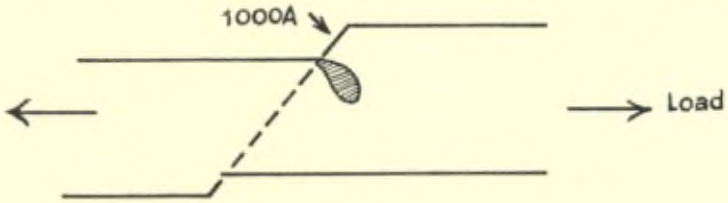

Fig. 7
Showing stress concentration at the edge of a slip band.

Round this notch there will certainly be a stress concentration, shown shaded in the figure. We suggest that the effect of this stress concentration may be to bring into operation other sources in the neighbourhood, for which the value of S_0 would normally have been too great for them to act. This gives an explanation of clustering which does not depend on any special characteristic of the sources, as it does in Seitz's model based on prismatic dislocations.

Another interesting fact is the following. The group at Cambridge, working with the electron microscope, has recently reported that only after mechanical polishing do widely spaced lines appear on which the total slip is c. 2000 A. If the polishing is purely electrolytic, the slip is much finer. The observations of Blewitt and Koehler ([29]) on the change of resistance of single crystals of ordered CuAu indicate, however, that the slip distance of the order of 1000 A is characteristic of the *interior* of lightly strained single crystals; the observations on electrolytically polished aluminium must be characteristic of the surface. I believe that a possible explanation can be found by assuming that the oxide layer on the surface is very effective in preventing dislocations from escaping. Therefore, as dislocations pile up against the surface, intense local stresses will be generated there. Now, if the surface has been polished mechanically, a surface layer will be full of dislocations. Plastic deformation can, therefore, occur involving slip-bands very closely spaced indeed. We may expect, then, that the strains set up by the piling up of dislocations from the primary slip-band can be relieved by *very local* plastic deformation of the surrounding metal as in fig. 8, perhaps without

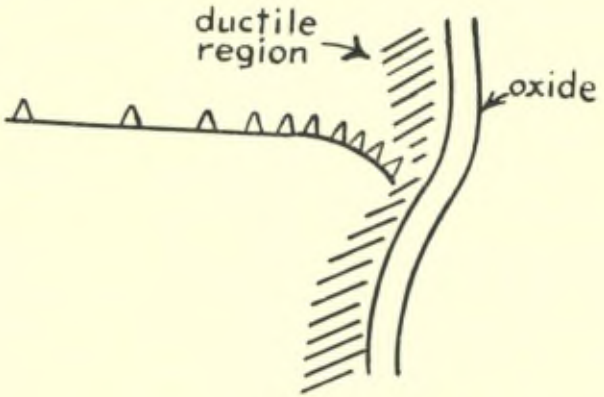

Fig. 8
Formation of slip zone on polished surface.

breaking the oxide. If on the other hand the surface layer has not been mechanically polished and is not full of dislocations, the stresses set up, before they break the oxide layer, will induce flow originating from neighbouring but more distant sources. If this hypothesis is correct, it will be very local slip bands originating in these sources which give the electrolytically polished surface its appearance.

This brings us to a consideration of the general effect of surfaces. If a single crystal were stressed uniformly, and if the surface presented no barrier to the escape of dislocations, one would expect just a few Frank-Read sources to operate, namely those with large values of x. The planes on which they would be would be too far apart for cross slip to occur — especially at low temperatures, where as has been shown by Cahn (5) [cf also Mott (2)] cross slip is not favoured. One would, then, especially at low temperatures, expect very considerable extensions to occur without work-hardening. Work-hardening would only begin when the stress became inhomogeneous owing to the effect illustrated in fig. 7. Some results of Andrade (5) on gold crystals, where no oxide film is to be expected, suggests that this is correct; slip with little or no hardening or asterisms can occur up to extensions of 30 %, and the effect is particularly marked at low temperatures.

Hardening, we believe, normally begins owing to some boundary which already exists, whether it be an oxide layer, a grain boundary or an occlusion. Once it begins new boundaries of the deformation band type are set up. Since the subsequent hardening is so little dependent on the initial conditions, a final theory will have to show that a few bands with big rotation in each gives the same hardening effect as a larger number with little rotation in each; it will also have to show that the deformation bands provide about the same resistance to glide in other planes as to glide in their own.

7. HEXAGONAL METALS

The hardening shown by hexagonal metals seems of a different type from that associated with deformation bands. If the above theory is correct, we should not expect hardening by this mechanism in the absence of cross slip; and cross slip is not to be expected in hexagonal metals.

It is possible that hardening is here connected with the formation

of vacancies, as suggested by Seitz in his report to this conference. On the other hand, it is possible that even in hexagonal crystals cross slip can occur over very short distances, so that one gets a much finer distribution of slip bands and deformation bands, the latter being not yet observed. Brown in Cambridge has however recently observed cross slip on cadmium crystals (unpublished).

REFERENCES

(1) F. C. Frank and W. T. Read, *Phys. Rev.*, **79**, p. 722 (1950).

(2) N. F. Mott, *Proc. Phys. Soc.* B, **64**, p. 729 (1951).

(3) W. M. Lomer, *Phil. Mag.* **42**, p. 1327 (1951).

(4) F. Röhm and A. Kochendörfer, *Zeits. f. Naturforschung*, **3a**, p. 648 (1948).

(5) E. N. da C. Andrade and C. Henderson, *Trans. Roy. Soc.*, **244**, p. 177 (1951).

(6) A. S. Nowick, *Phys. Rev.*, **82**, p. 551 (1951).

(7) R. Smoluchowski and H. Burgess, *Phys. Rev.*, **76**, p. 309 (1949).

(8) A. J. Bradley and A. Taylor, *Proc. Roy. Soc.*, **159**, p. 56 (1939).

(9) A. J. Bradley and G. C. Seager, *J. Inst. of Metals*, **64**, p. 1 (1939).

(10) C. Zener, *Acta Crystallographica*, **3**, p. 346 (1950).

(11) H. R. Paneth, *Phys. Rev.*, **80**, p. 708 (1950).

(12) G. J. Dienes, *J. Applied Phys.*, **21**, p. 1189 (1950).

(13) N. F. Mott, *Proc. Phys. Soc.*, **60**, p. 391 (1948).

(14) S. Smigelskas and E. O. Kirkendall, *Trans. Am. Inst. Min. Eng.*, **171**, p. 130 (1947).

(15) L. C. Correa and R. F. Mehl, *J. Metals (Metals Trans.)*, **19**, p. 155 (1951).

(16) F. Seitz, *Phys. Rev.*, **74**, p. 1505 (1948).

(17) F. Nabarro, « Bristol Conference on Strength of Solide », published by the Physical Society, p. 75 (1947).

(18) C. Herring, *J. Applied Physics*, **21**, p. 437 (1950).

(19) H. Udin, A. J. Shaler and J. Wulff, *J. Metals*, **1**, p. 186 (1949).

(20) Alexander, Kuczinski and Dawson, quoted by Herring (18).

(21) R. D. Heidenrich, and W. Shockley, « Bristol Conference on the Strength of Solids », p. 57 (1947).

(22) F. C. « Frank, Pittsburg Conference on Plastic Deformation of Crystalline Solids », **89**, published by O. N. R. (1950).

(23) N. F. Mott and F. Nabarro, « Bristol Conference on the Strength of Solids » (1947).

(24) P. W. Neurath and J. S. Koehler, *J. Applied Physics*, **22**, p. 621 (1951).

(25) A. H. Cottrell and B. A. Bilby, *Proc. Phys. Soc.*, **62A**, p. 49 (1949).

(26) E. Orowan, West of Scotland Iron and Steel Inst., p. 45 (1947).

(27) P. A. Beck, P. R. Sperry and Hu., Hsun, *J. Applied Phys.*, **21**, p. 150 (1950).

(28) A. F. Brown, *Nature*, **161**, p. 961 (1949).

(29) T. H. Blewitt and J. S. Koehler, « Pittsburg Conference on Plastic Deformation of Crystalline Solids », p. 77.

(30) R. Cahn, *J. Inst. Metals*, **18**, p. 129 (1951).

The Dynamics of Slip

by E. Orowan

Massachusetts Institute of Technology,
Cambridge, Massachusetts.

The main questions of the dynamics of slip are :

A. Why does slip occur at stresses so much below the usual theoretical estimate for the perfect crystal?

B. What determines the observed value of the yield stress, and what is the mechanism of strain hardening?

C. What is the cause of the formation of slip zones (slip bands)?

In what follows, first (in Part I) a brief critical summary of the present views will be given and then (Part II) a few new suggestions presented.

PART I

A. THE CAUSE OF THE DISCREPANCY BETWEEN THE CALCULATED AND OBSERVED VALUES OF THE YIELD STRESS

There are several difficulties in the way of attributing the discrepancy to stress concentration at random cracks after the fashion of the Griffith theory of brittle fracture.

1) All attempts to raise the yield stress by dissolving a surface layer and thus removing surface cracks seem to have failed. Whenever immersion in a solvent has an influence on the yield stress or the rate of slip under a given stress, it was shown to be due to the solution or deposition of surface impurities. Thus, surface cracks as a general cause of the discrepancy can be discounted.

2) Being due to random cracks, the strength of glassy materials shows considerable scatter : $\pm$ 20 or 25% is usual. The yield stress of crystalline materials, on the other hand, is reproducible, as a rule, within 2 or 3%. This would demand the presence of a vast number of (mainly internal) cracks. In commercial polycrystalline metals, such an abundance of cracks might perhaps be assumed;

this, however, could not be reasonably done for carefully grown single crystals whose yield stress, remarkably, seems to be more reproducible the better the crystal [1]. In contrast, the fracture stress of brittle materials becomes less reproducible the more carefully the number of cracks is reduced [2].

3) The length of cracks required for explaining the observed yield stress of soft crystals such as Zn or Cd by the elastic stress concentration theory often exceeds the diameter of the crystal.

Thermal stress fluctuations appear to be equally incapable of accounting for the discrepancy : the yield stress of metals increases only by factors of the order 2 to 4 as they are cooled from room temperature to the neighborhood of absolute zero. This might be attributed to the freezing-in of dislocations formed thermally at higher temperatures; however, the thermal formation of dislocations in an undisturbed crystal seems to be practically impossible at any temperature at which the crystal can exist. This follows from the circumstance that the elastic energy of a dislocation is of the order of 1 *e*V [3] per identity period, while the circumference of a stable dislocation loop at the observed values of the yield stress must contain hundreds of identity periods. Thus, the activation energy for the formation of a stable patch of slip must amount to hundreds of electron volts.

After the elimination of elastic stress concentrations and thermal stress fluctuations as main causes of the discrepancy, two possibilities remain. The first is to doubt the reality of the usual theoretical estimate of the yield stress. The present writer suggested that the usual assumption of a sinusoidal variation of the force between neighboring atomic planes with the amount of their tangential displacement could lead to wrong orders of magnitude if the atoms behaved as very hard spheres; in particular, the correct estimate of the yield stress must depend on the hardness of the atoms (the repulsion exponent) which does not occur at all in the conventional estimate based on the assumption of a sinusoidal variation of the shear force with the shear displacement. However, according to the calculation of Bragg and Lomer [4], the error of the conventional estimate cannot amount to more than a factor of 2 to 5 for metals of average hardness.

The dominating view at present is that the discrepancy is real and it is due to the presence of dislocations in all crystals so far observed. The assumption of a drastic defect such as is a dislocation

even in the most carefully produced crystals appears unplausible at first; however, two factors make it more acceptable. First, one or a few dislocations are sufficient to explain any amount of slip if they can multiply during deformation. Second, as it was shown by Sir Lawrence Bragg ([5]) and J. M. Burgers ([6]), boundaries between slightly disoriented regions in a nearly perfect crystal are arrays of dislocations from which slip may conceivably start.

The necessity of a multiplication (breeding) mechanism of dislocations ([7]) is a point of great importance in the theory of slip. Its only alternative would be to assume vast numbers of dislocations to be present in crystals before any plastic distortion. Since ductile metals like copper or gold can easily be extended to 100 or 1.000 times their initial length, hundreds of dislocations would have to be assumed in every atomic plane of an undistorted crystal to explain the observed shear strain without the assumption of a multiplication mechanism. This alternative, therefore, does not seem to deserve serious consideration.

Recently, Frank and Read ([8]) have discovered a mechanism by which unlimited amounts of slip can take place in a slip plane by the rotation of a dislocation anchored at the end of another dislocation not contained in the same slip plane. This « dislocation mill », however, cannot replace a multiplication mechanism, because it cannot cause slip to spread to other slip planes. In order to interpret the occurrence of slip in all planes in which it is observed without the assumption of a multiplication mechanism, one would have to postulate the presence of « dislocation mills » in a large fraction of all slip planes in a virgin crystal. This is as unlikely as the pre-existence of all dislocations observed to operate during plastic deformation. Consequently, the Frank-Read mechanism does not remove the necessity of a multiplication mechanism; in fact, it seems to demand a multiplication mechanism for dislocation mills. Such a mechanism will be suggested in the second part of this paper.

Very strong arguments for the existence of one or several multiplication mechanism are the phenomena of kinking and of the « punch-effect ». In kinking, large numbers of slip planes can operate almost simultaneously, and the slip may be confined to a narrow strip within each plane situated between the boundaries of the kink band. The amount of slip in an operative slip plane, and the spacings of the planes, are so small that, as a rule, slip markings cannot be observed microscopically. Since it would be very forced to assume

that dislocations of the required type pre-existed in all operative slip planes in the small area within the kink band, one is driven to the conclusion that a multiplication mechanism must have produced dislocations in those parts of the operative planes which lie withing the kink band, and that this mechanism must be capable of working with extreme rapidity.

The « punch-effect », observed by Jillson ([9]) and Smakula ([10]), is illustrated schematically in Fig. 1. This shows a fragment of a cylindrical Zn crystal (say, of 0.5 inch diameter), obtained from a longer rod by cleavage along the basal planes 1-1 and 2-2. If one of the basal faces (in Fig. 1 it is 1-1) is indented with a ball, the indentation runs across the basal planes and comes out as a protuberance on the opposite face 2-2. From the relatively sharp circumference of the protuberance it is evident that the indentation has propaged

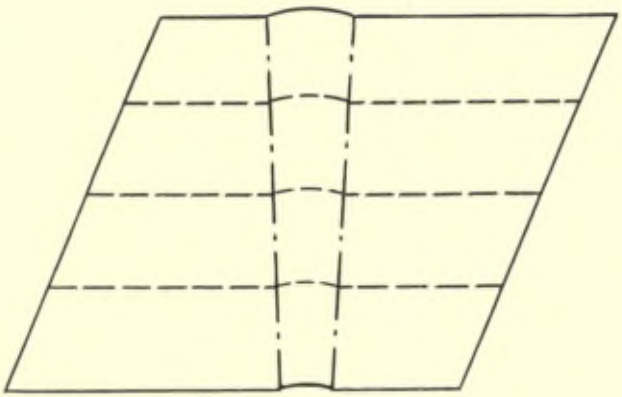

FIG. 1

along a well-defined approximately cylindrical channel in the crystal. The deformation is probably kinking, the wall of the channel representing the « plane » of kinking as indicated in Fig. 1. It may be combined with some twinning to allow the expansion of the basal planes within the indentation channel, required by their bulging. The assumption that this « punch-effect » is essentially kinking is supported by the observation that the diameter of the protuberance on face 2-2 is slightly larger than that of the indentation. Since the plane of kinking must approximately bisect the angle between the

parts of the slip plane inside and outside the kink band (Fig. 2), the indentation channel must slightly widen with increasing distance from the identation if its wall represents the plane of kinking. This agrees with the observation.

If the puch-effect is due to kinking, it represents additional support for the conclusion that there must exist a multiplication mechanism capable of acting very rapidly, not only within individual slip plane but normally to the slip planes. Beyond this, the punch-effect allows a further conclusion : it eliminates the earliest multiplication mechanism considered ([11]). This is the « reflection mechanism »; it assumes that a dislocation, arriving with high velocity at the surface of the crystal, overshoots the normal amount of slip by another identity period owing to its kinetic energy, and thus sends another dislocation back into the same slip plane. Since the deformation

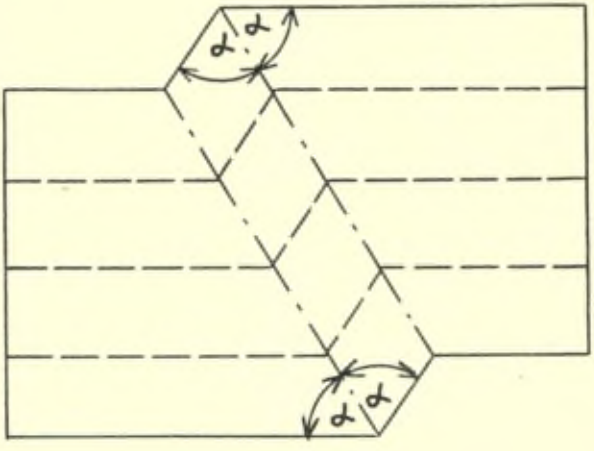

FIG. 2

in the punch-effect does not reach the surface of the crystal, the reflexion-mechanism cannot be at work.

The detailed elaboration of the dislocation theory of the discrepancy between calculated and observed yield stress must not let it forget that its foundation contains a weak point. The Griffith theory of brittle strength has received striking experimental verification when, by eliminating the worst cracks responsible for the usual

value of the tensile strength, the strength could be raised by factors up to 30 or 40. Nothing comparable with this has been observed in the case of slip. The only instance of an increase of yield stress by a treatment that may have reduced the effectiveness of dislocations was the thermal hardening of Zn and Cd crystals (12) (13) (14) in which a sharp yield point develops exceeding the usual yield stress by 30 to 50%; as soon as slip starts. the yield stress drops to its normal value. Cottrell (15) suggested that this would be a consequence of an immobilization of dislocations by impurity atoms; in fact, the phenomenon could be eliminated by avoiding traces of nitrogen in the metal. On this view, thermal hardening would be a direct proof of the weakening effect of dislocations. However, thermal hardening was never observed unless the heat treatment was preceded by a slight deformation, and this seems to contradict the view that it arises from the immobilization of dislocations by the adsorption of impurities; before deformation, there must have been fewer dislocations in the crystal and these ought to be, if anything, easier to immobilize by a given amount of impurity than the increased number of dislocations after plastic deformation. It looks rather as if the dislocations produced by the preliminary deformation acted as nuclei for the precipitation of an impurity phase which then acts as an obstacle to slip (16).

Apart from the slight increase of the yield stress in thermal hardening, no effects comparable to those supporting the Griffith theory have been observed. Even if it is granted that crystals of macroscopic size cannot be grown easily without defects, among which dislocations may occur, it is difficult to see why e. g., small globules of metals which can be produced readily down to colloidal dimensions, should contain dislocations. If they do not, they ought to be extremely hard if the current theoretical estimate of the yield stress is correct. Although no method is known for the determination of the hardness or yield stress of small globules, it would be remarkable if any abnormally high hardness had escaped accidental observation. There is a more positive evidence of lack of hardness in particles almost too small to contain dislocations : colloidal graphite, and probably also lead, are excellent lubricants. There is one series of reports (17) stating that the yield stress of certain steels tends towards the theoretically estimated order of magnitude as the deformed volume of the chip in milling decreases to submicroscopic dimensions; however, the uncertainties of the evaluation of the experiments

are too high to allow a judgment about the reality of the effect.

In view of these uncertainties it must be said that, as the weight of the theoretical superstructure increases, the need for experimental support for its foundations becomes more and more acute. Although the experiments required may be difficult, there is no reason why they should not be feasible.

B. THE FACTORS DETERMINING THE OBSERVED VALUE OF THE YIELD STRESS, AND THE MECHANISM OF STRAIN HARDENING

The primitive yield stress.

If the high value of the theoretically estimated yield stress is assumed to be real, there are several factors that may determine the low value of the yield stress. This value may represent :

1) The shear stress required for moving a free dislocation in an otherwise faultless crystal;

2) The shear stress needed for driving a dislocation through an internal stress field produced by other dislocations or by precipitated phases;

3) The shear stress for pressing the dislocation line through a gap between two obstacles, e. g., precipitated particles or centers of Frank-Read dislocation mills;

4) The critical stress at which the multiplication mechanism starts to work.

These possibilities will now be discussed briefly.

1) The first attempt at calculating the stress needed for moving a solitary dislocation was made by Peierls ([3]); the calculation was amplified by Nabarro ([3]). The main result of their considerations is that the stress needed for moving a free dislocation must depend on its length which depends strongly on delicate details of the interatomic forces, so that the approximations so far available are hardly sufficient for determining even the order of magnitude of the moving stress. There is a tendency nowadays to believe that the moving stress is much lower than the observed yield stress; this was first assumed by G. I. Taylor ([18]).

2) This assumption is the basis of Sir Geoffrey Taylor's theory

of strain hardening and of the Mott-Nabarro theory of precipitation hardening ([19]). The Taylor theory leads to the conclusion that the primitive yield stress (yield stress of the virgin crystal) is equal to the dislocation moving stress; in this respect, therefore, it coincides with the explanation mentioned under 1).

3) If there are two Frank-Read dislocation mills in a slip plane at a distance d, the shear stress needed for liberating a dislocation line connecting the two is ([22]) ([23]) :

$$\tau \approx 2G \frac{a}{d} \qquad (1)$$

where G is the shear modulus and a the atomic spacing. This is the two-dimensional analogue of the formule giving the pressure required for blowing a bubble from a nozzle of diameter d; the energy per unit length of the dislocation line corresponds to the surface energy of the bubble.

It has been suggested ([22]) that the primitive yield stress might be the stress given by eq. (1). In this case, it would be determined by the spacing of the double-mill. No suggestion has been made about the factors determining the spacing d in a virgin crystal and so the suggestion gives an element that may be used in a future theory rather than an explanation of the yield stress.

4) This possibility has apparently not been considered in the past; it will be discussed in the second part of this paper.

Strain hardening.

Until 1934, strain hardening was usually attributed to the generation of strongly disoriented and distorted regions in the crystal, i. e., of regions that are more difficult to deform than the uninjured parts of the lattice. In 1934, G. I. Taylor published his theory in which he suggested a different explanation of hardening; although this was more naive and less realistic than the old one, the elaboration of the theory contained a new element of great importance, namely, the realization that internal elastic stresses play a fundamental role in strain hardening.

Taylor assumed that the obstacles responsible for strain hardening were not generated in the course of the deformation but were present in the crystal from the beginning, in the form of walls impermeable to dislocations. He recognized that the presence of such walls did

not mean that plastic deformation was impossible; slip could start quite easily, but it was made more and more difficult by the increasing elastic resistance of the material. Thus, in Taylor's theory, strain hardening was similar to the gradually increasing force between a buffer-block and a car running against it : the real obstacle is the block which was present from the beginning, and the gradually increasing resistance to the car arises from the increasing elastic compression of the spring.

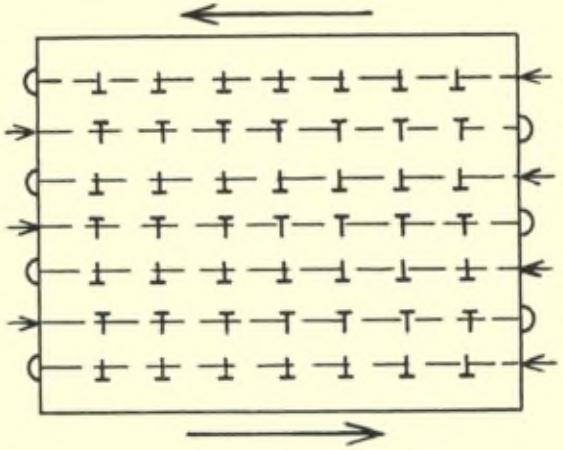

FIG. 3

The theory was elaborated quantitatively by assuming that the dislocations were distributed in the deformed crystal according to the scheme Fig. 3. The dashed horizontal lines represent operative slip planes; every second slip plane was assumed to be open to entering dislocations at its right hand end, but impenetrable at its left hand end, while the remaining operative planes behaved in the opposite manner. Consequently, every even-numbered plane accumulated, say, positive (⊥), every odd-numbered plane negative (⊤) dislocations which, according to Taylor's assumption, formed a simple rectangular lattice. Every dislocation was in the field of stress of all other dislocations; it was enclosed by the resulting internal stress in a potential trough. The yield stress Y was then the external stress needed for overcoming the internal stress barriers and lifting the dislocation out of the potential trough; by using a calculation,

made by Timpe, of the stress around a dislocation, Taylor showed that the internal stress barrier Y was inversely proportional to the spacing of the dislocations, i. e., proportional to the square root of their number N per unit of area. Obviously, the plastic strain was proportional to N; hence the yield stress Y and the plastic strain γ were connected by the relationship :

$$Y = C \sqrt{\gamma} \qquad (2)$$

which approximated the most common type of stress-strain curves. The constant C depended on the length of the slip plane over which the dislocations were free to move; if this was identified with the diameter of a single crystal or even with that of the grain in a common polycrystalline metal, however, the yield stress came out far too low. In order to obtain the observed magnitudes for Y, the free path of the dislocations had to be assumed to be of the order of 10^{-4} or 10^{-5} cm. This was identified with the spacing of a hypothetical mosaic structure, and it was assumed that the dislocations could not penetrate the block boundaries.

It would lead too far to point out the numerous conflicts of this theory with physical realities and even with logical consistency. A few may be mentioned, however. It has been shown by A.A. Griffith[23] that the assumption that dislocations can easily enter the lattice even at the lowest stresses is untenable; in reality, new dislocations cannot arise except at points of very strong stress concentrations. — If the spacing of the impermeable walls is compared with the spacing of the dislocation lattice, as a rule, the two turn out to be about equal; in other words, a mosaic block as illustrated in Fig. 3 would contain sometimes only one or two dislocations instead of the assumed extended lattice. This circumstance is serious because the dislocations in the neighboring blocks cannot belong to the same lattice; the signs of the dislocations in the same plane but on opposite sides of an impermeable wall must clearly be opposite. Finally, it was assumed in the theory that the ratio of the two spacings of the rectangular dislocation lattice remained constant, and the two spacings decreased proportionally with increasing strain. Obviously, however, this condition makes any continous increase of the dislocation density N and thus of the yield stress impossible; once a certain lattice is established, with N dislocations per unit area, the nearest geometrically similar lattice with a smaller spacing must contain

9N dislocations per unit area (because at least two new operative slip planes, a positive and a negative, have to be opened up between each two existing ones, and then the spacing in the planes must also be reduced to one-third of the previous value). Consequently, the impression that the mathematical formalism leading to eq. (2) resulted in a continuous stress-strain relationship was an illusion.

These difficulties, however, are not inherent in the fundamental idea of the theory; they arose only through the premature application of detailed mathematics to a very indeterminate physical basis. There is, of course, no doubt that the obstacles to the movement of dislocations are, as a rule, not pre-existent structural faults but injuries arising during deformation; it has also been found recently ([24]) that dislocations accumulating at obstacles do not form a lattice such as was assumed in the theory. However, the internal stress barrier due to the elastic interaction of two straight and parallel dislocations must be inversely proportional to their spacing, and the plastic strain must be approximately proportional to the density of the accumulated dislocations if dislocations cannot escape from the crystal. These simple facts may indeed be closely connected with the usual shape of stress-strain curves, and the first of them alone can account for the observed relationship between the spacing of slip bands and the yield stress (see below).

Since the publication of Taylor's theory, there has been no significant progress in the understanding of strain hardening. A new suggestion will be put forward in the second part of this paper.

C. ORIGIN AND SPACING OF SLIP ZONES (SLIP BANDS)

A remarkable feature of slip is the concentration of the deformation in thin zones, the slip zones (*). The spacings of these is much nearer to uniformity than to statistical randomness; with increasing temperature, it decreases for a given strain but remains about the same for a given value of the yield stress. Under certain circumstances [creep ([25]), oxidation hardening ([26])] slip lines can be absent, both at high and at low temperatures and rates of deformation.

(*) The more generally used name is « slip bands ». However, they are usually so thin that the word « Band » is a misnomer and may be interpreted as meaning the relatively undeformed layers between the slip zones.

There are two main possibilities for explaining this concentration of slip in narrow zones :

1) If slip is assumed to start at cracks or other relatively rare stress concentrations, the formation of slip zones must be expected since a crack can send a large number of dislocations into the crystal without any significant decrease of its stress concentration factor.

2) Slip zone formation is to be expected if a dislocation multiplication mechanism can produce new dislocations in the same slip plane, or if a Frank-Read dislocation mill is working in a plane.

The first possibility cannot be considered seriously at present, partly because slip is unlikely to originate at accidental cracks for the reasons given above, partly because it would hardly be compatible with the non-statistical distribution of the spacings of slip zones.

As regards the second possibility, both the reflexion mechanism of dislocation multiplication, and the so-called « Figure 8 » mechanism ([11]) could have led to strain concentration in slip zones; the probability that these mechanisms may play a significant role, however, does not appear to be high. Much more hopeful is the Frank-Read dislocation mill which could easily explain the formation of slip zones. The problem arising in this connection is that of the origin of dislocation mills. It cannot be assumed reasonably that the slip zones occur in positions determined by pre-existing dislocation mills; this would hardly be compatible with the non-statistical of their spacings. There is little doubt that the spacings are determined by the circumstance that significant movements of dislocations are inhibited within a certain surrounding of an existing slip zone by the stresses exerted by the dislocations accumulated in the zone (see below). If the slip zones are selected by such a mechanism, there must be far more slip planes potentially capable of developing them; and if only planes containing pre-existing dislocation mills could develop slip zones, the number of dislocation mills in a virgin crystal would have to be far higher than the observed number of slip zones. This seems very improbable, and the question arises whether dislocation mills are not formed during the plastic deformation, instead of being pre-existent. It will be shown in the second part of this paper that elementary features of slip point almost directly to a mechanism by which dislocation mills can arise and multiply during the deformation process.

The reason why slip zones are relatively regularly spaced, and why

the spacing decreases with increasing amount of plastic strain, i. e., with increasing yield stress, seems to be relatively simple. No doubt there must be large numbers of dislocations accumulated in every slip zone. This can be recognized directly from the fact that the slip line patterns on opposite sides of a deformed single crystal (e. g., of cylindrical crystals of Al, Zn, or Cd) are far from being identical as they would be if all, or most dislocations had disappeared after spreading slip over the whole slip plane. Any difference in the slip zone pattern on different sides of a single crystal, therefore, is a direct indication that many, or most, active dislocations have been trapped. Since, according to the Timpe-Koehler formula, the maximum shear stress produced by a dislocation in a parallel slip plane at distance r is :

$$\tau = \frac{Ga}{16\pi(1-\nu)} \cdot \frac{1}{r} \tag{3}$$

it is clear that no substantial movement of dislocations can take place within a distance :

$$d \approx \frac{Ga}{16\pi(1-\nu)} \frac{1}{\tau} \tag{3a}$$

of the slip zone if the applied resolved shear stress is Y. The minimum spacing of the slip zones, therefore, should be approximately the quantity d as given by eq. (3*a*). Experimental observations agree with this well enough; in a few cases, the constant of the inverse proportionality between Y and d has been found to be greater than the value in (3), but these measurements were made under creep conditions where unknown factors may have influenced the spacings.

It is seen that eq. (3*a*) and the Taylor theory of strain hardening are based on the same property of the elastic field around dislocations; in the present case, however, the order of magnitude of the effective spacing of the dislocations is directly observed, while in the Taylor theory it was a parameter of the theory not assumed to be susceptible of direct observation.

PART II

A. THE ORIGIN OF DISLOCATION MILLS

The Frank-Read dislocation mill arises when two edge dislocations having the same slip vector but lying in different slip lines meet. A simple way of producing this would be to press a rectangular punch into a crystal face perpendicular to the slip direction to the depth of one identity period (Fig. 4). Let the wavy rectangle inside the crystal represent the dislocation loop that marks the limit to

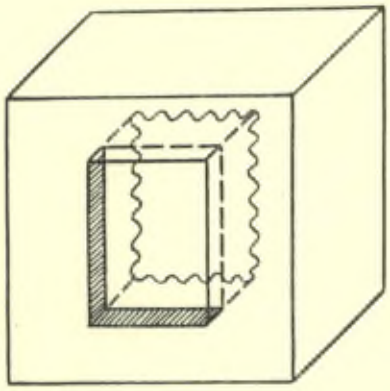

FIG. 4

which the slip caused by the punch has penetrated. The loop consists of two pairs of edge dislocations in two pairs of parallel slip planes; if one side of the dislocation rectangle is kept fixed, the adjoining sides can rotate around the points of intersection with the fixed side, and every full rotation (by 2) produces slip by one interatomic spacing in their slip planes. Clearly, the presence of two adjoining sides of the rectangle in Fig. 4 is sufficient for the mechanism to work; either of these sides may be kept fixed, and the other can then rotate in its own slip plane. Thus, the simplest type of dislocation mill is represented by Fig. 5; it can be regarded as arising from the indentation of a crystal face with a rectangular punch as above, but so that only two edges of the punch fall upon the crystal face.

Obviously, the indentation process just described cannot occur in natural or artificial crystals except as a rare accident, and the production of dislocation mills by irregularities of crystal growth

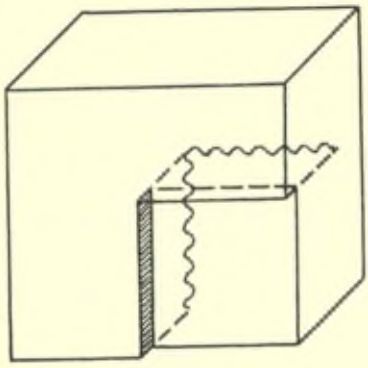

FIG. 5

does not seem to be much more likely. However, a phenomenon which is almost always observed during slip can easily be seen to lead to the creation of just those intersecting pairs of dislocations in different planes with a common slip direction which constitute a dislocation mill if one of the dislocations is kept fixed or at least retarded relative to the other. This is the phenomenon that has been called by Mathewson, Hibbard, and Maddin « cross slip ». It consists in slip branching off from the main slip plane into a subsidiary plane at an angle to it, the slip direction being the same in both planes. The typical appearance of the slip lines is shown schematically in Fig. 6 where 1′—1 and 2—2′ are the main slip planes, i. e., those in which the resolved shear stress is a maximum, and 1—2 is the subsidiary plane. As a rule, the subsidiary slip plane is only a short connection between two parallel main slip planes; the transition between the two kinds of slip planes is not a sharp angle but usually curved or finely stepped. At first sight, it may surprise that slip occurs in a plane in which the resolved shear stress, calculated in the usual way from the applied forces and the orientation of the crystal, is not a maximum. This, however, seems to have a trivial explanation. If slip commenced in the planes 1′—1 and 2—2′ in Fig. 6 independently and progressed towards the plane 1—2, the shear stress in

1—2, before slip started in this plane, must have reached a value far higher than that calculated with the usual formulae in which uniform distribution of stress and strain is assumed. The plane 1—2 therefore may have been, and probably was, the plane of the highest resolved shear stress in the region where the planes 1′—1 and 2—2′ met, at least before « cross » slip occurred in it ([27]).

Obviously, the planes active in cross slip have the same relative position and slip direction as the slip planes in Figs. 4 and 5; if, therefore, the slip processes in Fig. 6 do not occur simultaneously along every line perpendicular to the plane of the figure, they give rise to dislocations running along the broken line 1′—1—2—2′

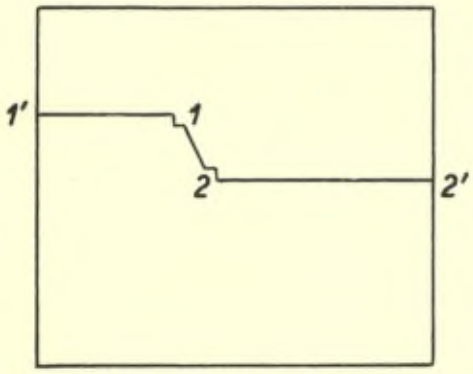

FIG. 6

which have the typical configuration of two dislocation mills at the points 1 and 2. All that is needed for the mill to start working is a retardation of the dislocation 1—2 relative to 1′—1 or 2—2′, or vice versa. If cross slip arises in the way just explained, however, such a retardation is bound to occur. The resolved shear stress in the subsidiary slip plane 1—2 can reach the critical yield value only so long as more slip has taken place along 1′—1 and 2—2′ than along 1—2; in particular, before slip starts in 1—2. After slip has started in it, the shear stress drops while it is always near the yield value in the main slip planes. There is a tendency, therefore, for slip in the subsidiary plane to progress more slowly than in the main slip planes. If this is so, all conditions of a dislocation mill are present.

Naturally, the amount of slip in the subsidiary plane need not be large enough to be microscopically observable; slip by one or two interatomic spacings, which escapes all observation, already gives dislocation mills in the two main slip planes 1′—1 and 2—2′.

The conclusion is that cross slip, however small in magnitude, must in all probability lead to the formation of dislocation mills in the operative main slip planes; in fact, cross slip would not produce dislocation mills only in the very unlikely case where slip in the main and subsidiary planes progressed synchronously in the slip direction. This case is purely hypothetical if the explanation of cross slip as given above is correct, because the yield stress in the subsidiary plane can then only be reached if slip in this plane is retarded.

B. STRAIN HARDENING

Every departure from straightness in a slip line must mean the presence of cross slip in the sense explained above, and, unless slip on the main and subsidiary planes is perfectly synchronous, cross slip implies all elements of a dislocation mill to be present. Consequently, the continued formation of dislocation mills in the slip zones during plastic deformation must be a very general feature of slip. How do the dislocation mills of a slip zone interfere with one another during the deformation? This is a particularly interesting subject for study; in this context, however, only a few simple points should be touched, without detailed explanation. The fixed arm (the « axis ») of a mill is a dislocation that may be positive or negative with respect to the slip direction and an arbitrarily fixed direction parallel to the fixed arm; correspondingly, the dislocation mills of a slip plane or slip zone are also either positive or negative. An easy consideration shows that the mobile arm of the mill is an edge dislocation only when it is normal to the slip direction, when it rotates by 90° into the slip direction, it becomes a screw dislocation, and after 180° rotation it is a pure edge dislocation again, but with an opposite sign. Consider now two mills in a plane, and let the mobile dislocations be parallel to the line connecting the centers. If the mills are of opposite signs and the mobile arms point in the same direction, they annihilate each other except on the line between the centers (Fig. 7*a*); this is the position of minimum energy in the absence of an applied stress. This case is realized in Fig. 4 where each hori-

zontal side of the dislocation rectangle represents the surviving part of the mobile arms of two mills of opposite sign, with their centers in the adjoining corners of the rectangle. If the mills are of the same sign, the position of minimum energy occurs when their

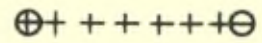

FIG. 7a

FIG. 7b

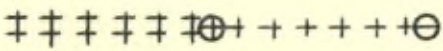

FIG. 7c

Slip direction vertical

mobile arms are antiparallel and, as before, parallel to the line joining the centers; in this case, the part of the connecting line between the centers contains no dislocation, while the remaining parts, between each of the centers and infinity are edge dislocations of opposite sign (Fig. 7*b*). If one of the mobile arms rotates by 180°, the configuration shown in Fig. 7*c* arises; this is of high energy, since the line marked with double crosses is a double dislocation. If a shear stress is applied, therefore, the two dislocations in Fig. 7*b* will rotate in the same sense, as indicated by the arrows, and they will tend to remain approximately parallel. After 180° rotation, they arrive at the initial configuration with the signs of the dislocations interchanged. On the other hand, if a shear stress is applied in the case shown by Fig. 7*a* (mills of opposite sign), the dislocation line

connecting the centers will bulge out and the bulge increases with increasing stress until it reaches a critical size. After this, the bulge suddenly increases, whips round and returns from the opposite side of the line connecting the centers into its initial position, as described by Frank and Read. As already mentioned, the process is analogous to the blowing of a bubble in a liquid from a nozzle; the present case is two-dimensional, the energy of the dislocation per unit length plays the role of the surface energy, and the shear stress that of the pressure. An easy consideration shows that the critical shear stress required for making the dislocation bulge whip around is ([20]) ([21]) ([8]).

$$\tau \approx 2G \frac{a}{d} \qquad (1)$$

where d is the distance between the two mills of opposite sign, G the shear modulus, and a the atomic spacing in the slip direction.

In the case of mills of equal sign, no corresponding resistance to the movement of the dislocations occurs so long as both arms are free to rotate. This is not generally the case. If, e. g., one arm is near surface or a grain boundary, it has a position of minimum energy when it is perpendicular to the surface (Fig. 8); it cannot rotate from this position without a large increase of its energy due to the necessary increase of its length (*). In such cases, the immobilized mill acts like a mill of opposite sign, and the rotating arms of other mills in the same plane have to be forced past it by bulging,

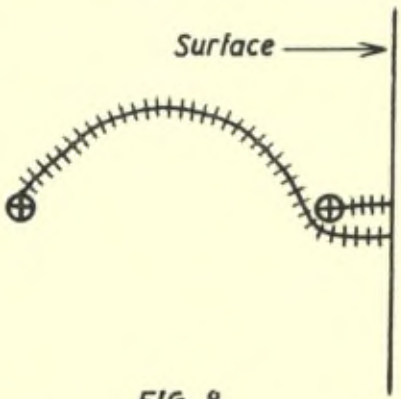

FIG. 8

(*) This immobility of mills near the surface makes one think of the spectacular increase of the plastic deformability of ionic crystals when they are progressively dissolved during the deformation process.

as indicated in Fig. 8. The shear stress required for this is of the order given by eq. (1).

From the points that have emerged from the discussion so far, a simple mechanism of strain hardening can be constructed which can account for several observed features of the process. Naturally, this may not be the only, or even the only important, mechanism of strain hardening; the relative importance of the various ways in which hardening can arise must be recognized from experiments. The present mechanism would work in the following manner :

1) When slip starts, it is accompanied by a certain amount of cross slip. As a rule, this is not observable microscopically owing to its small amount; however, even cross slip by one interatomic spacing, if arrested or retarded relatively to the main slip, represents a dislocation mill which can develop the main slip plane to a slip zone.

2) As cross slip continues at various points and the number of dislocation mills in the slip zone increases, the working of the mills in a slip plane or slip zone needs increasing stress owing to their mutual interference. If the number of the mills per unit area of the slip zone is N, their average distance is proportional to $1/\sqrt{N}$, and the shear stress required for driving the mills, according to eq. (1), is :

$$\tau = \text{const.} \sqrt{N} \tag{4}$$

The simplest assumption concerning the increase of N is that it is proportional to the strain γ; this would lead to :

$$\tau = Y = \text{const.} \sqrt{\gamma} \tag{5}$$

i. e., to a stress-strain curve of parabolic type, as in the theory of G. I. Taylor.

3) New slip zones cannot arise within a distance from an active slip zone given by eq. (3*a*). If the largest spacing between slip zones at a given moment is d_m, the condition for the creation of a new zone inside this spacing is that the shear stress must rise to the value τ determined by :

$$\tau \approx \frac{Ga}{8\pi(1-\nu)} \cdot \frac{1}{d_m} \cdot \tag{3b}$$

Accordingly, new slip zones appear in addition to slip continuing in some or all of the existing ones as the individual yield stress of the

active zones rises to a value at which (3*b*) is satisfied for one of the most widely spaced active zones.

4) When a new slip zone arises, it contains at first very few mobile dislocations which, therefore, can move easily. In other words, the activation energy per unit of shear strain is small in a newly opened up zone while it is high in an old zone with its densely entangled dislocations. Consequently,

a) if the temperature is high and/or the rate of deformation low, large amounts of slip develop in an active zone before new zones need be opened up; conversely, if the temperature is low or the strain rate high, the provision of activation energy for the old zones is difficult and new zones open up after relatively small strain in the old ones. — This is the general law observed in deformation by slip : at low temperatures and/or high strain rate, the zones are closely spaced and the strain per zone small, and vice versa.

b) Slip in a newly opened up zone is relatively rapid, while the old zones seem to be immobile and only careful observation can show that they are actually in slow movement. Creep at constant stress, in particular, used to progress mainly within the existing slip zones.

5) If the crystal is precipitation-hardened, relatively widely spaced slip zones may not arise because the stress needed for moving a dislocation over a plane is already so high that it can produce quite closely spaced slip planes before there is any substantial slip in one of them. In fact, since very closely packed slip planes very sparsely populated with dislocations do not behave as slip zones, and do not inhibit further slip in clearly defined surrounding region, any trace of slip zone formation may be absent. This may be the reason why in deformed copper with 0.6% Al., in which a surface layer has been oxidation hardened, the slip zones abruptly disappear at the boundary of the oxidation hardened layer and the deformation in this layer shows no trace of slip zone formation ([26]).

It may be added that a newly formed slip zone between two existing ones is provided from the beginning with about as many dislocation mills as the neighboring old zones : every mill axis connecting the old zones is cut by the new one and, as slip occurs in the new zone, it yields two dislocation mills of opposite sign. Since the number of the mills in an old zone is twice the number of mill axes on either side, the number of mills in the new zone will be about equal to that in the old ones. The new mills, however, are neither working at

first nor can they interfere much with the movement of dislocations. Until the amount of slip in the new zone has become considerable, the pairs of mills arising from the cutting of an existing axis are too closely spaced to be able to work, according to eq. (1). On the other hand, they cannot hinder too severely the movement of dislocations over them.

The propagation of slip to new slip planes.

Since the probability of Frank-Read dislocation mills arising during the growth of a crystal must be small, it seems that the only way known at present in which they are bound to be produced in quantities is that described in the preceding section (as a consequence of cross-slip). If, on the other hand, cross slip could only arise in the way just described, as a slip bridging two independent slip processes in different parallel planes, the formation of dislocation mills in these planes could not increase the number of the active slip planes, but only the magnitude of slip in them. Since the phenomenon of kinking shows that slip can spread extremely rapidly to a vast number of slip planes, without even extending over more than a fraction of their area, it is clear that a dislocation multiplication mechanism, different from the Frank-Read mechanism, must be at work.

Such a multiplication mechanism would be available if cross slip could arise from the deflection of the slip process into the subsidiary, and from this into another main, slip plane; in this way, a single dislocation in one plane would give at once two dislocation mills in two different main slip planes. Such a process could arise if the shear stress in the subsidiary slip plane, in front of the moving screw dislocation, would be raised to a high value by a thermal stress fluctuation; however, a more detailed consideration shows that the probability of such as event is very low because the slip is not deflected unless the shear stress in the subsidiary plane is raised to its high value over a sufficiently large area.

The next simplest possibility for a deflection of the slip process into a plane at an angle to its previous slip plane would be given if the shear stress in front of a running dislocation assumed its maximum value in planes inclined to the slip plane. At first sight, this would seem very improbable; the well known solutions of the stress distribution around a thin elliptical crack show that the maximum

tensile stress occurs in the plane of the crack if an external tension perpendicular to this plane is applied, and similarly the maximum shear stress in front of a dislocation occurs in the slip plane. If these solutions were generally valid, there could be no inherent

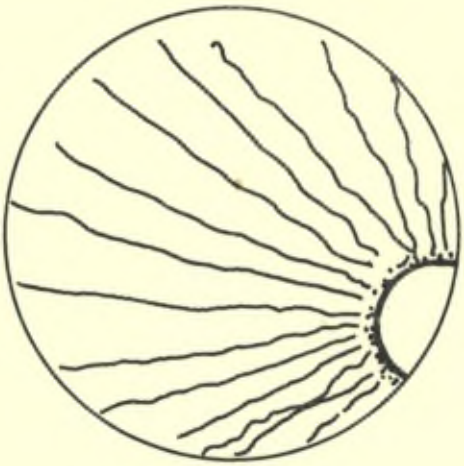

FIG. 9

tendency of a tensile crack or a slip process lo leave its own plane. However, a very weighty observation shows that such a tendency must be present under certain circumstances. This refers to the well known general phenomenon of specular fracture of brittle materials, glasses as well as crystals. If a glass rod is broken in tension, the surface of fracture is as indicated schematically in Fig. 9. It is smooth like a mirror (*) within a circle the center of which is the point where fracture has started (usually at the surface). At the circumference of this circle the surface begins to be matt and then rough; finally it goes over into coarse waves radiating from the origin of the fracture. The obvious interpretation of this phenomenon is that, when the crack has propagated to the circumference of the specular circle, it acquires a tendency to deviate from its plane. At different points of the circumference the deviation takes place in different directions; hence the waviness of the surface outside the circle. In some cases, the deviation occurs simultaneously upwards and downwards from

(*) Hence the name « specular » fracture.

the initial horizontal plane, so that a curved wedge falls out between the main fragments of the rod.

The tendency of the crack to be deflected from its plane might be attributed to the circumstance that, once its propagation starts, the rod is not under uniform tension but in tension combined with bending which may influence the stress distribution. That this is not the cause of specular fracture can be seen from the following simple experiment. A soda glass tube of about 6 mm diameter and

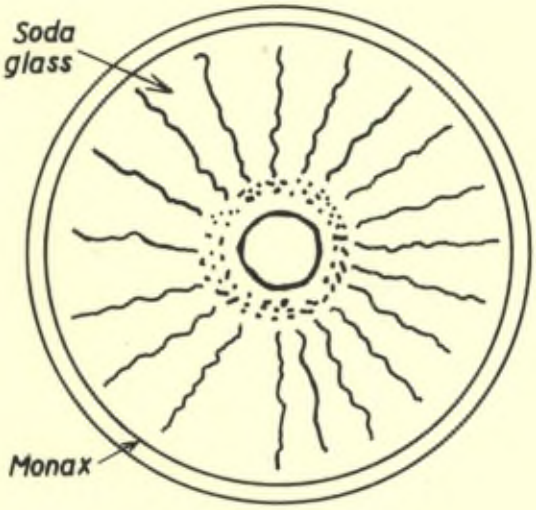

FIG. 10

a very thin capillary bore was coated in the flame with a very thin layer of « Monax » glass, the coefficient of thermal expansion of which is intermediate between soda and Pyrex glass. Within times ranging between minutes and weeks after the preparation of the coated capillary, this broke spontaneously under the internal stress due to the differential contraction of the two components, and the surface of fracture was of the type shown in Fig. 10. It showed a typical specular fracture, but the specular circle was concentric with the tube axis (since the soda glass was under tension, the fractures started at the wall of the capillary bore). Owing to the axial symmetry, there was no proper bending component present to which the tendency of the crack to be deflected could be attributed. The conclusion is,

then, that the crack acquires this tendency when it reaches a certain velocity; that is to say, the stress distribution in front of the running crack must differ from the static case in that the plane of maximum tensile stress is no longer the plane of the crack if this has reached a large enough velocity. This is strikingly confirmed by experiments on the fracture of cellophane sheets. If a cellophane sheet is put under tension after its center has been provided with a « crack » cut perpendicular to the tension by means of a pocket knife (Fig. 11)

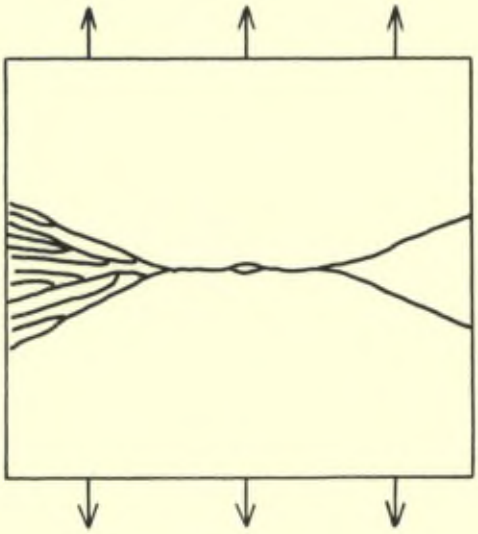

FIG. 11

the crack starts its propagation slowly, with abundant plastic deformation in a narrow zone at its edges which shows up strikingly between crossed polarizers; the direction of its propagation is exactly perpendicular to that of the tension. If the sheet is fairly humid, this type of propagation persists to the end; otherwise, however, it changes over at a critical crack length to a brittle type of fracture, with no plastic deformation at the edges. This is connected with a very rapid (practically instanteneous) propagation of the crack which now does not run perpendicularly to the tension but starts branching upwards and downwards in a very regular and somewhat spectacular manner. If the sheet is dry and the initial crack short, the tension needed for fracture is high, and in this case the crack branches dozens

of times, subdividing a triangular part of the sheet next to the initial crack into narrow strips (Fig. 11). This, clearly, is the two-dimensional manifestation of the phenomenon of specular fracture, and it shows strikingly that, with increasing velocity, the crack acquires a tendency to deviate from the direction of maximum applied tension which is the initial direction of its propagation.

A similar behavior of dislocations can be deduced from studies of the structure of moving dislocations made by Frenkel and Kontorova ([28]) and, independently, by Frank ([29]). It was found that the effective length of a running screw dislocation decreased with the velocity according to the quasi-relativistic relationship :

$$\Lambda = \Lambda_0 \sqrt{1 - v^2/v^2_{max}}; \qquad (6)$$

edge dislocations obeyed the same relationship approximately. Consider the edge dislocation first. At zero velocity, the maximum shear stress occurs in front of the dislocation in its slip plane. As the velocity increases, the dislocation contracts; since the material has to extend on one side, contract on the other side of the slip plane by one-half of the slip vector within the effective length of the dislocation, the tensile and compressive stresses in the slip direction in the dislocation must increase with the velocity of the dislocation. Since these stresses produce shear stresses in the planes intersecting the slip plane (the highest in the plane at 45° to the slip plane), the shear stress in the two 45° planes must increase with the velocity of the dislocation and tend towards infinity as the velocity approaches the limiting velocity of the dislocation. Since the « static » shear stress in the slip plane does not change substantially, the plane of maximum shear stress must be at 45° to it when the limiting velocity is nearly reached. Thus, dislocations must also have a tendency to leave their slip plane if their velocity becomes sufficiently high.

This conclusion has been verified by Mrs. E. H. Yoffe-Mann ([30]), who started from Eshelby's ([31]) solution of the problem of the uniformly moving dislocation and demonstrated that, in fact, the plane of maximum shear stress is the slip plane only so long as the velocity remains below about half of the Rayleigh velocity of the surface waves; for higher velocities, the plane of maximum shear stress swings out of the slip plane and approaches 45° as the velocity converges towards the limiting value which is the Rayliegh velocity. Mrs. Yoffe-Mann carried out a similar investigation of the problem

of the rapidly propagating tensile crack, and the results here were quite analogous.

There can be no doubt that the velocities of cracks in brittle materials can easily approach the theoretical limit. In the case of slip, however, an investigation by Leibfried ([32]) has led to the conclusion that dislocations cannot reach more than about 1/10 of the velocity of sound under usual conditions. Since half of the Rayleigh velocity is roughly one-quarter of the velocity of sound, the maximum velocity of dislocations in Leibfried's opinion is about one-half to one-third of the minimum required for a tendency of slip to leave its plane. This is a narrow margin, particularly in view of the circumstance that Leibfried's value is based on an order-of-magnitude estimate of the scattering cross section of a dislocation for elastic waves. Since the investigation contains several assumptions that, although reasonable, are nevertheless open to doubt, it seems that the inaccuracy of the result is greater than the narrow margin that stands between it and the possibility of the deflection of dislocations into an inclined slip plane.

The conditions for deflection of screw dislocations are somewhat more complicated than those for edge dislocations because here the maximum shear stress for a fast running dislocation must occur in a plane that does not intersect the slip plane in the dislocation line. However, as the limiting velocity is approached, the plane of maximum shear stress is bound to approach the plane that intersects the slip plane perpendicularly in the dislocation line itself; this follows directly from the quasi-relativistic contraction of the dislocation. Thus, a rapidly running screw dislocation in a cubic face centered metal will have a tendency to swing into the other octahedral plane of the same slip direction, in other words, if screw dislocations can reach high enough velocities, there must be a tendency for cross slip to arise without the necessity of independent slip started previously in two parallel slip planes, as described above. In this case, the deflection effect represents a mechanism for the production of dislocation mills.

Obviously, any tendency of either edge or screw dislocations to be deflected into another slip plane at high velocities represents a multiplication mechanism for dislocations (in addition to the mill production mechanism just mentioned). The deflection will take place only over a limited length of the dislocation front, so that only a tongue of slip of limited width swings into the inclined slip

plane. Since this is a subsidiary plane in which the applied shear stress is lower than in the main slip plane, the deflected slip will have an increased tendency to swing back into another main slip plane, parallel to the first one. Ultimately, slip must extend over the entire area of both main slip planes, while there may remain a bridge between them over which the slip process stepped from the one to the other. This bridge may consist of a slipped strip of the subsidiary plane, bounded by two screw dislocations at its sides, and two « corner dislocations » where the strip intersects the two main slip planes.

The primitive yield stress.

If such a deflection mechanism operates, therefore, it can produce all that is needed for explaining both the concentration of slip in slip zones, and the rapid propagation of slip from one plane to the next, as observed in kinking. In addition, it may conceivably give the answer to one of the most interesting and so far most unapproachable questions of slip : i. e., the question of what determines the primitive yield stress (the yield stress of the virgin crystal). If the experiments of Chalmers on « microcreep » are confirmed(*), they mean that very slight amounts of deformation can occur at stresses somewhat below the yield stress; the latter is merely the stress at which the amount of slip increases very suddenly. It may be that this rapid increase is due to the start of a multiplication mechanism which cannot work at lower stresses. If the multiplication mechanism is that of slip-deflection as just described, there must be a limiting stress below which it cannot work, namely, the stress at which the dislocations reach the critical velocity required for swinging into a subsidiary slip plane. At lower stresses, they take up a stationary velocity below the critical value, representing equilibrium between the work done by the applied stress and the elastic waves scattered as the dislocation progresses. Dislocations already present in the crystal could move at subcritical stresses and produce the phenomenon of micro-creep, if this is real; when the critical stress and thus the critical velocity of the dislocations is reached, the multiplication mechanism, including possibly a

(*) The phenomenon of " micro-creep " may possibly be due to the unavoidable excentricity of gripping the specimen in the testing apparatus.

mill-production mechanism, starts to work and produce the phenomenon of yielding.

SUMMARY

1) There is a curious lack of experimental evidence for the reality of the high theoretical estimate of the yield stress of crystals; new experiments for clearing up this point would be desirable.

2) If the reality of the discrepancy between calculated and observed yield stress is accepted, the only plausible way of accounting for it seems to be at present the assumption that every macroscopic crystal or polycrystalline metal contains at least a few dislocations, and that a mechanism for the multiplication of dislocations exists.

3) The Frank-Read « dislocation mill » alone cannot act as a multiplication mechanism spreading slip to other planes, as is observed in kinking; nor can the presence of a sufficient number of dislocation mills in an undeformed crystal be assumed. Consequently, there is need for a multiplication mechanism for dislocations capable of spreading slip to other planes, and a mechanism for producing dislocation mills. Both mechanisms could be replaced by one producing mills in slip planes not yet in operation.

4) Cross slip, as observed microscopically, is bound to produce dislocation mills in the two main slip planes, unless slip in the main and subsidiary planes progress exactly synchronously. If, however, cross slip arises from two independent slip processes in different planes being bridged by slip in an oblique subsidiary plane, mills can arise only in slip planes that are already in operation.

5) If dislocations can acquire velocities of the order of magnitude of the Rayleigh velocity, they must have at these velocities a tendency to swing into oblique slip planes. This would give both a multiplication mechanism of dislocations, and a mechanism for creating cross slip and thus dislocation mills in not yet operative slip planes.

The deflection effect is completely analogous to a similar effect occurring in the propagation of tensile cracks which is responsible for the characteristic features of brittle fracture (specular fracture).

6) The primitive yield stress may be the stress at which dislocations are accelerated to the critical velocity needed for the deflection mechanism of multiplication to act.

7) Strain hardening in single crystals seems to include two different effects. First, an increase of the operating stress of the dislocation mills in the slip zones, due to the increase of the number of mills with the slip, and the consequent decreases of the spacing of the obstacles between which the dislocations must be squeezed through by the applied stress. Second, the increase of the stress required for opening up new slip zones which is inversely proportional to the largest slip zone spacing present, and thus increases with the existing number of slip zones.

8) The picture of strain hardening just given leads, with the simplest assumptions, to stress-strain curves of simple parabolic type; it explains the decrease of the spacing of slip zones for a given strain with decreasing temperature and/or increasing rate of deformation; and it explains why strain hardening is much less rapid in hexagonal metals in which the available subsidiary slip planes have a higher yield stress than the basal plane, so that the number of cross-slips and thus the number of dislocation mills produced per unit of shear in the slip zones is less than in cubic metals.

REFERENCES

(1) E. N. da C. Andrade, and R. Roscoe, *Proc. Phys. Soc.*, London, **49,** p. 152. (1937),

(2) E. Orowan, *Zeits. f. Phys.*, **82** ,p. 235 (1933).

(3) R. Peierls, *Proc. Phys. Soc.*, London, **52,** p. 34 (1940); F. R. N. Nabarro, *Proc. Phys. Soc.*, London, **59,** p. 256 (1947).

(4) Sir Lawrence Bragg, and W. M. Lower, *Proc. Roy.Soc.*, *A***196,** p. 171 (1949); W. M. Lower, *ibid.*, p. 182.

(5) W. L. Bragg, *Proc. Phys. Soc.*, London, **52,** pp. 54, 105 (1940).

(6) J. M. Burgers, *Proc. Phys. Soc.*, London, **52,** p. 23 (1940).

(7) E. Orowan, *Zeits. f. Phys.*, **89,** p. 634 (1934).

(8) F. C. Frank and W. T. Read, *Phys. Rev.*, **79,** p. 722 (1950).

(9) O. C. Jillson, *Transaction A.I.M.E.*, **188,** p. 1009 (1950).

(10)

(11) F. C. Frank, Rep. Conf. on Strength of Solids, *Phys. Soc.*, London, p. 46 (1948); E. Orowan, Diploma Thesis, *Techn. Univ.*, Berlin-Charlottenburg, Feb., (1929), unpublished.

(12) E. Orowan, *Zeits. f. Phys.*, **89,** p. 614 (1934); *Proc. Phys. Soc.*, London, **52,** p. 8 (1940).

(13) C. L. Smith, *Nature*, **160,** p. 466 (1947).

(14) H. L. Wain, and A. H. Cottrell, *Proc. Phys. Soc.*, London, **63,** p. 339 (1950).

(15) A. H. Cottrell, Rep. Conf. on Strength of Solids, *Phys. Soc.*, London, p. 30 (1948).

(16) C. A. Edwards, D. L. Phillips and Y. H. Liu, *J. Iron Steel Inst.*, London, **147** (1943).

(17) W. R. Backer and M. C. Shaw, *Journ. Appl. Mech.*, **51**-SA-9.

(18) G. I. Taylor, *Proc. Roy. Soc.*, *A***145,** pp. 362-388 (1934).

(19) N. F. Mott and F. R. N. Nabarro, *Proc. Phys. Soc.*, London, **52,** p. 86 (1940).

(20) F. R. N. Nabarro, Symp. on Internal Stresses, *Inst. of Metals*, London, p. 248 (1947-1948).

(21) E. Orowan, Symp. on Internal Stresses, *Inst. of Metals*, London, p. 451 (1947-1948).

(22) N. F. Mott, N. R. C. Conf. on Imperfections and Grain Boundaries in Crystals; Pocono Manor, Oct. 1940 (in press).

(23) A. A. Griffith,

(24) J. D. Eshelby, F. C. Frank and F. R. N. Babarro, *Phil. Mag.*, **42,** p. 351 (1951).

(25) D. Hanson and J. Wheeler, *J. Inst. Metals*, **45,** p. 229 (1931).

(26) G. C. Smith and Dewhirst, *Research* (1950).

(27) E. Orowan, N. R. C. Conf. on Imperfections and Grain Boundaries in Crystals; Pocono Manor, Oct. 1950 (in press).

(28) J. Frenkel and T. Kontorova, *Phys. Zs. der Sovietunion*, **13,** p. 1 (1938).

(29) F. C. Frank, *Proc. Phys. Soc.*, London, **62,** p. 131 (1949).

(30) Mrs. E. H. Yoffe, to be published.

(31) J. D. Eshelby, *Proc. Phys. Soc.*, **62,** p. 307 (1949).

(32) G. Liebfried, *Zeits. f. Phys.*, **127,** p. 344 (1950).

Discussion des rapports de MM. Mott et Orowan

M. Kramers. — Can the development of cross-slip be watched under one miscroscope?

M. Orowan (Reply to Kramers). — Successive stages in cross-slip can be clearly seen in the papers of Yamaguchi published in 1928.

M. Dehlinger. — Für die Entstehung der Versetzungen sind bisher nur Modelle betrachtet worden, bei welchen die elastische Wechselwirkung eine Rolle spielt, die heute verhältnismässig gut berechnet werden kann. Dagegen wird die Mitwirkung der thermischen Schwingungen des Gitters kaum in Betracht gezogen, weil hiefür bisher kaum zuverlassige theoretische Grundlagen vorhanden waren. Experimentell ist aber der Einfluss der Temperatur auf die kritische Schubfestigkeit von Einkristallen deutlich zu sehen. Kochendörfer hat alle Messungen dieser Art zusammengestellt. Danach zeigt sich, dass der Temperaturverlauf durch die Differenz zweier Boltmann-Funktionen nach Becker-Orowan gut wiedergegeben wird. Wenn man also Versetzungswellen hat, wie sie soeben von Herrn Orowan beschrieben wurden, so wird man nicht nur deren Dämpfung zu beträchten haben. Es wird auch möglich sein, dass Verzetzungsswellen durch thermische Schwingungen verstärkt werden, oder dass Versetzungen, die an Gitterstörungen hängen geblieben sind, durch thermische Schwingungen weiter getrieben werden, d. h. dort neu antstehen.

Viel deutlicher sind diese Verhältnisse zu überblicken bei der Transformation einer allotropen Modifikation in eine andere durch Gleitvorgänge (Martensit, Au-Ca). Diese Vogänge gehen durch das ungestörte Gitter mit grösserer oder kleinerer Geschwindigkeit hindruch, bleiben aber an Gitterströrungen hängen. Auch hier handelt es sich um eine spezielle Art von Versetzungen.

M. Shockley. — In connection with professor Mott's discussion on the nature of slip bands and processes of multiplication of dislocations, I should like to refer to some observations of R. D. Heidenreich reported in Heidenreich and Shockley (1948). In brief by using Kikuchi lines as a measure of crystal perfection, Heidenreich established that intermittent stresses of high amplitude applied to an aluminium single crystal *destroyed perfection on the surface and not in the interior*. This was taken to imply that under these conditions *generation of dislocations occurred on the surface and not in the interior*. The experiments were preliminary and it was hoped that these publications would provoke research elsewhere. It is still to be hoped that such research will be undertaken, since the experiments, if proved sound and reproducible, must be taken account of in any theory of plastic deformation.

M. Mott. — I am surprised that Orowan considers there are not enough dislocations in crystals — beryl grown under geological conditions is a different case. A Frank-Read source is nothing unusual but is the commonest kind of section of dislocation.

M. Orowan. — Would you suggest that in the beryl or paraffin crystals shown by Frank only one of many dislocations present is visible.

M. Mott. — In the paraffin crystals they are probably all visible; I would suggest that if these crystals could be strained they would show only a few slip bands.

M. Orowan. — Guinier and Renniger have shown that some crystals are as perfect as can be shown by X-rays, yet the yield stress is not appreciably less. It seems most improbable that the yield stress is essentially determined by the dislocation spacing in the crystal, since it is not observed to depend markedly on the conditions of growth.

M. Mott. — It is not the spacing which determines the yield, but the length of the dislocation which lies in a given slip-plane. What determines this we do not know.

M. Frank. — If, as suggested by Orowan, an edge dislocation

is to be deflected out of its plane it must lave a dislocation at the point where it first deviated. This will necessitate a great deal of energy, and if we assume it will need the same energy, as the original one had, it will necessitate a velocity of V/C = 0.86.

I used to believe that dynamic multiplication of dislocations must occur, but besides the theoretical arguments which have been advanced against it, there have been several recent experimental attempts to find evidence of this, with only negative results. There is no conclusive decision yet, but for the present I prefer to explore the possibility of interpreting all the observed phenomena in terms of slow motions of dislocations, in ways of the kind described in professor Mott's paper.

M. Bragg. — Why is the deformation band so beautifully plane if the occurrence of the jamming is such a random process as you have described.

M. Mott. — The suggestion is that the first ones jamming encourage the others to do so in the same plane. This is explained in my Guthrie lecture.

M. Orowan. — Is it generally realised that deformation bands develop in a quite continuous manner?

M. Allen. — This discussion is concerned with points raised in the report by professor Mott and is based principally on experiments on the creep of pure aluminium at 200 °C carried out at the National Physical Laboratory by Mr. D. McLean.

The Character and Spacing of Deformation Bands.

The explanation of deformation bands put forward in Mott's Guthrie Lecture indicates that a deformation band should consist of a short stretch of bent lattice with a long stretch of lattice of original orientation on either side. A series of such bands is drawn in fig. 1*a* and the same set after polygonising is schown in fig. 1*b*. This character appears to obtain when deformation is carried out under suitably chosen conditions in single crystals (see fig. 10 in the Guthrie Lecture by N. F. Mott, *Proc. Phys. Soc.* 1951). There seems no reason why it should not obtain under more complicated conditions;

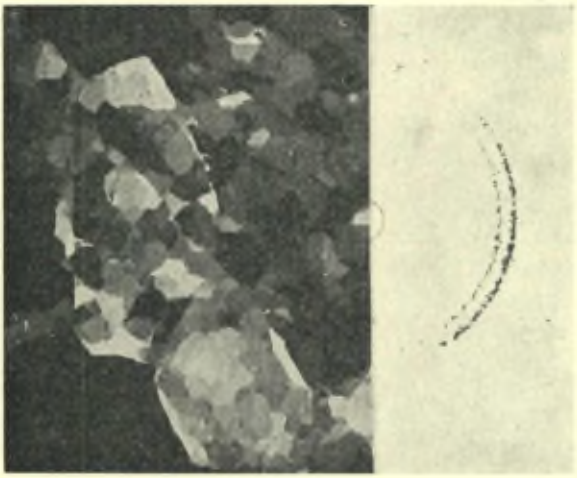

Fig. 1. — Polygonised (sub-crystal) structure developed during creep (50% extension in 1000 hrs. at 200 °C.
Left — micrograph × 100
Right — X-ray diagram.

Fig. 2. — Creep specimen extended 31 %.
Left — deformed surface.
Right — same field, section just below surface. × 100

Fig. 3 — Polygonised structure in cold rolled aluminium, reduced 50 % × 100

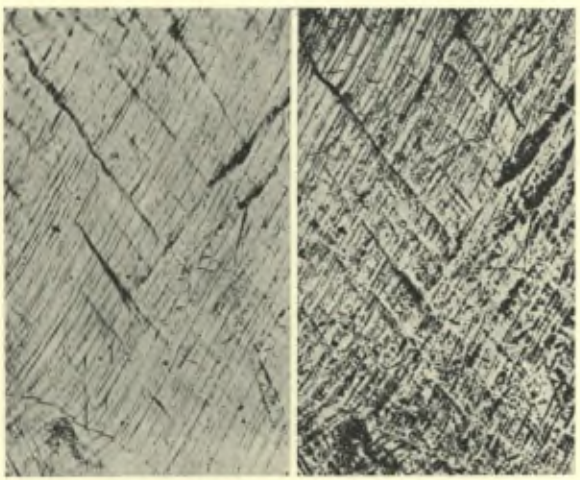

Fig. 4. — Originally polished surface after 31 % extension at 200 °C.
Left — in focus.
Right — out of focus, microscope stopped down. × 100

when two or three different directions of slip operate, two or three sets of well spaced deformation or polygonised bands should occur. This, however, does not appear to happer. Instead, the more regular bending depicted in somewhat idealised fashion in fig. 2 often occurs, and the sub-crystals formed after polygonisation are fairly uniform in size instead of being periodically thin and thick. The early work of Jenkins and Mellor (1) on iron showed this fairly uniform sub-crystal structure developing during creep. Similarly, the « call » structure that Wood and co-workers (2) and Wyon and Crussard (3) have shown on the surface of aluminium creep specimens, and which almost certainly delinsate the polygonised sub-crystal boundaries (*), have a fairly uniform size. Using an anodic oxidation technique in conjunction with a polarising microscope, these structures can be seen on sections of aluminium creep test specimens. Fig. 1 shows such a structure together with the X-ray pattern. Fig. 2 shows another field together with the appearance of the deformed surface; apparently the slip wasmainly in one direction. In this case banding occurs with a fairly regular spacing. An essentially similar structure is produced by cold rolling pure aluminium, as shown in fig. 3, so that this regularity occurs during both hot and cold deformation. Fig. 4 shows the appearance of an originally electro-polished surface after 30 per cent extension at 200 °C in a region where again slip was mainly in one direction. The appearance is closer to that indicated in the Guthrie Lecture. It will be noticed that the bands in one sense (actually the convex bands) are sharp, but those in the other sense are gradual. This was frequently, but not always, observed on the surface. As no indication of it was seen on sections, it is probably a surface effect. (The slide also shows the same area out of focus with the microscope stopped down to show up the « white line » structure.) Fig. 4 also shows the very regular spacing of deformation bands during creep. and Mr. McLean suggests that each deformation band is initiated by the preceding one, the first commencing near a grain boundary in a polycrystal. Polygonisation is generally observed to begin near a grain boundary.

(3) C. H. M. Jenkins and C. A. Mellor, *J.I.S.I.* 1935 (11), p. 179.

(2) C. R. Wilms and W. A. Wood, *J.I.M.* 1949, **75**, p. 693.

(1) G. Wyon and C. Crussard, *Revue Metallurgie*, 1951 (February), **78**, p. 121.

(*) Wood, of course does not agree with this.

The Nature of the Deformations taking place during the Creep of Aluminum.

These photographs have been obtained in the course of an investigation in which the contributions to the total deformation made by slip and grain boundary movement were measured. Grain boundary movement accounted for a very small proportion — not more than 5 or 10 per cent — of the total strain and in coarse grained specimens the prominent slip bands seen in fig. 4 accounted for about 50 per cent of the strain. These slip bands were spaced 10-30 μ apart, and the surfaces displacements were from 1/2 to 5 μ. The remainder of the deformation was accounted for by very fine slip in the material between the prominent slip bands, and visible only with phase contrast illumination under a very high magnification (fig. 5). The fine slip bands were spaced 1 μ or less apart, and produced surface displacements of 50 to 500 angstroms. Fig. 6 provides further evidence of the uniformly distributed shear between the prominent slip bands; the angle that the scratch across the slip bands makes with the direction of the slip bands alters as deformation proceeds. In fine grained specimens the fine slip accounts for nearly the whole of the deformation, prominent slip bands being rarely found.

The simultaneous existence of these two types of deformation will have to be accounted for by dislocation theory, and it is useful to consider how the two deformations appear when regarded as being due to the movements of dislocations. In the case of one particular coarse grained specimen the average displacement along the prominent bands was 10^{-4} cm in 1.000 hr, or 10^{-7} cm per hour, corresponding to a rate of passage of dislocations of $\frac{10^{-7}}{2.8 \times 10^{-8}}$ or 4 dislocations per hour. A roughly equal amount of deformation was produced by the finely distributed slip and if it is assumed that the fine slip bands were on the average about 10^{-5} on apart and that the dislocations producing the fine slip travelled about the same distance as those producing the prominent slip, the rate of passage of dislocations along them will have been about $4 \times \frac{10^{-5}}{20 \times 10^{-4}}$ per hour, or one dislocation in 50 hours. It seems necessary to postulate two types of dislocation source, one capable of producing dislocations at the higher rate and one producing them, under the same stress, at the lower rate. It was very difficult to decide how close the fine slip

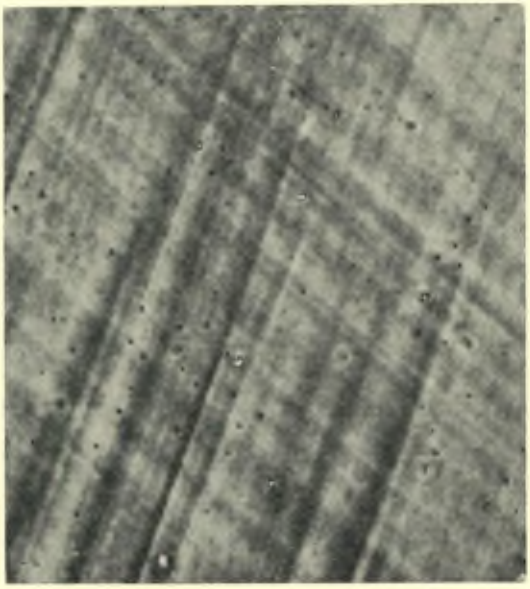

Fig. 5. — Phase-contrast micrograph showing fine slip. × 1500

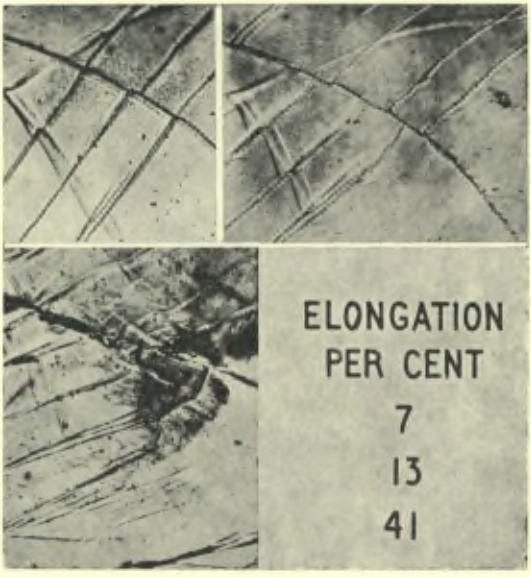

Fig. 6. — Showing shear in spaces between the prominent slip bands × 750

bands shown in fig. 5 might be. Fig. 5 was produced at an early stage of deformation. The fine bands later became impossible to see, and since from fig. 6 it is clear that the fine movement was continuing, it can only be concluded that new bands were continually being produced, and the spacings were becoming continually closer. It seems not impossible that this movement is due to the setting in motion of dislocations randomly distributed in the space between the slip bands, and that the greater density of slip in some parts of the space is merely statistical. It is probably that the dislocation in the prominent slip bands travel further than those in the fine slip bands, and the number of dislocations passing per hour in the fine slip bands may be somewhat undersetimated.

Creed and Polygonisation.

Professor Mott takes the view that the essential feature of « recovery » creep is the escape of the dislocations from the slip bands to form the boundary walls of polygonised areas. The occurrence of polygonisation during creep has been very evident in the work at the National Physical Laboratory, and an explanation has been attempted on the assumption that it is due to the capture of the dislocations associated with the fine slip by boundaries of the correct sign. The number (n) of dislocations per cm of the boundary is determined from the angular tilt at the boundary and given by $n = \frac{\theta}{\lambda}$ (θ = angular tilt; λ = unit slip distance caused by the passage of a single dislocation). These dislocations will have been gathered from an area d cms wide, where d is the distance between polygonisation boundaries, so that the density of dislocations will be $\frac{n}{d} = \frac{\theta}{d\lambda}$. The average distance moved by each dislocation will also be of the order of d, so that the shear due to each dislocation will be of the order of λd. Consequently the total shear will be of the order of $n\lambda \times \frac{\theta}{d\lambda} = \theta$.

Attempts to estimate the creep extension from measurements of angular tilt have been moderately successful. In a coarse grained specimen the creep strain attributed to the fine slip was 17 per cent, and from the measurements of angular tilt was estimated to be between 16 and 24 per cent. In a fine grained specimen the total creep strain, which was almost entirely due to fine slip (few coarse

slip bands being present) was 38 per cent. That estimated from the polygonisation tilts was 29 per cent. It is therefore probable that there is a very close connection between creep and polygonisation nevertheless polygonisation may follow creep rather than precede it and creep be possible without the dislocations producing it being gathered up into polygonisation boundaries.

M. Crussard. — Le professeur Mott a étudié ici un mécanisme d'écrouissage; les cross-slips et les bandes de déformation qui leur sont associées.

En réalité, il existe d'autres causes d'écrouissage. En effet, dans les monocristaux, en étudiant la forme exacte des courbes de traction, on observe :

— que jusqu'à 3-5 % d'allongement, il n'y a pas de bande de déformation marquée et que l'écrouissage est faible mais *existe tout de même*. (Les courbes des expériences de Röhm et Kockendörker se placent sur la prolongation de cette portion). Ceci prouve qu'un autre mécanisme, du genre de celui suggéré par F. Seitz, doit jouer;

— lorsqu'il y a double glissement dès le début, l'écrouissage est fort dès le début, mais croît ensuite très lentement, et il n'y a pas de bandes de déformation.

Dans les polycristaux, les bandes de déformation apparaissent rarement; les cross-slips n'apparaissent qu'après quelques pour cent d'allongement, et pourtant l'écrouissage est très fort dès le début.

Il semble donc qu'en pratique, la cause principale d'écrouissage réside, au début de la déformation, dans des obstacles tels que joints, pellicules d'oxydes superficielles et autres surfaces de discontinuité, qui bloquent des dislocations; ces dislocations à leur tour sont des obstacles pour les dislocations de tout autre système de glissement, recoupant le premier.

Je voudrais, d'autre part, signaler une difficulté dans la théorie des cross-slips proposée par le professeur Mott : lorsqu'on observe au microscope un cristal en cours de déformation, on voit les deux bouts de bandes de glissement et le cross-slip qui les joint apparaître en même temps (disons en moins d'une demi-seconde). Il faudrait admettre que plusieurs sources de Frank-Read soient mises en mouvement simultanément dans un même plan, ce qui paraît peu

probable. Je serais donc plutôt en faveur d'un mécanisme de bifurcation à partir d'une source unique, peut-être l'action de quelques dislocations bloquées sur un plan de glissement anormal (unpredicted slip) recoupant le plan de glissement normal. Dans certains cas j'ai même réservé un petit élément de glissement analogue à un cross-slip, mais qui, au lieu de rejoindre deux bandes de glissement, se trouvent simplement à la fin d'une bande.

M. Hollomon. — The surface effects described by Mott probably can be interpreted in terms of a network of dislocations, each segment of which acts as a Frank-Read source (*). For interior sources the critical stress for the generation of loops will be

$$\tau/G \gtrsim b/L$$

where G is the shear stress, b the Burgers vector, end L the distance between pinning points. A surface source, however, will be pinned only at one end and because of line tension the free end of the dislocation segment will be perpendicular to the surface. Thus a surface source can be thought to be pinned at an image point outside the crystal. The effective length of a surface source is then twice its actual length. Since the distribution of lengths of segments in the interior and at the surface will be similar ordinarily surface sources will begin to generate loops at a stress about one-half that for the interior sources.

Thus the initial flow stress for single crystals with uncontaminated surfaces will be governed by the lengths of the longer surface sources. Oxide particles or films may pin the free ends of such segments and raise the flow stress by as much as a factor of two. After considerable deformation of single crystals the lengths of interior sources govern the flow stress and surface treatments should have little effect.

(*) J. C. Fisher, discussion to paper « Creep Behavior of Zinc Modified by Copper in the Surface Layer », by M. R. Pickus and E. R. Parker, *Journal of Metals*, September 1951.

TABLE DES MATIÈRES

Pages

Le Neuvième Conseil de Physique 7

Rapports et discussions.

Cyril Stanley SMITH. — Interfaces Between Crystals 11
Discussion 45

G.W. RATHENAU. — Grain Growth Observed by Electron Optical Means 55

W.G. BURGERS. — Recrystallization and Grain Growth in Solid Metals 73
Discussion 157

E. RUDBERG. — Recent Work on Solid State Transformation in Sweden 167
Discussion 188

A. GUINIER. — Les défauts de périodicité dans les réseaux des solutions solides 197
Discussion 231

Werner KÖSTER. — Neuere Untersuchungen zur Frage der Aushärtung 235
Discussion 262

Jean LAVAL. — Sur l'élasticité du milieu cristallin 273
Discussion 313

F.C. FRANK. — Crystal Growth and Dislocations 315
Discussion 336

C. CRUSSARD. — Etude des interférences des ondes d'agitation thermique dans les cristaux : application à l'activation des transformations 345
Discussion 370

Frederick SEITZ. — On the Generation of Vacancies by Moving Dislocations 377
Discussion 408

V. DEHLINGER. — Diskussionsbeitrag zur Theorie der Versetzungen. . 415
Discussion 420

G. BORELIUS. — Calorimetric Studies of Isothermal Recovery 427
Discussion 429

W. SHOCKLEY. — Dislocation Models of Grain Boundaries 431
Discussion 485

H. COTTRELL. — The Yield Point in Single Crystal and Polycrystalline Metals 487
Discussion 504

N.F. MOTT. — Diffusion, Work-hardening, Recovery and Creep . . . 515

E. OROWAN. — The Dynamics of Slip 535
Discussion 566